Molecular and biochemical characterisation of isoprene metabolism by *Variovorax* sp. WS11

Robin Dawson, BSc, MRes

A thesis submitted to the school of Environmental Sciences in fulfilment of the requirements for the degree of Doctor in Philosophy.

July 2021

University of East Anglia

School of Environmental Sciences

Norwich, UK

Abstract

Isoprene is the most abundant non-methane volatile organic compound (VOC), with over 500 Tg C yr^{-1} produced worldwide. Terrestrial plants, particularly trees, are the main sources of isoprene, and soils are currently the largest known sink for atmospheric isoprene. The work described in this thesis aimed to characterise the isoprene metabolic pathway used by the novel Gram negative bacterium, *Variovorax* sp. WS11. Isoprene monooxygenase (IsoMO), the plasmid-encoded soluble diiron monooxygenase (SDIMO) first identified in *Rhodococcus* sp. AD45, was characterised in *Variovorax* sp. WS11 by targeted mutagenesis and heterologous expression of the IsoMO-encoding genes, *isoABCDEF*. Linear alkynes selectively inhibited isoprene oxidation by different SDIMO enzymes, with octyne inhibiting isoprene oxidation by IsoMO and acetylene inhibiting the co-oxidation of isoprene by the soluble methane monooxygenase (sMMO). These findings provided avenues for further studies of isoprene degrading communities in soils.

Analysis of the proteome of isoprene-grown *Variovorax* sp. WS11 allowed the prediction of the full isoprene metabolic pathway. Propionyl-CoA was predicted as a metabolic intermediate due to the significant expression of peptides which catalyse the methylcitrate cycle and the methylmalonyl-CoA pathway. These data indicated that *Variovorax* sp. WS11 incorporates isoprene-derived carbon via a different metabolic pathway than *Rhodococcus* sp. AD45, in which the genes encoding these pathways were not expressed during growth on isoprene. Further molecular and biochemical analyses are required to confirm the roles of the putative methylmalonyl-CoA and methylcitrate pathways in isoprene metabolism.

The expression of the *iso* metabolic gene cluster was regulated by two LysR-type transcriptional regulators, with targeted mutations indicating that *dmlR_4* encoded a transcriptional activator and *dmlR_5* encoded a transcriptional repressor. Isoprene metabolism was differentially regulated in the presence of alternative carbon sources, with glucose repressing the expression of the *iso* gene cluster and pyruvate stimulating expression of *isoA* and the apparent activity of IsoMO.

Table of Contents

List of Tables

List of Figures

Declaration

I declare that the work presented in this thesis was conducted by me under the direct supervision of Professor J. Colin Murrell. Results obtained by, or with help from, others have been acknowledged in the relevant section. None of the work presented has been previously submitted for any other degree.

Robin Dawson

Acknowledgements

I would like to thank the European Research Council for funding my PhD project. I am endlessly grateful to my supervisor, Professor Colin Murrell, for his support and guidance over the course of my PhD, and for pushing me to perform as best I can. I would also like to thank current and past members of the Murrell group for their advice in so many aspects of my project. To Professor Jonathan Todd, I am very grateful for his advice and guidance in molecular genetics techniques. Also, thanks are due to Dr Andrew Crombie for his patience and advice on many occasions.

To my family and friends, who never miss an opportunity to let me know that they are proud of me, no thanks could ever be enough. And finally, to my fiancée, Abbie, whose emotional support and endless patience have made it possible for me to reach the completion of this project.

Abbreviations

ABS: Activator binding site

ACC: 1-aminocyclopropane-1-carboxylic acid

AHL: Acyl-homoserine lactone

ANI: Average nucleotide identity

ATCC: American Type Culture Collection

ATP: Adenosine triphosphate

BLAST: Basic Local Alignment Search Tool

bp: base pairs

CCR: Carbon catabolite repression

cDNA: Complementary deoxyribonucleic acid

CDP-ME: Methylerythritol cytidyl diphosphate

cfu: Colony forming units

ChIP-Seq: Chromatin immunoprecipitation with sequencing

CoA: Coenzyme A

CoM: Coenzyme M

C_T: Cycle threshold

DCE: *cis*/*trans*-1,2-dichloroethylene

DEPC: Diethyl pyrocarbonate

DMAPP: Dimethylallyl pyrophosphate

DMSO: Dimethyl sulfoxide

DNA: Deoxyribonucleic acid

DTT: Dithiothreitol

DXP: Deoxyxylulose

EPS: Extracellular polysaccharide

GC: Gas chromatography

gDNA: Genomic deoxyribonucleic acid

GMBA: 2-glutathionyl-2-methyl-3-butenoic acid

GmR: Gentamicin resistance gene (*aacC1*)

GOI: Gene of interest

GSH: Glutathione (reduced)

GSSG: Glutathione disulfide (oxidised)

GST: Glutathione *S*-transferase

H^{CP}: Henry's law constant

HEPES: 4-(2-hydroxyethyl)-1-piperazineethanesulfonic acid

HGMB: 1-hydroxy-2-glutathionyl-2-methyl-3-butene

HMBPP: 3-methyl-butenyl-1-diphosphate

HTH: Helix-turn-helix

hu: Photochemical oxidation

IPP: Isopentyl diphosphate

IsoMO: Isoprene monooxygenase

Isoprene: 2-methyl-1,3-butadiene

IspS: Isoprene synthase

KanR: Kanamycin resistance/resistant

kpb: kilobase pairs

LC: Liquid chromatography

LTTR: LysR-type transcriptional regulator

m/sec: Undefined unit applied to bead-beating machines developed by MP Biomedicals (Section 7.4.2)

MarR: Multiple antibiotic resistance regulator

MDH: Methanol dehydrogenase

MEcPP: 2-C-methyl-D-erythritol-2,4-cyclodiphosphate

MEP: Methylerythritol 4-phosphate

mg(dw): Milligrams of dry weight

min: Minute

MMOH-α: Soluble methane monooxygenase oxygenase component, α-subunit

MMOB: Soluble methane monooxygenase regulatory/coupling protein component

MMOR: Soluble methane monooxygenase oxidoreductase component

mpb: megabase pairs

mRNA: Messenger ribonucleic acid

MS: Mass spectrometry

MVA: Mevalonate

NAD: Nicotinamide adenine dinucleotide (oxidised)

NADH: Nicotinamide adenine dinucleotide (reduced)

nmol: Nanomoles

NMS: Nitrate mineral salts

OD_{540}: Optical density, measured at 540 nm

OH: Hydroxyl radical

OMI: Ozone monitoring instrument

PAR: Photosynthetically available radiation

PCR: Polymerase chain reaction

pMMO: Particular methane monooxygenase

ppb: parts per billion

ppbv: parts per billion by volume

PQQ: Pyrroloquinoline quinone

R: Standard/regular DNase treatment by Turbo DNase (Thermo Fisher Scientific) (Section 7.4.2)

RA: Relative abundance

RAST: Rapid Annotations Using Subsystems Technology

RBS: Regulatory binding site

RIN: RNA integrity number

RNA: Ribonucleic acid

rRNA: ribosomal RNA

RPM: Revolutions per minute

RT-qPCR: Reverse transcription quantitative polymerase chain reaction

RT: Room temperature (specific to Chapter 3)

SDIMO: Soluble diiron monooxygenase

SDS: Sodium dodecyl sulfate

sMMO: Soluble methane monooxygenase

SOA: Secondary organic aerosol

sRNA: Small ribonucleic acid

T: Treated (specific to Section 7.4.2)

TBE: Tris Borate EDTA

TMT: Tandem mass tagging

To4MO: Toluene 4-monooxygenase

ToMOD: Toluene/*o*-xylene monooxygenase

U: Untreated (specific to Section 7.4.2)

V: Vigorous DNase treatment by Turbo DNase (Thermo Fisher Scientific) (Section 7.4.2)

VOC: Volatile organic compounds

WS11: Willow soil isolate number 11

XaMO: Alkene monooxygenase from *Xanthobacter* sp. Py2

1. Introduction

1.1. Isoprene – a highly abundant volatile organic compound

Volatile organic compounds (VOC) are highly abundant components of the atmosphere, produced from a myriad of biogenic and anthropogenic sources. The most abundant non-methane VOC is undoubtedly isoprene (2-methyl-1,3-butadiene), the simplest hemiterpene unit consisting of a methylated 4-carbon chain with two terminal alkene groups. With an estimated annual production of 550 Tg C yr^{-1} (Guenther *et al*. 2006, 2012, Sindelarova *et al*. 2014), the importance of isoprene cannot be understated. The vast majority of isoprene production is biogenic, with an estimated 90% produced by terrestrial plants (Sharkey *et al*. 2008, Sindelarova *et al*. 2014).

1.1.1. Atmospheric chemistry of isoprene

Isoprene is highly reactive due to its twin carbon=carbon double-bonds. According to the composition of the local atmosphere, the half-life of isoprene and the products of its oxidation can be highly varied (Atkinson & Arey 2003, Seinfeld & Pandis 2006). Hydroxyl radicals (OH) initiate nucleophilic attack on the C=C bonds of isoprene, giving isoprene an estimated half-life of only 1.7 hours (Seinfeld & Pandis 2006, Wennberg *et al*. 2018, Berndt *et al*. 2019). Other known atmospheric reactants with isoprene include ozone, resulting in a predicted half-life of 1.3 days, and nitrate radicals (NO_3), giving isoprene an atmospheric half-life of only 0.8 hours (Seinfeld & Pandis 2006, Kwan *et al*. 2012, Wennberg *et al*. 2018). Interactions of isoprene with SO_2 and NO_2 also contribute to the formation of secondary organic aerosol (SOA) (Edney *et al*. 2005, Kleindienst *et al*. 2006, Wennberg *et al*. 2018), diverse particulate matter which can provide the nuclei for cloud condensation (Claeys *et al*. 2004). Such interactions have been demonstrated in both laboratory-based and environmental studies, wherein the specific photooxidation products of isoprene caused significant increases in SOA when exposed to NO_2 or SO_2 (Figure 1.1) (Edney *et al*. 2005, Kleindienst *et al*. 2006, Nestorowicz *et al*. 2018). Two markers for SOA production by isoprene are 2-methylerithritol and 2-methylthreitol (Claeys *et al*. 2004). The production of these compounds is strongly correlated with the diurnal production of isoprene, with a peak in summer months consistent with the temperature effect on isoprene biogenesis (described in Section 1.2.3) (Plewka *et al*. 2006, Kleindienst *et al*. 2007a, Li *et al*. 2018a, Lantz *et al*. 2019b). It should be noted that Nozière *et al*. (2011) have challenged the significance of the above compounds as a marker for abiotic SOA production since their enantiomeric analysis of 2-methyl-tetrols indicated that a significant proportion was of biological origin.

Each reaction produces a variety of compounds with differing implications for the local atmosphere. The addition of OH to isoprene at any of the double-bond associated carbons (Barket *et al*. 2004) produces, with the further addition of O_2, isoprene peroxy radicals of varying forms (Liu *et al*. 2016). These react in turn with hydroperoxyl radicals (HO_2), producing hydroxyhydroperoxides, or with NO_x ($NO + NO_2$) to produce methyl vinyl ketone and methacrolein (Barket *et al*. 2004, Liu *et al*. 2016, Seinfeld & Pandis, 2006). Subsequent products of the reactions of isoprene peroxy radicals include SOA, formaldehyde, and diverse particulate organic matter (Atkinson & Arey, 2003, Carlton *et al*.

2009, Liu *et al*. 2016). The local concentration of NO_x drives further reactions of the organic peroxy radicals. In the presence of NO, NO_2 is generated which is then photolyzed to produce O_3 (Barket *et al*. 2004, Squire *et al*. 2015) at a rate which is predicted to be dependent on NO_2 formation from NO radicals (Biesenthal *et al*. 1997). The accumulation of O_3 as a result of isoprene-dependent reactions in areas of mid/high-NO_x, typically in industrialised or highly residential areas, impacts upon local air quality (Trainer *et al*. 1987, Barket *et al*. 2004, Silva *et al*. 2016). In areas of low NO_x, such as in rural or unpopulated areas, isoprene reacts directly with O_3 which, when combined with photolysis, results in decreased O_3 (Jenkin *et al*. 2015).

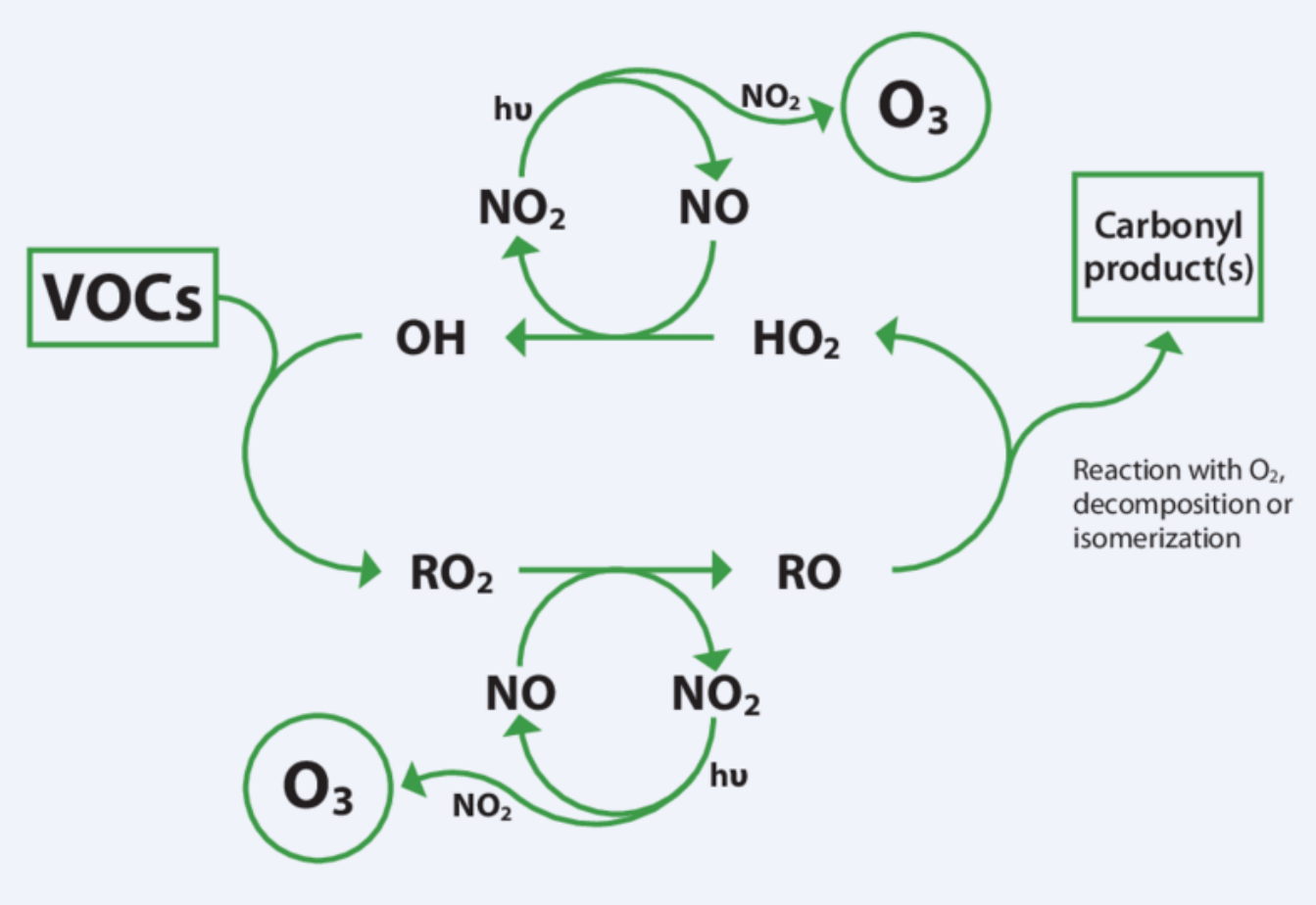

Figure 1.1. Atmospheric chemistry of isoprene and other VOC driven by photochemical oxidation (hu) (taken from Jenkin & Hayman, 1999).

1.1.2. **Direct and indirect measurement of atmospheric isoprene**

The measurement of atmospheric isoprene and the fate of isoprene remains a frequently updated area of research. A combination of laboratory-based (Kleindienst *et al*. 2006, Kleindienst *et al*. 2007, Kroll *et al*. 2005, 2006), direct measurement (Bolas et al. 2020, Otu-Larbi et al. 2020) and indirect measurement (Fu *et al*. 2019, Kaiser *et al*. 2018, Wolfe *et al*. 2016) studies have attempted to resolve the maelstrom of chemical processes driving the atmospheric flux of isoprene. Much progress has stemmed from the deployment of new technologies on land and in space. A frequently used model is MEGAN2.1 (Guenther *et al*. 2006, 2012), which attempts to predict the net release of biogenic isoprene. These predictions are hampered by uncertainties in many factors, including the uncertainty of

direct measurements and lacking knowledge of the factors influencing VOC cycling (Robinson et al. 2005, Arneth et al. 2008, Stone et al. 2011, Guenther et al. 2012, Bolas et al. 2020).

Direct measurement of isoprene typically relies on gas chromatography. When conducted *in situ*, this requires sophisticated equipment, a steady power supply, and gas cylinders sufficient to support on-line analysis (Bolas et al. 2020, Gómez et al. 2020). Recent studies using the iDirac apparatus have demonstrated field isoprene measurements in a range of areas, including the Malaysian Borneo and various sites across England (Bolas et al. 2020, Otu-Larbi et al. 2020). Otu-Larbi *et al*. (2020) demonstrated the ability of this apparatus to record continuous measurements at specific intervals at four different heights of a forest canopy, providing temporal resolution to isoprene emission data during a mild drought. Other methods are available which do not rely on *in situ* sampling capabilities, including "grab samples" which can be deployed over relatively large areas and collected for later analysis. A hinderance of this technique is the lack of temporal resolution, a significant drawback when attempting to record the cycling of VOC (Robinson *et al*. 2005).

Laboratory-based analyses of the photooxidation products of isoprene have informed current methods of indirect quantification of isoprene. A key reaction which has been used to develop satellite-based approaches is that of isoprene and NO_x which, in NO_x-rich areas, produces significant quantities of formaldehyde (Kaiser *et al.* 2018, Wolfe *et al.* 2016). This fact has provided the basis for many top-down isoprene measurement studies. Using the ozone monitoring instrument (OMI), researchers have attempted to infer changes in isoprene emissions over time by using measurements of atmospheric formaldehyde (Kaiser *et al.* 2018, Wolfe *et al.* 2016, Zhu *et al.* 2017). Limitations of this method were discussed by Fu *et al*. (2019). The isoprene-dependent formation of formaldehyde is governed by the availability of NO_X, limiting the utility of these indirect measurements in non-industrialised areas (Wolfe *et al.* 2016) or over the ocean. Further complicating these top-down approaches is the incomplete knowledge of the cycling of other VOC and their influence on formaldehyde production (Fu *et al*. 2019), and also the significant variation between local-to-regional emission models (Arneth *et al*. 2008, 2011, Kaiser *et al*. 2018). The uncertainty of the formaldehyde-measuring method was claimed to be between 10-50% (Fu *et al*. 2019). The recent demonstration of direct measurements of isoprene by remote infrared sensing over the Amazon rainforest may lead to greater accuracy in measuring atmospheric isoprene (Fu *et al*. 2019), although the technical limitations identified in this study call for further investigation. The combined application of direct isoprene measurement and top-down formaldehyde measurement have allowed for greater confidence when measuring isoprene in areas which have low NO_X concentrations, a limitation when using methods which rely solely on the measurement of formaldehyde (Fu *et al*. 2019).

Modelling of VOC cycling is hindered by many difficulties, not least of which is the incomplete understanding of the products of the oxidation of VOC in the atmosphere. Isoprene, for example, forms many peroxy radicals depending on the site of hydroxyl radical attack within the carbon skeleton (Barket *et al*. 2004, Liu *et al*. 2016), and the second-generation products and beyond are still not entirely understood (Carlton *et al*. 2009, Wennberg *et al*. 2018). Further

discrepancies between modelled isoprene cycling and direct measurements are believed to stem from incomplete knowledge relating to environmental and biological factors. Missing environmental factors which influence isoprene emission (see below), such as local temperature and CO_2 concentration, may introduce discrepancies in model predictions, while the lack of data relating to basal rates of isoprene emission by trees is believed to provide the greatest uncertainty (Arneth *et al*. 2008, Kaiser *et al*. 2018). Kaiser *et al*. (2018) argue that the lack of such knowledge has led to significant biases in prediction of VOC cycling by the well-known MEGAN2.1 model (Guenther *et al*. 2006, 2012).

1.1.3. **Atmospheric implications of isoprene production**

Global cycling of isoprene is believed to produce a variety of effects on local and regional climate according to the concentrations of available atmospheric compounds with which isoprene can react. It would also stand to reason that blooms of isoprene would cause a range of effects on the local atmosphere, such as during biomass burning (Li *et al.* 2018) or algal blooms (Hu *et al*. 2013). The depletion of hydroxyl radicals by isoprene indirectly increases the lifetime of methane (CH_4) (Wang & Shallcross 2000, Sanderson *et al*. 2003), thereby contributing to the warming effect imposed by this potent greenhouse gas. Methane typically persists for approximately 10 years in the atmosphere (National Research Council, 2010, Nisbet *et al.* 2016), with hydroxyl radicals playing a key role in mitigating the residence time. As has already been mentioned, isoprene can have significant effects on local air quality depending on the availability of reactive compounds. In areas of mid/high-NO_x, one of the end-products of isoprene oxidation is O_3 (Atkinson & Arey 2003, Monks *et al*. 2015), which is known to impact greatly on human health if present in excessive quantities (World Health Organization 2000, Forouzanfar *et al*. 2015). The formation of SOA by the reactions of isoprene with NO_2 and SO_2 can contribute to a cooling effect due to the radiative shielding provided by clouds (Claeys *et al*. 2004). It has been posited that the production of BVOC produces a net negative radiative forcing effect (Unger 2014), although a more recent study argues that this failed to account for the full radiative effects of atmospheric aerosols (Scott *et al*. 2018). While isoprene undoubtedly exerts varied influences on local and regional atmospheric chemistry and climate, more work is needed to fully evaluate the net climatic effects of this abundant VOC.

Terrestrial plants are the primary source of biogenic isoprene (as described in Section 1.2) (Seinfeld & Pandis 2006, Guenther *et al*. 2012). Recent years have seen significant changes in land use which reflect societal needs, such as for food and biofuel crops (Ellis *et al*. 2010, Gunarso *et al*. 2013). Malaysian oil palm plantations are a striking example. Between 2000-2010, approximately 230,000 ha of native forest were replaced with oil palm every year (Gunarso *et al*. 2013). Oil palm trees are known to be exceptionally high producers of isoprene, producing approximately 172.9 µg isoprene/gdw of leaves/h (Nicholas Hewitt & Street, 1992, Kesselmeier & Staudt, 1999). This translates to an estimated 7800 µg isoprene m^{-2} h^{-1} in oil palm plantations (Misztal *et al*. 2011), representing a significant hotspot for isoprene production. Ambient isoprene concentrations over such plantations can reach up to 12 ppbv (Silva *et al*. 2016). These isoprene hotspots may have significant, albeit localised, impacts on the atmosphere due to the chemical interactions described above. For example, photochemical smog has been observed

in areas of increased isoprene emission (Bru *et al*. 2012, Lantz *et al*. 2019a). However, the long-term impacts of atmospheric isoprene increasing concurrent with the expansion of oil palm plantations have not been fully described. Hardacre *et al*. (2013) predicted a global change in atmospheric isoprene concentration of <1 ppb, while other studies have predicted significant impacts on air quality in certain urban environments (Silva *et al*. 2016). O_3 levels were predicted to rise by 3-4.5 ppbv in such areas by 2020 (Silva *et al*. 2016). Predicted increases in SOA concentrations also reach as much as 3.5 μg m^{-3} in models of oil palm expansion (Silva *et al*. 2016). More work is needed to determine the effects of increasing isoprene concentrations, particularly relating to its influence on global climate.

1.2. **Production of isoprene and factors affecting isoprene biosynthesis**

1.2.1. **Biosynthesis of isoprene by a variety of organisms**

Isoprene is synthesised by a wide variety of organisms, with production reported in plants (Loreto & Velikova 2001, Sharkey & Yeh 2001, Laothawornkitkul *et al*. 2008, Wiberley *et al*. 2009, Jardine *et al*. 2020), bacteria (Kuzma *et al*. 1995, Fall & Copley 2000, Wagner *et al*. 2000), fungi (Bäck *et al*. 2010), animals (DeMaster & Nagasawa 1978, Deneris *et al*. 1985), algae (Bonsang *et al*. 1992, Shaw *et al*. 2010, Exton *et al*. 2013), and corals (Dawson *et al*. 2021). Considerable variation in isoprene biosynthesis exists between each group, and plants in particular are noted for significant variation in emission rates down to species level. The American oak, for example, is a high-producer of isoprene, while many European oaks do not produce isoprene at all (Sharkey *et al*. 2008). Approximately 90% of isoprene is produced by terrestrial plants (Figure 1.2). Although the vast majority of isoprene is produced by tropical trees (Guenther *et al*. 2006, 2012, Sharkey *et al*. 2008), only 20-38% of tropical tree species are believed to emit isoprene (Jardine *et al*. 2020). Isoprene emission rates range from approximately <1 μg g^{-1} dry weight leaves h^{-1} (μg/gdw leaves/h) in ash species (*Sorbus scopulina* and *Fraxinus caroliniana*) to 172.9 μg/gdw leaves/h by oil palm trees (Hewitt & Street, 1992, Kesselmeier & Staudt, 1999). Other terrestrial plants known to produce isoprene include mosses (Hanson *et al.* 1999), ferns (Tingey *et al*. 1987), and even commercial crops such as oat and sugar beet (Sharkey *et al*. 2008). Cumulatively, terrestrial plants generate an estimated 499-535 Tg isoprene yr^{-1} (Seinfeld & Pandis 2006, Guenther *et al*. 2012), the majority of which is produced by leaves. Recent studies have identified isoprene production in the roots of trees such as poplar, albeit at a significantly lower rate than in the leaves (van Doorn *et al*. 2020).

By contrast, aquatic isoprene biosynthesis accounts for a relatively small, but not insignificant, proportion of the global isoprene budget (reviewed by Dawson *et al.* 2021). Estimates range from 0.1-11.6 Tg C yr^{-1}, making it difficult to definitively state the impact of aquatic isoprene biosynthesis on the isoprene biogeochemical cycle (Palmer & Shaw 2005, Arnold *et al*. 2009, Luo & Yu 2010, Shaw *et al*. 2010). Known contributors to aquatic isoprene production are bacteria (Shaw *et al*. 2010), microalgae (Dani et al. 2017, Steinke et al. 2018), dinoflagellates (Bentlage *et al*. 2016), and phytoplankton (Arnold *et al*. 2009, Shaw *et al*. 2010), with further contributions from seaweeds and corals (Shaw *et al*. 2010, Dawson *et al*. 2021).

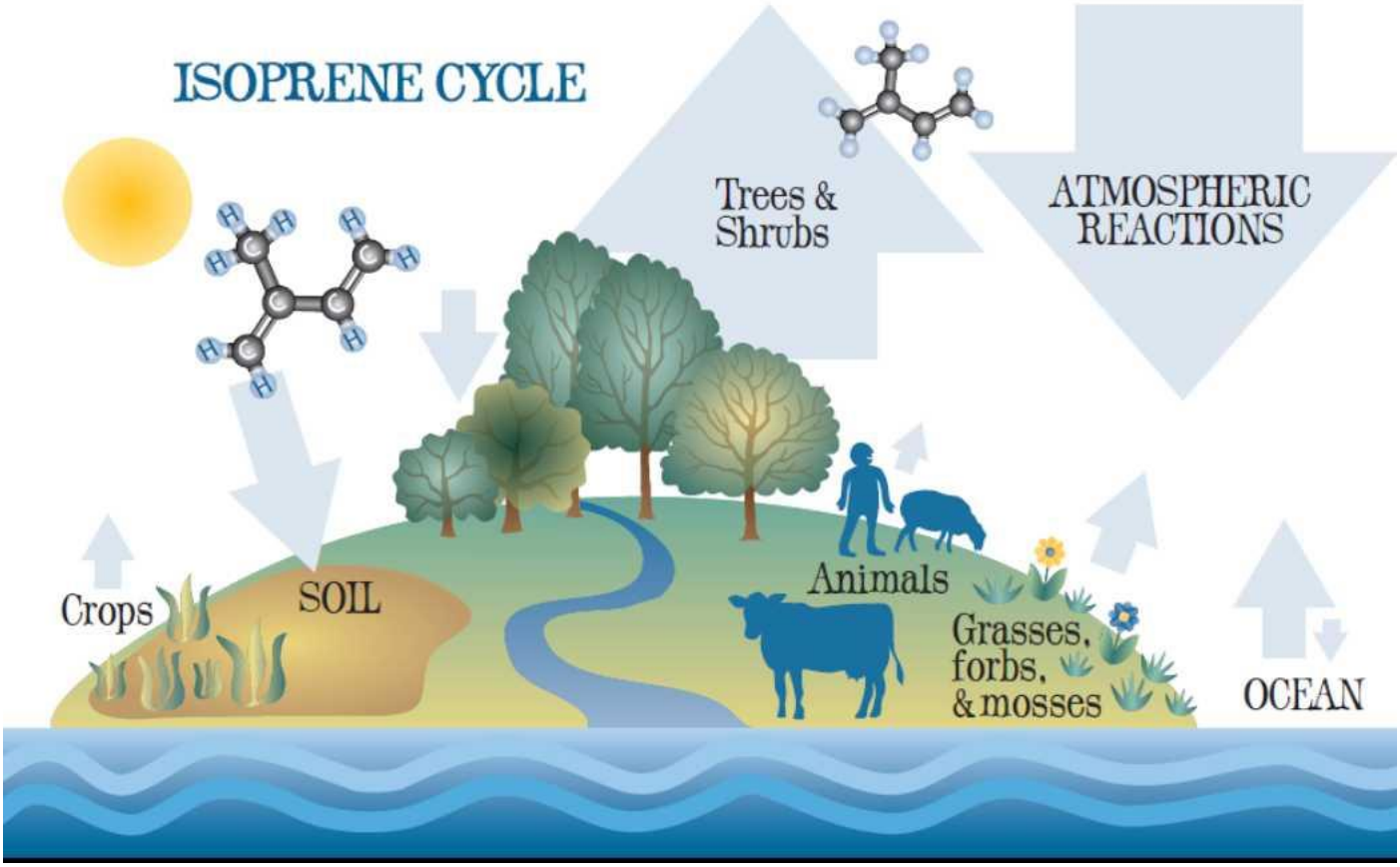

Figure 1.2. Global isoprene biogeochemical cycle, demonstrating the major sources and sinks of isoprene (taken from Mcgenity *et al.* 2018).

1.2.2. **Isoprene biosynthetic pathways**

Isoprene synthase (IspS), a divalent cofactor-dependent enzyme, catalyses the formation of isoprene from dimethylallyl pyrophosphate (DMAPP) (Lantz *et al.* 2019, Silver & Fall, 1995). The biosynthetic pathways responsible for the formation of this critical isoprene precursor, or its isomer isopentyl diphosphate (IPP), have been the subject of study for many years. Two distinct pathways for the formation of DMAPP/IPP have been characterised (Figure 1.3) (Zhao *et al.* 2013). The mevalonate pathway, described in animals, fungi, archaea, and the cytosol of higher plants begins with the condensation of two acetyl coenzyme A (CoA) units to form acetoacetyl-CoA. This is condensed with a third acetyl-CoA unit and the product is reduced to form mevalonate (MVA). Mevalonate 5-phosphate is generated by two consecutive kinase enzymes, and subsequently converted to IPP by an ATP-coupled decarboxylation reaction. IPP:DMAPP isomerase catalyses the interconversion of IPP and DMAPP. The methylerythritol 4-phosphate (MEP) pathway, described in bacteria, green algae, and plant plastids, was reviewed by Zhao *et al*. (2013). Initially, glyceraldehyde 3-phosphate and pyruvate are combined in a thiamine diphosphate-dependent reaction to form deoxyxylulose (DXP). DXP is converted to MEP, the first committed product of the MEP pathway, by reductive isomerisation. MEP is then converted to methylerythritol cytidyl diphosphate (CDP-ME) by combination with cystidine 5'-triphosphate, then CDP-ME is phosphorylated and cyclised to form MEcPP (2-C-methyl-D-erythritol-2,4-cyclodiphosphate). Ring cleavage and reductive dehydration form 3-methyl-butenyl-1-diphosphate (HMBPP), which is finally converted to IPP and DMAPP (Zhao *et al.* 2013). Production of isoprene by roots has not been linked to

either the MEP or mevalonate pathway at present. This is significant when considering that the MEP pathway is localised in the chloroplast and requires photosynthetic electron transport (Li & Sharkey, 2013, Rasulov *et al.* 2009, Weise *et al.* 2013), while the roots are located belowground and do not have the same access to photosynthetic electrons. This may account for the fact that isoprene production by poplar roots is approximately 100-fold lower than isoprene production by poplar leaves (van Doorn *et al*. 2020).

1.2.3. **Factors affecting isoprene biogenesis**

Many factors influence the expression of isoprene synthase, including light, temperature, and CO_2 (Lantz *et al*. 2019a). The dependence of isoprene emission on light can be linked directly to the availability of MEP pathway components, as the MEP pathway has been demonstrated to rely entirely on photosynthetic electron transport (Li & Sharkey, 2013, Rasulov *et al.* 2009, Weise *et al.* 2013). Garcia *et al*. (2019) demonstrated this by chemically inhibiting photosynthetic electron transport to prevent isoprene emission. A well-known feature of isoprene emission by plants is the "post-illumination burst" in which an isoprene-emitting plant is suddenly deprived of light, causing an immediate cessation of isoprene emission until, approximately 5 minutes later, all remaining DMAPP in the chloroplasts is converted to isoprene (Li & Sharkey, 2013, Rasulov *et al.* 2009, Weise *et al.* 2013). This has even been demonstrated in transgenic tobacco engineered to express IspS, in which its native MEP precursor pool was directed into a post-illumination burst (Zuo *et al.* 2019).

The effect of temperature on isoprene emission can be linked to the optimum of IspS, which is approximately 45 ^{o}C (Lantz *et al.* 2019). A common observation in isoprene emitters is an increase in the rate of emission with increasing temperature (Monson *et al.* 2016, Rosenstiel *et al.* 2004, Sanadze & Kalanadze, 1966). Conversely, CO_2 is a potent inhibitor of isoprene emission at relatively low concentrations (Feng *et al.* 2019, Loreto & Sharkey, 1990, Monson & Fall, 1989). Two main hypotheses attempted to rationalise this observation. First was the inhibition of the MEP pathway due to limited phosphate availability (McClain & Sharkey 2019). Second was competition for pyruvate by the phosphoenolpyruvate carboxylase, which is stimulated at high CO_2, to deprive the MEP pathway of metabolic precursors (Rosenstiel *et al*. 2004). Each theory has since been refuted (Lantz *et al.* 2019). Lantz *et al*. (2019) suggested that Ca^{2+} spikes involved in the stomatal response to CO_2 may, in turn, regulate the MEP pathway, although no evidence has been provided in support of this.

Long-term changes to the capacity of plants for isoprene emission may differ from the short-term response of isoprene emission to certain stimuli. A lack of photosynthetically available radiation (PAR) during growth can lower the overall capacity of a plant for isoprene emission (Hanson & Sharkey, 2001a, 2001b, Lantz *et al.* 2019). This is demonstrated in part by the observed gradient of isoprene emission in the canopy of trees. Sharkey *et al*. reported significant drops in isoprene emission capacity with decreasing PAR at lower heights within the canopies (Sharkey *et al.* 1996). Temperature also has long-term influences on the capacity for isoprene emission, a fact which may drive significant changes in global isoprene emissions over time (Lehning *et al.* 1999). For instance the CO_2 effect which inhibits isoprene emission is now know to be alleviated or overruled by increasing temperature (Lantz *et al.* 2019).

Many studies have attempted to account for this in models of isoprene emission as global temperatures increase, although there is currently no consensus on the net effects. Hantson *et al*. (2017) posited that changing land use will result in significant declines in long-term isoprene emission, while Lantz *et al*. (2019) believe that it is first necessary to elucidate the mechanism of CO_2 suppression before models can be accurately adjusted.

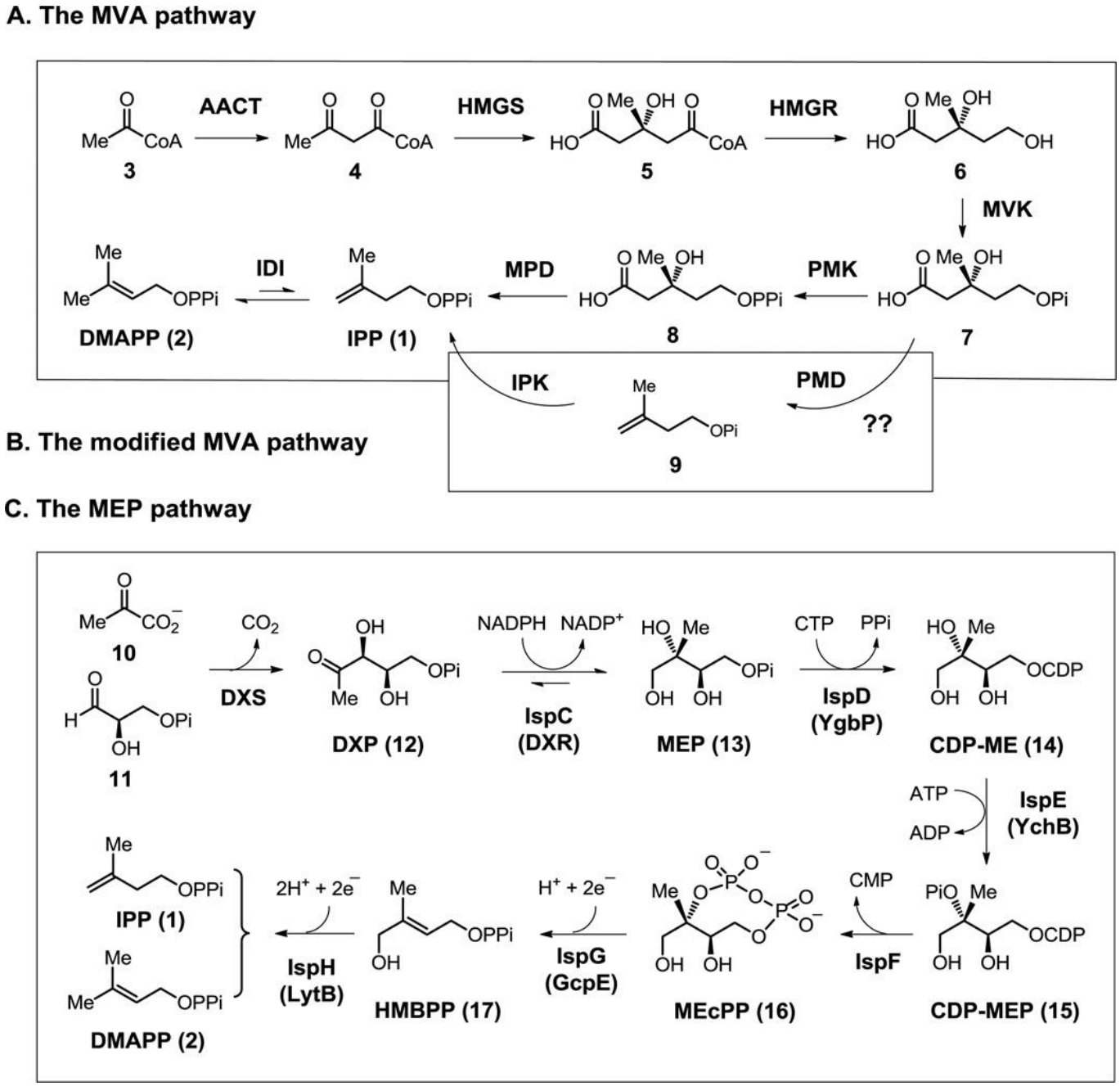

Figure 1.3. Biosynthetic pathways responsible for the production of the isoprene precursor DMAPP from alternative starting substrates glyceraldehyde 3-phosphate or acetyl-CoA (taken from Zhao *et al.* 2013).

1.3. **Roles of isoprene biosynthesis**

1.3.1. **Chemical interference to prevent isoprene biosynthesis**

Studies into the role of isoprene biosynthesis are yet to designate a core function or set of functions to the producing organism. The metabolic cost of producing a single molecule of DMAPP is 20 ATP and 14 NADPH (Sharkey

& Yeh 2001), strongly indicating the significance of isoprenoid biosynthesis, although this cannot be solely attributed to isoprene due to the fact that DMAPP from the MEP pathway also supplies the synthesis of carotenoids and other terpenes (Harrison *et al*. 2013). 1.3-2% of net productivity are estimated to be spent on isoprene production under normal conditions (Guenther *et al.* 1995, Lantz *et al.* 2019, Sharkey & Yeh, 2001), while as much as 10-20% of photosynthetically fixed carbon is used under certain stressed conditions (Guenther *et al*. 1995, Harley *et al*. 1996). Physiological and fitness-related roles were initially tested by chemically inactivating isoprene production using fosmidomycin, a herbicidal agent which inhibited the production of DMAPP and therefore inhibited isoprenoid biosynthesis (Lantz *et al.* 2019, Loreto & Velikova, 2001, Sharkey *et al.* 2001, Sharkey & Singsaas, 1995). 90% of isoprene production was inhibited after less than 1 hour in *Phragmites australis* leaf experiments (Loreto & Velikova 2001), although others such as *Populus nigra* required much longer incubations (Zeidler *et al*. 1998). *Phragmites australis* (common-reed) demonstrated significant sensitivity to ozone stress after fosmidomycin-treatment (Loreto & Velikova 2001). Exogenously supplied isoprene was able to alleviate stress caused by long-term exposure to low levels of ozone (100 nl L^{-1}), with a lesser protective effect in short-term cases of acute exposure (300 nl L^{-1}). Ozone damages plant tissues by generating reactive oxygen species (Pell *et al*. 1997, Ryan *et al*. 2014). Ozone stress in fosmidomycin-fed leaves was followed by the accumulation of H_2O_2 to high levels, and isoprene was reported to have a H_2O_2-quenching effect (Sharkey & Yeh 2001, Sharkey *et al*. 2001). However, it should be noted that H_2O_2 also accumulated in fosmidomycin-fed leaves which were not challenged by ozone. This may be due to wider deleterious effects caused by fosmidomycin poisoning. Sharkey *et al*. (2001) reported that fosmidomycin did not inhibit photosynthesis for several hours after exposure, but it would stand to reason that any inhibition of core photosynthetic apparatus after this point would have knock-on effects on wider plant processes. It has since been reported that fosmidomycin inhibition of the MEP pathway also hinders non-isoprene-related processes, such as the synthesis of abscisic acid (Barta & Loreto 2006). Abscisic acid is a phytohormone involved in many processes, including plant development and responses to abiotic stresses (Shu *et al.* 2018). This observation brings the physiological data gathered during fosmidomycin treatment into question.

1.3.2. **Physiological roles of biogenic isoprene**

For many years, isoprene has been reported to protect plants against heat and light stresses (Lantz *et al.* 2019, Sharkey *et al.* 2001, Singsaas *et al.* 1997, Velikova *et al.* 2006). Sensitivity of the photosynthetic apparatus of plants was observed after fosmidomycin treatment, and this was alleviated by an exogenous supply of isoprene. Stress tolerance due to isoprene was observed in kudzu, white and red oaks (Singsaas *et al*. 1997, Sharkey *et al*. 2001), and Oriental plane (Velikova *et al*. 2006), and also in non-isoprene-emitters such as the common bean, *Phaseolus vulgaris* (Sharkey *et al*. 2001). Many studies did not provide physiological evidence for these protective effects, but posited that the effects were likely to be due to direct intercalation of isoprene into thylakoid membranes. Singsaas *et al*. (1997) calculated the physiological concentration of isoprene which could be accumulated within plant membranes at approximately 20 µl L^{-1}. Logan *et al*. (1999) supplied 18-21 µl L^{-1} isoprene to spinach thylakoid membranes and phosphatidylcholine liposomes, but this failed to induce any detectable changes in the physiology of the membranes. The stabilisation hypothesis was further disproved by the demonstration that, when thylakoid

membranes and phosphatidylcholine liposomes were supplied with isoprene to 20 µl L^{-1}, the internal concentration of isoprene was approximately 2 orders of magnitude lower than assumed (Harvey *et al*. 2015). Only 60 isoprene molecules were present per million lipid molecules. The physiological concentration of isoprene within membranes was therefore too low to affect membrane dynamics, even in high-emitters of isoprene.

1.3.3. **Molecular analyses of the role of biogenic isoprene**

Further study of the protective role of isoprene required the development of techniques which specifically targeted the isoprene biosynthetic pathway without causing unrelated changes to plant phenotype, as described in fosmidomycin treatments. Inhibitory RNA (RNAi) were used to depress the expression of IspS in grey poplar, causing an increased sensitivity of the photosynthetic apparatus to heat stress (Behnke *et al*. 2007). Contrary to previous observations, non-emitting grey poplar was more tolerant of oxidative stress than the wild-type isoprene emitter (Behnke *et al*. 2009). This was addressed in terms of the upregulation of alternative antioxidants in the absence of *ispS* expression, particularly ascorbate, which was reported to have a greater O_3-quencing effect than isoprene (Behnke *et al*. 2009). However, Vickers *et al*. (2009) challenged the observations in the RNAi-inhibited lines as, due to the long generation time of grey poplar, the studies were conducted in first-generation transgenic plants. Transgenic lines demonstrate altered stress responses due to the transformation process which can persist for several generations (Molinier *et al*. 2006). 4th generation transgenic *Nicotiana tabacum* (tobacco) expressing *ispS* from *Populus alba* (white poplar) under the control of a *lac* promoter produced isoprene at levels comparable to that of the wild-type *P. alba* (0.5-18 nmol isoprene m^{-2} s^{-1}) (Vickers *et al*. 2009). Transgenic *N. tabacum* exhibited significantly smaller increases in the thermotolerance of photosynthetic apparatus in the isoprene-emitting plants when compared to previous fosmidomycin-based studies. However, when considered over the course of the full experiment rather than individual stress events, two higher-emitting plants demonstrated an improvement in net photosynthesis (Vickers *et al*. 2009). This may indicate that the impacts on thermotolerance demonstrated in fosmidomycin studies may have been exacerbated by knock-on effects on non-isoprene-related processes. Protection against oxidative stress by isoprene was evidently dependent on the level of isoprene production. When fumigated with ozone, *N. tabacum* either initially accumulated and subsequently lost H_2O_2, or failed to accumulate H_2O_2 in the highest emitting lines (Vickers *et al*. 2009). Rather than being attributed to a physiological role such as intercalation within thylakoid membranes, Vickers *et al*. (2009) reported an increase in the relative proportion of reduced ascorbate in high-emitting *N. tabacum* compared to the azygous, non-emitting control. This may result in the isoprene-emitting plants having a greater antioxidant capacity (Asada 1992, Baier *et al*. 2005). This contradicts the data of Behnke *et al*. (2009) which reported an upregulation in ascorbate in non-isoprene-emitting grey poplar resulting in a protective phenotype. More recent studies using the same transgenic *N. tabacum* identified growth deficits as a result of isoprene emission under drought stress, although the plant's photosynthetic apparatus was protected (Ryan *et al*. 2014). Proteomic analyses of the roots of transgenic non-isoprene-emitting poplar indicated similar changes in redox signalling as in the leaves (van Doorn *et al*. 2020). Non-isoprene-emitting poplar exhibited increased lateral root growth compared to wild-type isoprene-emitting poplar, coinciding with an upregulation of superoxide dismutases to alleviate ROS-related stress. However, van Doorn *et al*. (2020) noted that the alternative

protective mechanisms were less effective at maintaining redox balance in the roots of the transgenic non-emitting poplar as was isoprene in the roots of the native isoprene-emitter.

1.3.3.1. **Regulatory effects of biogenic isoprene**

Current studies are attempting to characterise the potential role of isoprene in the regulation of gene expression. A microarray study by Harvey and Sharkey (2016) demonstrated that, even in the non-emitting *Arabidopsis thaliana*, exogenous isoprene was able to elicit changes in gene expression. This argument becomes more compelling when considering that *A. thaliana* and *N. tabacum* engineered to express IspS demonstrated similar changes in gene expression (Zuo *et al*. 2019). Genes influenced by isoprene emission or fumigation have previously been summarised (Lantz *et al.* 2019), and many have confirmed roles in the tolerance of plants against various stressors including heat, light, and oxidation. There are currently no confirmed mechanisms which explain the influence of isoprene on gene expression. However, isoprene affected ATP-synthase activity within the thylakoid membranes of transgenic *A. thaliana* (Velikova *et al*. 2011), suggesting that isoprene may influence signal transduction pathways by interacting with membrane-bound proteins (Harvey & Sharkey 2016).

1.4. **Anthropogenic production of isoprene**

Anthropogenic isoprene production accounts for an estimated 100 Tg C yr^{-1} (Atkinson & Arey 2003). A significant quantity of isoprene is produced by the rubber industry (approximately 0.8 Tg C yr^{-1}) due to isoprene forming the basis of natural and synthetic runner (natural rubber is *cis*-1,4-polyisoprene) (Greve 2000, Steinbüchel 2003, Yang *et al*. 2011, Li *et al*. 2018b). The majority of industrially-produced isoprene is derived from petroleum-based sources, resulting in many laboratories dedicating research towards the engineering of existing biological pathways to produce isoprene with less environmental impact (Yang *et al.* 2011, Zhao *et al.* 2011). *Escherichia coli* has been engineered to express IspS from *Populus nigra*, allowing the conversion of DMAPP produced from the native *E. coli* MEP pathway (Section 1.2.2) into isoprene (Zhao *et al.* 2011). When co-expressed with MEP-pathway enzymes from *B. subtilis*, isoprene was accumulated to 314 mg L^{-1} (Zhao *et al.* 2011). *E. coli* was also engineered to co-express IspS from *Populus alba* along with the MVA pathway from *Saccharomyces cerevisiae*, leading to the accumulation of 532 mg isoprene L^{-1} under fermentation conditions (Yang *et al*. 2011). As a basic hemiterpene unit, isoprene has the potential to be employed in many areas of industry including aviation fuels (Rosenkoetter *et al*. 2019), isoprenoid-based pharmaceuticals (George *et al*. 2015), pesticides, and more (Li *et al.* 2018). The replacement of petroleum-based isoprene sources with environmentally-friendly alternatives was discussed by Wang *et al.* (2016), including the use of catalytically-driven production using non-petroleum feedstocks. Approximately 7 million tons of natural rubber are produced each year of an estimated 20 million tons of total rubber production (Steinbüchel 2003, Yang *et al*. 2011). Unlike the synthesis of synthetic rubber, natural rubber is sourced almost exclusively from the rubber-producing plant *Hevea brasiliensis* (Steinbüchel 2003, Men *et al*. 2019), 75% of which is dedicated to the production of vehicle tyres. Men *et al*. (2019) discussed the current state of natural rubber production with particular emphasis on the need to develop a better understanding of the natural rubber biosynthetic pathway. Genetic engineering to

allow the microbial production of natural rubber, or optimising *in vitro* synthesis strategies, may reduce the reliance on *H. brasiliensis* which has high requirements for growth (Men *et al*. 2019).

Aside from industry-related isoprene production, human activity is known to result in the release of isoprene into the atmosphere. Motor exhaust is a key example, as atmospheric isoprene measurements are higher by roadsides than in other urban areas (Barletta *et al*. 2002, Durana *et al*. 2006, Hellén *et al*. 2012). Further to this, human activities such as smoking releases an estimated 134.9 ± 27.9 µg isoprene per cigarette (Liu *et al.* 2010).

1.5. **Biological consumption of isoprene – ecology and isolation of isoprene degraders**

1.5.1. **Identification of soil as a sink for isoprene degradation**

Microbial oxidation of isoprene using the SDIMO family of enzymes has been demonstrated for many years. Methanotrophs expressing the soluble methane monooxygenase (sMMO) and *Xanthobacter* spp. grown on propene all oxidised isoprene but were unable to use it as the sole source of carbon and energy (Hou *et al*. 1981, Crombie 2011). *Nocardia* sp. IP1 was capable of growing on isoprene by using an alternative monooxygenase which oxidised isoprene or 1,3-butadiene at either alkene group on the dialkene chains, generating varied epoxide products (Van Ginkel *et al*. 1987). Ewers *et al*. (1990) also demonstrated the ability of known type cultures *Rhodococcus erythropolis* JE 88 and *Alcaligenes denitrificans* ssp. *Xylosoxidans* JE 75 to consume isoprene as the sole source of carbon and energy. The latter observations came as a result of the search for microorganisms which could degrade chlorinated ethenes, thereby demonstrating the versatility of the isoprene degrading bacteria.

In spite of the identification of isoprene degrading bacteria, it was widely accepted that atmospheric chemistry represented the primary route for isoprene removal. Soils were suggested to be the first biological sink for isoprene (Cleveland & Yavitt 1997, 1998). A combination of laboratory- and field-based studies demonstrated that temperate forest soils were capable of consuming 385 ppbv isoprene to levels which were lower than ambient isoprene concentrations within a forest canopy (<3-10 ppbv) (Cleveland & Yavitt 1997). This consumption was curtailed by autoclaving the soils, demonstrating that the activity was biological in nature. From these data, the authors estimated that soils consumed approximately 20.4 Tg isoprene yr^{-1}. However, this estimate assumed a constant 24-hour consumption of isoprene by soils, something which is highly unlikely when considering the light-dependent nature of isoprene biosynthesis (Cleveland & Yavitt, 1997, Li & Sharkey, 2013, Weise *et al.* 2013). A second study demonstrated that 500 ppbv isoprene could be degraded to less than 5 ppbv by temperate soils (once again prevented by autoclaving) in a manner which demonstrated a temperature optimum of 30 ^{o}C (Cleveland & Yavitt 1998), further decreasing the likelihood of a constant rate of isoprene consumption by soils over a 24-hour period. The isolation of a novel isoprene-degrading *Arthrobacter* sp. was also reported (Cleveland & Yavitt 1998). Novel isoprene degrading bacteria have also been isolated from aquatic environments. *Rhodococcus* sp. AD45, a strain which has since become the model for molecular analyses of the isoprene metabolic pathway, was isolated from freshwater sediment (van Hylckama Vlieg *et al*. 1998). *Rhodococcus* sp. AD45, like the isoprene degraders reported by Ewers *et al*. (1990), was isolated for its potential to perform biological transformations of chlorinated ethenes

(van Hylckama Vlieg *et al.* 1998). This novel strain was capable of detoxifying epoxides due to a specific glutathione *S*-transferase. This GST has since been identified as a part of the isoprene metabolic pathway (van Hylckama Vlieg *et al*. 1998, 1999, 2000, Crombie *et al*. 2015). This is discussed in detail in Section 1.6.

The work of Cleveland and Yavitt was disputed on the basis that non-atmospheric isoprene concentrations were used in the soil studies (Fall & Copley 2000). The concentration of isoprene even in the canopy of a high-emitting forest is unlikely to exceed 4-10 ppbv (Goldstein *et al*. 1998), but this concentration would be significantly diluted in the air between leaves and soils. It was argued that soil-residing isoprene degraders could only act as a sink for isoprene produced by microorganisms in soil (Fall & Copley 2000). Gray *et al*. (2015) addressed this in part by demonstrating that isoprene degraders in soils were capable of consuming between 2-200 ppbv isoprene. Enrichments of soils with different concentrations of isoprene were coupled with increases in the relative abundance of specific bacterial taxa and even fungal taxa (Gray *et al.* 2015). However, this did not necessarily confirm that each of the more abundant taxa contained *bona fide* isoprene degraders. Cross-feeding occurs when breakdown products of a certain metabolic pathway or pathways leak from the metabolising organisms and support the growth of other organisms which may not be capable of metabolising the initial substrate (Krause *et al*. 2017). A well-described example is the cross-feeding of methylotrophic bacteria when enriching for methanotrophic populations with methane (Krause *et al*. 2017). This may also be the case for enrichments with isoprene, necessitating the use of labelled substrates to determine the active population of isoprene degraders within a given environment.

1.5.2. **Diversity of isoprene degrading microorganisms in terrestrial and aquatic environments**

Recent studies have begun to demonstrate the wealth of bacterial taxa capable of isoprene degradation. El Khawand *et al*. (2016) enriched garden soil and horse chestnut leaves with 0.5% (v/v) isoprene with the aim of isolating novel isoprene degrading bacteria, and enriched willow soil with 0.5% (v/v) ^{13}C-labelled isoprene with the aim of identifying the dominant isoprene degrading taxa by DNA-stable isotope probing (DNA-SIP). DNA-SIP relies on the incorporation of a labelled substrate into the DNA of the metabolising organism, allowing the separation of labelled (heavy) DNA from unlabelled (light) DNA by ultracentrifugation using a caesium chloride gradient (Radajewski *et al*. 2000, Dumont & Murrell 2005, Nkongolo & Narendrula-Kotha 2020). This distinguished the active isoprene degrading community from potential cross-feeders. Sequencing of the 16S rRNA gene sequences from the heavy fraction of isoprene-enriched willow soil demonstrated a significant increase in the relative abundance (RA) of Actinobacteria, of which 88% were *Rhodococcus* spp. A further 6.5% (RA) was comprised of *Comomonas* spp. and *Variovorax* spp., organisms which had not previously been identified as isoprene degraders (El Khawand *et al*. 2016).

Further investigations of isoprene degraders were conducted in soils and leaves of various origins, including poplar, willow, greenhouse-based and Malaysian oil palms, and tropical trees such as *Madhuca latifolia* and *Tectona grandis* (Carrión *et al.* 2018, Crombie *et al.* 2018, Larke-Mejía *et al.* 2019, Singh *et al.* 2019). Many of these studies reported the isolation of novel isoprene degraders following enrichment with isoprene. *Pseudomonas, Arthrobacter* and *Bacillus* were isolated from the leaves and soils of tropical trees, although they were not able to support growth

above 500 ppmv isoprene (Singh *et al.* 2019). While this study indicated that isoprene was oxidised by these tropical isolates due to the generation of hydroxyl and carboxylic acid groups (Singh *et al.* 2019), it did not provide any genetic or biochemical basis for isoprene oxidation. Other studies made use of cultured isoprene degraders to develop molecular probes which were able to detect isoprene degrading bacteria in environmental samples. These probes targeted the alpha-subunit of the isoprene monooxygenase (IsoMO) oxygenase component, encoded by *isoA* (van Hylckama Vlieg *et al*. 2000, Crombie *et al*. 2015, El Khawand *et al*. 2016). IsoA is discussed in greater detail in Section 1.6.4. Studies of isoprene degrading taxa in environmental samples frequently detected Gram positive Actinobacteria in high abundance, particularly from the genera *Mycobacterium* and *Rhodococcus*. 99.8% of *isoA* sequences from ash leaf enrichments with 25 ppmv isoprene were determined to be *Rhodococcus*-like (Carrión *et al*. 2018), while willow leaf enrichments with 25 ppmv isoprene contained a RA of 50.7% *isoA* and 49.3% *isoA* relating to *Mycobacterium* and *Rhodococcus*, respectively (Carrión *et al*. 2018). Crombie *et al*. (2018) used two enrichments with 500 ppmv and 150 ppmv isoprene, each followed by DNA-SIP, to demonstrate the variety of non-Actinobacterial isoprene degraders on poplar leaves. Members of the Comamonadaceae increased from 3% RA to 16% RA of the labelled community between the first and second enrichments, of which the majority were *Variovorax* spp. A separate poplar leaf enrichment using 50 ppmv isoprene also identified 5.8% RA *isoA* sequences relating to *Variovorax* spp. (Carrión *et al*. 2018), while an enrichment of the soil in a tyre dump determined that the majority of *isoA* sequences were *Variovorax*-like (Carrión *et al*. 2018). Larke-Mejia *et al*. (2019) studied willow soil at a decreased enrichment concentration of 25 ppmv isoprene. As a result, non-Actinobacterial isoprene degraders were isolated and detected in significantly greater abundance than in previous studies. Members of the Comamonadaceae increased from 8-12% RA after 6 days of enrichment to 21-30% after 7 days. Approximately 90% of the labelled community were of the order Burkholderiales, with *Ramlibacter spp.* and *Variovorax spp*. collectively accounting for 72% and 59% of the labelled community after 6 and 7 days of enrichment, respectively. Surprisingly, *Rhodococcus spp.* accounted for approximately 4.5% of the labelled community (Larke-Mejía *et al*. 2019). This study led to the isolation of many novel isoprene degrading Actinobacteria; *Nocardioides* sp. WS12 and a further 11 *Rhodococcus* spp. Novel Gram negative isoprene degraders were also isolated; *Ramlibacter* sp. WS9, and *Variovorax* sp. WS11. *Sphingopyxis* sp. OPL5 was subsequently isolated from an enrichment of oil palm leaves taken from Kew Gardens (London, UK) (Larke-Mejía *et al*. 2019). These data indicated that, while Actinobacteria such as *Rhodococcus* spp. are highly abundant isoprene degraders in the environment, Gram negative isoprene degrading bacteria may also comprise a significant proportion of the isoprene sink in soils. As oil palm trees are high producers of isoprene (Hewitt *et al.* 2009), a Malaysian oil palm plantation was investigated for the abundance of isoprene degrading bacteria (Carrión *et al*. 2020). Novel isoprene degrading genera were highly enriched by ^{13}C-isoprene in soils, including *Rhodoblastus, Thiomonas*, *Sphingomonas* and *Pelomonas*. This study identified significant differences between the communities of soil-residing isoprene degraders from oil palm and willow soils (Carrión et al. 2018, 2020, Larke-Mejía et al. 2019). *Rhodococcus*, *Variovorax*, and *Sphingopyxis*, major isoprene-degrading genera in temperate soils, comprised less than 1% of the enriched community in the tropical soil. Study of the oil palm phyllosphere after enrichment with ^{13}C-isoprene identified *Gordonia* and *Zoogloea* as the dominant genera (Carrión *et al*. 2020).

Acuña Alvarez *et al*. (2009) demonstrated the greater isoprene degrading potential of sediments over water samples in estuarine environments. It was also noted that the rate of isoprene uptake increased significantly when samples were challenged with lower concentrations of isoprene. Sampling locations with lower ambient concentrations of isoprene were associated with a more rapid rate of isoprene consumption during enrichment experiments (Acuña Alvarez *et al*. 2009). These data may indicate inhibition of isoprene degrading communities at excessive concentrations of isoprene. Aquatic enrichments led to the isolation of four new isoprene degraders of the genera *Rhodococcus*, *Xanthobacter*, *Gordonia* and *Dyadobacter* (Acuña Alvarez *et al*. 2009). This study was able to effectively demonstrate the ability of aquatic isoprene degraders to consume isoprene produced at environmentally relevant concentrations by the aquatic isoprene producing microalgae *Dunaliella teriolecta* and *Phaeodactylum tricornutum* (Acuña Alvarez *et al*. 2009). A later study reported the enrichment of samples from the same estuary with 0.5% (v/v) isoprene, and performed DNA-SIP to investigate the active isoprene degrading community (Johnston *et al*. 2017), once again identifying that Actinobacteria were dominant at higher enrichment concentrations of isoprene. Continued studies using a range of enrichment concentrations of isoprene, particularly at lower concentrations, may identify a greater diversity of aquatic isoprene degraders.

Alignment of translated IsoA amino acid sequences from isolated isoprene degraders against the corresponding α-oxygenase components of other SDIMO provided some indication of the phylogenetic organisation of the SDIMO expressed by these bacteria (Figure 1.4). IsoA-based phylogeny provided an interesting insight into the likelihood of acquisition of isoprene metabolism by horizontal gene transfer. Many IsoA sequences from *Rhodococcus spp.* were grouped together despite the diversity of isolation sites (freshwater sediment, leaves, soils), but some *Rhodococcus*-specific IsoA sequences were separated by the IsoA sequences from other Gram positive isoprene degraders (Figure 1.4). IsoA sequences from Gram negative isoprene degraders were also separated from Gram positive by the alkene monooxygenase alpha subunit (XamoA) of *Xanthobacter* sp. Py2, potentially indicating a greater diversity in IsoA sequences between the more unrelated organisms. The IsoA sequences from *Variovorax* sp. WS11 and *Ramlibacter* sp. WS9, two Gram negative isoprene degraders isolated from willow soil (Larke-Mejía *et al*. 2019), were grouped very close together despite being from different genera.

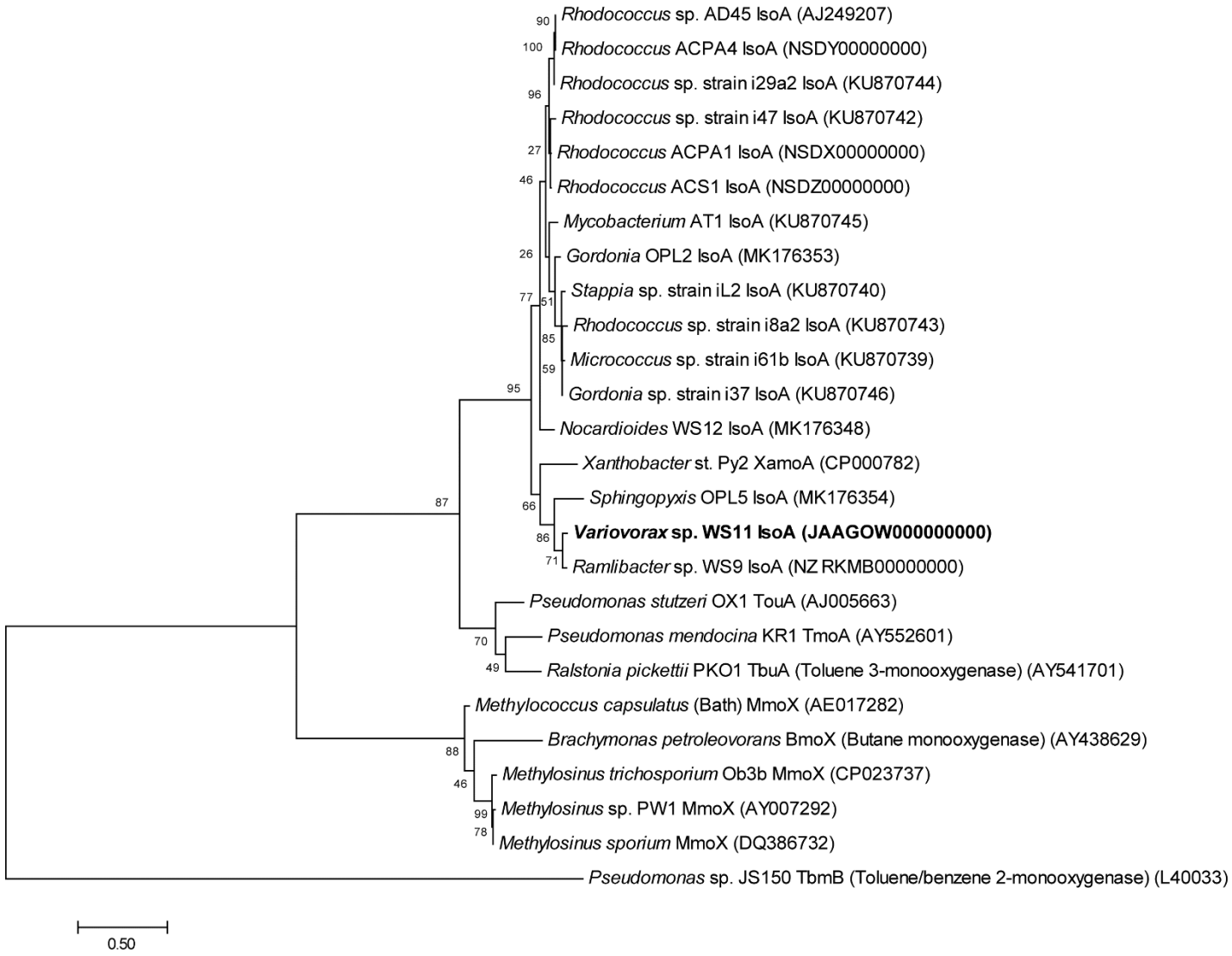

Figure 1.4. Phylogenetic organisation of translated amino acid sequences of the α subunit of the oxygenase from these SDIMO. The tree was draw using the Maximum Likelihood programme in Mega7 (Kumar *et al*. 2016). Bootstrap values (500 replications) are shown at the nodes. Branch lengths are measured as the number of substitutions per site (taken from Dawson *et al.* 2020).

1.6. **Soluble diiron monooxygenases (SDIMO) family of enzymes**

1.6.1. **Structural classifications of SDIMO**

SDIMO enzymes catalyse the oxidation of a range of aliphatic and aromatic hydrocarbons (Leahy *et al.* 2003, Shu *et al.* 1997, Tinberg & Lippard, 2009). These proteins can be broadly organised into six groups according to the organisation of subunits and electron transport components (Table 1.1) (Leahy *et al*. 2003, Coleman *et al*. 2006). Shared by all SDIMO is the oxygenase subunit which contains the non-heme diiron centre of the active site (Leahy *et al*. 2003). Molecular oxygen is activated at Fe(III) by NAD(P)H-derived electrons, producing an intermediate which attacks the hydrocarbon substrate and liberates H_2O (Shu *et al.* 1997, Tinberg & Lippard, 2011, Wang *et al.* 2017). The oxygenase component may be tetrameric $(\alpha\beta)_2$ or hexameric $(\alpha\beta\gamma)_2$ according to the SDIMO sub-class (Table 1.1). Further SDIMO components facilitate the transfer of electrons from NAD(P)H to the diiron centre (Stirling &

Dalton 1979, Ross & Rosenzweig 2017). All SDIMO sub-classes employ an oxidoreductase with a NAD(P)H/FAD-binding domain and two electron-transfer cofactors, FAD and [2Fe-2S] (Lund & Dalton 1985, Ross & Rosenzweig 2017). The subsequent electron-transfer step differs between three- and four-component SDIMO (Figure 1.5). In three-component SDIMO such as the soluble methane monooxygenase (sMMO), the reductase binds directly to the oxygenase and reduces Fe(III) to Fe(II), allowing the activation of molecular oxygen (Lund & Dalton, 1985, Wang *et al.* 2017). The reductase of four-component SDIMO, such as the toluene 4-monooxygenase, is incapable of directly binding to the oxygenase component (Blazyk *et al*. 2005), instead shuttling the electrons to a ferredoxin which contains a Rieske-type [2Fe-2S] prosthetic group. This then transfers the electrons to the diiron centre (Blazyk *et al*. 2005). A final component shared by all SDIMO is a small effector/regulatory protein which lacks cofactors but is implicated in various processes which influence catalysis, including the control of substrate access to the active site (Wallar & Lipscomb 2001, Song *et al*. 2011, McCormick & Lippard 2012, Lee *et al*. 2013, Liang & Lippard 2014).

1.6.2. **Roles of SDIMO components and regulation of substrate oxidation**

Oxidation of hydrocarbon substrates can vary significantly between SDIMO classes due to the presence or absence of different components, and also due to the inherent differences in amino acid sequence identity between the different enzymes. The oxygenase/hydroxylase α-subunit is the most highly conserved (58% - >80% identity) (Leahy *et al*. 2003). This makes sense when considering the critical function of the α-oxygenase subunit; this contains the diiron centre of the active site and requires the conservation of many amino acid residues in order to maintain catalytic function and substrate specificity (Leahy *et al*. 2003, Petkevičius *et al*. 2019). Other oxygenase components can vary significantly between SDIMO types. Classes 4-6 do not contain a γ-oxygenase subunit, and those that do can share as little as 15% identity (Saeki *et al*. 1999, Kotani *et al*. 2003, Sazinsky *et al*. 2004, He *et al*. 2017). The mechanism of substrate oxidation by SDIMO was best described for the sMMO of *Methylococcus capsulatus* (Bath). Electrons are transferred from NADH to the oxidoreductase component (MMOR), where they are sequentially transferred through the FAD and [2Fe-2S] cofactors (Lund & Dalton 1985, Ross & Rosenzweig 2017), and finally to the diiron centre of the alpha subunit of the oxygenase component (MMOH-α) (Banerjee *et al.* 2019, Lee *et al.* 2013, Shu *et al.* 1997, Stirling & Dalton, 1979, Tinberg & Lippard, 2009). The reduced diiron(II) centre activates molecular oxygen, producing a diiron(III) peroxo intermediate which rapidly breaks down to produce the Q species (IV) (Banerjee *et al.* 2019, Shu *et al.* 1997, Tinberg & Lippard, 2010, Tinberg & Lippard, 2009). The Q species attacks the highly stable C-H bond of methane to produce methanol (Shu *et al.* 1997, Tinberg & Lippard, 2009). The mechanism of methane oxidation by the sMMO has been extensively reviewed (Ross & Rosenzweig 2017, Banerjee *et al*. 2019).

The regulatory component (MMOB), also known as the coupling protein, serves several functions which influence catalysis. MMOB directly competes with MMOR for the same binding site on the oxygenase component, thereby preventing reduction of the diiron centre and inhibiting substrate oxidation (Lee *et al.* 2013, Liu *et al.* 1995, Sirajuddin & Rosenzweig, 2015). The N-terminus of MMOB becomes well-ordered upon binding to MMOH. This was hypothesised to act as an anchor for MMOB, reducing the likelihood of being out-competed by MMOR (Blazyk *et al*. 2005, Lee *et al*. 2013). However, binding of MMOB to MMOH is also known to increase both the rate of substrate

oxidation by sMMO and the substrate specificity of the enzyme (Froland *et al.* 1992, Liu *et al.* 1995a, 1995b, Rinaldo *et al.* 2007, Sirajuddin & Rosenzweig, 2015). The regulatory components of the four-component toluene 4-monooxygenase (To4MOD) and toluene/*o*-xylene monooxygenase (ToMOD) also compete with their respective Rieske-type ferredoxin components for binding to the oxygenase component (Bailey *et al.* 2012, Bailey *et al.* 2008a, Fox *et al.* 1991, Wang & Lippard, 2014). Liang and Lippard (2014) demonstrated a concentration-dependent inhibition of electron transfer between the ferredoxin (ToMOC) and oxygenase (ToMOH) components of the toluene/*o*-xylene monooxygenase. A sub-stoichiometric concentration of ToMOD was hypothesised to cause a conformational change in ToMOH which increased substrate and dioxygen access to the active site (Rinaldo *et al*. 2007, Liang & Lippard 2014). This control over electron transfer by ToMOD was suggested to prevent unnecessary activation of oxygen by ToMOH (Fox *et al.* 1991, Wang *et al.* 2014). Different methods have been suggested for the control of substrate oxidation by To4MOD. Binding of To4MOD to the oxygenase component controls substrate specificity by altering the size of the aromatic substrate channel, preventing import of aromatic substrates to the active site (Bailey *et al.* 2012, Bailey *et al.* 2008a). This binding also enhances the rate of oxidation by increasing access of dioxygen to the Fe(III) centre, and also by inducing persistent conformational changes in To4MOH which enhance binding of To4MOC (Bailey *et al.* 2008a, McCormick & Lippard, 2012, Song *et al.* 2011).

1.6.3. **Substrate specificity and enantioselectivity**

The substrate ranges of different SDIMO classes are highly varied and often overlap. The sMMO is capable of oxidising terminal and sub-terminal alkanes, alkenes, haloalkanes, cyclic hydrocarbons and aromatic hydrocarbons (Colby *et al*. 1977, Higgins *et al*. 1979, Leak & Dalton 1987, Green & Dalton 1989, Fox *et al*. 1990, Sirajuddin & Rosenzweig 2015). This is believed to be due to the exceptional level of oxidising potential of the sMMO (Lipscomb 1994). However, methanotrophs expressing sMMO are only capable of growing on methane, meaning that the co-oxidation of these alternative hydrocarbons may cause the accumulation of toxic or inhibitory oxidation products (Breuer *et al.* 2004, van Hylckama Vlieg *et al.* 1998). This was also noted in studies which assessed the viability of SDIMO-expressing bacteria during the remediation of trichloroethylene (TCE)-contaminated sites. While *M. trichosporium* OB3b was capable of degrading TCE, it was rapidly inactivated by the accumulation of epoxide products (van Hylckama Vlieg *et al.* 1996, 1997). The sMMO of *Methylocella silvestris* BL2 and *Methylococcus capsulatus* (Bath) are capable of co-oxidising isoprene, presumably to a corresponding epoxide (Crombie 2011, Dawson *et al*. 2020). Other SDIMO are noted for their significantly greater stereospecificity (Gallagher *et al*. 1997, Breuer *et al*. 2004, Nichol *et al*. 2015) and typically smaller, although not insignificant, substrate ranges (Leahy *et al*. 2003). For example, the three-component toluene 2-monooxygenase expressed by *Burkholderia cepacia* G4 oxidises both phenol and toluene to their respective hydroxylated derivatives (Shields *et al*. 1989, Rui *et al*. 2004). The toluene 4-monooxygenase, a four-component SDIMO, is capable of oxidising a wide range of halogenated, cyclic, and aliphatic alkenes, but is incapable of oxidising phenol (Bailey *et al.* 2008b, McClay *et al.* 1996, Nichol *et al.* 2015, Yen *et al.* 1991).

Various alkene monooxygenases have been studied for their ability to oxidise alkenes to enantiospecific epoxides (Breuer *et al.* 2004, Cheung *et al.* 2013, Gallagher *et al.* 1997, Nichol *et al.* 2015, Saeki *et al.* 1999, Zhou *et al.* 1999). This fact has made the SDIMO family of enzymes a potentially useful resource to industry, as the use of biological catalysts may generate high concentrations of a single chiral compound rather than a racemic mixture. *Rhodococcus rhodochrous* B-276 was studied in detail for its ability to oxidise a large range of aliphatic alkenes, from C3 to over C13, as well as chlorinated alkenes and styrene (Gallagher *et al*. 1997, Breuer *et al*. 2004, Fosdike *et al*. 2005). Likewise, the four-component alkene monooxygenase of *Xanthobacter* sp. Py2 oxidises both substituted and unsubstituted alkenes, as well as benzene, toluene, and phenol (Zhou *et al.* 1999). However, there are several drawbacks in attempting to industrialise the use of SDIMO. Firstly, attempting to harvest mid-point products of a metabolic pathway is hindered by the need to engineer or partially inhibit onward steps of the pathway. This is less pronounced in cases where the desired product is produced by co-oxidation, although this raises the issue of toxicity caused by the accumulated product (Fox *et al*. 1990, Oldenhuis *et al*. 1991, van Hylckama Vlieg *et al*. 1996, 1997, Nichol *et al*. 2015). Secondly, the enzyme in question must be expressed in an organism which is easy to manipulate and grow, such as *E. coli*. This is hindered by the fact that SDIMO are composed of multiple subunits which contain various cofactors, and each subunit must be correctly folded in order to retain function (Mitchell *et al*. 2002, Bailey *et al*. 2008a). While many studies have reported difficulties in expressing SDIMO in *E. coli* (Champreda *et al.* 2004, van Hylckama Vlieg *et al.* 2000, Zhou *et al.* 1996, 1999), some evidence suggests that co-expression with chaperone proteins may enhance protein folding and activity (Furuya *et al*. 2013, McCarl *et al*. 2018). The need to improve our understanding of the structure and function of SDIMO has led to numerous studies reporting the engineering of active site components to tailor substrate specificity (Lock *et al.* 2017, Mitchell *et al.* 2002, Nichol *et al.* 2015, Petkevičius *et al.* 2019, Smith *et al.* 2002, Wang & Lippard, 2014). In time, this may lead to a greater ability to utilise these enzymes in the remediation of hydrocarbon-contaminated sites, and the synthesis of valuable chiral compounds.

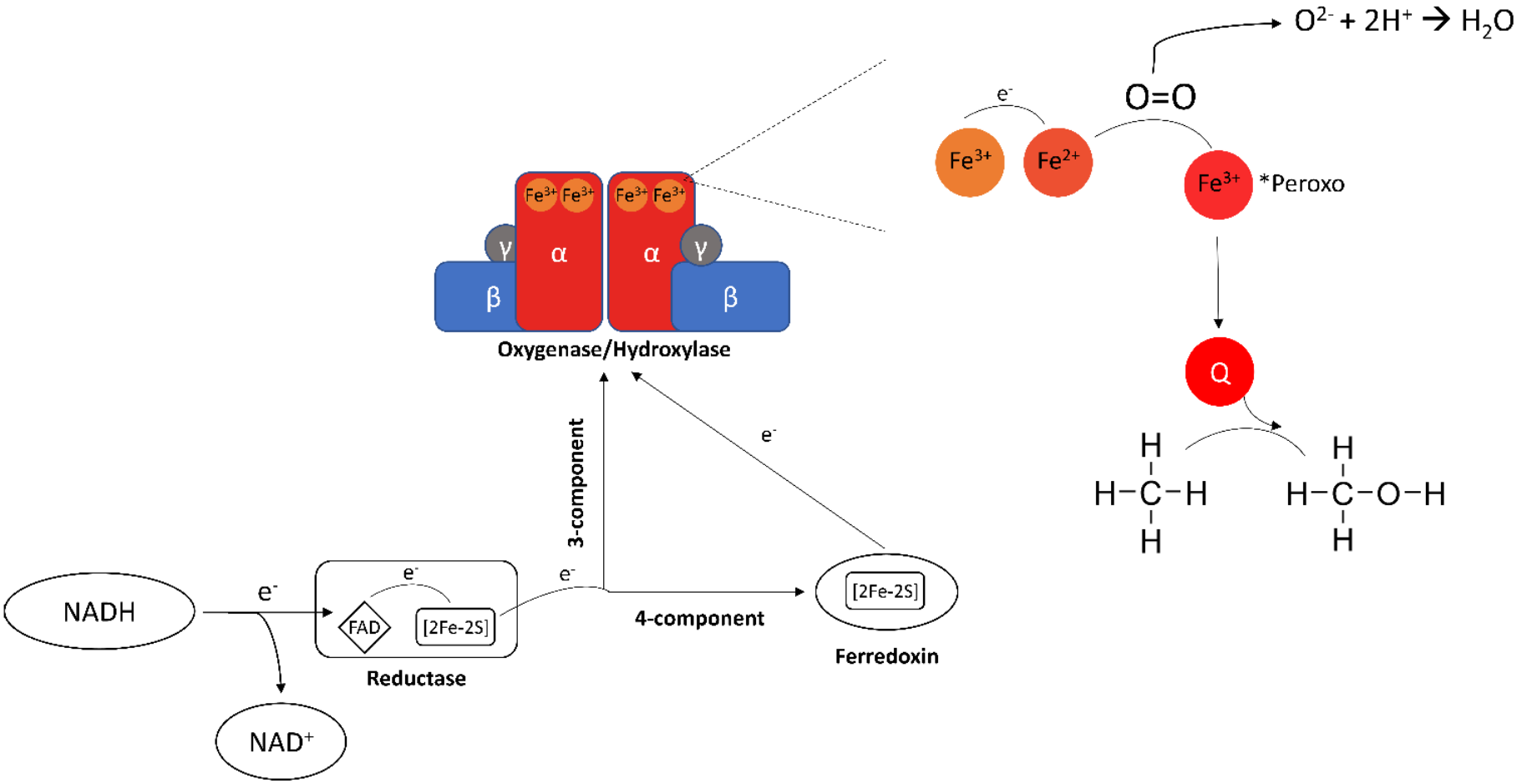

Figure 1.5. Shuttling of electrons via SDIMO electron transport proteins from NADH to the diiron centre of the active site, leading to substrate oxidation by the diiron (IV) Q species (Shu *et al.* 1997, Tinberg & Lippard, 2009). The coupling protein has been excluded for the sake of simplicity.

Table 1.1. SDIMO groups categorised according to the structural units and accessory proteins.

SDIMO Group	Example enzyme	Producing organism	Example Reaction	Subunit organisation	References
1	Phenol hydroxylase	*Pseudomonas* sp. CF600	Phenol → Catechol	$\alpha_2\beta_2\gamma_2$, C, R	(Shingler *et al*. 1989)
2	Toluene 4-monooxygenase	*Pseudomonas mendocina* KR1	Toluene → *p*-cresol	$\alpha_2\beta_2\gamma_2$, C, R, F	(Yen *et al*. 1991)
	Alkene monooxygenase	*Xanthobacter* sp. Py2	Alkene → epoxide	$\alpha_2\beta_2\gamma_2$, C, R, F	(Small & Ensign 1997)
	Isoprene monooxygenase	*Rhodococcus* sp. AD45	Isoprene → Epoxyisoprene	$\alpha_2\beta_2\gamma_2$, C, R, F	(van Hylckama Vlieg *et al.* 2000)
3	Soluble methane monooxygenase	*Methylococcus capsulatus* (Bath)	Methane → Methanol	$\alpha_2\beta_2\gamma_2$, C, R	(Colby *et al*. 1977)
4	Alkene monooxygenase	*Rhodococcus rhodochrous* B-276*	Propene → Propene oxide	$\alpha_2\beta_2$, C, R	(Saeki *et al*. 1999)
5	Propane monooxygenase	*Gordonia* sp. TY5	Propane → 2-propanol	$\alpha_2\beta_2$, C, R	(Kotani *et al*. 2003)
6	Dioxane monooxygenase	*Mycobacterium dioxanotrophicus* PH-06	1,4-dioxane → 1,4-dioxane-2-ol	$\alpha_2\beta_2$, C, R	(He *et al*. 2017)

**Rhodococcus rhodochrous* B-276 was originally classified as *Nocardia corallina* B-276

C – Coupling/effector protein

R – NAD-dependent oxidoreductase ([2Fe-2S] + FAD)

F – Rieske-type ferredoxin ([2Fe-2S])

1.6.4. **Isoprene monooxygenase**

The first example of an SDIMO involved in a dedicated isoprene metabolic pathway rather than a co-oxidative process was described by van Hylckama Vlieg *et al*. (2000). *Rhodococcus* sp. AD45 was isolated from an isoprene-enrichment culture of freshwater sediment due to its ability to degrade *cis* and *trans*-1,2-dichloroethylene (DCE) (van Hylckama Vlieg *et al.* 1998). Unlike co-oxidations of chlorinated ethenes reported in other studies (Van Ginkel *et al.* 1987, van Hylckama Vlieg *et al.* 1996), *Rhodococcus* sp. AD45 was not inhibited by the resulting epoxide products due to the expression of a glutathione *S*-transferase (GST) (van Hylckama Vlieg *et al.* 1998, 1999). The initial oxidation of isoprene and DCE were performed by a putative 4-component alkene monooxygenase, encoded by the genes *isoA-F* (van Hylckama Vlieg *et al.* 2000). This novel enzyme showed striking similarity to the alkene monooxygenase of *Xanthobacter* sp. Py2 in terms of genetic organisation and identity at the amino acid level (Small & Ensign, 1997, van Hylckama Vlieg *et al.* 2000). Using the available structural information from other SDIMO, it was predicted that the oxygenase component of IsoMO (IsoABE) consisted of an $\alpha_2\beta_2\gamma_2$ conformation (van Hylckama Vlieg *et al.* 2000). Electrons were delivered by a NADH-dependent oxidoreductase (IsoF) to a Rieske-type ferredoxin (IsoE), with regulation of catalytic activity by a coupling protein which lacked any prosthetic groups (IsoD) (van Hylckama Vlieg *et al.* 2000). IsoMO catalysed the epoxidation of isoprene to form 3,4-epoxy-3-methyl-1-butene (henceforth epoxyisoprene) (van Hylckama Vlieg *et al.* 1999, 2000), which was then detoxified by the activity of a glutathione *S*-transferase and further metabolised by the enzymes encoded by other genes found in the vicinity of *isoA-F* (Figure 1.6) (van Hylckama Vlieg *et al.* 1998, 1999, 2000). The *iso* metabolic genes are described in Section 1.6.1 and depicted in Figure 1.8.

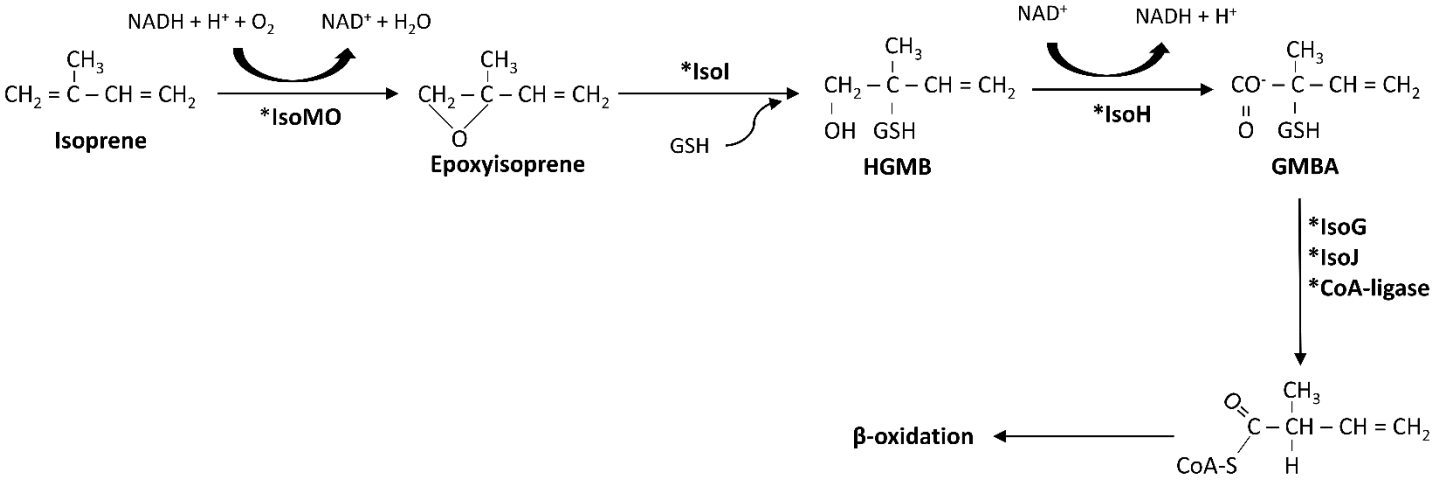

Figure 1.6. The isoprene oxidation pathway used by *Rhodococcus* sp. AD45 (adapted from van Hylckama Vlieg *et al.* 2000).

Since the discovery of IsoMO in *Rhodococcus* sp. AD45, many species of isoprene degrading bacteria have been isolated from various environmental samples (as described in Section 1.5). A lack of conservation of IsoMO components between distinct bacterial taxa is evident when comparing representative Gram positive and Gram

negative isoprene degraders (Figure 1.7). Using the translated amino acid sequences of the IsoMO from *Variovorax* sp. WS11 as a query (Larke-Mejía *et al*. 2019, Dawson *et al*. 2020), the most closely-related IsoMO was contained by another Gram negative isoprene degrader, *Ramlibacter* sp. WS9 (Larke-Mejía *et al*. 2019). The IsoA component of the IsoMO from *Variovorax* sp. WS11 retained 73% identity with the IsoA components from *Rhodococcus* sp. AD45 and *Nocardioides* sp. WS12, as well as with the alkene monooxygenase α-oxygenase component (XamoA) from *Xanthobacter* sp. Py2. When IsoA from *Variovorax* sp. WS11 was compared to IsoA from *Ramlibacter* sp. WS9, 91.8% of amino acid residues were conserved (Figure 1.7). Phylogenetic organisation of IsoA components also demonstrated the relatedness of the IsoA sequences from *Variovorax* sp. WS11 and *Ramlibacter* sp. WS9 (Figure 1.4), as each was clustered on the same branch separately from all Gram positive IsoA sequences (Dawson *et al*. 2020). Curiously, XamoA was positioned between the Gram negative and Gram positive IsoA sequences, possibly indicating a greater degree of separation between the distant isoprene degrading species. As expected, other IsoMO components shared a lower degree of identity than did the IsoA components (Figure 1.7). Leahy *et al*. (2003) reviewed the evolutionary relationships between SDIMO components and found that α-oxygenase components tended to be much more highly conserved, most likely due to the need to retain active site functionality. Coordination of the diiron centre of the soluble methane monooxygenase requires four glutamate and two histidine residues (Rosenzweig *et al*. 1997, Ross & Rosenzweig 2017). The same coordinating residues were also identified in the α-oxygenase component of the toluene 4-monooxygenase (Bailey *et al.* 2008a). Substitutions of certain active site residues caused significant effects on substrate recognition and regiospecificity (Pikus *et al*. 1997, Canada *et al*. 2002, Tao *et al*. 2004, Petkevičius *et al*. 2019), demonstrating the critical relationship between the composition of the oxygenase α-subunit of SDIMO and the substrate range of the enzyme. Other SDIMO components tend to show a much greater degree of diversity, although the IsoB-F components of *Variovorax* sp. WS11 and *Ramlibacter* sp. WS9 all shared over 60% amino acid identity (Figure 1.7).

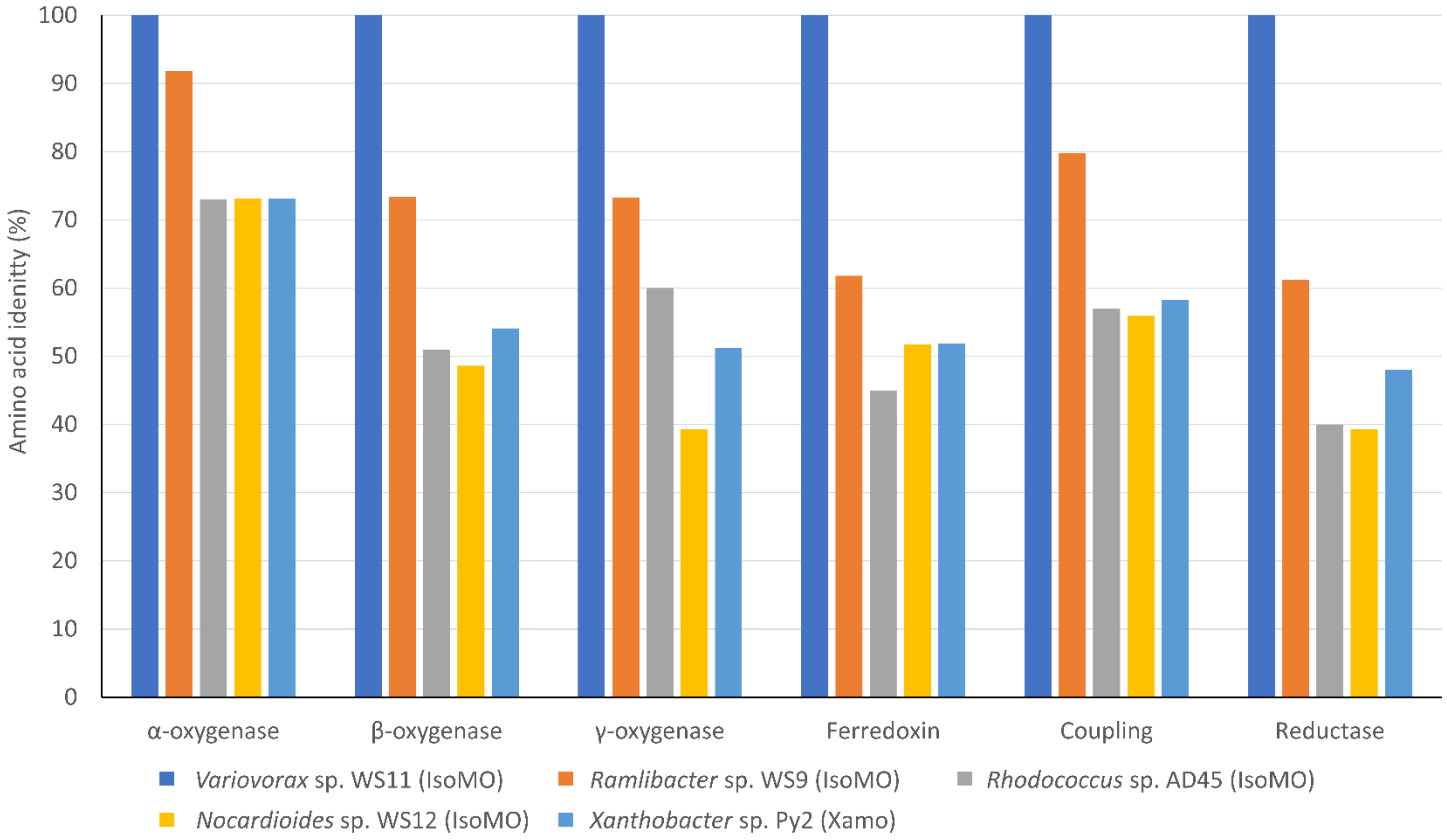

Figure 1.7. Identity of translated amino acid sequences of IsoMO subunits and alkene monooxygenase subunits (Xamo: *Xanthobacter* sp. Py2) against the IsoMO subunits of *Variovorax* sp. WS11.

1.7. **Bacterial metabolic pathways for the degradation of isoprene**

1.7.1. **Bacterial oxidation of isoprene**

An aerobic pathway for the degradation of isoprene was first described by van Hylckama Vlieg *et al.* (1999, 2000) (Figure 1.6). The initial oxidation of isoprene to epoxyisoprene was catalysed by IsoMO with an enantiomeric excess of 95% (*R*)-epoxyisoprene (van Hylckama Vlieg *et al.* 1999, 2000). Initial studies using *Rhodococcus* sp. AD45 attempted to confirm the functionality of IsoMO from this bacterium by heterologously expressing all genes involved in isoprene metabolism in *E. coli*, *Xanthobacter* spp., *Pseudomonas* spp. or *Burkholderia* spp. (van Hylckama Vlieg *et al.* 2000). However, no isoprene degradation was detected in any of these hosts. Crombie *et al*. (2015) confirmed the necessity of IsoMO in isoprene metabolism by constructing an *isoA* deletion mutant of *Rhodococcus* sp. AD45, thereby abolishing isoprene metabolism. The epoxidation of isoprene was followed by the detoxification of epoxyisoprene by conjugation with glutathione, catalysed by a homodimeric glutathione *S*-transferase (IsoI), forming 1-hydroxy-2-glutathionyl-2-methyl-3-butene (HGMB) (van Hylckama Vlieg *et al.* 1998, 1999, 2000). IsoI did not have activity with all tested epoxides, instead exhibiting the greatest activity towards epoxyisoprene, and 1,2-epoxyhexane was capable of completely inhibiting IsoI activity and also growth on isoprene by *Rhodococcus* sp. AD45 (van Hylckama Vlieg *et al.* 1998, 1999). Epoxyisoprene was converted to HGMB with an enantiomeric excess of 70-80% (van Hylckama Vlieg *et al.* 1999). Subsequent metabolism of HGMB required a homodimeric NAD^+-dependent dehydrogenase, IsoH (van Hylckama Vlieg *et al.* 1999, 2000). This enzyme shared homology with the

epoxide carboxylase proteins found in *Xanthobacter* sp. Py2 (Allen & Ensign, 1999, van Hylckama Vlieg *et al.* 2000). IsoH catalysed two sequential oxidation steps, yielding 2NADH and 2-glutathionyl-2-methyl-3-butenoic acid (GMBA). The specificity of IsoH towards glutathione-conjugated compounds was confirmed, although a conjugate of epoxypropane and glutathione was oxidised at a significantly lower rate than HGMB (van Hylckama Vlieg *et al.* 1999). Subsequent steps of the isoprene metabolic pathway remain to be characterised. It has been theorised that GMBA is further metabolised by a manner which resembles isoleucine metabolism (Jimenez-Diaz *et al.* 2017, van Hylckama Vlieg *et al.* 2000). This would begin with the formation of a CoA-thioester of GMBA, followed by the removal of glutathione by the as-yet uncharacterised glutathione *S*-transferase, IsoJ. This enzyme was confirmed to be active towards two known substrates of glutathione *S*-transferase enzymes, 1,2-dichloro-4-nitrobenzene (DCNB) and 1-chloro-2,4-dinitrobenzene (CDNB), although IsoJ had no activity towards products of isoprene metabolism (van Hylckama Vlieg *et al.* 2000). Even when adding purified GMBA to crude extracts of isoprene-grown *Rhodococcus* sp. AD45, no glutathionyl groups were liberated and no carboxylation was evident (van Hylckama Vlieg *et al.* 2000). It was predicted that the resultant compound would be broken down by β-oxidation to yield acetyl-CoA (Massey *et al*. 1976, Jimenez-Diaz *et al*. 2017).

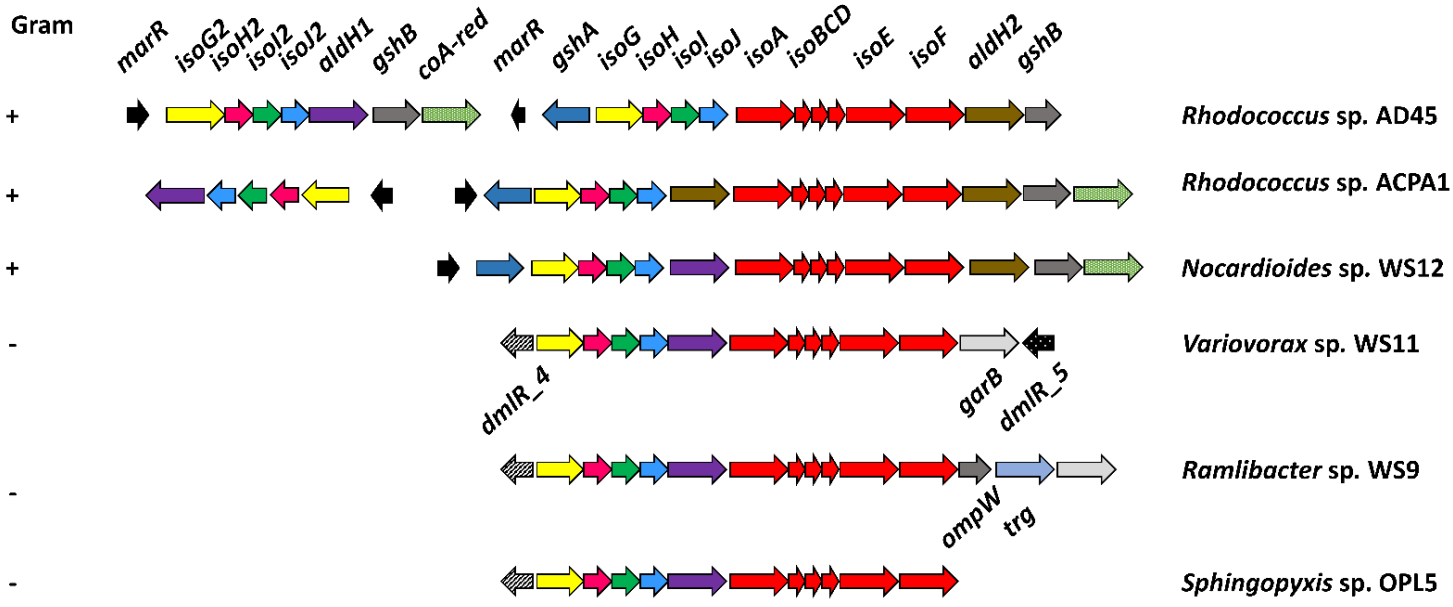

Figure 1.8. Comparison of the *iso* metabolic gene clusters of three Gram positive and three Gram negative isoprene degraders. *isoG*: putative CoA-transferase, *isoH*: HGMB dehydrogenase, *isoI*: glutathione *S*-transferase, *isoJ*: glutathione *S*-transferase, *aldH*: putative aldehyde dehydrogenase, *isoA*: IsoMO α-oxygenase subunit, *isoB*: IsoMO γ-oxygenase subunit, *isoC*: IsoMO ferredoxin component, *isoD*: IsoMO coupling protein, *isoE*: IsoMO β-oxygenase component, *isoF*: IsoMO reductase component, *gshA*: putative glutamate-cysteine ligase, *gshB*: putative glutathione synthetase, *garB*: putative glutathione-disulfide reductase, *marR*: putative multiple antibiotic resistance-type transcriptional regulator, *dmlR*: putative LysR-type transcriptional regulator, *ompW*: putative outer membrane protein, *trg*: putative methyl-accepting transducer domain-containing protein, *coA-red*: putative CoA-disulfide reductase.

As more isoprene degraders have been identified, a common trait of glutathione-dependence has been inferred due to the conservation of glutathione biosynthesis or recycling genes in the *iso* metabolic gene clusters of distinct isoprene degrading bacteria (Figure 1.8) (McGenity *et al*. 2018, Larke-Mejía *et al*. 2019, Dawson *et al*. 2020). The use of glutathione in *Rhodococcus* sp. AD45 was worthy of note due to the fact that most Gram positive bacteria tend to use alternative low molecular weight thiols, such as mycothiol (Johnson *et al.* 2009, Lienkamp *et al.* 2020). Epoxypropane formation by the alkene monooxygenase of *Rhodococcus rhodochrous* B-276 is followed by conjugation with coenzyme M (CoM), catalysed by an epoxyalkane:coM transferase (Ensign, 2001, Krum & Ensign, 2000, Liu & Mattes, 2016). Isoprene-grown *Rhodococcus* sp. AD45 accumulated approximately 2 mM glutathione in the cytoplasm (van Hylckama Vlieg *et al.* 1998). At present, no isoprene-degrading bacterium has been identified which lacks IsoI or IsoH, indicating that glutathione biosynthesis must be conserved.

1.7.2. **Regulation of isoprene metabolism**

Isoprene metabolism by *Rhodococcus* sp. AD45 was initially shown to be induced in the presence of isoprene (van Hylckama Vlieg *et al.* 2000). The regulation of isoprene metabolism in *Rhodococcus* sp. AD45 was characterised in greater detail by Crombie *et al*. (2015). Transcriptome analysis revealed a core cluster of 22 genes which were significantly upregulated when *Rhodococcus* sp. AD45 was induced by either isoprene or epoxyisoprene. When induced, these genes accounted for over 25% of transcripts, demonstrating the importance of the *iso* metabolic gene cluster and associated accessory genes (Figure 1.8) (Crombie *et al*. 2015). Given the rapidity of the epoxyisoprene-induced response compared to the isoprene-induced response, and considering the fact that the induced set of genes were common after induction by both isoprene and epoxyisoprene, it was hypothesised that epoxyisoprene was the primary inducer of *iso* metabolic genes rather than isoprene. A mutant strain of *Rhodococcus* sp. AD45 which lacked an intact copy of *isoA*, therefore rendering it incapable of oxidising isoprene to epoxyisoprene, lacked any transcriptional of the *iso* genes when supplemented with isoprene but was still strongly induced by epoxyisoprene (Crombie *et al*. 2015). Therefore, it was suggested that either epoxyisoprene or a subsequent metabolic product of isoprene metabolism was responsible for inducing the expression of these transcripts (Crombie *et al*. 2015). Other genes involved in isoprene metabolism include a putative *marR*-type transcriptional regulator, *marR2*, which was upregulated 19-fold when *Rhodococcus* sp. AD45 was supplemented with isoprene (Crombie *et al*. 2015). This family of proteins is typically associated with antibiotic resistance mechanisms (*marR*: *m*ultiple *a*ntibiotic *r*esistance *r*egulator), but examples of *marR* controlling metabolic pathways involved in the degradation of aromatic compounds and environmental toxins are also available (Wilkinson & Grove 2006). *marR2* is located upstream of the *iso* metabolic gene cluster and is transcribed in the opposite direction (Figure 1.8), indicating a potential regulatory role. Further characterisation of the regulation of isoprene metabolism in a Gram negative isoprene degrading bacterium was described by Dawson *et al*. (2020) (and is described in Chapter 6, Section 6.5.1, Chapter 7, and Chapter 8).

1.7.3. **Organisation and conservation of *iso* metabolic gene clusters**

All genome-sequenced isoprene degrading bacteria isolated by the Murrell, Janssen, and McGenity groups contain a core set of genes involved in isoprene degradation that have been characterised in detail, *isoGHIJABCDEF* (Crombie *et al.* 2018, Dawson *et al.* 2020, El Khawand *et al.* 2016, Johnston *et al.* 2017, Larke-Mejía *et al.* 2019, van Hylckama Vlieg *et al.* 2000). *iso* metabolic gene clusters have not been detected in the isoprene degraders and co-oxidisers isolated by other groups at the time of writing (Srivastva *et al*. 2015, 2017, Singh *et al*. 2019). There is compelling evidence to suggest that isoprene metabolism was acquired in many isolates by horizontal gene transfer. The *iso* metabolic gene clusters of *Rhodococcus* sp. AD45 and *Variovorax* sp. WS11 are located on megaplasmids, and the *iso* cluster of *Rhodococcus* sp. AD45 was associated with a relatively large number of transposase sequences (Crombie *et al*. 2015, Dawson *et al*. 2020). A review of the evolution of SDIMO by Leahy *et al*. (2003) noted that approximately half of the SDIMO gene clusters included in their study were plasmid-encoded. All isolated isoprene degraders contain at least one copy of an *aldH* (aldehyde dehydrogenase) gene within the *iso* gene cluster, often between *isoJ* and *isoA* (Figure 1.8) (Crombie *et al*. 2018, McGenity *et al*. 2018, Larke-Mejía *et al*. 2019, Dawson *et al*. 2020). In *Rhodococcus* sp. AD45, *aldH1* was predicted to encode a glyceraldehyde 3-phosphate dehydrogenase, while *aldH2* was predicted to encode a 4-hydroxymuconic semialdehyde dehydrogenase (Crombie *et al*. 2015). While no role for *aldH1/aldH2* has been confirmed in isoprene metabolism, the ubiquity of *aldH* genes within *iso* metabolic gene clusters indicates an essential role. Glutathione was required for isoprene metabolism in *Rhodococcus* sp. AD45 (van Hylckama Vlieg *et al.* 1998, 1999, 2000), and the genes required for glutathione biosynthesis (*gshAB*) are conserved in the *iso* metabolic gene clusters of Gram positive isoprene degraders (Figure 1.8). However, the *iso* metabolic gene clusters of Gram negative bacteria do not contain glutathione biosynthesis genes. The glutathione biosynthesis genes of *Variovorax* sp. WS11 were located on the chromosome while the *iso* gene cluster was plasmid-encoded (Dawson *et al*. 2020). This disparity can be rationalised according to the apparent rarity of glutathione in Gram positive bacteria (Johnson *et al*. 2009, Lienkamp *et al*. 2020). It is possible that the ability of Gram positive isoprene degraders to synthesise glutathione, a trait which is essential to isoprene metabolism, was acquired in the same event as the ability to metabolise isoprene, as evidenced by the proximity of the requisite genes (Figure 1.8).

A curious trait of some Gram positive isoprene degraders is the duplication of *isoGHIJ* (Crombie *et al*. 2015), genes required for the isoprene metabolic pathway following the epoxidation of isoprene (van Hylckama Vlieg *et al.* 1998, 1999). A greater variety of genome-sequenced Gram positive and Gram negative isoprene degraders are required to determine whether this is purely a Gram positive trait. No roles have been confirmed for the second copies of *isoGHIJ*, although it is possible that some Gram positive isoprene degraders require additional genes related to the use of glutathione in order to cope with the toxic oxidation product of isoprene metabolism, epoxyisoprene. Another trait which may be conserved in Gram positive isoprene degraders is the presence of genes with putative functions in the use of CoA. These include a phenylacetate-CoA ligase upstream of the *iso* metabolic gene cluster of *Rhodococcus* sp. AD45, and a putative CoA-disulfide reductase in each Gram positive *iso* gene cluster (Figure 1.8). The relevance of these genes is supported when considering the putative CoA-transferase roles of *isoG* and *isoG2* (Crombie *et al*. 2015). Each *iso* metabolic gene cluster has one or more putative transcriptional regulators close to

the primary metabolic genes (Figure 1.8), although the family of transcriptional regulators differs between Gram positive and Gram negative isolates. Gram positive isoprene degraders employ putative MarR-type transcriptional regulators, while Gram negative isoprene degraders use putative LysR-type transcriptional regulators (LTTRs), annotated as *dmlR* (*D-m*alate *m*etabolism *r*egulator) (Figure 1.8). LTTRs are more commonly associated with the regulation of metabolic processes than are the MarR-type regulatory proteins (Alekshun & Levy 1999, Maddocks & Oyston 2008). Each regulatory gene is typically found close to, and divergently transcribed from, the gene(s) it controls (Alekshun & Levy 1999, Maddocks & Oyston 2008). This is supported by the location and orientation of *marR* and *dmlR* genes on each *iso* metabolic gene cluster, with the exception of *Nocardioides* sp. WS12 which has a single copy of *marR* transcribed in the same orientation as the *iso* genes (Figure 1.8).

1.7.4. **Alternative mechanisms of isoprene metabolism**

1.7.4.1. **Reductive isoprene metabolism**

Initial evidence for an anaerobic pathway of isoprene reduction was presented by Kronen *et al*. (2019). Isoprene was demonstrated to act as an electron acceptor for acetogenesis by an enrichment culture primarily composed of *Acetobacterium* spp. This process required H_2 and HCO_3^-, and resulted in the enrichment culture producing less acetate than cultures which lacked isoprene (Kronen *et al*. 2019), leading to the hypothesis that reductive isoprene metabolism acted as an energy-conservation process. This reductive process liberated a range of methyl butenes which were not present in cultures which were not supplied with isoprene. As present, no metabolic pathway or essential genes for the reductive metabolism of isoprene have been characterised.

1.7.4.2. **Lyase-dependent isoprene oxidation**

Rohwerder *et al.* (2020) identified genes involved in the metabolism of 2-hydroxyisobutyrate immediately upstream of the *iso* metabolic gene cluster of *Rhodococcus* sp. ACPA4 (Crombie *et al.* 2017). They suggested an alternative mechanism of isoprene oxidation which does not require glutathione, instead using a lyase-dependent method which follows the pathway of isobutene metabolism (Rohwerder *et al*. 2020). Functional confirmation of the proposed pathway is required.

1.8. **Project aims**

The overall aim of the work detailed in this thesis was to characterise the novel isoprene degrader, *Variovorax* sp. WS11. This work was conducted with the context of all previous characterisation of the molecular underpinnings of isoprene metabolism being described in *Rhodococcus* sp. AD45, a Gram positive Actinobacterium, meaning that very few comparative studies of isoprene metabolism have been reported.

The initial aim of this project was to study the physiology of *Variovorax* sp. WS11, both as this related to the metabolism of isoprene and to the optimum growth conditions which would allow this novel bacterium to be most effectively employed as a model organism in laboratory-based studies. The genome of *Variovorax* sp. WS11 was analysed with the aim of identifying the physiological capabilities of this bacterium. The substrate specificity of the

isoprene monooxygenase for diverse alkene substrates was previously described in *Rhodococcus* sp. AD45 (Sims 2020), and an aim of this project was to conduct a comparative study using *Variovorax* sp. WS11 in a whole-cell system, thereby comparing the specificity of isoprene monooxygenase in distinct model bacteria. A key aim of the physiology-based studies in *Variovorax* sp. WS11 was to demonstrate an effective method to distinguish between isoprene oxidation by the isoprene monooxygenase and by another representative soluble diiron monooxygenase. The soluble methane monooxygenase was chosen for reference due to the reports of the inhibition of this enzyme by alkynes (Prior & Dalton 1985). To fulfil this aim, linear alkynes were selected to specifically inhibit substrate oxidation by the IsoMO and sMMO.

A key aim of this project was to further characterise the isoprene metabolic pathway first identified by van Hylckama Vlieg *et al*. (2000). This aim was approached by studying the proteome of isoprene-grown *Variovorax* sp. WS11, compared with uninduced cells and cells grown using succinate. This aimed to identity the full range of proteins which were differentially expressed specifically during growth on isoprene, thereby allowing the prediction of a full isoprene metabolic pathway. The mechanism for assimilation of carbon from isoprene was unknown prior to these experiments.

Characterisation of isoprene metabolism through molecular biology approaches was a critical aim of this project, as this would serve as a basis for comparison with the molecular mechanism of isoprene metabolism identified in *Rhodococcus* sp. AD45. These characterisation studies were conducted through a combination of targeted mutagenesis of the isoprene monooxygenase α-oxygenase component (*isoA*) and expression of the isoprene monooxygenase in a heterologous host. This aimed to demonstrate whether the conventional isoprene metabolic pathway (*isoGHIJABCDEF*) first identified in *Rhodococcus* sp. AD45 was active in *Variovorax* sp. WS11, and whether this pathway was essential to the ability of this bacterium to metabolise isoprene.

Finally, an aim of this project was to characterise the regulation of isoprene metabolism. This previously understudied area of isoprene metabolism research had only been described in any detail in a single study using *Rhodococcus* sp. AD45 (Crombie et al. 2015). The regulation isoprene metabolism in *Variovorax* sp. WS11 was initially studied using activity-based assays to identify the expression of isoprene monooxygenase under a range of growth conditions, followed by studies of the transcription of the *iso* metabolic gene cluster. Analysis of the transcriptome of *Variovorax* sp. WS11 was planned with the aim of identifying the full complement of genes which were differentially transcribed during growth on isoprene or alternative growth conditions. Specific transcriptional regulators were identified in the *iso* metabolic gene cluster of *Variovorax* sp. WS11, and targeted mutagenesis was employed with the aim of identifying the functions of the respective genes (*dmlR_4* and *dmlR_5*). Further experiments were designed with the aim of identifying the specific mechanisms of transcriptional control exerted by these regulators.

2. Materials and Methods

Some of the methods listed below were reported by Dawson *et al*. (2020). Unless otherwise indicated, experimental procedures were optimised and conducted by R. Dawson.

2.1 Materials

Molecular biology-grade and analytical-grade materials were obtained from Sigma-Aldrich (St Louis, MO, USA), Thermo Fisher Scientific (Waltham, MA, USA), Merck (Kenilworth, NJ, USA), or Melford (Chelsworth, Ipswich, UK). Gases were obtained from Sigma-Aldrich, Apollo Scientific (Bredbury, Cheshire, UK), or CK Special Gases Ltd (Newton Unthank, UK). Custom oligonucleotides were obtained from Thermo Fisher Scientific.

2.2 Cultivation and maintenance of bacterial cultures

Bacterial strains and plasmids are shown in Table 2.1. All culture density measurements were recorded using a UV-1800 spectrophotometer (Shimadzu, Milton Keynes, UK).

2.2.1 Antibiotics

Antibiotics were prepared as solutions in distilled water and sterilised by syringe filter as above. Antibiotic solutions were added to growth media at the following concentrations: kanamycin 50 μg ml^{-1}, gentamicin 10 μg ml^{-1}, streptomycin 50 μg ml^{-1}, spectinomycin 50 μg ml^{-1}, and ampicillin 100 μg ml^{-1}, unless stated otherwise. Antibiotic solutions were maintained at -20 °C.

2.3 Growth and manipulation of *Escherichia coli*

E. coli strains used in this study (Table 2.1) were maintained in LB medium. While not in use, *E. coli* strains were maintained at -80 °C in a combination of LB medium and 10% (v/v) glycerol. Starter cultures were prepared by transfer of an individual colony from LB agar into 10 ml of LB medium and incubation overnight at 37 °C with shaking at 180 revolutions per minute (rpm). These cultures were then manipulated according to the specific experimental requirements.

2.3.1 Preparation and transformation of chemically competent *E. coli*

1 ml of starter culture of the relevant *E. coli* strain was transferred to 100 ml SOB medium, which was then incubated at 37 °C with shaking at 180 rpm until the OD_{600} measured 0.35. The cells were spun in a centrifuge, pre-cooled to 4 °C, at 2,000 x *g* for 10 minutes. The supernatant was removed and the cell pellet was resuspended in 60 ml of chilled chemical competence buffer. This was incubated on ice for 20 minutes before centrifuging as before. The cell pellet was resuspended in 4 ml of chilled chemical competence buffer and incubated for a further 20 minutes on ice before 200 μl aliquots were snap-frozen in liquid nitrogen. Chemically competent *E. coli* were stored at -80 °C until required.

Chemically competent cells were thawed on ice and 50 µl aliquots were gently mixed with 50-100 ng of plasmid DNA or DNA ligation mix. The mixture was incubated on ice for 30 minutes and then heat shocked at 42°c for 45 seconds before immediately transferring to ice. Heat shocked cells were promptly mixed with 950 µl of SOC medium and allowed to recover for 1 hour at 37 °C, 180 rpm. Transformed cells were then transferred to selective LB agar and incubated for 18 – 24 hours at 37 °C.

2.4 **Growth and manipulation of *Variovorax* sp. WS11**

2.4.1 **Growth of *Variovorax* sp. WS11**

Variovorax sp. WS11 was routinely maintained in Ewers medium with 1% (v/v) gaseous isoprene in the headspace of a 120 ml glass vial, sealed by a butyl rubber stopper and an aluminium crimp top. Cultures were incubated at 30°c with shaking at 160 rpm. Sugars and carboxylic acids were used as growth substrates at 10 mM. The purity of cultures was routinely checked by a combination of light microscopy using a Zeiss Axoiskop 50 microscope, 130 VA Type B (Carl Zeiss Ltd, Cambridge, UK), and streaking of liquid cultures for single colonies on R2A agar (Oxoid, Thermo Fisher). Long-term stocks of *Variovorax* sp. WS11 were maintained at -80 °c in a combination of Ewers medium and 10% (v/v) glycerol.

2.4.2 **Preparation and transformation of *Variovorax* sp. WS11 according to established protocols**

Genetic techniques for use in *Variovorax* sp. WS11 were enabled by optimising the preparation of electrocompetent cells. A method initially described for use in *Variovorax paradoxus* EPS (Pehl *et al*. 2012) was partially modified, found to be successful, and was further optimised to improve the transformation efficiency of *Variovorax* sp. WS11.

Variovorax sp. WS11 was grown in 50 ml Ewers medium with 10 mM succinate until an OD_{540} of 0.6 was reached. Cultures were incubated at 4 °C for 24 hours and then spun at 4,000 x *g* for 30 minutes in a pre-cooled centrifuge. The supernatant was removed and the pellet resuspended in an equal volume of chilled 300 mM sucrose. The culture was centrifuged as before and resuspended in chilled 300 mM sucrose. The culture was then centrifuged as before and resuspended in 1:10 the original volume of chilled 300 mM sucrose. The culture was centrifuged as before and resuspended in 1:100 the original volume of chilled 300 mM sucrose. 100 µl of electrocompetent *Variovorax* sp. WS11 was mixed with 100 ng of the relevant DNA and transformed in a 2 mm gap cuvette by exponential decay electroporation at 2.5 kV, 200 Ω, 25 µF. Transformed cells were resuspended in 900 µl of Ewers medium with 10 mM succinate and allowed to recover at 30 °C for 1.5 hours with shaking at 160 rpm before transferring to Ewers agar with 10 mM succinate and the appropriate selective agent.

2.4.3 **Optimised preparation and transformation of *Variovorax* sp. WS11**

Variovorax sp. WS11 was grown in 50 ml Ewers medium with 10 mM succinate until an OD_{540} of 0.6 was reached. Cells were incubated at 4 °C for 48 hours and then spun at 6,000 x *g* for 10 minutes in a pre-cooled centrifuge. The supernatant was removed and the pellet resuspended in an equal volume of chilled, sterile distilled water. This cell suspension was then centrifuged at 6,000 x *g* for 10 minutes at 4 °C and the pellet resuspended in 10 ml chilled,

sterile distilled water. This was then centrifuged as above and the final pellet resuspended to 1-2 ml in of chilled 10% (v/v) glycerol. This was stored as 100 µl aliquots at -80 °C or used immediately for electroporation by the above protocol. The final modification was the extension of the recovery period from 1.5 to 3 hours before transferring transformants to selective Ewers agar.

2.5 **Growth and manipulation of *Rhodococcus* sp. AD45**

2.5.1 **Growth of *Rhodococcus* sp. AD45**

Rhodococcus sp. AD45 was maintained in Ewers medium with 1% (v/v) isoprene. All growth conditions and purity checks were conducted as outlined in section 2.4.1.

Table 2.1. Bacterial strains used in this study.

Strain	Description	Reference
Escherichia coli Top10	F– *mcrA,* Δ(*mrr-hsdRMS-mcrBC*) Φ80*lacZ*ΔM15, Δ*lacX74, recA1, araD139, Δ(ara leu) 7697, galU, galK, rpsL (StrR), endA1, nupG*	Invitrogen
E. coli DH5-α	Δ*lacZ* ΔM15, Δ(*lacZYA-argF*) U169, *recA1*, *endA1*, *hsdR17*(*rK-mK+*), *supE44*, *thi-1*, *gyrA96*, *relA1*	NEB
E. coli 803	Strain used for routine transformations	(Wood *et al*. 1966)
E. coli Rosetta 2 (pLysS)	*E. coli* BL21 derivative designed to enhance expression of rare codons. pLysS expresses T7 lysozyme to depress auto-expression of cloned genes by the T7 RNA polymerase	Sigma-Aldrich
Variovorax sp. WS11	Gram negative isoprene degrader, isolated from willow soil	(Larke-Mejía *et al*. 2019)
Variovorax sp. WS11 Δ*isoA*	Non-isoprene-degrading *Variovorax* sp. WS11 with targeted deletion of isoprene monooxygenase α-oxygenase component (IsoA)	(Dawson *et al*. 2020)
Variovorax sp. WS11 Δ*dmlR_4*	Non-isoprene degrading *Variovorax* sp. WS11 with targeted deletion of putative regulatory gene *dmlR_4*	This study
Variovorax sp. WS11 Δ*dmlR_5*	Isoprene-degrading *Variovorax* sp. WS11 with targeted deletion of putative regulatory gene *dmlR_5*	This study
Variovorax sp. WS11 Δ*rif*	*Variovorax* sp. WS11 which had acquired spontaneous resistance to rifampicin	This study
Variovorax sp. WS11 Δ*nitro*	*Variovorax* sp. WS11 which had acquired spontaneous resistance to nitrofurantoin	This study
Variovorax paradoxus EPS	Non-isoprene degrading species of *Variovorax*, previously characterised for its ability to produce biofilms.	(Pehl *et al*. 2012)
Rhodococcus sp. AD45	Gram positive isoprene degrader, isolated from freshwater sediment	(van Hylckama Vlieg *et al*. 1998)
Rhodococcus sp. AD45-id	Non-isoprene degrading *Rhodococcus* sp. AD45 with targeted loss of the megaplasmid containing all *iso* genes	(Crombie *et al*. 2015)
Methylococcus capsulatus (Bath)	Wild-type methane-oxidising bacterium	(Whittenbury *et al*. 1970)

2.5.2 **Preparation and transformation of electrocompetent *Rhodococcus* sp. AD45**

Electrocompetent *Rhodococcus* sp. AD45 was prepared as described previously (Crombie *et al*. 2015). In brief, a 50 ml culture was grown in Ewers medium with 10 mM succinate to an OD_{540} of 0.6, cooled on ice, and harvested by centrifugation at 2,500 x *g* for 15 minutes at 4 °C. This culture was washed twice in chilled water and re-suspended in 1 ml of 10% (w/v) glycerol. 100 µl aliquots were electroporated by an exponential decay protocol at 2.5 kV, 800 Ω, 2.5 µF in a 2 mm gap cuvette. Cells were recovered for 4 hours in 1 ml Ewers medium with 10 mM succinate before transferring to selective agar.

2.6 **Growth of *Variovorax* sp. WS11 in an isoprene-fed fermentor**

Variovorax sp. WS11 was inoculated at mid-exponential phase into 400 ml Ewers medium in a 2 litre flask with 1% (v/v) headspace isoprene. Once an OD_{540} >0.3 had been reached, this culture was used to inoculate a 4 litre working volume fermentor (Electrolab, Tewkesbury, UK), demonstrated in Figure 2.1 (Dawson *et al*. 2020). Optimal growth conditions were maintained throughout growth (30 °C, 160 rpm, pH 6.0). Aerobic conditions were maintained by a constant airflow at 2.4 L min^{-1}. A constant flow of isoprene into the fermentor unit was maintained by passing a 1 ml min^{-1} flow of air through liquid isoprene in a 30 ml glass vial, maintained on ice and sealed by a butyl rubber stopper (Dawson *et al*. 2020). Culture purity was routinely checked as described in Section 2.4.1.

At intervals of approximately 2 days, 3 litres of isoprene-grown *Variovorax* sp. WS11 was siphoned into chilled, sterilised bottles and promptly centrifuged at 7,000 rpm at 4 °C for 10 minutes in an Avanti J-20 high speed centrifuge (Beckman Coulter, Pasadena, CA) using a JLA 8.1000 rotor (Beckman Coulter). The supernatant was discarded and the pellet was made into a slurry by the addition of 4 ml of ice-cold 50 mM HEPES, pH 6.0. Excessive washing of cells was avoided due to the observation of significantly reduced isoprene uptake activity after one or more washes (described in Section 3.4.2.2). Snap-frozen cell pellets were formed by releasing droplets of cell slurry from a disposable Pasteur pipette into liquid nitrogen. Cell pellets were promptly stored at -80 °C until required. The fermentor culture was restored to a 4-litre volume by addition of fresh Ewers medium.

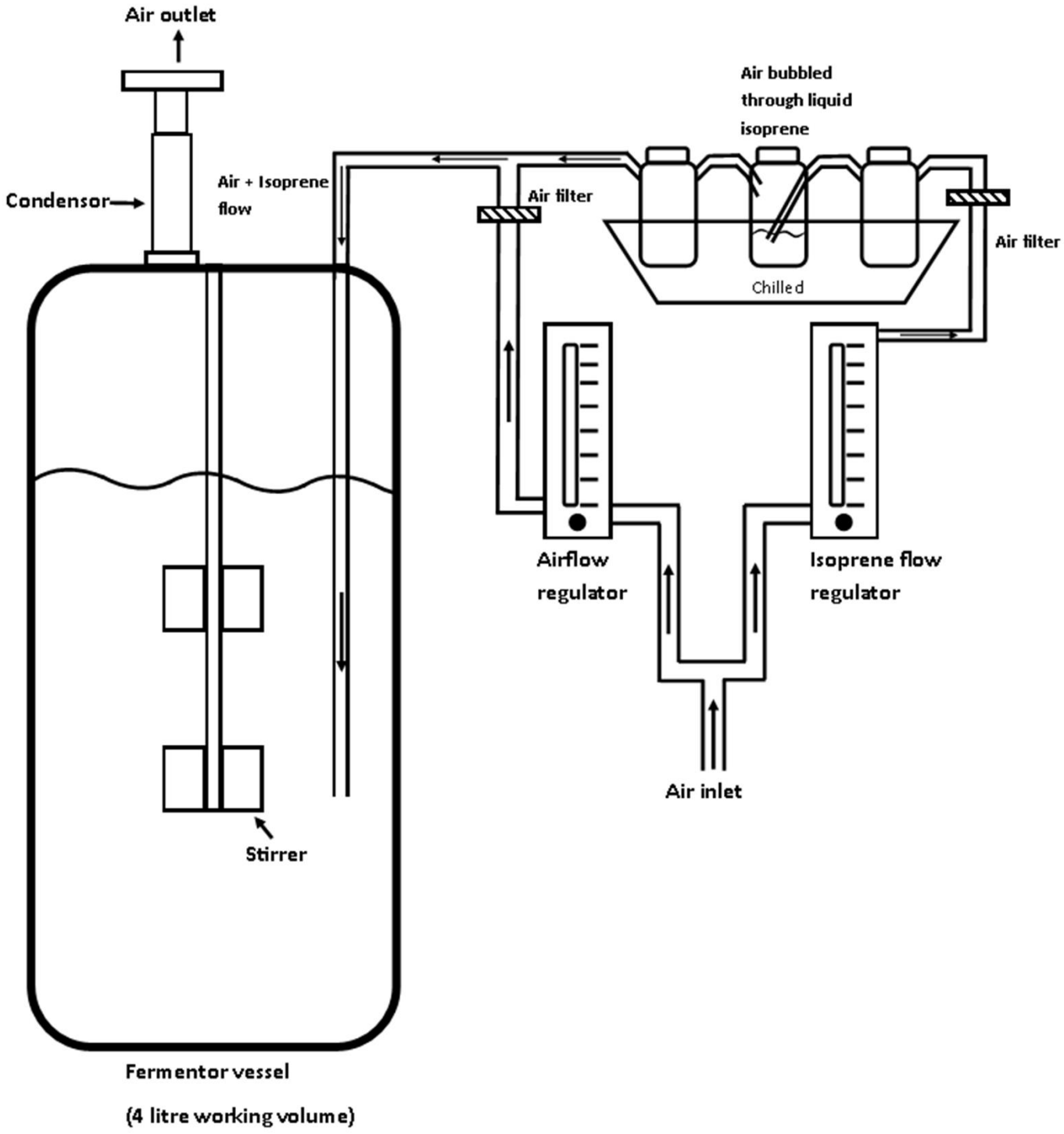

Figure 2.1. Schematic representation of an isoprene-fed fermentor (Dawson *et al*. 2020).

2.6.1 **Optimisation of Antifoam supply during growth on isoprene**

After approximately 120 hours of growth, a significant mass of bubbles was produced on the surface of the fermentor culture. This was dispersed by adding the silicone-based Antifoam A (Sigma Aldrich) at 0.25 ml L^{-1}, whereas an organic antifoaming agent, Antifoam 204 (Sigma Aldrich), inhibited the growth of *Variovorax* sp. WS11.

2.7 **Extraction of deoxyribonucleic acid (DNA)**

2.7.1 **Genomic DNA from WS11**

Variovorax sp. WS11 was grown in 50 ml Ewers medium with 10 mM succinate at 30 ^{o}C with shaking at 160 rpm to a final OD_{540} of 0.6. The culture was centrifuged at 3,000 * *g* for 10 minutes at 4^{o}c and genomic DNA was extracted using a Genomic Tip 100/G DNA isolation kit (Qiagen, Manchester, UK) and corresponding DNA buffers (Qiagen). Genomic DNA extraction was conducted according to the manufacturer's instructions.

2.7.2 **Plasmid DNA extraction from *E. coli***

E. coli starter cultures were prepared as described in Section 2.3, supplemented by a selective agent specific to the plasmid in question. Starter cultures were centrifuged at 6,000 * *g* for 10 minutes and the supernatant was discarded. Plasmid DNA was extracted using a GeneJET Plasmid Miniprep Kit (Thermo Fisher) according to the manufacturer's instructions. Plasmid DNA concentration and quality were determined as described in Section 2.8.1. Mid-scale plasmid DNA preparations, or extraction of low copy-number vectors, were conducted using a Plasmid Plus Midi Kit (Qiagen) according to the manufacturer's instructions.

2.8 **Nucleic acids techniques**

2.8.1 **Quantification of DNA/RNA**

DNA and RNA concentrations were calculated by using a NanoDrop spectrophotometer (Thermo Fisher), with nucleic acid purity being predicted according to the ratio of absorbances at 230 nm, 260 nm, and 280 nm. Nucleic acid quality was further estimated by separation of a known quantity of nucleic acid by agarose gel electrophoresis (Section 2.8.5) and studying the extent of degradation.

2.8.2 **Polymerase chain reaction (PCR)**

PCR reactions were prepared on ice in a 50 µl reaction volume using either a DreamTaq DNA polymerase (Thermo Scientific) or Q5 high-fidelity DNA polymerase (NEB, Hitchin, UK). A typical master mix (1x) contained 1x buffer supplemented with an appropriate divalent cation, dNTPs (0.2 mM), forward and reverse primers (0.4 µM), and the relevant DNA polymerase at the concentration recommended by the manufacturer. PCR amplification was typically achieved by the steps demonstrated in Table 2.2 using a DNA Engine Tetrad 2 (Bio-Rad, Hercules, CA). Degenerate primers designed to amplify the 16S rRNA gene (Lane 1991) and M13 universal primers (Invitrogen) were routinely used under these conditions (Table 2.3).

Table 2.2. Typical polymerase chain reaction cycling conditions.

Step	Temperature (°C)	Time
Initial Denaturation	95	3 minutes
25 – 25 cycles	95	30 seconds
	NA	30 seconds
	72	1 minute/kb
Final Extension	72	7 minutes

NA: annealing temperature is not available due to the variability of this condition depending on the primers used.

Typical conditions were altered in the case of PCR using colony biomass directly as a template for amplification (henceforth colony PCR). The PCR mastermix was amended to contain 0.07% (w/v) BSA and 5% (v/v) DMSO per 50 µl reaction. Furthermore, the initial denaturation step was increased to 10 minutes to ensure that genetic material was made available for amplification by PCR.

Table 2.3. Degenerate primers routinely used in this study.

Primer Name	Sequence (5'--3')	Reference/Origin
27F	AGAGTTTGATCMTGGCTCAG	(Lane 1991)
1492R	TACGGYTACCTTGTTACGACTT	
M13F	GTAAAACGACGGCCAG	Invitrogen
M13R	CAGGAAACAGCTATGAC	

2.8.3 **Cloning and sub-cloning techniques: Restriction**

Digestion of DNA by restriction enzymes was typically conducted using 1 µg of template DNA in a 20 µl reaction. DNA was digested by the relevant FastDigest restriction enzyme (Thermo Fisher) for 1 hour at 37 °C. Where possible, the reaction was inactivated by heat treatment before continuing with further applications of the digested DNA. Digested DNA was cleaned by column-based purification in a HighPure PCR product purification kit (Roche, Welwyn Garden City, UK) and eluted DNA was quantified and quality-checked as described in Section 2.8.1. Where necessary, such as in the case of sub-cloning a linear DNA fragment into a vector, linearised vector DNA was prevented from self-ligating by treatment with FastAP thermosensitive alkaline phosphatase (Thermo Scientific) for the final 30 minutes of digestion in a FastDigest reaction. Where FastDigest restriction enzymes were not used, FastAP thermosensitive alkaline phosphatase treatment was conducted using linearised, purified vector DNA in a separate reaction using FastAP buffer (Thermo Scientific) according to the manufacturer's instructions. The linear, dephosphorylated DNA was then purified as described previously.

2.8.4 **Cloning and sub-cloning techniques: Ligation**

Following digestion by compatible restriction enzymes and column-based purification, vector and insert DNA were combined at a molar ratio between 1:1 and 1:5. Ligation was achieved using T4 DNA ligase (Thermo Fisher) at room temperature for 1 hour. The ligated DNA mixture was used directly to transform *E. coli* Top10 as described in Section 2.3.1.

Genes of interest synthesised directly using Q5 high fidelity polymerase were separated by agarose gel electrophoresis, as described in Section 2.8.5, and the DNA was extracted from the agarose gel and purified using a HighPure PCR product purification kit according to the manufacturer's instructions. As Q5 high-fidelity polymerase produces DNA which lacks overhanging bases at either the 5' or 3' terminus, gel-extracted PCR products were ligated directly with pJET1.2/blunt using the CloneJET PCR Cloning Kit (Thermo Fisher) according to the manufacturer's instructions. Ligation mixtures were used to transform *E. coli* Top10 as described in Section 2.3.1. Plasmids were extracted from transformants as described in Section 2.7.2, and DNA inserts could then be excised from pJET1.2/blunt using an appropriate combination of restriction enzymes, as described in Section 2.8.3. DNA inserts were then ligated into an appropriate vector which had been digested with a complementary combination of restriction enzymes (prepared as described in Section 2.8.3). This process is described with greater specificity in later chapters.

2.8.5 **Agarose gel electrophoresis**

Agarose was added to 1X Tris Borate EDTA (TBE) buffer to a final concentration of 0.5-1.0% (w/v), heated to homogeneity, and mixed with 0.5 µg ml^{-1} ethidium bromide. Approximately 100 ng of DNA was separated on an agarose gel by electrophoresis and the size of bands were estimated by reference against a GeneRuler 1 kb DNA ladder (Thermo Fisher). When separating RNA by agarose gel electrophoresis, 2 µg of RNA was loaded and the size of rRNA bands were compared against a GeneRuler 1 kb DNA ladder after separation by electrophoresis at 60 V at 4 ^{o}C. Gels were visualised using a ChemiDoc XRS System (Bio-Rad, Hercules, CA, USA).

2.8.6 **Genome sequencing and analysis**

The genome of *Variovorax* sp. WS11 was sequenced and assembled by MicrobesNG (University of Birmingham, UK) using the Enhanced Genome Sequencing service. The genome sequence was produced by a combination of technologies; long-read scaffolds were produced by Oxford Nanopore sequencing, and Illumina HiSeq was used to produce short-read sequences using a 250 bp paired end protocol. Trimming of Illumina adapters was conducted using Trimmomatic 0.30 with a sliding window quality cutoff of Q15 (Bolger *et al*. 2014). Genome assembly was performed using Unicycler v0.4.0 (Wick *et al*. 2017). The genome of *Variovorax* sp. WS11 was annotated by the RAST annotation pipeline, http://rast.theseed.org/FIG/rast.cgi (accessed on 16/05/2019) (Aziz *et al*. 2008, Overbeek *et al*. 2014, Brettin *et al*. 2015).

2.9 **Targeted mutagenesis and complementation**

Variovorax sp. WS11 was the subject of targeted mutagenesis experiments according to Schäfer *et al*. (1994). pK18mobsacB was selected as the vector backbone to facilitate marker-exchange mutagenesis. Due to this vector being based on the pMB1 replicon, it can only replicate stably in *E. coli* (Sutcliffe 1979) and therefore any phenotypic traits (e.g. kanamycin resistance) conferred to *Variovorax* sp. WS11 must be due to complete insertion of the suicide construct into the site of mutagenesis by homologous recombination.

2.9.1 **Double homologous recombination**

Suicide vectors were prepared in pK18mobsacB to facilitate targeted deletion by marker exchange mutagenesis. 400-600 bp regions of the gene of interest, overlapping the translational start and stop codons, were synthesised by PCR using Q5 high-fidelity polymerase (Qiagen) and cloned directly into pJET1.2/blunt (refer to Section 2.8.4.). These flanking regions were excised by restriction enzymes and sequentially sub-cloned into pK18mobsacB, which itself had been digested by corresponding restriction enzymes and dephosphorylated to prevent self-ligation. *aacC1*, encoding a gentamicin acetyltransferase which conferred gentamicin resistance (Wohlleben *et al*. 1989), was cloned directly between the two flanking regions within pK18mobsacB. *aacC1* was derived from two sources; p34S-Gm by direct restriction using *Xba*I in a non-orientation-dependent manner (Dennis & Zylstra 1998), or pCM351 by PCR-dependent synthesis (Marx & Lidstrom 2002) and subsequent digestion by *Xba*I and sub-cloning into pK18mobsacB between the flanking regions. The latter method had the advantage of including *loxP* sites immediately upstream and downstream of *aacC1*, allowing the excision of *aacC1* subsequent to mutagenesis (Marx & Lidstrom 2002). Uptake of the suicide construct into *Variovorax* sp. WS11 was facilitated by electroporation (Section 2.4.3.), allowed to recover as described previously, and spread on Ewers agar with 10 mM succinate, 50 µg/ml kanamycin and 10 µg/ml gentamicin. Antibiotic resistant colonies were confirmed to have gained the full pK18mobsacB backbone within Megaplasmid 1 (as described in Chapter 6) by colony PCR using primers specific to the site of mutagenesis.

Transformants were verified by PCR and grown in Ewers medium with 10 mM succinate in the presence of kanamycin to ensure that a stable recombination event had occurred. Kanamycin resistant cultures were serially-diluted to 10^{-5} in sterile water and spread onto R2A agar in the absence of antibiotics. Single colonies were grown in Ewers medium in the absence of antibiotic. The latter two steps were performed in the absence of selection pressure to encourage a second recombination event, thereby excising the pK18mobsacB vector. Cultures were spread directly onto Ewers agar with 10 mM succinate, 10 µg/ml gentamicin, and 5% (w/v) sucrose. Gentamicin selected against a reversion to wild-type, while sucrose selected against maintenance of the pK18mobsacB backbone due to lethal levansucrase activity encoded by *sacB* (Schäfer *et al*. 1994). Stable maintenance of *aacC1* within the gene of interest, causing inactivation of the gene, was confirmed by three factors: maintenance of gentamicin resistance, loss of kanamycin resistance, and a positive PCR screen using primers indicated in Chapter 6, Table 6.1 and Chapter 8, Table 8.1.

2.9.2 **Complementation**

In order to establish beyond doubt that phenotypic differences in *Variovorax* sp. WS11 mutants were caused by the inactivation of the specifically targeted gene, the native gene was expressed from a vector using the native promoter of the gene in question. In each case, the gene of interest with appropriate flanking regions was synthesised by PCR using the Q5 high-fidelity polymerase. Each gene was cloned into pJET1.2/blunt as described in Section 2.8.4 and sub-cloned into pBBR1MCS-2 (Kovach *et al*. 1995) which had been digested with complementary restriction enzymes and dephosphorylated as described in Section 2.8.3. Mutant strains of *Variovorax* sp. WS11 were prepared for electrocompetence (as described in Section 2.4.3) and transformed with their respective complementation constructs in pBBR1MCS-2, with selection for transformants by spreading on Ewers agar with 10 mM succinate and kanamycin.

2.10 **Extraction of total RNA from WS11**

Unless otherwise stated, *Variovorax* sp. WS11 was grown in 50 ml Ewers medium using three biological replicates per condition to an OD_{540} of 0.6 (30°c, 160 rpm). Cultures were centrifuged at 6,000 * *g* for 10 minutes at 4 °C and the pellet was immediately transferred to ice. RNA was then extracted by the hot acid-phenol method (Gilbert *et al*. 2000). All glassware, water, and solutions required for RNA extraction were treated with 0.1% (v/v) diethyl pyrocarbonate (DEPC) by incubation at 37 °C overnight, followed by autoclaving. All DNA was removed from the extracted RNA by treatments with RNase-free DNase (Qiagen), followed by a purification step using an RNeasy spin column (Qiagen) according to the manufacturer's instructions. The absence of detectable DNA was confirmed by polymerase chain reaction using primers designed to amplify the 16S ribosomal RNA (rRNA) gene (Section 2.8.2, Table 2.3).

2.10.1 **Time-course induction of *iso* metabolic gene expression**

Variovorax sp. WS11 was grown in 50 ml Ewers medium using 10 mM succinate as the sole source of carbon and energy to an OD_{540} of approximately 0.6. Cultures were centrifuged at 6,000 x *g* for 10 minutes at 4 °C and the supernatant discarded. Cell pellets were resuspended in fresh Ewers medium without a carbon source, then immediately centrifuged as above. Washed cell pellets were gently resuspended in an equal volume of fresh Ewers medium with no carbon source and incubated at 30 °C with shaking at 160 rpm for 1 hour, with the exception of the experiments described in Section 7.5.3. This period of starvation aimed to deplete intracellular stores of carbon, thereby decreasing the time required to induce expression of the *iso* metabolic genes. Starved cultures were induced under one condition for a set period of time: substrate-free (20 minutes, 1 hour, 6 hours, 24 hours), 10 mM succinate (20 minutes, 1 hour, 6 hours, 24 hours), 1% (v/v) isoprene (20 minutes, 1 hour, 6 hours, 24 hours), 0.01% (w/v) epoxyisoprene (10 minutes, 20 minutes, 2 hours, 4 hours). At each of the indicated timepoints, 10 ml of culture was removed by sterile syringe and mixed well with 2 volumes of RNAprotect (Qiagen). Following 5 minutes of incubation at room temperature, treated cultures were centrifuged at 5,000 x *g* for 10 minutes at 4 °C. The supernatant was discarded, and protected cells were immediately stored at -80 °c. After no longer than 5 days, RNA was extracted from thawed cell pellets using TRIzol Reagent (Thermo Fisher Scientific) according to the

manufacturer's protocol. All DNA was removed by a single treatment with RNase-free DNase (Qiagen), and treated RNA was then purified using an RNeasy minikit (Qiagen).

2.10.2 **Induction of gene expression by non-growth substrates**

In cases where a non-growth substrate was tested for its ability to induce the expression of *iso* metabolic genes, *Variovorax* sp. WS11 was initially grown in Ewers medium using 10 mM glucose or 10 mM succinate to an OD_{540} of 0.6. Cultures were centrifuged and washed twice in an equal volume of 50 mM HEPES (pH 6.0), and washed cells were resuspended in an equal volume of fresh Ewers medium with no carbon source. After incubation at 30 ^{o}C with shaking at 160 rpm for 2 hours, cells were exposed to a carbon source which could not act as a growth substrate, such as epoxyisoprene. Induced cultures were incubated as above for a further 2 hours, and then were harvested by centrifugation at 6,000 x *g* for 10 minutes at 4 ^{o}C. Total RNA was then extracted from the cell pellets as described in Section 2.10.

2.10.3 **Complementary DNA synthesis**

Complementary DNA (cDNA) was synthesised using 500 ng of purified RNA as a template. cDNA was synthesised using Superscript III reverse transcriptase (Invitrogen, Waltham, MA, USA), primed for amplification using random hexamers (Fermentas, Waltham, MA, USA), according to the manufacturer's instructions. Each RNA sample was prepared for cDNA synthesis in duplicate, with one sample containing reverse transcriptase and a negative control containing no reverse transcriptase. Both the cDNA and negative control samples were used as templates for each condition during RT-qPCR (described in Section 2.11.).

2.11 **Quantitative reverse transcriptase PCR (RT-qPCR)**

Quantitative PCR (qPCR) was performed in 20 µl reactions using a StepOnePlus instrument (Applied Biosystems, Foster City, CA, USA), using Sensifast SYBR Hi-ROX master mix (BioLine, London, UK). 2 µl of template cDNA or the corresponding negative no-reverse transcriptase control were used as a template for qPCR amplification. The amplification protocol used in this study is recorded in Table 2.4. This qPCR amplification protocol was designed with the aid of Dr. M. Farhan Ul-Haque. Melt curve analysis was used to ensure that fluorescence readings corresponded to the synthesis of specific products. Each biological replicate for each growth/induction condition was tested by RT-qPCR using a further three technical replicates. Changes in target gene expression were calculated relative to a suitable reference housekeeping gene according to the comparative C_T method (Schmittgen & Livak 2008). The comparative C_T method calculates the relative change in expression of a gene of interest (e.g. *isoA*, *isoG*) compared to an internal reference gene (*rpoB*), also compared to the relative expression of the same genes under a different condition (e.g. succinate-grown vs. isoprene-grown) (Schmittgen & Livak 2008). Efficiencies of qPCR primers are detailed in Section 7.4.1. R^2 values of standard curves were calculated by plotting the Log(template quantity) against C_T value. Average qPCR primer efficiencies are: *qisoA*_2F:*qisoA*_2R (95.3±1.4%, R^2=0.99), *qrpoB_1F*:*qrpoB_2R* (96.5±11.1%, R^2=0.98±0.02) , *qisoG_F*:*qisoG_R* (94.4±0.7%, R^2=0.99).

Table 2.4. Real-time PCR amplification, followed by melt curve analysis. An asterisk (*) indicates the step at which fluorescence was recorded.

Step	Temperature (°C)	Time
Initial Denaturation	95	3 minutes
40 cycles	95	20 seconds
	60	60 seconds
	81*	60 seconds
Melt Curve Analysis	95	15 seconds
	60	1 minute
	95^{T}	15 seconds

* Fluorescence was recorded during this step.

^{T} Melt curve analysis was recorded during this step. The temperature was increased with recording of fluorescence at 0.3 °C intervals.

2.12 **Whole transcriptome analysis by RNA-seq**

Cell cultures were prepared as described in Section 2.10.1, and RNA was sent to Novogene (UK) Company limited (Cambridge, UK). RNA quality was assessed by an Agilent 2100 Bioanalyser (Agilent) with an RNA Integrity Number (RIN) cut-off of 6.0. RNA was sequenced using an Illumina HiSeq 1000 at Novogene (Cambridge, UK). Data processing and bioinformatics analyses were all conducted by Novogene, UK.

2.13 **Preparation of cell extracts for mass spectrometry analysis**

Variovorax sp. WS11 was grown in 100 ml Ewers medium with 10 mM succinate or 1% (v/v) isoprene to an OD_{540} of 0.6 in a sealed 2 litre flask, using three biological replicates for each condition. Cells were centrifuged at 7,000 rpm for 10 minutes at 4 °C in an Avanti J-20 high-speed centrifuge (Beckman Coulter) using a JLA 8.1000 rotor (Beckman Coulter). The supernatant was removed and the pellet resuspended in an equal volume of ice-cold 50 mM HEPES (Formedium). The washed cultures were re-centrifuged under the same conditions and the cell pellets resuspended in 1 ml of ice-cold 50 mM HEPES, pH 7.0, with 10 mM dithiothreitol (DTT) and 200 mM NaCl. SIGMA*FAST* Protease Inhibitor Cocktail Tablets (EDTA-Free, Sigma Aldrich) were added to the HEPES buffer according to the manufacturer's instructions. Cell suspensions were broken by three passages through a pre-chilled French Pressure Mini at 20,000 psi, medium ratio. Cell extracts were centrifuged at maximum speed in a conventional benchtop centrifuge at 4 °C for 30 minutes. The supernatant was stored separately and the cell pellet was resuspended in an equal volume of ice-cold 50 mM HEPES. Cell extracts were stored at -20 °C until required.

2.13.1 **Analysis of the expression of Iso peptides over time**

Variovorax sp. WS11 was inoculated in 1 L Ewers medium in 2 litre flasks with 10 mM succinate and grown to an OD_{540} of 0.6, using two biological replicates for each condition. Cells were centrifuged as described in Section 2.13 and were then washed in an equal volume of Ewers medium. Cells were re-centrifuged and resuspended in fresh Ewers

medium, then starved for 1 hour at 30 °C with shaking at 160 rpm. Two replicates of 200 ml of uninduced cells (0 hours post-starvation) were removed. The remaining cells were supplemented with either 10 mM succinate or 1% (v/v) isoprene, using two biological replicates for each condition. 200 ml of cells were harvested after 6 hours, 24 hours, and 30 hours. All cells were centrifuged at 7,000 rpm for 10 minutes at 4 °C, and the total protein content was extracted as described in Section 2.13. Samples were frozen at -20 °C and transported for analysis. All samples were fractionated and labelled using a TMT 16plex Label Reagent set (Thermo Fisher). Samples were analysed by mass spectrometry using an OrbiTrap system by Dr Gerhard Saalbach (John Innes Centre). Data were processed using Proteome Discoverer software (Thermo Fisher).

2.14 **Measurement of headspace isoprene by gas chromatography (GC)**

A gas-tight glass syringe (Agilent, Cheadle, UK) was used to pierce the butyl rubber stopper of a sealed vial and 50 µl of headspace gas was removed. This was injected into a 7820A gas chromatograph (Agilent) and measured according to the method described by Crombie *et al.* (2015).

2.15 **Activity of isoprene monooxygenase**

2.15.1 **Isoprene uptake assays**

Variovorax sp. WS11 was grown in 20 ml Ewers medium using a defined carbon source or a combination of a carbon source at 10 mM with 1% (v/v) headspace isoprene, using three biological replicates per condition. Cells were grown to mid-exponential phase, typically requiring incubation at 30 °C for 16-20 hours when growing using sugars or carboxylic acids or 30-50 hours when growing using isoprene, and were centrifuged at 6,000 * *g* for 10 minutes at 4 °C. The supernatant was discarded and cells were resuspended in 1 ml of chilled 50 mM HEPES (pH 6.0). Cell density was adjusted to an OD_{540} of 10 in 1 ml using 50 mM HEPES and sealed in a 30 ml vial using a butyl rubber stopper. Suspended cells were initially heated to 30 °C for 3 minutes using a temperature-controlled water bath with shaking at 160 rpm. Approximately 300 ppm isoprene was injected into the headspace and the suspension was incubated for a further 1 minute before sampling 50 µl of headspace using a gas-tight syringe (Agilent) and injecting into a Fast Isoprene Sensor (Hills-Scientific, Boulder, CO, USA). Further 50 µl headspace samples were taken and measured by Fast Isoprene Sensor at 3-minute intervals for 1 hour.

2.15.2 **Calculation of affinity of IsoMO for isoprene (K_m)**

Small, sealed aliquots of liquid isoprene were incubated in a 37 °C water bath for 5 minutes and fitted with a pierceable lid. Isoprene standards were prepared to 1% and 10% (v/v) headspace by injecting headspace isoprene from the heated aliquots into pre-sealed 120 ml vials. *Variovorax* sp. WS11 cell pellets (refer to Section 2.6) were thawed and resuspended to an OD_{540} of 1.0 in 1 ml and sealed in a 30 ml vial. A lower cell density was required to conduct isoprene uptake assays when using fermentor-grown cells due to the higher rates of isoprene uptake observed by these cells when compared to batch-grown *Variovorax* sp. WS11 (discussed in Section 7.2). Cells were pre-warmed to 30 °C by incubation in a temperature-controlled water bath for 3 minutes before adding one of five volumes of isoprene from the 1% or 10% (v/v) isoprene standards; 0.2 ml, 0.4 ml, 0.6 ml, 0.8 ml, or 1.0 ml

headspace. Isoprene-amended vials were incubated for a further 1 minute at 30 °C and a 50 µl headspace sample was measured by gas chromatography. Further 50 µl headspace samples were taken at 5-minute intervals for 15 minutes in order to calculate the initial rate of isoprene uptake. The initial rate of isoprene uptake was plotted against the initial concentration of isoprene and used to calculate K_m (µM) and V_{max} (nmol min^{-1} mg dry $weight^{-1}$) by Michaelis-Menten plots.

2.15.3 **Oxygen electrode**

Variovorax sp. WS11 was grown in 400 ml Ewers medium as described in Section 2.6, using either 10 mM glucose or 10 mM succinate as the sole source of carbon and energy. These cultures were centrifuged at 7,000 rpm using a high-speed centrifuge in a JLA 10.500 rotor for 10 minutes at 4 °C, and cell slurries were formed in 4 ml of 50 mM HEPES (pH 6.0) and drop-frozen in liquid nitrogen as described in Section 2.6. Isoprene-grown cells were prepared in a fermentor as described in Section 2.6. Substrate-induced rates of oxygen consumption by whole cells were determined by a Clark oxygen electrode (Rank Brothers Ltd, Cambridge, UK) (Clark *et al.* 1953). The reaction chamber held 3 ml of aerated 50 mM HEPES, pH 6.0, heated to 30 °C by a circulating water jacket and maintained with a steady agitation by a magnetic stirrer. The oxygen electrode was calibrated by comparison against oxygen-saturated 50 mM HEPES (pH 6.0) (Green & Hill, 1984) and oxygen-depleted buffer. The latter was achieved by the addition of sodium diothionite to reduce all available oxygen to water within the reaction chamber.
Variovorax sp. WS11 cell pellets grown using isoprene, glucose, or succinate were thawed and starved in a small volume of 50 mM HEPES (pH 6.0) at room temperature for up to 2 hours in order to decrease the observed endogenous rate of oxygen consumption. Starved cells were added to the reaction chamber to a final OD_{540} of 2.0. Following the detection of a stable endogenous rate of oxygen uptake, water saturated with the substrate of interest was added to the reaction chamber to a final substrate concentration of 100 µM. Alkene concentrations in water were prepared in sealed 30 ml vials, and the dissolved concentration of each alkene was calculated according to the Henry's law constants (H^{CP}) reported by Sander *et al*. (2015). Endogenous rates of oxygen consumption were subtracted from the substrate-added rate of oxygen consumption, resulting in substrate-induced rates of oxygen consumption for specific substrates by whole cells of *Variovorax* sp. WS11, recorded using three biological replicates per substrate, per growth condition.

2.15.4 **Alkyne inhibition of IsoMO**

Isoprene uptake assays were conducted as described in Section 2.15.1 from a single batch of drop-frozen, isoprene-grown cells of *Variovorax* sp. WS11. Gaseous alkynes (C2-C4) were prepared for addition to isoprene uptake assays by sparging a submerged, water-filled 120 ml vial with the relevant alkyne until all water had been displaced. These vials were sealed and used as stocks of 100% headspace alkyne. The volume of each alkyne required in the headspace to reach an aqueous concentration of 50 µM in 1 ml of liquid within a 30 ml vial was calculated according to gas-liquid partitioning with reference to the relevant Henry's law constants of each alkyne. Acetylene – 4.1 x 10^{-4} mol/m^3 Pa; propyne – 9.3 x 10^{-4} mol/m^3 Pa; butyne - 5.4 x 10^{-4} mol/m^3 Pa (Sander 2015). C6-C8 alkynes were

prepared as 1% (v/v) stock solutions in DMSO. Control samples were injected with DMSO alone after timepoint 3, or were not injected with any inhibitory agent.

50 µl of headspace isoprene was measured by gas chromatography at 5-minute intervals for 10 samples using an Agilent 7820A gas chromatograph. After measuring timepoint 3, 11 minutes after adding 300 ppm isoprene, an alkyne was added to an aqueous concentration of 50 µM. The inhibited rate of isoprene uptake (timepoints 5-10) were calculated relative to the initial, uninhibited rate of isoprene uptake (timepoints 1-3). The percentage of inhibition of isoprene uptake by C2-C4 alkynes was calculated as the average of three biological replicates ± standard deviation about the mean. The percentage of inhibition of isoprene uptake by C6-C8 alkynes were calculated as the mean inhibition of isoprene uptake by alkynes subtracted by the mean inhibition of isoprene uptake by DMSO (1.4 ± 7.2% initial isoprene uptake) ± standard deviation about the mean.

2.15.5 **Alkyne inhibition of sMMO**

Methylococcus capsulatus (Bath) was grown by Dr A. Crombie using methane as the sole source of carbon and energy according to published protocols (Nielsen *et al.* 1996), with the expression of the soluble methane monooxygenase (sMMO) over the particulate methane monooxygenase measured by naphthalene (Brusseau *et al*. 1990). The culture was maintained at the optimum conditions for growth on methane in a 2 litre fermentor (New Brunswick, Eppendorf, Stevenage, UK). Cells were drop-frozen in liquid nitrogen and stored at -80 ^{o}C. *M. capsulatus* (Bath) was thawed (by R. Dawson) and resuspended in 1 ml of 50 mM phosphate, pH 7.0, with 20 mM sodium formate supplied to provide sufficient reducing power to support the co-oxidation of non-growth substrates. As a proxy for the oxidation of methane by sMMO, the oxidation of propylene to propylene oxide was measured by gas chromatography (Colby *et al*. 1977). This was conducted under the same conditions as the isoprene uptake assay, with resuspended *M. capsulatus* (Bath) being pre-heated to 30 ^{o}C for 3 minutes before spiking with 1 ml of headspace propylene from a 1% (v/v) stock. Isoprene uptake assays using *M. capsulatus* (Bath) expressing the sMMO were conducted by the above method with three biological replicates. Inhibition of both isoprene oxidation and propylene oxidation by sMMO were tested using 50 µM acetylene and 50 µM octyne, including DMSO and uninhibited controls. It was noted that DMSO alone caused significant inhibition of the oxidation of propylene and isoprene by sMMO ($p=0.02$). The inhibition of sMMO-catalysed propylene oxidation and isoprene oxidation by octyne was adjusted accordingly by subtracting 25.2 ± 6% and 27.4 ± 5% respectively from the mean percentage of inhibition.

2.16. **Statistical analysis**

Data were typically presented as the mean of three biological replicates ± standard deviation, as indicated in the respective figure legends. Where this was not the case, the number of biological replicates is stated. Statistical analyses were as follows. Comparisons of relative expression data between different conditions were conducted by Students *t* test. Comparisons of specific reaction rates (such as rates of isoprene uptake) or levels of growth between two conditions were conducted by *t* test for the comparison of two means. Statistical significance was indicated by a

p value ≤ 0.05. Differences in peptide abundance were calculated by Proteome Discoverer software (Thermo Scientific), with p-values calculated using the background-based *t* test. This method was suitable for non-replicated data (proteome data were calculated as the average of two biological replicates), and identifies significant changes in peptide abundance (p≤0.05) compared to the ratio of abundance of the background population of peptides between the given conditions (ThermoFisher 2017).

3. **Physiology and Growth of *Variovorax* sp. WS11**

3.1. **Introduction**

Variovorax spp. are Gram negative β-proteobacteria of the Comamonadaceae family. This genus is frequently noted for two reasons; symbiotic associations with plants, and the degradation of xenobiotic compounds (Satola *et al*. 2013). The former was reviewed by Garcia Teijeiro *et al.* (2020). *Variovorax paradoxus* 5C-2, initially isolated from the roots of *Brassica juncea* L. Czern in cadmium-contaminated soil, significantly increased the shoot biomass of pea plants. This plant growth promoting ability may relate to previous observations of other *Variovorax* spp. colonising the roots of some plants and also influencing phytohormone levels (Natsagdorj *et al.* 2019, Sun *et al.* 2018). *Variovorax* spp. also indirectly influence plant survival, as Hong *et al*. (2017) reported antagonistic activity of the endophytic *Variovorax paradoxus* KB5 against the model phytopathogen *Pseudomonas syringae* pv. Tomato DC3000 (Xin & He, 2013). Competition by *Variovorax* spp. in soils and on plant roots is thought to be influenced by its modulation of quorum sensing. This relates to the production and excretion of quorum sensing molecules among *Variovorax* spp. and the metabolic degradation of acyl-homoserine lactone to impede signalling by other species (Leadbetter & Greenberg 2000, Garcia Teijeiro *et al*. 2020).

The metabolic versatility and bioremediative properties of *Variovorax* spp. have been reported frequently in recent years, typically due to the isolation of this genus from contaminated environments. *Variovorax* sp. MAK3 was isolated from groundwater which was contaminated by coal-tar following enrichment with ^{13}C-labelled benzene (Posman *et al*. 2017). This novel strain was predicted to metabolise benzene by using a ring-hydroxylating dioxygenase enzyme (Posman *et al*. 2017). Aromatic compounds with similar structures are also degraded by this genus. *Variovorax boronicumulans* HAB-30 was enriched and isolated from TCE-contaminated soil according to its ability to co-metabolise phenol (Aziz *et al.* 2020). *o*-dimethyl phthalate was also degraded by a co-culture of *Achromobacter denitrificans* and *Variovorax* sp. BS1 (Prasad 2017). The degradation of known industrial contaminants by *Variovorax* spp. may make this genus very useful when establishing bioremediation strategies. This was demonstrated by Zheng *et al*. (2018), as *Variovorax* spp. identified in petroleum-contaminated soil were capable of degrading C9-C30 alkanes at a range of efficiencies. *Variovorax* spp. are also known to degrade pesticide compounds; *V. boronicumulans* CGMCC 4969 degraded thiacloprid and acetamiprid (Sun *et al.* 2018), while *Variovorax* sp. WDL1, composed of two near-isogenic sub-populations, utilised a megaplasmid-encoded linuron degradation pathway (Werner *et al*. 2020). In the latter case, only one component of the *Variovorax sp.* WDL1 population was capable of linuron degradation (Albers *et al*. 2018).

Both rich and defined growth media have been used in the cultivation of *Variovorax* spp. (Futamata *et al*. 2005, Pehl *et al*. 2012, Prasad 2017, Sun *et al*. 2018a, Natsagdorj *et al*. 2019). The metabolic versatility and adaptability of *Variovorax* spp. permits the use of a range of growth conditions. Studies typically report the cultivation of *Variovorax* spp. at 30 ^{o}C with shaking to maintain aerobic conditions (Pehl *et al*. 2012, Prasad 2017, Meinert *et al*. 2018,

Fredendall *et al*. 2020). However, phylogenetic analyses of arctic environments indicate that *Variovorax* spp. are also capable of surviving on glacial ice (Ciok *et al*. 2016, Weiland-Bräuer *et al*. 2016). Further evidence that *Variovorax* spp. are robust against a range of temperatures was presented by Natsagdorj *et al*. (2019) as the rhizosphere-associated *Variovorax* sp. HRRK 170 was capable of growth between 10-30 ^{o}C, although 40 ^{o}C inhibited growth. Many studies report cultivation at circumneutral pH (Futamata *et al*. 2005, Prasad 2017), but *Variovorax* sp. HRRK 170 was also capable of growth between pH 5.0 - 10.0 (Natsagdorj *et al*. 2019).

Isoprene degrading bacteria have been isolated from many environmental samples (as described in Section 1.4), with a variety of growth media used in the cultivation of terrestrial isoprene degraders. Studies of the model isoprene degrader *Rhodococcus* sp. AD45 used MMY medium (van Hylckama Vlieg *et al*. 1998) or other minimal media (Dorn *et al*. 1974, Crombie *et al*. 2015), while more recent enrichment studies have used MAMS medium (Schaefer *et al*. 2002, Johnston *et al*. 2017) or CBS medium (El Khawand *et al*. 2016). Ewers medium (described in Section 2.2.1) was used by Larke-Mejia *et al*. (2019) to enrich and subsequently cultivate the first Gram negative isoprene degrading bacteria *Variovorax* sp. WS11 and *Ramlibacter* sp. WS9, and was used for the cultivation of *Variovorax* sp. WS11 throughout this project.

3.2. **Specific chapter aims and objectives**

The research detailed in this chapter was conducted with the aim of developing *Variovorax* sp. WS11 as a viable model bacterium for the study of isoprene metabolism. Initially, a key objective of this project was to optimise the conditions for the growth of this bacterium in batch and large-scale fermentor cultures, as sufficient biomass was required for physiological and biochemical studies of isoprene metabolism in *Variovorax* sp. WS11. Once ideal growth conditions had been established, whole-cell isoprene uptake and inhibition-based assays were developed with the aim of characterising the isoprene monooxygenase in *Variovorax* sp. WS11 compared to that of *Rhodococcus* sp. AD45. Finally, a key aim of this study was to characterise the isoprene metabolic pathway through the use of a proteomics study, thereby identifying the mechanism of incorporation of isoprene-derived carbon into central metabolism.

1. Study the range of sugars, carboxylic acids, and alkenes capable of supporting the growth of *Variovorax* sp. WS11.
2. Characterise the ability of *Variovorax* sp. WS11 to metabolise isoprene with respect to previous experiments in *Rhodococcus* sp. AD45 (e.g. toxicity of isoprene at elevated concentrations, substrate specificity of IsoMO).
3. Use linear alkynes to inhibit the oxidation of substrates by the IsoMO from *Variovorax* sp. WS11, and compare these data with the inhibition of substrate oxidation by a well-characterised SDIMO.
4. Analyse the proteome of isoprene-grown *Variovorax* sp. WS11 compared to growth on succinate. Verify predictions of the isoprene metabolic pathway made in *Rhodococcus* sp. AD45, particularly relating to the incorporation of isoprene-derived carbon via β-oxidation.

3.3. **Hypothesis**

DNA-SIP studies have indicated that *Variovorax* spp. are abundant members of isoprene-degrading communities, making *Variovorax* sp. WS11 a suitable model bacterium for the study of isoprene metabolism. Much of the work described in this chapter was conducted with the knowledge that *Variovorax* sp. WS11 contained a full *iso* metabolic gene cluster (detailed in Chapter 4). The presence of this gene cluster led to the hypothesis that *Variovorax* sp. WS11 would assimilate isoprene through a similar method to *Rhodococcus* sp. AD45, described by van Hylckama Vlieg *et al*. (2000). The proteome of isoprene-grown *Variovorax* sp. WS11 confirmed that the whole isoprene metabolic gene cluster was expressed during growth on isoprene, and led to the hypothesis that isoprene-derived carbon is incorporated via propionyl-CoA using the methylcitrate and methylmalonyl-CoA pathways.

3.4. **Methods**

3.4.1. **Optimising the growth of *Variovorax* sp. WS11**

Initial characterisation of the physiology of *Variovorax* sp. WS11 was conducted at pH 6.5, buffered using a phosphate solution, following the same guidelines as Larke-Mejía *et al*. (2019). Cultures were maintained at 30 °C with shaking at 160 rpm to ensure aeration. Routine growth of *Variovorax* sp. WS11 was conducted in 20 ml Ewers medium using 1% isoprene (v/v) in the headspace of a sealed 120 ml vial. The cellular morphology of *Variovorax* sp. WS11 changed depending on the growth conditions. Cultures which were maintained under the above conditions and were maintained at approximately 1% isoprene (v/v) most frequently presented as small, almost coccoid cells (Figure 3.1A), despite *Variovorax* spp. previously being identified as rod-shaped (Kim *et al*. 2006, Natsagdorj *et al*. 2019). This morphology was altered when grown to late-exponential/stationary phase, when the culture had become substrate-limited and was likely to be undergoing stress-related adaptations (Jaishankar & Srivastava 2017). In these cultures, cells were often longer with some extending in a manner which may indicate failure to divide efficiently (Figure 3.1B). Colony morphology was routinely checked as described in Section 2.4.1. Changing cell morphology was previously reported in *Variovorax dokdonensis* DS-43, which was reported as having both oval and rod-shaped cells (Im *et al*. 2010).

It was quickly noted that aggregates of cells formed in liquid culture, and initial optimisations of growth conditions were based on the assumption that this was a sign of stress. When visually inspected by microscopy, *Variovorax* sp. WS11 cells were present in combinations of the normal compact morphology and also as longer, partially segmented cells (Figure 3.1C). These were mixed with large plaques of aggregated material.

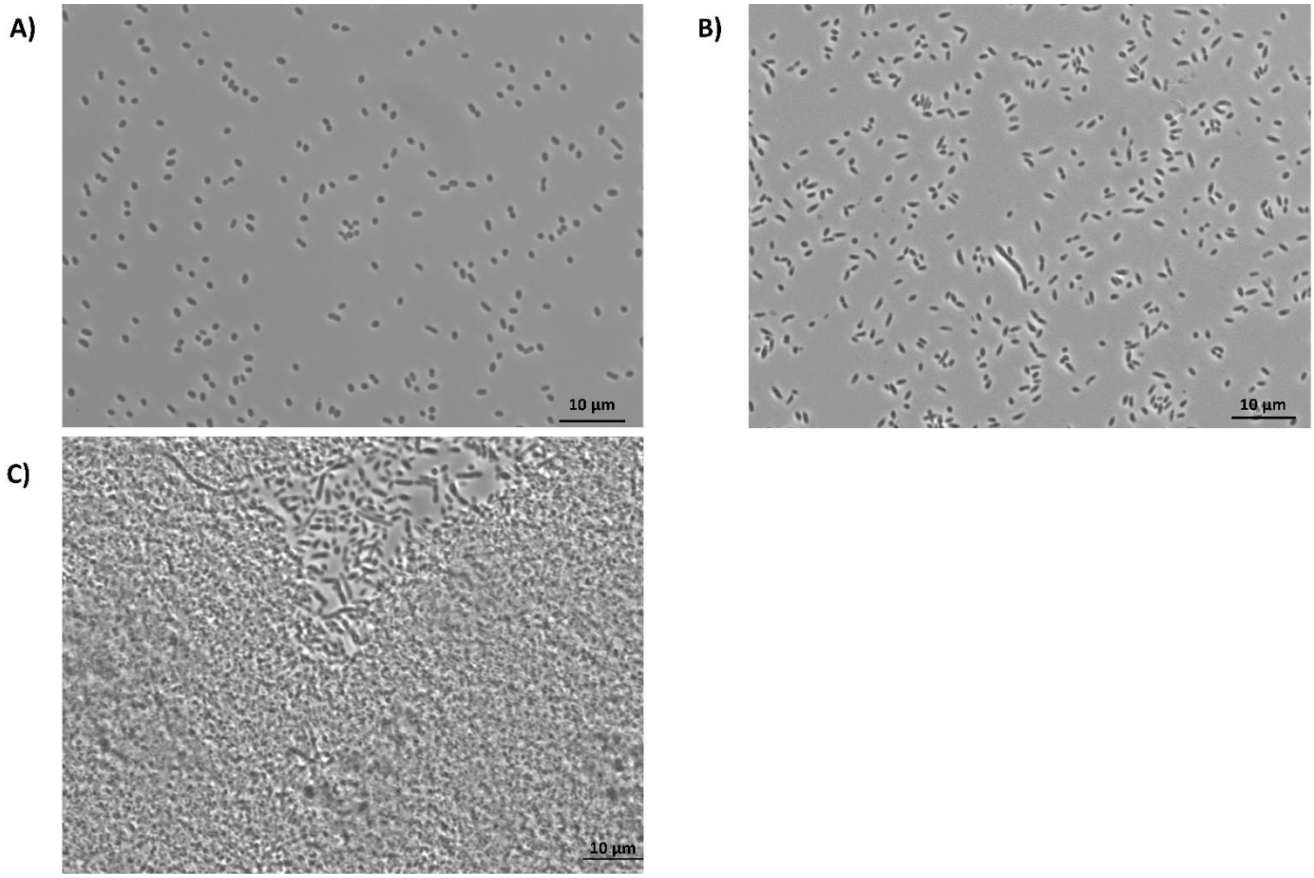

Figure 3.1. A) Isoprene-grown *Variovorax* sp. WS11, maintained under the recommended conditions with excess isoprene to maintain growth. B) *Variovorax* sp. WS11 grown using 10 mM glucose as the sole carbon source. C) Aggregated material extracted from a liquid culture of *Variovorax* sp. WS11. 1000x magnification.

The original growth conditions were reinvestigated in order to determine the cause of the apparent stress to *Variovorax* sp. WS11. Ewers medium was previously buffered to pH 6.5 using phosphate, so a growth experiment was established using phosphate adjusted to pH 6.0, 6.5, 7.0, 7.5, 8.0, or 8.5. There was very little difference in growth observed between pH 6.0-8.5, but the culture incubated at pH 6.0 reached the highest final OD_{540} of 0.54 (Figure 3.2). The root-associated *Variovorax* sp. HRRK 170 was previously grown at a pH range of 5.0 – 10.0 (Garcia Teijeiro *et al*. 2020), indicating that this genus is robust against changes in pH. Routine cultures of *Variovorax* sp. WS11 were subsequently buffered to pH 6.0, as this appeared to be closer to the optimum pH for this strain (Figure 3.2). However, it should be noted that the difference in maximum OD_{540} between *Variovorax* sp. WS11 grown at pH 6.0 and the original pH 6.5 was not statistically significant ($p= 0.17$, determined by *t* test). During the isolation of isoprene degraders from willow soil, MAMS vitamins (Kanagawa *et al*. 1982) were added to Ewers medium at 0.1% (v/v) (Larke-Mejía *et al*. 2019). This medium component was determined to be essential to the growth of *Variovorax* sp. WS11, as the exclusion of the vitamin solution (described in Section 2.2.1) resulted in a total cessation of growth in liquid culture. Alternative growth media were also tested for suitability in cultivating *Variovorax* sp. WS11. Nitrate mineral salts (NMS) medium, typically used in the cultivation of methanotrophs (Whittenbury 1981), was modified to contain ammonium nitrate in place of potassium nitrate (A-NMS) and was used to support the growth of *Variovorax* sp. WS11 with 10 mM glucose. *Variovorax* sp. WS11 reached an OD_{540} of 0.27 after 24 hours, increasing to 0.65 after

96 hours of incubation at 30 °C. When grown under the same conditions using Ewers medium, *Variovorax* sp. WS11 reached an OD_{540} of 1.10 after 24 hours. Therefore, Ewers medium was selected for continued use in the cultivation of *Variovorax* sp. WS11. The optimum growth conditions of *Variovorax* sp. WS11 were further interrogated by varying the temperature and level of agitation. *Variovorax* sp. WS11 was initially isolated at 30 °C with shaking at 160 rpm (Larke-Mejía *et al*. 2019). Growth under these conditions was compared to growth at 22 °C, with or without shaking (Figure 3.3). These data indicated that there was no significant difference between the maximum OD_{540} of *Variovorax* sp. WS11 at 22 °C or at 30 °C ($p=0.08$, determined by *t* test), consistent with the observation by Garcia Teijeiro *et al*. (2020) that *Variovorax* sp. HRRK 170 was capable of growth between 10 – 30 °C. Agitation of the cultures had a much more pronounced impact on growth. Regardless of the growth temperature, static cultures failed to reach the same OD_{540} as the cultures which were shaken at 160 rpm (Figure 3.3). The maximum OD_{540} of *Variovorax* sp. WS11 at 30 °C was significantly lower in the absence of shaking at 160 rpm ($p\leq0.01$), while the decrease in maximum OD_{540} of cultures at room temperature was not statistically significant ($p=0.13$). *Variovorax* spp. are aerobic, and studies typically report the cultivation of this genus with shaking between 120 – 180 rpm, likely due to the requirement for sufficient aeration (Han *et al.* 2011, Meinert *et al.* 2018, Posman *et al.* 2017, Prasad, 2017, Zheng *et al.* 2018). Increases in temperature above 30 °C were detrimental to growth. When *Variovorax* sp. WS11 was incubated with 10 mM glucose at 30 °C and 37 °C, the culture which was incubated at 37 °C reached an OD_{540} of 0.15 compared to an OD_{540} of 1.1 at 30 °C.

None of the tested conditions were able to prevent the formation of cell aggregates. However, a correlation between culture density and clumping of cells was detected. It is therefore likely that *Variovorax* sp. WS11 forms cell aggregates as a result of stress due to some form of substrate or nutrient limitation. Similar yellow cell clumps were also detected during the growth of *Variovorax paradoxus* NBRC 15149 on 1,4-dioxane (Tusher *et al*. 2020).

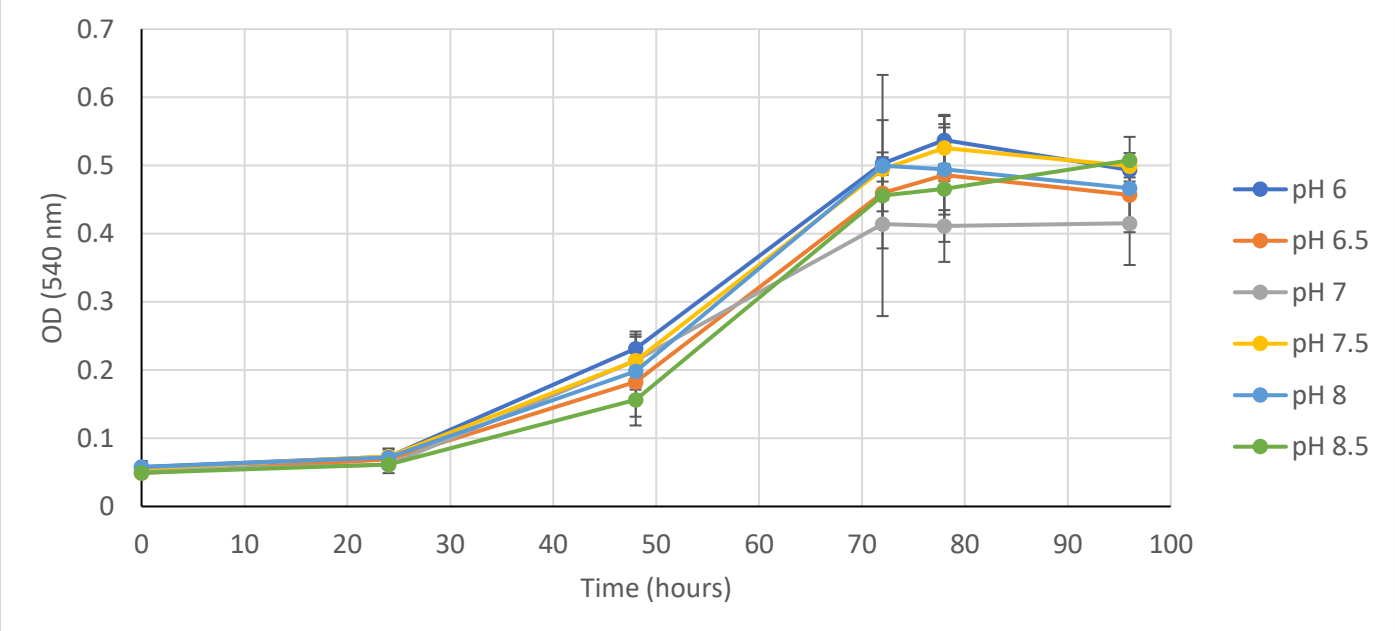

Figure 3.2. Growth of *Variovorax* sp. WS11 on 1% isoprene (v/v), buffered with phosphate to pH 6.0 – 8.5. These data were calculated as the average of three biological replicates ± standard deviation.

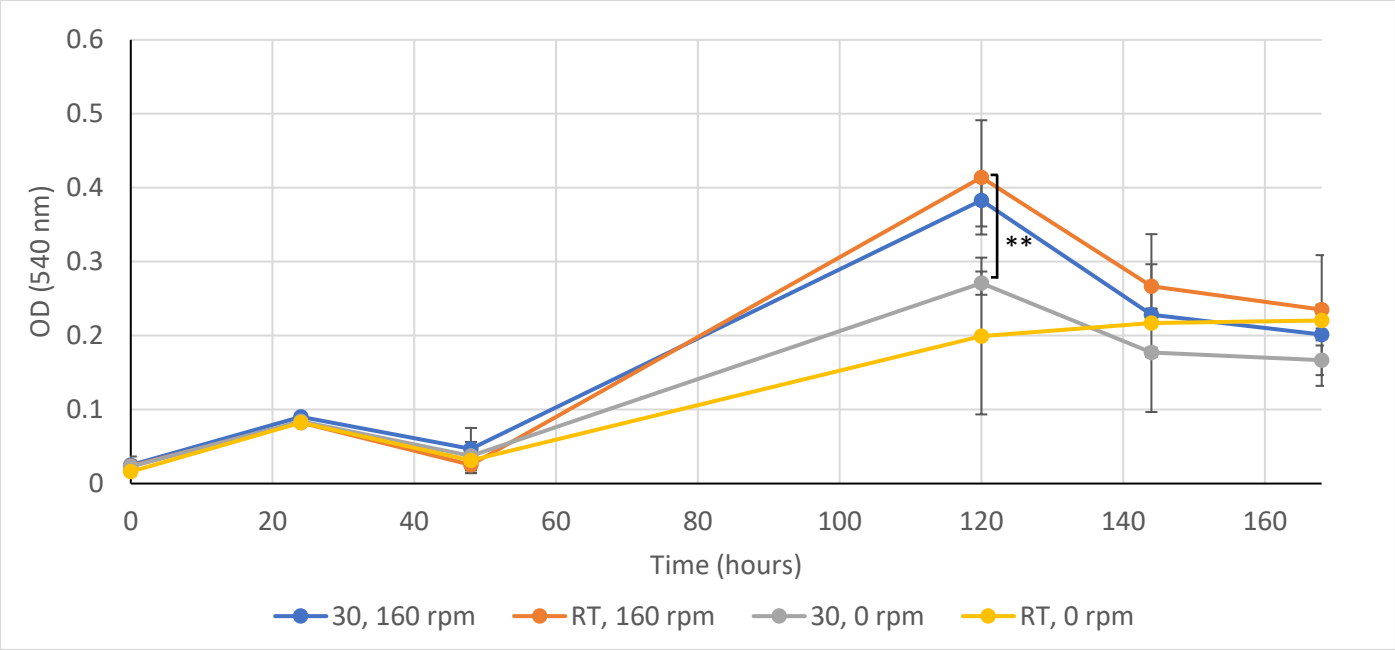

Figure 3.3. Growth of *Variovorax* sp. WS11 on 1% (v/v) isoprene at 30 °C (30) or 22 °C (RT) with shaking at 160 rpm or without agitation. These data were calculated as the average of three biological replicates ± standard deviation. An asterisk denotes a statistically significant difference between the indicated conditions (** p≤0.01, determined by *t* test).

3.4.2. **Large-scale cultivation of *Variovorax* sp. WS11**

3.4.2.1. **Optimisation of fermentor conditions**

Variovorax sp. WS11 was inoculated from an isoprene-grown culture into a 2 L flask containing 400 ml Ewers medium, supplemented with liquid isoprene which evapourated to create a headspace concentration of approximately 1% (v/v). Once the culture had reached mid-exponential phase, this was used as the inoculum for 4 litres of Ewers medium in a fermentor (as described in Section 2.6). The optimum conditions described for the growth of *Variovorax* sp. WS11 were maintained throughout growth, and samples were taken regularly to record the OD_{540} (Figure 3.11) and pH of the culture.

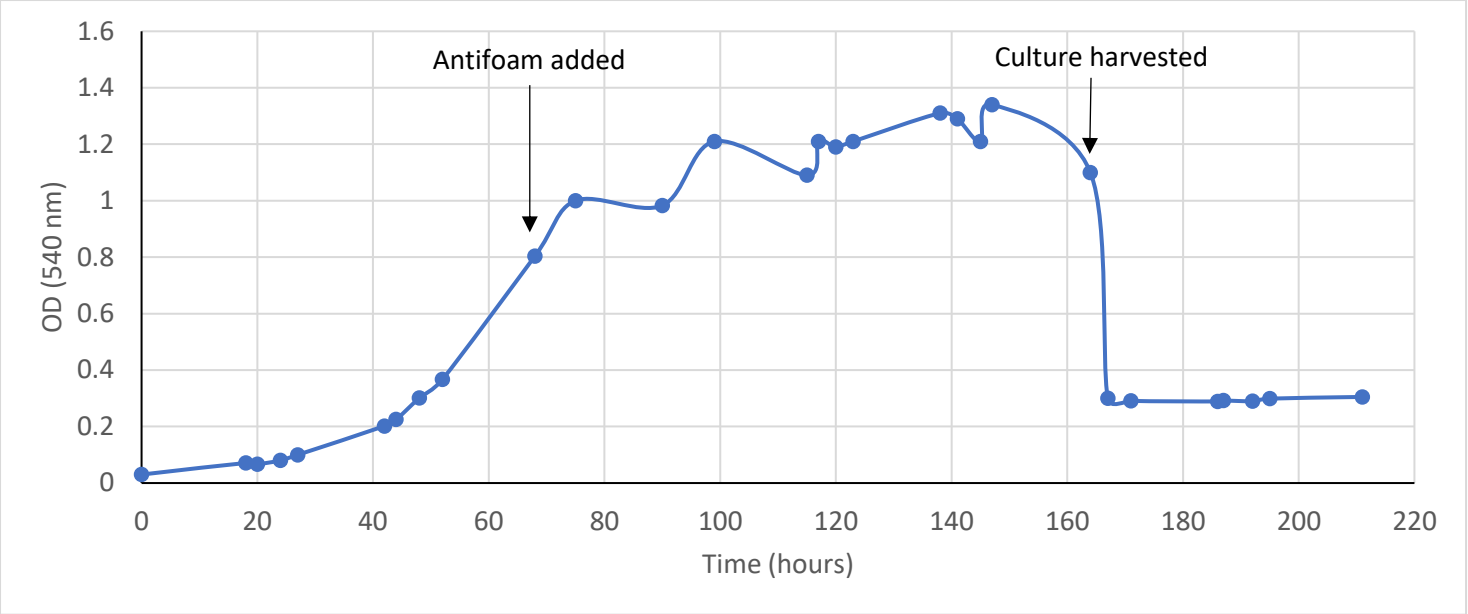

Figure 3.4. Growth of *Variovorax* sp. WS11 in an isoprene-fed fermentor. Antifoam 204 was added after 76 hours. N=1 (single biological replicates).

A constant supply of oxygen and isoprene was maintained in the fermentor to support the growth of *Variovorax* sp. WS11 (Chapter 2, Figure 2.1). A significant quantity of bubbles and foam were produced by the fermentor culture after approximately 70 hours of incubation. An organic antifoaming agent (Antifoam 204, Sigma-Aldrich) was added at 0.25 ml L^{-1} (as described in Section 2.6.1). Addition of Antifoam 204, a polypropylene-based polyether mixture, was followed almost immediately by a decline in the rate of growth of *Variovorax* sp. WS11 (Figure 3.4). Inhibition of cell cultures by Antifoam 204 was recorded in Chinese hamster ovarian cell lines (Velugula-Yellela *et al*. 2018), and methanol uptake by *Methylosinus trichosporium* OB3b was also inhibited by Antifoam 204 (Adegbola 2008). According to the product specification (Sigma), no inhibition of the growth of well-characterised model organisms was detected. Growth of *Variovorax* sp. WS11 was not recovered after incubation for a further 80 hours (Figure 3.4). It was initially thought that the high OD_{540} of the fermentor culture had resulted in a cessation of growth. Three litres of culture were harvested and replaced by three litres of fresh Ewers medium. No growth was detected in the subsequent 40 hours, confirming that Antifoam 204 had caused a lasting inhibition of growth.

In order to confirm the inhibitory properties, smaller cultures were prepared in the presence and absence of Antifoam 204. *Variovorax* sp. WS11 was grown with 10 mM succinate and supplemented with 1x or 10x the concentration of Antifoam 204 used in the fermentor (Figure 3.5). 1x Antifoam 204 inhibited growth on succinate for approximately 5 days before rapid growth was detected. 10x Antifoam 204 consistently inhibited growth on succinate for the duration of the experiment, although not by a statistically significant margin compared to 1x Antifoam 204 ($p=0.06$). These data confirmed that Antifoam 204 was inhibitory to the growth of *Variovorax* sp. WS11, but could not verify a dose-dependent relationship between the concentration of Antifoam 204 and the level of inhibition.

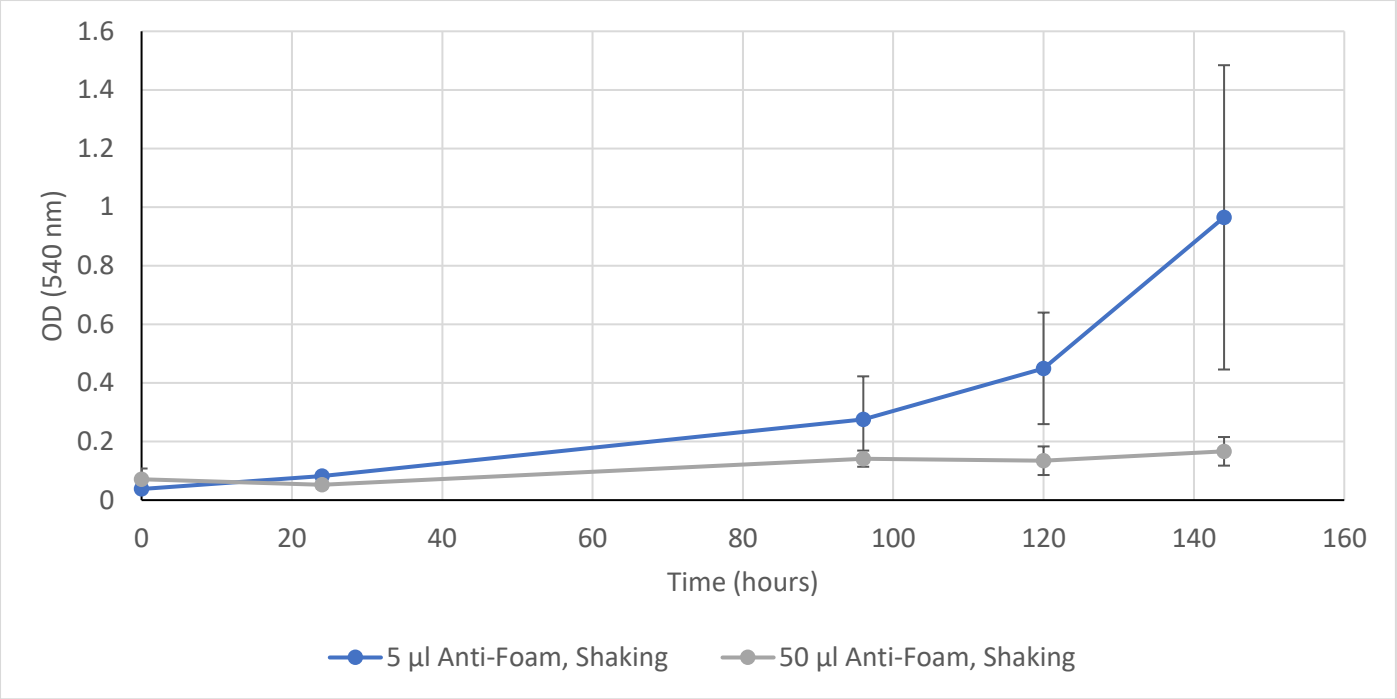

Figure 3.5. Growth of *Variovorax* sp. WS11 on 10 mM succinate, supplemented with 0.25 ml L^{-1} (5 µl, 1x) or 2.5 ml L^{-1} (50 µl, 10x) Antifoam 204. These data were calculated as the average of three biological replicates ± standard deviation.

An alternative antifoaming agent was required for subsequent fermentor preparations. Antifoam A (Sigma), a silicone polymer solution, was added to *Variovorax* sp. WS11 with 1% (v/v) isoprene (Figure 3.6). The growth of *Variovorax* sp. WS11 was almost identical when using 1% isoprene or 1% isoprene + Antifoam A. As expected, Antifoam 204 (control) inhibited the growth of *Variovorax* sp. WS11 on isoprene. The reason for the differences in growth between the organic and silicone-based antifoam agents is unclear. A review of the effects of antifoaming agents suggested that membrane compositions may be affected in certain organisms, although there has been no mechanistic evidence to support this (Routledge 2012).

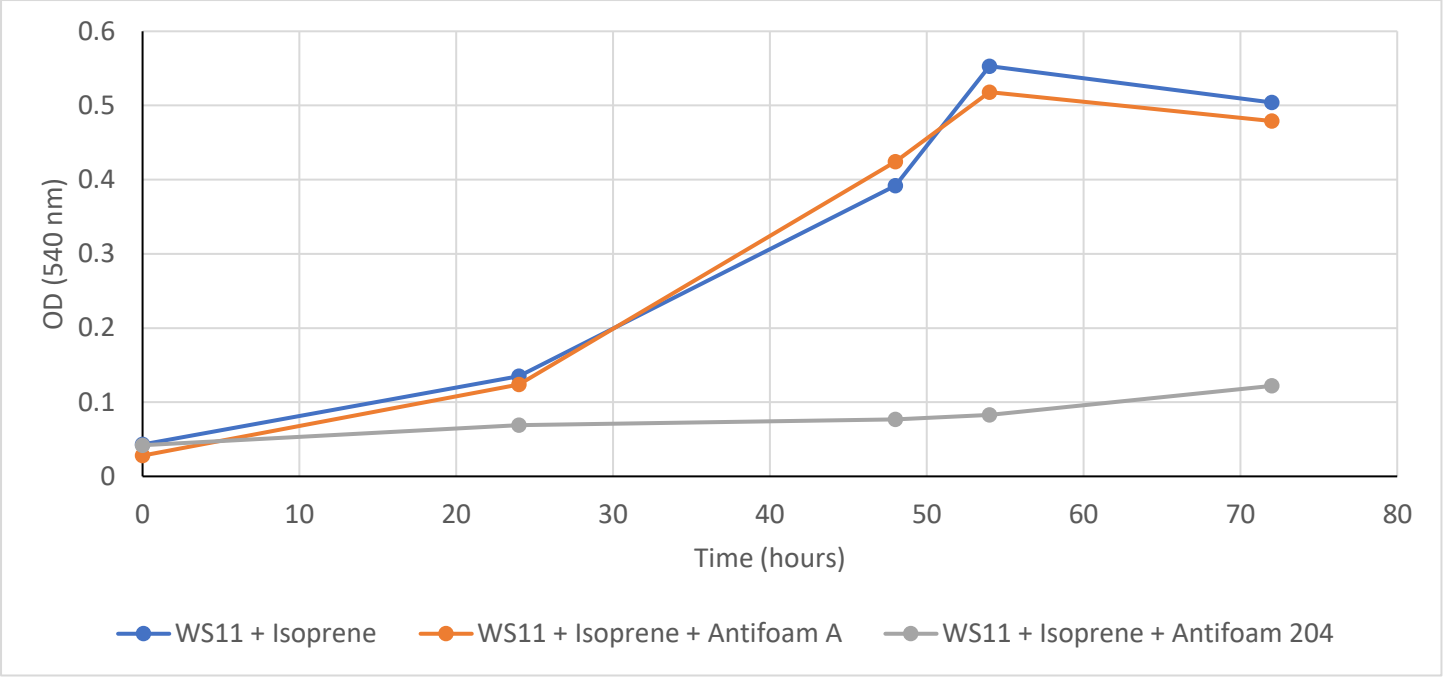

Figure 3.6. Growth of *Variovorax* sp. WS11 on 1% (v/v) isoprene supplemented with 0.25 ml L^{-1} Antifoam A or 0.25 ml L^{-1} Antifoam 204. N=1 (single biological replicates).

In a second fermentor-based experiment, *Variovorax* sp. WS11 initially grew at a relatively slow rate until approximately 80 hours post-inoculation (Figure 3.7). The rate of growth was higher after harvesting, without a second lag period, indicating a stable rate of growth on isoprene had been achieved. The dissolved oxygen content (dO_2) of the fermentor culture decreased continuously in spite of alterations to agitation and the rate of aeration, confirming that *Variovorax* sp. WS11 was conducting rapid aerobic metabolism. This was consistent with the oxygen requirement of IsoMO (van Hylckama Vlieg *et al*. 2000). During each fermentor experiment, *Variovorax* sp. WS11 formed thick aggregates on all static fixtures (baffle, probes, etc.), consistent with the previous observations of clumped cells forming in small-scale liquid cultures, indicating that *Variovorax* sp. WS11 forms biofilms. *Variovorax paradoxus* EPS was characterised for its ability to form biofilms, although *Variovorax* sp. WS11 does not share the related swarming function (Jamieson *et al*. 2009, Pehl *et al*. 2012, Fredendall *et al*. 2020).

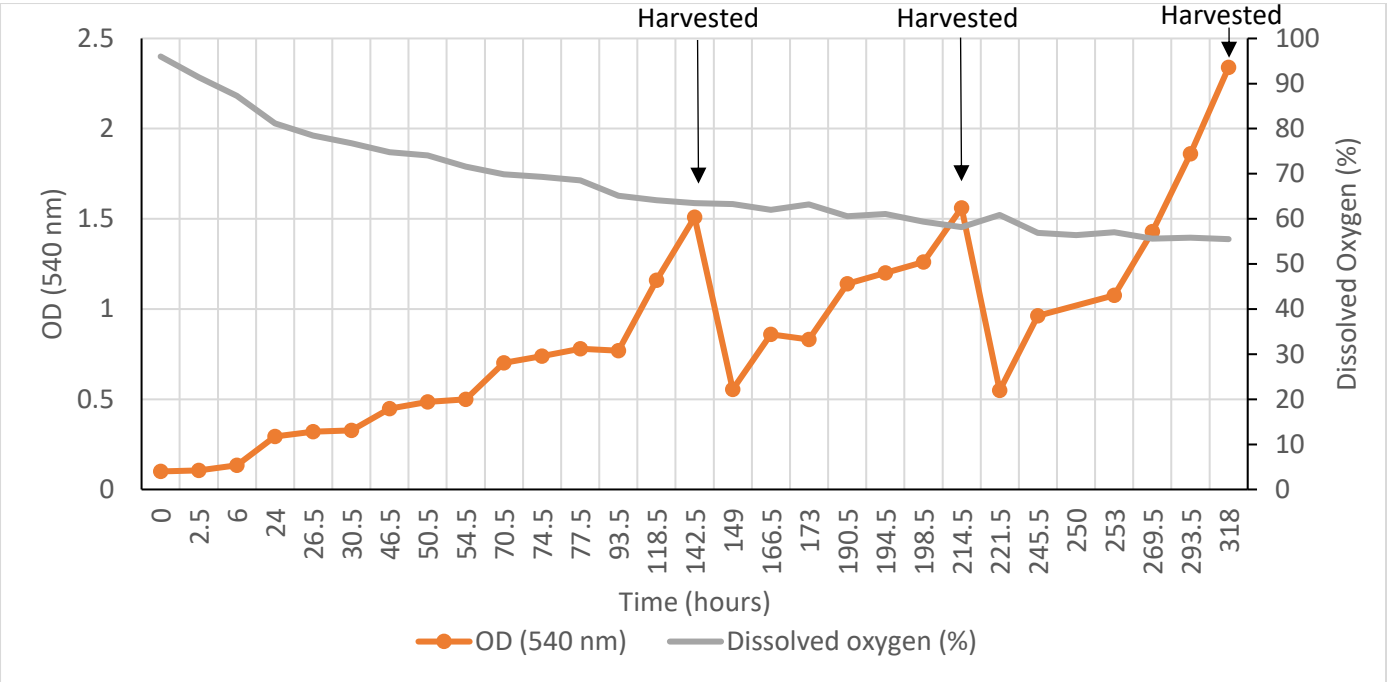

Figure 3.7. Growth of *Variovorax* sp. WS11 in an isoprene-fed fermentor, supplemented with Antifoam A after 100 hours. N=1 (single biological replicates).

3.4.2.2. **Harvesting and storage of fermentor-grown *Variovorax* sp. WS11**

Variovorax sp. WS11 was harvested from the isoprene-fed fermentor by centrifugation in a high-speed centrifuge (as described in Section 2.6). The cell slurry was washed twice in 50 mM phosphate, pH 6.0, and drop-frozen in liquid nitrogen. Isoprene uptake activity of cells was tested using an oxygen electrode (Section 3.5.5). Compared to a pre-harvest activity of 25.0 nmol isoprene/min/mg, washed cells had no detectable rate of isoprene uptake. Further harvests confirmed that isoprene uptake activity was consistently lost after this harvesting procedure; as a pre-harvest uptake rate of 30.6 nmol min^{-1} mg dry $weight^{-1}$ decreased to 0.8 nmol min^{-1} mg dry $weight^{-1}$.

It was theorised that the loss of isoprene uptake by *Variovorax* sp. WS11 was due to stress caused by excessive centrifugation and washing. A fermentor batch was centrifuged and re-suspended in a small volume of 50 mM phosphate buffer, followed by freezing without washing steps. The rate of isoprene uptake of thawed cells was 27.8 nmol min^{-1} mg dry $weight^{-1}$, indicating that reduced stress during the harvesting procedure was required to maintain activity. Further optimisation of the harvesting procedure is detailed in Table 3.1. The use of 10% (w/v) glycerol was attempted as a protective measure against stress during the drop-freezing and thawing procedure. However, this decreased the rate of isoprene uptake to only 15% of the rate without glycerol. Alternative buffers were tested for the resuspension of *Variovorax* sp. WS11 and for the subsequent oxygen electrode trials. 50 mM HEPES, adjusted to pH 6.0, consistently resulted in an increased rate of isoprene uptake. Subsequent harvesting of the fermentor was conducted by centrifuging *Variovorax* sp. WS11 as previously described, resuspending the pellet in a small volume of 50 mM HEPES (pH 6.0) to form a cell slurry, and drop-freezing in liquid nitrogen without washing or further centrifugation steps. *Variovorax* sp. WS11 consistently retained activity after thawing, with an average isoprene uptake rate of 31.5 nmol min^{-1} mg dry $weight^{-1}$.

Table 3.1. Optimisation of fermentor-harvesting conditions. Isoprene uptake of harvested cells was tested using a Clark oxygen electrode. N=1 (single biological replicates).

Harvesting Conditions	Isoprene uptake (nmol min^{-1} mg dry $weight^{-1}$)
50 mM Phosphate, pH 6.0 (twice-washed)	0.8
50 mM Phosphate, pH 6.0	27.8
50 mM Phosphate + 10% Glycerol	4.3
50 mM HEPES, pH 6.0	37.4

3.5. **Results and discussion**

3.5.1. **Colony morphology and motility**

Due to the changes in cell morphology, culture purity was routinely checked by a combination of plating on rich R2A agar and visual inspection by microscopy. Colonies were typically small, round, and yellow. The colouring was likely to be due to concentrations of carotenoid pigments (Willems *et al*. 1991, Ciok *et al*. 2016). However, if plates had been left at 22°C or refrigerated at 4 °C for some time, colony edges became less defined and spread in a manner which resembled biofilm formation and swarming in *Variovorax paradoxus* EPS (Pehl *et al*. 2012). The genome of *Variovorax* sp. WS11 (described in Chapter 4) was analysed for genes typically associated with bacterial motility, such as flagella biosynthesis (*flh, flg, fli*) and motor genes (*mot*) (Kane *et al*. 2007, Osterman *et al*. 2015). Flagella genes (*flgA-J*) were present, with almost all *fli* genes (*fliCDEFGIKLMNOPQRS*), and *mot* genes (*motAB*) also detected (Figure 3.8A). This indicated that *Variovorax* sp. WS11 may be capable of synthesising and motorising flagella (Figure 3.8B), so motility was tested as described in *Variovorax paradoxus* EPS (Jamieson *et al*. 2009, Pehl *et al*. 2012). Briefly, 20 µl of liquid culture, grown to mid-exponential phase, was plated on soft Ewers agar (0.3% (w/v) agarose) or soft nutrient agar (0.3% (w/v) agarose) with 10 mM glucose, succinate, or sorbitol. Jamieson *et al*. (2009) reported that motility was enhanced in *Variovorax paradoxus* EPS when the agar contained carboxylic acids such as succinate compared to agar which contained sugars. Motility was not observed after 2 weeks at 30 °C. This indicates that the disruption of colonies over time may be due to biofilm formation, as nutrient deficiency may result in stress responses in colonies. It is curious that many recognised motility-associated genes are clustered in the genome of *Variovorax* sp. WS11 (Figure 3.8A) without any motility being observed. Genes with predicted roles in chemotaxis were also present between the *flgJ* and *flgK* genes, and also downstream of the *motAB* genes. This indicated that *Variovorax* sp. WS11 would use motility as a means of swarming towards nutrient sources, as in *Variovorax paradoxus* EPS (Pehl *et al*. 2012). There are many potential explanations for the lack of motility in *Variovorax* sp. WS11, such as the use of incorrect conditions to induce swarming or mutation of motility-encoding genes causing inactivation or downregulation of expression.

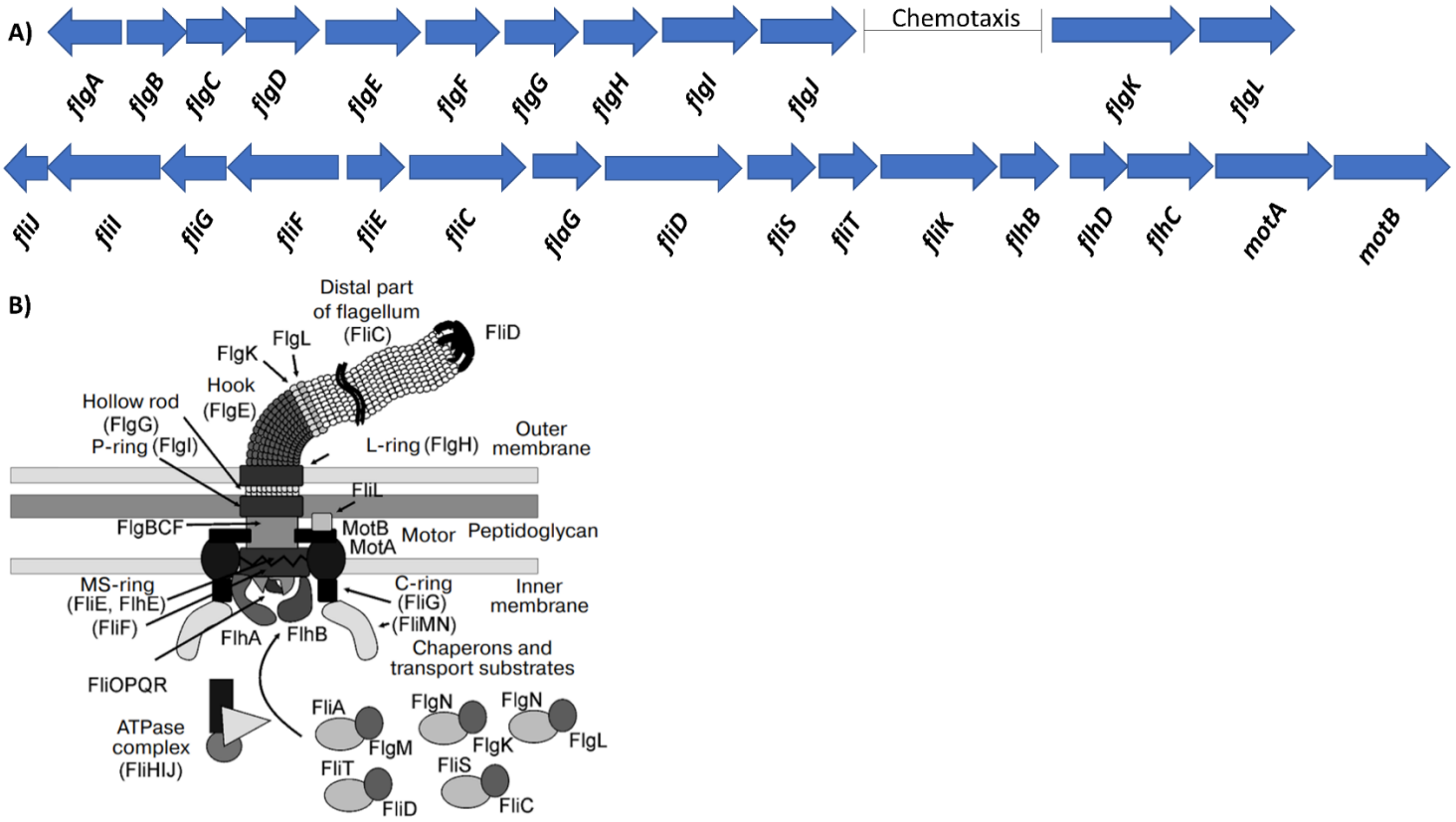

Figure 3.8. (A) Putative flagella biosynthesis (*flg/fli/flih*) genes and motor (*mot*) genes detected in the genome of *Variovorax* sp. WS11. (B) Schematic representation of flagellum structure (taken from Osterman *et al.* 2015).

3.5.2. **Resistance of *Variovorax* sp. WS11 to high isoprene concentrations**

Isoprene degrading bacteria have been isolated and cultivated at a range of isoprene concentrations. Larke-Mejía *et al*. (2019) reported the isolation of *Variovorax* sp. WS11 at 1% isoprene (v/v) following the initial enrichment from willow soil at 25 ppmv isoprene. Other studies often used lower concentrations for general cultivation; water- and sediment-isolates were typically incubated at 0.5% (v/v) isoprene (Johnston *et al*. 2017), while the model isoprene degrader *Rhodococcus* sp. AD45 was grown using 0.6% (v/v) (van Hylckama Vlieg *et al*. 1998, Crombie *et al*. 2015). Crombie *et al*. (2015) noted that concentrations of isoprene exceeding 2% (v/v) inhibited the growth of *Rhodococcus* sp. AD45. Apparent isoprene degraders isolated from tropical soil and leaves were incapable of growth above 0.5% (v/v) isoprene (Srivastva *et al*. 2017, Singh *et al*. 2019).

In order to determine whether high concentrations of isoprene were inhibitory to the growth of *Variovorax* sp. WS11, cultures were incubated with 1%, 4%, and 10% (v/v) headspace isoprene (Figure 3.9). The Henry's law constant (H^{cp}) for the saturated concentration of isoprene in water is 0.013 (Sander 2015), so the dissolved concentration cannot exceed 13 mM under standard temperature and pressure. Increasing the headspace concentration of isoprene would cease to have an effect once the point of aqueous saturation was reached, indicating that the 4% and 10% isoprene vials should have had approximately equal concentrations of dissolved isoprene in the media. However, growth of *Variovorax* sp. WS11 was impeded when incubated with 10% (v/v) isoprene compared to 4% (v/v) isoprene ($p=0.04$) (Figure 3.9). There was very little difference in the maximum OD_{540}

of *Variovorax* sp. WS11 with 1% (v/v) isoprene compared to 4% (v/v) isoprene (p=0.07), demonstrating that *Variovorax* sp. WS11 had a higher threshold before showing signs of toxicity due to high concentrations of isoprene.

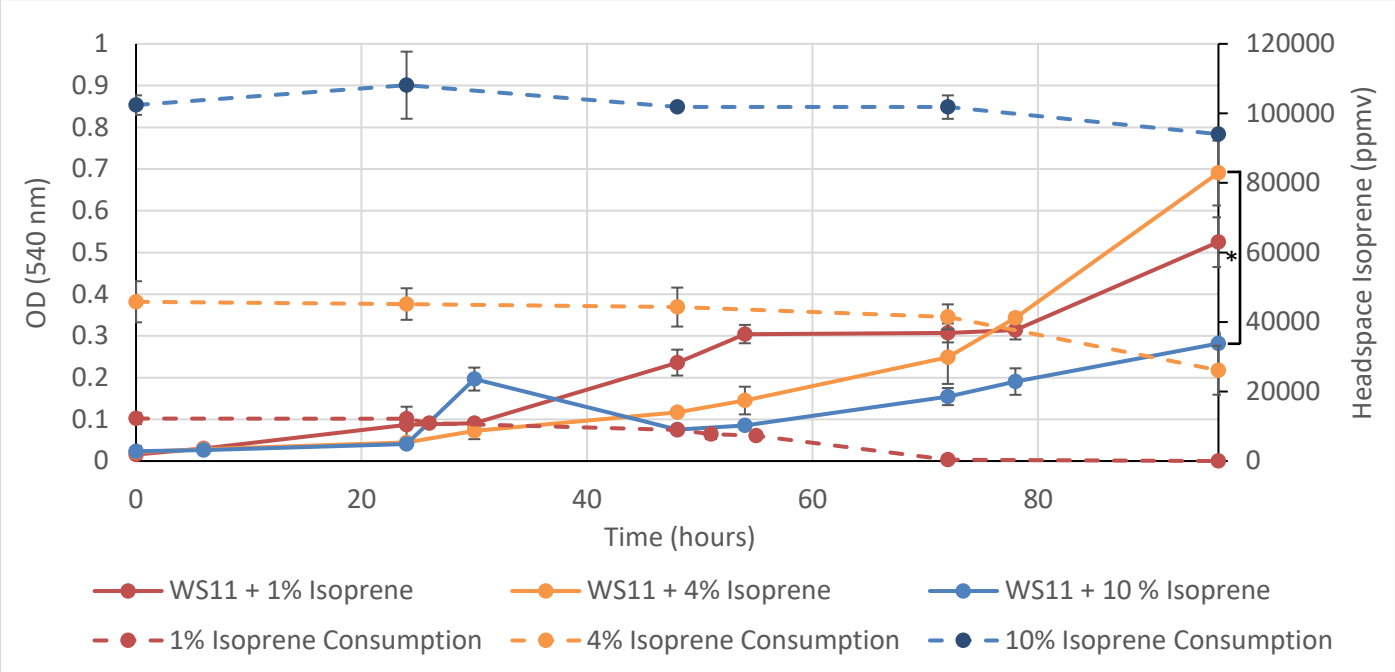

Figure 3.9. Growth of *Variovorax* sp. WS11 at 1% (red), 4% (orange), and 10% (blue) isoprene. Solid lines represent the OD_{540} of cultures, dotted lines of the same colour represent the concentration of isoprene in the headspace of the corresponding vial (ppmv). These data were calculated as the average of three biological replicates ± standard deviation. Asterisks denote a statistically significant difference between the indicated conditions ($p \leq 0.05$).

3.5.3. Growth of *Variovorax* sp. WS11 on diverse carbon sources

As has been described in Section 3.1, *Variovorax* spp. are frequently reported for their metabolic versatility. Known growth substrates include sugars and sugar alcohols, carboxylic acids, thiol-substituted compounds and alkenes (aliphatic and aromatic) (Brandt *et al.* 2014b, Futamata *et al.* 2005, Jamieson *et al.* 2009, Pehl *et al.* 2012, Satola *et al.* 2013). *Variovorax paradoxus* B4 was characterised for its ability to degrade mercaptosuccinate to succinate and sulfite (Brandt *et al.* 2014b, 2015), while *Variovorax paradoxus* EPS used an aryl alkyl sulfoxidase which also performed co-oxidations on many compounds, including styrene (Tischler *et al*. 2018). Before our study, no *Variovorax* sp. had been reported with the ability to grow on isoprene as the sole source of carbon and energy.

Variovorax sp. WS11 was prepared for growth assays differently according to the tested growth substrate. To test for growth on sugars and carboxylic acids, *Variovorax* sp. WS11 was initially grown in Ewers medium using 10 mM glucose as the sole source of carbon and energy. Alkene and epoxide growth tests were prepared by initially growing *Variovorax* sp. WS11 using 1% (v/v) isoprene as the sole source of carbon and energy. All cultures were harvested at approximately mid-exponential phase and used to inoculate fresh Ewers medium with a sugar, carboxylic acid, alkene, sugar alcohol, or epoxide substrate (Table 3.2). Cultures were incubated for a maximum of 1 week before recording the OD_{540} with the exception of the alkene and epoxide-supplemented cultures, which were incubated for

up to 3 weeks. With the exception of lactose and sucrose, all sugars tested were capable of supporting the growth of *Variovorax* sp. WS11 to a high OD_{540} when supplied at a concentration of 10 mM. Sorbose was a relatively poor growth substrate, while sorbitol was a better substrate for growth. This may indicate that sugar alcohols are more readily incorporated as growth substrates by *Variovorax* sp. WS11, although this is not supported by the literature. A comparison of the growth substrates of seven *Variovorax* spp. by Jin *et al*. (2012) demonstrated that only two of seven strains could use D-sorbitol as a growth substrate. They identified carboxylic acids to be more commonly used as growth substrates than sugars, although a wider range of substrates must be tested in order to confirm whether this is true for *Variovorax* sp. WS11. Taurine, an amino sulfonic acid, tested as a growth substrate due to the study of the genome of *Variovorax* sp. WS11 (described in Chapter 4), was capable of supporting growth. Salicylic acid and the sodium salt were incapable of supporting growth in spite of the genome-derived evidence presented in Chapter 4. The same was observed for methanesulfonate, ethanesulfonate, catechol, and naphthalene, which were not growth substrates. The latter was surprising as previous evidence suggested the ability of *Variovorax* spp. to grow on naphthalene as the sole source of carbon and energy (Martirani-Von Abercron *et al*. 2017).

Further study of the growth substrates used by *Variovorax* sp. WS11 could focus on the use of alkanesulfonates and other organosulfur compounds. As was described earlier, *Variovorax paradoxus* B4, *V. paradoxus* S110, and *V. paradoxus* EPS have been characterised for their ability to metabolise sulfur. Other examples of organosulfur metabolism have been described in *Variovorax* spp. (Brandt *et al.* 2014a, 2014b, Han *et al.* 2011, Heine *et al.* 2019), including the degradation of mercaptosuccinate, taurine, 3,3-thiodipropionic acid, and aromatic sulfonates (Brandt, *et al.* 2014a, Han *et al.* 2011, Satola *et al.* 2013). Evidence for mercaptosuccinate metabolism by *Variovorax* sp. WS11 was found in the genome sequence, as a hypothetical protein had over 80% amino acid identity with the mercaptosuccinate dioxygenase of *V. paradoxus* B4 (Altschul *et al.* 1990, Brandt *et al.* 2014b). This protein was located with a putative molybdopertin molybdenumtransferase, known to be essential to growth on mercaptosuccinate by *V. paradoxus* B4 (Brandt *et al.* 2014a, 2014b).

Table 3.2. Carbon and energy sources capable of supporting the growth of *Variovorax* sp. WS11 (adapted from Dawson *et al.* 2020).

Substrate	Level of Growth
Sugars/other hydrocarbons (10 mM)	
Glucose	+++
Fructose	+++
Sucrose	+
Maltose	++
D-xylose	++
L-arabinose	+++
L-sorbose	+
D-sorbitol	+++
Lactose	-
Glycerol	++
Taurine	++
Carboxylic Acids (10 mM)	
Sodium pyruvate	+++
L-malate	-
Tri-sodium-citrate	+++
Potassium acetate	++
Sodium malate	-
Methylmalonate	-
Sodium propionate	+++
Potassium glutamate	+++
Sodium succinate	++
Sodium salicylate	-
Sodium methanesulfonate	-
Ethanesulfonic acid	-
Potassium phthalate	-
Vanillate	-
Alkenes/Epoxides (0.1% w/v)	
Ethylene (1% v/v)	-
Propylene (1% v/v)	-
Isoprene (1% v/v)	++
1-butene (1% v/v)	-
2-methyl-3-butene	-
1,3-butadiene (1% v/v)	-
1-pentene	-
1,4-pentadiene	-
3-methyl-1,4-pentadiene	-
Hexene	-
1,2-epoxyhexane	-
Epoxyisoprene	-
Styrene	-
Naphthalene	-
Limonene	-
Catechol	-

- refers to no growth; + refers to OD_{540} 0.1-0.3; ++ refers to OD_{540} 0.3-0.8; +++ refers to OD_{540} >0.8.

3.5.4. **Toxicity of isoprene-like compounds**

It was curious that *Variovorax* sp. WS11 was incapable of growing on any of the tested alkenes other than isoprene (Table 3.2), particularly when considering that 1,3-butadiene and isoprene (2-methyl-1,3-butadiene) share very similar structures. 2-methyl-3-butene also failed to act as a growth substrate. The lack of growth on 1,2-epoxyhexane was expected as van Hylckama Vlieg *et al*. (1998) reported that this epoxide inhibited the activity of IsoI, and also inhibited growth on isoprene by *Rhodococcus* sp. AD45. However, the lack of growth on epoxyisoprene was unexpected. *Variovorax* sp. WS11 possesses a full *iso* metabolic gene cluster including *isoI* and *isoH* (Chapter 1, Figure 1.8), indicating the ability of this bacterium to detoxify epoxyisoprene and to incorporate GMBA into central metabolism (Chapter 1, Figure 1.6). It was theorised that, although epoxyisoprene was a potent inducer of *iso* gene expression in *Variovorax* sp. WS11 (Dawson *et al.* 2020, Chapter 7), the toxicity of epoxyisoprene was sufficient to inhibit growth before the Iso metabolic proteins could be expressed to a high enough level. Further complicating matters was the reactivity of epoxides in aqueous solution; the epoxide ring is highly susceptible to nucleophilic attack and therefore is prone to being rapidly degraded (McClay et al. 2000, Faiz & Zahoor 2016). Therefore, it is unlikely that epoxyisoprene would be present in solution for long enough to support extended growth of *Variovorax* sp. WS11. Short-term toxic effects of epoxyisoprene were demonstrated by inoculating isoprene-grown *Variovorax* sp. WS11 with 1% (v/v) isoprene with three concentrations of liquid epoxyisoprene, 0.005%, 0.01%, and 0.05% (w/v). 0.05% (w/v) epoxyisoprene was sufficient to completely inhibit the growth of *Variovorax* sp. WS11, and the difference in maximum OD_{540} between cultures grown with 0.05% (w/v) epoxyisoprene and the other conditions was statistically significant ($p \leq 0.01$). 0.01% (w/v) epoxyisoprene caused an extended lag period before exponential growth could be achieved (Figure 3.10), although this was not statistically significant compared to 0.005% epoxyisoprene after 48 hours ($p=0.19$). When grown on isoprene, *Variovorax* sp. WS11 should have full expression of the *iso* metabolic gene cluster and active synthesis of glutathione. van Hylckama Vlieg *et al*. (1998) measured approximately 2 mM glutathione in the cytoplasm of isoprene-grown *Rhodococcus* sp. AD45, and if *Variovorax* sp. WS11 also accumulated significant levels of glutathione when growing on isoprene then excess epoxyisoprene should be conjugated with glutathione by IsoI (van Hylckama Vlieg *et al*. 1998, 1999). The observed inhibition may indicate that the addition of relatively high concentrations of epoxyisoprene causes damage to cellular components or proteins, as observed in the sMMO-mediated oxidation of trichloroethene (Fox *et al*. 1990). Methane oxidation by *Methylosinus trichosporium* OB3b was totally inhibited by the products of TCE oxidation (Chu & Alvarez-Cohen 1999).

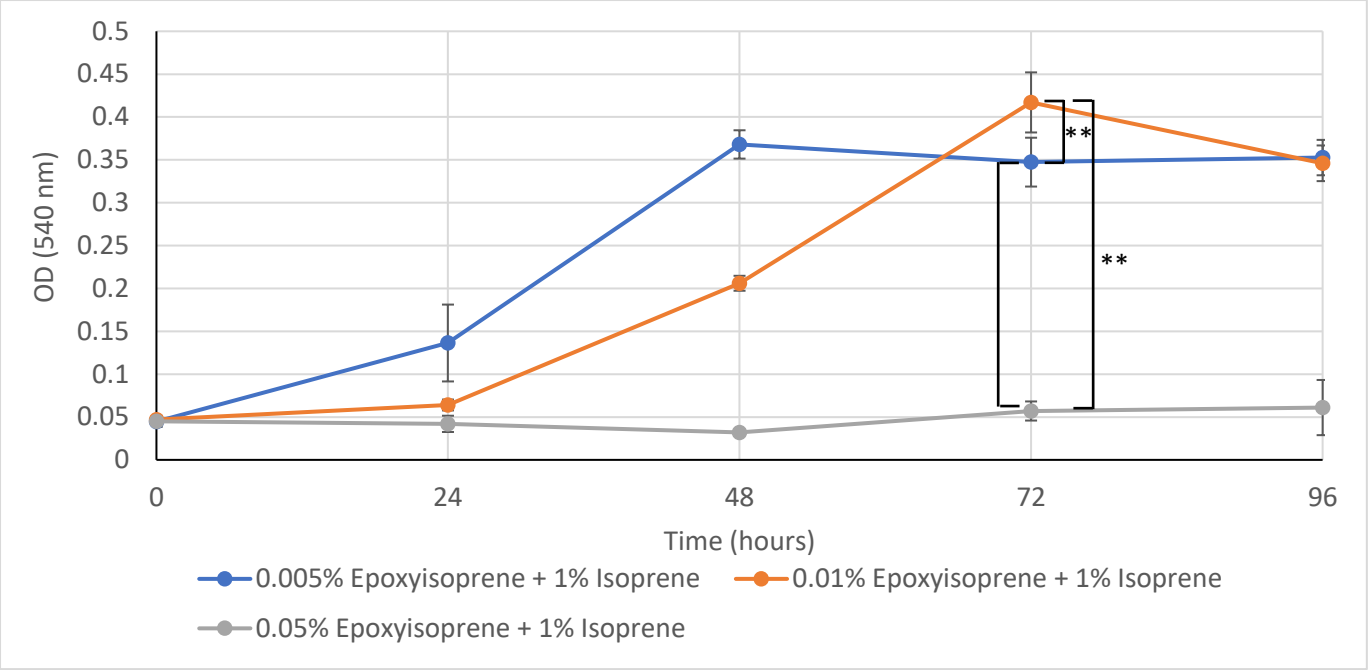

Figure 3.10. Growth of *Variovorax* sp. WS11 with 1% (v/v) isoprene and different concentrations of epoxyisoprene. These data were calculated as the average of three biological replicates ± standard deviation. An asterisk denotes a statistically significant difference between indicated conditions (** p≤0.01), determined by *t* test.

1,3-butadiene failed to support the growth of *Variovorax* sp. WS11 when added as the sole source of carbon and energy (Table 3.2). *Rhodococcus* sp. AD45 was able to grow on 1,3-butadiene (Sims, L., Personal Communication), albeit at a slower rate than growth on isoprene. 1,3-butadiene was expected to support the growth of *Variovorax* sp. WS11 due to the structural similarities with isoprene, and also due to the fact that the isoprene monooxygenases of *Rhodococcus* sp. AD45 (Sims 2020) and *Variovorax* sp. WS11 both oxidise 1,3-butadiene at a similar rate to isoprene (as described in Section 3.5.5) (Sims 2020). Potential reasons for the lack of growth on 1,3-butadiene were considered.

Crombie *et al*. (2015) demonstrated that the *iso* metabolic genes of *Rhodococcus* sp. AD45 were significantly upregulated by epoxyisoprene but not by isoprene. It was therefore hypothesised that, although 1,3-butadiene was oxidised by the IsoMO of *Variovorax* sp. WS11, the epoxide product was not capable of inducing expression of the *iso* metabolic genes. This would, in turn, result in the accumulation of the reactive epoxide (Fox *et al*. 1990, van Hylckama Vlieg *et al*. 1998). Alternatively, the specificity of IsoI for epoxyisoprene may prevent the conjugation of epoxides of 1,3-butadiene with glutathione (van Hylckama Vlieg *et al*. 1999). It was unknown which epoxide product would be formed by IsoMO, although the toluene 2-monooxygenase of *Burkholderia cepacaia* G4 and toluene 4-monooxygenase of *Pseudomonas* sp. ENVBF1 each converted 1,3-butadiene to butadiene monoepoxide rather than butadiene diepoxide (McClay et al. 2000). van Hylckama Vlieg *et al*. (1999) noted that *Rhodococcus* sp. AD45 mainly oxidised isoprene to epoxyisoprene at the 3,4- position, while isoprene degrading *Nocardia* sp. IP1 produced epoxides at the 1,2-, 3,4-, and 1,2,3,4- positions (Van Ginkel *et al*. 1987). 1,3-butadiene acted as a weak inducer of *iso* gene expression by *Variovorax* sp. WS11, more than 10-fold less than the induction by isoprene (as described in

Chapter 7). It is possible that 1,3-butadiene or an epoxide product of 1,3-butadiene could act as an inducer of isoprene metabolism, but it is unclear which epoxide would be produced by *Variovorax* sp. WS11.

Following the assumption that 1,3-butadiene and its oxidation products were not able to induce *iso* gene expression, it was theorised that *Variovorax* sp. WS11 would be able to consume 1,3-butadiene concurrently with isoprene. This was based, in part, on the observation of van Hylckama Vlieg *et al*. (1998, 1999) that the IsoI protein of *Rhodococcus* sp. AD45 catalysed the conjugation of various epoxides with glutathione, not just epoxyisoprene. With isoprene present to induce expression of IsoMO and the epoxide-detoxifying apparatus (IsoI, IsoH), epoxides of 1,3-butadiene may be assimilated into central metabolism. When isoprene and 1,3-butadiene were added concurrently, all growth on isoprene ceased (Figure 3.11). This indicated toxicity caused directly by the presence of 1,3-butadiene, so cultures were also prepared with 10 mM glucose and 10 mM pyruvate and supplemented with 1,3-butadiene (Figure 3.11). Different levels of inhibition were observed for each substrate. Growth on isoprene was entirely inhibited, while growth on glucose and pyruvate were approximately halved. *Variovorax* sp. WS11 typically grows to an OD_{540} >1.0 after 24-48 hours of incubation with 10 mM pyruvate or 10 mM glucose at 30 ^{o}C, indicating a toxic effect of 1,3-butadiene. In the case of isoprene-grown cells, it was likely that IsoMO had either become inhibited or was no longer being synthesised. As *Variovorax* sp. WS11 was added from a mid-exponential phase isoprene-grown culture, it was expected that sufficient glutathione would have been synthesised to detoxify butadiene epoxide. However, the inhibition of growth on glucose and pyruvate may indicate a different inhibitory effect caused by 1,3-butadiene, as there would be no previous expression of the *iso* metabolic genes. 1,3-butadiene and its oxidation products have previously been shown to exert toxic effects on many types of cells (Albertini *et al*. 2010, Ashizawa *et al*. 2012). Without the enzymatic oxidation of 1,3-butadiene by IsoMO, the inhibition of glucose- and pyruvate-grown cells indicates non-enzymatic oxidation processes in *Variovorax* sp. WS11, or potentially enzymatic degradation by processes unrelated to the *iso* metabolic gene cluster. However, the differing degrees of inhibition between isoprene-grown cells and the alternative substrates indicated that the rapid enzymatic oxidation of 1,3-butadiene is a greater source of inhibitory products.

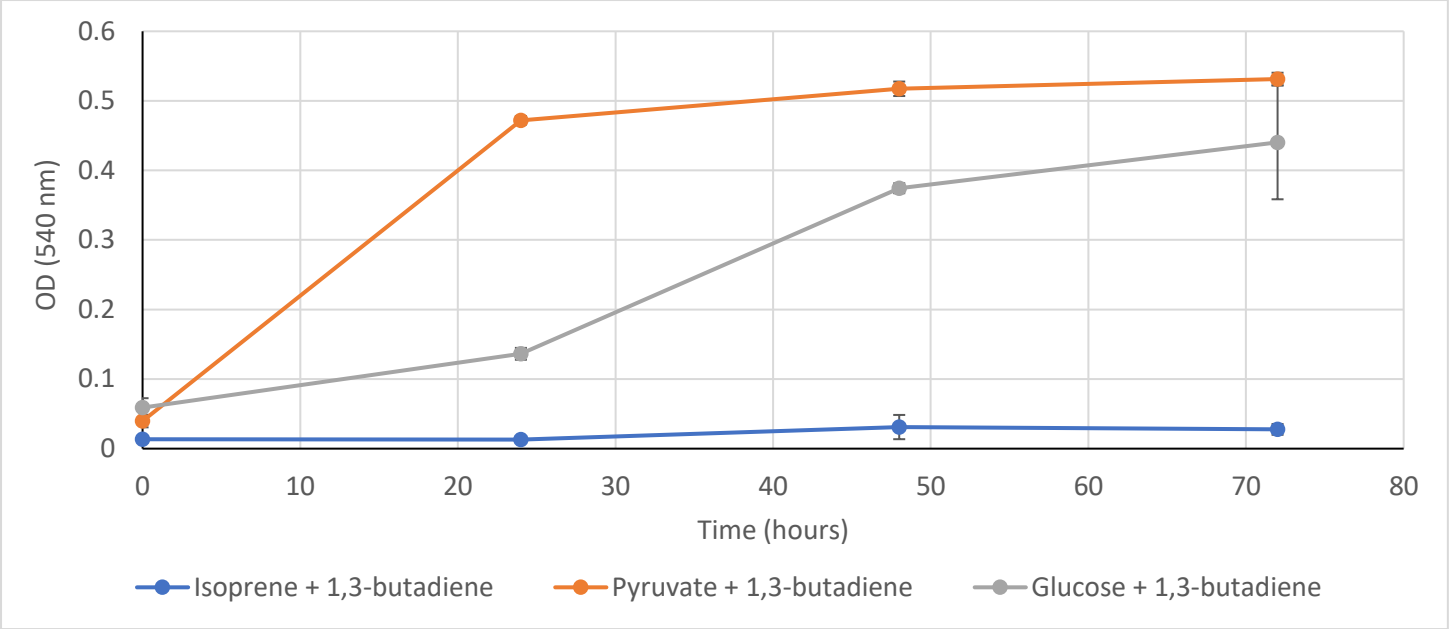

Figure 3.11. Growth of *Variovorax* sp. WS11 with combinations of 1,3-butadiene with 1% (v/v) isoprene, 10 mM glucose, or 10 mM pyruvate. These data were calculated as the average of three biological replicates ± standard deviation.

As the concurrent addition of isoprene and 1,3-butadiene was inhibitory to the growth of *Variovorax* sp. WS11, it was theorised that 1,3-butadiene would be coincidentally metabolised if added to a culture which was currently growing on isoprene. This was based on the requirement of glutathione for the detoxification of epoxides, and also the requirement for active IsoI and IsoH, all of which would be present during growth on isoprene. Cultures were established with 1% (v/v) isoprene, and 1% (v/v) 1,3-butadiene was added after 30 hours. The isoprene-only culture had consumed isoprene to a sub-detection level by 72 hours' incubation, and the increase in OD_{540} had slowed, indicating that *Variovorax* sp. WS11 was becoming substrate-limited (Figure 3.12). The 1,3-butadiene-ammended culture had approximately 0.2% (v/v) isoprene remaining after 72 hours, and the OD_{540} was still increasing. The rate of isoprene consumption between 30 – 48 hours was also slower when compared to the isoprene-only culture. This indicated that isoprene and 1,3-butadiene were competing for the active site of IsoMO. The similar rates of oxidation of isoprene and 1,3-butadiene by IsoMO support this observation (as described in Section 3.5.5). These data indicated that 1,3-butadiene was incorporated as cellular biomass, particularly when considering the higher final OD_{540} of the cultures amended with isoprene and 1,3-butadiene. This experiment was repeated with a higher initial concentration of isoprene in order to confirm the continued incorporation of 1,3-butadiene into isoprene-grown *Variovorax* sp. WS11 (Figure 3.13). As before, the consumption of isoprene was faster in the isoprene-only culture when compared with the combination of isoprene and 1,3-butadiene, further indicating competition for the active site of IsoMO by each substrate. The final OD_{540} of *Variovorax* sp. WS11 with both isoprene and 1,3-butadiene was significantly higher than that of the isoprene-only culture ($p \leq 0.01$), confirming the coincident use of 1,3-butadiene as a source of carbon and energy. The decrease in the rate of growth shortly after adding 1,3-butadiene was likely to be due to stress caused by butadiene epoxide. However, the increase in growth rate from 54 –72 hours' growth indicated that *Variovorax* sp. WS11 overcame the inhibition by 1,3-butadiene. Further study of the incorporation of

1,3-butadiene by *Variovorax* sp. WS11 would be greatly informed by quantifying the concentrations of oxidised and reduced glutathione in cells amended with isoprene or a combination of 1,3-butadiene and isoprene.

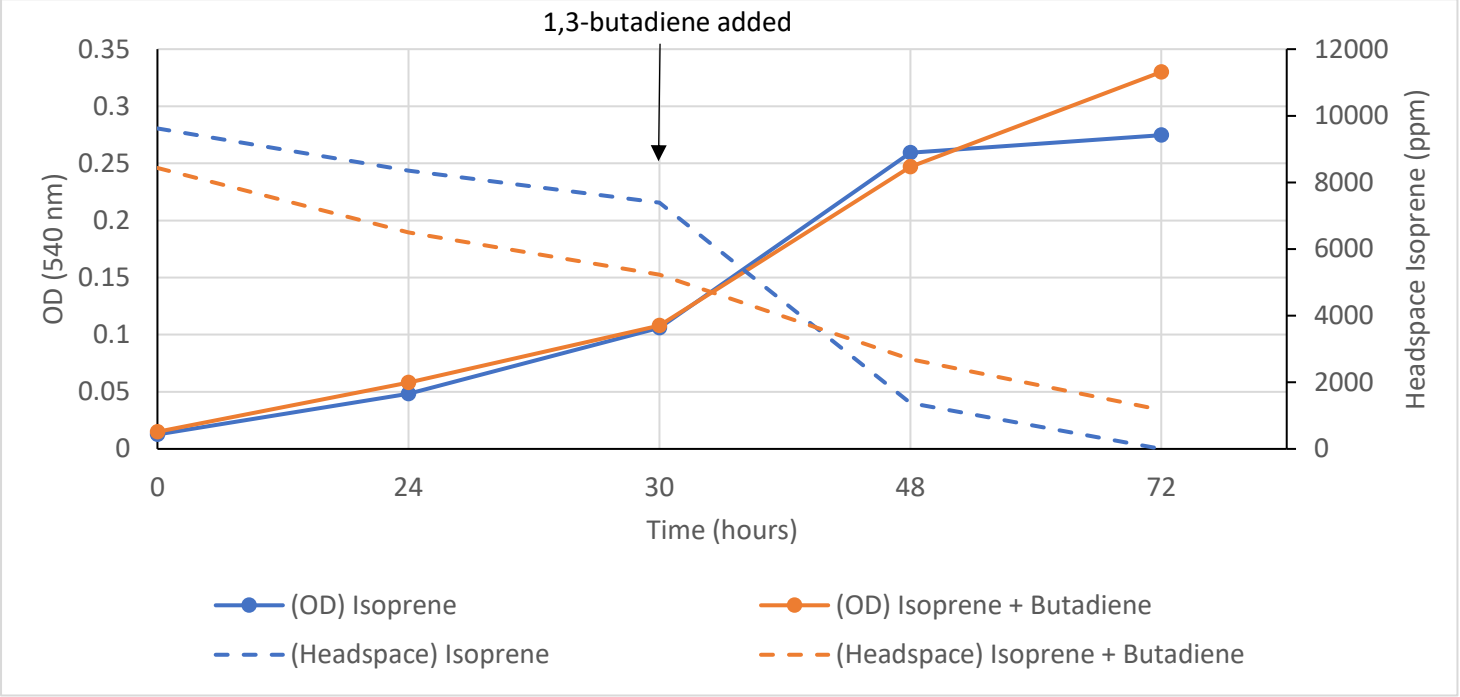

Figure 3.12. Addition of 1,3-butadiene to isoprene-grown *Variovorax* sp. WS11. N=1 (single biological replicates).

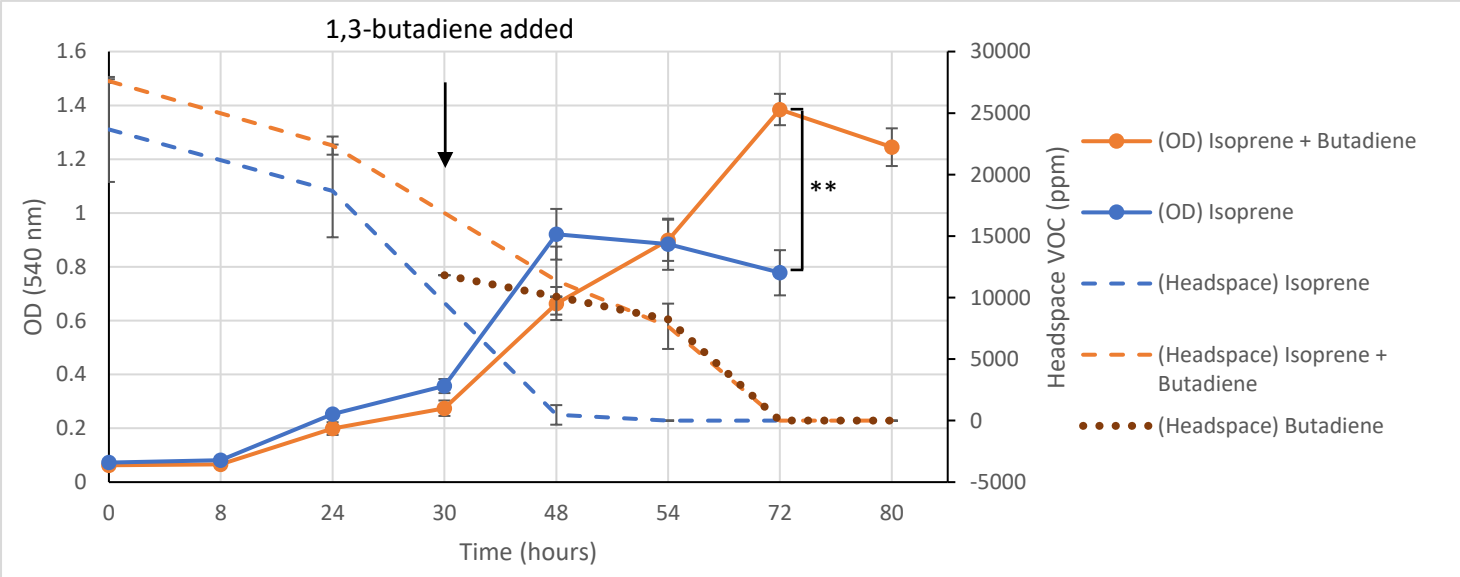

Figure 3.13. Concurrent consumption of 1,3-butadiene and isoprene by *Variovorax* sp. WS11. These data were calculated as the average of three biological replicates ± standard deviation. An asterisk indicates a statistically significant difference between conditions (** p≤0.01).

Collectively, these data indicated that *Variovorax* sp. WS11 was capable of using 1,3-butadiene as a source of carbon and energy only when isoprene was present to drive expression of the *iso* metabolic gene cluster. However, it was possible that butadiene epoxide or a subsequent product of metabolism may be capable of propagating the

continued induction of the *iso* genes once isoprene had run out. This was studied by adding a higher concentration of 1,3-butadiene to a culture with a lower concentration of isoprene (Figure 3.14). The basis for this was the assumption that *Variovorax* sp. WS11 would continue to consume the remaining isoprene and begin the consumption of 1,3-butadiene as demonstrated in Figure 3.13. This would be followed either by the cessation of growth if oxidation products of 1,3-butadiene could not upregulate *iso* gene expression, or by continued growth if the *iso* genes were expressed. Consumption of isoprene slowed after adding 1,3-butadiene, as did the rate of growth, as observed previously (Figure 3.13). The concentration of 1,3-butadiene in the headspace of the cultures decreased slightly, indicating oxidation by IsoMO (Figure 3.14). This was followed by a cessation of growth and isoprene consumption by *Variovorax* sp. WS11. As isoprene and 1,3-butadiene compete for the active site of IsoMO, it is likely that excess 1,3-butadiene resulted in a greater proportion of butadiene epoxide being produced compared to epoxyisoprene. This would result in a lower level of expression of the *iso* metabolic gene cluster, resulting in butadiene epoxide accumulating and exerting toxic effects. These data indicated that the downstream products of butadiene metabolism are incapable of inducing *iso* gene expression. Instead, the observed metabolism of 1,3-butadiene (Figure 3.13) likely occurred as a coincidence of the active isoprene metabolic pathway.

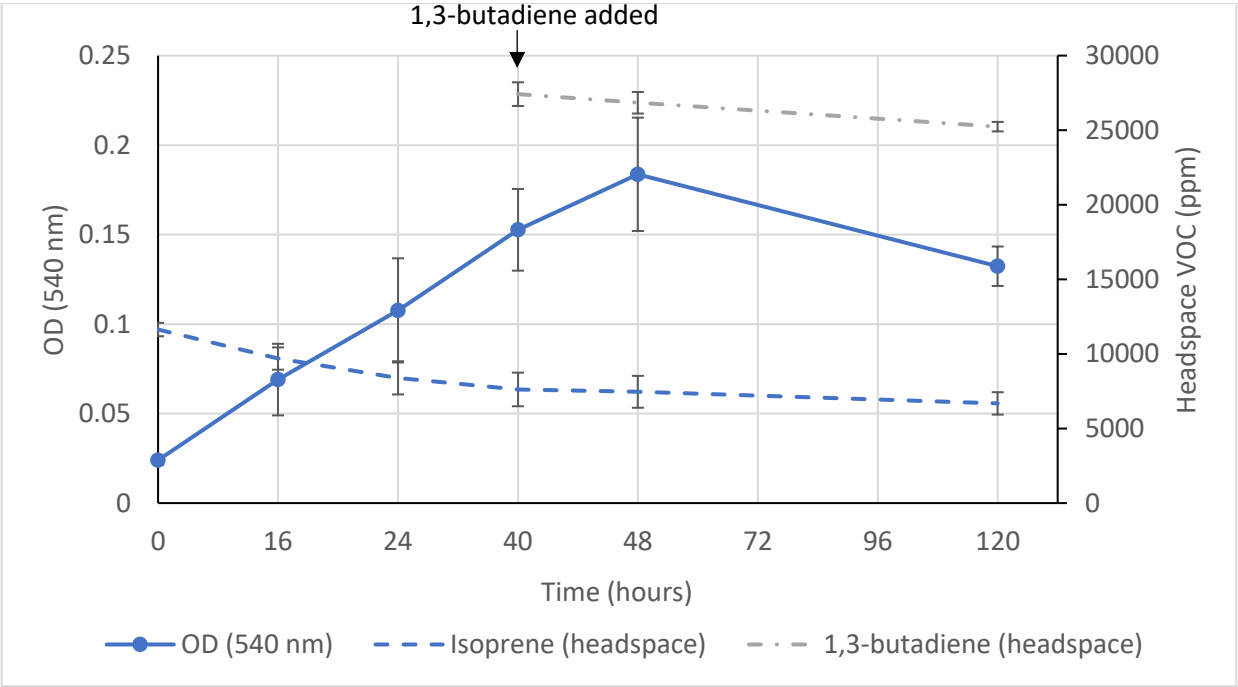

Figure 3.14. Growth of *Variovorax* sp. WS11 on isoprene, supplemented with excess 1,3-butadiene after 24 hours. These data were calculated as the average of three biological replicates ± standard deviation.

It is likely that the observed growth on, and consumption of, 1,3-butadiene when applied mid-growth on isoprene occurred as a result of cross-specificity of its oxidation products with enzymes from the isoprene metabolic pathway. This indicated that *Variovorax* sp. WS11 may be able to incorporate carbon from more alkene substrates if isoprene is also present to induce the expression of the *iso* metabolic genes. However, the presence of isoprene was not sufficient to prevent the toxicity of epoxyisoprene to *Variovorax* sp. WS11 (Figure 3.14). As well as *Rhodococcus* sp. AD45, five Gram positive isoprene degraders grow using epoxyisoprene (Johnston 2014). *Rhodococcus* sp. AD45

contains duplicated copies of *isoG*, *isoH*, *isoI*, and *isoJ*, the products of which are predicted to catalyse the steps of isoprene metabolism after the formation of epoxyisoprene by IsoMO (Crombie *et al*. 2015). The presence of these duplicates, particularly *isoI* which encodes a glutathione *S*-transferase known to detoxify epoxyisoprene by conjugation with glutathione (van Hylckama Vlieg *et al*. 1999), may account for the apparent resistance of *Rhodococcus* sp. AD45, and other Gram positive isoprene degraders, to epoxyisoprene. Overall, these data indicated that the isoprene metabolic pathway is capable of incorporating alternative, similarly structured alkenes into central metabolism so long as isoprene is present at a higher concentration to maintain the supply of inducing metabolites such as epoxyisoprene.

3.5.5. **Substrate oxidation range of *Variovorax* sp. WS11**

The ability of whole cells of *Variovorax* sp. WS11 to oxidise isoprene and other carbon sources was tested using a Clark oxygen electrode (Clark *et al.* 1953). Previous studies reported the use of oxygen electrodes when measuring substrate oxidation by bacteria which express SDIMO. For example, toluene oxidation by the toluene 2-monooxygenase of *Burkholderia cepacia* G4 was measured as a function of oxygen consumption within the sealed reaction chamber of the electrode (Yeager *et al*. 1999). Isoprene-grown cells of *Variovorax* sp. WS11 from the fermentor were added to the reaction chamber as described in Section 2.15.3. The endogenous rate of oxygen uptake was relatively high immediately after thawing, a trait which was not detected in pre-harvest cells. It was theorised that the stress of centrifugation and freezing resulted in the sheering of some cells, releasing metabolites which intact cells could use. Freeze-thawing is a documented method of bacterial cell lysis (Shehadul Islam *et al*. 2017), and would result in the observed increase in the endogenous rate of oxygen uptake by the surviving cells. A similar trait was observed in smaller-scale harvests of glucose- and succinate-grown *Variovorax* sp. WS11. In order to test this, thawed glucose-grown *Variovorax* sp. WS11 were challenged with 100 µM glucose immediately after thawing and after 1 hour with stirring at room temperature in the absence of substrate (Table 3.3). It was assumed that starved cells would use any metabolites released from stress-sheered cells, resulting in a lower endogenous rate of oxygen uptake over time. The endogenous oxygen uptake by glucose-grown cells decreased approximately 5-fold after 1 hour, while the substrate-added rate of oxygen uptake remained almost unchanged. The substrate-induced rate of oxygen uptake appeared to be almost four-fold greater after starvation for 1 hour (Table 3.3) due to the relative difference between the endogenous and substrate-added rates changing rather than an increase in the rate of substrate oxidation. As starved cells were likely to demonstrate a more accurate rate of oxygen uptake than freshly thawed cells, oxygen uptake assays were performed using cells which were starved for 1-2 hours.

Table 3.3. Endogenous and glucose-induced rates of oxygen uptake by glucose-grown *Variovorax* sp. WS11. N=1 (single biological replicates).

Length of Starvation (hours)	Endogenous O_2-uptake (nmol/sec)	Substrate-added O_2-uptake (nmol/sec)	Substrate-induced O_2-uptake (nmol min^{-1} mg dry $weight^{-1}$)
0	2.5	3.2	30.6
1	0.6	3.5	118.3

Isoprene-grown *Variovorax* sp. WS11 oxidised a wide range of aliphatic and aromatic alkenes (Figure 3.15) (Dawson *et al*. 2020), as was previously observed in *Rhodococcus* sp. AD45 (van Hylckama Vlieg et al. 2000, Sims 2020). Glucose- and succinate-grown cells had no detectable rate of oxidation of alkenes. Isoprene was oxidised at an average rate of 31.5 nmol min^{-1} mg dry $weight^{-1}$ by isoprene-grown cells, and 1,3-butadiene was oxidised at 86.4% of this rate (p=0.13, determined by *t* test). This supported the hypothesis that isoprene and 1,3-butadiene compete for the active site of IsoMO when *Variovorax* sp. WS11 was incubated with a combination of isoprene and 1,3-butadiene (Figure 3.13, Figure 3.14). Shorter-chain alkenes such as ethylene and propylene were oxidised at lower rates than the longer chain alkenes, indicating that the IsoMO of *Variovorax* sp. WS11 has a greater affinity for long-chain hydrocarbons. The greatest rate of oxidation of a non-isoprene substrate was observed for 1-octene, an eight-carbon alkene. Similar substrate ranges have been observed in other SDIMO. The three-component alkene monooxygenase of *Rhodococcus rhodochrous* B-276 oxidised C3-C13 alkenes, including aromatic alkenes such as styrene (Gallagher *et al*. 1997, Breuer *et al*. 2004). The sMMO of *M. trichosporium* OB3b catalysed the co-oxidation of propene, butene, 1,3-butadiene, and pentene, with further oxidation up to C7 of alkenes, while the toluene 4-monooxygenase of *Pseudomonas mendocina* KR1 oxidised C3-C8 alkenes also including 1,3-butadiene (Higgins et al. 1979, Green & Dalton 1989, Ono & Okura 1990, McClay et al. 2000). It has been well-established that SDIMO possess broad substrate ranges, and the IsoMO of *Variovorax* sp. WS11 exhibited a characteristically broad substrate range. A curious trait of this IsoMO was an increase in the rate of substrate oxidation with the addition of side chains (Figure 3.15). For example, isoprene (2-methyl-1,3-butadiene) and 3-methyl-1,4-pentadiene were oxidised at higher rates than their respective unmethylated alkenes, although these differences were not statistically significant (p=0.13 and p=0.07, respectively). However, the rate of oxidation of 1,3-butadiene was significantly greater than butene (p=0.01). This relationship was particularly striking when comparing the oxidation of aromatic and cyclic hydrocarbons with their branched derivatives. There was no detectable rate of oxidation of benzene or cyclohexene by isoprene-grown *Variovorax* sp. WS11, but the addition of a methyl, ethyl, propyl, or hydroxyl group resulted in an increase in the rate of substrate-induced oxygen uptake (Figure 3.15). Many SDIMO also catalyse the epoxidation or hydroxylation of aromatic or cyclic hydrocarbons. Cyclohexene and methylcyclohexene were co-oxidised by the sMMO of *M. trichosporium* OB3b (Leak & Dalton 1987), unlike IsoMO which was incapable of oxidising cyclohexene in whole cells (Dawson *et al*. 2020). *Mycobacterium* sp. ELW1 also utilised a monooxygenase which preferentially oxidised branched hydrocarbons, as the growth on 2-methypropene was faster than the growth on 1- and 2-butene (Kottegoda *et al*. 2015). Aromatic hydrocarbons such as benzene, toluene, *o*-xylene, ethylbenzene, and styrene are

oxidised by many types of SDIMO (Green & Dalton 1989, Whited et al. 1991, Bertoni et al. 1996, Zhou et al. 1999, McClay et al. 2000, Oelschlägel et al. 2018). Other bacterial multicomponent monooxygenases have been shown to form epoxides from methylated alkenes, including another terpene-related monooxygenase, pinene monooxygenase of *Pseudomonas fluorescens* (Leak *et al*. 1992).

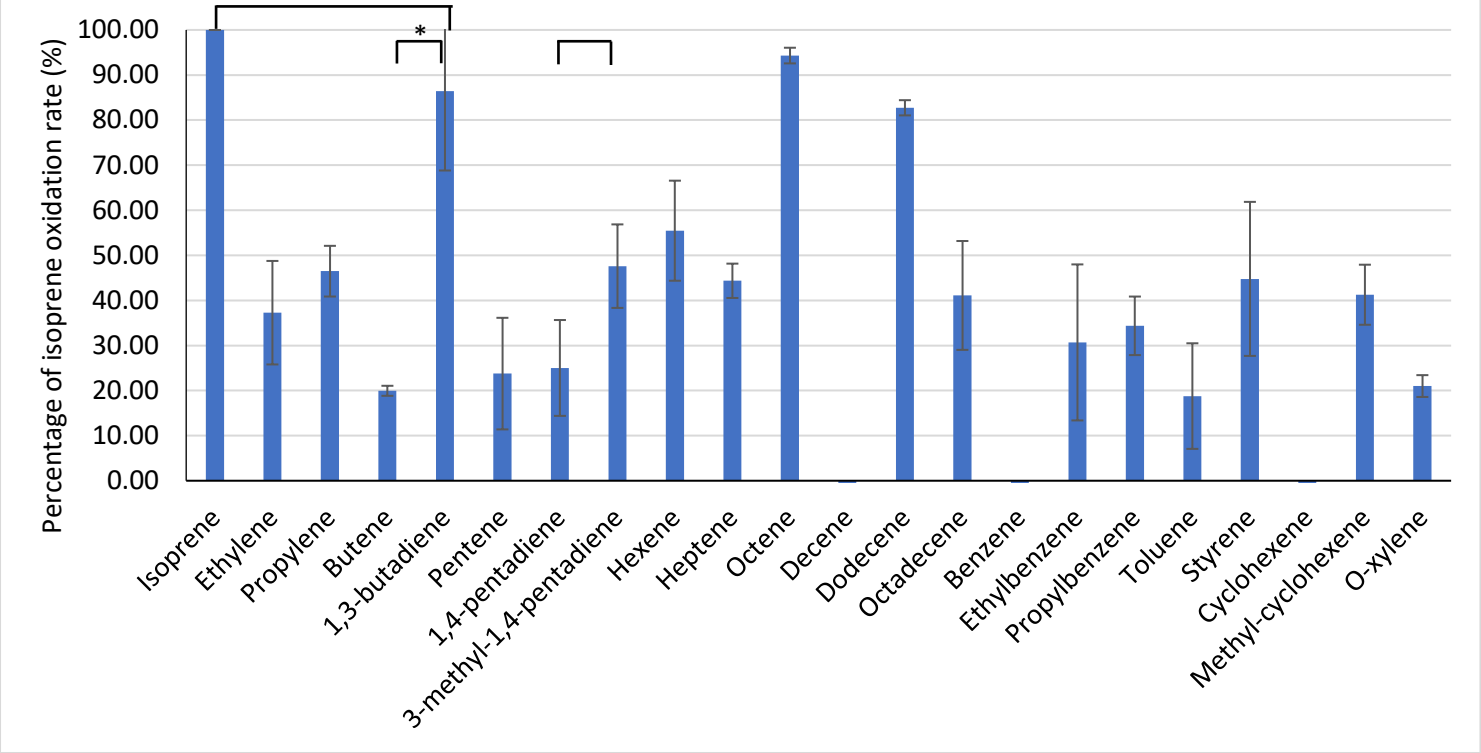

Figure 3.15. Substrate-induced rates of oxygen uptake by whole-cells of isoprene-grown *Variovorax* sp. WS11. Oxidation rates are presented relative to the average rate of isoprene oxidation, 31.5 nmol min^{-1} mg dry $weight^{-1}$ (taken from Dawson *et al.* 2020). These data were calculated as the average of three biological replicates ± standard deviation. Asterisks indicate a statistically significant difference between the indicated conditions ($p \leq 0.05$).

3.5.6. **Inhibition of isoprene monooxygenase by linear alkynes**

It has been known for many years that alkynes are mechanism-based inhibitors of SDIMO, requiring the active turnover of both alkyne and oxygen in order to exert an inhibitory effect (Prior & Dalton 1985, Small & Ensign 1997, Yeager *et al*. 1999, Hamamura *et al*. 2001). It therefore stands to reason that there should be a relationship between the substrate specificity of the SDIMO in question and the relative potency of an alkyne inhibitor of similar structure. For example, the sMMO of *Methylococcus capsulatus* (Bath) oxidises methane at a high rate, but the rate of substrate oxidation decreases with increasing carbon chain length (Colby *et al*. 1977). Similarly, 3% (v/v) acetylene is sufficient to completely inhibit the activity of the sMMO, but the strength of inhibition decreased for propyne and butyne (Prior & Dalton 1985). Initial reports of the three-component alkene monooxygenase of *R. rhodochrous* B-276 suggested that it was not inhibited even by 50% (v/v) acetylene, while a similar concentration of propyne inhibited up to 70% of alkene-oxidising activity (Gallagher *et al*. 1997). A later study confirmed that acetylene was a weak inhibitor of the growth of *R. rhodochrous* B-276 on propene, while propyne and butyne were potent inhibitors

(Fosdike *et al*. 2005). A correlation between substrate specificity and the strength of inhibition by alkynes was also identified for the putative isobutylene monooxygenase of *Mycobacterium* sp. ELW1 (Kottegoda *et al*. 2015).

The IsoMO of *Variovorax* sp. WS11 tended to oxidise longer-chain alkenes at a higher rate than shorter-chain alkenes (Figure 3.15). For example, ethylene was oxidised at less than 40% of the rate of isoprene, while octene was oxidised at over 90% of the rate of isoprene oxidation. Therefore, it was expected that the IsoMO of *Variovorax* sp. WS11 would be weakly inhibited by short-chain alkynes such as acetylene but strongly inhibited by long-chain alkynes such as octyne. This was supported by the findings of Dr. A. Johnston (2014), as the growth of *Gordonia polyisoprenivorans* i37 and *Mycobacterium holderi* i29a2 on isoprene was not affected by the presence of acetylene, indicating that acetylene was not an inhibitor of IsoMO. 50 µM acetylene inhibited isoprene uptake by whole cells of *Variovorax* sp. WS11 to an average of 6.5% of the control rate. 50 µM Propyne and 50 µM butyne inhibited isoprene uptake by whole cells of *Variovorax* sp. WS11 to 53.1% and 87.4% of the control rate, respectively (Figure 3.16). The trend of increasing inhibition continued, as an average of 94.7% of isoprene uptake was inhibited by 50 µM octyne. The difference in inhibition of IsoMO by acetylene and octyne was statistically significant ($p \leq 0.01$). The IsoMO of *Rhodococcus* sp. AD45 and *Gordonia polyisoprenivorans* i37 were similarly not inhibited by 50 µM acetylene (Johnston, 2014, Sims, L., 2020), but propyne inhibited 70% of isoprene uptake by the IsoMO of *Rhodococcus* sp. AD45 compared to only 53% for the IsoMO of *Variovorax* sp. WS11 (Sims 2020). The IsoMO of *Rhodococcus* sp. AD45 was inhibited to a similar degree by C3-C8 alkynes, correlating with the similar rates of oxygen uptake induced by the corresponding alkenes.

Several SDIMO have been identified which catalyse the co-oxidation of isoprene, including the sMMO of *M. silvestris* BL2 (Crombie 2011). The IsoMO of *Variovorax* sp. WS11 is a four-component SDIMO with a different substrate oxidation specificity than the three-component sMMO. Therefore, it was expected that the use of alkyne inhibitors would be sufficient to distinguish between the oxidation of isoprene by the IsoMO and sMMO of *Variovorax* sp. WS11 and a representative methanotroph, respectively. The sMMO of *M. capsulatus* (Bath) is known to be inhibited by acetylene (Stirling & Dalton 1979). Therefore, this sMMO was chosen as a comparative SDIMO. The sMMO of *M. capsulatus* (Bath) co-oxidised isoprene at an initial rate of 1.38 ± 0.15 nmol min^{-1} mg dry $weight^{-1}$. In order to validate the experimental conditions, the well-characterised co-oxidation of propylene to propylene oxide by sMMO (Richards *et al*. 1994) was used as a proxy for methane oxidation. Acetylene and octyne, the least and most potent inhibitors of isoprene oxidation by IsoMO, respectively, were selected as inhibitors of the sMMO. As expected, 50 µM acetylene inhibited propylene oxidation and isoprene oxidation by the sMMO to 96.2% and 99.1% of the control rates, respectively. The latter was 15-times the strength of inhibition of isoprene oxidation by the IsoMO, and this difference was determined to be statistically significant by *t* test ($p \leq 0.05$), strongly indicating that acetylene would facilitate the differentiation between isoprene degraders and isoprene co-oxidisers which use sMMO. 50 µM acetylene only inhibited 6.5% of isoprene oxidation by the IsoMO compared the control rate (Figure 3.16), while 50 µM octyne was sufficient to inhibit 95.5% of isoprene oxidation by the IsoMO in whole cells of *Variovorax* sp. WS11, a statistically significant difference when compared between each SDIMO ($p \leq 0.01$). These data demonstrated the

relationship between the substrate oxidation profile of SDIMO and the inhibition by alkynes of corresponding carbon chain length, and also indicates the potential of alkynes as probes to distinguish between different classes of SDIMO-utilising bacteria.

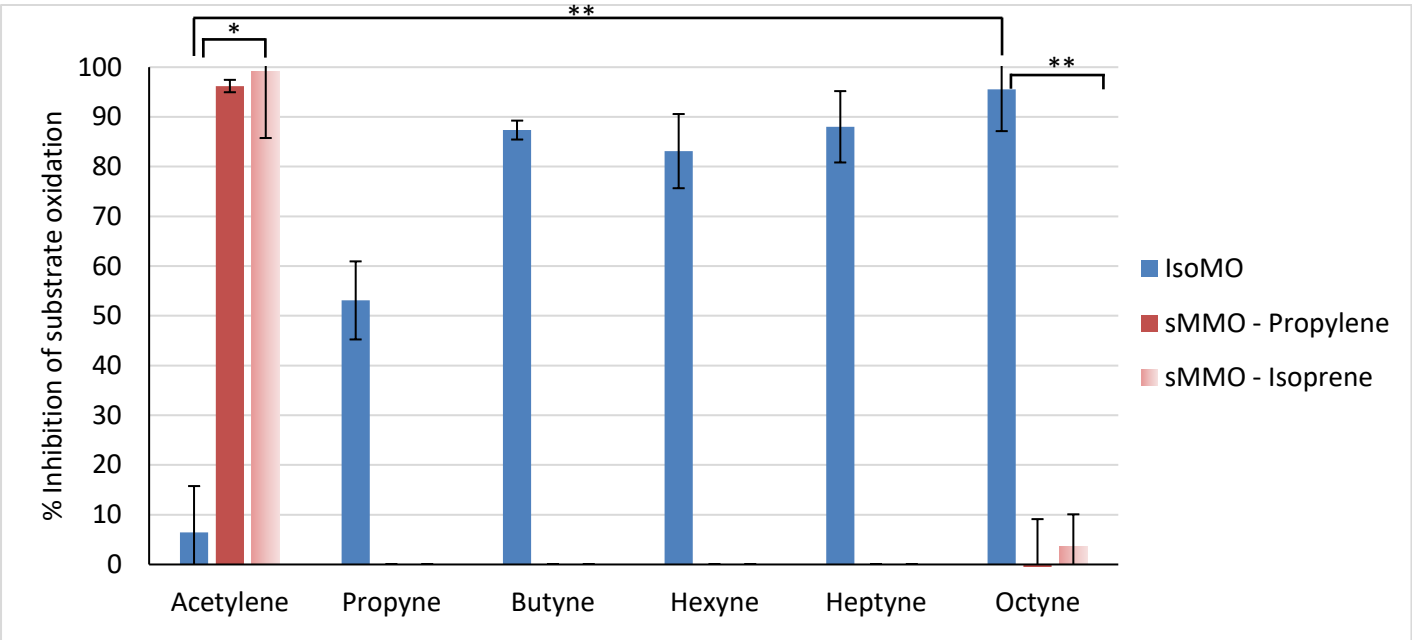

Figure 3.16. Inhibition of the IsoMO of *Variovorax* sp. WS11 and the sMMO of *M. capsulatus* (Bath) by 50 µM of linear 1-alkynes (taken from Dawson *et al.* 2020). These data were calculated as the average of three biological replicates ± standard deviation. Asterisks denote a statistically significant difference between the indicated conditions (* p≤0.05, **p≤0.01).

Isoprene is a 4-carbon dialkene chain with a sub-terminal methyl group. As the IsoMO of *Variovorax* sp. WS11 exhibited the highest rate of oxidation for isoprene compared to other alkenes (Figure 3.15), it was theorised that an alkyne of corresponding structure would be an effective inhibitor of isoprene oxidation. 2-methyl-1-buten-3-yne is an alkyne which is identical to isoprene with the exception of the alkene group at position 3 being substituted for an alkyne group. It was initially expected that the resemblance to isoprene would make this alkyne a highly effective inhibitor of isoprene uptake, but the inhibition was less than half that of 1- and 2-butyne (Figure 3.17), a statistically significant decrease in inhibition (p≤0.05). This was likely to be due to the ability of the IsoMO of *Variovorax* sp. WS11 to perform oxidations at either end of the isoprene chain. In approximately 50% of cases, this may result in the oxidation of a non-inhibitory alkene group rather than the alkyne group, explaining the observed lack of inhibition. Previous studies have demonstrated changes in the effectiveness of alkynes according to the location of the alkyne group. For example, the toluene 2-monooxygenase of *B. cepacia* G4 was inhibited more effectively by 2- and 3-alkynes than the corresponding 1-alkynes (Yeager *et al.* 1999). Interestingly, 1-butyne and 2-butyne were almost identical in their inhibition of the IsoMO of *Variovorax* sp. WS11 (Figure 3.17), indicating that this SDIMO has similar activity towards sub-terminal alkene groups as well as primary alkenes.

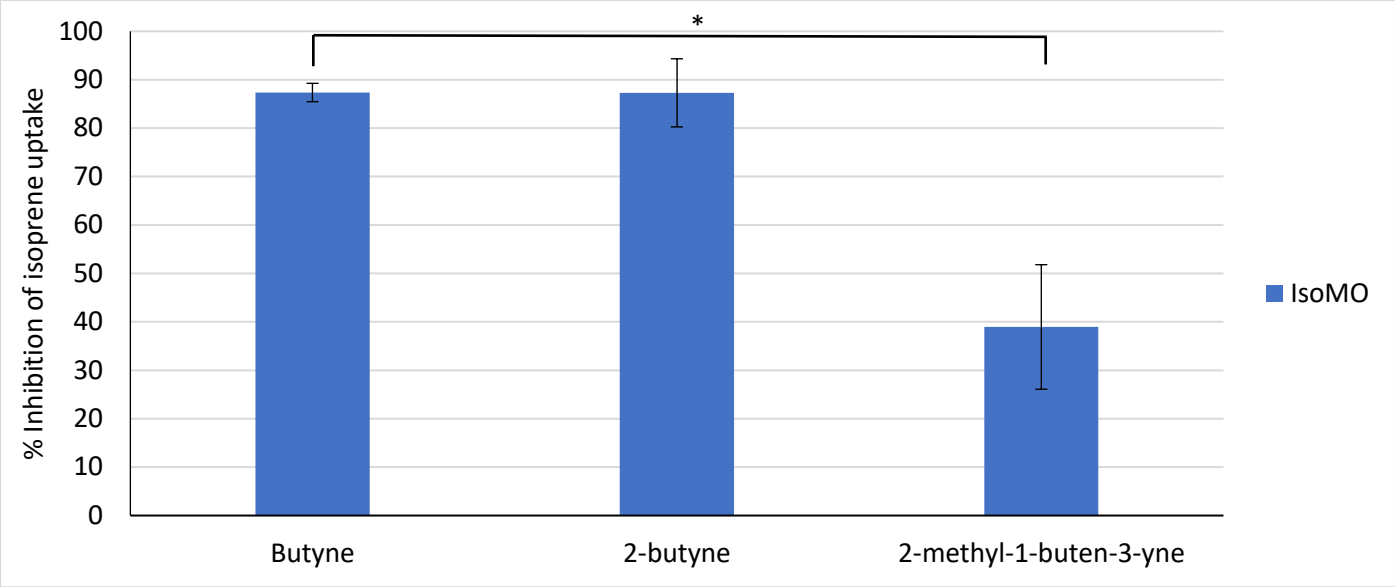

Figure 3.17. Inhibition of isoprene oxidation by the IsoMO of *Variovorax* sp. WS11 by 1- and 2-butyne, and 2-methyl-1-buten-3-yne. These data were calculated as the average of three biological replicates ± standard deviation. Asterisks denote a statistically significant difference between the indicated conditions (* p≤0.05).

3.5.7. **Analysis of the proteome of isoprene-grown *Variovorax* sp. WS11**

Relatively little mechanistic detail is available to describe the isoprene metabolic pathway, with the only confirmed intermediate metabolites being reported by van Hylckama Vlieg *et al*. (1998, 1999) over 20 years ago. These metabolites are depicted in Figure 1.6. *isoG*, *isoJ* and *aldH* are all associated with the *iso* metabolic gene cluster (Figure 1.8) but currently do not have confirmed roles in isoprene metabolism. IsoG and IsoJ, along with an unconfirmed CoA-ligase, were predicted to catalyse the conversion of GMBA to 2-methyl-3-butenyl-CoA, although the latter product is unconfirmed (van Hylckama Vlieg *et al*. 2000). The level of abundance of Iso metabolic peptides in an isoprene degrading bacterium remains largely unknown, although van Hylckama Vlieg *et al*. (1999) and Crombie *et al*. (2015) demonstrated that peptides and transcripts associated with the isoprene metabolic pathway were highly upregulated in *Rhodococcus* sp. AD45. During purification, IsoH and IsoI were predicted to comprise 16% and 8% of total soluble proteins in *Rhodococcus* sp. AD45, respectively (van Hylckama Vlieg *et al*. 1999, 2000), and transcriptome analysis indicated that the *iso* metabolic gene cluster of this species comprised over 25% of transcripts after induction by either isoprene or epoxyisoprene.

Analysis of the proteome of an isoprene degrading bacterium would provide valuable information about the mechanisms of isoprene metabolism, particularly relating to the assimilation of GMBA into central metabolism. van Hylckama Vlieg *et al*. (2000) suggested β-oxidation as a likely mechanism, similar to the degradation of isoleucine via tiglyl-CoA to acetyl-CoA and propionyl-CoA (Massey et al. 1976). As *Variovorax* sp. WS11 contains an *iso* metabolic gene cluster which is related to that of *Rhodococcus* sp. AD45 (Chapter 1, Figure 1.6), it was determined that this bacterium represented a suitable model for the analysis of peptides involved in isoprene metabolism.

3.5.7.1. Initial analysis of differentially expressed peptides in *Variovorax* sp. WS11

Variovorax sp. WS11 was prepared for mass spectrometry analysis as described in Section 2.13. Unfractionated samples were prepared for Tandem Mass Tagging (TMT) using a TMTsixplex Isobaric Label Reagent Set (Thermo Fisher), with mass spectrometry run using OrbiTrap by Dr. Gerhard Saalbach (John Innes Centre, Norwich, UK). Iso metabolic peptides were highly upregulated when grown on isoprene compared to growth on succinate (Figure 3.18), confirming the observation that isoprene metabolism is inducible in *Variovorax* sp. WS11 (discussed in Chapters 6 and 7). The most upregulated peptides were IsoG and IsoH, which were 250-times more abundant in isoprene-grown cells compared to succinate-grown cells (Figure 3.18), as determined by calculating the ratio of abundance of peptides under each growth condition. By comparison, the IsoMO peptides were upregulated to a lesser extent, with abundance ratios between 20-111.

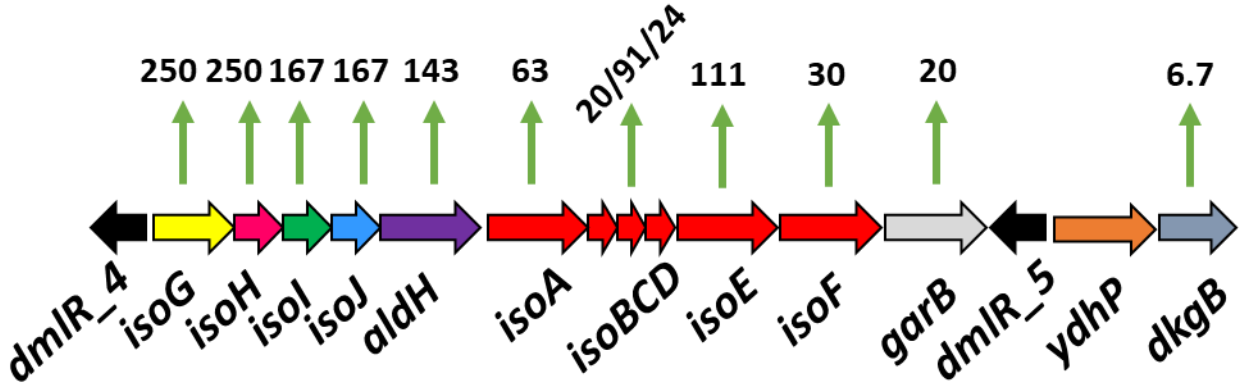

Figure 3.18. Relative abundance of peptides related to the *iso* metabolic gene cluster in *Variovorax* sp. WS11, with the presented values representing the relative abundance of each peptide (abundance ratio) after growth on isoprene compared to succinate. These data were calculated as the average of three biological replicates.

The relative abundance of each peptide provided valuable insights into the differential expression of each component of the *iso* metabolic gene cluster. However, the total abundance of each peptide was also relevant as this indicated the resting level of expression of the *iso* genes and also the abundance of the Iso peptides relative to the whole proteome of *Variovorax* sp. WS11. The overall abundance of each Iso peptide was significantly higher during growth on isoprene ($p \leq 0.01$, calculated by background based *t* test), as expected, with IsoH present at the greatest abundance of 746,833,473. However, several Iso peptides were also relatively abundant when grown on succinate (Figure 3.19). This was particularly evident for IsoGHI and AldH. IsoMO oxygenase components (IsoABE) were more abundant during growth on succinate than the accessory components (IsoCDF), with IsoA present at the highest abundance of 1,071,767 (Figure 3.19). By comparison, IsoC had an abundance of 50,244. This indicated that *Variovorax* sp. WS11 maintained a moderate level of expression of all Iso metabolic peptides, even in the absence of isoprene, but highly expressed these peptides in the presence of isoprene. This indicated a mechanism of sensing isoprene in order to increase the expression of the *iso* metabolic gene cluster. In *Rhodococcus* sp. AD45, epoxyisoprene is a significantly stronger inducer of *iso* gene expression than isoprene (Crombie *et al*. 2015), as discussed in Chapter 6 (Chapter 6, Section 6.5.1). Therefore, maintaining a low level of IsoMO expression to convert

environmental concentrations of isoprene to epoxyisoprene would result in sudden, large increases in expression of the *iso* metabolic gene cluster. Likewise, the toxicity of epoxyisoprene would be dangerous without IsoI and IsoH present to detoxify the epoxide group and form HGMB and GMBA, respectively, accounting for the relatively high basal level of abundance of these peptides (Figure 3.22) (van Hylckama Vlieg *et al*. 1998, 1999).

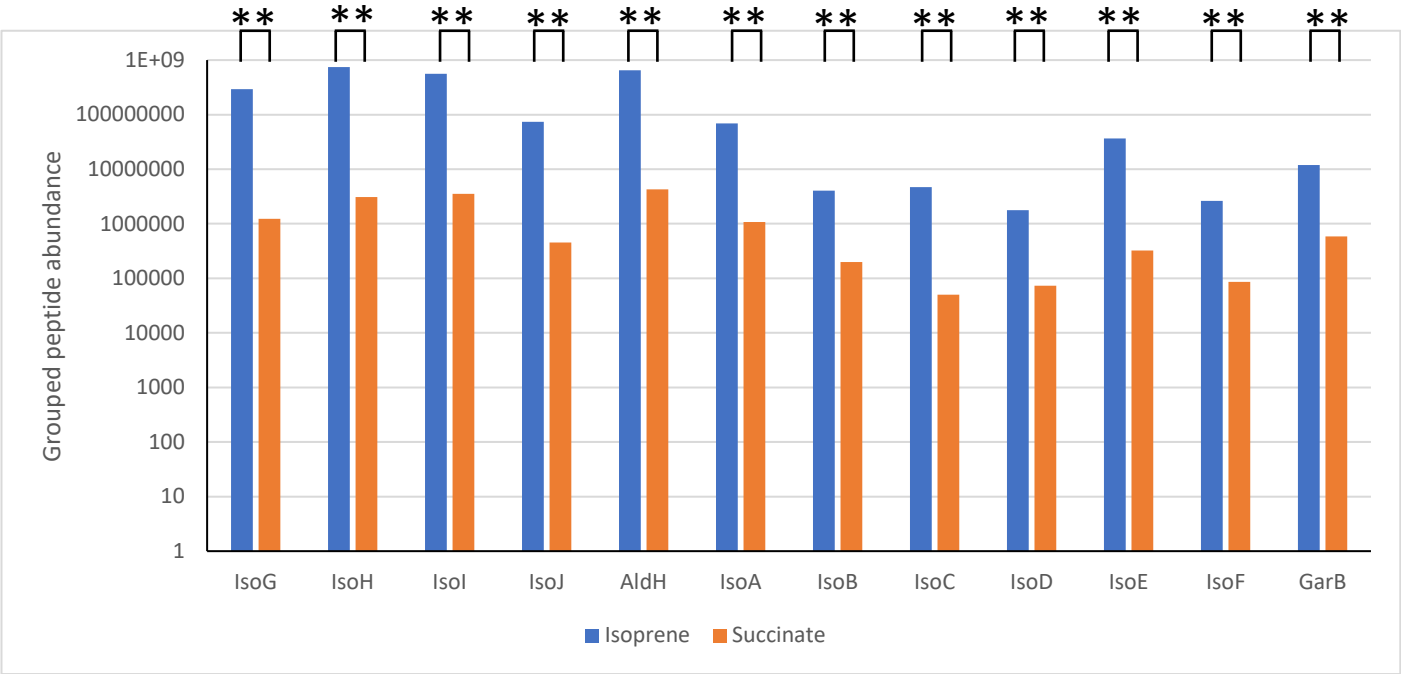

Figure 3.19. Grouped total abundances of each Iso-related peptide during growth on isoprene or succinate. These data were calculated as the average of three biological replicates. Asterisks denote a statistically significant difference between the indicated conditions (** p≤0.01).

Genes which were not previously identified in Gram positive isoprene degraders such as *Rhodococcus* sp. AD45 were also upregulated, namely *garB* and *dkgB*. These encode a putative glutathione-disulfide reductase and 2,5-diketo-D-gluconic acid reductase B, respectively. DkgB plays a role in the reduction of 2,5-diketogluconate to 2-ketogluconate, part of the ascorbate biosynthesis pathway (Sun *et al.* 2018). GarB, however, catalyses the NAD(P)H-dependent reduction of glutathione disulfide to glutathione, replenishing reduced glutathione which acts as an antioxidant (Janes & Schulz 1990, Deponte 2013). The latter has the most easily-understandable role in isoprene metabolism, as glutathione is required to detoxify epoxyisoprene to form HGMB, catalysed by IsoI (van Hylckama Vlieg *et al*. 1998, 1999, 2000). Therefore, GarB may replenish intracellular stores of reduced glutathione, allowing the detoxification process to continue. The genome of *Variovorax* sp. WS11 contains three copies of *garB*, each with less than 50% identity at the amino acid level with the others (Table 3.4). When analysed by the protein-based Basic Local Alignment Search Tool (BLASTp), all three *garB* genes had the same predicted domains (Altschul *et al*. 1990). These were a pyruvate/2-oxoglutarate dehydrogenase complex, a small NADH binding domain, and a glutathione-disulfide reductase domain. The only difference in domain composition was that *garB_1* and *garB_2* contained a plant-like glutathione-disulfide reductase domain while *garB_3* contained an animal/bacterial-like glutathione disulfide domain. GarB_1 is likely to be widespread in *Variovorax* spp., as BLASTp analysis identified homologous peptides almost entirely within this genus. The *garB_1* and *garB_2* genes were both located on the chromosome of

Variovorax sp. WS11, and *garB_2* was primarily related to non-*Variovorax*-specific peptides when studied by BLASTp analysis. However, *garB_3* was highly related (87%) to a glutathione-disulfide reductase gene found in a metagenome-derived *Variovorax* spp. from an isoprene-enriched poplar phyllosphere study (accession no. RZL94151) (Crombie *et al*. 2018). Overall, this suggests that *Variovorax* sp. WS11 has gained at least two non-genus-specific glutathione-disulfide reductase genes, likely to aid in the recycling of reduced glutathione (Deponte 2013). Only *garB_3* (elsewhere referred to as *garB*) was located with the *iso* metabolic gene cluster, indicating that other metabolic pathways may require specific systems to recycle reduced glutathione.

Table 3.4. Percentage identity and percentage coverage (shown in brackets) of translated glutathione disulfide reductase genes in *Variovorax* sp. WS11, determined by BLASTp analysis (Altschul *et al*. 1990). *garB_3* is located downstream of the *iso* metabolic gene cluster.

	garB_1	*garB_2*	*garB_3 (iso)*
garB_1	100 (100)	47.2 (64)	45.3 (60)
garB_2	47.2 (64)	100 (100)	42.9 (57)
garB_3 (iso)	45.3 (60)	42.9 (57)	100 (100)

All *iso* metabolic genes in *Variovorax* sp. WS11 are located on a megaplasmid (discussed in Chapter 4). Initial analysis of the proteome indicated that a mixture of peptides encoded on megaplasmid 1 and on the chromosome were upregulated when grown on isoprene. Some of these genes were related to the β-oxidation pathway suggested by van Hylckama Vlieg *et al*. (2000), with predicted functions including fatty acid CoA-ligase, methylmalonyl-CoA mutase, propionyl-CoA carboxylase, and enoyl-CoA hydratase (Jimenez-Diaz *et al.* 2017). However, the relative abundances of these peptides were typically between 3-10, compared to growth on succinate. All of these genes were located on the chromosome of *Variovorax* sp. WS11. A cluster of four peptides were upregulated on isoprene compared to succinate with roles in the methylcitrate cycle, a pathway which combines propionyl-CoA and oxaloacetate to form 2-methylcitrate (Eoh & Rhee 2014), yielding succinate and pyruvate. All of these peptides were upregulated when grown using isoprene, with relative expressions between 3.44-6.58, and were located on Megaplasmid 1. As the methylcitrate pathway requires propionyl-CoA, a compound which is formed through the β-oxidation pathway, and the genes were located on the same plasmid as the *iso* metabolic gene cluster, it is likely that *Variovorax* sp. WS11 uses the methylcitrate pathway to assimilate isoprene-derived carbon.

3.5.7.2. **Differential expression of Iso peptides over time in *Variovorax* sp. WS11**

The data discussed in Section 3.5.7.1 were retrieved from OrbiTrap analyses run on unfractionated samples, reducing the coverage of individual peptides, and no information was retrieved regarding isoprene-induced changes in peptide abundance over time. New samples were prepared in order to study the degree of expression of Iso metabolic peptides over time (as described in Section 2.13.1). The degree of upregulation in peptide expression was

calculated by using uninduced (Timepoint 0) samples as a baseline. Expression of Iso peptides was not significantly increased after growth on succinate at any of the tested timepoints ($p \geq 0.05$), although IsoI expression increased 2.57-fold after 24 hours (Figure 3.21). IsoI also exhibited the fastest increase in expression during growth on isoprene, with a significant increase of 5.16-fold after 6 hours, compared to the uninduced control ($p \leq 0.01$, determined by background-based *t* test) (Figure 3.20). All Iso metabolic peptides were significantly upregulated above the uninduced control after 24 hours of growth on isoprene ($p \leq 0.01$), with IsoI and IsoB expression increasing between 2- and 12.5-fold more than other Iso peptides. These encode a glutathione *S*-transferase, responsible for the glutathione-dependent detoxification of epoxyisoprene, and the IsoMO γ-oxygenase subunit, respectively (van Hylckama Vlieg *et al*. 2000, Leahy *et al*. 2003). Aside from IsoB, the peptides which catalyse the steps of isoprene metabolism after the formation of epoxyisoprene by IsoMO were the most highly expressed. This indicated the relative importance of the subsequent steps in isoprene metabolism when compared to the initial oxidation of isoprene. The ferredoxin component of IsoMO, IsoC, was the only Iso peptide to be present at a lower abundance after 30 hours of growth on isoprene compared to 24 hours. IsoC is predicted to act as a shuttle for electrons between the reductase component (IsoF) and oxygenase component (IsoABE) of isoprene monooxygenase, as found in other SDIMO (Leahy *et al*. 2003, Blazyk *et al*. 2005). The decrease in expression of IsoC is particularly curious when considering the fact that all other Iso peptides increased in abundance from 24 to 30 hours (Figure 3.20, Figure 3.22). It is interesting to note that the expression of IsoA and IsoD initially decreased after 6 hours of growth on isoprene, while the peptides which catalyse the subsequent steps of the pathway were all upregulated. The decrease in IsoA abundance, especially, may indicate an initial requirement of the cell to increase the abundance of the epoxide-detoxifying apparatus before upregulating the expression of IsoMO, thus preventing dangerous accumulations of epoxyisoprene.

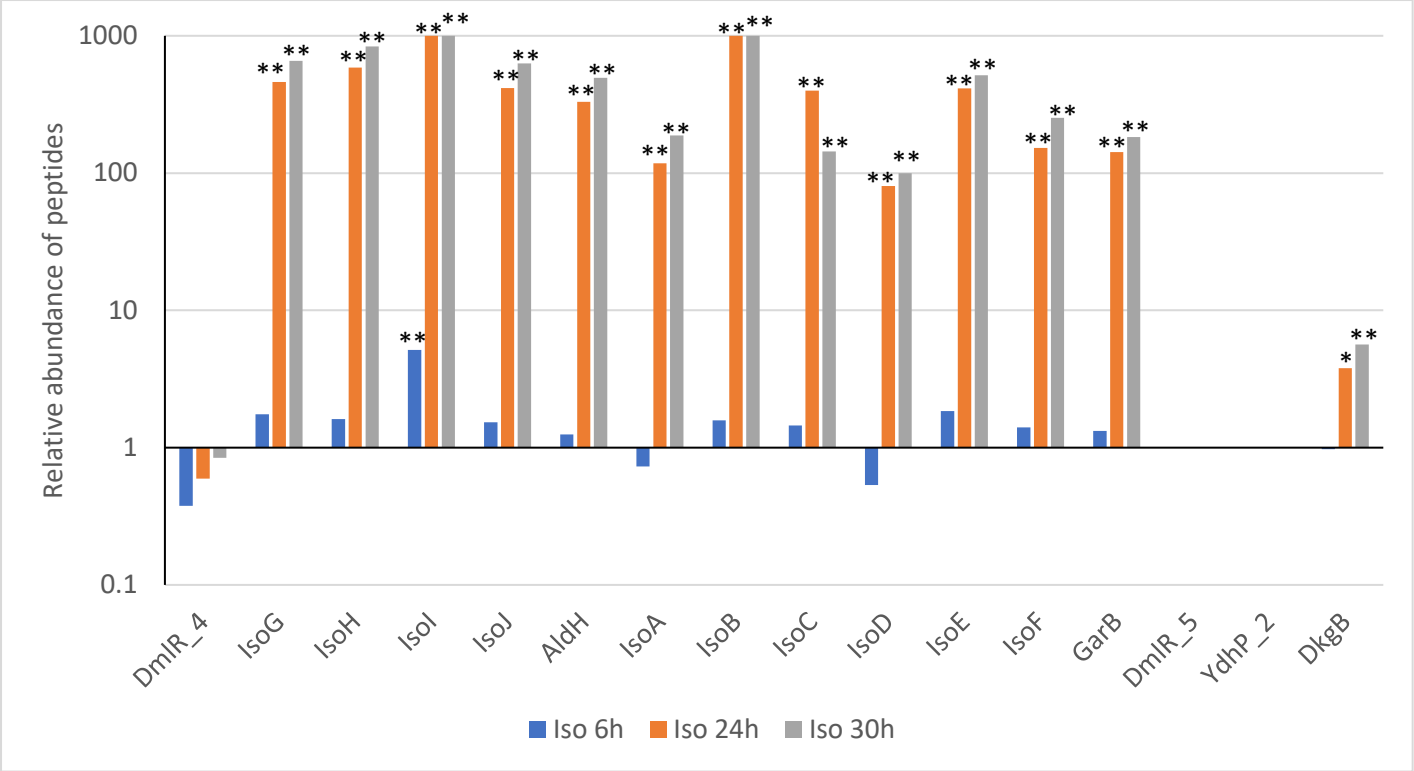

Figure 3.20. Ratio of abundance of peptides encoded by the *iso* metabolic gene cluster over time during growth on isoprene, compared to the uninduced control. These data were calculated as the average of two biological replicates. Asterisks indicate a statistically significant difference between the indicated condition and the uninduced control (* p≤0.05, ** p≤0.01).

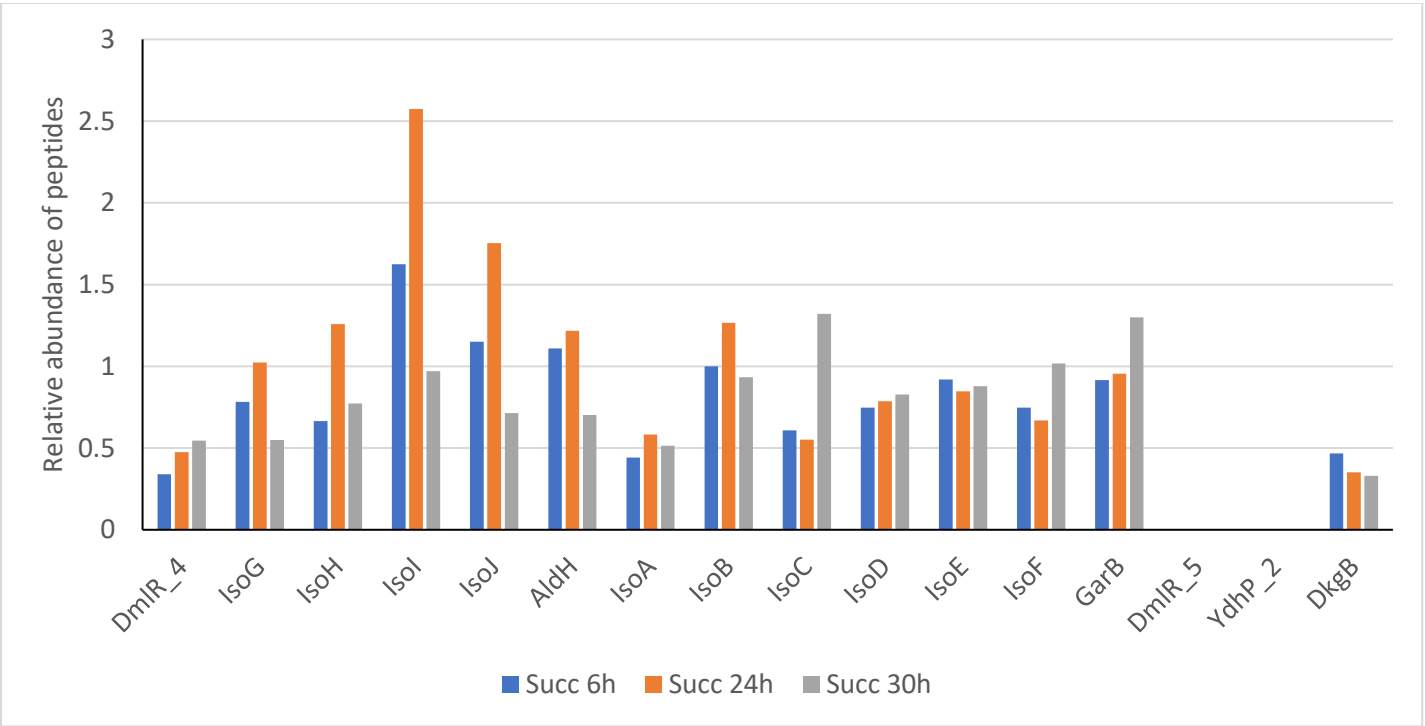

Figure 3.21. Ratio of abundance of peptides encoded by the *iso* metabolic gene cluster over time during growth on succinate, compared to the uninduced control. These data were calculated as the average of two biological replicates.

IsoGHI and IsoA were all present at higher abundances than IsoJ and the other IsoMO components in the uninduced control (Figure 3.22). These more abundant peptides may play roles in the ability of *Variovorax* sp. WS11 to sense isoprene, and in the initial response of this bacterium to the catabolism of isoprene. IsoA encodes the α-oxygenase component of IsoMO, containing the active site of the enzyme (Leahy *et al*. 2003), and would therefore be essential to catalyse the initial oxidation of isoprene to epoxyisoprene, which in turn would induce the expression of the whole *iso* metabolic gene cluster (Crombie *et al*. 2015). IsoI catalyses the detoxification of epoxyisoprene (van Hylckama Vlieg *et al*. 1998, 1999, 2000), and would therefore be necessary to prevent toxic effects to *Variovorax* sp. WS11 caused by the epoxide. GarB, a putative glutathione-disulfide reductase, was present at approximately the same abundance as the IsoMO components in the uninduced and isoprene-induced samples, further indicating the role of this protein in isoprene metabolism (described in Section 3.5.7.1). Maintaining a low level of expression of all Iso peptides in the absence of isoprene would allow *Variovorax* sp. WS11 to initially sense and respond to the presence of isoprene while also preventing toxicity due to epoxyisoprene accumulation. In this context, the initial decrease in IsoA expression concurrent with increases in IsoGHIJ expression during the first 6 hours of growth on isoprene indicated that *Variovorax* sp. WS11 was preparing for the accumulation of toxic epoxyisoprene caused by isoprene oxidation (Figure 3.20). Curiously, DmlR_5 and YdhP_2 peptides were not detected in the proteome of *Variovorax* sp. WS11 under any of the tested conditions.

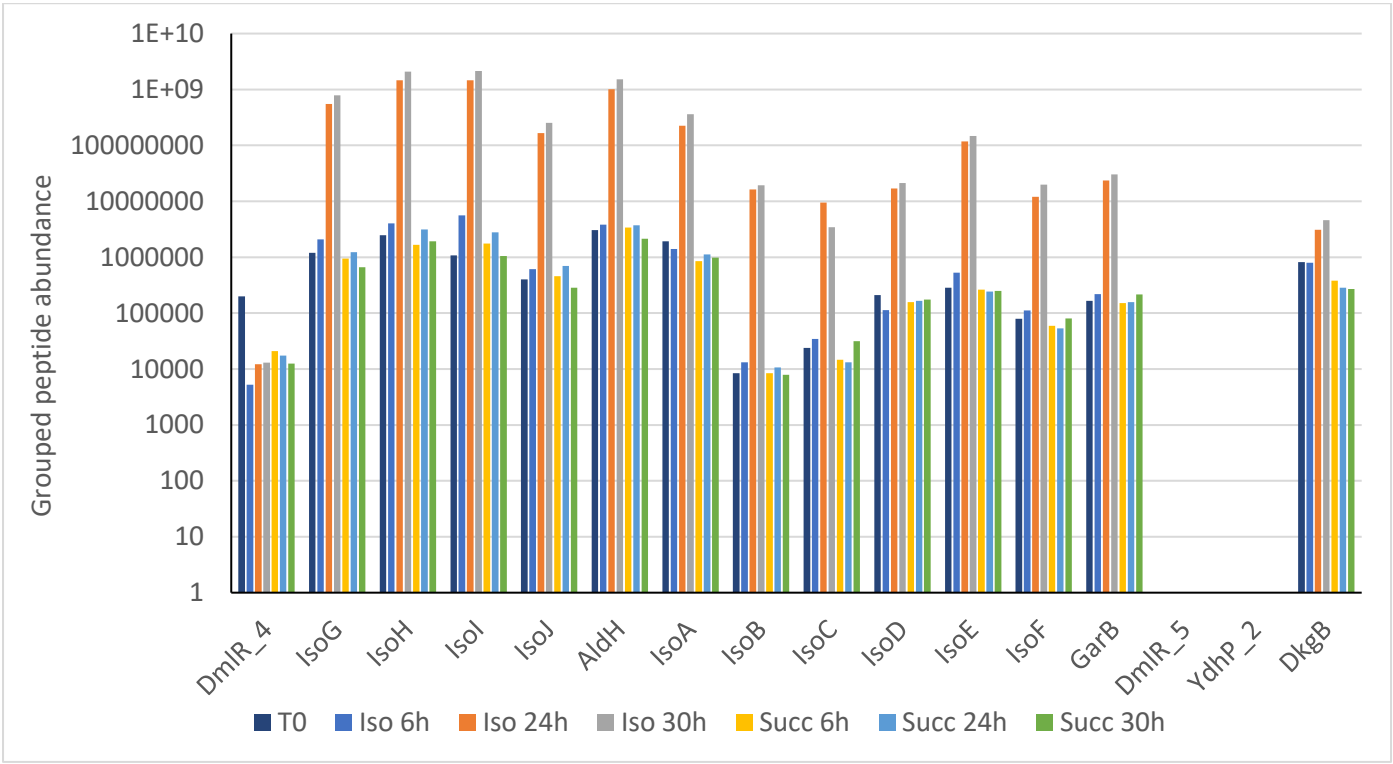

Figure 3.22. Abundance of individual peptides encoded by the *iso* metabolic gene cluster during growth on isoprene or succinate, compared to the uninduced control (T0). These data were calculated as the average of two biological replicates.

3.5.7.3. **Abundance and differential expression of peptides relating to β-oxidation**

Peptides encoded by many gene clusters were differentially expressed when *Variovorax* sp. WS11 was grown on isoprene. Many of these were related to the oxidation of fatty acids, supporting the hypothesis by van Hylckama Vlieg *et al*. (2000) that isoprene metabolism may resemble isoleucine catabolism due to the use of β-oxidation. Metabolism of fatty acids by β-oxidation reduces the length of a carbon skeleton by liberating acetyl-CoA, producing shorter CoA-thioesters (Jimenez-Diaz *et al*. 2017). A CoA-thioester is initially formed by conjugation of the carboxylic acid chain with CoA, catalysed by a fatty acid-CoA ligase. FAD-dependent oxidation of the fatty acid chain occurs due to an acyl-CoA dehydrogenase, followed by the hydration of the newly formed C=C double-bond by an enoyl-CoA hydratase (Figure 3.23). A 3-hydroxyacyl-CoA dehydrogenase then catalyses the NAD^+-dependent oxidation of the hydroxyl group to a ketone group, followed by thiolysis catalysed by a 3-ketoacyl-CoA thiolase.

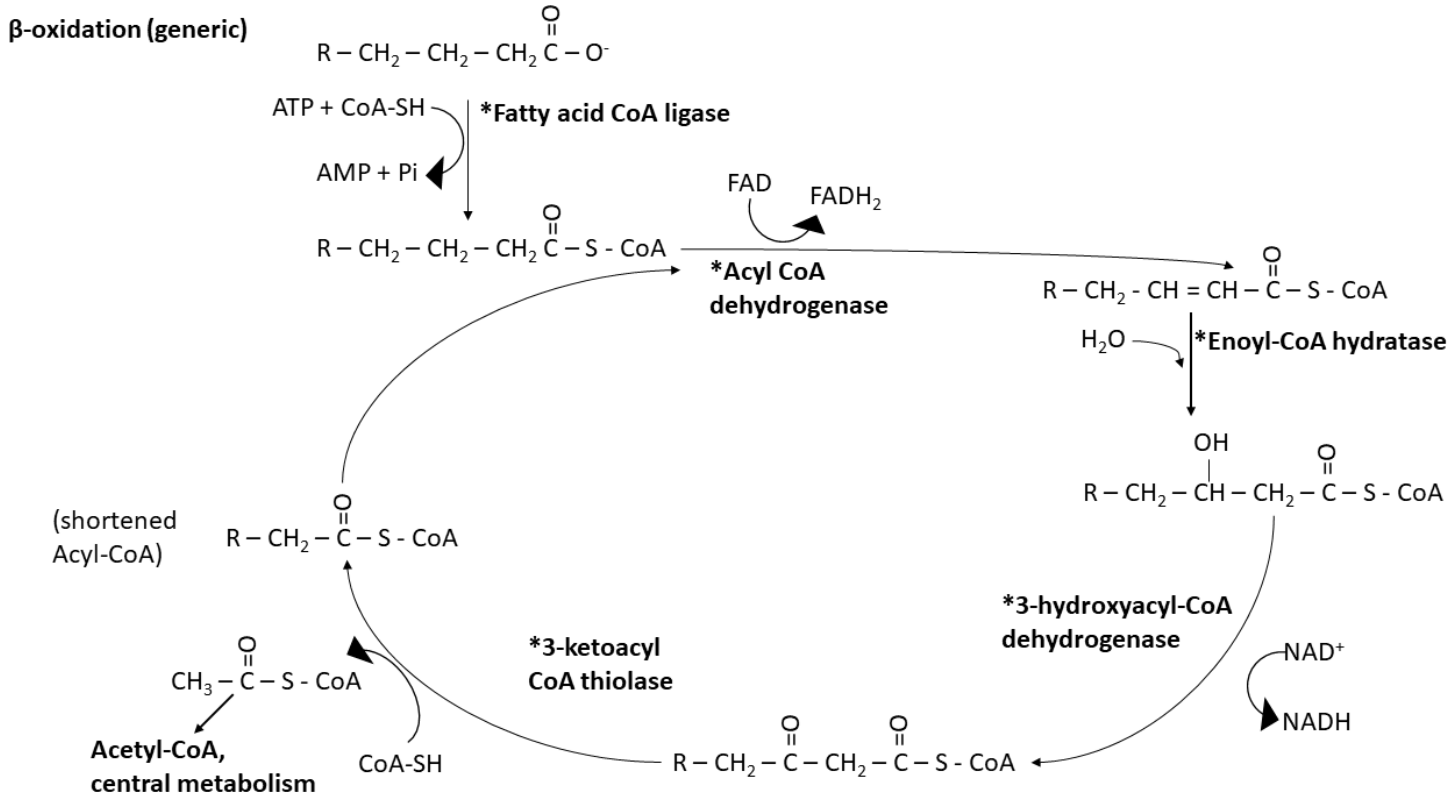

Figure 3.23. Generic scheme of β-oxidation, breaking down a long-chain fatty acid to acetyl-CoA and a shorter-chain fatty acid. Adapted from Jimenez-Diaz *et al*. (2017). An asterisk denotes the name of the enzyme which catalyses the reaction in question.

Expression of the above peptides, with the exception of 3-hydroxyacyl-CoA dehydrogenase and 3-ketoacyl-CoA thiolase, increased significantly during growth on isoprene ($p \leq 0.01$) (Table 3.5), indicating the viability of this metabolic pathway in isoprene metabolism. Two isoprene-induced copies of a long-chain fatty-acid CoA ligase were present at different sites in the genome of *Variovorax* sp. WS11, each located with other genes related to fatty acid metabolism. It should be noted that, although 3-hydroxyacyl-CoA dehydrogenase was downregulated over the

course of growth on isoprene, the overall abundance of this protein was very high, decreasing from 9,399,514 to 6,982,277 between 6 hours and 30 hours. For comparison, the abundance of several IsoMO components was approximately 10,000,000 after induction. Two 3-ketoacyl-CoA thiolase peptides were present at different abundances (Table 3.5). In descending order in Table 3.5, the abundances of the 3-ketoacyl-CoA thiolase peptides changed from 4,636,017 to 5,924,182, and 59,264,989 to 47,538,806 between 6 and 30 hours of growth on isoprene. Therefore, although only the former gene was upregulated during growth on isoprene, it is likely that the sheer abundance of these peptides, particularly of the latter enzyme candidate, resulted in the contribution of a 3-ketoacyl-CoA thiolase to β-oxidation in *Variovorax* sp. WS11.

Table 3.5. Peptides with predicted roles in β-oxidation expressed by *Variovorax* sp. WS11 during growth on isoprene (Iso) or succinate (Succ) at 6 hours (6h), 24 hours (24h), or 30 hours (30h) post-inoculation. Peptides which were significantly expressed during growth on isoprene are indicated in bold ($p \leq 0.01$). These data were calculated as the average of two biological replicates.

Peptide	Iso-6h	Iso-24h	Iso-30h	Succ-6h	Succ-24h	Succ-30h
LcfB (long-chain fatty acid-CoA ligase)	0.81	**14.20**	**37.18**	0.59	0.57	0.47
LcfB (long-chain fatty acid-CoA ligase)	**21.36**	**22.25**	**20.74**	4.43	3.10	2.97
Acyl-CoA dehydrogenase	1.64	**18.98**	**25.18**	0.43	1.88	1.53
Probable 3-hydroxyacyl-CoA dehydrogenase	0.92	0.71	0.69	0.36	0.38	0.58
3-ketoacyl-CoA thiolase	1.01	1.30	1.29	1.1	1.02	1.52
3-ketoacyl-CoA thiolase	1.15	0.91	0.92	0.94	0.97	0.99

3.5.7.4. **Predicting the isoprene metabolic pathway in *Variovorax* sp. WS11 using proteomic data**

A scheme of isoprene metabolism was proposed by Dr. A. Crombie (Figure 3.24). This predicted metabolic pathway did not utilise many of the enzymes required for the β-oxidation pathway suggested by Van Hylckama Vlieg *et al*. (2000), instead using an acetyl-CoA acetyltransferase to generate propionyl-CoA and acetyl-CoA (Figure 3.24). A key step of β-oxidation is the incorporation of a CoA moiety, which was suggested to be catalysed by IsoG, identified by BLASTp as a putative CoA transferase with potential racemase activity (Altschul *et al*. 1990, van Hylckama Vlieg *et al*. 2000, Crombie *et al*. 2015). No CoA donor has been discovered at the time of writing. Glutathione must be liberated in order for the CoA-conjugated intermediate to be incorporated into central metabolism. This is likely to be catalysed by IsoJ, a putative glutathione *S*-transferase which demonstrated no activity towards HGMB (van Hylckama Vlieg *et al*. 2000). Oxidised glutathione-disulfide (GSSG) would then be regenerated to reduced glutathione using GarB (Deponte 2013). Subsequent activity by an enoyl-CoA hydratase would hydroxylate the C=C bond at position 4, forming a sub-terminal hydroxyl group (Agnihotri & Liu 2003). Alternatively, following the ligation of GMBA with CoA by IsoG, or potentially by a fatty acid CoA ligase, the alkene group at position 4 could be hydroxylated by an enoyl-CoA hydratase, and glutathione could then be removed by IsoJ. Following the generation of a hydroxylated intermediate by enoyl-CoA hydratase, a second step requiring IsoH or AldH was proposed in which NAD^+ or $NADP^+$, respectively was used to oxidise the sub-terminal hydroxyl to a C=O group, followed by thiolysis by the addition of a

second CoA group by an acetyl-CoA acetyltransferase (Jimenez-Diaz *et al*. 2017). This would form acetyl-CoA and propionyl-CoA.

Isoprene-derived propionyl-CoA could be assimilated into central metabolism by two mechanisms: conversion to succinate via methylmalonyl-CoA (Halarnkar & Blomquist 1989, Wongkittichote *et al*. 2017), or assimilation through the methylcitrate cycle (Eoh & Rhee 2014). The former route would be initiated by the conversion of propionyl-CoA to methylmalonyl-CoA, catalysed by the biotin-dependent propionyl-CoA carboxylase (Wongkittichote *et al*. 2017). Propionyl-CoA carboxylase was expressed with a relative peptide abundance of 11.3 after 30 hours of growth on isoprene, supporting the use of this reaction. *accA1* (encoding acetyl-/propionyl-CoA carboxylase) is located immediately downstream of biotin synthesis genes which were also upregulated during growth on isoprene, providing further credence to this theory. A vitamin B_{12}-dependent methylmalonyl-CoA mutase, which was expressed at an abundance of 5.3 after 30 hours on isoprene compared to the uninduced control, would then catalyse the conversion of methylmalonyl-CoA to succinyl-CoA (Wongkittichote *et al*. 2017). Finally, succinate-CoA ligase catalyses the ATP-dependent removal of CoA-SH, forming succinate. The α-subunit of succinate-CoA ligase was initially upregulated with an abundance of 10.7 after 6 hours on isoprene, falling to 4.5 after 30 hours.

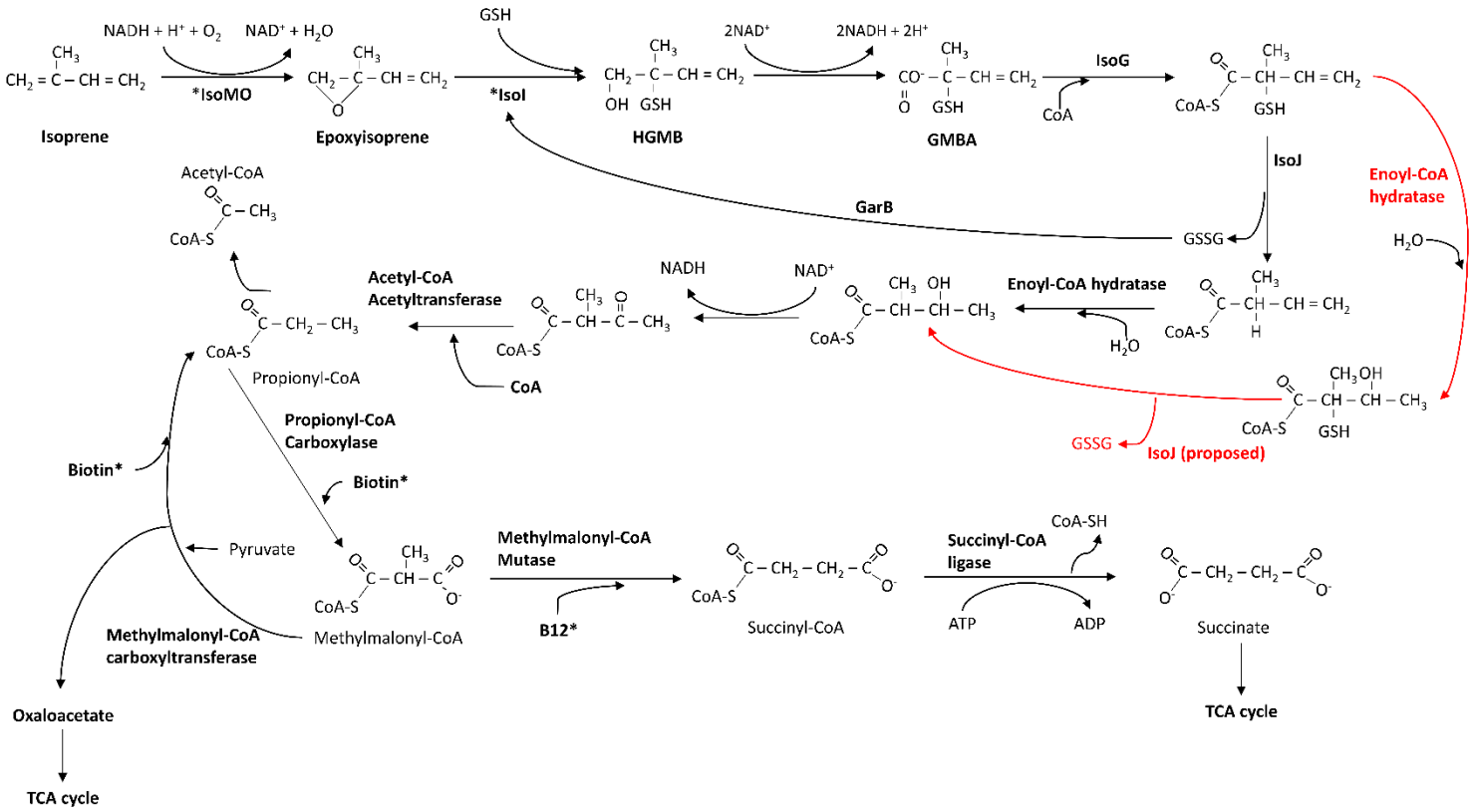

Figure 3.24. Isoprene metabolic pathway proposed by Dr. A. Crombie, in which IsoG and IsoJ act as a CoA-ligase and a glutathione *S*-transferase, respectively. Enzymatic steps were inferred using available proteomic data. The vitamin cofactors, biotin and vitamin B12 (Vit B12) are indicated with asterisks. Red arrows denote alternative, plausible metabolic reactions.

The second potential route of propionyl-CoA assimilation into central metabolism involves the methylcitrate pathway (Figure 3.25). Previous studies have identified this as an essential pathway for the metabolism of propionyl-CoA derived from β-oxidation of odd-chain fatty acids (Eoh & Rhee 2014, Dolan *et al*. 2018). The methylcitrate cycle requires specific enzymes; methylcitrate synthase, methylisocitrate lyase, 2-methylaconitate isomerase, and aconitate hydratase (Eoh & Rhee 2014). With the exception of aconitate hydratase, the expression of each of these proteins was significantly upregulated ($p \leq 0.01$) when *Variovorax* sp. WS11 was grown on isoprene, and downregulated when grown on succinate (Table 3.6). The genes which encode these enzymes were all located on megaplasmid 1, with the exception of the chromosomally-encoded aconitate hydratase, the same plasmid which contains the *iso* metabolic gene cluster (described in Chapter 4). From this, it can be inferred that isoprene metabolism by *Variovorax* sp. WS11 progresses via propionyl-CoA (as in Figure 3.25), which is then converted to pyruvate and succinate by the plasmid-encoded methylcitrate cycle (Table 3.6). However, an alternative route of propionyl-CoA assimilation via methylmalonyl-CoA cannot be discounted (as described above). The implication that *Variovorax* sp. WS11 assimilates isoprene via the methylcitrate and methylmalonyl-CoA pathways indicates that metabolism of isoprene in this bacterium diverged from *Rhodococcus* sp. AD45, as analysis of the transcriptome of *Rhodococcus* sp. AD45 after induction by isoprene or epoxyisoprene did not identify increased expression of isocitrate lyase, malate synthase, genes associated with methylmalonyl-CoA assimilation, or methylcitrate pathway-encoding genes (Crombie *et al*. 2015). Although transcriptomic and proteomic data cannot be directly compared, a difference in the methods of assimilation of isoprene-derived carbon skeletons is indicated.

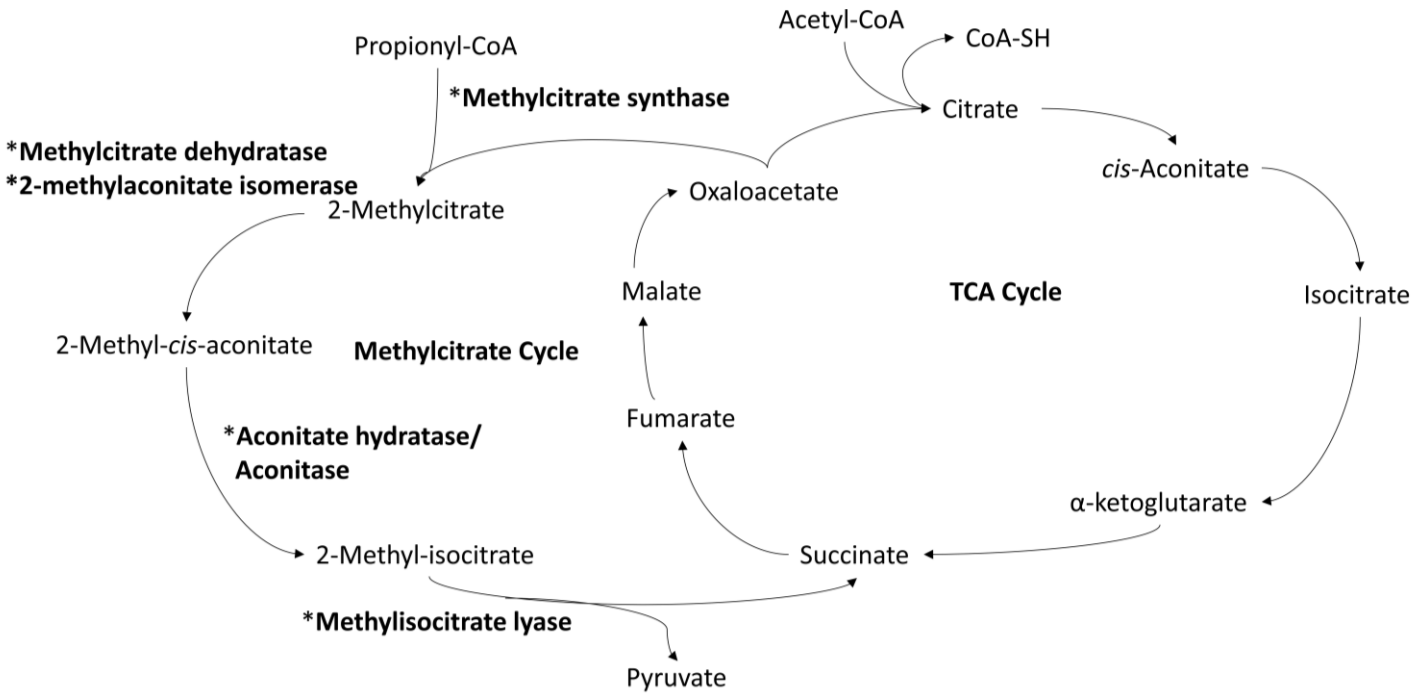

Figure 3.25. Methylcitrate cycle converting propionyl-CoA, which is produced by β-oxidation of odd-chain fatty acids, and oxaloacetate to succinate and pyruvate (adapted from Dolan *et al.* 2018).

Table 3.6. Relative abundance of methylcitrate cycle-related enzymes during growth of *Variovorax* sp. WS11 on isoprene or succinate, compared to the uninduced control. Peptides which were significantly expressed during growth on isoprene are indicated in bold (p≤0.01). These data were calculated as the average of two biological replicates.

Description	Isoprene-6h	Isoprene-24h	Isoprene-30h	Succinate-6h	Succinate-24h	Succinate-30h
2-methylcitrate synthase	0.81	**93.80**	**111.16**	0.72	0.79	0.65
2-methylcitrate synthase	0.71	**81.79**	**91.41**	0.93	0.64	0.26
2-methylcitrate dehydratase	0.86	**43.94**	**71.89**	0.69	0.72	0.89
2-methyl-aconitate isomerase	1.37	**32.87**	**56.83**	0.46	0.45	0.40
Methylisocitrate lyase	0.72	**23.79**	**41.64**	0.21	0.39	0.23
Aconitate hydratase A	1.05	1.46	1.12	0.45	0.48	0.32
Aconitate hydratase B	1.01	1.40	1.41	2.00	2.03	2.15

3.5.7.5. Roles of biotin and vitamin B12 in the growth of *Variovorax* sp. WS11 using isoprene

Incorporation of isoprene by the metabolic pathway proposed in Figure 3.24 indicated a role for both biotin and vitamin B12. The highly expressed propionyl-CoA carboxylase (described in Section 3.5.7.4) catalyses the biotin-dependent formation of methylmalonyl-CoA (Wongkittichote *et al*. 2017). The reverse reaction, catalysed by methylmalonyl-CoA carboxyltransferase (Figure 3.24), is also biotin-dependent (Carey *et al*. 2004). The latter enzyme was expressed 19.1-times more after 30 hours of growth on isoprene compared to the uninduced control. While biotin is supplied in MAMS vitamins (Section 2.2.1), biotin synthase was significantly upregulated during the growth of *Variovorax* sp. WS11 on isoprene (p≤0.01), with a relative peptide abundance of 8.4 after 30 hours of growth. During growth on succinate, biotin synthase was only upregulated after 6 hours. Collectively, these data indicated the importance of biotin in isoprene metabolism, and also indicated that *Variovorax* sp. WS11 may synthesise biotin *de novo* in order to sustain growth on isoprene.

Vitamin B12 is required for the activity of methylmalonyl-CoA mutase, an enzyme which catalyses the conversion of methylmalonyl-CoA to succinyl-CoA (Takahashi-Iñiguez *et al*. 2012). Approximately 30 genes have been identified with roles in vitamin B12 (cobalamin) biosynthesis (Roth *et al*. 1993, Raux *et al*. 1996), but only 5 *cob* genes (*cobDGNSU*) were located in the genome of *Variovorax* sp. WS11, each at different locations, indicating the inability of this bacterium to synthesise vitamin B12 *de novo*. Instead, vitamin B12 (cyanocobalamin) was supplied as a part of the MAMS vitamins solution (Section 2.2.1). The predicted isoprene metabolic pathway suggests that *Variovorax* sp. WS11 would be able to continue metabolising isoprene even under conditions of vitamin B12 limitation, as the biotin-dependent methylmalonyl-CoA carboxyltransferase would allow the continued generation of carbon skeletons via oxaloacetate (Figure 3.24). The methylcitrate cycle would also provide an alternative method for the incorporation of isoprene in the absence of vitamin B12, as propionyl-CoA would be introduced into the TCA cycle via methylcitrate (Figure 3.25), bypassing succinyl-CoA as an intermediate and negating the need for vitamin B12.

It was previously observed that the exclusion of the MAMS vitamin solution prevented the growth of *Variovorax* sp. WS11 in liquid culture (described in Section 3.4.1). MAMS vitamin solution was modified to exclude either biotin, vitamin B12, or both vitamins, and *Variovorax* sp. WS11 was grown in Ewers medium with 1% (v/v) isoprene, supplied with one of the three modified MAMS vitamins solutions (Figure 3.26). Growth on isoprene was unaffected by the loss of biotin. Within 48 hours, *Variovorax* sp. WS11 had reached a final OD_{540} of approximately 0.4, likely due to the expression of biotin synthase facilitating the incorporation of propionyl-CoA via propionyl-CoA carboxylase and methylmalonyl-CoA carboxyltransferase (Carey *et al*. 2004). A slight decrease in the rate of growth on isoprene was observed when *Variovorax* sp. WS11 was deprived of vitamin B12 (Figure 3.26). Methylmalonyl-CoA mutase requires vitamin B12 (Takahashi-Iñiguez *et al*. 2012), meaning that *Variovorax* sp. WS11 may not have been able to synthesise succinyl-CoA directly from methylmalonyl-CoA. However, the fact that *Variovorax* sp. WS11 was still able to grow to a final OD_{540} of 0.38 indicated that isoprene-derived carbon was still incorporated via either the biotin-dependent methylmalonyl-CoA pathway (Figure 3.24) or the methylcitrate cycle (Eoh & Rhee 2014). When growing under conditions of vitamin B12-deficiency, *Variovorax* sp. WS11 may also generate pyruvate via the methylcitrate cycle which could then act as a substrate for the generation of oxaloacetate by methylmalonyl CoA-carboxyltransferase (Carey *et al*. 2004). Likewise, the generation of succinate by the methylcitrate cycle would bypass the vitamin B12-dependent generation of succinyl-CoA from methylmalonyl-CoA. When deprived of both biotin and vitamin B12, *Variovorax* sp. WS11 demonstrated the greatest decrease in growth on isoprene (Figure 3.26), significantly lower from 40-46 hours than the vitamin B12-deprived culture ($p \leq 0.05$). After 46 hours, the biotin-deprived culture had grown to a significantly higher OD_{540} than the other conditions ($p \leq 0.05$), indicating that the loss of vitamin B12 had the greatest impact on growth. The OD_{540} of cultures grown in the absence of both vitamins were approximately equal to the unhindered cultures after 64 hours of growth, but the increased lag period and slower growth rate indicated that *Variovorax* sp. WS11 was required to adopt a less efficient strategy for growth on isoprene. These data indicated that biotin supplied in MAMS vitamins was sufficient to partially complement the growth of *Variovorax* sp. WS11 in the absence of vitamin B12, while cultures grown in the absence of both vitamins had to synthesise biotin *de novo* to support growth on isoprene.

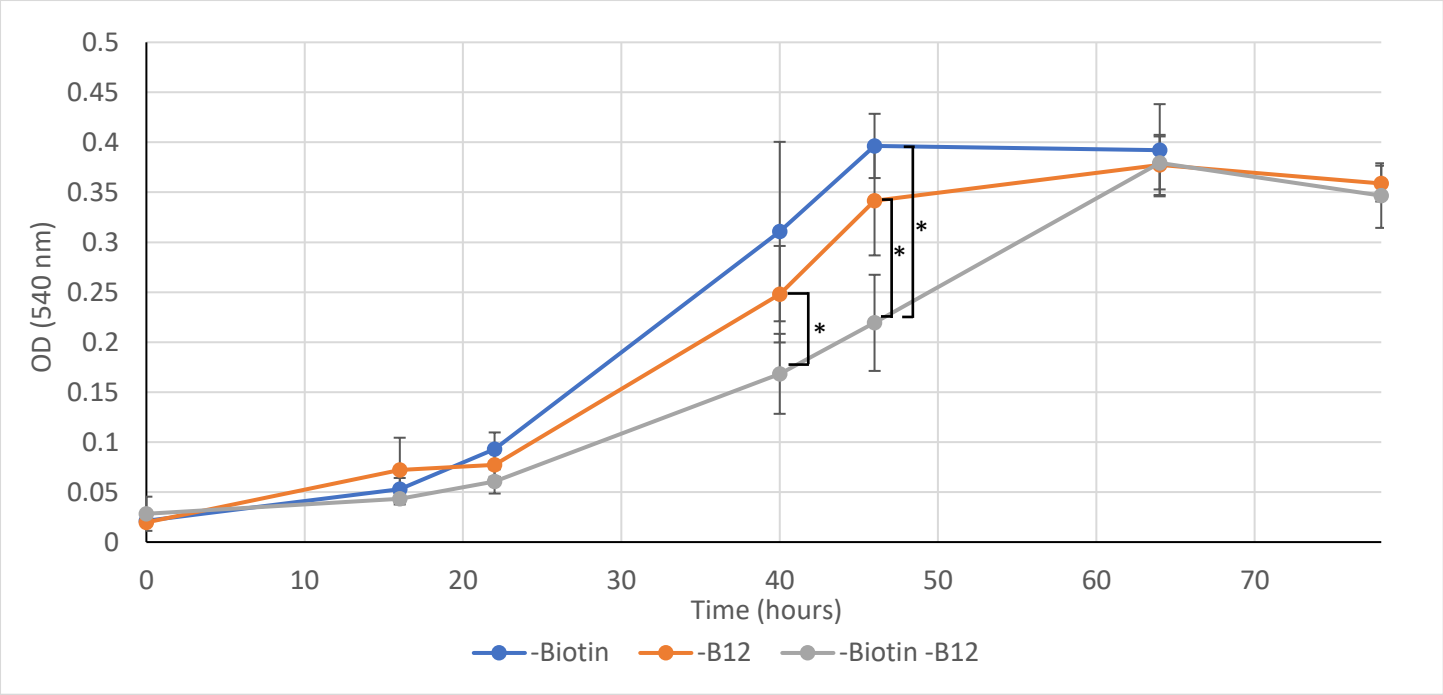

Figure 3.26. Growth of *Variovorax* sp. WS11 on 1% (v/v) isoprene when deprived of exogenously-supplied biotin (-Biotin), vitamin B12 (-B12), or both vitamins (-Biotin -B12). Error bars represent the standard deviation about the mean of three biological replicates. Asterisks denote a statistically significant difference between the indicated conditions (* $p \leq 0.05$).

As the loss of vitamin B12 had varying effects on the growth of *Variovorax* sp. WS11 on isoprene, depending on the presence or absence of exogenously-supplied biotin, a further growth experiment was conducted using 10 mM succinate as the sole source of carbon and energy. As expected, *Variovorax* sp. WS11 grew without apparent detrimental effects when deprived of biotin (Figure 3.27). However, growth on succinate was significantly impaired in the absence of vitamin B12 or in the absence of both vitamins ($p \leq 0.01$). This indicated that the presence of biotin was insufficient to facilitate the use of an alternative metabolic pathway as in isoprene metabolism. Vitamin B12 is not directly required by the enzymes of the core TCA cycle (Kennedy 2016), instead only acting as an essential cofactor for the formation of succinyl-CoA from methylmalonyl-CoA in the context of isoprene-fed growth. Therefore, it was not immediately obvious why the absence of vitamin B12 caused such a detrimental effect in *Variovorax* sp. WS11.

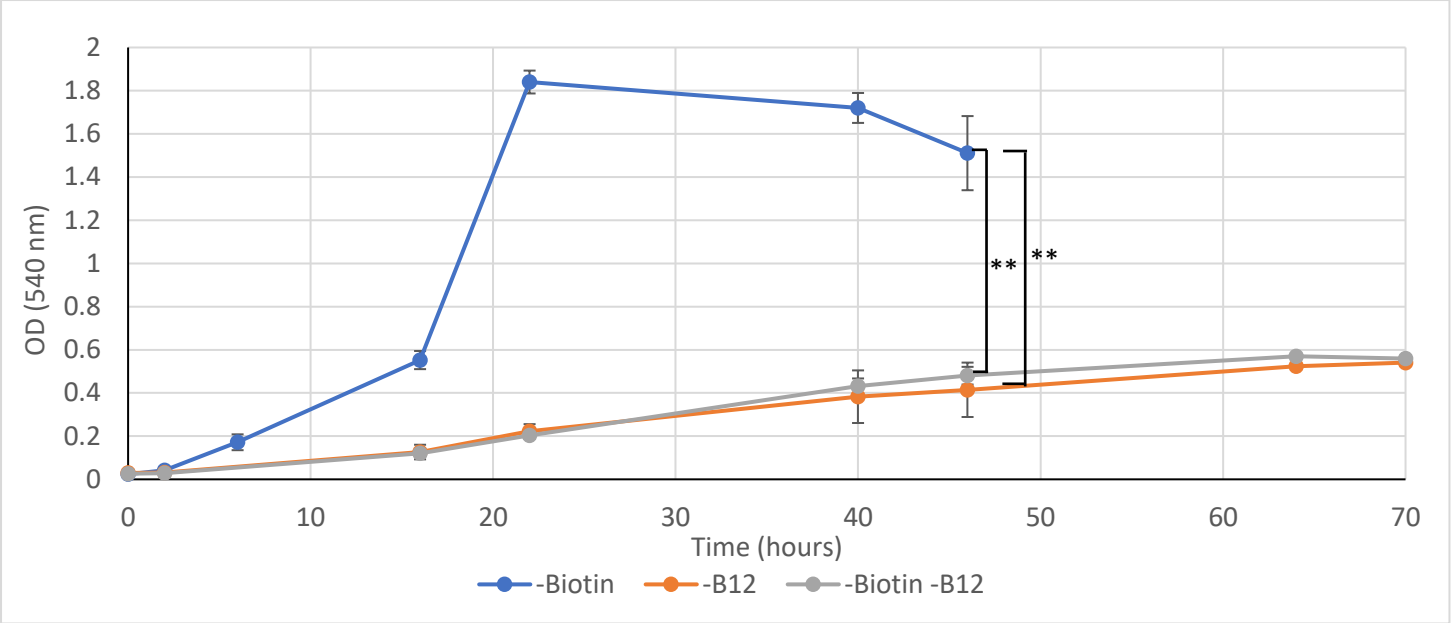

Figure 3.27. Growth of *Variovorax* sp. WS11 on 10 mM succinate when deprived of exogenously-supplied biotin (-Biotin), vitamin B12 (-B12), or both vitamins (-Biotin -B12). Error bars represent the standard deviation about the mean of three biological replicates. Asterisks denote a statistically significant difference between the indicated conditions (** p≤0.01).

MAMS vitamins was modified to contain 10-times the original concentration of biotin, vitamin B12, or both vitamins (Figure 3.28). None of these conditions resulted in a detectable change in the rate of growth of *Variovorax* sp. WS11 on isoprene, even when vitamin B12 was removed from the high-biotin vitamin solution. These data indicated that increased concentrations of biotin were sufficient to overcome any growth impediment resulting from the lack of vitamin B12. This may be due to an increase in the activity of the biotin-dependent enzymes propionyl-CoA carboxylase and methylmalonyl-CoA carboxyltransferase (as described above), facilitating the incorporation of isoprene-derived carbon via oxaloacetate.

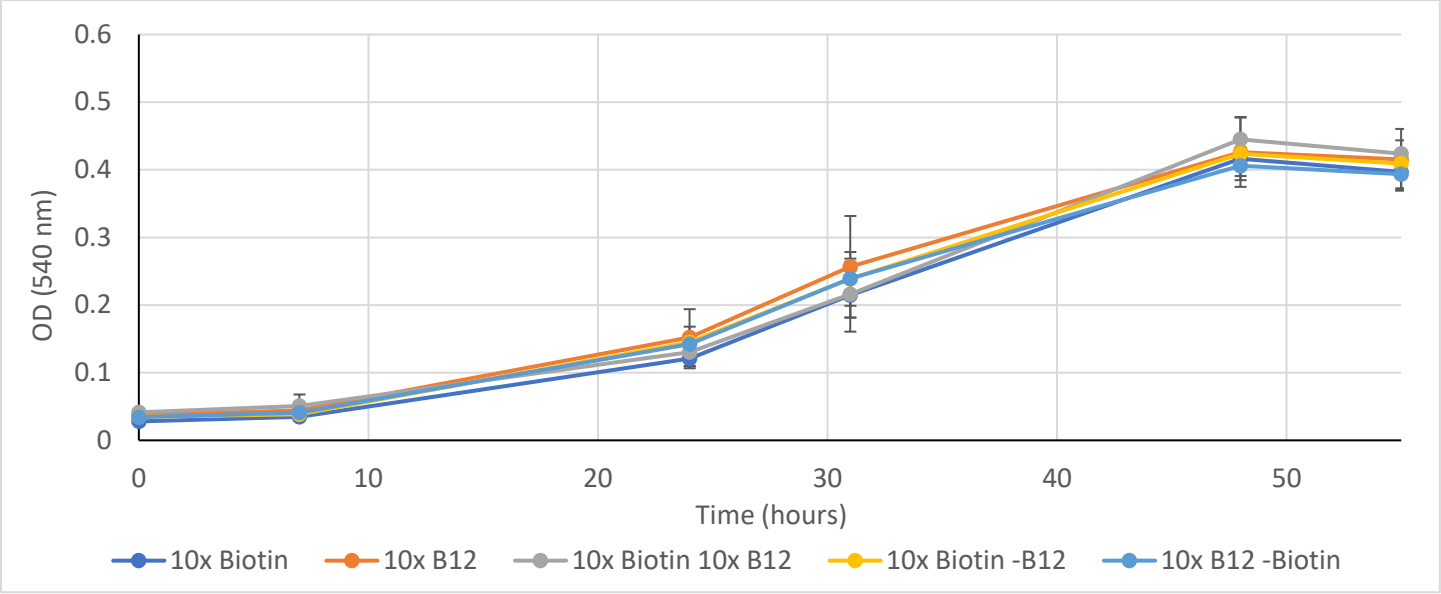

Figure 3.28. Growth of *Variovorax* sp. WS11 on 1% (v/v) isoprene when supplied with increased concentrations of biotin or vitamin B12. Error bars represent the standard deviation about the mean of three biological replicates.

When grown using 10 mM succinate in the presence of increased concentrations of biotin or vitamin B12, no changes in the rate of growth of *Variovorax* sp. WS11 were detected. Growth was significantly slowed over the first 24 hours when vitamin B12 was excluded from the vitamin solution ($p \leq 0.01$) (Figure 3.29). Unlike in the previous experiment (Figure 3.27), *Variovorax* sp. WS11 was able to reach the same final OD_{540} as the other cultures when supplied with 10x the normal concentration of biotin (Figure 3.29). These data indicated a role of biotin in the incorporation of succinate-derived carbon by *Variovorax* sp. WS11.

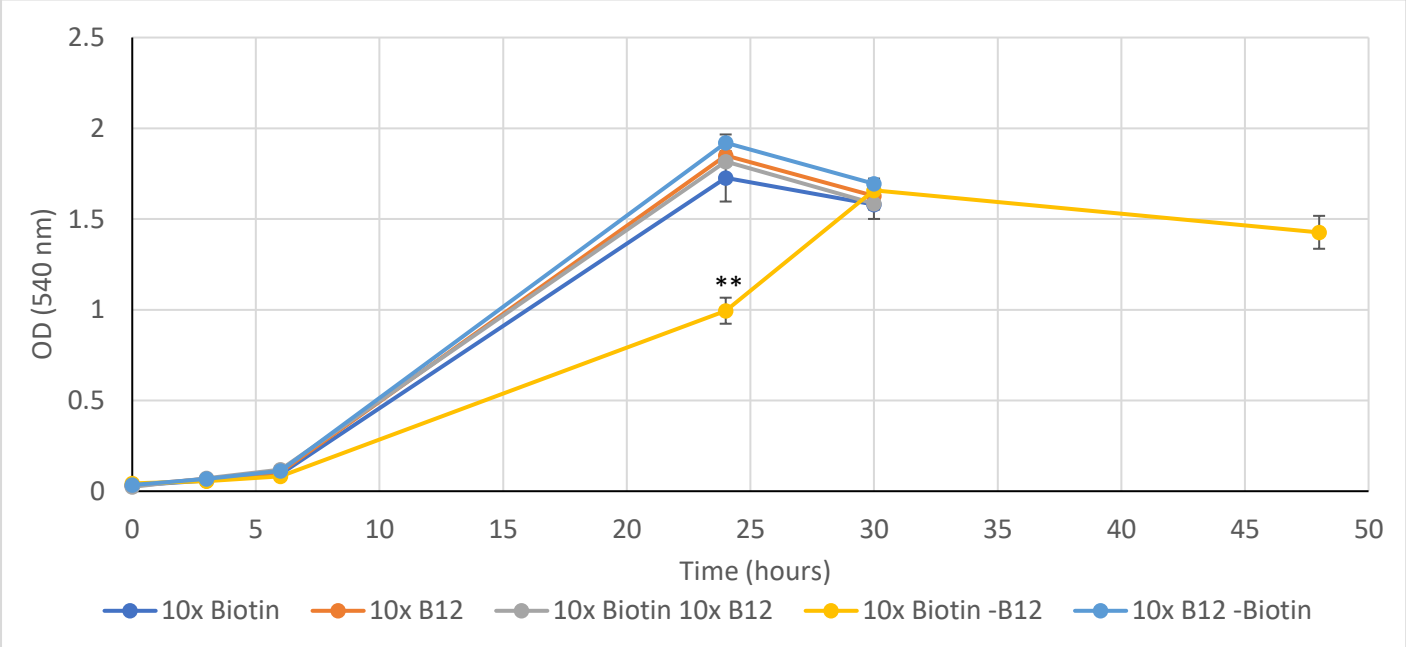

Figure 3.29. Growth of *Variovorax* sp. WS11 on 10 mM succinate when supplied with increased concentrations of biotin or vitamin B12. Error bars represent the standard deviation about the mean of three biological replicates. Asterisks indicate a statistically significant difference between the conditions (** $p \leq 0.01$).

3.5.7.6. **Proteomics analysis indicates copper/cation stress in *Variovorax* sp. WS11**

During growth on both isoprene and succinate, a group of genes which encoded proteins with roles in copper stress resistance were located on a single, significantly expressed gene cluster on the chromosome ($p \leq 0.01$) (Figure 3.30, Table 3.7). YhjQ, which encodes an uncharacterised copper-binding protein, was one of the most highly upregulated peptides during growth on isoprene (Table 3.7). Other highly expressed peptides were copper resistance protein A (*copA_2*), a copper-exporting ATPase (*copA_3*), a periplasmic chaperone which was predicted to act in conjunction with *copA_3* (*cusF*), an outer membrane efflux protein (*tolC*), and a putative plastocyanin (*petE*). The latter had a predicted role as an electron transfer protein. Two hypothetical proteins were also present, one of which (*hypoth_2*) was significantly upregulated during growth on isoprene ($p \leq 0.05$). BLASTp analysis of the translated amino acid sequence of *hypoth_2* failed to identify any conserved sequences (Altschul *et al*. 1990), preventing predictions of the function of this gene. Maintaining appropriate intracellular copper concentrations to facilitate Cu-requiring reactions, while also preventing toxic accumulations of Cu, is essential to bacterial survival (Bondarczuk & Piotrowska-Seget 2013), but the relative level of expression of these genes when *Variovorax* sp. WS11 was grown on isoprene compared to succinate may indicate copper stress under the tested conditions (Table 3.7). The only source of copper supplied in Ewers medium was part of the SL-6 trace elements solution (Quayle & Pfennig 1975), with 1 mg L^{-1} $CuCl_2.2H_2O$, equivalent to 6.8 µM, added at a 1:1000 ratio (Section 2.2.1). A study of copper-related proteome data in other β-proteobacteria stated that copper usage in this class was largely related to aerobic respiration, with small plastocyanin-like proteins being abundant in environmental bacteria (Antoine *et al*. 2019). A predicted plastocyanin (PetE) was also one of the most highly upregulated peptides when *Variovorax* sp. WS11 was grown on isoprene. Overall, these data indicated that the abundance of copper-related peptides in *Variovorax* sp. WS11 under each growth condition occurred as a result of aerobic metabolism rather than copper-induced stress.

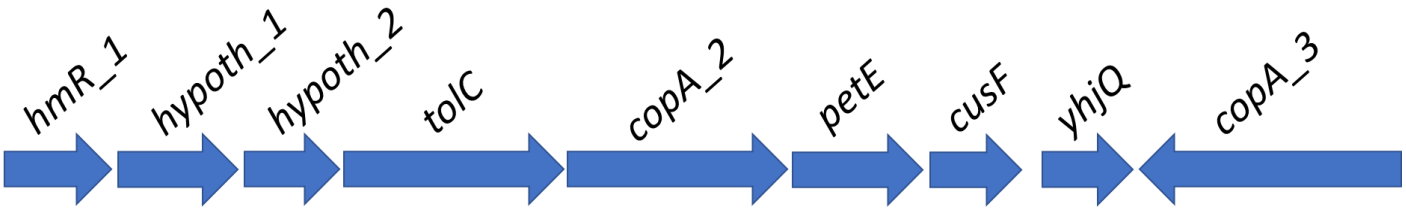

Figure 3.30. Cluster of copper-related genes in *Variovorax* sp. WS11 which were highly upregulated during growth on isoprene and succinate.

Table 3.7. Relative abundance of copper-related proteins (depicted in Figure 3.30) during growth on isoprene or succinate compared to the uninduced control. These data were calculated as the average of two biological replicates. Data presented in bold were present at a significantly greater abundance in the indicated condition/timepoint compared to the uninduced control (p≤0.01).

Description	Isoprene-6h	Isoprene-24h	Isoprene-30h	Succinate-6h	Succinate-24h	Succinate-30h
hmR_1	**76.01**	**98.04**	**67.62**	**37.61**	**21.14**	**20.78**
hypoth_1	NA	NA	NA	NA	NA	NA
hypoth_2	4.21	**9.05**	**7.42**	**6.02**	3.21	2.93
tolC	NA	NA	NA	NA	NA	NA
copA_2	**8.49**	**11.88**	**10.68**	**8.96**	**6.66**	**6.54**
petE	**133.30**	**236.65**	**195.60**	**93.04**	**63.45**	**53.01**
cusF	**65.36**	**95.30**	**75.77**	**66.24**	**56.49**	**42.46**
yhjQ	**155.06**	**247.89**	**222.01**	**27.39**	**37.46**	**65.17**
copA_3	**24.43**	**11.75**	**20.02**	2.79	1.12	1.97

3.6. **Conclusions**

The work described in this chapter was conducted with the initial aim of optimising the growth of *Variovorax* sp. WS11. This was essential, as the generation of high-biomass cultures facilitated the physiological and biochemical characterisation of this novel isoprene degrading bacterium. Growth of *Variovorax* sp. WS11 was supported at a broad range of pH, consistent with previous observations of *Variovorax* spp. (Natsagdorj *et al*. 2019, Garcia Teijeiro *et al*. 2020), although overall growth was improved slightly by adjusting the pH of cultures to 6.0. Ewers medium, initially used by Larke-Mejía *et al*. in the isolation of isoprene degrading bacteria (Larke-Mejía *et al*. 2019), was the most effective growth medium tested. Contrary to previous work with *Rhodococcus* sp. AD45, *Variovorax* sp. WS11 was capable of sustained growth on a range of isoprene concentrations, with limited growth even occurring at 10% (v/v) isoprene. Growth of *Variovorax* sp. WS11 was effectively scaled up to a four litre volume in an isoprene-fed fermentor, the first published example of such a system (Dawson *et al*. 2020). Initial challenges with the large-scale cultivation of *Variovorax* sp. WS11 related to the excessive production of foam in the fermentor unit and also to the strategy for harvesting cells. The use of a silicone-based Antifoam agent was sufficient to prevent excessive foaming while also retaining growth. The adaptation of the harvesting protocol to minimise centrifugation and washing steps prevented the loss of isoprene oxidation activity due to stress, allowing the subsequent characterisation of the substrate oxidation and alkyne inhibition profiles of IsoMO using the same batch of cells. This aimed to reduce inter-sample variability.

Variovorax sp. WS11 grew on a range of sugars and carboxylic acids, consistent with the metabolic versatility demonstrated by other members of this genus (Leadbetter & Greenberg 2000, Pehl *et al*. 2012, Satola *et al*. 2013). Despite the broad substrate oxidation range of the IsoMO of *Variovorax* sp. WS11, the only alkene capable of

supporting growth was isoprene. Therefore, other non-isoprene alkenes co-oxidised by IsoMO likely resulted in toxic accumulations of epoxide products which would inhibit growth (van Hylckama Vlieg *et al*. 1996, 1997). However, 1,3-butadiene was also consumed by *Variovorax* sp. WS11 when isoprene was present at greater concentrations, likely due to the need for isoprene-derived metabolites to induce the expression of the *iso* metabolic pathway.

The IsoMO of *Variovorax* sp. WS11 oxidised all but two of the tested alkenes with varying levels of effectiveness. Short-chain alkenes were oxidised at a slower rate than longer-chain alkenes, unlike the IsoMO of *Rhodococcus* sp. AD45 which oxidised C2-C7 alkenes at a similarly low rate (Sims, 2020). Linear, cyclic, and aromatic hydrocarbons with side-chains were oxidised by *Variovorax* sp. WS11 at an increased rate compared to the unbranched derivatives. This may explain why the SDIMO in *Variovorax* sp. WS11 is used in the isoprene metabolic pathway rather than supporting growth on an alternative, unbranched alkene. Inhibition of IsoMO by linear alkynes correlated with the rate of substrate oxidation by the corresponding alkenes, as acetylene (C2) was the least effective inhibitor of isoprene uptake while octyne (C8) was the most effective. This differed from propylene and isoprene oxidation by the sMMO of *M. capsulatus* (Bath), as these processes were almost entirely inhibited by acetylene but were poorly inhibited by octyne. This fact may allow for in-depth studies of soil communities. It has been estimated that 20.4 Tg C yr^{-1} isoprene are consumed by soils (Cleveland & Yavitt 1997, 1998), but no study has yet identified the proportion of isoprene degradation by co-oxidisers compared to the proportion of consumption by true isoprene degraders. By applying acetylene or octyne to an isoprene-consuming soil sample, the relative consumption of isoprene by each group could be calculated. Previous studies have used acetylene and octyne on soil samples to differentiate between the activity of ammonia oxidising bacteria and archaea, each of which use a copper-containing multicomponent monooxygenase (Taylor *et al*. 2017), demonstrating the potential effectiveness of this strategy.

van Hylckama Vlieg *et al*. (1999, 2000) initially identified the *iso* metabolic gene cluster and demonstrated the roles of IsoA-F, IsoI, and IsoH in the conversion of isoprene to GMBA. IsoG and IsoJ were not assigned roles in isoprene metabolism, although IsoJ was identified as a glutathione S-transferase with no activity towards the isoprene-derived glutathione conjugate HGMB (van Hylckama Vlieg *et al*. 2000). Analysis of the proteome of *Variovorax* sp. WS11 confirmed that all Iso peptides were significantly upregulated during growth on isoprene ($p \leq 0.05$), strongly indicating that IsoG and IsoJ catalyse reactions in the isoprene metabolic pathway. Analysis of the proteome of isoprene-grown *Variovorax* sp. WS11 identified several putative isoprene metabolic pathways beyond the reactions reported by van Hylckama Vlieg *et al*. (2000). The generation of the intermediate propionyl-CoA is very likely as this compound is a common substrate for the methylmalonyl-CoA and methylcitrate pathways (Carey *et al*. 2004, Eoh & Rhee 2014). Further analysis of the isoprene metabolic pathway could be conducted via the strategic generation of targeted knockouts within the *iso* gene cluster, followed by liquid chromatography with mass spectrometry (LC-MS) to identify accumulated metabolites. IsoG and IsoJ are clear candidates for deletion, as the significant expression of these peptides during growth on isoprene confirmed a role for each gene product in isoprene metabolism (Figure 3.21).

In summary, *Variovorax* sp. WS11 is a highly-adaptable isoprene degrader, capable of growing under a range of conditions but with a strict requirement for aeration. The optimised conditions for cultivation of *Variovorax* sp. WS11 provided the basis for in-depth analysis of the molecular basis of isoprene metabolism, discussed in subsequent chapters. Analysis of the proteome of isoprene-grown *Variovorax* sp. WS11 has provided valuable insights into the isoprene metabolic pathway.

4. Analysis of the genome of *Variovorax* sp. WS11

4.1. Introduction

The genomes of *Variovorax* spp. are approximately 6 Mbp with a GC content of 67-68% (Aziz *et al.* 2020, Brandt *et al.* 2014b, Han *et al.* 2011, Öztürk *et al.* 2020). The diverse metabolic capabilities of *Variovorax* spp. are reflected in the abundance of metabolic genes in the genomes of sequenced isolates, often encoded on plasmids or chromids (secondary chromosomes which do not contain essential genes) (Harrison *et al*. 2010, Ciok *et al*. 2016, Öztürk *et al*. 2020). For example, chromid 1 of *Variovorax paradoxus* B4 (Table 4.1) encodes genes putatively required for autotrophic growth (Brandt *et al.* 2014a). A comparative study of a number of *Variovorax* genomes identified a clade of phylogenetically diverse linuron-degrading species, the majority of which contained the genes associated with linuron catabolism on one or more plasmids (Öztürk *et al*. 2020). Chromids and multiple plasmids were commonly identified in sequenced isolates of *Variovorax* spp., ranging from 0.02 – 1.4 Mbp (Table 4.1) (Brandt *et al.* 2014b, Dejonghe *et al.* 2003, Han *et al.* 2011, Öztürk *et al.* 2020, Satsuma, 2010, Werner *et al.* 2020), with *Variovorax* sp. WDL1 containing five plasmids (Dejonghe *et al*. 2003). Some plasmids have been noted due to a high density of insertion sequences (Öztürk *et al*. 2020). In the *Variovorax* sp. WDL1 plasmid pWDL1-1, the linuron-degradation genes were flanked by *IS1071*, forming a composite transposon (Öztürk *et al*. 2020, Werner *et al*. 2020). This organisation was conserved for the chromosomal- and plasmid-encoded linuron catabolism genes of other *Variovorax* species (Bers *et al*. 2011, Öztürk *et al*. 2020). The presence of other insertion sequences was reported in other plasmid-encoded metabolic gene clusters, such as the terephthalate dioxygenase (*tph*) and benzoate 1,2-dioxygenase of pWDL1-3 (Öztürk *et al*. 2020). The genomes of many *Variovorax* species contain putative or confirmed oxygenase genes. *Variovorax paradoxus* EPS degraded styrene using a two-component styrene monooxygenase, an enzyme which also exhibited sulfoxidase activity (Tischler *et al*. 2018). *Variovorax boronicumulans* HAB-30 also produced oxygenase enzymes to degrade aromatic compounds, with phenol being degraded to catechol by a phenol hydroxylase and further metabolised by a catechol 2,3-dioxygenase or catechol 1,2-dioxygenase (Aziz *et al.* 2020) . The genetic basis for the metabolic diversity of *Variovorax* spp. has begun to be characterised, but there is still much to be learned. For example, Öztürk *et al*. (2020) identified highly conserved regions on the plasmids of linuron-degrading *Variovorax* species, particularly relating to the abundance and placement of insertion sequences. The role of horizontal gene transfer in the degradation of xenobiotic compounds by *Variovorax* spp. is yet to be studied.

Comparisons of the *iso* metabolic gene clusters of verified isoprene degraders and metagenome-derived sequences has highlighted the level of conservation of isoprene metabolism at the genetic level. A core cluster of 10 genes, *isoGHIJABCDEF* (Chapter 1, Figure 1.8), has been detected in all sequenced isolates, and metagenome studies have allowed the reconstruction of partial or whole *iso* gene clusters (Larke-Mejía *et al*. 2019). A conserved set of accessory genes has so far been detected in most isoprene degraders, with key differences between Gram positive and Gram negative isolates (as described in Section 1.6.1). For example, all known Gram positive isoprene degraders

have the genes required for glutathione biosynthesis (*gshAB*) within the *iso* metabolic gene cluster (Chapter 1, Figure 1.8), and many also encode two distinct aldehyde dehydrogenases (*aldH*). The duplication of *isoGHIJ* in many Gram positive isolates, particularly Rhodococci, also represents a deviation from the conserved core of the *iso* metabolic gene cluster seen in Gram negative bacteria.

A currently underrepresented area of study is the proportion of isoprene degraders which employ plasmid-encoded *iso* metabolic gene clusters. The first example of plasmid-encoded isoprene metabolism was described in *Rhodococcus* sp. AD45, with all genes required for isoprene metabolism encoded on a single >300 kbp megaplasmid (van Hylckama Vlieg *et al*. 2000, Crombie *et al*. 2015). While no other examples had been identified in isoprene degraders at that time, plasmid-encoded SDIMO enzymes had already been identified in various cases (Leahy *et al*. 2003, Crombie *et al*. 2015). These include the alkene monooxygenase of *Rhodococcus rhodochrous* B-276 (Saeki *et al*. 1999), the phenol hydroxylases of some *Pseudomonas* strains (Herrmann *et al*. 1987, Shingler *et al*. 1989, Nordlund *et al*. 1990), and the alkene monooxygenase of *Xanthobacter* sp. Py2 (Krum & Ensign, 2001, Zhou *et al.* 1999). This demonstrated the diversity of plasmid-encoded SDIMO, as these examples represent different SDIMO classes comprised of various combinations of subunits (as described in Section 1.5) (Chapter 1, Table 1.1). At the beginning of this project, the genome of *Variovorax* sp. WS11 was available as a single chromosome composed of 581 contigs with an estimated sequence contamination of 5.8%. Phylogeny based on the 16S rRNA gene sequence indicated that *Variovorax* sp. WS11 was most closely related to *Variovorax* sp. RA8 (99.9% nucleotide identity) (Altschul *et al*. 1990). *Variovorax* sp. OPL2.2 was subsequently isolated from oil palm leaves (see below), which had 100% identity with the 16S rRNA gene of *Variovorax* sp. WS11 and an average nucleotide identity (ANI) of 99.9% (Carrión *et al*. 2020). *Variovorax* sp. OPL2.2 was the second isoprene degrading strain of *Variovorax* to be isolated, and was confirmed to be of the same species as *Variovorax* sp. WS11 (Carrión et al. 2020). Further comparisons of *Variovorax* sp. WS11 with other *Variovorax* spp. can be made when considering the distribution of tRNA-encoding genes. The plasmids of linuron-degrading *Variovorax* spp. all contained tRNA genes, with some encoding the tRNA required for all proteinogenic amino acids (Öztürk *et al*. 2020). This was less pronounced in *Variovorax* sp. WS11, with only one asparaginyl-tRNA being encoded on megaplasmid 2.

Table 4.1. General genome features of characterised *Variovorax* spp.

Isolate	Size (Mbp)	GC Content (%)	Coding Sequences	tRNA
***Variovorax* sp. WS11** (Crombie *et al*. 2018, Larke-Mejía *et al*. 2019, Dawson *et al*. 2020)				
Chromosome	6.1	68.2	5930	47
Megaplasmid 1	1.1	64.4	1222	
Megaplasmid 2	1.3	66.6	1293	1
***Variovorax* sp. RA8** (Satsuma 2010, Öztürk *et al*. 2020)				
Chromosome	6.5	67.2	6035	48
Plasmid 1	0.43	64.9	382	
Plasmid 2	0.43	64.2	404	26
Plasmid 3	0.07	61.2	58	
***Variovorax* sp. WDL1** (Dejonghe *et al*. 2003, Bers *et al*. 2011, Öztürk *et al*. 2020)				
Chromosome	6.7	67.2	6250	50
Plasmid 1	0.82	62.5	812	43
Plasmid 2	0.57	63.5	527	26
Plasmid 3	0.21	63.7	193	
Plasmid 4	0.02	62.6	17	
Plasmid 5	0.02	62.6	24	

Table 4.1. Continued.

***Variovorax paradoxus* S110** (Han *et al*. 2011)				
Chromosome 1	5.6	67.6	5265.0	46.0
Chromid 1	1.1	67.0	1040.0	15.0
***Variovorax paradoxus* B4** (Brandt *et al.* 2019, Brandt *et al.* 2014a, 2014b)				
Chromosome 1	5.8	67.2	5331.0	46.0
Chromid 1	1.4	66.9	1264.0	2.0
***Variovorax paradoxus* EPS** (Han *et al*. 2013, Fredendall *et al*. 2020)				
Chromosome	6.6	66.5	5944.0	57.0
***Variovorax boronicumulans* HAB-30** (Aziz *et al.* 2020)				
Chromosome	6.7	68.4	6084.0	49.0

Chromosome, chromid, and plasmid information were obtained from the NCBI Genome database, https://www.ncbi.nlm.nih.gov/genome/ (accessed on 12/05/2020).

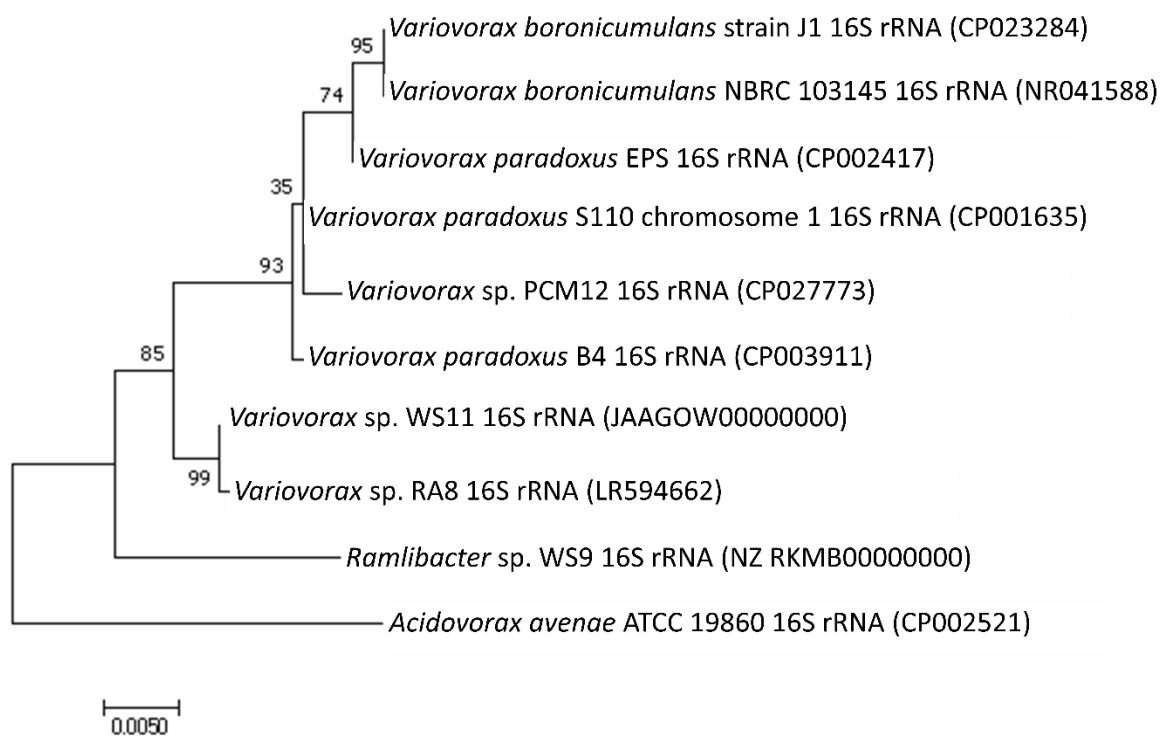

Figure 4.1. Phylogenetic relationship between *Variovorax* sp. WS11 and other characterised *Variovorax* spp., based on nucleotide identity of near complete 16S rRNA gene sequences. Bootstrap values (500 replications) are shown at the nodes (adapted from Dawson *et al.* 2020). Phylogenetic analysis was run using the Maximum Likelihood method based on the Tamura-Nei model (Tamura & Nei 1993), using the standard parameters in MEGA7 (Kumar et al. 2016).

4.2. **Specific chapter aims and objectives**

The studies detailed in this chapter were conducted with the aim of identifying the genetic basis of isoprene metabolism in *Variovorax* sp. WS11. This was approached by BLAST analyses using the representative *iso* metabolic genes from *Rhodococcus* sp. AD45 as query sequences. Broader analysis of the genome of *Variovorax* sp. WS11 was made possible by genome sequencing using a combination of Illumina and Oxford Nanopore techniques. Annotation of the genome using RAST and MicroScope platforms (Aziz et al. 2008, Overbeek et al. 2014, Vallenet et al. 2019) were conducted with aim of predicting the physiological and metabolic potential of *Variovorax* sp. WS11, supplementing the physiological analysis described in Chapter 3.

1. Using the genome of *Variovorax* sp. WS11, infer the metabolic and physiological potential of this novel isoprene degrading bacterium. Experimentally validate the most likely physiological and metabolic traits, indicated by the presence of clusters of genes with similar organisation to previously characterised examples.
2. Study the genome of *Varoivorax* sp. WS11 compared with the published genomes of other *Variovorax* spp. and other isoprene degraders with the aim of gaining insight into the acquisition of the *iso* metabolic gene cluster in *Variovorax* sp. WS11.

4.3. Hypothesis

It was hypothesised that, due to the isolation of *Variovorax* sp. WS11 in an isoprene-enriched community under aerobic conditions, this novel bacterium would metabolise isoprene through a similar mechanism to that first described in *Rhodococcus* sp. AD45. *Variovorax* spp. are a metabolically versatile genus, leading to the further hypothesis that the genome of *Variovorax* sp. WS11 would reflect a wide range of potential growth substrates and potential physiological responses to varying stimuli.

4.4. Results and discussion

4.4.1. Studying the annotated genome of *Variovorax* sp. WS11

The first genome sequence of *Variovorax* sp. WS11 was 8.57 Mbp, with a GC content of 67.2%. This was within the expected GC range of *Variovorax* spp., but the genome was much longer than other members of this genus (Table 4.1). The genome of *Variovorax* sp. WS11 was re-sequenced by a combination of Illumina (short-reads) and Oxford Nanopore (long-reads) as described in Section 2.8.6. The chromosome of *Variovorax* sp. WS11 was assembled into three contigs, with two circular megaplasmids of 1.1 and 1.3 Mbp identified by Bandage software (Version 0.8.1). Analysis by tBLASTn (Altschul *et al*. 1990) identified the whole *iso* metabolic gene cluster of *Variovorax* sp. WS11 on Megaplasmid 1, similar to the location of the *iso* metabolic gene cluster of *Rhodococcus* sp. AD45 on a megaplasmid (Crombie *et al*. 2015). The chromosome was 6.08 Mbp, falling within the typical range of *Variovorax* genomes (Table 4.2). CheckM analysis predicted that the genome was 98.3% complete with 1.2% contamination. While the majority of coding sequences were present on the chromosome, the distribution of genes relating to different subsystems varied greatly between the chromosome and plasmids. 4.7 and 4.5% of coding sequences on the chromosome and megaplamsid 1, respectively, were assigned to carbohydrate metabolism, whereas 7.5% of coding sequences on megaplasmid 2 were assigned to this subsystem (Table 4.2). The fatty acid, lipids, and isoprenoids subsystem only comprised 2.1% of chromosomal coding sequences, while megaplasmids 1 and 2 contained 5.8 and 5.7%, respectively. These data indicated roles for each megaplasmid in the general metabolic processes of *Variovorax* sp. WS11. This is consistent with other studies that have identified the genes required for various metabolic pathways on plasmids in *Variovorax* spp. (Satola *et al*. 2013, Öztürk *et al*. 2020).

Table 4.2. General features of the *Variovorax* sp. WS11 genome, identified by MicroScope annotation software https://mage.genoscope.cns.fr/microscope (accessed 20/05/2019) (Vallenet *et al*. 2019). Taken from Dawson *et al.* 2020.

Feature	**Chromosome**	**Megaplasmid 1**	**Megaplasmid 2**
Size (bp)	6,084,916	1,100,013	1,304,680
G+C Content	68.2	64.4	66.6
Number of Contigs	3	1	1
L50	2		
N50	1,304,680		
Completeness (CheckM - %)	98.3		
Contamination (CheckM - %)	1.2		
Gene - RAST-Predicted			
No. of coding sequences (total)	5,930	1,222	1,293
No. of genes with assigned function	3,958	596	776
No. genes without assigned function	1,972	626	517
No. rRNAs	6		
No. tRNAs	47		1
No. of pseudogenes	26		

Subsystem	**Chromosome**	**Plas 1**	**Plas 2**
Cofactors, Vitamins, Prosthetic Groups, Pigments	147	6	1
Cell Wall and Capsule	27	0	0
Virulence, Disease and Defence	57	2	3
Potassium metabolism	13	0	0
Photosynthesis	0	0	0
Miscellaneous	45	1	6
Phages, Prophages, Transposable elements, Plasmids	6	0	0
Membrane Transport	179	35	36
Iron acquisition and metabolism	3	0	0
RNA Metabolism	44	5	1
Nucleosides and Nucleotides	48	1	13
Protein Metabolism	137	0	1
Cell Division and Cell Cycle	0	0	0
Motility and Chemotaxis	12	0	0
Regulation and Cell signalling	56	9	12

Table 4.2. Continued.

Secondary Metabolism	5	0	0
DNA Metabolism	94	2	2
Fatty Acids, Lipids, and Isoprenoids	125	71	74
Nitrogen Metabolism	15	1	19
Dormancy and Sporulation	1	0	0
Respiration	111	21	33
Stress Response	89	1	5
Metabolism of Aromatic Compounds	100	21	20
Amino Acids and Derivatives	338	9	19
Sulfur Metabolism	23	5	23
Phosphorus Metabolism	36	0	1
Carbohydrates	277	55	97

Variovorax sp. WS11 and *Variovorax* sp. OPL2.2, isolated from willow soil and oil palm leaves, respectively, share identical organisation of the *iso* metabolic gene clusters, and the *isoA* genes share 99.4% identity at the deduced amino acid level (Carrión *et al*. 2020). The genome of *Variovorax* sp. OPL2.2 is 8.5 Mbp, composed of 50 contigs with 98.4% completeness. When considering the typical size of a genome in *Variovorax* spp., as well as the abundance of plasmids and chromids (Table 4.1), it is likely that *Variovorax* sp. OPL2.2 also uses a plasmid-encoded *iso* metabolic gene cluster.

4.4.2. **Chromosomal and plasmid-encoded oxygenase genes in *Variovorax* sp. WS11**

The genome of *Variovorax* sp. WS11 was studied by a combination of visual inspection and annotation by RAST software (Aziz *et al.* 2008, Overbeek *et al.* 2014). Many genes were annotated as monooxygenases or dioxygenases involved in the metabolism of aromatic compounds and aliphatic alkanesulfonates. Individual genes were ignored due to the likelihood of mis-annotation. However, genes which were present in conjunction with related genes, such as multiple oxygenase components, ferredoxin and reductase components or transport-related genes, were analysed with respect to published, characterised genes. The organisation of putative oxygenase genes is depicted in Figure 4.2.

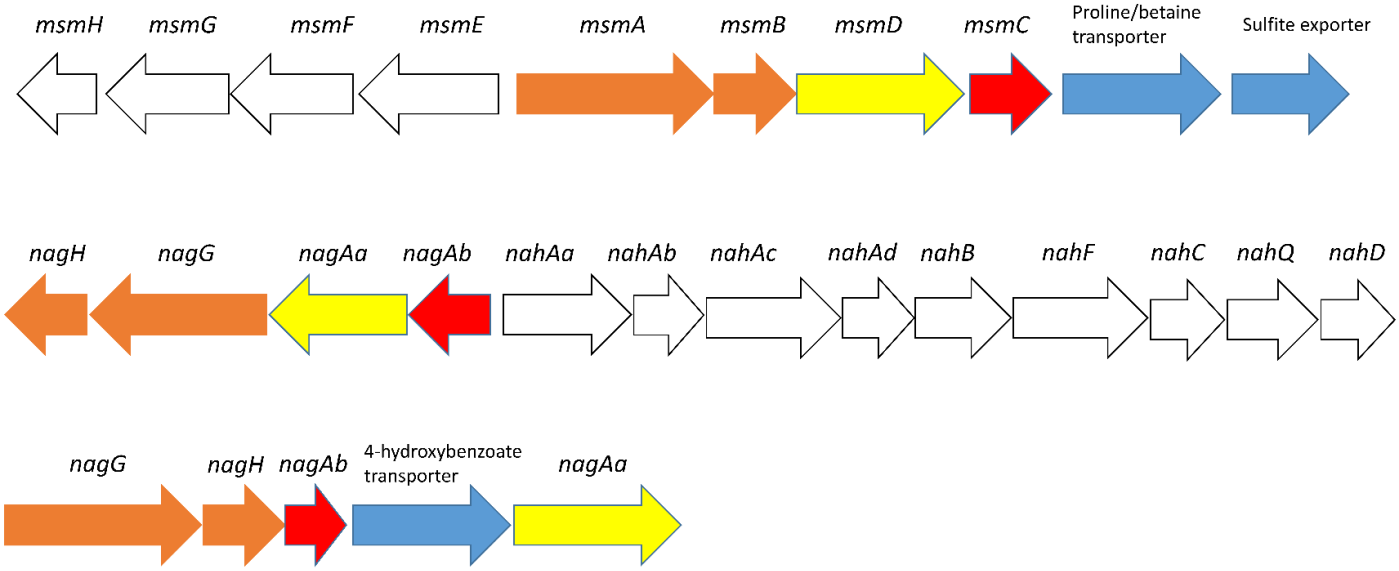

Figure 4.2. Organisation of putative methanesulfonate (*msm*), salicylate (*nagGH*), and naphthalene (*nagAcAd*) metabolic genes (taken from Dawson *et al.* 2020). White arrows represent essential genes which were absent from the putative metabolic gene cluster.

4.4.2.1. ***Protocatechuate 3,4-dioxygenase***

Protocatechuate 3,4-dioxygenase catalyses the breakage of O_2 and subsequent addition of each oxygen atom to an aromatic ring, typically catechols, phthalates and hydroxybenzoates (Contzen & Stolz 2000). Protocatechuate is also a product of the oxidation of toluene by the toluene 4-monooxygenase (Whited *et al*. 1991, Tao *et al*. 2004). Protocatechuate 3,4-dioxygenase has also been associated with the metabolism of sulfonated aromatics (Contzen & Stolz 2000), making this suitable for analysis in *Variovorax* sp. WS11. A putative protocatechuate 3,4-dioxygenase (*pcaGH*) was detected on the chromosome of *Variovorax* sp. WS11. These genes shared 38.3% and 50.9% amino acid identity with the functional α- and β-oxygenase components from *Agrobacterium tumefaciens* (PcaG and PcaH, respectively) (Altschul *et al*. 1990, Contzen & Stolz 2000). The moderately high amino acid identity of the β-component may indicate a conserved oxygenase function. However, accessory genes such as *pcaBCDIJ*, encoding a lactonizing enzyme (*pcaB*), decarboxylase (*pcaC*), hydrolase (*pcaD*) and transferase (*pcaIJ*) (Parke 1995, Contzen & Stolz 2000), were not present in *Variovorax* sp. WS11. The only other *pca* gene adjacent to the putative *pcaGH* was *pcaQ*, a LysR-type transcriptional regulator which induces *pca* gene expression in response to muconate (Parke 1996). While it is possible that these genes are active, non-isoprene alkenes did not support the growth of *Variovorax* sp. WS11 (Chapter 3, Table 3.2), although a range of aromatic and sulfonated hydrocarbons may still be tested. Given the involvement of protocatechuate in the metabolism of toluene (Whited *et al*. 1991, Tao *et al*. 2004), the presence of genes involved in the degradation of protocatechuate may indicate a historic/vestigial toluene metabolic pathway in *Variovorax* sp. WS11.

4.4.2.2. ***Benzoate 1,2-dioxygenase***

The Rieske-type benzoate 1,2-dioxygenase catalyses the O_2-dependent oxidation of benzoate to 1-carboxy-1,2-*cis*-dihydroxycyclohexa-3,5-diene (Wolfe *et al*. 2002). This requires the interaction of a reductase (*benC*) and dehydrogenase (*benD*) for the subsequent formation of catechol (Wolfe *et al*. 2002). Putative copies of each gene were located on the chromosome of *Variovorax* sp. WS11. The identity of the translated amino acid sequences were 24-30% for these components (Altschul *et al*. 1990), indicating mis-annotation as a benzoate 1,2-dioxygenase. While the clustering of these putative aromatic ring-dioxygenase genes indicates a currently undiscovered function, IsoMO is currently the only active oxygenase in *Variovorax* sp. WS11 known to oxidise aromatic hydrocarbons (such as toluene, ethylbenzene, propylbenzene, styrene, and o-xylene) (Chapter 3, Figure 3.15), as *Variovorax* sp. WS11 only performed these oxidations when grown on isoprene. However, it is possible that the tested conditions have not allowed for expression of the putative benzoate 1,2-dioxygenase genes, as many other genes involved in benzoate metabolism were annotated elsewhere on the chromosome and on megaplasmid 2. Chromosomal genes included putative ATP-binding proteins involved in benzoate transport, a benzoate ring-cleaving hydrolase, and a benzoate CoA-ligase. The use of ATP-type transporters in the metabolism of benzoate has been described previously (Michalska *et al*. 2012, Choudhary *et al*. 2017). Curiously, genes involved in the anaerobic degradation of benzoate were annotated on megaplasmid 2 (Pelletier & Harwood 1998), despite there only being a few cases of *Variovorax* spp. growing anaerobically (Yoon *et al*. 2006, Im *et al*. 2010). These genes included dehydrogenases, a hydrolase, and a ligase involved in the metabolism of cyclohexanecarboxyl-CoA.

4.4.2.3. ***Alkanesulfonate monooxygenase and dioxygenase***

Many *Variovorax* spp. have been characterised for their ability to metabolise aliphatic sulfonates (Satola *et al*. 2013, Wübbeler *et al*. 2015, Brandt *et al*. 2019). Sulfur transporters were commonly observed during visual inspection of the chromosome and megaplasmids of *Variovorax* sp. WS11 (Carver *et al*. 2012). A putative methanesulfonate monooxygenase was identified on the chromosome, with the large and small oxygenase subunits identified along with reductase and ferredoxin components (*msmABCD*) (Figure 4.2). These were queried against *msmABCD* from *Methylosulfonomonas methylovora* (Marco *et al*. 1999, Jamshad *et al*. 2006), with the highest amino acid identity (55%) detected for the oxygenase α-subunit (MsmA). Characterised methanesulfonate-degraders have copies of *msmEFGH* which collectively encode an ABC-transporter (Jamshad *et al*. 2006). These genes were not present with the putative methanesulfonate monooxygenase genes in *Variovorax* sp. WS11, but copies were detected by tBLASTn analysis on the chromosome and on megaplasmid 2, using the ratified genes from *M. methylovora* as query sequences (Altschul *et al*. 1990). MsmA was further investigated by alignment against confirmed MsmA amino acid sequences, demonstrating the presence of the conserved Rieske motif (CXH-X_{26}-CXXH) (Figure 4.3) (Marco *et al*. 1999). These analyses strongly indicated the presence of an active methanesulfonate monooxygenase in *Variovorax* sp. WS11. However, 5 mM sodium methanesulfonate and 5 mM ethanesulfonate did not support the growth of *Variovorax* sp. WS11 under the tested conditions (Chapter 3, Table 3.2).

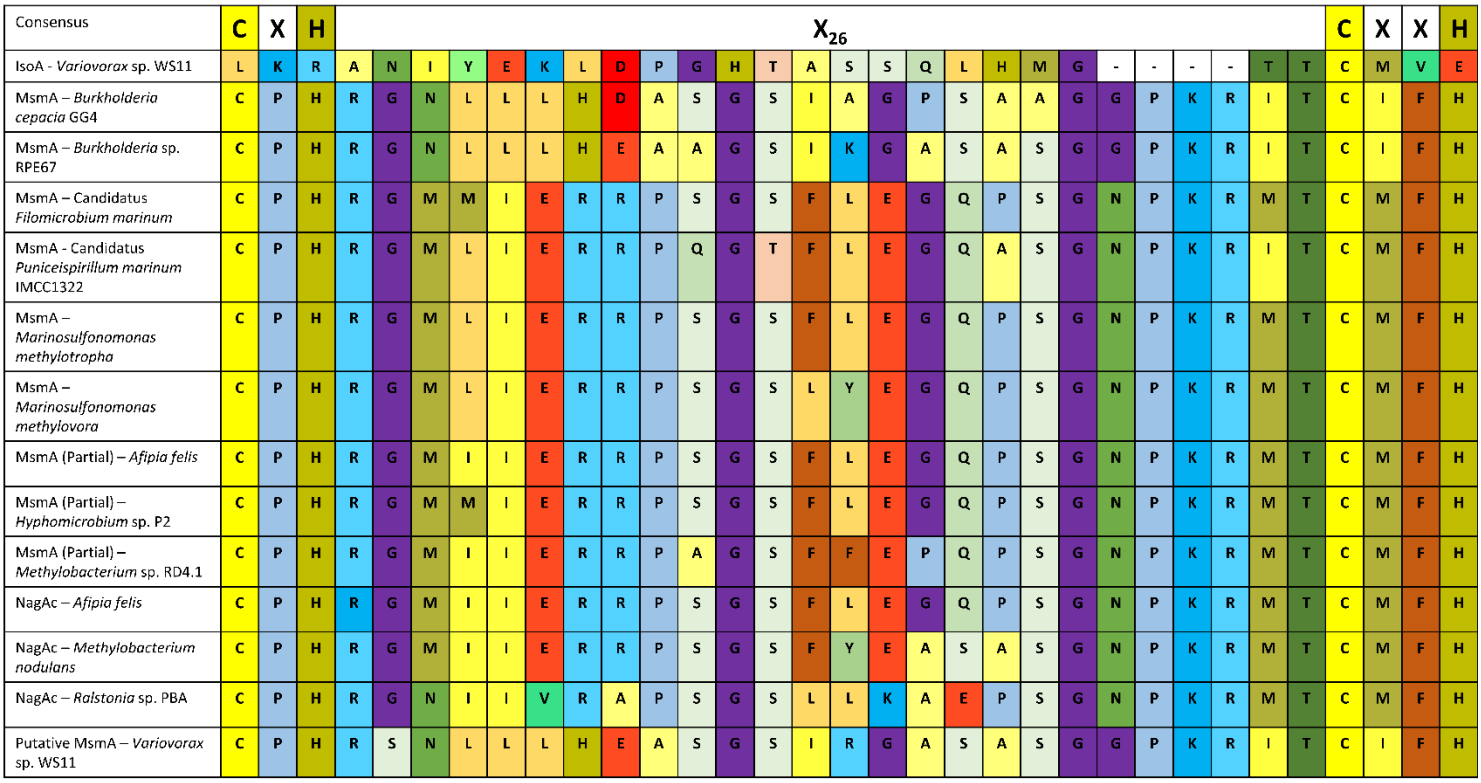

Figure 4.3. Alignment of the deduced amino acid sequences of putative and confirmed Rieske-type oxygenase alpha subunits, including MsmA (methanesulfonate monooxygenase) and NagAc (aromatic ring hydroxylating dioxygenase). The non-heme diiron monooxygenase alpha subunit IsoA was included for comparison. Each colour corresponds to a specific amino acid.

Taurine, an aliphatic sulfonate, supported the growth of *V. paradoxus* B4 (Carbajal-rodríguez *et al*. 2011). Genes encoding a putative α-ketoglutarate-dependent taurine dioxygenase (*tauD*) (Eichhorn *et al*. 1997) were detected on the chromosome of *Variovorax* sp. WS11. An ABC-type transporter (*tauABC*) was distant from *tauD* on the chromosome of *Variovorax* sp. WS11, potentially indicating a mis-annotation. Organosulfonate ABC transporter genes were also located on megaplasmid 2. *Variovorax* sp. WS11 was inoculated in Ewers medium with 10 mM taurine, resulting in moderate growth (Chapter 3, Table 3.2). It is unclear whether the identified *tauABCD* genes were responsible, or whether taurine was metabolised by an alternative method such as the putative methanesulfonate monooxygenase described above. Functional confirmation through targeted mutagenesis or expression of candidate *tauABCD* genes in a heterologous host is required to determine the genetic components of taurine metabolism in *Variovorax* sp. WS11. Collectively, the analyses of the genome of *Variovorax* sp. WS11 indicate a wide, as-yet uncharacterised potential for degradation of organosulfur compounds.

4.4.2.4. ***Salicylate 5-hydroxylase/ Naphthalene 1,2-dioxygenase***

The enzymatic oxidation of naphthalene to salicylate is conducted by the naphthalene 1,2-dioxygenase (*nagAaAbAcAd*), followed by the further oxidation of salicylate by a salicylate 5-hydroxylase (*nagGH*) (Yen *et al.* 1991, Yen & Gunsalus, 1985, Zhou *et al.* 2001). Essential genes for these pathways may be co-transcribed as a single operon (Zhou *et al.* 2001) or transcribed separately (Yen & Gunsalus 1985). Although no naphthalene-degrading

strain of *Variovorax* has been isolated, varied studies have linked this genus to naphthalene degradation. A biofilm community formed around a naphthalene crystal was largely composed of *Variovorax* spp., and *Variovorax* was a dominant component of the enriched community in a DNA-SIP experiment using ^{13}C-labelled naphthalene in soils (Madsen 2011, Martirani-Von Abercron *et al*. 2017). The genome of *Variovorax* sp. WS11 contained various genes with putative roles in naphthalene and salicylate degradation (Figure 4.2). Two gene clusters encoding a putative salicylate 5-hydroxylase (*nagGH*) were located on megaplasmid 2 and on the chromosome. One was located with putative naphthalene 1,2-dioxygenase reductase and ferredoxin components (*nagAaAb*) but not the dioxygenase genes themselves (*nagAcAd*), possibly indicating the loss of naphthalene degradation genes from a complete cluster. No growth was observed when *Variovorax* sp. WS11 was inoculated in Ewers medium with 5 mM sodium salicylate (Chapter 3, Table 3.2). Due to the lack of a complete naphthalene-degradation gene cluster, it was unlikely that *Variovorax* sp. WS11 would be able to grow on naphthalene as the sole source of carbon and energy. Consequently, when tested, 5 mM naphthalene was unable to support growth.

Many of the putative oxygenase genes in the genome of *Variovorax* sp. WS11 were previously identified in other *Variovorax* spp. An aromatic-ring hydroxylating dioxygenase was identified in *Variovorax* sp. MAK3, potentially accounting for the ability of this isolate to degrade $_{13}$C-benzene in coal-tar contaminated soils (Posman *et al*. 2017). Likewise, *Variovorax paradoxus* strains B4, S110, and EPS each have chromosomal copies of an alkanesulfonate monooxygenase (*ssuD*) (Altschul *et al*. 1990). As many of the putative oxygenase genes identified in other *Variovorax* spp. were also identified in *Variovorax* sp. WS11, albeit as incomplete or inactive gene clusters, it is likely that redundant genes and processes were lost by *Variovorax* sp. WS11, or an ancestor of this species, during the process of adapting to a new niche.

4.4.3. **Genome-guided study of the physiology of *Variovorax* sp. WS11**

As described above, a combination of annotation-based and visual inspections were used to infer from the genome the metabolic and physiological potential of *Variovorax* sp. WS11. Using the genomes of other characterised *Variovorax* spp. as the basis for study, specific physiological traits of *Variovorax* sp. WS11 were investigated. For example, the abundance of genes involved in flagella biosynthesis on the genome of *Variovorax* sp. WS11 led to the investigation of motility on soft agar (Chapter 3, Figure 3.8).

4.4.3.1. ***Methanol dehydrogenase***

Two co-located genes on the genome of *Variovorax* sp. WS11 were annotated as methanol dehydrogenase (MDH), with one being characterised as a lanthanide-dependent *xoxF*. The latter gene had 67% amino acid identity with the translated XoxF gene from *Methylorobum extorquens* AM1 (Nakagawa *et al*. 2012), while the former had 70% identity with the MDH large subunit of *Methylosinus trichosporium* OB3b (Farhan Ul Haque *et al*. 2016). Genes involved in the synthesis of pyrroloquinoline quinone (PQQ) (Keltjens *et al*. 2014), a known cofactor of the related MDH *mxaF*, were located close to the MDH genes (Schmidt *et al*. 2010, Wu *et al*. 2015). As the lanthanide-dependent MDH was located with the genes required for PQQ synthesis (Deng *et al*. 2018), it was unclear whether

an active MDH would be Ca^{2+}-dependent or lanthanide-dependent. Therefore, *Variovorax* sp. WS11 was tested for growth on 0.1% and 1% methanol (Aristar) in the presence or absence of 5 µM lanthanum, supplied as $LaCl_3$ (Krause *et al*. 2017, Lv *et al*. 2020), or 2 g L^{-1} $CaCl_2.2H_2O$. Liquid cultures were prepared in 10 ml Ewers medium or NMS medium (Whittenbury *et al*. 1970), and solid agar was prepared using the same media. Methanol was supplied to agar plates by adding small volumes of methanol onto cotton wool and incubating the plates with the cotton wool in sealed chambers. This worked under the assumption that all methanol would volatilise and become available to the agar. No growth was detected on methanol under any of these conditions. *Variovorax* sp. WS11 was capable of growing under all of the above conditions with 10 mM glucose, confirming that the conditions were appropriate and the lack of growth on methanol was due to no either a non-functional MDH and/or a lack of a C1 assimilation pathway.

4.4.3.2. ***Plant-growth promotion***

Variovorax spp. have previously been identified in endophytic and epiphytic associations with plant roots and leaves (Han *et al.* 2011, Hong *et al.* 2017, Natsagdorj *et al.* 2019, Surette *et al.* 2003), although the ability of *Variovorax* sp. WS11 to exploit either niche is currently unexplored. For example, *V. boronicumulans* CGMCC 4969 synthesised the phytohormone salicylate (Liu *et al*. 2013), and *Variovorax paradoxus* have been linked to the prevention of ethylene accumulation in plants (Belimov *et al*. 2001, 2009). Ethylene biosynthesis is stimulated in response to certain stressors, such as drought, via the production of 1-aminocyclopropane-1-carboxylic acid (ACC) (Glick *et al*. 1998, Belimov *et al*. 2009). ACC deaminase (*acdS*) has been identified in the genomes of several *Variovorax* spp., linking this genus to the promotion of plant growth by mitigating stress responses (Belimov *et al*. 2009, Garcia Teijeiro *et al*. 2020, Han *et al*. 2011, Natsagdorj *et al*. 2019). The genome of *Variovorax* sp. WS11 was studied by tBLASTn analysis using the deduced amino acid sequence of *acdS* from *Variovorax paradoxus* S110 (Altschul *et al*. 1990, Kamala-Kannan *et al*. 2010). *Variovorax* sp. WS11 contains a gene annotated as *acdS* which shared 90% deduced amino acid identity with AcdS from *V. paradoxus* S110, strongly indicating ACC deaminase activity and therefore promotion of plant growth. While the IsoMO from *Variovorax* sp. WS11 directly catalyses the oxidation of ethylene, the rate of substrate oxidation was relatively low (Chapter 3, Figure 3.15), indicating that the indirect removal of ethylene by ACC deaminase activity would be more likely than direct removal by IsoMO. Further to this, the co-oxidation of ethylene to ethylene oxide would likely be toxic to *Variovorax* sp. WS11.

Biofilm formation has previously been identified as a key aspect of the colonisation of plants by bacteria (Bloemberg & Lugtenberg 2004), a trait which has since been linked to plant growth promotion by *Variovorax* sp. HRRK 170 (Natsagdorj *et al*. 2019). Biofilm formation has been identified in diverse *Variovorax* spp. (Jamieson *et al*. 2009, Pehl *et al*. 2012, Martirani-Von Abercron *et al*. 2017, Natsagdorj *et al*. 2019), and the abundance of flagella and pilus-related genes in the genome of *Variovorax* sp. WS11, combined with the observation of adherence to solid fixtures in the fermentor (as described in Chapter 3), strongly indicated the ability of *Variovorax* sp. WS11 to establish biofilms (Conrad *et al*. 2011). Further contributing to the coordination of population-level activities such as biofilm

formation, the chromosome of *Variovorax* sp. WS11 contains *luxRI* homologues which encode the regulation and synthesis of the quorum sensor acyl-homoserine lactone (AHL) (Egland & Greenberg 2001).

4.4.4. ***Conserved and varied aspects of the iso metabolic gene cluster***

4.4.4.1. ***Organisation of the iso metabolic gene cluster***

All characterised isoprene degrading bacteria share a conserved cluster of 10 *iso* metabolic genes, *isoGHIJABCDEF* (as described in Section 1.6.3). The presence and organisation of accessory genes can differ greatly between isoprene degraders (Chapter 1, Figure 1.8). For example, the *iso* metabolic gene clusters of all sequenced Gram negative bacteria contain a single copy of *aldH*, encoding an aldehyde dehydrogenase, between *isoJ* and *isoA*. (Crombie *et al*. 2018, Larke-Mejía *et al*. 2019, Carrión *et al*. 2020, Dawson *et al*. 2020), while the *iso* metabolic gene clusters of most Gram positive isoprene degraders contain *aldH1* and *aldH2*, typically located at opposite ends of the *iso* cluster (Crombie *et al*. 2015). In *Rhodococcus* sp. AD45, *aldH1* encoded a putative glyceraldehyde 3-phosphate dehydrogenase (Maceachran & Sinskey 2013), while *aldH2* encoded a putative 4-hydroxymuconic semialdehyde dehydrogenase (Moonen *et al*. 2008, Crombie *et al*. 2015). AldH from *Variovorax* sp. WS11 shared the greatest identity at the deduced amino acid level with AldH1 from *Rhodococcus* sp. AD45 (52.7%), compared to only 26.1% identity with AldH2 (Dawson *et al*. 2020). To date, *aldH* has not been assigned a role in isoprene metabolism, although transcription of *aldH1* and *aldH2* was upregulated by both isoprene and epoxyisoprene in *Rhodococcus* sp. AD45 (Crombie *et al*. 2015). The Gram positive isoprene degrader *Nocardioides* sp. WS12, isolated from willow soil (Larke-Mejía *et al*. 2019, Gibson *et al*. 2020), had only a single copy of *aldH* between *isoJ* and *isoA* (Chapter 1, Figure 1.8).

Genes involved in glutathione biosynthesis were detected in the *iso* metabolic gene clusters of Gram positive bacteria (Chapter 1, Figure 1.8) (van Hylckama Vlieg *et al*. 2000, Crombie *et al*. 2015). *gshAB*, encoding a glutamate-cysteine ligase and a glutathione synthetase (Smirnova & Oktyabrsky 2005, Wongsaroj *et al*. 2018) respectively, were located in identical positions relative to the *iso* metabolic genes. *gshA* was divergently transcribed from the *iso* metabolic gene cluster, with the exception of *Nocardioides* sp. WS12 (Larke-Mejía *et al*. 2019). The *iso* metabolic gene clusters of Gram negative bacteria do not contain *gshAB*, although the epoxide-detoxifying glutathione *S*-transferase (*isoI*) was still present (Larke-Mejía *et al*. 2019, Dawson *et al*. 2020). *gshAB* were located on the chromosome of *Variovorax* sp. WS11 rather than megaplasmid 1, and were co-localised with a potassium transport protein. This makes sense when considering the role of glutathione in osmoprotection (McLaggan *et al*. 1990). As described in Section 1.6.1, prokaryotic glutathione biosynthesis is found primarily in Gram negative bacteria (Smirnova & Oktyabrsky, 2005). Gram positive bacteria tend to detoxify reactive compounds such as epoxides using alternative low molecular weight thiols (Johnson *et al*. 2009, Lienkamp *et al*. 2020). Due to the presence of *gshAB* on the plasmid-encoded *iso* metabolic gene cluster in *Rhodococcus* sp. AD45, it is likely that glutathione biosynthesis was horizontally acquired as a means of protecting Gram positive isoprene degraders against epoxide toxicity. The duplication of *isoGHIJ* in isoprene-degrading species of *Rhodococcus*, and also a second copy of *gshB* in *Rhodococcus* sp. AD45, indicated an increased requirement for the mitigation of stress caused by isoprene metabolism. IsoI and

IsoH have confirmed roles in isoprene metabolism subsequent to the oxidation of isoprene by IsoMO (van Hylckama Vlieg *et al*. 1998, 1999, 2000). *isoGHIJ2* are yet to be assigned roles in isoprene metabolism, although IsoGHJ2 all share 99% amino acid identity with the primary gene copies and IsoI2 shares 79% identity with IsoI (Crombie *et al*. 2015). Transcriptome analysis also demonstrated that the primary and secondary copies of *isoGHIJ* were transcribed to equal levels (Crombie *et al*. 2015). It is therefore likely that the duplicated genes involved in the subsequent steps of isoprene metabolism aid in the prevention of epoxide accumulation during the metabolism of isoprene. As the *iso* metabolic gene clusters of Gram negative isoprene degraders have single copies of *isoGHIJ* and no copies of *gshAB*, it is likely these bacteria possess better-adapted mechanisms for mitigating epoxyisoprene-induced stress. A glutathione-related gene which is present in the *iso* metabolic gene clusters of Gram negative isoprene degraders, but not in Gram positive isoprene degraders, is glutathione-disulfide reductase (*garB*). Glutathione-disulfide (GSSG) is an oxidised form of glutathione which is formed as a result of glutathione's role as an antioxidant (Janes & Schulz 1990). GSSG is then reduced to its active form by an NAD(P)H-dependent reaction, catalysed by GarB. GarB expression in *Variovorax* sp. WS11 was significantly upregulated after 30 hours of growth on isoprene ($p \leq 0.01$), with a relative peptide abundance of 183 compared to an uninduced control (Chapter 3, Figure 3.20). This clearly indicated a role for GarB in isoprene metabolism, likely as a method of recycling oxidised GSSG to reduced glutathione (Janes & Schulz 1990). The gene with the closest homology to *garB* in the *iso* metabolic gene cluster from *Rhodococcus* sp. AD45, predicted by tBLASTn (Altschul *et al*. 1990), was a putative FAD-dependent oxidoreductase, provisionally identified as a CoA-disulfide reductase. These reductases shared 28.2% identity at the amino acid level, indicating different functions. The *iso* metabolic gene cluster from a metagenome-derived *Gordonia* sp. also contained a putative CoA-disulfide reductase, indicative of a conserved function in Gram positive isoprene degraders (Carrión *et al*. 2020). A CoA-disulfide reductase was previously identified as a thiol recycling mechanism in another Gram positive bacterium, *Staphylococcus aureus* (delCardayre *et al*. 1998), although that enzyme was NADPH-dependent as with GarB (Janes & Schulz 1990). The role of a CoA-disulfide reductase in the metabolism of isoprene by *Rhodococcus* sp. AD45 is unclear, although it is likely that both Gram positive and Gram negative isoprene degraders use thiol-recycling mechanisms.

Variovorax spp. are commonly identified in natural, commercial, and xenobiotic-contaminated soils (Aziz *et al*. 2020, Lu *et al*. 2019, Öztürk *et al*. 2020, Zheng *et al*. 2018), and also in the phyllosphere and leaves of plants (Leadbetter & Greenberg 2000, Hong *et al*. 2017, Garcia Teijeiro *et al*. 2020). With this in mind, it is curious to consider that only two sequenced isolates of *Variovorax* contain an *iso* metabolic gene cluster. Isoprene is a highly abundant volatile organic compound (Guenther *et al*. 2006, 2012, Sindelarova *et al*. 2014), and xenobiotic-degradation genes in *Variovorax* spp. are likely to be horizontally transferred due to the common association with plasmids and insertion sequences (Öztürk *et al*. 2020). *Variovorax* spp. have been identified in the isoprene degrading communities of a variety of environmental samples through DNA-SIP (El Khawand *et al*. 2016, Carrión *et al*. 2018, 2020, Crombie *et al*. 2018, Larke-Mejía *et al*. 2019), but the paucity of sequenced isolates prevents a detailed summary of the diversity of isoprene-degrading strains of *Variovorax*.

4.4.4.2. ***Putative regulators of isoprene metabolism***

The regulatory gene(s) located upstream of the core *iso* metabolic gene cluster differs between Gram positive and Gram negative isoprene degrading bacteria. Gram positive isoprene degraders contain 1-2 copies of a *marR*-type transcriptional regulator upstream of *isoG*, while all sequenced Gram negative isolates contain a LysR-type transcriptional regulator (*dmlR*) immediately upstream of *isoG* (Chapter 1, Figure 1.8). A present, only isoprene degrading *Variovorax* spp. contain a second copy of *dmlR* downstream of *garB* (Carrión *et al*. 2020, Dawson *et al*. 2020). MarR- and LysR-type transcriptional regulators (MTTR and LTTR, respectively) share a similar mode of action, in which a co-inducer or co-repressor, typically a constituent of the metabolic pathway which is regulated, binds to the regulator to alter the specificity of DNA-binding (Maddocks & Oyston 2008). Comparison by BLAST at the deduced amino acid level strongly indicated a conserved function for the LTTR upstream of *isoG*, henceforth referred to as *dmlR_4* after the copy found in *Variovorax* sp. WS11. DmlR_4 from *Variovorax* sp. WS11 shared 100%, 92.8%, and 72.3% identity with the same gene from *Variovorax* sp. OPL2.2 (Carrión *et al*. 2020), a metagenome-derived isoprene-degrading *Variovorax* sp. (Crombie *et al*. 2018), and *Ramlibacter* sp. WS9 (Larke-Mejía *et al*. 2019), respectively. The translated DmlR_4 gene from *Variovorax* sp. WS11 only shared 30.7% identity with DmlR_5, located downstream of *isoF*, although conserved regions identified by BLASTp analysis indicate that DmlR_5 is also a LTTR (Altschul *et al*. 1990). These regions include a helix-turn-helix DNA-binding domain and a LysR substrate-binding domain (reviewed by Maddocks & Oyston, 2008). DmlR_5 shared 82% identity with the homologous gene in a metagenome-derived isoprene-degrading *Variovorax* sp. (Crombie *et al*. 2018), and 87% identity with a LTTR from *Variovorax* sp. RA8. The latter strain is not a known isoprene degrader and the genome contains no *iso* metabolic gene cluster. The highest identity of *dmlR_5* with a non-*Variovorax* bacterium was detected in *Pseudorhodoferax* sp. Leaf267 (81%), an isolate from the phyllosphere of *A. thaliana*. In this bacterium, the *dmlR_5* homolog was upstream of, and divergently transcribed from, genes involved in the synthesis of a type IV secretion system. The high amino acid identity (>70%) of DmlR_5 with many non-isoprene degrading species of bacteria indicate that this gene does not share the same role as *dmlR_4*, and may instead act as a non-specific regulator of various processes. Molecular analysis of the roles of *dmlR_4* and *dmlR_5* in isoprene metabolism in *Variovorax* sp. WS11 is described in Chapter 8.

4.5. **Conclusions**

The genome of *Variovorax* sp. WS11 was sequenced through a combination of short-reads and long-reads techniques, leading to the identification of a chromosome (composed of three contigs) and two circular megaplasmids (Table 4.2). Annotation by RAST software (Aziz *et al*. 2008, Brettin *et al*. 2015, Overbeek *et al*. 2014) followed by subsystems analysis indicated that each megaplasmid contained genes involved in the metabolism of sulfur, aromatic compounds, carbohydrates, and lipids (Table 4.2). These subsystems were consistent with previous reports of other *Variovorax* spp. degrading the above compounds through various metabolic processes (Aziz *et al*. 2020, Brandt *et al*. 2014a, Carbajal-rodríguez *et al*. 2011, Dawson *et al*. 2020, Satola *et al*. 2013). The closest relative of *Variovorax* sp. WS11, according to nucleotide identity of the 16S rRNA gene sequence, was the isoprene-degrading *Variovorax* sp. OPL2.2 (100% identity). With an ANI of 99%, *Variovorax* sp. OPL2.2 was determined to be

of the same species as *Variovorax* sp. WS11, likely accounting for the high degree of conservation of both amino acid identity and genetic organisation of their respective *iso* metabolic gene clusters (Carrión *et al*. 2020).

In summary, the genome of *Variovorax* sp. WS11 is organised in a similar manner to other characterised *Variovorax* spp., as essential metabolic processes encoded on the chromosome appear to be augmented by the presence of large plasmids. Megaplasmids 1 and 2 contained many genes with predicted roles in a variety of metabolic processes (Table 4.2). The full *iso* metabolic gene cluster of *Variovorax* sp. WS11 was located to a single portion of megaplasmid 1, as in *Rhodococcus* sp. AD45 (Crombie *et al*. 2015), although the critical glutathione biosynthesis genes were located on the chromosome. Comparative genomics analysis may provide valuable insights into the conservation of the predicted methylcitrate and methylmalonyl-CoA pathways in the assimilation of isoprene by diverse isoprene degrading bacteria.

5. Optimising genetics systems in *Variovorax* sp. WS11

5.1. Introduction

At the beginning of this project, *Rhodococcus* sp. AD45 was the only model bacterium used for the study of isoprene degradation. The initial identification of the *iso* metabolic gene cluster by van Hylckama Vlieg *et al*. (2000) and the subsequent molecular and transcriptomic analysis of isoprene metabolism by Crombie *et al.* (2015) were all conducted in this bacterium. The identification of a greater diversity of isoprene degraders through culture-dependent and culture-independent techniques (as described in Section 1.4.2) necessitated the development of a new model organism to provide a basis for comparative studies. One aim of this project was to study the similarities and differences between the mechanisms of isoprene metabolism by phylogenetically diverse species of bacteria. *Variovorax* sp. WS11 was the first Gram negative isoprene degrader to be characterised (Dawson *et al*. 2020) and served as a basis for comparison with the Gram positive *Rhodococcus* sp. AD45. A reverse genetics approach was required to link phenotypic functions with candidate genes. In order to achieve this, a reliable method of introducing DNA into *Variovorax* sp. WS11 was required. The only example of the transformation of an isoprene degrader before this study was described in *Rhodococcus* sp. AD45 (Crombie *et al*. 2015). Electroporation was used to introduce a suicide vector into *Rhodococcus* sp. AD45 in order to delete *isoA*, thereby abolishing isoprene metabolism.

Previous studies in non-isoprene degrading *V. paradoxus* TBEA6, *V. paradoxus* EPS, and *V. paradoxus* B4 used conjugation as a means of mobilising DNA from *Escherichia coli* S17-1 λpir into the recipient bacterium (Carbajal-rodríguez *et al*. 2011, Pehl *et al*. 2012, Schürmann *et al*. 2013, Fredendall *et al*. 2020). These either used the spot-agar mating technique (Friedrich *et al*. 1981) or conjugation on a filter membrane (Pehl *et al*. 2012, Fredendall *et al*. 2020). Transformation of *V. paradoxus* EPS was also conducted by electroporation (Pehl *et al*. 2012). There are benefits to using conjugation over electroporation, and vice versa. Conjugation typically has a higher rate of success than electroporation and requires no preparation of the recipient cells to induce competence (Cadoret *et al*. 2014, Zeaiter *et al*. 2018). Conjugative systems also include secretins which make the DNA used for transformation resistant to digestion by restriction endonucleases within the recipient cell (Chen *et al*. 2005). Drawbacks of conjugation include the requirement for a vector which contains a specific origin of transfer and a conjugative pilus which facilitates genetic transfer between donor and recipient bacteria (Chen *et al*. 2005, Cadoret *et al*. 2014). In cases where the donor DNA contains an origin of transfer but no conjugative machinery (F-factor), the use of a helper plasmid with promiscuous conjugative machinery facilitates the transfer of DNA (Stabb & Ruby 2002). Also, conjugation requires a selection method to prevent the proliferation of the donor bacterium, and potential 'helper' bacterium, potentially necessitating the prior creation of an antibiotic resistant strain of the recipient bacterium. The use of nutrient-deficient (auxotrophic) *E. coli* strains circumvents this issue, as *E. coli* S17-1 λpir is deficient for the synthesis of proline and histidine (Parke 1990). Electroporation, which increases membrane permeability through the application of an electrical field, has a lower efficiency of transfer of DNA into the recipient cell. However, the advantage of this technique is the ability to use small quantities of DNA without the need for plasmid-encoded

conjugative machinery (Cadoret *et al*. 2014). Drawbacks of electroporation as a method of DNA delivery primarily relate to the specific preparation of cells and the variable success rates between different species of bacteria. Electrocompetent cells must first be prepared, with some studies recommending the inclusion of stabilising agents such as sucrose or glycerol (Chassy *et al*. 1988, Crombie 2011, Pehl *et al*. 2012), but a sufficiently low solute concentration must also be used to prevent arcing in electroporation cuvettes. The electrical field must be strong enough to destabilise cell membranes, invariable resulting in the death of a proportion of the population, but not so strong as to exceed the optimum for transformation (Chassy *et al*. 1988). These considerations must be applied to the optimisation of electroporation protocols for each strain tested, making electroporation more labour-intensive to prepare.

5.2. Specific chapter aims and objectives

In this chapter, the optimisation of *Variovorax* sp. WS11 as a model organism for the study of isoprene metabolism is described. Study of the molecular basis of isoprene metabolism required the ability to reliably transform *Variovorax* sp. WS11 with non-native DNA. Therefore, the work detailed in this chapter was conducted with the aim of developing genetics techniques such as electroporation and conjugation. Also, the susceptibility of *Variovorax* sp. WS11 to conventional antibiotics was studied, thereby identifying the range of plasmid vectors which would be suitable for future studies in this bacterium.

1. Establish protocols which allow the genetic transformation of *Variovorax* sp. WS11.
2. Study the profile of antibiotic susceptibility/resistance in *Variovorax* sp. WS11, facilitating the use of suitable plasmid vectors in further experiments.

5.3. Hypothesis

Previous studies in *Variovorax* spp. have described the transformation of members of this genus through both electroporation and conjugation. Therefore, it was hypothesised that *Variovorax* sp. WS11 was a suitable model bacterium for genetic studies of the *iso* cluster due to the relative ease of genetic manipulations in previously-characterised members of this genus. The ability to transform *Variovorax* sp. WS11 would enable valuable comparative studies with *Rhodococcus* sp. AD45, which will be essential to fully understand the molecular mechanisms which contribute to the function of the *iso* gene cluster.

5.4. Methods

5.4.1. Optimising the transformation of *Variovorax* sp. WS11 by electroporation

The benefits of electroporation over conjugation as a means of bacterial transformation relate to the suitability of many plasmids for this process (Cadoret *et al*. 2014). Also, the lack of a donor bacterium increases the ease of isolating the desired transformants. However, cells had to be specifically prepared to induce electrocompetence. *Variovorax* sp. WS11 was grown to mid/late exponential phase in Ewers medium with 10 mM succinate, then transferred to 50 ml of fresh Ewers medium with 10 mM succinate and grown to an OD_{540} of 0.4. The culture was

incubated on ice for 15 minutes and then washed twice in 5 ml ice-cold water (centrifugation at 6,000 x *g*, 15 minutes, 4 °C). The cell pellet was resuspended in 1 ml of 10% (w/v) glycerol. 100 µl aliquots were transformed with 110 ng of pBBR1MCS-2 (KanR, 5,144 bp) (Kovach *et al*. 1995), a plasmid previously used in the complementation of genetic mutations in other species of *Variovorax* (Pehl *et al*. 2012, Schürmann *et al*. 2013). *Variovorax* sp. WS11 was electroporated in a 2 mm gap cuvette under the standard conditions described in Section 2.4 (2.5 kV, 200 Ω, 2.5 µF). Cells were recovered for 3 hours in Ewers medium with 10 mM succinate and spread on R2A agar with 50 µg/ml kanamycin to select for plasmid uptake. An average electroporation frequency of 1.36 x 10^4 colony forming units (cfu)/µg plasmid DNA was calculated by counting the kanamycin resistant colonies after incubation at 30 °C for 5 days. Increasing the resistance of the electroporation to 400 Ω increased the frequency to 1.99 x 10^4 cfu/µg plasmid DNA, while decreasing the voltage to 2.2 kV decreased the electroporation frequency to 1.05 x 10^4 cfu/µg. When *Variovorax* sp. WS11 was electroporated in the absence of pBBR1MCS-2, no kanamycin resistant colonies were obtained.

In order to confirm that the observed resistance to kanamycin was due to the uptake of pBBR1MCS-2, *Variovorax* sp. WS11 was grown in Ewers medium with 10 mM succinate (+50 µg/ml kanamycin) to an OD_{540} of approximately 1.0 and cells were harvested by centrifugation. Plasmid DNA was extracted as described in Section 2.8.2. pBBR1MCS-2 was digested with *Bgl*II and *Hind*III as described in Section 2.8.3. *In silico* simulation of this digestion predicted the formation of two DNA fragments of 1,437 and 3,707 bp. Uncut and digested pBBR1MCS-2 were separated by agarose gel electrophoresis (as described in Section 2.8.5) and visualised (Figure 5.1).

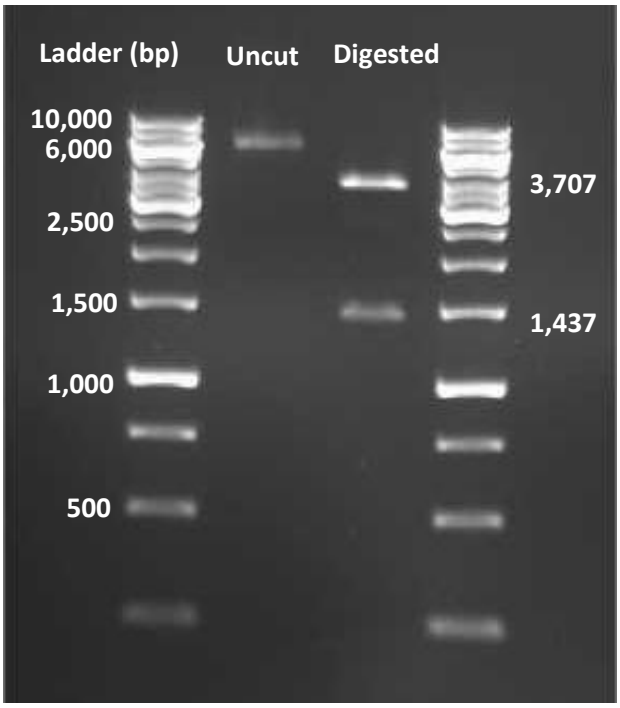

Figure 5.1. Restriction digestion of pBBR1MCS-2 with *Bgl*II and *Hind*III. pBBR1MCS-2 was extracted from *Variovorax* sp. WS11.

Although *Variovorax* sp. WS11 was successfully transformed under the above conditions, the electroporation frequency with pBBR1MCS-2 was quite low. Certain variables were considered when optimising the electroporation procedure; the preparation of electrocompetent cells, the electroporation conditions, and the recovery conditions. *V. paradoxus* EPS was previously prepared for electroporation as described in Section 2.4.2 (adapted from the protocol described by Smith & Iglewski, 1989), with the exception that *V. paradoxus* EPS was previously grown in YE medium and recovered on YE agar (Pehl *et al*. 2012). As this protocol maintained *V. paradoxus* EPS in the same medium throughout, further transformation experiments were conducted using Ewers medium to grow *Variovorax* sp. WS11, Ewers medium to recover electroporated cells, and Ewers agar to grow transformants. This aimed to reduce any stress to the cells which could be caused by switching between minimal and rich media. Key differences between this protocol and the initial electroporation protocol used for *Variovorax* sp. WS11 were as follows; the inclusion of an incubation period at 4 ^{o}C for 24 hours before washing, longer centrifugation periods (30 minutes), and washing and resuspension in 300 mM sucrose (Orwin, P, personal communication, Pehl *et al*. 2012). Sucrose was frequently included in electroporation protocols as an osmoprotectant (Holo & Nes 1989, Pyne *et al*. 2013, Takaku *et al*. 2020). Cells were electroporated at 2.5 kV with a variation in the resistance and recovery time (Table 5.1). The frequency of electroporation increased above the initial transformation conditions. Surprisingly, increasing the resistance to 400 Ω did not increase the electroporation frequency as before, with the frequency decreasing from 8.24×10^4 to 6.24×10^4 cfu/µg (Table 5.1). The frequency of electroporation increased more than 2-fold when the recovery time was increased from 1 hour to 3 hours, but there was little to no difference between the electroporation frequency after 3 hours and 5 hours of recovery. Once again, when *Variovorax* sp. WS11 was electroporated in the absence of pBBR1MCS-2, no kanamycin resistant colonies were recovered.

Table 5.1. Optimising electroporation conditions according to the protocol described for *V. paradoxus* EPS (Pehl *et al*. 2012). N=1 (single biological replicates).

Cells incubated at 4^{o}c for 24 hours, resuspended in 300 mM sucrose					
Voltage (kV)	**Resistance (Ω)**	**Capacitance (µF)**	**Recovery Time (hours)**	**Colonies (cfu)**	**Electroporation Frequency (cfu/µg plasmid DNA)**
2.5	200	2.5	1	425	3.86×10^4
2.5	200	2.5	3	906	8.24×10^4
2.5	200	2.5	5	894	8.13×10^4
2.5	400	2.5	3	686	6.24×10^4

These data indicated that the ideal electroporation conditions were 2.5 kV, 200 Ω resistance, 2.5 µF capacitance, with recovery for 3 hours. Subsequent optimisation of electroporation conditions focused on the preparation and washing of electrocompetent cells. The transformation efficiency of *V. paradoxus* EPS was improved by incubation at 4 ^{o}C for 24 hours before electroporation (Orwin, P., personal communication), although the reason for this was unknown. *Variovorax* sp. WS11 was incubated for 48 hours at 4 ^{o}C, and 300 mM sucrose was substituted for 10% glycerol. Each condition improved the efficiency of transformation (Table 5.2). As described previously, increasing

the resistance of electroporation caused a successive decrease in the electroporation frequency. Increasing the voltage from 2.5 to 2.8 kV also caused a decrease in the frequency of electroporation. Centrifugation and excessive washing of *Variovorax* sp. WS11 was previously found to hinder the rate of substrate oxidation by whole cells (as described in Chapter 3). This was predicted to be due to stress caused by repeated pelleting and resuspension leading to the shearing of cells. Therefore, the centrifugation steps during the preparation of electrocompetent cells were adapted from the previously described method (Chapter 2, Section 2.4.2) to decrease the length of centrifugation from 30 minutes to 10 minutes. The optimised transformation conditions were described in Section 2.4.3.

Table 5.2. Optimisation of electroporation conditions by varying the voltage and resistance of electroporation, and the preparation of electrocompetent cells. N=1 (single biological replicates).

Cells incubated at 4°c for 48 hours, resuspended in 10% glycerol					
Voltage (kV)	**Resistance (Ω)**	**Capacitance (μF)**	**Recovery Time (hours)**	**Colonies (cfu)**	**Electroporation Frequency (cfu/μg plasmid DNA)**
2.5	200	2.5	3	2,488	2.26×10^5
2.5	400	2.5	3	1,352	1.23×10^5
2.5	600	2.5	3	692	6.29×10^4
2.8	400	2.5	3	1,564	1.42×10^5

5.4.2. **Optimising the transformation of *Variovorax* sp. WS11 by conjugation**

Conjugation was primarily used as the means of transformation in previous studies of *Variovorax* spp. Targeted mutagenesis in *V. paradoxus* TBEA6 was enabled by mobilising a suicide vector from *E. coli* S17-1 by the spot agar mating technique (Friedrich *et al*. 1981, Schürmann *et al*. 2013). The same method was subsequently used to mobilise pBBR1MCS-5 into *V. paradoxus* TBEA6 when complementing the targeted mutation. Conjugation via spot-agar mating was successfully employed in *V. paradoxus* B4 (Carbajal-rodríguez *et al*. 2011). *V. paradoxus* EPS was also transformed by conjugation with *E. coli* S17-1 λpir by bi-parental mating on a sterile filter membrane (Pehl *et al*. 2012, Fredendall *et al*. 2020). *E. coli* S17-1 λpir simplifies the conjugation process due to the requirement for supplementation with proline and histidine in order to support growth (Parke 1990). By excluding these vitamins during the selection of transconjugants, the growth of the *E. coli* donor strain can be prevented without the use of an antimicrobial agent, avoiding the need for a recipient strain with a natural or acquired resistance to a specific antibiotic.

Before conjugation could be attempted in *Variovorax* sp. WS11, the medium components used in the growth and selection of the donor and recipient bacteria had to be tested. Growth of *E. coli* S17-1 λpir was previously selected against by excluding proline and histidine from the growth medium (Parke 1990). As MAMS vitamins do not contain proline or histidine (as described in Section 2.2.1), *E. coli* S17-1 was streaked onto Ewers medium with a range of carbon sources (Table 5.3). While growth was not supported on isoprene, *E. coli* S17-1 was able to grow on Ewers

medium with 10 mM citrate or 10 mM glucose, with or without vitamin supplementation. While isoprene may have provided a counter-selection sufficient to prevent the growth of *E. coli* S17-1, *Variovorax* sp. WS11 grew very slowly on Ewers agar with isoprene. In fact, *Variovorax* sp. WS11 grew to approximately the same level when inoculated on Ewers agar with no carbon source, indicating scavenging of media components. Previous studies with *V. paradoxus* EPS used M9 agar for the selection of transformants after conjugation. M9 agar was prepared according to the standard recipe described by the American Type Culture Collection (ATCC). MAMS vitamins and various carbon sources were included or excluded as described in Table 5.3. *Variovorax* sp. WS11 consistently failed to grow on M9 agar regardless of the carbon source, while *E. coli* S17-1 was able to grow on glucose or citrate in the presence of vitamins. As the media composition was not sufficient to select for the growth of only *Variovorax* sp. WS11, antibiotic agents were considered.

Table 5.3. Growth of the donor (*E. coli* S17-1) and recipient (*Variovorax* sp. WS11) bacteria in preparation for conjugation. MAMS vitamins were either included (Vits) or excluded (No Vits) from the agar. Growth (+), no growth (-), or poor growth (~) are recorded.

	Ewers + isoprene		**Ewers + 10 mM citrate**		**Ewers + 10 mM glucose**	
	Vits	No Vits	Vits	No Vits	Vits	No Vits
***Variovorax* sp. WS11**	+	-	+	~	+	~
***E. coli* S17-1**	-	-	+	~	+	~

While the antibiotic susceptibility profile of *Variovorax* sp. WS11 indicated that chloramphenicol, tetracycline, or ampicillin could be used as selective agents during conjugation with *E. coli* S17-1, these antibiotics are typically required as selective agents for routinely used plasmids. Also, the putative spectinomycin resistant mutant of *Variovorax* sp. WS11 had not retained a resistance phenotype. Therefore, an alternative antibiotic was required to suppress the growth of the donor *E. coli* S17-1. Rifampicin and nitrofurantoin are two antibiotics with potent activity against *E. coli* (Campbell *et al*. 2001, Alanazi *et al*. 2018). Rifampicin inhibits the DNA-dependent RNA polymerase (Campbell *et al*. 2001), while nitrofurantoin exerts a poorly characterised bactericidal effect by acting on many cellular components (Huttner *et al*. 2015). *Variovorax* sp. WS11 was grown in Ewers medium with 10 mM succinate to late-exponential phase and serially diluted across a 10-fold dilution series. Cells were spread on R2A agar supplemented with 50 µg/ml rifampicin (prepared as 50 mg/ml in 70% (v/v) methanol) or supplemented with 35 µg/ml nitrofurantoin (prepared as 35 mg/ml in 70% (v/v) ethanol). Colonies were transferred to Ewers medium with 10 mM glucose, supplemented with the appropriate antibiotic. Resistance to nitrofurantoin or rifampicin was confirmed by repeated sub-culture into Ewers medium with the same antibiotic.

pBBR1MCS-2 was selected for the optimisation of conjugation protocols as this plasmid contains a *mob* region which facilitates conjugative transfer (Kovach *et al*. 1995). The initial conjugation protocol was as follows. *Variovorax* sp. WS11 was grown in 20 ml Ewers medium with 10 mM succinate in the presence of nitrofurantoin or rifampicin. *E. coli* S17-1, containing pBBR1MCS-2, was grown in 5 ml LB with kanamycin to select for plasmid retention. Cells were grown to approximately equal densities, accounting for the differences in the volume of each culture, and samples were serially diluted and plated on R2A agar for cell counting. The remaining cells were washed twice in 50 mM phosphate buffer (pH 6.0 and pH 7.0 for *Variovorax* sp. WS11 and *E. coli* S17-1, respectively) to remove any antibiotics. Cells were mixed in equal volumes and adsorbed onto a 0.2 µm sterile filter membrane (Millipore, Merck, Kenilworth, NJ, USA) by applying a vacuum. The filter was washed twice using 50 ml phosphate buffer (pH 7.0) and placed on an R2A agar plate in the absence of antibiotic for 24 hours at 30 °C. This incubation period aimed to allow time for conjugation events to occur. The filter membrane was washed in 10 ml phosphate buffer to resuspend all cells, and the mixture was serially diluted and spread on Ewers agar with 10 mM succinate, 50 µg/ml kanamycin and either 50 µg/ml rifampicin or 50 µg/ml nitrofurantoin (depending on the spontaneous resistant mutant of *Variovorax* sp. WS11 which was used). Transconjugants were counted and compared to the initial numbers of untransformed *Variovorax* sp. WS11 in order to calculate the efficiency of conjugation (Table 5.4).

Table 5.4. Efficiency of conjugative transfer of pBBR1MCS-2 from *E. coli* S17-1 (donor) to *Variovorax* sp. WS11 (recipient). Mutants of *Variovorax* sp. WS11 were resistant to either rifampicin (*Variovorax* sp. WS11 Δ*rif*) or nitrofurantoin (*Variovorax* sp. WS11 Δ*nitro*). N=1 (single biological replicates).

Conjugative Plasmid	**Anti-*E. coli* selective agent**	**Donor:Recipient Ratio**	**Transconjugants/ml**	**Efficiency of Conjugation**
pBBR1MCS-2	Rifampicin	5:8	4.51×10^{6}	1.80×10^{-4}
pBBR1MCS-2	Nitrofurantoin	5:0.3	8.15×10^{5}	3.26×10^{-5}

The efficiency of conjugation was quite low in both cases. *Variovorax* sp. WS11 Δ*rif* was present in excess compared to the donor, and *E. coli* S17-1 was present in excess compared to the *Variovorax* sp. WS11 Δ*nitro*. *Variovorax* sp. WS11 Δ*rif* had approximately 10-fold greater efficiency of conjugation. Whether this was due to the choice of antibiotic or due to the ratio of donor to recipient was unclear, but further optimisation was conducted using *Variovorax* sp. WS11 Δ*rif*. Pehl *et al*. (2012) described the conjugation of *V. paradoxus* EPS with *E. coli* S17-1 λpir. Further transformations of *Variovorax* sp. WS11 by conjugation were conducted according to the same method. *Variovorax* sp. WS11 Δ*rif* and *E. coli* S17-1 were grown as before and washed in 50 mM phosphate buffer supplemented with 10 mM $MgSO_4$. As before, the cell cultures were serially diluted and spread on R2A agar for cell counts. Divalent cations have previously been found to increase conjugation efficiency in other species of bacteria, accounting for the inclusion of $MgSO_4$ (Johnson & Grossman 2016, Sakuda *et al*. 2018). The cell suspensions were combined in 10 mM $MgSO_4$ and adsorbed onto a sterile 0.2 µm filter membrane by applying a vacuum, then the filter membrane was washed twice with 50 ml of 10 mM $MgSO_4$. The membrane was incubated on an R2A agar plate at 30 °C for 24 hours and then washed in 10 ml of 10 mM $MgSO_4$. The wash solution was serially diluted and spread on Ewers agar with 10 mM succinate, 50 µg/ml kanamycin, and 50 µg/ml rifampicin. The efficiency of conjugation

was approximately 100-fold higher than the previous method (Table 5.5). Repeating this method achieved a conjugation efficiency of 2.6 x 10^{-2}. The duplicate conjugation experiments indicated that transformation of *Variovorax* sp. WS11 Δ*rif* by this protocol was reproducible. This protocol was repeated in *Variovorax paradoxus* EPS. This strain was found to be resistant to 35 μg/ml tetracycline during an unrelated experiment, and tetracycline was therefore included as a selectable marker to prevent the growth of *E. coli* S17-1. This protocol transformed *V. paradoxus* EPS with a conjugation frequency of 4.06 x 10^{-2}, indicating that this adapted method was suitable for the transformation of at least two species of *Variovorax*.

Table 5.5. Efficiency of conjugation of *Variovorax* sp. WS11 with *E. coli* S17-1 under the optimised conditions described by Pehl *et al*. (2012). N=1 (single biological replicates).

Conjugative Plasmid	**Anti-*E. coli* selective agent**	**Donor:Recipient Ratio**	**Transconjugants/ml**	**Efficiency of Conjugation**
pBBR1MCS-2	Rifampicin	10:3	3.9 x 10^{7}	1.3 x 10^{-2}
pBBR1MCS-2	Rifampicin	15:2	7.8 x 10^{7}	2.6 x 10^{-2}

5.5. Results and discussion

5.5.1. Antibiotic susceptibility testing

Genetic manipulations typically require the introduction of a selection pressure in order to identify successful transformants and to select against the growth of non-transformants. A simple and often used selectable trait is antibiotic resistance, typically encoded on the donated plasmid. The natural antibiotic resistance profile of a bacterium therefore restricts the range of plasmids available for use in genetic manipulations. No genes involved in antibiotic resistance were identified in the genome of *Variovorax* sp. WS11 during annotation using the MicroScope platform (Aziz *et al*. 2008, Overbeek *et al*. 2014, Brettin *et al*. 2015, Vallenet *et al*. 2019). The susceptibility of *Variovorax* sp. WS11 to antibiotics was tested by preparing R2A agar supplemented with a range of antibiotics at the concentrations described in Section 2.2.2. The tested antibiotics were primarily broad-spectrum protein synthesis inhibitors and β-lactam antibiotics; ampicillin, kanamycin, gentamicin, streptomycin, spectinomycin, tetracycline, and chloramphenicol (Arenz & Wilson 2016, Polikanov *et al*. 2018). Each antibiotic was prepared across a 2-fold dilution series from 1x concentration (described in 2.2.2) to 0.125x concentration in R2A agar. *Variovorax* sp. WS11 was grown in Ewers medium with 10 mM glucose to mid-exponential phase and serially diluted across a 10-fold series to 10^{-7}. Cell suspensions from each dilution were spread on R2A agar, amended with antibiotics, and incubated for 96 hours at 30 °C. Plates which had too many colonies to count were excluded. Cell counts from the 10^{-3}, 10^{-4}, and 10^{-5} dilutions were recorded (Figure 5.2). The aminoglycoside antibiotic kanamycin was a successful inhibitor of *Variovorax* sp. WS11 in all trials, while ampicillin was not an effective inhibitor (Carrión, O., unpublished). Chloramphenicol was completely inhibitory at 35 μg/ml and 17.5 μg/ml, but not at 8.75 μg/ml or 4.38 μg/ml. Tetracycline was also not inhibitory at 8.75 μg/ml and 17.5 μg/ml (Figure 5.2).

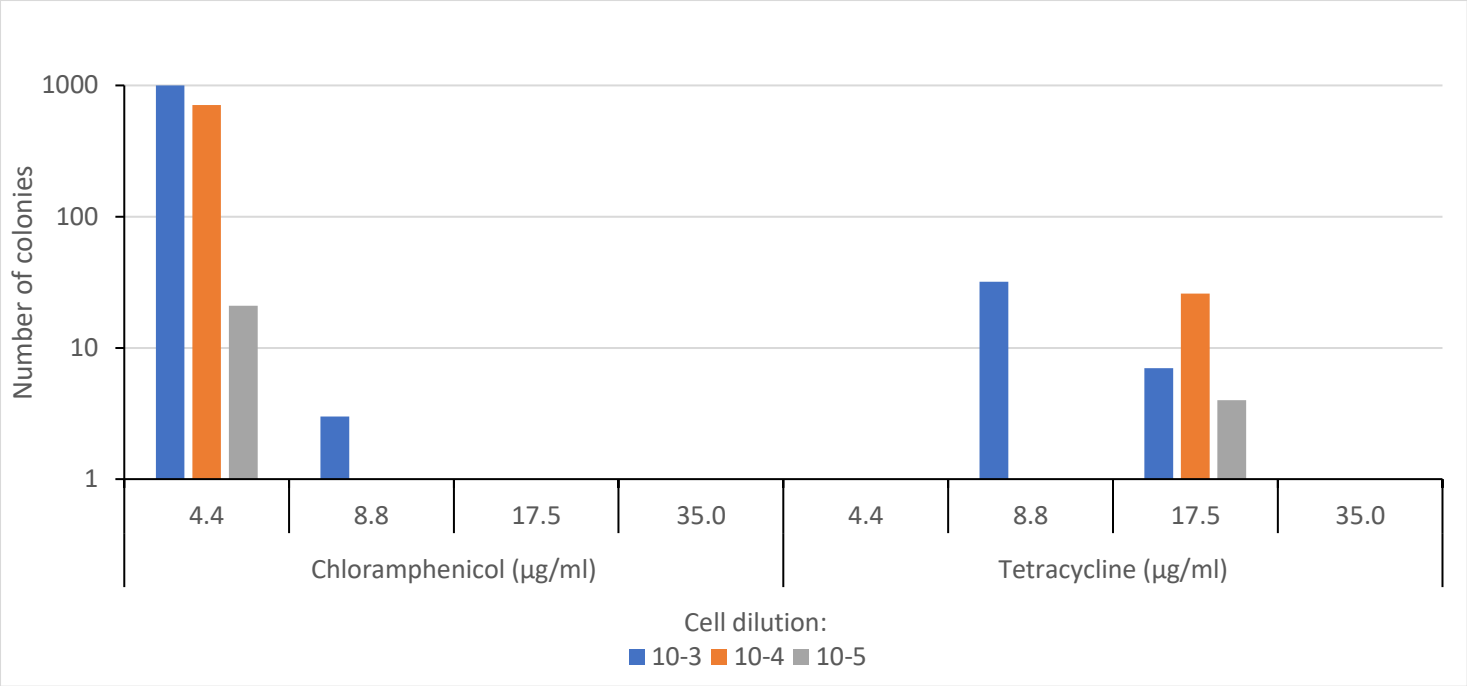

Figure 5.2. Susceptibility of *Variovorax* sp. WS11 to antibiotics. Colonies on R2A agar were recorded for a 2-fold dilution series of each antibiotic. N=1 (single biological replicates).

The thermal stability of antibiotics must be considered when applying to a relatively slow-growing organism like *Variovorax* sp. WS11. Colonies were typically visible on R2A agar after 5-7 days, while certain antibiotics are only stable for a few days. Ampicillin, for example, is only stable for up to 3 days in culture (Ivashkiv 1973). Tetracycline was also unsuitable as a selective agent, potentially due to the relatively short half-life of this antibiotic (12 hours in phosphate buffer at 24 °C) (Ali 1984). In spite of the thermal stability of chloramphenicol in liquid, growth of *Variovorax* sp. WS11 was not inhibited at the lowest tested concentrations, indicating a low-level of resistance (Franje *et al*. 2010). Gentamicin and kanamycin consistently inhibited the growth of *Variovorax* sp. WS11 on R2A agar at all tested concentrations. While streptomycin and spectinomycin typically inhibited the growth of *Variovorax* sp. WS11 at all tested concentrations, there some were instances of colonies forming at low concentrations of these antibiotics. Colonies were transferred from spectinomycin-supplemented agar and streptomycin-supplemented agar to Ewers medium with 1% (v/v) isoprene and 50 µg/ml spectinomycin or 50 µg/ml streptomycin. Moderate growth was observed in the presence of spectinomycin, with *Variovorax* sp. WS11 reaching an OD_{540} of 0.19 after 6 days. However, subsequent attempts to grow *Variovorax* sp. WS11 with spectinomycin failed, indicating that no stable resistance phenotype had been established. Colonies from the streptomycin-supplemented plate reached an OD_{540} of 0.09, indicating that a stable mutation had not been achieved. Previous studies have linked spontaneous resistance to spectinomycin and streptomycin to mutations in the 30S subunit of the bacterial ribosome (Maness *et al*. 1974, Criswell *et al*. 2006). The temporary resistance of *Variovorax* sp. WS11 to spectinomycin may also be due to a mutation in the 30S rRNA, although the instability of this resistance may indicate a detrimental effect of this mutation on cell fitness.

5.6. **Conclusions**

The work described in this chapter was conducted with the aim of developing *Variovorax* sp. WS11 as a suitable model organism for the study of isoprene metabolism. Molecular studies of the genetic and biochemical basis for isoprene metabolism required efficient, reproducible genetics systems to facilitate the manipulation of *Variovorax* sp. WS11. The susceptibility of this strain to antibiotics was studied as antibiotic resistance is a common selectable trait used in the transformation of bacteria. Kanamycin and gentamicin consistently inhibited the growth of *Variovorax* sp. WS11 on R2A agar. The stability of antibiotics for 5 days or more was required due to the slow growth of *Variovorax* sp. WS11 on agar, preventing the use of less-stable antibiotics such as ampicillin (Ivashkiv 1973). Ampicillin failed to inhibit the growth of *Variovorax* sp. WS11 (Carrión, O., unpublished).

Spontaneous rifampicin-resistant mutants of *Variovorax* sp. WS11 were generated by spreading high-density cell cultures on R2A agar supplemented with 50 µg/ml rifampicin. *Variovorax* sp. WS11 Δ*rif* demonstrated stable resistance to rifampicin in liquid media but the initial conjugation efficiency was very low (Table 5.3). The efficiency was improved when using the protocol previously described for *V. paradoxus* EPS (Pehl *et al*. 2012), with the highest recorded efficiency of 1.3×10^{-2} (Table 5.4). This protocol was validated in *V. paradoxus* EPS, which achieved a conjugation efficiency of 4.06×10^{-2}. Therefore, conjugation was a suitable technique for the transformation of *Variovorax* sp. WS11.

Transformation of *Variovorax* sp. WS11 by electroporation was successful when using an adapted version of the protocol described for *V. paradoxus* EPS (Pehl *et al*. 2012). Due to the relative ease of preparing large stocks of electrocompetent *Variovorax* sp. WS11, which could be maintained at -80 ^{o}C until required, and because a second selectable marker such as rifampicin was not required to isolate transformants, electroporation was chosen as the preferred transformation method for the remainder of this project. By adapting the reported transformation protocols designed for other *Variovorax* spp., *Variovorax* sp. WS11 can be reliably transformed with relatively high efficiencies. This enabled the molecular analysis of isoprene metabolism in this new model bacterium, as described in Chapters 6, 7 and 8.

6. Molecular and biochemical analysis of isoprene metabolism by *Variovorax* sp. WS11

6.1. Introduction

The *iso* metabolic gene cluster has consistently been detected in the genomes of sequenced isoprene degraders. This cluster encodes an isoprene monooxygenase (*isoABCDEF*), two glutathione *S*-transferases (*isoI*, *isoJ*), a dehydrogenase (*isoH*), and a putative racemase/CoA-transferase (*isoG*). At the beginning of this project, isoprene monooxygenase (IsoMO) was the best-characterised component of isoprene metabolism, with only three studies describing the functions of IsoH, IsoI, and IsoJ, with no functional characterisation of IsoG (Crombie *et al*. 2015, van Hylckama Vlieg *et al*. 1998, 1999, 2000). However, analysis of the proteome of *Variovorax* sp. WS11 confirmed that IsoGHIJ were highly expressed during the growth of this bacterium on isoprene (described in Chapter 3).

IsoMO is a four-component SDIMO (as described in Section 1.5), composed of a non-heme diiron oxygenase (IsoABE), a Rieske-type ferredoxin (IsoC), a reductase (IsoF), and a coupling protein (IsoD) which lacks a cofactor. The genes encoding IsoMO (*isoABCDEF*) were first identified in *Rhodococcus* sp. AD45 (van Hylckama Vlieg *et al*. 2000). However, no activity was observed when expressing these genes in *E. coli* from a gene library in pLAFR3 (van Hylckama Vlieg *et al*. 2000). The average size of these cosmid library inserts was 23 kbp, while the *iso* metabolic gene cluster of *Rhodococcus* sp. AD45, encompassing all 22 genes upregulated in the presence of isoprene (Crombie *et al*. 2015), measures approximately 27 kbp. This indicates that *E. coli* may not have received the entire *iso* metabolic gene cluster, therefore preventing metabolism of isoprene by *E. coli*. Crombie *et al*. (2015) provided the first functional evidence that IsoMO was essential to isoprene metabolism in *Rhodococcus* sp. AD45. *isoA* was inactivated by targeted mutagenesis, abolishing the growth of *Rhodococcus* sp. AD45 on isoprene.

Previous studies have reported difficulties when attempting to express and/or purify functional SDIMO in a heterologous host, particularly in *E. coli* (Champreda *et al*. 2004, McCarl *et al*. 2018). For example, expression of the alkene monooxygenase from *X. autotrophicus* Py2 in *E. coli* was unsuccessful (Zhou *et al*. 1996, Zhou *et al*. 1999). The sMMO is one of the best-characterised SDIMO. However, while individual components of sMMO have been expressed in *E. coli* (West *et al*. 1992, Park *et al*. 2018), activity of the whole sMMO is only observed when expressed in a methanotroph (Smith *et al*. 2002, Lock *et al*. 2017). A recent study by McCarl *et al*. (2018) reported that the activity of the ethene monooxygenase from *Mycobacterium chubuense* NBB4 doubled when it was co-expressed in *Pseudomonas putida* with chaperonins from *M. chubuense* NBB4 or *E. coli*. GroEL, a well-characterised chaperonin, was also essential for the correct folding of the oxygenase component of other SDIMO (Furuya *et al*. 2012, 2013). The co-expression of IsoMO with chaperonins may facilitate functional expression of IsoMO in *E. coli*. Significant progress in the expression of the IsoMO from *Rhodococcus* sp. AD45 was achieved by the development of the homologous expression strain, *Rhodococcus* sp. AD45-id (isoprene deficient) (Crombie *et al*. 2018). Strain AD45-id lacks the *iso* cluster-containing megaplasmid, and as a result is incapable of growth on isoprene. Almost all

components of the IsoMO have been expressed in soluble form in *Rhodococcus* sp. AD45-id, with only the reductase component (IsoF) proving recalcitrant to purification (Lockwood & Sims, unpublished, Sims, 2020).

This study aimed to identify the similarities and differences in the mechanisms of isoprene degradation between the Gram positive *Rhodococcus* sp. AD45 and the Gram negative *Variovorax* sp. WS11. *Variovorax* sp. WS11 contains an *iso* metabolic gene cluster with considerable similarity to that of *Rhodococcus* sp. AD45 (as described in Chapter 4), strongly indicating a conserved mechanism of isoprene metabolism. This was interesting when considering that *Rhodococcus* sp. AD45 and *Variovorax* sp. WS11 are phylogenetically distinct and were isolated from different environments (freshwater sediment and willow soil, respectively). Before the analysis of the proteome of isoprene-grown *Variovorax* sp. WS11, limited information was available regarding the metabolism of isoprene after the production of GMBA (Crombie *et al*. 2015, van Hylckama Vlieg *et al*. 1998, 1999, 2000), and many genes present on the *iso* metabolic gene cluster, including *isoG, isoJ, aldH* and *garB*, still have no confirmed function in isoprene metabolism.

6.2. **Specific chapter aims and objectives**

The molecular basis for isoprene metabolism in *Variovorax* sp. WS11 was studied, and the results are detailed in this chapter. These studies were conducted with the aim of performing a detailed comparison of the mechanisms of isoprene metabolism between *Variovorax* sp. WS11 and *Rhodococcus* sp. AD45. Additionally, the isoprene monooxygenase from *Variovorax* sp. WS11 was expressed in a heterologous, non-isoprene-degrading host bacterium with the aim of confirming the function of this essential *iso* component in isoprene metabolism. Finally, the affinity of the isoprene monooxygenase for isoprene was studied compared to the IsoMO from other isoprene degrading bacteria. This aimed to provide an indication of the affinity of IsoMO from bacteria isolated from distinct ecological niches.

1. Confirm the essential/non-essential role of the *iso* metabolic gene cluster in the ability of *Variovorax* sp. WS11 to assimilate isoprene by using targeted mutagenesis.
2. Confirm the specific function of IsoMO from *Variovorax* sp. WS11 through expression in a heterologous host, as described previously (Crombie et al. 2018, Sims 2020).
3. Study the kinetics of isoprene oxidation by IsoMO, and use these data to infer the sensitivity of IsoMO for isoprene from an isoprene degrader from willow soil compared to alternative environments (e.g. aquatic, leaf).

6.3. **Hypothesis**

The identification of the *iso* metabolic gene cluster in *Variovorax* sp. WS11 (detailed in Chapter 4) supported the hypothesis that this novel isoprene degrader assimilated isoprene through the same mechanism as *Rhodococcus* sp. AD45. This hypothesis was further explored in Chapter 6 through a combination of genetics and molecular approaches. It was hypothesised that the IsoMO from *Variovorax* sp. WS11 would have a lower affinity for isoprene

than the IsoMO from *Rhodococcus* sp. AD45. This was due to the fact that *Variovorax* sp. WS11 was isolated from the soil around a willow tree, with willow producing relatively large amounts of isoprene, while *Rhodococcus* sp. AD45 was isolated from freshwater sediment. If *Variovorax* sp. WS11 had adapted to a niche with a greater availability of isoprene than *Rhodococcus* sp. AD45, this may be reflected in the affinity of the respective IsoMO enzymes for isoprene.

6.4. **Methods**

6.4.1. **Assembly of a suicide construct in pK18mobsacB**

The targeted deletion of a gene can be achieved through a number of methods (Kaniga *et al*. 1991, Xu & Zhang 2016). Marker-exchange mutagenesis was chosen due to the relative ease of selecting for a mutant phenotype (Poteete *et al*. 2006, Farhan Ul Haque *et al*. 2016). This was achieved by double-homologous recombination, a process which relies on the introduction of two DNA sequences into a suicide vector which are identical to flanking regions of the gene of interest (Figure 6.1) (Xu & Zhang 2016). The introduction of a selectable marker between the flanking regions, typically a gene which encodes resistance to an antibiotic (Poteete *et al*. 2006), allows the insertion of the antibiotic resistance gene within the gene of interest, disrupting and inactivating it. The suicide vector used in this study was pK18mobsacB (Schäfer *et al*. 1994). pK18mobsacB was constructed using pBR322, a vector which is restricted to replication in *E. coli* (Bolivar *et al*. 1977). *sacB* encodes levansucrase, an enzyme which causes a lethal response to sucrose when expressed (Steinmetz *et al*. 1985).

The development of a reliable genetics system in *Variovorax* sp. WS11 (as described in Chapter 5) facilitated the introduction of DNA into this strain, and the availability of a genome sequence allowed the use of targeted mutagenesis. The region upstream of *isoA*, overlapping with the start codon of *isoA* and the stop codon of *aldH*, was amplified by PCR using the primers *isoA*.up.fwd and *isoA*.up.rev (Table 6.1). These primers introduced *Bam*HI and *Xba*I restriction sites at the 5' and 3' ends of this flanking region, respectively. The region downstream of *isoA*, overlapping with the stop codon of *isoA* and the start codon of *isoB*, was amplified by PCR using the primers *isoA.*down.fwd and *isoA*.down.rev (Table 6.1). These primers incorporated 5'-*Xba*I and 3'-*Hin*dIII restriction sites. The upstream and downstream flanking regions, termed A and B, respectively, were individually cloned into pJET1.2 (as described in Section 2.8.4). Flank A was excised from pJET1.2 by digestion with *Xba*I and *Bam*HI, and pK18mobsacB was linearised by digestion with *Xba*I and *Bam*HI, followed by ligation of the purified Flank A and pK18mobsacB (as described in Sections 2.8.3 and 2.8.4). The ligation mixture was mobilised into *E. coli* Top10 by heat shock (as described in Section 2.3.1), and the cells were subsequently spread on LB agar with 50 µg/ml kanamycin to select for maintenance of pK18mobsacB:*isoA*.up. This consistently resulted in very few colonies forming on kanamycin-supplemented agar, despite *E. coli* Top10 initially being used to replicate the empty pK18mobsacB vector. Those few colonies that did form were grown in LB with 50 µg/ml kanamycin and the plasmids were extracted as described in Section 2.7.2. Vector DNA was digested with *Xba*I and *Bam*HI to excise Flank A, and the resulting mixture was separated by agarose gel electrophoresis (as described in Section 2.8.5). Flank A was expected to have a size of approximately 500 bp, while pK18mobsacB is 5.7 kbp (Schäfer *et al*. 1994), but the digested DNA product consisted

of only pK18mobsacB with no excised insert (Figure 6.1). This problem persisted until *E. coli* DH5-α was used instead of *E. coli* Top10 as the recipient bacterium.

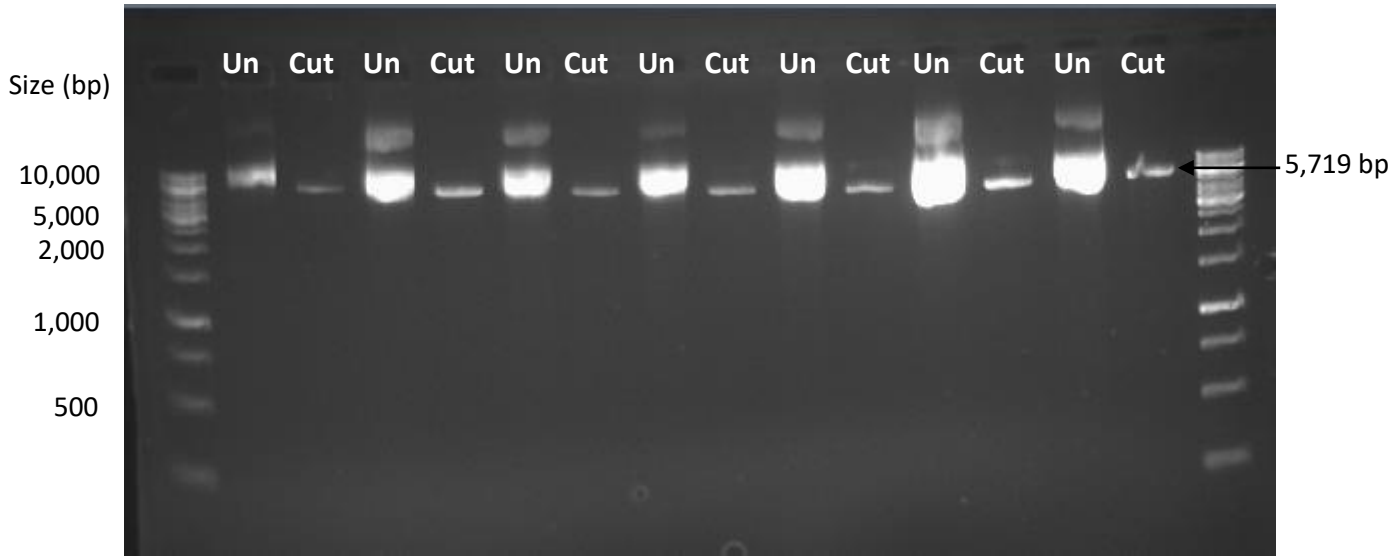

Figure 6.1. Putative pK18mobsacB:*isoA*.up vectors digested with *Xba*I and *Bam*HI (Cut) with their respective uncut (Un) vectors to act as references.

The synthesis of Flank A, the digestion of pJet:*isoA*.up and pK18mobsacB, and the transformation procedure were conducted as described previously. The transformation of *E. coli* DH5-α with the ligation mixture resulted in many colonies forming on LB agar with 50 µg/ml kanamycin, each of which contained pK18mobsacB:*isoA*.up (Figure 6.2).

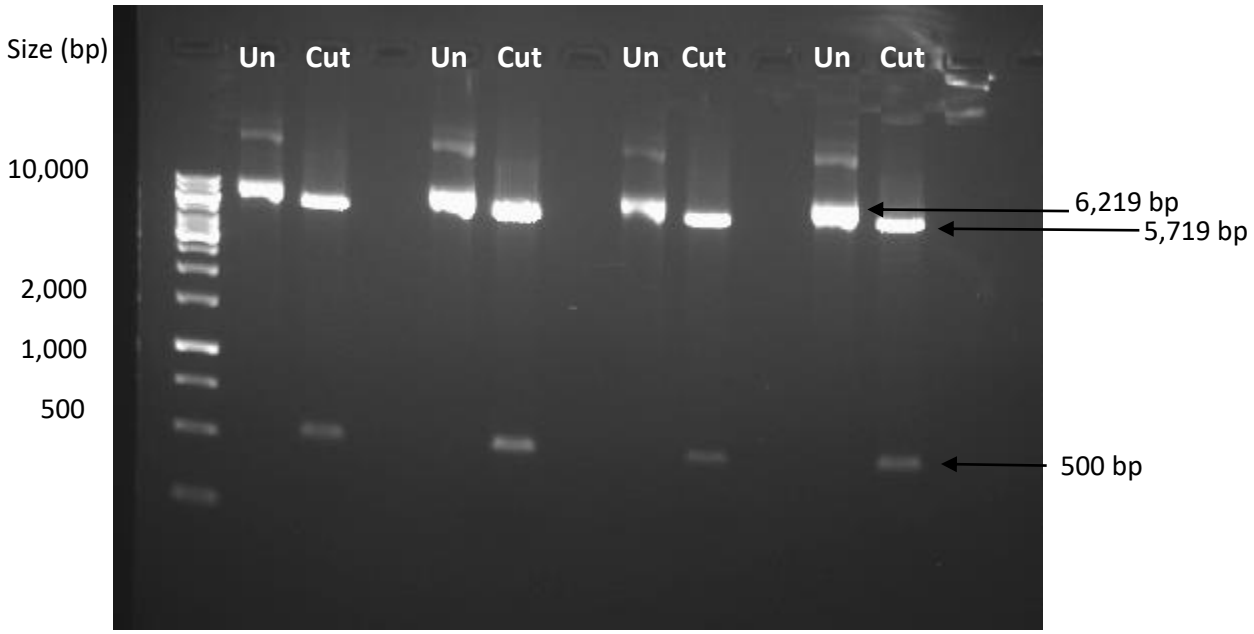

Figure 6.2. pK18mobsacB:*isoA*.up (Un) digested with *Xba*I and *Bam*HI (Cut), producing linear pK18mobsacB (5.7 kbp) and Flank A (500 bp).

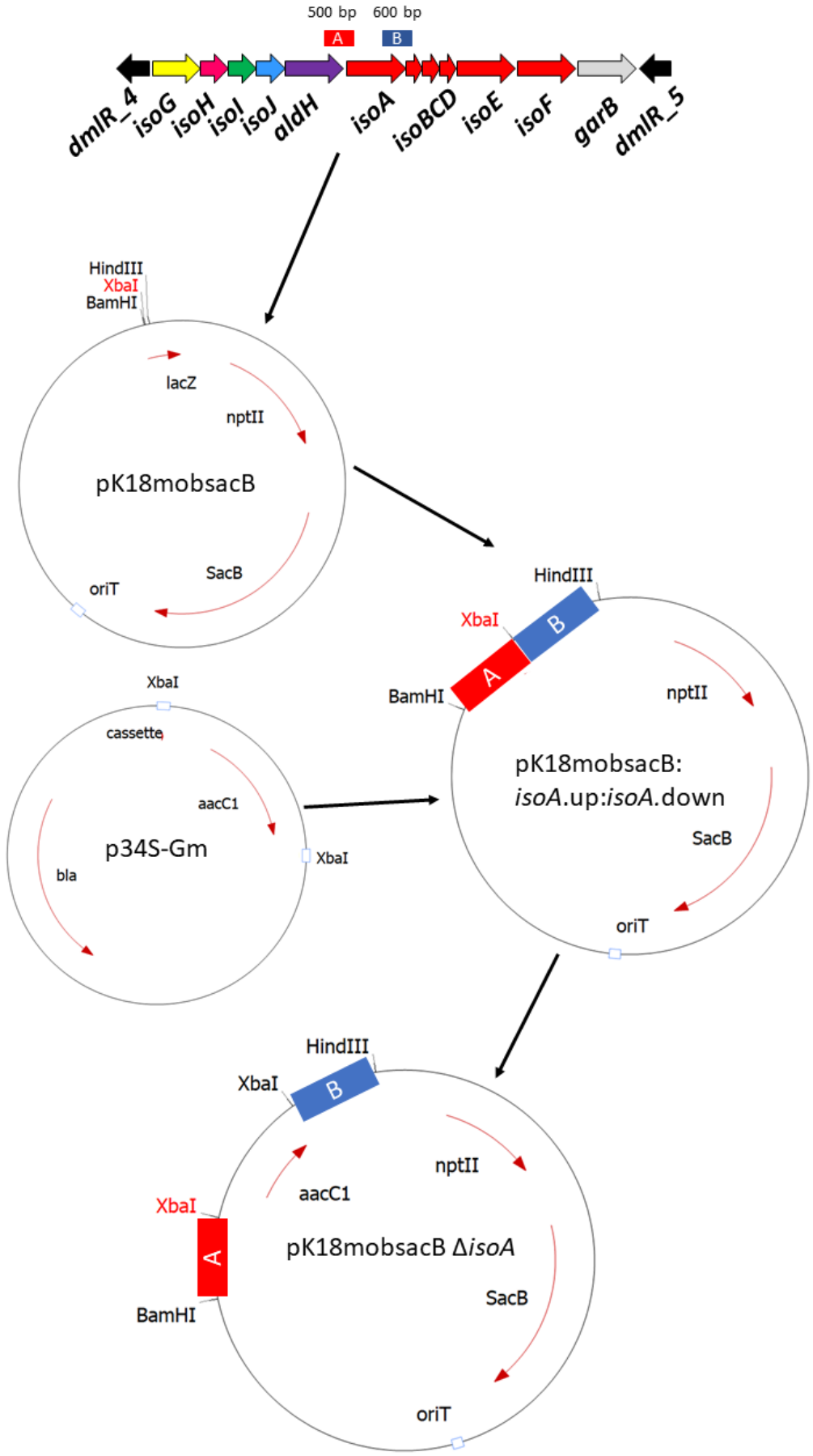

Figure 6.3. Assembly of a suicide vector in pK18mobsacB with upstream and downstream flanking regions of *isoA* (A and B, respectively) on either side of a gene which encodes gentamicin resistance (*aacC1*).

With the cloning procedure validated in *E. coli* DH5-α, Flank B was sub-cloned from pJET1.2 into pK18mobsacB:*isoA*.up. *aacC1*, encoding a gentamicin 3-N-acetyltransferase, was excised from p34S-Gm by digestion with *Xba*I (Dennis & Zylstra 1998). This gene was sub-cloned into the *Xba*I site between Flank A and Flank B in pK18mobsacB, producing pK18mobsacB Δ*isoA* (Figure 6.3).

6.4.2. **Deletion of *isoA* by double-homologous recombination**

pK18mobsacB Δ*isoA* was mobilised into *Variovorax* sp. WS11 by electroporation as described in Section 2.4.3. pK18mobsacB contains an RP4 origin of replication, meaning that replication of this vector is only possible in the enterobacteriaceae (Bolivar *et al*. 1977, Schäfer *et al*. 1994). Therefore, *Variovorax* sp. WS11 would not gain stable resistance to kanamycin from pK18mobsacB alone. This was confirmed by transforming *Variovorax* sp. WS11 with pK18mobsacB with no insert, as no colonies formed on Ewers agar with 50 μg/ml kanamycin. Colonies formed in the presence of kanamycin when *Variovorax* sp. WS11 was transformed with pK18mobsacB Δ*isoA*, something which would only be possible if a recombination event at Flank A or Flank B had occurred (Figure 6.4, Figure 6.5), introducing the whole suicide vector into the genome of *Variovorax* sp. WS11. Colonies were screened for this single-recombination event by PCR using colony biomass directly as the template for amplification. Recombination at Flank A was screened for by primers A-screen_fwd and A-screen_rev (Figure 6.4), and recombination at Flank B was screened for by primers B-screen_fwd and B-screen_rev (Figure 6.5). The primers used to screen for the recombination events are listed in Table 6.1. Due to the locations of B-screen_fwd and B-screen_rev, these primers were also used to screen for a double-recombination event leading to the deletion of *isoA*. Recombinations were consistently detected at Flank B in kanamycin-resistant colonies.

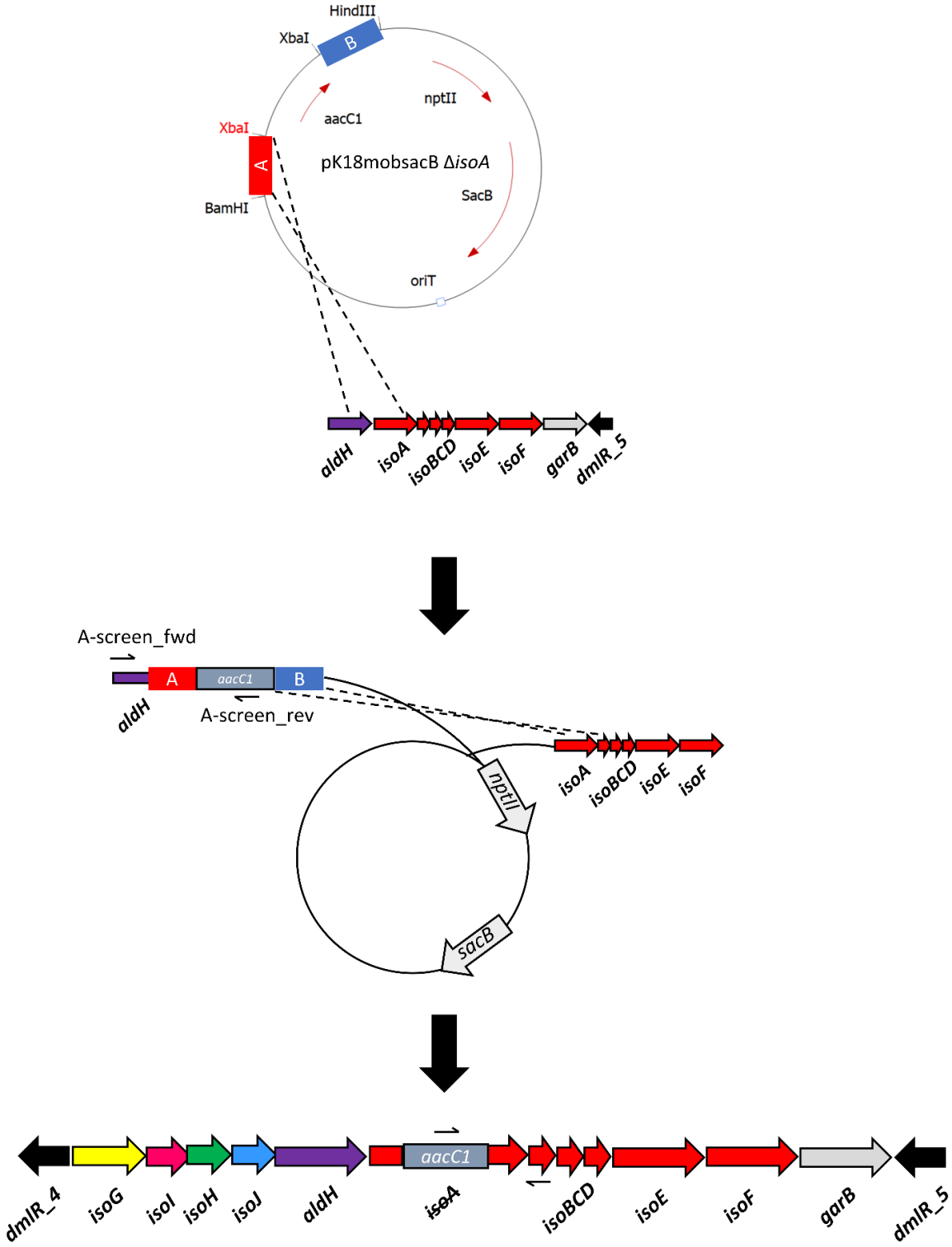

Figure 6.4. Deletion of *isoA* by recombination at Flank A, including the locations of primers to screen for the single-recombination event (half-arrows).

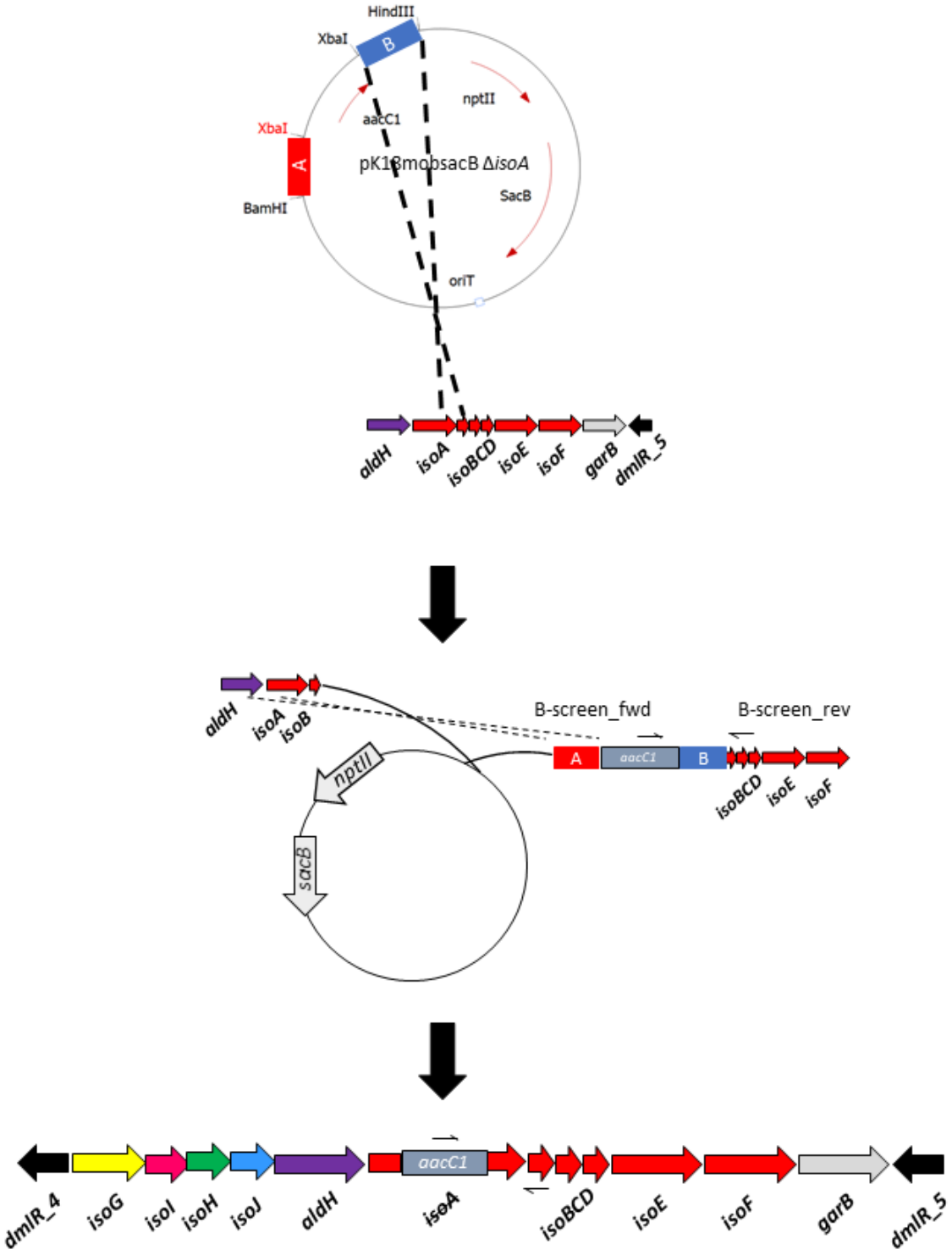

Figure 6.5. Deletion of *isoA* by recombination at Flank B, including the locations of primers to screen for the single-recombination event (half-arrows).

PCR-validated colonies were transferred to Ewers medium with 10 mM succinate and 50 µg/ml kanamycin and incubated at 30 °C with shaking at 160 rpm. Cultures were grown to an OD_{540} of 0.5-0.8, demonstrating that the resistance of *Variovorax* sp. WS11 to kanamycin was stable, and serially diluted across a 10-fold dilution series. Diluted cells were spread on R2A agar in the absence of antibiotic (as described in Section 2.9.1). Individual colonies

were transferred to Ewers medium in the absence of antibiotic to remove all selection pressure for the maintenance of pK18mobsacB, thereby encouraging a second recombination event. This would result in either a reversion to the wild-type, the most likely outcome (Heap *et al*. 2012), or a recombination at the second flanking region, replacing the original copy of *isoA* with the inactivated copy. Selection pressure was required to ensure that the second recombination event had occurred, and that *Variovorax* sp. WS11 did not revert to the wild type. After growth on R2A agar and subsequently in Ewers medium without antibiotic, *Variovorax* sp. WS11 was spread on Ewers agar with 10 µg/ml gentamicin and 5% (w/v) sucrose. The presence of sucrose is lethal to Gram negative bacteria which express *sacB* (Steinmetz *et al*. 1985), resulting in the death of any cells which retained the pK18mobsacB backbone. Gentamicin resistance, encoded by *aacC1*, would only be retained by cells which had undergone a second recombination event but had not reverted to wild-type (Figure 6.4, Figure 6.5).

In order to confirm that a stable mutation had occurred in *isoA*, three tests were conducted. Firstly, gentamicin-resistant and sucrose-resistant colonies of *Variovorax* sp. WS11 were streaked on R2A agar with either kanamycin or gentamicin (Figure 6.6). Colonies which were resistant to gentamicin but sensitive to kanamycin had lost the pK18mobsacB vector backbone, evidenced by the loss of *nptII* (neomycin/kanamycin resistance). These colonies were then used directly as the templates for PCR using the primers B-screen_fwd and B-screen_rev. B-screen_fwd was designed to anneal within *aacC1* and B-screen_rev annealed in *isoB* downstream of Flank B. Therefore, the correct PCR product could not be produced if wild-type *Variovorax* sp. WS11 was used as the template for the PCR reaction. PCR products of the same size could therefore only formed by double-recombination colonies or colonies which had only undergone a single recombination event at Flank B (Figure 6.7). Finally, colonies which had lost resistance to kanamycin but retained *aacC1* within *isoA* were inoculated in Ewers medium with 1% (v/v) isoprene.

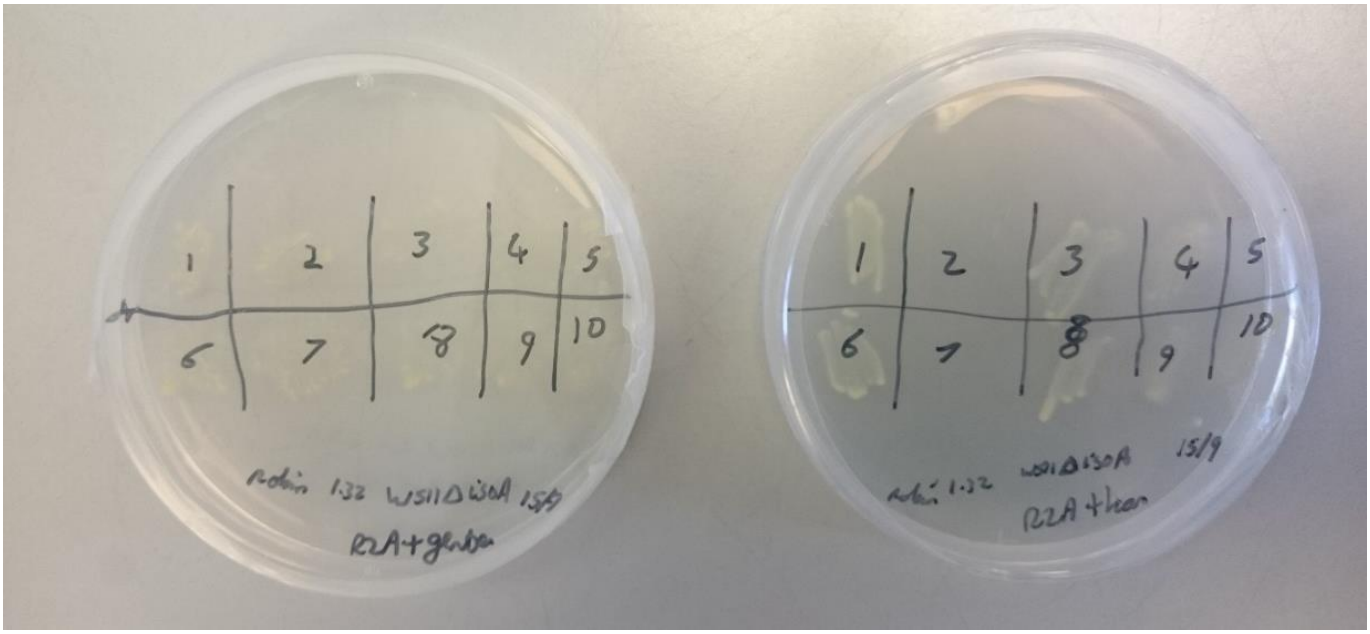

Figure 6.6. Streaking gentamicin-resistant colonies of *Variovorax* sp. WS11 Δ*isoA* on R2A agar with 50 µg/ml kanamycin or 10 µg/ml gentamicin.

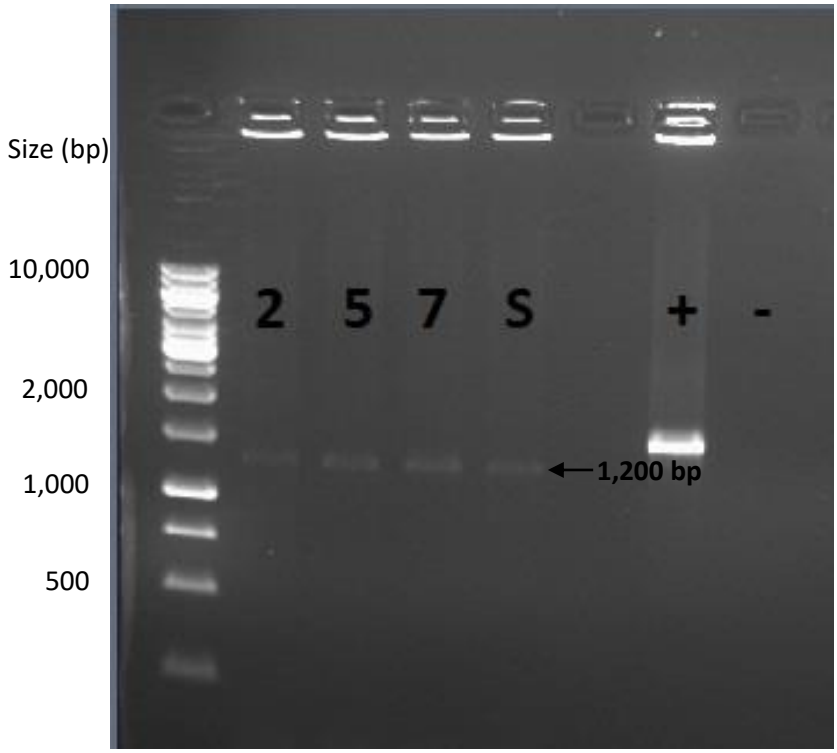

Figure 6.7. Screening for the double-recombination event using *Variovorax* sp. WS11 Δ*isoA* colony biomass directly as the template for the reaction. Colonies 2, 5, and 7 (Figure 6.6) were used, including one single-recombination colony as a size reference (S). The PCR reaction was validated by using primers specific to the 16S rRNA gene in the presence (+) or absence (-) of colony biomass.

6.4.3. **Inducing the expression of IsoMO from pTipQC1**

IsoMO from *Variovorax* sp. WS11 was synthesised by Q5 high-fidelity polymerase using the primers *isoAF*_fwd and *isoAF*_rev (Table 6.1), including *Pci*I and *Bam*HI restriction sites at the termini. All attempts to clone *isoA-F* directly into pJET1.2/blunt (as described in Section 2.8.4) were unsuccessful, possibly as a result of the length of the insert DNA measuring over 4.5 kbp. Instead, *isoA-F* was directly digested using *Pci*I and *Bam*HI, and pTipQC1 was digested using *Nco*I and *Bam*HI, with FastAP phosphatase used to dephosphorylate the linearised pTipQC1 vector before ligation (as described in Section 2.8.3). The digested product and vector were ligated as described in Section 2.8.4, and the resulting vector (henceforth pTipQC1:*iso11*) was used to transform *Rhodococcus* sp. AD45-id as described previously (Crombie *et al*. 2018). *Rhodococcus* sp. AD45-id was also transformed using empty pTipQC1 to demonstrate that isoprene oxidation was not conferred by the vector backbone.

Expression of the cloned genes in pTipQC1 occurred from a thiostrepton-inducible promoter (P_{tipA}) (Nakashima & Tamura 2004). Crombie *et al*. (2018) reported the induction of *iso* metabolic genes from *Rhodococcus* sp. AD45-id at an on OD_{540} of 0.6, with induction from pTipQC1 using 1 µg/ml thiostrepton (prepared as a 20 mg/ml solution in DMSO). The cells were induced overnight at 25 °C, a decrease from the growth temperature of 30 °C. Isoprene uptake assays were conducted at room temperature in static cultures. Initial attempts to express *isoA-F* in *Rhodococcus* sp. AD45-id from pTipQC1:*iso11* were conducted under the same growth and induction conditions,

while isoprene uptake assays were conducted as described in Section 2.15.1. While isoprene oxidation was detected in whole cells, it occurred at a lower rate than in *Variovorax* sp. WS11 (Figure 6.8). Optimisation of this protocol began with adjustments to the concentration of thiostrepton, the antimicrobial compound used to induce expression from P_{tipA}, as it was hypothesised that this compounds may cause stress to the induced cells (Nakashima & Tamura 2004, Bagley *et al*. 2005). Concentrations of thiostrepton above and below 1 µg/ml resulted in a lower rate of isoprene oxidation (Figure 6.8). Therefore, further tests were conducted with induction of IsoMO expression using 1 µg/ml thiostrepton.

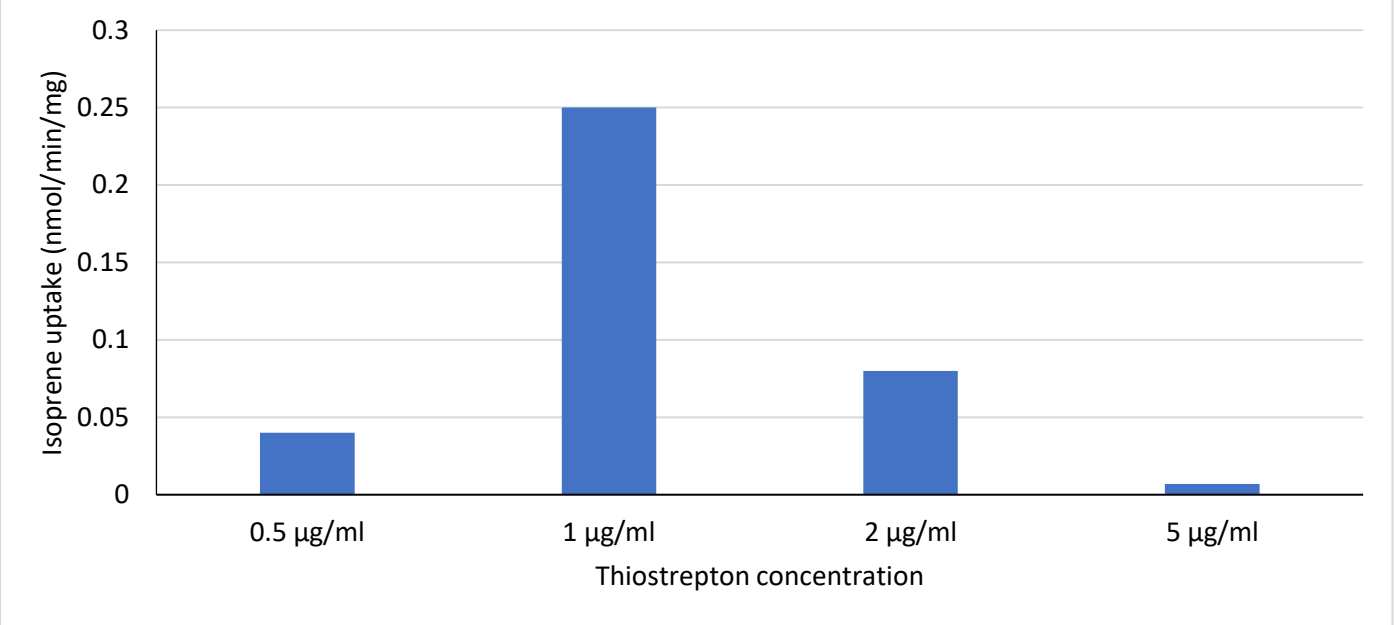

Figure 6.8. Induction of isoprene oxidation by IsoMO, varied by the concentration of the inducer thiostrepton. N=1 (single biological replicates).

The length of time after induction by thiostrepton was also tested, as overnight incubation may have been unnecessary if maximum expression could be reached within a shorter period of time. Isoprene oxidation was greater at each tested timepoint after 0 hours, indicating that overnight incubation may be too long for optimum expression of genes from the P_{tipA} promoter (Figure 6.9). The greatest level of expression, 0.82 nmol min^{-1} mg dry $weight^{-1}$, was recorded after 6 hours. Curiously, this rate was halved after a further 2 hours. Further experiments were conducted with an induction length of 6 hours.

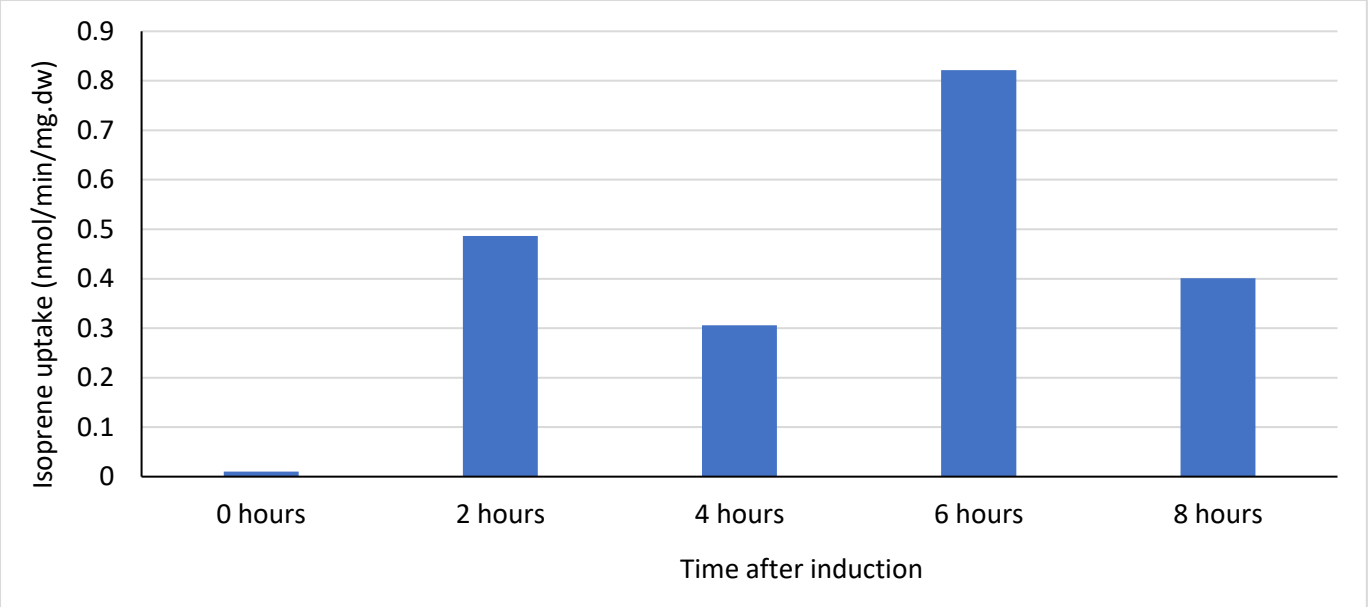

Figure 6.9. Induction of isoprene oxidation from pTipQC1:*iso11* by 1 µg/ml thiostrepton, varied by the time after induction. N=1 (single biological replicates).

Table 6.1. Primers relating to the experiments discussed in this chapter.

Primer	Sequence (5'--3')	Function	Reference
isoA.up_fwd	ATCAGGATCCCATGGGCCCGGACATCCCATTCG	Synthesis of the 5' flanking region of *isoA* for insertion into pK18mobsacB.	(Dawson *et al*. 2020)
isoA.up_rev	TGACTCTAGACGGCAGAAGCGGCTCTGCATCG		
isoA.down_fwd	ATCATCTAGAACATGGCGCAGACCTACC	Synthesis of the 3' flanking region of *isoA* for insertion into pK18mobsacB.	(Dawson *et al*. 2020)
isoA.down_rev	CTTAAAGCTTGATCGGCACCGTACACTC		
A-screen_fwd	CCATGAACTCTCCCGAAATC	Identification of single crossover recombination at Flank A in the formation of an *isoA* mutant of *Variovorax* sp. WS11.	(Dawson *et al*. 2020)
A-screen_rev	CGGAGACTGCGAGATCATAG		
B-screen_fwd	TCGTGAGTTCGGAGACGTAG	Identification of single crossover recombination at Flank B in the formation of an *isoA* mutant of *Variovorax* sp. WS11.	
B-screen_rev	ACGTCGAAGCACTCCATCTC		
*isoA*_fwd	ATGAGGTACCCCTTGCTGAGCCGAGACGACTG	Expression of *isoA-F* from *Variovorax* sp. WS11 in pBBR1MCS-2 from the vector's *lac* promoter.	This study.
*isoAF*_rev	ATCAGGATCCCGATGGCGATCAGCTCGTAG		
*isoAprom*_fwd	ATCAGGTACCTTCCGACATCGATCGCGCAACC	Expression of *isoA-F* from *Variovorax* sp. WS11 in pBBR1MCS-2 from the native flanking region, including 200 bp of *aldH*.	(Dawson *et al*. 2020)
*isoFprom*_rev	TGATGGATCCCGATGGCGATCAGCTCGTAGTG		
*isoA(gib)*_fwd	CGGCCGCTCTAGAACTAGTGTTGTCATCAAAGAAATCGATC	Synthesis of *isoA-F* for subsequent insertion into pBBR1MCS-2 with the flanking region upstream of *isoG* by Gibson assembly.	This study.
*isoF(gib)*_rev	AGACAAGAAAGAGACAACCATGAGCTTG		
*isoG1*_fwd	TGGTTGTCTCTTTCTTGTCTCCTGGTTG	Synthesis of the flanking region upstream of *isoG* for subsequent insertion into pBBR1MCS-2 *isoA-F* by Gibson assembly.	This study.
*isoG1*_rev	AGGGAACAAAAGCTGGGTACCCATCTAGTCTTGTCCCG		
*isoAF*_fwd	ATGAACATGTCCTTGCTGAGCCGAGACGACTG	Synthesis of *isoA-F* for subsequent	(Dawson *et al*. 2020)

*isoAF*_rev	ATCAGGATCCCGATGGCGATCAGCTCGTAG	cloning into pTipQC1.	
*aacC1*_fwd	TCTAGAGTTCCGCGCACATTTCCC	Synthesis of GmR with flanking *loxP* sites, using pCM351 as a template.	This study.
*aacC1*_rev	TCTAGAAGCGCGTTTCCGAGAACC		

6.5. **Results and discussion**

6.5.1. ***Variovorax* sp. WS11 Δ*isoA* cannot grow on isoprene but responds to isoprene and epoxyisoprene**

isoA encodes the α-oxygenase subunit of IsoMO and contains the diiron active site. Therefore, deletion of *isoA* by targeted mutagenesis would abolish all IsoMO activity, preventing the oxidation of isoprene to epoxyisoprene. Crombie *et al*. (2015) first demonstrated this in *Rhodococcus* sp. AD45, confirming that IsoMO was essential to the growth of *Rhodococcus* sp. AD45 on isoprene. However, the *iso* metabolic genes were still upregulated in response to epoxyisoprene, but not isoprene, indicating that epoxyisoprene or a subsequent product of isoprene metabolism was responsible for inducing the expression of the *iso* metabolic gene cluster in *Rhodococcus* sp. AD45. It was likely that the deletion of *isoA* would also prevent the growth of *Variovorax* sp. WS11 on isoprene.

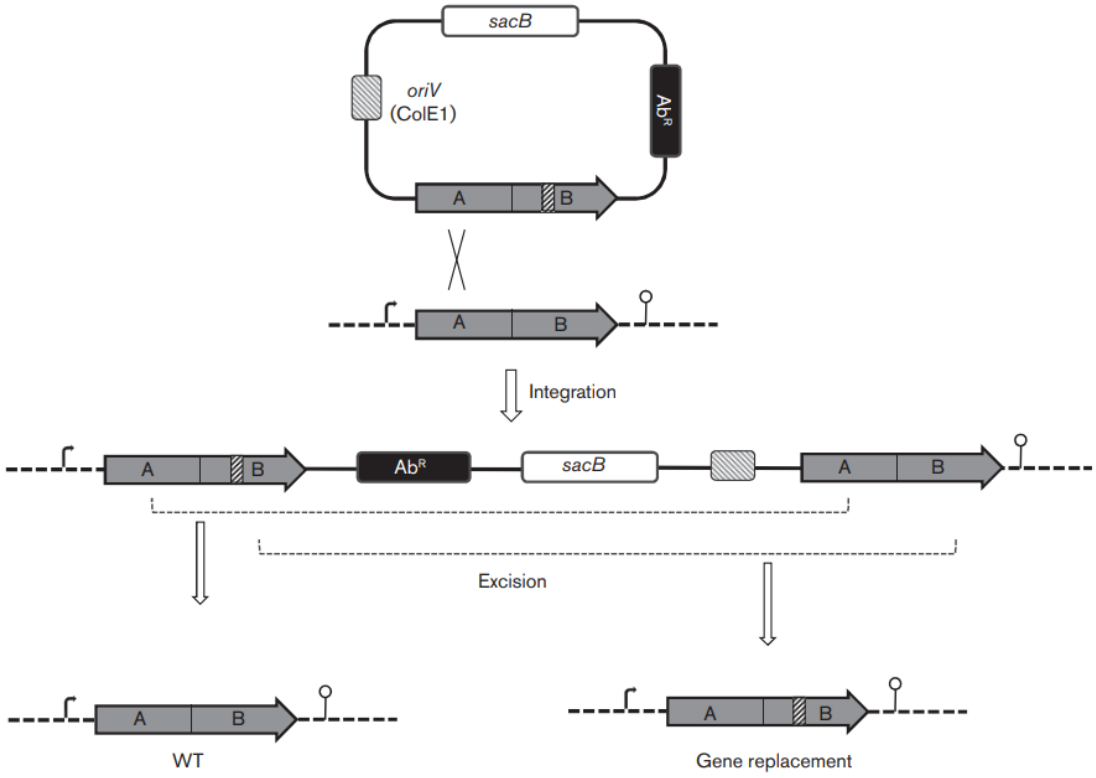

Figure 6.10. Targeted replacement of a gene (AB) with an altered gene copy by double-homologous recombination. Excision of the suicide plasmid is achieved by counter-selection due to sensitivity to sucrose caused by expression of levansucrase, encoded by *sacB* (taken from Biswas, 2015).

Variovorax sp. WS11 which contained an inactive copy of *isoA*, henceforth *Variovorax* sp. WS11 Δ*isoA*, failed to grow in Ewers medium with 1% (v/v) isoprene (Figure 6.11), resulting in a significant difference between the growth of

WS11Δ*isoA* and wild-type *Variovorax* sp. WS11 on isoprene (p≤0.01). This confirmed that IsoMO is essential to the growth of *Variovorax* sp. WS11 on isoprene, as the activity of this enzyme is dependent on the diiron active site at *isoA* (Crombie *et al*. 2015, Leahy *et al*. 2003, van Hylckama Vlieg *et al*. 2000).

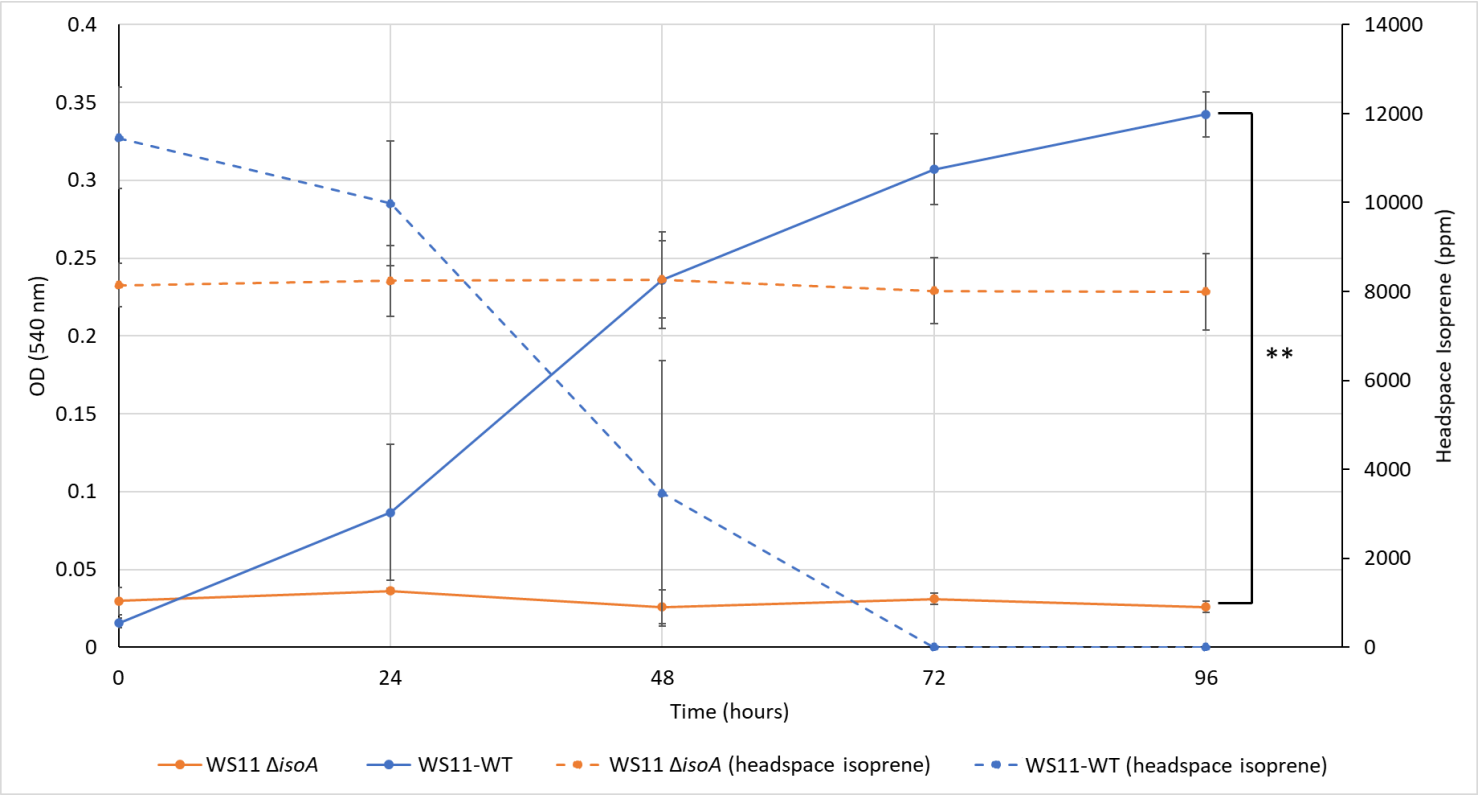

Figure 6.11. Growth of wild-type *Variovorax* sp. WS11 (WS11-WT) and a mutant which lacks *isoA* (WS11 Δ*isoA*) on isoprene. Consumption of isoprene was measured by sampling headspace isoprene (ppm) by GC. Error bars represent the standard deviation about the mean of three biological replicates. Asterisks denote a statistically significant difference between the indicated conditions (** p≤0.01).

Expression of the *iso* metabolic genes in *Rhodococcus* sp. AD45 Δ*isoA* was induced by epoxyisoprene but not by isoprene, demonstrating that isoprene was not the primary inducer of isoprene metabolism (Crombie *et al*. 2015). Instead, either epoxyisoprene or a subsequent product of isoprene metabolism induced expression of *isoG-F*. As *Variovorax* sp. WS11 Δ*isoA* had no active isoprene monooxygenase, isoprene could not be oxidised to epoxyisoprene. Therefore, isoprene and epoxyisoprene were tested as inducers of *iso* metabolic gene expression in *Variovorax* sp. WS11 Δ*isoA*. Induction of *iso* gene expression was tested by reverse transcriptase quantitative PCR (RT-qPCR), with cells being prepared as described in Section 2.10.2 with certain exceptions. *Variovorax* sp. WS11 Δ*isoA* was grown to an OD_{540} of 0.6 with 10 mM succinate, then cells were washed and starved for 2 hours at 30 °C with shaking at 160 rpm before supplementing with either 10 mM succinate, 0.1% (w/v) epoxyisoprene, or 1% (v/v) isoprene. The cultures were incubated for a further 2 hours at 30 °C with shaking at 160 rpm, then total RNA was extracted as described in Section 2.10. All contaminating gDNA was removed by treatment with DNase (as described in Section 2.10), then expression of the *iso* metabolic genes was studied by RT-qPCR as described in Section 2.11. The design and optimisation of qPCR primers specific to *isoG* and *rpoB* is described in Section 7.4.1.

Both isoprene and epoxyisoprene induced the expression of the *iso* metabolic genes in *Variovorax* sp. WS11 Δ*isoA* (Figure 6.11). As *isoA* had been deleted by targeted mutagenesis, *isoG* was selected as the target for RT-qPCR. The primers used to amplify *isoG* (q*isoG_1F*:q*isoG_1R*) and *rpoB* (q*rpoB_1F:*q*rpoB_1R*) are shown in Table 7.7. The introduction of *aacC1* into *isoA* was likely to have caused a polar mutation which would inactivate *isoBCDEF* (Blume *et al*. 1968), meaning that only the upstream genes *isoGHIJ* would still be active. As *Variovorax* sp. WS11 Δ*isoA* was unable to oxidise isoprene to epoxyisoprene, any expression of the *iso* metabolic genes in the presence of isoprene would be caused by isoprene alone rather than any of the subsequent products of isoprene metabolism. *isoG* was induced 6.3-fold by isoprene, relative to *rpoB*, while epoxyisoprene induced the expression of *isoG* 146-fold (Figure 6.12). Both isoprene and epoxyisoprene significantly upregulated the expression of *isoG*, as determined by *t* test ($p \geq 0.05$), but epoxyisoprene was a significantly more potent inducer of *iso* gene expression than was isoprene ($p \leq 0.05$). The induction of *iso* gene expression was much greater in the presence of a complete isoprene oxidation pathway (Figure 6.13). Isoprene induced an increase in the expression of *isoA* and *isoG* expression in wild-type *Variovorax* sp. WS11 by 397.87±36.62 and 1888.42±218.82, respectively, relative to *rpoB* (Figure 6.13). Both *Variovorax* sp. WS11 and *Variovorax* sp. WS11 Δ*isoA* expressed *isoG*, and likely also *isoHIJ*, and were therefore expected to be able to detoxify epoxyisoprene, while only wild-type *Variovorax* sp. WS11 was capable of isoprene oxidation. The lower level of expression of *isoG* by *Variovorax* sp. WS11 Δ*isoA* indicated a decreased ability to respond to the presence of epoxyisoprene when *isoA* was deleted, likely due to the introduction of a polar mutation causing a decrease in the expression of the genes downstream of *isoA*. A putative glutathione disulfide reductase gene (*garB*) is located immediately downstream of *isoF*. GarB was significantly expressed during growth on isoprene (Chapter 3, Figure 3.20), and was predicted to recycle glutathione disulfide to the reduced form, the antioxidant glutathione, during growth on isoprene (Chapter 3, Figure 3.24), allowing the continued detoxification of epoxyisoprene. The introduction of a polar mutation in *isoA* may have inactivated *garB*, preventing the regeneration of glutathione and exacerbating the toxicity of epoxyisoprene in *Variovorax* sp. WS11 Δ*isoA*.

Similarities and differences can be observed between the expression of *iso* metabolic genes in *Variovorax* sp. WS11 and *Rhodococcus* sp. AD45. Most significantly, expression of *isoG* in *Rhodococcus* sp. AD45 Δ*isoA* was not induced at all by isoprene but was significantly upregulated by epoxyisoprene (Crombie *et al*. 2015). This indicates that the regulators of *iso* metabolic gene expression in each model isoprene degrader have different affinities for the products of the isoprene oxidation pathway. The LysR-type transcriptional regulators from *Variovorax* sp. WS11 and the MarR-type transcriptional regulator from *Rhodococcus* sp. AD45 (Crombie *et al*. 2015) must be investigated further to determine the relative responses of each regulator to the products of isoprene metabolism. Although *marR2* was upregulated when *Rhodococcus* sp. AD45 was incubated in the presence of isoprene and epoxyisoprene, the mechanism of action of this regulator is currently unknown (Crombie *et al*. 2015). Interactions of the intermediate compounds of a metabolic pathway with the regulator of that pathway have been described previously. For example, allolactose binds to the repressor of the *lac* operon (LacI) to de-repress expression of the *lac* genes (Matthews & Nichols 1997). This has also been observed for metabolic pathways which involve SDIMO.

TbuT from *Ralstonia pickettii* PKO1 regulates the expression of the toluene 3-monooxygenase operon when in the presence of toluene (Byrne & Olsen 1996, Leahy *et al*. 1997). Although many metabolic pathways which involve the degradation of alkenes and epoxides have been described, there is currently little information available regarding the regulation of these pathways.

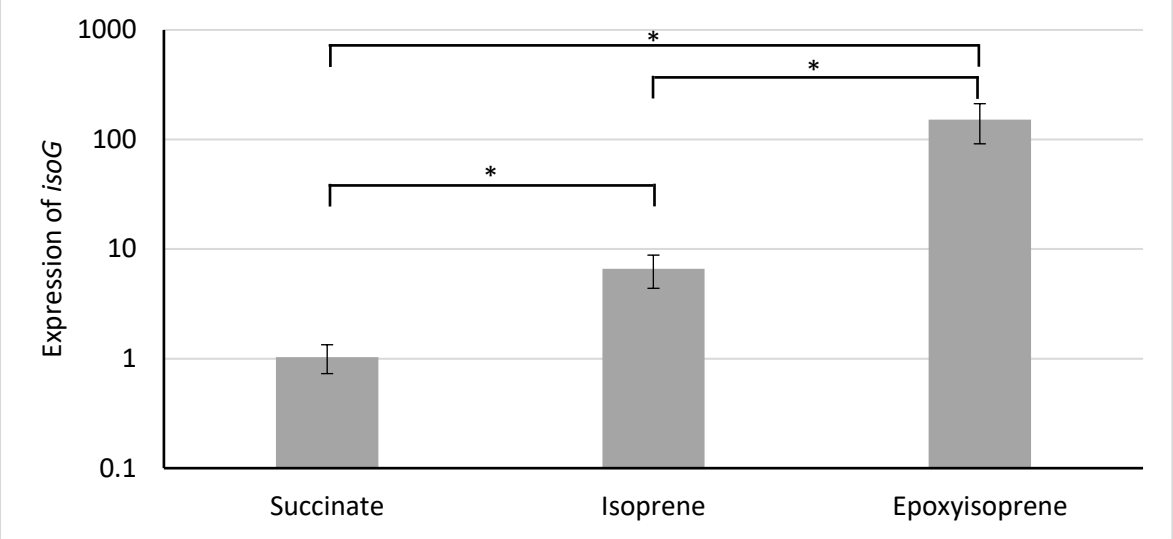

Figure 6.12. Expression of *isoG* by *Variovorax* sp. WS11 Δ*isoA,* induced by 1% (v/v) isoprene or 0.1% (w/v) epoxyisoprene after 2 hours, relative to the expression of *rpoB*. Error bars represent the standard deviation about the mean of three biological replicates. Asterisks denote a statistically significant difference between the indicated conditions (* p≤0.05).

6.5.1.1. **Induction of *iso* metabolic genes by downstream products of isoprene metabolism**

Epoxyisoprene induced a significantly greater change in expression of *iso* metabolic genes in *Variovorax* sp. WS11 and *Rhodococcus* sp. AD45 than isoprene (Crombie *et al*. 2015, Dawson *et al*. 2020). When wild-type *Variovorax* sp. WS11 was incubated with 1% (v/v) isoprene and 0.1% (w/v) epoxyisoprene for 2 hours, *isoA* was induced by 188.95±113.27 and 1542.13±866.62 respectively (relative to *rpoB*), while *isoG* was induced by 342.41±254.3 and 3651.98±1925.7 respectively (relative to *rpoB*) (Chapter 7, Figure 7.13). This led to the hypothesis that either epoxyisoprene or a subsequent product of isoprene metabolism, such as HGMB or GMBA (Chapter 1, Figure 1.6), was the primary inducer of isoprene metabolism (Crombie *et al*. 2015). HGMB was chemically synthesised from epoxyisoprene by NewChem Technologies Ltd (Newcastle, UK) at a ratio of 1:5 with an unrelated regioisomer. Impure HGMB was tested for its ability to induce expression of the *iso* metabolic genes of *Variovorax* sp. WS11, as described in Section 6.5.1.1. Briefly, succinate-grown cultures of *Variovorax* sp. WS11 were washed in 50 mM HEPES (pH 6.0) and starved in Ewers medium for 1 hour without a carbon source. Starved cells were split into separate 120 ml vials and induced with either 10 mM succinate, 1% (v/v) isoprene, or 200 µM HGMB for 2 hours. The latter was added to a total concentration of 1 mM, of which 1:5 parts were HGMB. RNA was extracted from induced cells as described in Section 2.10. cDNA was synthesised as described in section 2.10.3, and RT-qPCR was conducted as described in Section 2.11. HGMB induced the expression of *isoA* and *isoG* by 7.54±2.53 and 9.50±3.2, respectively

(relative to *rpoB*). While the induction of *iso* metabolic genes by HGMB was significant compared to succinate-induced cells (determined by *t* test, p≤0.05), the level of expression of each gene was much lower than in isoprene-induced cells (Figure 6.13) and epoxyisoprene-induced cells (Chapter 7, Figure 7.13). Therefore, epoxyisoprene was determined to be the primary inducer of *iso* metabolic gene expression in *Variovorax* sp. WS11. Isoprene and HGMB are weaker inducers, approximately equal in potency when inducing the expression of *isoG*. A mechanism of induction of isoprene metabolism may be hypothesised according to these data. The presence of isoprene induces a low level of *iso* metabolic gene expression in *Variovorax* sp. WS11, resulting in a relatively low level of accumulation of Iso peptides in *Variovorax* sp. WS11 cells. IsoMO then catalyses the oxidation of isoprene to epoxyisoprene, which in turn induces a significant increase in *iso* metabolic gene expression, resulting in a greater amount of IsoMO and associated Iso metabolic proteins accumulating in the cell to facilitate isoprene metabolism. This could provide an advantage when sending environmental concentrations of isoprene.

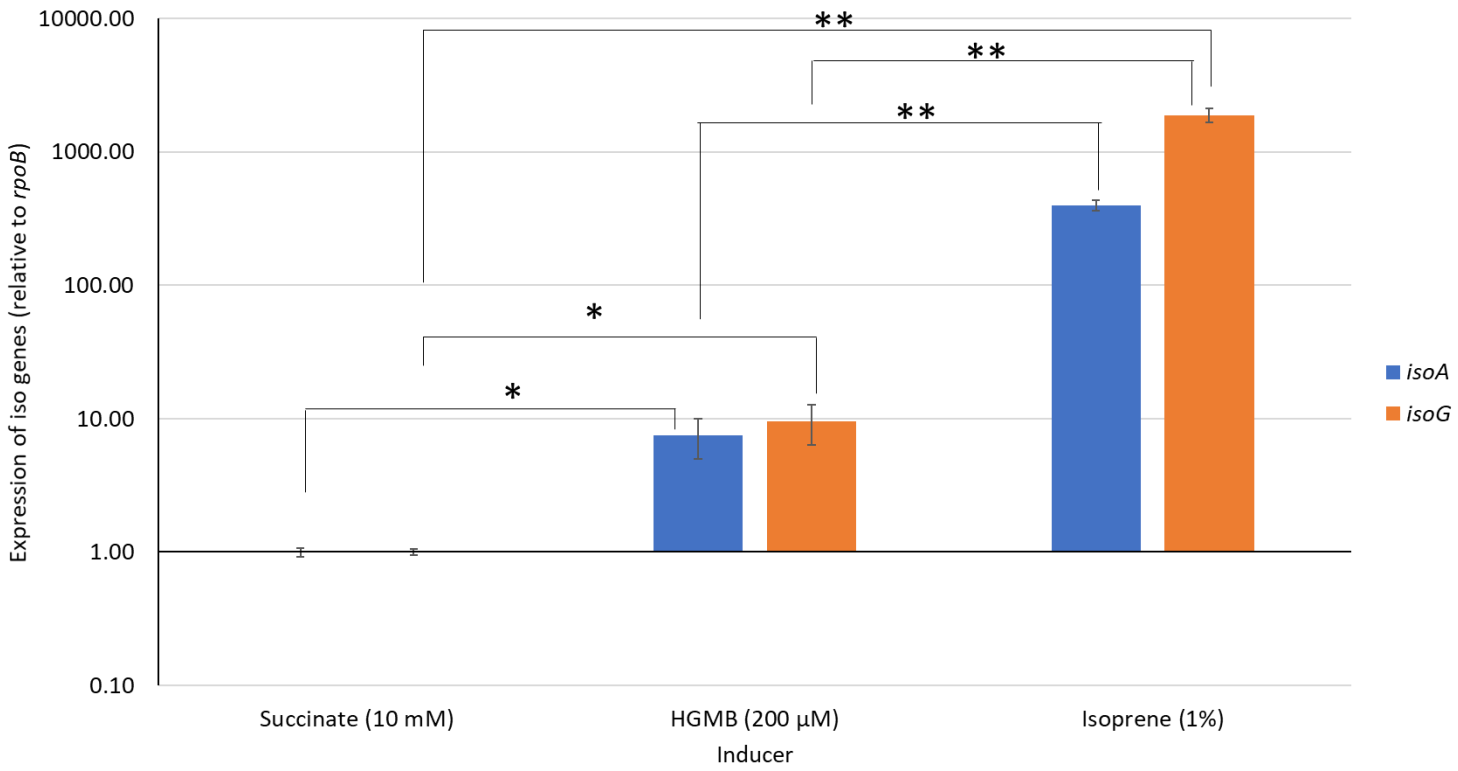

Figure 6.13. Induction of *iso* metabolic gene expression in wild-type *Variovorax* sp. WS11 by 1% (v/v) isoprene or 200 µM HGMB after 2 hours, normalised to the expression of *rpoB*. Error bars represent the standard deviation about the mean of three biological replicates. Asterisks denote a statistically significant difference between the indicated conditions (* p≤0.05, ** p≤0.01).

6.5.2. **Restoration of isoprene oxidation in *Variovorax* sp. WS11 Δ*isoA* by complementation**

In order to confirm beyond all doubt that *Variovorax* sp. WS11 Δ*isoA* no longer grew on isoprene due to the inactivation of IsoMO, rather than disruption of other processes due to the mutation process, growth on isoprene was complemented by re-introduction of *isoA-F* into *Variovorax* sp. WS11 on a plasmid. pBBR1MCS-2 was selected for the complementation process as this vector was previously used in the complementation of mutants of *V.*

paradoxus EPS (Kovach *et al*. 1995, Pehl *et al*. 2012). Initially, *isoA-F* was cloned directly into pBBR1MCS-2 without including the native flanking region 5' of *isoA*. The primers used in the synthesis of *isoA-F* are listed in Table 6.1. The multiple cloning site of pBBR1MCS-2 is located immediately downstream of a *lac* promoter, but the lack of a *lacI* gene prevented the repression of the cloned genes. As a result, the cloned *isoA-F* genes would be expressed at a constitutive, low level (Kovach *et al*. 1995). This level of expression was incapable of restoring the wild-type phenotype, as *Variovorax* sp. WS11 Δ*isoA* was unable to grow on isoprene as the sole source of carbon and energy. The same was also observed for *Variovorax* sp. WS11 Δ*isoA* transformed with the vector only (Figure 6.14). However, it was hypothesised that the level of expression of IsoMO would still be sufficient to restore isoprene oxidation. McCarl *et al.* (2018) previously expressed ethene monooxygenase in *Pseudomonas putida* according to this method, albeit with variable results. The most stable results in the latter study were obtained by scraping colonies from plates immediately after transformation with pBBR1MCS-2 containing the ethene monooxygenase genes, followed by epoxidation assays using the pooled biomass (McCarl *et al*. 2018). *Variovorax* sp. WS11 Δ*isoA* was transformed by electroporation with pBBR1MCS-2:*isoA-F* according to the method described in Section 2.4.3. Freshly transformed colonies were scraped directly into 50 mM HEPES and adjusted to an OD_{540} of 10.0. Isoprene uptake assays were conducted as described in Section 2.15.1. Isoprene was removed from the headspace at a rate of 1.65±0.4 nmol min^{-1} mg dry $weight^{-1}$, indicating that isoprene monooxygenase was expressed in active form from the pBBR1MCS-2 *lac* promoter.

6.5.2.1. **Growth on isoprene can be complemented by expression of *isoA-F* from native promoters**

As the expression of isoprene metabolism is inducible rather than constitutive in *Variovorax* sp. WS11 (as described in Chapter 7), transcription of *iso* metabolic genes from a native promoter must be responsive to growth on isoprene or alternative substrates. The *lac* promoter in the pBBR1MCS-2 vector would not respond appropriately to growth conditions, potentially resulting in the lack of growth on isoprene. Primers were re-designed to include the native intergenic space between *isoA* and *aldH*, including 200 bp of *aldH* overlapping with the stop codon of the latter gene. *isoAprom*_fwd and *isoFprom*_rev (described in Table 6.1) were used to synthesise *isoA-F* with the native flanking region, including *Kpn*I and *Bam*HI restriction sites. This construct, measuring approximately 4,900 bp, was cloned directly into pBBR1MCS-2 after digestion with the above restriction enzymes. The resulting vector (pBBR1:*isoAp*:*isoA-F*) was used to transform *Variovorax* sp. WS11 Δ*isoA*. Growth on isoprene was restored to approximately the same level as wild-type *Variovorax* sp. WS11 (Figure 6.14), although the maximum OD_{540} was lower than the wild-type ($p \leq 0.05$), strongly indicating the presence of a promoter within the synthesised flanking region.

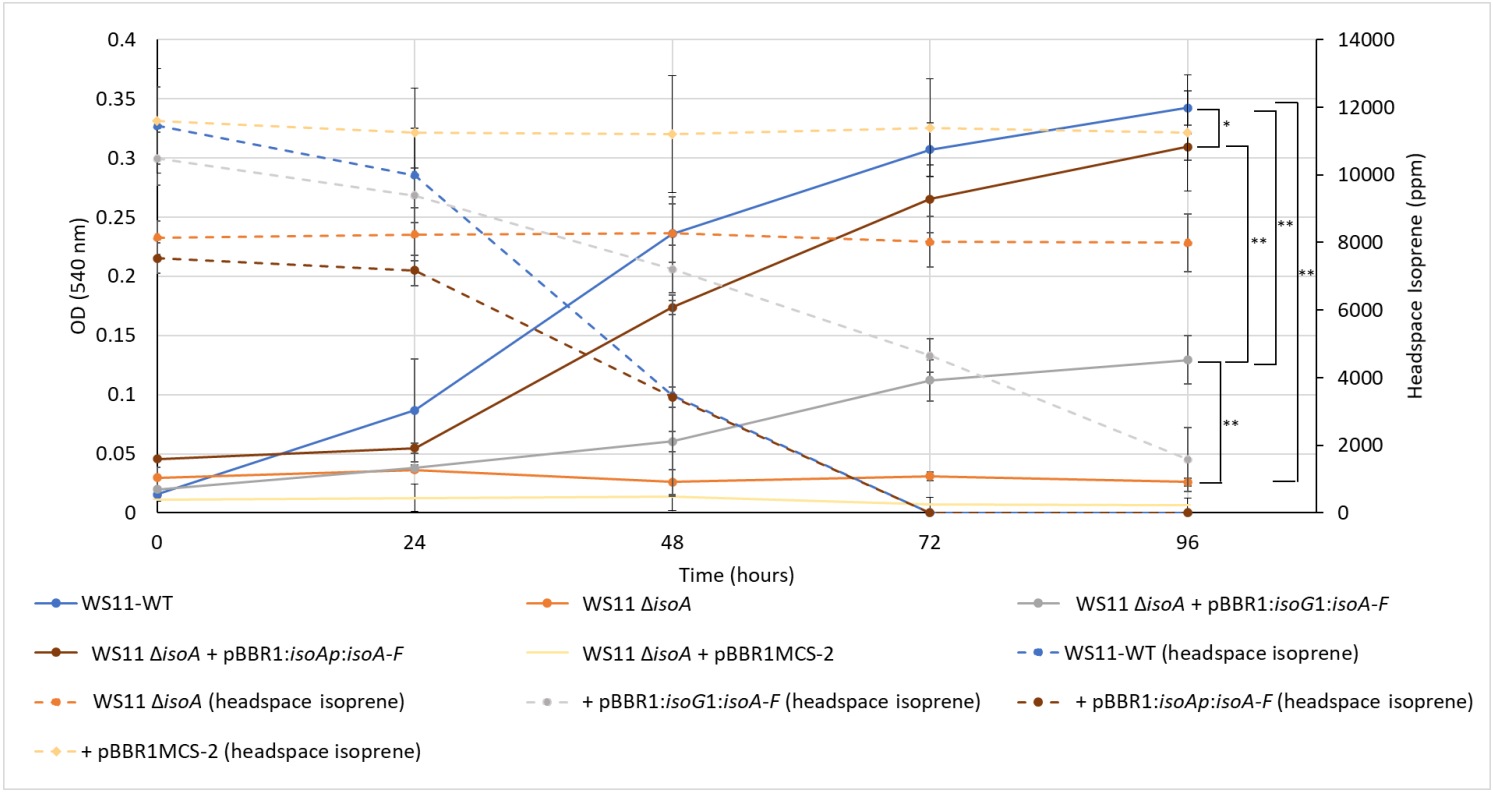

Figure 6.14. Growth of *Variovorax* sp. WS11 Δ*isoA* on isoprene, complemented by expression of *isoA-F* from pBBR1MCS-2 driven by native promoters. Headspace isoprene was measured by gas chromatography (GC). Error bars represent the standard deviation about the mean of three biological replicates. Asterisks denote a statistically significant difference between the indicated conditions (* p≤0.05, ** p≤0.01).

Prior to this work, an isoprene-inducible promoter had already been identified upstream of *isoG* by Dr. O. Carriòn-Fonseca (referred to as *isoG1*). This raised the possibility that two isoprene-inducible promoters were present in the *iso* metabolic gene cluster of *Variovorax* sp. WS11. The *isoG1* promoter was assessed for its ability to drive the expression of *isoA-F* while *Variovorax* sp. WS11 *ΔisoA* was incubated in the presence of isoprene. *isoG1* was cloned into pBBR1MCS-2 in the native orientation, and inserted immediately upstream of *isoA-F*. *isoG1* was synthesised by PCR using the primers *isoG1*_fwd and *isoG1*_rev (described in Table 6.1), and *isoA-F* was synthesised using the primers *isoA*(gib)_fwd and *isoF*(gib)_rev. pBBR1MCS-2 was linearised by digestion with *Kpn*I and *Bam*HI and was combined with the latter PCR products by Gibson assembly (Gibson *et al*. 2009, 2010) according to the manufacturer's instructions (NEBuilder HiFi DNA Assembly Master Mix, New England Biolabs). *Variovorax* sp. WS11 Δ*isoA* was transformed with pBBR1:*isoG1*:*isoA-F* by electroporation. This vector was sufficient to restore significant growth of *Variovorax* sp. WS11 Δ*isoA* on isoprene (p≤0.01) (Figure 6.14), although only to approximately one half of the final OD_{540} achieved by wild-type *Variovorax* sp. WS11 or *Variovorax* sp. WS11 Δ*isoA* with pBBR1:*isoAp*:*isoA-F* (p≤0.01). These data indicated that the *iso* metabolic gene cluster of *Variovorax* sp. WS11 contained two isoprene-responsive promoters (Figure 6.15), each of which was regulated to a different degree.

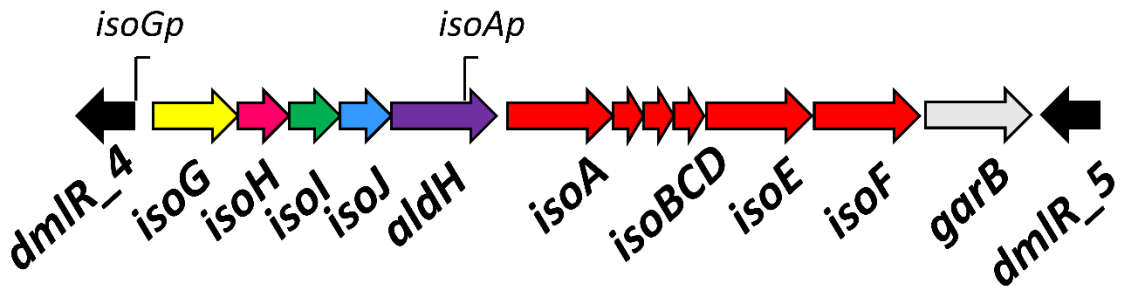

Figure 6.15. *iso* metabolic gene cluster of *Variovorax* sp. WS11, including the approximate locations and proposed orientations of the *isoG1* and *isoAp* promoters.

6.5.3. **Heterologous expression of IsoMO in *Rhodococcus* sp. AD45-id**

As has been described previously, the expression of SDIMO in a heterologous host is often unsuccessful or is only successful when attempting to purify and characterise individual SDIMO components (Champreda *et al*. 2004, McCarl *et al*. 2018, Zhou *et al*. 1996, 1999). Crombie *et al*. (2018) were able to express active IsoMO from *Rhodococcus* sp. AD45 by using a homologous host, *Rhodococcus* sp. AD45-id. Also, *isoA-F* from a *Variovorax*-specific metagenome bin was synthesised and cloned into pTipQC1 (Nakashima & Tamura 2004, Crombie *et al*. 2018). Both the *Rhodococcus*-specific and *Variovorax*-specific *isoA-F* were expressed in active form in *Rhodococcus* sp. AD45-id, with the latter oxidising approximately 200 ppm isoprene in 140 minutes. The successful expression of a whole IsoMO may have been made possible due to the fact that *Rhodococcus* sp. AD45 is a native isoprene degrader, although strain AD45-id lacked the megaplasmid which encodes the *iso* metabolic gene cluster. A role of chaperones in the successful expression of SDIMO was suggested by McCarl *et al*. (2018), a role which may account for the observed expression as *Rhodococcus* sp. AD45-id may have still encoded chaperones required for the correct folding of individual IsoMO components.

Rhodococcus sp. AD45-id expressing IsoMO from pTipQC1:*iso11* oxidised isoprene as an average rate of 0.56±0.09 nmol min^{-1} mg dry $weight^{-1}$, significantly greater than cells transformed with pTipQC1 only which had no detectable rate of isoprene oxidation ($p \leq 0.05$) (Figure 6.16). The rate of isoprene oxidation was consistently lower in *Rhodococcus* sp. AD45-id than in *Variovorax* sp. WS11. There are several potential reasons for this reduction in activity. Firstly, inducing *isoA-F* from the P_{tipA} promoter would result in a different level of expression of *isoA-F* than in wild-type *Variovorax* sp. WS11, as expression in the native bacterium occurs from the two *iso* promoters (Figure 6.15), driven by the products of isoprene metabolism rather than thiostrepton. Secondly, without the full *iso* metabolic pathway (Chapter 1, Figure 1.6), *Rhodococcus* sp. AD45-id would not be able to regenerate reducing power after the initial oxidation of isoprene to epoxyisoprene. van Hylckama Vlieg *et al.* (2000) predicted that the NAD^+ was recycled to NADH during the two sequential oxidation steps catalysed by IsoH, forming GMBA from HGMB. As a result, while a native isoprene-degrading bacterium would be able to replenish a pool of reducing power during isoprene metabolism, *Rhodococcus* sp. AD45-id would become limited. Finally, no codon-optimisation was conducted when designing the expression system pTipQC1:*iso11*. This may have reduced the efficiency of transcription and translation when expressing *isoA-F* from *Variovorax* sp. WS11, a Gram negative β-proteobacterium,

in *Rhodococcus* sp. AD45-id, a Gram positive actinobacterium. Homologous expression of the *Rhodococcus* sp. AD45 IsoMO from pTipQC1 in *Rhodococcus* sp. AD45-ID achieved a rate of 0.12 nmol min^{-1} mg dry $weight^{-1}$, compared to 8.39 nmol min^{-1} mg dry $weight^{-1}$ in wild-type *Rhodococcus* sp. AD45 (Sims 2020). The failure of *Rhodococcus* sp. AD45 to regain its native rate of isoprene oxidation when expressing its own IsoMO was indicative of a decrease in the activity of some IsoMO components, or that IsoMO is less abundant when expressed from the P_{tipA} promoter. The same relative decrease in the rate of isoprene oxidation when *Rhodococcus* sp. AD45-ID expressed IsoMO from *Variovorax* sp. WS11 indicated the same issues.

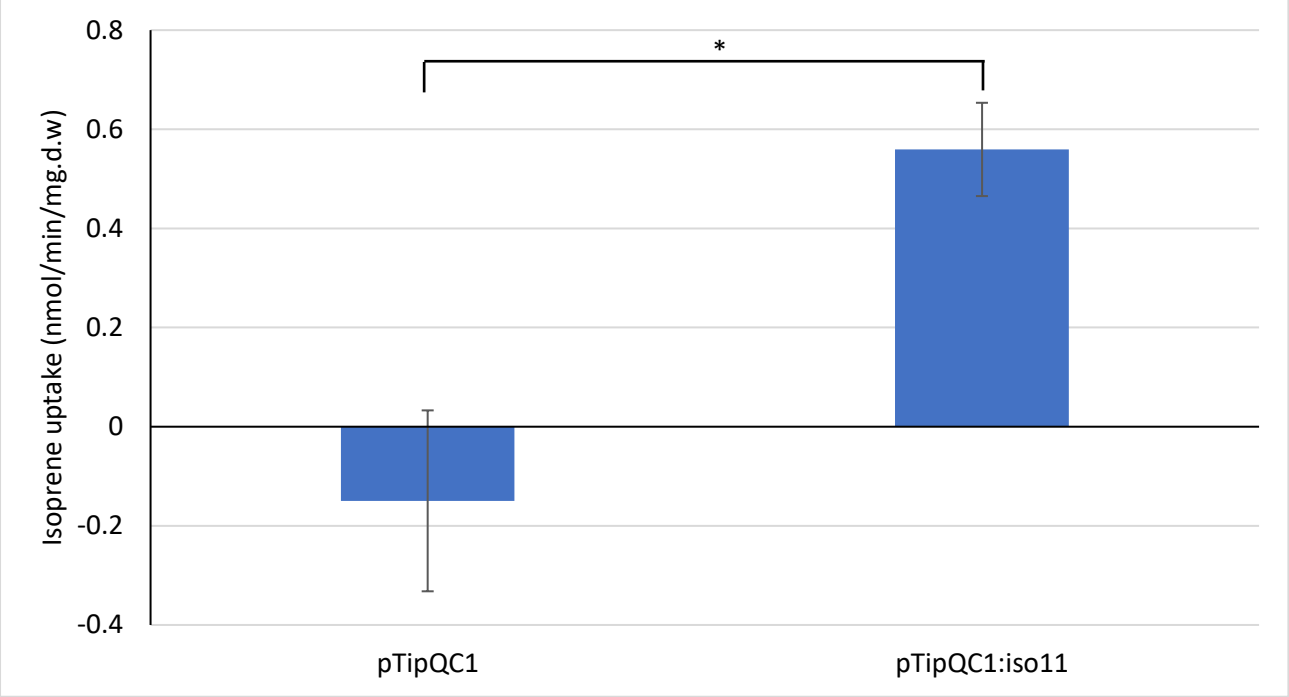

Figure 6.16. Oxidation of isoprene by IsoMO, expressed from pTipQC1:*iso11* 6 hours after induction by 1 µg/ml thiostrepton. Error bars represent the standard deviation about the mean of three biological replicates. An asterisk denotes a statistically significant difference between the indicated conditions ($p \leq 0.05$).

isoA-F from *Rhodococcus* sp. AD45 was only functionally expressed in the homologous expression system in *Rhodococcus* sp. AD45-id, with attempts to express these genes in heterologous strains consistently being unsuccessful (van Hylckama Vlieg *et al*. 2000, Crombie *et al*. 2015). Similarly, Lloyd *et al*. (1999) previously reported the expression of the sMMO in methanotrophs which normally only express the particulate methane monooxygenase (pMMO). Further attempts to express and purify the sMMO from *E. coli* has only been successful for individual components (West *et al*. 1992, Lock *et al*. 2017). A common issue with the expression of foreign proteins in *E. coli* is the aggregation of the expressed peptides in inclusion bodies and the failure to incorporate the correct cofactors (Rosano & Ceccarelli 2014). This was observed when attempting to express the reductase component of toluene 4-monooxygenase in *E. coli*, with the addition of exogenous FAD cofactor improving the activity of the partially purified enzyme (Pikus *et al*. 1996). The relatively poor rates of isoprene oxidation from pTipQC1:*iso11*

indicated that IsoMO components may have been improperly folded in the heterologous host, an issue which may be overcome in future studies by the inclusion of a chaperone of chaperones during expression (McCarl *et al.* 2018).

6.5.3.1. **Failed expression of *isoA-F* in *E. coli***

Although *E. coli* is a common host for expression of recombinant proteins, many studies have reported inactivity when attempting to express SDIMO in *E. coli* (Champreda *et al*. 2004, Mccarl *et al*. 2018, van Hylckama Vlieg *et al*. 2000, Zhou *et al*. 1996, 1999). *isoA-F* from *Variovorax* sp. WS11 had been prepared in two vectors, pTipQC1 and pBBR1MCS-2, with expression driven from one of three promoters; P_{tipA}, *isoAp*, and *isoG1*. *E. coli* Rosetta 2 PlysS (Novagen) was used as a host for the expression of *isoA-F* from each vector. *E. coli* Rosetta 2 is a derivative of the common expression strain *E. coli* BL21 which is suited for expression of codons which are rarely used by *E. coli*. In spite of this, *E. coli* Rosetta 2 was unable to oxidise isoprene when *isoA-F* expression was induced by 1 µg/ml thiostrepton (Figure 6.17). Expression from the P_{tipA} promoter was previously only reported in actinobacteria such as *Rhodococcus* spp. and *Streptomyces* spp., so it may be the case that this promoter was unsuitable for expression in *E. coli* (Holmes *et al*. 1993, Chiu *et al*. 2001, Crombie *et al*. 2018).

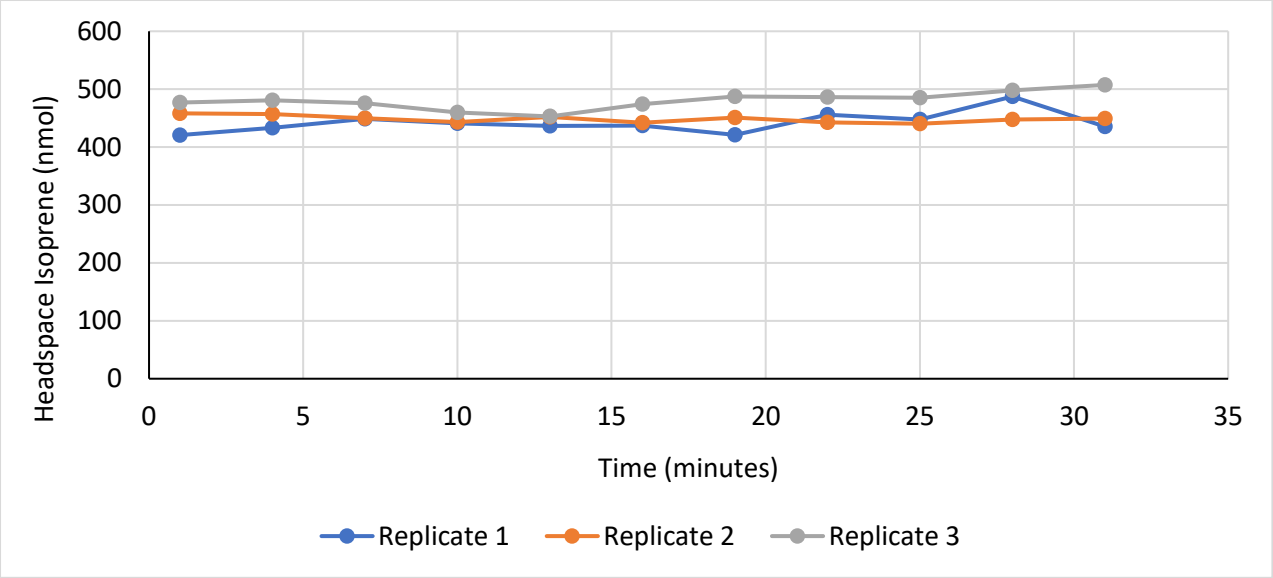

Figure 6.17. Testing expression of *isoA-F* in *E. coli* Rosetta 2 by analysis of headspace isoprene. IsoMO was expressed from pTipQC1 and induced by 1 µg/ml thiostrepton. Each data series represents a single biological replicate.

Growth on isoprene or oxidation of isoprene were not detected in *E. coli* Rosetta 2 after transformation with either pBBR1:*isoAp*:*isoA-F* or pBBR1:*isoG1*:*isoA-F*. The genome of *E. coli* Rosetta 2 was unlikely to contain the genes encoding the necessary isoprene-responsive regulatory proteins, decreasing the likelihood of successful transcription from the *iso* promoters. Even when expressing the majority of *iso* metabolic genes and co-localised regulatory proteins and related promoters from a contiguous piece of DNA, *E. coli* could not utilise the isoprene metabolic pathway from *Rhodococcus* sp. AD45 (van Hylckama Vlieg *et al*. 2000).

6.5.4. **Kinetics of isoprene oxidation by the IsoMO of *Variovorax* sp. WS11**

With relatively few isolated isoprene degrading species of bacteria currently available, there was little information available with regards to the affinity of IsoMO for isoprene. The only well-characterised isoprene-degrading bacterium was *Rhodococcus* sp. AD45, which was initially studied by van Hylckama Vlieg *et al*. (1998, 1999, 2000) and was further-characterised by Sims *et al*. (Sims *et al.* unpublished). Recent studies have begun to characterise IsoMO from three isoprene degrading bacteria; *Variovorax* sp. WS11, *Rhodococcus* sp. AD45, and *Sphingopyxis* sp. OPL5 (Dawson *et al*. 2020, Larke-Mejía *et al*. 2020, Sims 2020). Assays have typically been conducted in whole-cells, as 3- and 4-component SDIMO have often proved recalcitrant to purification and reconstitution, and functional complementation has been achieved by combining the components from multiple SDIMO (Champreda *et al*. 2004, Mccarl *et al*. 2018, van Hylckama Vlieg *et al*. 2000, Zhou *et al*. 1996, 1999). This is likely to be as a result of the cofactors which are required for activity in each of the components of SDIMO; the oxygenase component requires a diiron cofactor, the ferredoxin component requires a Rieske-type [2Fe-2S] cluster, and the reductase requires an NAD^+ cofactor and non-Rieske [2Fe-2S] cluster (Colby *et al*. 1977, Leahy *et al*. 2003, Miura & Dalton, 1995).

The kinetics of isoprene oxidation by IsoMO in whole-cells of *Variovorax* sp. WS11 was tested according to the method described in Section 2.15.2. The same batch of isoprene-grown *Variovorax* sp. WS11 was used for each isoprene uptake assay when gathering these kinetics data to reduce inter-sample variability. Isoprene stocks were prepared in 120 ml vials at 1% (v/v) and 10% (v/v) headspace isoprene. Volumes of isoprene headspace between 0.2 ml and 1 ml were transferred to sealed 30 ml vials containing 1 ml of isoprene-grown *Variovorax* sp. WS11 at an OD_{540} of 1.0. The rate of isoprene uptake was measured for 15 minutes using a gas chromatograph (Agilent). These data were analysed using a Michaelis-Menten plot (Figure 6.18). The K_m in whole-cells of *Variovorax* sp. WS11 (K_m apparent) and the V_{max} for isoprene oxidation were calculated using Hyper32 software (University of Leeds, Leeds, UK). The version used in this study was 1.0.

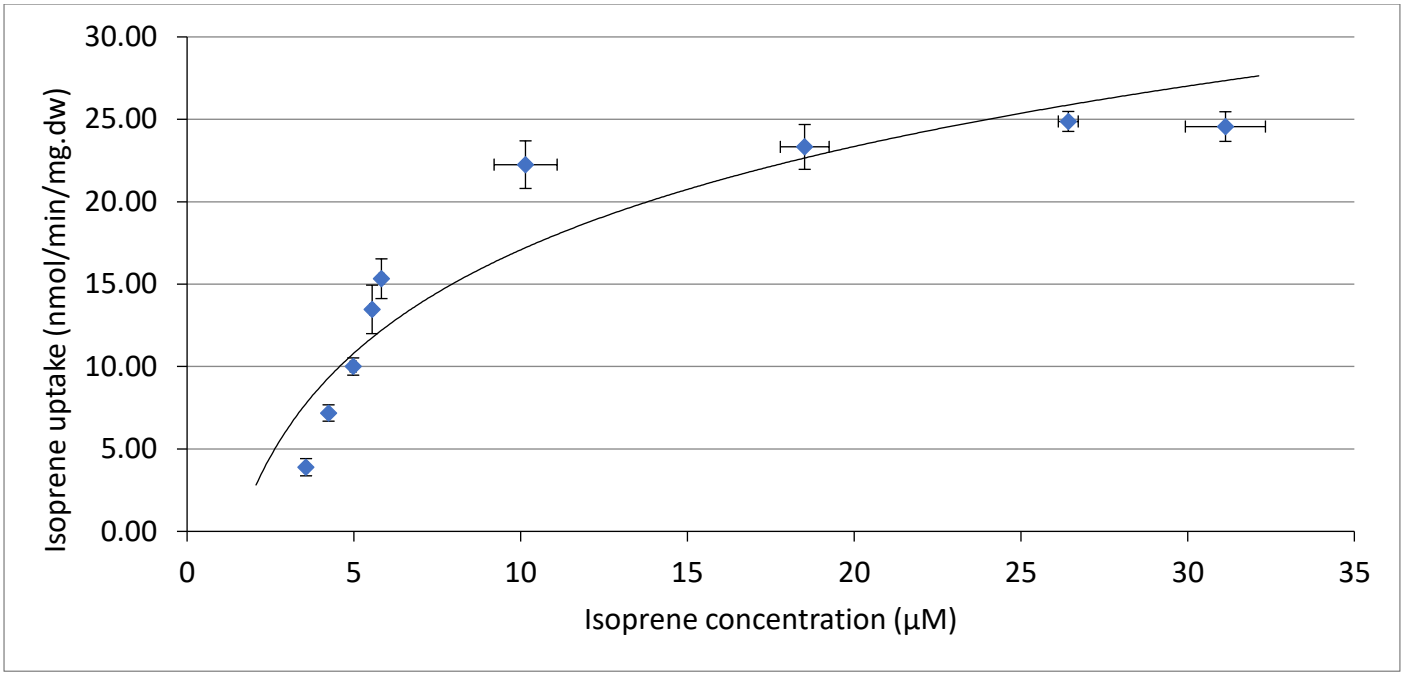

Figure 6.18. Michaelis-Menten kinetics analysis of the rate of isoprene uptake plotted against the concentration of isoprene. Horizontal error bars represent the standard deviation in isoprene concentration, while vertical error bars represent the standard deviation in the rate of isoprene uptake.

The K_m of IsoMO from *Variovorax* sp. WS11 was 10.53±3.89 µM with a V_{max} of 35.39±5.71 nmol min^{-1} mg dry $weight^{-1}$ (Figure 6.18). Curiously, the apparent V_{max} indicated by Hyper32 software was greater than the Michaelis-Menten plot indicated, as the rate of isoprene oxidation appeared to plateau at approximately 25 nmol min^{-1} mg dry $weight^{-1}$ (Figure 6.18). However, a V_{max} of 35.39±5.71 appeared to be the most reliable when considering that the average rate of isoprene uptake by *Variovorax* sp. WS11 in whole cells was 31.5 nmol min^{-1} mg dry $weight^{-1}$ when incubated with 100 µM isoprene (Chapter 3, Figure 3.15), a concentration which exceeded the K_m by far. These data were very similar to the oxidation of trichloroethylene by the toluene 2-monooxygenase from *Burkholderia cepacia* G4, which had a K_m and V_{max} of 12 µM and 37 nmol min^{-1} mg $protein^{-1}$, respectively (Newman & Wackett 1997). This IsoMO had a lower affinity for isoprene than the IsoMO from *Rhodococcus* sp. AD45, which had a K_m between 0.8-2.9 µM and a V_{max} between 43.9-76 nmol min^{-1} mg dry $weight^{-1}$ (van Hylckama Vlieg *et al*. 1998, Sims 2020). IsoMO has been partially purified from *Rhodococcus* sp. AD45 using the *Rhodococcus* sp. AD45-id expression system, with the purified oxygenase component achieving rates of up to 18 nmol min^{-1} mg $IsoABE^{-1}$ (Sims 2020). IsoMO from *Variovorax* sp. WS11 had a lower affinity for isoprene and a higher V_{max} than the IsoMO from *Sphingopyxis* sp. OPL5, which measured 2.53 µM and 10.28 nmol min^{-1} mg dry $weight^{-1}$, respectively (Larke-Mejía *et al*. 2020). The affinity for isoprene of IsoMO from *Sphingopyxis* sp. OPL5, a Gram negative isoprene degrader isolated from oil palm leaves, was very similar to that of *Rhodococcus* sp. AD45, a Gram positive bacterium isolated from freshwater sediment (van Hylckama Vlieg *et al*. 1998, Larke-Mejía *et al*. 2020), although the maximum rate of isoprene oxidation was approximately four-times lower in *Sphingopyxis* sp. OPL5. The increased affinity for isoprene of the IsoMO from *Rhodococcus* sp. AD45 and *Sphingopyxis* sp. OPL5 may indicate a requirement for scavenging of isoprene in nature when compared to the lower affinity of IsoMO from *Variovorax* sp. WS11 for isoprene. As *Sphingopyxis* sp. OPL5 was

isolated from oil palm leaves, one of the highest producers of isoprene in nature (Hewitt & Street 1992, Kesselmeier & Staudt 1999, Silva *et al*. 2016), a potential requirement for scavenging of isoprene when compared to other isoprene degrading bacteria is surprising. For comparison, partially purified 4-component alkene monooxygenase from *R. rhodochrous* B-276 had a K_m of 235 µM for propene and a V_{max} of 245 U/mg protein, where 1 unit equated to the amount of enzyme required to form 1 nmol propene oxide/min (Gallagher *et al*. 1997), and the toluene 4-monooxygenase of *Pseudomonas mendocina* KR1 had a K_m and V_{max} for toluene of 53 µM and 1.7 nmol min^{-1} mg $protein^{-1}$, respectively (Tao *et al*. 2005). These data indicate that IsoMO has a relatively high affinity for isoprene when compared to other four-component SDIMO, although a true comparison would require the purification of IsoMO rather than activity assays in whole cells.

Surveys of isoprene degrading bacteria in their native environments will be required in order to fully understand any relationship between the kinetics of isoprene oxidation and the native environmental conditions, although it would stand to reason that isoprene degraders native to low-isoprene ecosystems would require IsoMO with a much higher affinity for isoprene in order to scavenge low environmental concentrations. Therefore, the kinetics of isoprene oxidation require much greater study.

6.6. **Conclusions**

The research described in this chapter aimed to improve our understanding of isoprene metabolism in *Variovorax* sp. WS11, as this was the first well-characterised isoprene degrader which could be compared with *Rhodococcus* sp. AD45. Mutagenesis and genetics experiments were conducted with the aim of characterising IsoMO from *Variovorax* sp. WS11. Targeted mutagenesis had previously only been conducted on *isoA* in *Rhodococcus* sp. AD45. Isoprene oxidation by *Variovorax* sp. WS11 was found to be dependent on a *Rhodococcus* sp. AD45-like isoprene monooxygenase. Deletion of *isoA* prevented all growth on isoprene, as described by Crombie *et al*. (2015), and growth on isoprene was restored to different levels when *isoA-F* was expressed *in trans* using two isoprene-inducible promoters (Figure 6.14). Induction of *isoA-F* from *isoAp* more closely resembled the growth of wild-type *Variovorax* sp. WS11 on isoprene, while expression from *isoG1* only permitted growth to half of the wild-type level. Transcriptional analysis by RT-qPCR indicated a difference in the regulation of *iso* gene expression between *Rhodococcus* sp. AD45 and *Variovorax* sp. WS11, as *iso* gene expression in *Variovorax* sp. WS11 Δ*isoA* was significantly induced by both isoprene and epoxyisoprene ($p \leq 0.05$), although epoxyisoprene was a significantly more potent inducer than isoprene ($p \leq 0.05$) (Figure 6.12). Additionally, the use of synthetic HGMB failed to induce *iso* gene expression to the same level as the epoxide (Figure 6.13). Collectively, these observations suggest that epoxyisoprene is the most important inducer of *iso* gene expression, but that isoprene is capable of inducing the initial expression of the *iso* metabolic gene cluster in *Variovorax* sp. WS11. This could provide an advantage when sensing environmental concentrations of isoprene.

The expression of *isoA-F* from *Variovorax* sp. WS11 in a heterologous host was achieved, albeit at a low rate (Figure 6.16). *Rhodococcus* sp. AD45-id was the only successful expression system, likely due to the fact that *Rhodococcus*

sp. AD45 is a native isoprene degrading bacterium (van Hylckama Vlieg *et al*. 2000, Crombie *et al*. 2015). This expression system only gained a low rate of isoprene oxidation, potentially due to the incorrect folding of IsoMO components. The co-expression of a specific chaperone or group of chaperones may facilitate the correct folding of IsoMO, as well as aiding the incorporation of the correct cofactors in each component (Leahy *et al*. 2003, McCarl *et al*. 2018). This may improve the expression of IsoMO from *Variovorax* sp. WS11 in *Rhodococcus sp.* AD45-id, or in a more closely related *Variovorax* spp. Kinetics characterisation in *Variovorax* sp. WS11 was conducted in whole cells, with a K_m(apparent) of 10.53±3.89 µM and a V_{max} of 35.39±5.71 nmol min^{-1} mg dry $weight^{-1}$. This indicated that the IsoMO of *Variovorax* sp. WS11 had a lower affinity for isoprene than the IsoMO of *Rhodococcus* sp. AD45, which had an apparent K_m between 0.8 and 2.88 µM (van Hylckama Vlieg *et al*. 1998, Sims 2020).

Overall, the work presented in this chapter improved our understanding of the metabolism of isoprene by *Variovorax* sp. WS11 and identified key similarities in the mechanism of isoprene metabolism used by this novel bacterium and the established model organism, *Rhodococcus* sp. AD45. Differences in the expression of the *iso* metabolic gene cluster were identified, and a need for a greater understanding of the kinetics of isoprene oxidation by IsoMO was evident.

7. Regulation of isoprene metabolism by *Variovorax* sp. WS11

7.1. Introduction

Transcriptional control of SDIMO gene expression has been best-described for three-component SDIMO such as the sMMO. In this case, the ratio of copper to cellular biomass determined whether the genes encoding the pMMO or sMMO were expressed (Nielsen *et al*. 1996, Murrell *et al*. 2000). This switch was controlled by a σ^N-dependent transcriptional activator (Stafford *et al*. 2003). In the case of the facultative methanotroph *Methylocella silverstris* BL2, which only expressed the sMMO, alternative carbon sources repressed the expression of the sMMO (Smirnova & Dunfield 2018). Other classes of SDIMO are regulated by different mechanisms. For example, expression of the toluene 3-monooxygenase of *Ralstonia pickettii* PKO1 is regulated by a transcriptional activator, TbuT, which regulates expression according to the presence of aromatic and chlorinated aliphatic hydrocarbons (Byrne & Olsen 1996). The toluene 4-monooxygenase, which catalyses the oxidation of toluene to *p*-cresol (Yen *et al*. 1991), is moderately similar to the IsoMO and is also a group 2 SDIMO (Chapter 1, Table 1.1). However, little information is available with regards to the transcriptional regulation of this enzyme. The 4-component alkene monooxygenase from *Xanthobacter* sp. Py2 is very similar to IsoMO, as the α-oxygenase component (XamoA) shares 73.1% identity with IsoA from *Variovorax* sp. WS11 (Altschul *et al*. 1990). In fact, phylogenetic analysis indicated that the IsoA component of the *Variovorax* sp. WS11 IsoMO is more similar to XamoA than to other IsoA components from Gram positive isoprene degraders (Chapter 1, Figure 1.4). However, due to the lack of studies into the transcriptional control of the XaMO metabolic gene cluster, it is difficult to make inferences into the potential transcriptional control of the *iso* metabolic gene cluster.

Regulation of isoprene metabolism has only been reported by Crombie *et al*. (2015) through a transcriptome study in a single bacterium. When *Rhodococcus* sp. AD45 was challenged with isoprene and epoxyisoprene, a core cluster of 22 contiguous genes was significantly upregulated, collectively accounting for 25% of the transcriptome. These included the core *iso* metabolic genes, *isoGHIJABCDEF*, two copies of aldehyde dehydrogenase (*aldH*), glutathione biosynthesis genes (*gshAB*), *marR* (*m*ultiple *a*ntibiotic *r*esistance *r*egulator)-type and *gntR*-type transcriptional regulators. Surprisingly, no genes relating to the methylcitrate or methylmalonyl-CoA pathways were significantly induced by isoprene or epoxyisoprene when compared to a succinate-induced control (Crombie *et al*. 2015). These metabolic pathways were significantly expressed during the growth of *Variovorax* sp. WS11 on isoprene ($p \leq 0.05$) (Chapter 3, Table 3.6). Expression of the *iso* metabolic genes in *Rhodococcus* sp. AD45 was induced by epoxyisoprene rather than isoprene, although Crombie *et al*. (2015) hypothesised that a subsequent product of isoprene metabolism may act as an inducer. 2-glutathionyl-2-methyl-3-butene (HGMB) was a poor inducer of isoprene metabolism in *Variovorax* sp. WS11 (Figure 6.11), with *isoA* and *isoG* only induced marginally more by this metabolic intermediate than by isoprene alone (Figure 6.10). Transcriptional control of isoprene metabolism is likely to be different in *Rhodococcus* sp. AD45 and *Variovorax* sp. WS11 for a number of reasons. Firstly, Crombie *et al*. (2015) reported that the *iso* metabolic gene cluster of *Rhodococcus* sp. AD45 was co-transcribed from a single operon.

Subsequent mutagenesis and complementation studies in *Variovorax* sp. WS11 identified two isoprene-inducible promoters in the Gram negative *iso* gene cluster (Figure 6.12, Figure 6.13). The *iso* metabolic gene cluster of *Rhodococcus* sp. AD45 is also much larger than that of *Variovorax* sp. WS11, containing duplicated copies of *isoGHIJ*, glutathione biosynthesis genes, and multiple classes of regulatory genes (*marR* and *gntR*). In *Rhodococcus* sp. AD45, *marR2* and *gntR* were differentially expressed in the presence of isoprene (Crombie *et al*. 2015). *marR*-type transcriptional regulators typically regulate genes by binding to a promoter between two or more divergently transcribed genes (Wilkinson & Grove 2006, Perera & Grove 2010). *marR* genes negatively autoregulate their own transcription, thereby preventing accumulation of the regulatory protein within the cell, and respond to the binding of specific ligands (Wilkinson & Grove 2006, Perera & Grove 2010). These types of regulation were previously identified in *Rhodococcus jostii* RHA1, in which *p*-hydroxycinnamate metabolism was induced by the binding of *p*-courmaryol-CoA to a *marR*-type transcriptional regulator (Otani *et al*. 2016). Although catabolic pathways regulated by *marR*-type transcriptional regulators tend to relate to aromatic compounds (Wilkinson & Grove 2006), the presence of two *marR* copies in the *iso* metabolic gene cluster of *Rhodococcus* sp. AD45, and the significant upregulation of *marR2* during growth on isoprene (Crombie *et al*. 2015), indicated a role for this regulator in isoprene metabolism. *gntR*-type transcriptional regulators may act as transcriptional repressors of metabolic pathways, particularly in the absence of substrates of the pathway in question (Tropel & van der Meer 2004). *gntR* was only upregulated in *Rhodococcus* sp. AD45 after four hours of growth on isoprene (Crombie *et al*. 2015). This may indicate a role for this putative transcriptional regulator in controlling gene expression during the initial stages of isoprene metabolism.

The isoprene metabolic gene cluster of *Variovorax* sp. WS11 contains two putative LysR-type transcriptional regulatory genes, *dmlR_4* and *dmlR_5* (Chapter 1, Figure 1.8). The difference in the types of transcriptional regulator in the Gram positive and Gram negative *iso* metabolic gene clusters may indicate differences in the respective mechanisms of regulating gene expression, especially when considering the single promoter system of *Rhodococcus* sp. AD45 and the dual-promoter system of *Variovorax* sp. WS11. The mechanisms of action of *dmlR_4* and *dmlR_5* are discussed in Chapter 8. The research described in this chapter aimed to study the regulation of *iso* metabolic gene expression in *Variovorax* sp. WS11. A combination of IsoMO activity assays in whole cells and gene expression studies by RT-qPCR were conducted in order to determine the level of expression of *iso* metabolic genes under a variety of growth conditions. Finally, a transcriptome experiment was designed with the aim of determining the full range of genes which are differentially expressed during the growth of *Variovorax* sp. WS11 on isoprene. When compared with the proteome of isoprene-grown *Variovorax* sp. WS11 (discussed in Chapter 3), this final experiment aimed to provide insights into the range of metabolic reactions which comprise the isoprene metabolic pathway.

7.2. **Specific chapter aims and objectives**

The work conducted in this chapter aimed to provide the first evidence for the transcriptional control of isoprene metabolism in *Variovorax* sp. WS11. This was approached through a combination of IsoMO activity assays, conducted in whole cells, and studies of *iso* metabolic gene expression by RT-qPCR. Finally, a whole transcriptome

experiment was designed with the aim of identifying the full range of genes which were differentially expressed under conditions of growth on isoprene compared to growth under alternative conditions, and also to use this information with respect to the proteomics data analysed in Chapter 3 to indicate the regulation of isoprene metabolism. However, technical challenges associated with the extraction of RNA from *Variovorax* sp. WS11 required the additional aim of optimising the extraction of high quality RNA.

1. Study the conditions under which isoprene metabolism is expressed/repressed in *Variovorax* sp. WS11.
2. Optimise RNA extraction conditions using *Variovorax* sp. WS11 with the aim of conducting a whole transcriptome experiment.
3. Using the transcriptome of isoprene-grown *Variovorax* sp. WS11, compared to other growth conditions, validate and supplement the findings from the study of the proteome of *Variovorax* sp. WS11 (detailed in Chapter 3).

7.3. **Hypothesis**

The regulation of isoprene metabolism at the transcriptional level has not previously been described, making it difficult to form early hypotheses with regards to this work. However, it was initially hypothesised that the oxidation of isoprene, and by extension the expression of the *iso* metabolic gene cluster, would be affected by the availability of alternative carbon sources, similar to the preferential utilisation of glucose controlled by carbon catabolite repression (CCR) (Brückner & Titgemeyer 2002). Additionally, insights gained from the proteome of isoprene-grown *Variovorax* sp. WS11 (detailed in Chapter 3) led to the hypothesis that the transcriptome of isoprene-grown *Variovorax* sp. WS11 would support the assimilation of isoprene through the methylcitrate and methylmalonyl-CoA pathways.

7.4. **Methods**

7.4.1. **Optimisation of RT-qPCR primers and reaction conditions**

Before commencing with RT-qPCR, qPCR primers were required to amplify a target gene and a housekeeping gene, or genes, within the parameters of the qPCR protocol. *isoA* was the most obvious target gene to calculate the relative expression of the *iso* metabolic gene cluster, as *isoA* encodes the highly-conserved active site of IsoMO (Leahy *et al*. 2003, Crombie *et al*. 2015). *isoG* was also selected as the target gene for the analysis of expression of *iso* metabolic genes in *Variovorax* sp. WS11 Δ*isoA* (Chapter 6, Figure 6.12), although this was conducted later than the experiments described here (described in Section 6.5.1). Housekeeping genes were assessed for suitability with respect to previous studies. Genes such as *rpoB* (DNA-directed RNA polymerase subunit B), *gmK* (guanylate kinase), *gyrA* (DNA gyrase subunit A), and the 16S rRNA gene were frequently cited as stably-expressed reference genes for use in qPCR (Neretin *et al*. 2003, Bragonzi *et al*. 2005, Nieto *et al*. 2009, McMillan & Pereg 2014, Wen *et al*. 2016, Bai *et al*. 2020). Despite the fact that the 16S rRNA gene was frequently reported as a reference gene, the critical function of the RNA product of this gene in protein expression means that the level of 16S rRNA expression must vary according to the level of protein expression in a cell at a given time (Clark *et al*. 2019). Further to this, different

species of bacteria may contain differing copy numbers of the 16S rRNA gene (Větrovský & Baldrian 2013). Previous studies have also suggested that the 16S rRNA gene was an unfavourable housekeeping gene for qPCR (Vandecasteele *et al*. 2001, Wen *et al*. 2016). Primers were designed which were specific to the *rpoB*, *gmk*, and *gyrA* genes, as well as for the target genes *isoA* and *isoG*. Primer design was conducted using Primer Express software (version 3.0.1, Applied Biosystems, Foster City, CA, USA), with primers designed for amplification using a SYBR Green mastermix with standard amplification parameters. A single pair of primers was created initially for *isoA* (q*isoA*_F:q*isoA*_R), *rpoB* (q*rpoB*_F:q*rpoB*_R), *gmK* (q*gmk*_F:q*gmk*_R), and *gyrA* (q*gyrA*_F:q*gyrA*_R) (Table 7.7).

Initially, the suitability of these primers for qPCR was determined by using standard concentrations of complementary DNA (cDNA) derived from RNA extracted from *Variovorax* sp. WS11 (as described in Sections 2.10 and 2.10.3). cDNA standards were prepared by adjusting the RNA concentration to approximately 100 ng/µl (standard 1), assuming a 1:1 conversion of RNA to cDNA during treatment with Superscript III reverse transcriptase (Thermo Fisher), and subsequently by diluting this cDNA across a ten-fold dilution series four times in nuclease-free water, making five standards. 2 µl of each standard was used as the template for qPCR analysis, using three technical replicates. qPCR was conducted as described in Section 2.11 with a key difference; a two-step amplification protocol was used with the cycle threshold (C_T) value recorded during the amplification step. Control reactions with no template were included to ensure that the mastermix was not contaminated. C_T values, transformed by a Log_{10} scale, were plotted against each cDNA standard (Figure 7.2). Primer efficiency was calculated using the following calculation, where E represents the efficiency (%), and the slope was calculated by plotting a standard curve using the Log (sample quantity) against average C_T value.

$$E = \left(10^{-\frac{1}{slope}} - 1\right) * 100$$

Table 7.1. Efficiency of qPCR primers. Repl 1 and Repl 2 denote individual biological replicates.

Primer target	Efficiency (%) – Repl 1	Efficiency (%) – Repl 2
isoA	102.99	393.42
rpoB	89.24	71.96
gyrA	80.60	97.69
gmk	100.48	63.91

The average efficiency of the qPCR primers varied from 80.6-102.99%, (Table 7.1), calculated using three technical replicates. With primer efficiencies for qPCR ranging from 90-110% typically deemed as acceptable (Kirschneck *et al*. 2017, Stephan *et al*. 2019), *rpoB* and *gyrA* were unsuitable for further use in RT-qPCR. A second biological replicate was used to confirm the suitability of *isoA* and *gmk*, but the primer efficiencies were very different and no longer fit within the accepted range of 90-110%. Additionally, melt curve analysis of the *isoA* primers indicated non-specific

binding to targets other than *isoA*-encoding cDNA, as the peak of fluorescence decreased from 92.13 °C to approximately 82 °C at the lowest concentrations of cDNA template (Figure 7.2).

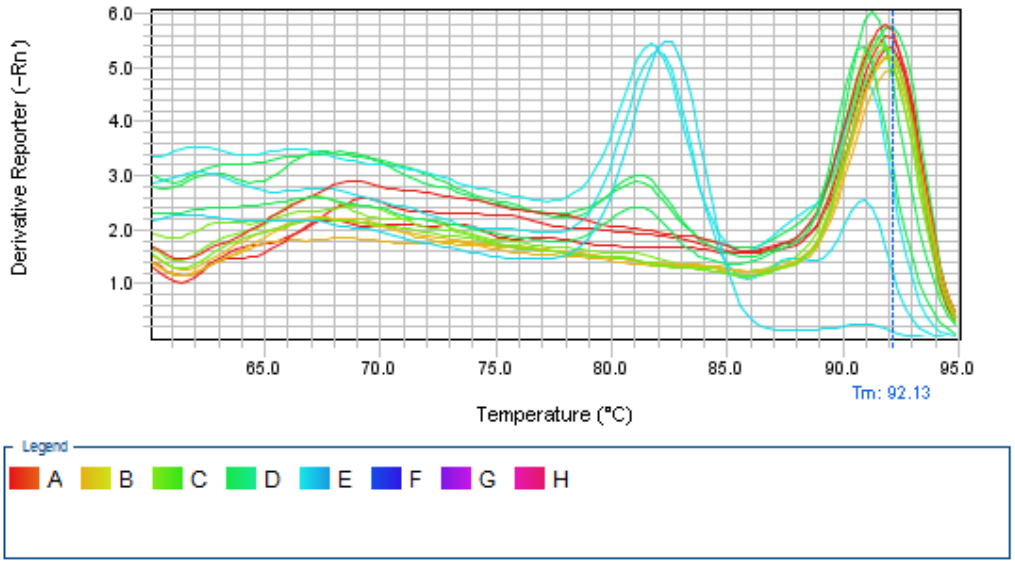

Figure 7.1. Melt curve analysis of *qisoA_F* and *qisoA_R* dissociation from a cDNA template.

The poor performance of these primers may have been caused by several issues. qPCR primer design guidelines typically recommend the amplification of an amplicon between 75-200 bp in order to prevent the amplified region from being obscured by potential primer dimers (Thornton & Basu 2011). The amplicons produced by the first primer pairs were relatively small, measuring between 56-71 bp (Table 7.7). Alternatively, the Primer Express software only designed the primers to be specific to the genes of interest without taking into account any other regions of homology in the genome of *Variovorax* sp. WS11. This mistake may have allowed non-specific amplification to occur, resulting in the non-specific melt-curve analysis seen in Figure 7.1, and contributing to the poor primer efficiency (Table 7.1).

New qPCR primers were designed for each of the four targets of interest, initially beginning with the design of multiple primers specific to each target using Primer Express software, followed by specificity-related quality tests using Primer-BLAST (Ye *et al*. 2012). Re-designed primers were tested for specificity against the target gene, while the genome database of *Variovorax* sp. WS11 was included as a specificity parameter. Pairing of the primer with non-specific targets, particularly at the 3' end of the primer, was a criterion for failure. Primers which were unlikely to amplify any non-specific targets were selected for further testing, with two primer pairs selected for *isoA*, *gyrA*, and *rpoB*. Designing *gmk*-specific primers was unsuccessful, as all tested primer pairs were predicted to amplify several non-specific regions of DNA. Re-designed primer pairs were tested using cDNA from isoprene-grown *Variovorax* sp. WS11 as a template for amplification.

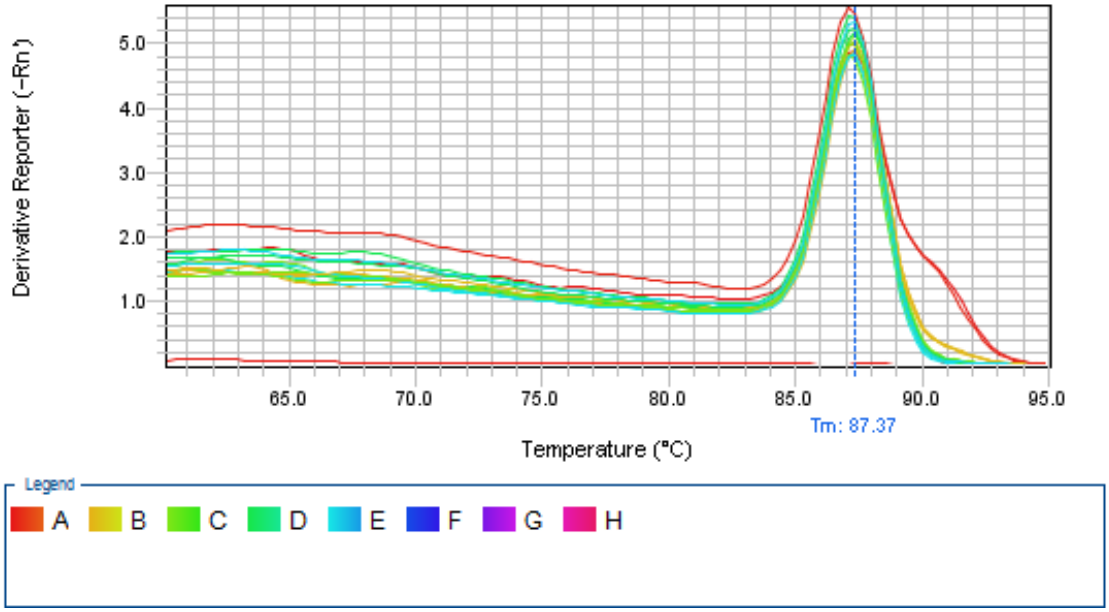

Figure 7.2. Melt curve analysis of q*isoA*_2F and q*isoA*_2R dissociation from a cDNA template.

Table 7.2. Efficiency of redesigned *isoA*- and *rpoB*-specific primers, presented as the average of three biological replicates ± standard deviation.

Primer target	Average efficiency (%)
isoA	95.3±1.4
rpoB	96.5±11.1

Initially, *rpoB*-specific qPCR primers were relatively inefficient when using the standard, two-step qPCR protocol (Table 7.1). This protocol consisted of holding at 95 °C for 10 minutes, then 40 cycles of 95 °C for 15 seconds and 60 °C for 60 seconds, followed by melt-curve analysis (Chapter 2, Table 2.4). No significant non-specific peaks were present to indicate amplification of other targets (Figure 7.4). Increasing the read-temperature from 61 °C to 81 °C in an adapted three-step protocol (Chapter 2, Table 2.4) improved the efficiency of *rpoB* to an average of 96.5%, allowing q*rpoB*_1F and q*rpoB*_1R to be used for RT-qPCR. q*isoA*_2F and q*isoA*_2R were suitable for RT-qPCR, as the melt-curve analysis indicated that no non-specific products were produced (Figure 7.3), and the efficiency of the primers fell within the acceptable range (Table 7.2). Subsequent analysis of RT-qPCR data was conducted using the comparative C_T method (Schmittgen & Livak 2008). The comparative C_T method ($\Delta\Delta C_T$) studies the qPCR signal for a specific target gene under the treatment and control conditions, with respect to the expression of a housekeeping gene under the same conditions, and uses this to calculate the fold-change in expression of the target gene. This method was recommended for ease of use compared to the inclusion of standard curves, although the use of this method was contingent on the efficiency of the qPCR primers falling within the acceptable range (Table 7.2). The comparative C_T method required the use of a single internal control gene, so *rpoB* was selected and consistently included as the reference for fold-change in gene expression.

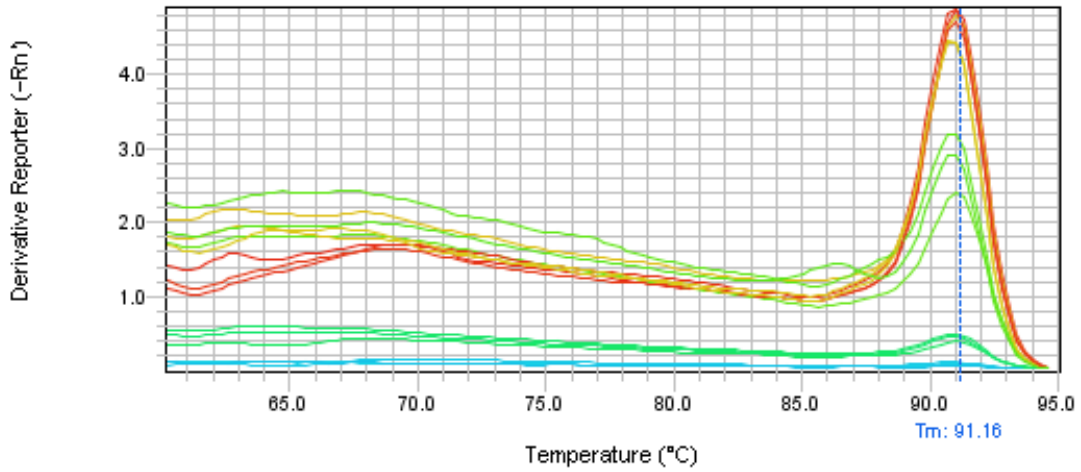

Figure 7.3. Melt curve analysis of q*rpoB*_1F and q*rpoB*_1R dissociation from a cDNA template.

Primers specific to *isoG* were designed as described previously. cDNA standards were prepared and the efficiency of the primers was tested as described above. q*isoG*_1F and q*isoG*_1R (Table 7.7) amplified *isoG* under the optimised reaction conditions with sufficient efficiency for use in RT-qPCR (Table 7.3). The *isoG*-specific qPCR primers were subsequently used to test the relative level of expression of *isoG* by *Variovorax* sp. WS11 Δ*isoA* after exposure to isoprene and epoxyisoprene (Chapter 6, Figure 6.12).

Table 7.3. Efficiency of *isoG*-specific primers, presented as the average of three biological replicates ± standard deviation.

Primer target	Average efficiency (%)
isoG	94.4±0.7

7.4.2. **Optimisation of RNA extraction conditions**

Novogene (Cambridge, UK) was selected to perform whole-transcriptome analysis by mRNA sequencing. 51 samples were required for the transcriptome analysis, comprising an uninduced control and four induced conditions, with four timepoints selected for each induced condition (Section 2.10.1). The chosen conditions were 10 mM succinate, no substrate (starved and stressed control), 1% (v/v) isoprene, and 0.01% (w/v) epoxyisoprene. This concentration of epoxyisoprene was chosen in order to account for the difference between the concentrations of isoprene and epoxyisoprene. According to Henry's law, a 1% (v/v) headspace concentration of isoprene produces a concentration of 0.13 mM in liquid due to liquid-gas partitioning (Sander 2015). Epoxyisoprene, however, would have a concentration of 0.1 M if added at the concentration used in previous experiments (0.1% (w/v)). By decreasing the amount of epoxyisoprene in the cultures to 0.01% (w/v), epoxyisoprene would still be present at a greater initial concentration than isoprene but would also rapidly degrade in water.

The samples had to be stored between the harvesting of cells and extraction of the RNA due to the number of samples required. RNAprotect Bacteria Reagent (Qiagen, Manchester, UK) was used according to the manufacturer's

instructions. Pelleted, protected cells were stored at -80 °C for less than 1 week before RNA was extracted. The extraction procedure had to be optimised in order to achieve the required concentration and quality (determined by RNA integrity number, RIN) of RNA for sequencing by Novogene (≥3 µg, RIN ≥6.0). A smaller volume of cells was used than in previous experiments (10 ml rather than 50 ml) due to the required ratio of 2:1 RNAprotect to cell culture. Initially, RNA was extracted by the hot phenol protocol (Gilbert *et al*. 2000) and contaminating DNA was removed using a Turbo DNA-free kit (Thermo Fisher Scientific, Waltham, MA, USA). While the use of acidic phenol should select for the extraction of RNA over DNA (Chomczynski & Sacchi 1987), the lack of an RNA-purification column allowed a certain amount of contaminating DNA to remain in the samples. The Turbo DNA-free kit was recommended for ease of use and the lack of time-consuming purification steps required by on-column protocols. The Turbo DNA-free kit was initially tested by using standard concentrations of genomic DNA (Figure 7.4). A routine protocol (37 °C, 30 minutes, 2.5 µl DNase in 50 µl of gDNA sample) or a vigorous protocol (37 °C, 2 x 30 minutes, 2 x 2.5 µl DNase in 50 µl of gDNA sample) was used to digest the DNA samples. The routine protocol (R1-R3) was sufficient to degrade up to 100 ng of gDNA in 50 µl after 30 minutes, but the strong 16S rRNA band present in the 500 ng sample lane (R3) indicated that this protocol was insufficient for use in samples with heavy contamination of DNA (Figure 7.4). The vigorous protocol (V1-V3) was sufficient to remove 50-500 ng of gDNA after 30 minutes.

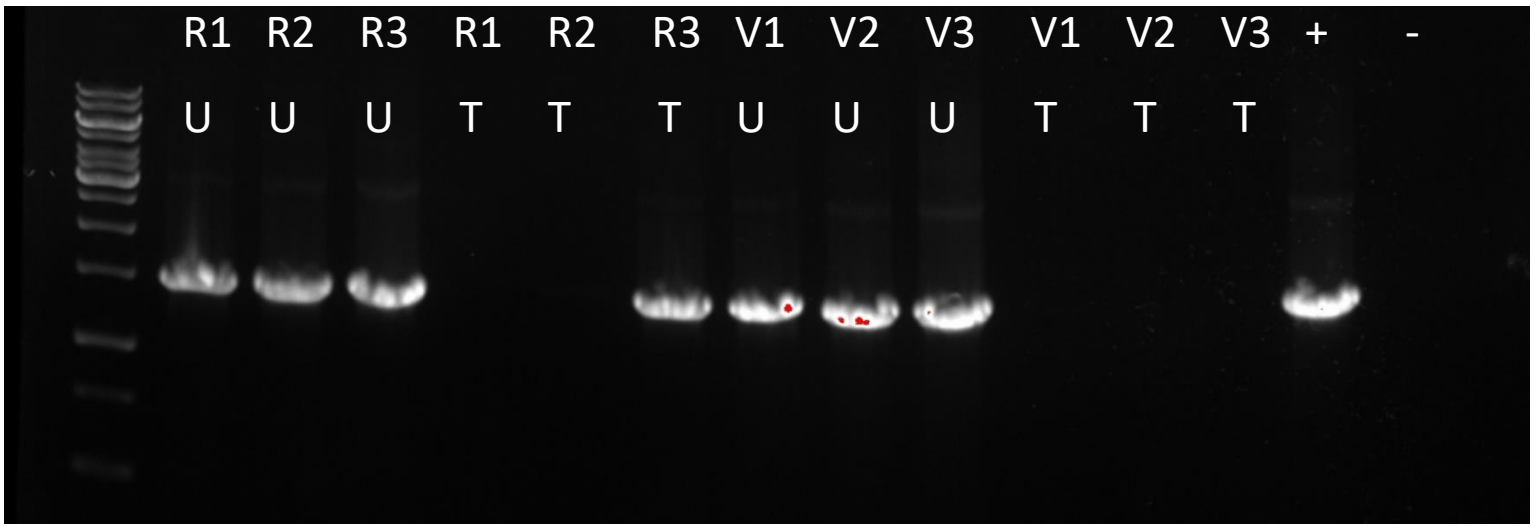

Figure 7.4. Evidence of genomic DNA contamination after treatment with a Turbo DNA-free kit using either a routine protocol (R1, R2, R3 – single treatment 2.5 µl DNase, 30 minutes at 37 °C) or a vigorous protocol (V1, V2, V3 – two successive treatments with – 2.5 µl DNase, 30 minutes at 37 °C). DNA concentrations were 50 ng (R1,V1), 100 ng (R2,V2), or 500 ng (R3,V3), with untreated (U) samples compared to treated (T) samples. Contamination by genomic DNA was tested by PCR using genes specific to the 16S rRNA gene, using a positive genomic DNA control (+) or a negative control with no template (-).

Cell cultures were prepared according to the timepoints described in Section 2.10.1, but RNA was extracted using the hot-phenol protocol described in Section 2.10. Contaminating DNA was removed by the Turbo DNA-free kit using

the vigorous treatment protocol. All samples were confirmed to be DNA-free and were sent to Novogene for quality control checks. Approximately 50% of the samples were of insufficient quality for further analysis. This was likely to be due to two reasons. Firstly, the RNA samples were extracted and frozen at -80 ^{o}C, then thawed for DNase treatment and subsequently re-frozen for shipment to Novogene. The act of freeze-thawing may have decreased the quality of the RNA. Further RNA extraction protocols used a combination of the RNA extraction and DNase treatment protocols before freezing the samples, preventing any thawing of the RNA. Secondly, the treatment protocol required the incubation of the RNA samples at 37 ^{o}C. RNA is very easily degraded, particularly at elevated temperatures (discussed by Fabre *et al*. 2014).

In a second experiment, samples were prepared as described above and immediately treated by the Turbo DNA-free kit, with aliquots taken prior to freezing for quantification using a Nanodrop spectrophotometer (Thermo Fisher). One-third of samples retained contaminating gDNA after using the vigorous protocol. These samples were unsuitable for RNA-sequencing, necessitating further troubleshooting. An alternative DNase was needed due to the requirement of the Turbo DNA-free kit to be incubated at 37 ^{o}C for extended periods, likely causing the decreased quality of RNA samples. Quality control reports from Novogene also identified the presence of 5S rRNA in some samples, meaning that purification of the samples would be required in order to prevent the rRNA from influencing the sequencing and analysis processes (Novogene UK, personal communication).

The length of time required to remove contaminating DNA caused RNA samples to degrade excessively. As the phenol:chloroform extraction protocol was allowing excessive amounts of gDNA to remain in the samples, necessitating the use of vigorous DNase protocols, further RNA extractions were conducted using the RNeasy minikit (Qiagen). This kit was compatible with RNase-free DNase (Qiagen), which operated at room temperature. Initially, *Variovorax* sp. WS11 was grown in 10 ml Ewers medium to a final OD_{540} of either 0.6 or 1.0, using either 10 mM succinate or 1% (v/v) isoprene as the sole source of carbon and energy. The cells were broken by a single bead-beating step using a Lysing Matrix B bead-beating tube (MP Biomedicals), consistent with the cell breakage method previously used in the hot acid-phenol protocol (described in Section 2.10), and RNA was extracted using an RNeasy minikit according to the manufacturer's instructions. Contaminating DNA was removed using the RNase-free DNase kit, following either the on-column protocol or the off-column protocol (according to the manufacturer's instructions), or the Turbo DNA-free kit vigorous protocol.

Table 7.4. RNA concentration and purity, determined by Nanodrop spectrophotometer.

Sample	Concentration (ng/µl)	260/280	260/230	DNA-free?
1.Succinate, OD=0.6, on-column digestion	426.8	2.14	2.01	N
2.Isoprene, OD=0.6, on-column digestion	708.4	2.17	2.18	N
3.Succinate, OD=1.0, on-column digestion	889.3	2.17	2.36	Y
4.Isoprene, OD=1.0, on-column digestion	652.2	2.17	1.66	N
5.Succinate, OD=1.0, Turbo DNase	991.6	1.98	1.92	Y
6.Isoprene, OD=1.0, Turbo DNase	510.4	2.01	1.78	Y
7.Succinate, OD=0.6, off-column digestion	414.8	2.18	1.45	N
8.Succinate, OD=0.6, off-column digestion	601.3	2.16	1.59	N

The density of the cell culture used in the extraction protocol influenced the amount of RNA apparently retrieved from the samples (Table 7.4), although the concentration of RNA purified from cultures with an OD_{540} of 0.6 were sufficient to meet the concentration of RNA required by Novogene. A single bead-beating step in a Lysing Matrix B tube at 6.0 m/sec using a FastPrep-24 5G sample preparation system (MP Biomedicals) for 30 seconds was sufficient to break the cells previously, but the samples described in Table 7.4 only displayed weak rRNA bands when separated by agarose gel electrophoresis (Figure 7.5). 2 µg of RNA samples were loaded into each well and separated by electrophoresis at 60 V for 90 minutes in a temperature-controlled room, maintained at 4 ^{o}C. This aimed to minimise the heating of the samples by the electrophoresis process, as this would cause degradation and smearing of the RNA. Several features of the agarose gel analysis indicated issues with the preparation of RNA when using the RNeasy mini kit (Figure 7.5). Firstly, the brightness observed in the wells indicated contamination of the samples by proteins. As each sample had been purified using the RNA purification columns in the RNeasy mini kit, the presence of proteins was surprising. Additionally, the faintness of the ribosomal RNA (rRNA) bands indicated poor quality of the RNA samples. The apparent concentrations of RNA recorded by Nanodrop analysis may have been artificially increased due to the presence of proteins and also contaminating DNA, as the on-column and off-column protocols using RNase-free DNase did not reliably remove contaminating DNA from any of samples (Table 7.4).

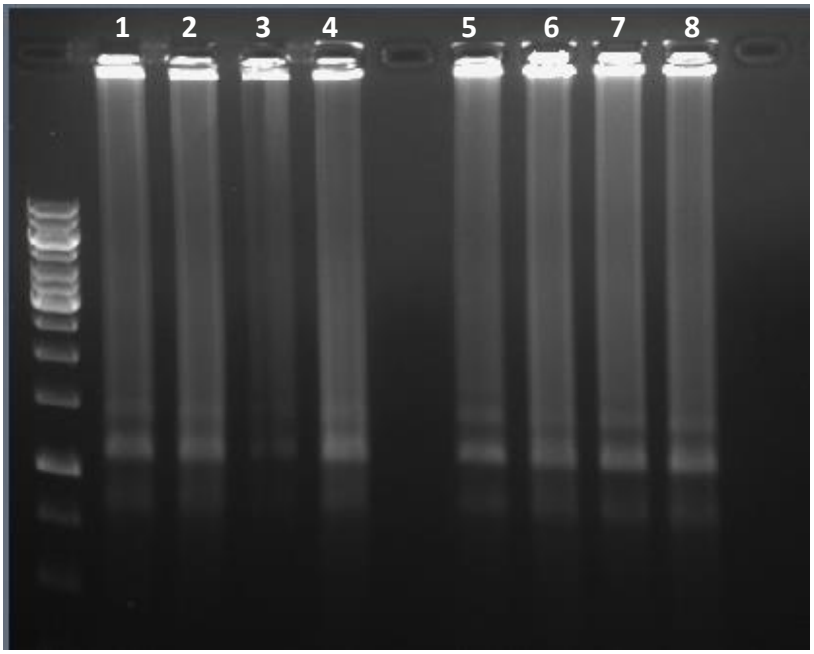

Figure 7.5. Quality of RNA samples described in Table 7.4, analysed by agarose gel electrophoresis.

The hot phenol method was used for further extractions of RNA from *Variovorax* sp. WS11 (Gilbert *et al*. 2000). Genomic DNA was removed from the RNA samples by two rounds of treatment using RNase-free DNase, using the off-column protocol. Each RNA sample was prepared according to varied methods in an attempt to identify any steps of RNA preparation which were promoting RNA degradation, or which were allowing contaminating DNA to remain in the sample. Cells were prepared at an initial density of either 0.6 or 1.0. As phenol carryover can inhibit the activity of enzymes (discussed by Tavares *et al*. 2011), including DNase, a second chloroform extraction step was included in the RNA extraction protocol for samples 5 and 6 (Table 7.5). No visible difference was observed in RNA concentration or quality (Figure 7.6), indicating that a second chloroform-extraction step was not necessary. The volume of DNase added to the samples was also varied from 5 µl to 10 µl, as previous samples were inconsistently degraded by RNase-free DNase when using 2.5 µl of DNase in 100 µl suspensions of RNA in nuclease-free water (following the manufacturer's instructions). Contaminating DNA was fully removed from all 6 samples after two rounds of DNase treatment, confirming that 5 µl of DNase was sufficient (Table 7.5).

Table 7.5. RNA concentration and quality, as determined by a nanodrop spectrophotometer. Contamination by DNA was tested by PCR using primers specific to the 16S rRNA gene. These data are represented in Figure 7.6.

Sample	Concentration (ng/µl)	260/280	260/230	DNA-free?
1. OD_{540} = 1.0, 5 µl DNase, 2x off-col	327	2.18	2.09	Y
2. OD_{540} = 1.0, 10 µl DNase, 2x off-col	409.4	2.16	2.22	Y
3. OD_{540} = 1.0, 5 µl DNase, 1x on-col, 2x off-col	307.9	2.17	2.23	Y
4. OD_{540} = 0.6, 5 µl DNase, 1x on-col, 1x off-col	122.3	2.0	1.45	Y
5. OD_{540} = 0.6, 2x chloroform, 5 µl DNase, 2x off-col	176.3	2.15	1.4	Y
6. OD_{540} = 0.6, 2x chloroform, 10 µl DNase, 2x off-col	263.2	2.17	1.72	Y

The quality of the RNA samples was greatly improved after extraction by the acidic phenol:chloroform method when compared to the RNeasy mini kit (Figure 7.6). rRNA bands were well-defined with very little smearing, and no evidence of protein contamination was seen in the wells, indicating that this method of RNA extraction and preparation was more suitable for the preparation of samples for RNA-seq.

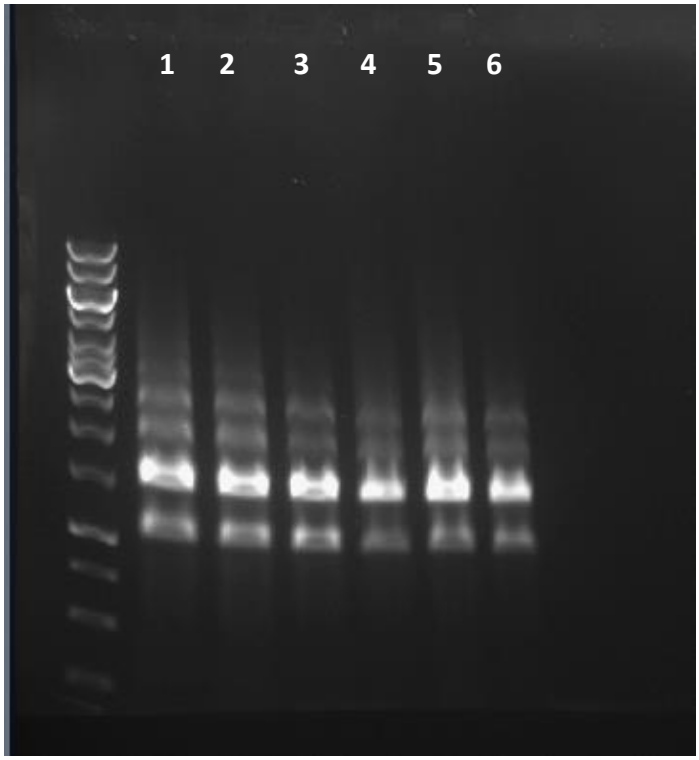

Figure 7.6. Quality analysis of the RNA described in Table 7.5 by agarose gel electrophoresis.

6 of 51 samples were suitable for RNA-seq, with the remaining 45 samples having insufficient RIN values for further analysis. The amount of DNA in the samples after phenol:chloroform extraction necessitated two rounds of DNase treatment coupled with column-based purification by the RNeasy minikit after each incubation with DNase. RNA extraction by the TRIzol reagent (ThermoFisher Scientific) was subsequently used to lyse *Variovorax* sp. WS11 and extract total RNA (according to the manufacturer's instructions). The instructions from Thermo Fisher were unspecific with regards to the drying of the RNA pellets and the solubilisation of RNA. The incubation temperature and length of time of the re-solubilisation step were varied in initial trials, although little difference in the quality of RNA samples was observed across the tested conditions (Figure 7.7). Samples 5 and 6 were vortexed during the resuspension step in order to test RNA recovery and RNA quality compared to flicking tubes during resuspension (samples 1-4). This aimed to determine whether RNA degradation would be exacerbated by mechanical perturbation. The greatest quantity of RNA was recovered in samples 4 and 5 (Table 7.6), indicating that a longer drying step combined with a lower resuspension temperature were the ideal conditions. Interestingly, only a single DNase treatment step (using the off-column protocol with RNase-free DNase, as described above) was required to remove all detectable DNA from the TRIzol-extracted samples, halving the length of time required for manipulations of the RNA at room temperature. As this was likely to increase the quality of the RNA samples, the substrate-switched time-course experiment was repeated using the TRIzol reagent (as described in Section 2.10.1).

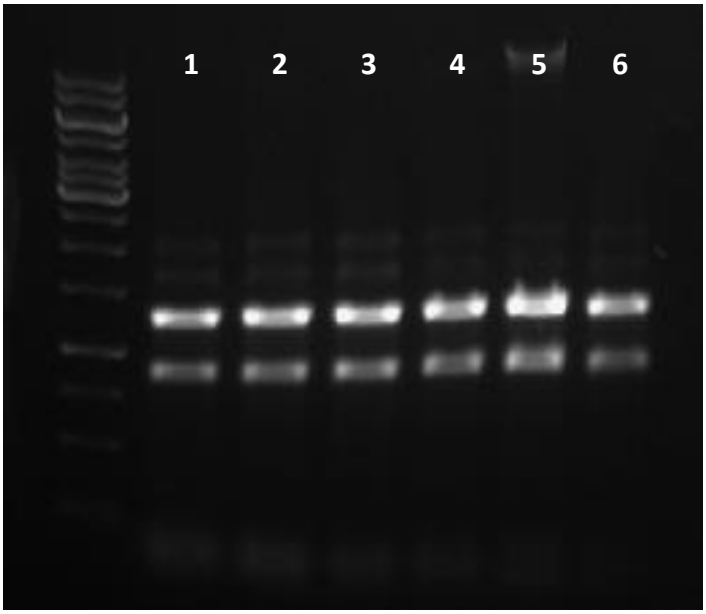

Figure 7.7. Quality of the RNA described in Table 7.6 after extraction by the TRIzol reagent, analysed by agarose gel electrophoresis.

Table 7.6. Concentration and quality of the RNA samples shown in Figure 7.7, as determined by agarose gel electrophoresis. Contamination by DNA was tested by PCR using primers specific to the 16S rRNA gene.

Sample	Concentration (ng/µl)	260/280	260/230	DNA-free
1. 5 minutes drying, 5 minutes @ 60 °C	385.7	1.99	1.93	Y
2. 10 minutes drying, 5 minutes @ 60 °C	962.3	2.00	2.29	Y
3. 5 minutes drying, 10 minutes @ 55 °C	663.2	1.98	2.09	Y
4. 10 minutes drying, 10 minutes @ 55 °C	1761.5	2.08	2.26	Y
5. 8 minutes drying, 10 minutes @ 55 °C	2128.8	2.06	2.22	Y
6. 8 minutes drying, 5 minutes @ 60 °C	726.5	1.97	2.07	Y

RIN values from TRIzol-extracted RNA were sufficient to continue with RNA-sequencing. The samples were being analysed at the time of writing this thesis.

Table 7.7. Primers used in the studies described in this chapter.

Primer name	Primer Sequence (5'--3')	Product length (bp)	Primer function
q*isoA*_F	GGCGGTGAAGAACTTTTTCG	58	Initial primers designed to amplify *isoA* during RT-qPCR
q*isoA*_R	CGCGGCTTCGATGCA		
q*rpoB*_F	GCGAAGTGCCGCTCATG	56	Initial primers designed to amplify *rpoB* during RT-qPCR
q*rpoB*_R	GCGCTCTGTGCCGTTGAT		
q*gyrA*_F	GACTGGATCGATCAGCTCTTCA	61	Initial primers designed to amplify *gyrA* during RT-qPCR
q*gyrA*_R	GGTTGGAGAAGCACAGGATGTAG		
q*gmk*_F	CACGCGCCAACGAATTC	71	Initial primers designed to amplify *gmk* during RT-qPCR
q*gmK*_R	CGCCTTCAGGTCGAAAAGTG		
q*isoA*_1F	GTTCATGCTCGAATGGGTGG	213	Alternative primers designed to amplify *isoA*.
q*isoA*_1R	GGGTACTTCTCGTTGAGCCA		
q*isoA*_2F	GATGTCTCGTTCTGGCGTTC	157	Successful primers designed to amplify *isoA*.
q*isoA*_2R	ACCCGTAGTCCTTCATCGTG		
q*rpoB*_1F	TGCAGGCCATTTACACCAAC	220	Successful primers designed to amplify *rpoB*.
q*rpoB*_1R	TTGAACTTCATGCGACCGAC		
q*rpoB*_2F	CTGGAACGGCTACAACTTCG	203	Alternative primers designed to amplify *rpoB*, unsuccessful.
q*rpoB*_2R	CGACGTAGATGATCCCGGAT		
q*gyrA*_1F	GACCAAGGAAGACGACTGGA	159	Successful primers designed to amplify *gyrA*.
q*gyrA*_1R	GGGAACATGTTGACGATCGG		
q*gyrA*_2F	CTCAACAACGACTGGAACCG	220	Alternative primers designed to amplify *gyrA*, unsuccessful.
q*gyrA*_2R	CGAGCCGAATTTCCGTGTAG		
q*isoG*_1F	AAGACCATGAGCAACCAGGA	233	Successful primers designed to amplify *isoG*.
q*isoG*_1R	GCCGTTGTTCTCGACTTCAA		
q*isoG*_2F	GCAACAAGGAATGGATCGGA	225	Alternative primers designed to amplify *isoG*, unsuccessful.
q*isoG*_2R	GATGGGTCAGCACTTCGTTT		

7.5. **Results and discussion**

7.5.1. **Differential expression of isoprene metabolism**

The regulation of isoprene metabolism in *Variovorax* sp. WS11 was initially studied with regards to the functional activity of isoprene oxidation when compared between growth conditions. Analysis of the proteome of isoprene-grown *Variovorax* sp. WS11 confirmed that the abundance of Iso metabolic peptides increased significantly during growth on isoprene when compared to succinate-grown or uninduced controls ($p \leq 0.01$) (as described in Section 3.5.7.4). This indicated that isoprene metabolism was inducible in *Variovorax* sp. WS11, although Iso metabolic peptides were still moderately abundant during growth on succinate (Chapter 3, Figure 3.22). Isoprene oxidation by *Variovorax* sp. WS11 was studied by isoprene uptake assays in whole cells after growth using a range of carbon

sources (as described in Section 2.15.1). 1% (v/v) isoprene, 10 mM glucose, 10 mM fructose, 10 mM succinate, 10 mM pyruvate, and a combination of each sugar or carboxylic acid with 1% (v/v) isoprene were chosen as the appropriate conditions for testing. Cells grown in batch culture were harvested at an OD_{540} of approximately 0.6, washed in 50 mM HEPES (pH 6.0) and resuspended to a final OD_{540} of 10.0 in 50 mM HEPES (pH 6.0).

Variovorax sp. WS11 oxidised isoprene when grown using isoprene, a combination of pyruvate and isoprene, and a combination of succinate and isoprene (Figure 7.8). This contrasts with previous observations in *Rhodococcus* sp. AD45, where isoprene oxidation was repressed after growth using a combination of succinate and isoprene (Crombie *et al*. 2015). The lack of isoprene oxidation when *Variovorax* sp. WS11 was grown on succinate alone confirmed that the baseline level of abundance of Iso metabolic proteins (Chapter 3, Figure 3.22) was not sufficient to catalyse a detectable rate of isoprene metabolism (Figure 7.8). Alternatively, another form of repression may have been active due to the presence of the more energetically favourable substrate. The difference in isoprene oxidation rates between isoprene-grown and succinate+isoprene-grown *Variovorax* sp. WS11 was relatively small and not statistically significant ($p>0.05$), but the decrease in the average rate of isoprene oxidation when grown on succinate+isoprene indicated that succinate may be a weak repressor of isoprene metabolism (Figure 7.8). However, the rate of isoprene oxidation increased more than 2-fold when *Variovorax* sp. WS11 was grown on pyruvate+isoprene compared to isoprene alone ($p\leq0.05$). This could be explained by pyruvate acting as a reductant to maintain levels of NADH within the cell. This was previously described for the oxidation of methane by the sMMO of *Methylosinus trichosporium* OB3b, in which sodium formate acted as a co-substrate which stimulated the rate of methane oxidation (Brusseau *et al*. 1990). When grown on a combination of a sugar with isoprene, *Variovorax* sp. WS11 did not oxidise isoprene (Figure 7.8), a significant reduction when compared to the isoprene-grown cells ($p\leq0.05$). The role of carbon catabolite repression in the sequential utilisation of carbon sources is well established, with glucose typically recognised as the most efficient, and therefore first-metabolised, carbohydrate (Brückner & Titgemeyer 2002). CCR is the most likely explanation for the lack of isoprene oxidation during the growth of *Variovorax* sp. WS11 using a combination of a sugar with isoprene (Figure 7.8), with glucose and fructose representing more efficient sources of carbon and energy than isoprene. It should also be noted that the rate of isoprene oxidation by *Variovorax* sp. WS11 during growth on isoprene was more than 20-fold lower in these individual batch cultures than in the isoprene-fed fermentor cultures (Chapter 3, Figure 3.15). In the latter case, *Variovorax* sp. WS11 consumed isoprene at an average rate of 31.52±5.52 nmol min^{-1} mg dry $weight^{-1}$ cells, compared to an average of 1.51±0.64 nmol min^{-1} mg dry $weight^{-1}$ by the 20 ml cultures used in this experiment. This was previously observed in *Rhodococcus* sp. AD45, which also oxidised isoprene at a higher rate after growth in the isoprene-fed fermentor compared to individual small-scale cultures (Sims 2020). This enhancement of isoprene oxidation is likely to be as a result of the frequent supply of fresh Ewers medium and the continuous introduction of O_2 and isoprene (Chapter 2, Figure 2.1). Growth of *Variovorax* sp. WS11 in sealed 120 ml vials limited the amount of O_2 available for aerobic respiration, and isoprene oxidation as a result, thereby limiting the maximum rate of substrate oxidation.

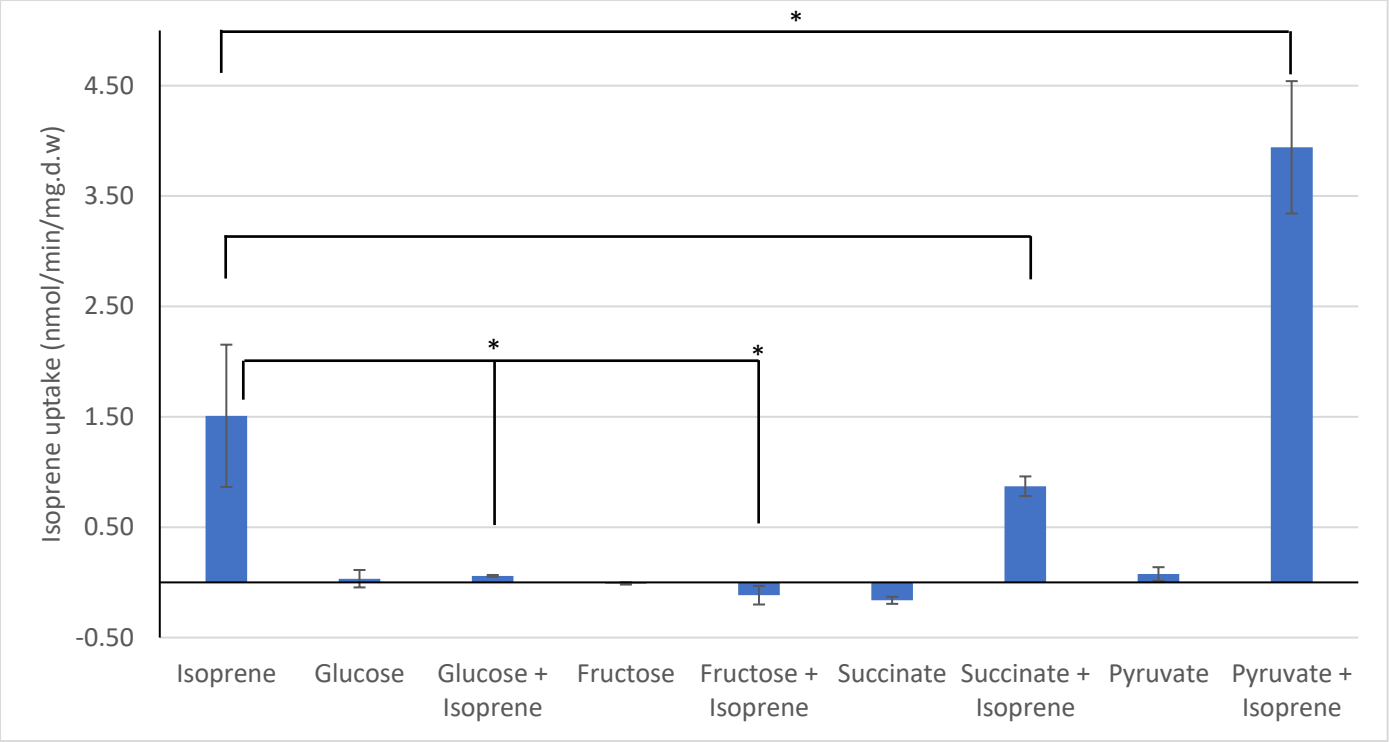

Figure 7.8. Oxidation of isoprene by whole cells of *Variovorax* sp. WS11 after growth on varied carbon sources. Error bars represent the standard deviation about the mean of three biological replicates. Asterisks denote a statistically significant difference between the indicated conditions ($p \leq 0.05$).

7.5.2. **Differential expression of *iso* metabolic genes under different growth conditions**

Differences in the rate of isoprene oxidation were evident when *Variovorax* sp. WS11 was grown on combinations of isoprene with sugars or carboxylic acids (Figure 7.8), confirming that isoprene metabolism was inducible in this bacterium. However, it was unclear whether the control of IsoMO activity occurred at the level of transcription or translation. Transcriptional regulation allows bacteria to respond rapidly to an environmental stimulus, with mRNA being synthesised within minutes or hours to a significant degree (Browning & Busby 2016). Repression of transcriptional initiation can occur through a number of mechanisms. For example, this may be due to promotion of mRNA-degradation, or by direct binding of repressor proteins to the RNA polymerase to block its activity (Rojo 1999, Payankaulam *et al*. 2010). Translational control also allows rapid adaptation of bacteria to stimuli, typically through RNA-dependent mechanisms. Small RNA (sRNA)-dependent repression, which may occur by the direct binding of sRNA to mRNA, prevents activity at the ribosome binding site (RBS) (Azam & Vanderpool 2018). RNA-binding proteins may also be expressed along with the regulated operon which, in turn, exert an autoregulatory role (Babitzke *et al*. 2009, Geissmann *et al*. 2009). The role of transcriptional repression of isoprene metabolism in *Variovorax* sp. WS11 was tested by RT-qPCR. This had not previously been demonstrated in an isoprene-degrading bacterium, as the most relevant observation available prior to this study was the repression of IsoMO activity by succinate in *Rhodococcus* sp. AD45 rather than repression of transcription of *iso* metabolic genes (Crombie *et al*. 2015).

7.5.2.1. **Expression of *isoA* in the presence of a combination of substrates**

Variovorax sp. WS11 was grown in Ewers medium with 1% (v/v) isoprene, 10 mM glucose, or 10 mM glucose + 1% (v/v) isoprene, with three biological replicates per condition. Cells were harvested at an OD_{540} of 0.6, and total RNA was extracted as described in Section 2.10. cDNA was synthesised from the RNA as described in Section 2.10.3, and RT-qPCR was conducted as described in Section 2.11 *isoA* and *rpoB* were selected as the targets for amplification, using primers q*isoA*_2F:q*isoA*_2R and q*rpoB*_1F:q*rpoB*_1R. Three biological replicates of each cDNA target were analysed using a further three technical replicates, and the relative change in expression of *isoA* was calculated relative to *rpoB* using the comparative C_T method (Schmittgen & Livak 2008). Using the expression of *isoA* in glucose-grown cells as a baseline (1.31±1.04), the expression of *isoA* during growth on glucose+isoprene decreased to an average of 0.14±0.09 (Figure 7.9), although this was not a statistically significant decrease according to *t* test (p=0.12). When grown on isoprene, the expression of *isoA* increased significantly to a value of 581.64±174.96, relative to *rpoB* (p=0.005). These data support the initial observations derived from the isoprene uptake study (Figure 7.8), as a combination of glucose and isoprene repressed the expression of *isoA* and therefore prevented activity of IsoMO. This was likely to be a result of CCR caused by the presence of glucose (Brückner & Titgemeyer 2002).

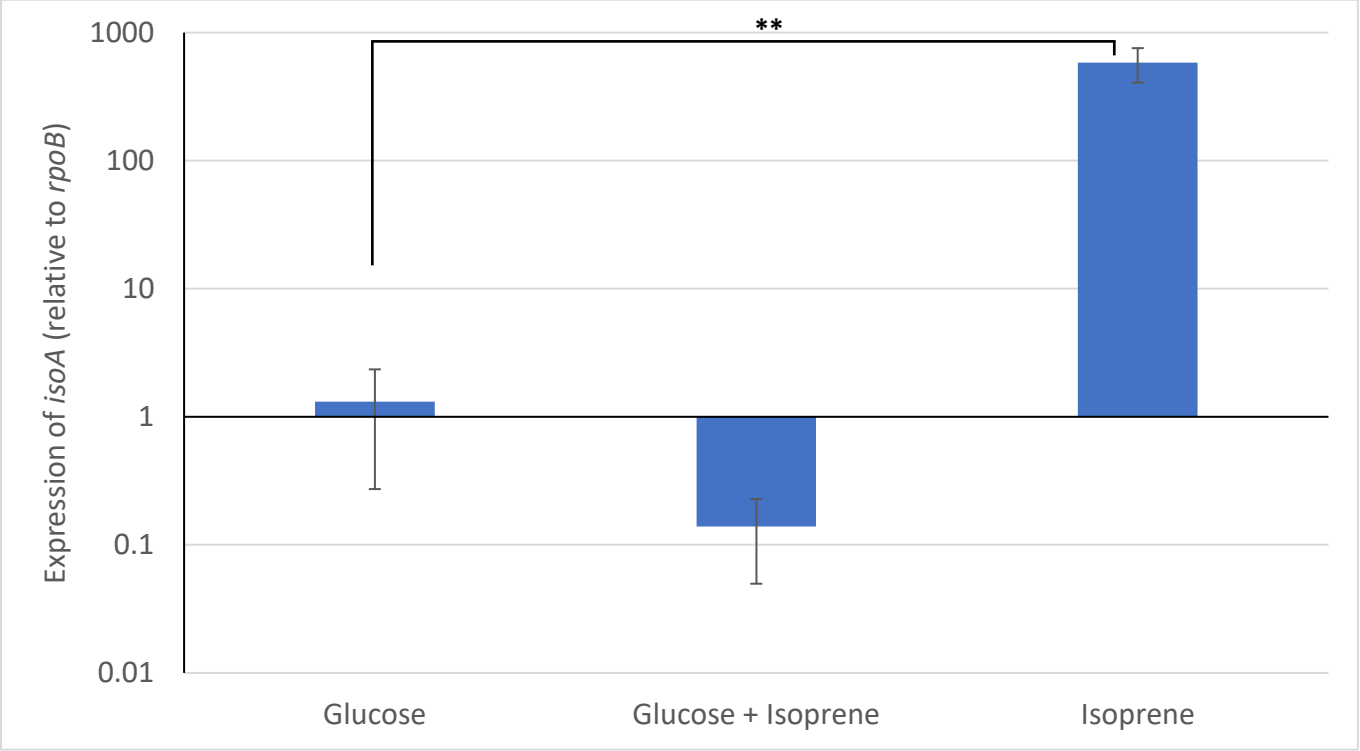

Figure 7.9. Expression of *isoA* by *Variovorax* sp. WS11 during growth on different carbon sources, relative to *rpoB*. An asterisk represents statistically significant expression of *isoA* (** p≤0.01) compared to the glucose-grown baseline. Error bars represent the standard deviation about the mean of three biological replicates.

Variovorax sp. WS11 was grown on fructose, fructose+isoprene, succinate, succinate+isoprene, pyruvate, and pyruvate+isoprene, consistent with the data shown in Figure 7.8. RNA was extracted from these cells as described

previously, and cDNA was prepared. The single carbon sources fructose, succinate and pyruvate, served as the relative baseline level of expression of *isoA* for comparison with cells grown on a combination of that substrate with isoprene. Expression values were 1.00±0.12, 1.04±0.38, and 1.01±0.15, respectively (Figure 7.10). As expected, combinations of a carboxylic acid with isoprene did not totally repress the expression of *isoA*, consistent with the rates of isoprene oxidation observed when *Variovorax* sp. WS11 was grown using these substrates (Figure 7.8, Figure 7.10). *isoA* was transcribed to a significantly greater degree in the presence of isoprene when compared to each baseline condition ($p \leq 0.05$), such as succinate+isoprene compared to succinate-only. The relative levels of expression of *isoA* were also consistent with the observations made during the isoprene uptake assays; *Variovorax* sp. WS11 oxidised isoprene at a greater rate during growth on pyruvate+isoprene than it did during growth on succinate+isoprene (Figure 7.8). *isoA* was also expressed to a greater degree during growth on pyruvate+isoprene than during growth on succinate+isoprene (Figure 7.10), measuring 374.93±112.78 compared to 29.57±11.76, respectively, further indicating that succinate may be a weak repressor of isoprene metabolism by *Variovorax* sp. WS11. Pyruvate may also stimulate isoprene metabolism, as isoprene oxidation was greater during growth on pyruvate+isoprene than on isoprene alone (Figure 7.8). This may have been as a result of pyruvate providing additional reducing power to the cells, as in the case of sodium formate acting as a reductant for *M. trichosporium* OB3b during methane oxidation (Brusseau *et al*. 1990).

Unlike glucose, which prevented the activity of IsoMO by repressing *isoA* expression, fructose prevented IsoMO activity but still allowed significant expression of *isoA*, with expression of 257.16±17.07 relative to *rpoB* ($p \leq 0.01$). The mode of regulation of isoprene metabolism by fructose is unclear, although typical carbon catabolite repression or mRNA degradation appear to be unlikely when considering the continued transcription of *isoA*. Instead, a form of post-transcriptional or post-translational regulation is most likely. In the former case, repression of translation by small antisense RNA may be responsible for the prevention of isoprene oxidation, although this has not currently been described in any isoprene degrading bacterium. The mechanism of regulation of isoprene metabolism by fructose requires further study.

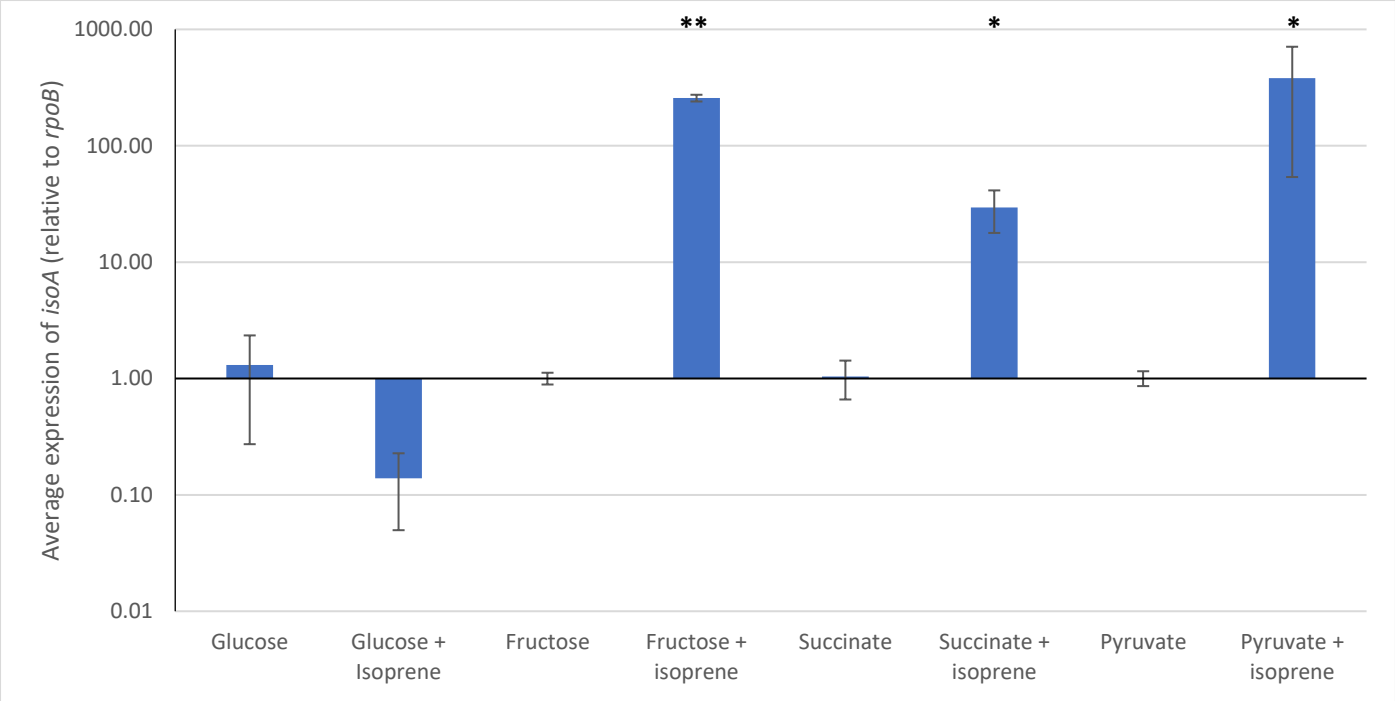

Figure 7.10. Expression of *isoA* by *Variovorax* sp. WS11 during growth on a combination of a sugar or carboxylic acid with isoprene, relative to *rpoB*. Asterisks denote statistically significant expression of *isoA* (* p≤0.05, ** p≤0.01) compared to the respective baseline conditions. Error bars represent the standard deviation about the mean of three biological replicates.

7.5.3. **Induction of *iso* metabolic genes by alternative alkenes**

Isoprene and epoxyisoprene were known to induce the expression of the *iso* metabolic gene cluster in *Variovorax* sp. WS11 (Chapter 6, Figure 6.12). Due to the wide substrate specificity of IsoMO in *Variovorax* sp. WS11 (Chapter 3, Figure 3.15), it was possible that various alkenes or the respective epoxides may induce the expression of IsoMO. However, isoprene was the only alkene which was able to support the growth of *Variovorax* sp. WS11 as the sole source of carbon and energy (Chapter 3, Table 3.2), and epoxyisoprene was known to inhibit the growth of *Variovorax* sp. WS11 when present at sufficient concentrations (Chapter 3, Figure 3.10). 1,3-butadiene, a similar compound to isoprene (2-methyl-1,3-butadiene), was only metabolised when isoprene metabolism was already active due to the presence of isoprene (Chapter 3, Figure 3.13), and only when present at a similar concentration to isoprene (Chapter 3, Figure 3.14). In order to study changes in *iso* metabolic gene expression by alternative alkenes, short-term gene induction studies were required, eliminating the requirement for *Variovorax* sp. WS11 to grow on the substrate in question.

Preparation of cells for induction of transcription was performed as described in Section 2.10.2. After starvation of washed cells in order to deplete intracellular stores of carbon, *Variovorax* sp. WS11 was supplied with 10 mM glucose, 1% (v/v) isoprene, or 1% (v/v) 1,3-butadiene, then incubated for 2 hours at 30 °C with shaking at 160 rpm. RNA was extracted as described in Section 2.10, and cDNA was synthesised as described in Section 2.10.3. It should be noted that one of the three biological replicates of RNA from glucose-induced *Variovorax* sp. WS11 was heavily

degraded and therefore could not be included in the analysis. RT-qPCR analysis was conducted using primers targeting *isoA* and *rpoB* for two biological replicates of cDNA from glucose-induced cells and three biological replicates of cDNA from isoprene-induced and 1,3-butadiene-induced cells (Figure 7.11).

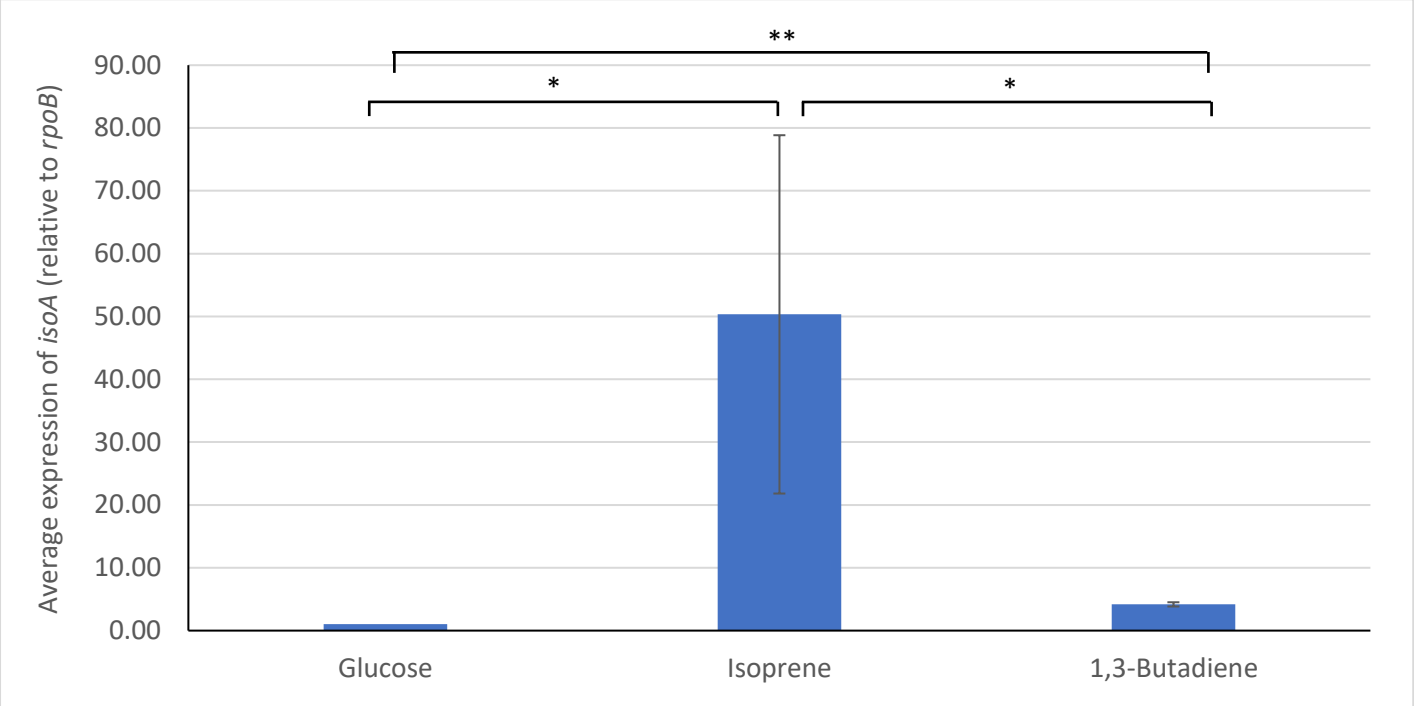

Figure 7.11. Expression of *isoA* by *Variovorax* sp. WS11 after induction by glucose, isoprene, or 1,3-butadiene for 2 hours, relative to *rpoB*. Error bars represent the standard deviation about the mean of three biological replicates. Asterisks denote a statistically significant difference between indicated conditions (* $p \leq 0.05$, ** $p \leq 0.01$).

isoA expression was significantly increased to a relative value of 50.33±28.53 by isoprene after 2 hours ($p \leq 0.05$), while 1,3-butadiene induced *isoA* by 4.18±0.34, relative to *rpoB* (Figure 7.11). The induction of *isoA* by 1,3-butadiene was low but statistically significant ($p \leq 0.01$) with respect to *isoA* expression in glucose-grown cells. The expression of *isoA* induced by isoprene was very low when compared to the induction of *isoA* relative to succinate-grown cells as a baseline (Chapter 6, Figure 6.13), as *isoA* expression was upregulated by 397.87±36.62, relative to *rpoB* after 2 hours. There were several differences between these experiments which may account for this deviation. Primarily, the difference in the initial growth substrate was likely to introduce some variation. Glucose was known to be a significant repressor of isoprene metabolism and *isoA* expression ($p \leq 0.01$), while succinate did not totally repress the expression of *isoA*, and isoprene was still oxidised by *Variovorax* sp. WS11 during growth on succinate+isoprene (Figures 7.8 & 7.10). Therefore, it is possible that growing *Variovorax* sp. WS11 on glucose caused sufficient repression of the *iso* metabolic gene cluster to prevent a significant increase in *isoA* expression during this 2-hour experiment, while succinate may only be a weak repressor of *iso* gene expression (Figure 7.10). The length of starvation and the number of washes may also be factors. *Variovorax* sp. WS11 was starved for 2 hours during this experiment, which may have caused sufficient stress to *Variovorax* sp. WS11 to hinder the response to the inducing substrates. The isoprene- and epoxyisoprene-induction study described in Section 6.5.1 was conducted after these

experiments with the insight that only 1 hour of starvation was necessary (Carriòn, O., personal communication). Therefore, *Variovorax* sp. WS11 was likely to have been stressed to a lesser degree after only 1 hour of starvation, resulting in more rapid expression of *isoA*. Washing and repeated centrifugation of *Variovorax* sp. WS11 places stress upon the cells and decreases the ability of this bacterium to oxidise isoprene, as described in Section 3.4.2.2. Expression of *isoA* after induction by isoprene or 1,3-butadiene was calculated for cells which had been washed twice in 50 mM HEPES, which would have placed stress upon the cells. This excessive washing was likely to reduce the turnover of isoprene to epoxyisoprene by *Variovorax* sp. WS11, with the latter compound inducing the greatest expression of the *iso* metabolic genes. Subsequent experiments, such as those described in Section 3.4.2.2, used a single washing step to minimise this stress. The high error of the isoprene-induced expression of *isoA* may be a result of stresses on the bacterium caused by the cell-preparation procedures (Figure 7.11).

As the induction of *isoA* by 1,3-butadiene proved the concept that the *iso* metabolic genes in *Variovorax* sp. WS11 were induced by isoprene-like alkenes, 3-methyl-1,4-pentadiene was also tested for its ability to induce *iso* gene expression (as described in Section 2.10.2), as this compound was structurally very similar to isoprene. 1,2-epoxyhexane was also tested for its ability to induce *iso* gene expression. Epoxyhexane was previously shown to irreversibly inhibit the activity of IsoI in *Rhodococcus* sp. AD45 (van Hylckama Vlieg *et al*. 1998), but the epoxide derivative of isoprene is a potent inducer of *iso* gene expression. IsoMO was not induced by the presence of 0.1% (w/v) epoxyhexane, indicating that the presence of an epoxide ring alone was not sufficient to induce the expression of the *iso* metabolic gene cluster (Figure 7.12). 3-methyl-1,4-pentadiene induced the expression of *isoA* by 3.79±3.86, relative to *rpoB*. The relatively high degree of error, combined with the lack of statistical significance ($p=0.41$), means that 3-methyl-1,4-pentadiene cannot be definitively identified as an inducer of *iso* gene expression. 3-methyl-1,4-pentadiene was oxidised by IsoMO at 48.04% of the rate of isoprene (Chapter 3, Figure 3.15), indicating the importance of carbon chain-length in the activity of IsoMO. It is possible that carbon chain-length also influences the effectiveness of an inducer of *iso* gene expression.

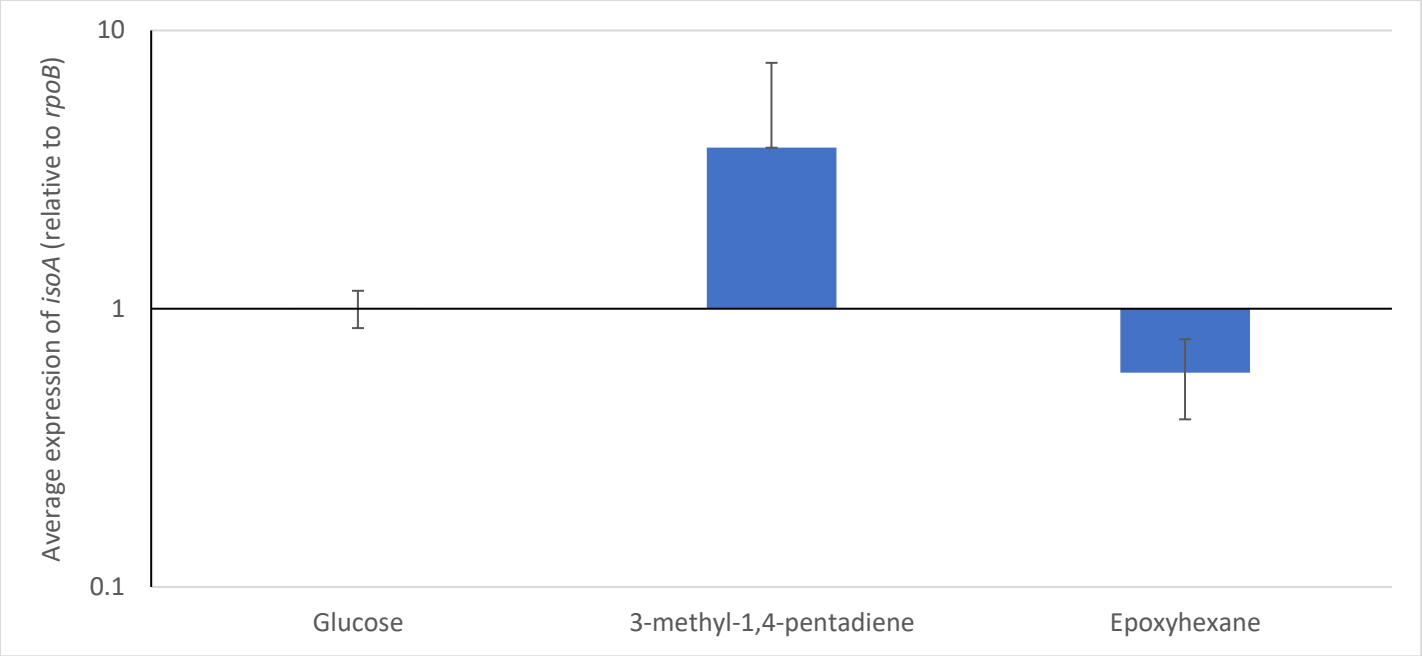

Figure 7.12. Expression of *isoA* by *Variovorax* sp. WS11 2 hours after induction by 10 mM glucose, 0.1% (w/v) 3-methyl-1,4-pentadiene, or 0.1% (w/v) 1,2-epoxyhexane, relative to *rpoB*. Error bars represent the standard deviation about the mean of three biological replicates.

Transcription of the *iso* metabolic gene cluster evidently differs between *Variovorax* sp. WS11 and *Rhodococcus* sp. AD45. Isoprene acted as an inducer of isoprene metabolism in *Variovorax* sp. WS11 (Chapter 6, Figure 6.12), although epoxyisoprene was the strongest inducer of *iso* metabolic gene expression (Chapter 6, Figure 6.12). By comparison, isoprene metabolic genes in *Rhodococcus* sp. AD45 were not induced by isoprene (Crombie *et al*. 2015). This may be due to the difference in the affinity for the metabolic intermediates of isoprene metabolism. Also, while *Rhodococcus* sp. AD45 used 1,3-butadiene and epoxyisoprene as growth substrates (Sims, L., personal communication), the growth of *Variovorax* sp. WS11 was inhibited in the presence of these compounds (described in Section 3.5.4). In spite of this, both 1,3-butadiene and epoxyisoprene significantly upregulated the expression of the *iso* metabolic genes in *Variovorax* sp. WS11 (Figure 7.11, Figure 6.12) indicating the affinity of these compounds for the transcriptional regulators which control isoprene metabolism. However, the low level of expression of *isoA* when *Variovorax* sp. WS11 was incubated with 1,3-butadiene indicated a low affinity of *iso*-specific transcriptional regulators for this compound. The structure of the inducing compound was evidently important for the strength of the gene expression, as 3-methyl-1,4-pentadiene induced little to no expression of isoprene metabolic genes (Figure 7.12).

7.5.4. **Whole transcriptome analysis of *Variovorax* sp. WS11**

Analysis of the proteome of *Variovorax* sp. WS11 identified the full range of peptides expressed during growth on isoprene compared to succinate. The whole *iso* metabolic gene cluster was highly expressed and translated during growth on isoprene but not on succinate (Chapter 3, Figure 3.20, Figure 3.21). A proposed mechanism of assimilation of GMBA, the glutathione-conjugated aldehyde intermediate of isoprene metabolism, into central metabolism was

also supported by the proteomic analysis (as described in Section 3.5.7.4). However, the proteome alone did not provide a full indication of the changes in gene expression when *Variovorax* sp. WS11 was initially exposed to isoprene, or changes in gene expression over time during growth on isoprene. This is, in part, due to the short half-life of mRNA compared to peptides, and also due to post-transcriptional regulation and modifications which may cause the transcriptome to differ significantly from the proteome (Haider & Pal 2013). A response to the presence of isoprene would also be significantly faster at the level of transcription when compared to translation. For example, after 6 hours of incubation in the presence of isoprene, only IsoI was expressed to a significantly greater degree in *Variovorax* sp. WS11 when compared to the uninduced control ($p \leq 0.01$). A complete understanding of the transcriptional and translational responses of *Variovorax* sp. WS11 in the presence of isoprene may inform further studies into the unconfirmed mechanisms by which isoprene is incorporated into central metabolism.

7.5.4.1. **Optimisation of a substrate-switched time-course experiment**

Previous RT-qPCR studies in *Variovorax* sp. WS11 used end-point conditions in which RNA was extracted from a whole culture (as described in Section 2.10). While these experiments were sufficient to calculate relative changes in the expression of *isoA* and *isoG* when *Variovorax* sp. WS11 was grown on isoprene (Figure 7.9; Chapter 6, Figure 6.13) or exposed to epoxyisoprene (6.12), little indication was given of the change in expression of the whole *iso* metabolic gene cluster over time. Proteomic analysis indicated that only IsoI was significantly upregulated after 6 hours of growth on isoprene ($p \leq 0.01$) (Chapter 3, Figure 3.20), expressed at an abundance of 5.52 compared to the uninduced control, while RT-qPCR analysis confirmed that the expression of *isoA* and *isoG* were significantly increased after only 2 hours ($p \leq 0.05$) (Figure 6.12). This emphasised the need for an understanding of both transcription and translation of the *iso* metabolic gene cluster during the exposure of *Variovorax* sp. WS11 to isoprene.

A time-course strategy for the induction of *iso* metabolic genes was devised in which succinate-grown cells were washed in an equal volume of Ewers medium (to reduce stress which may be caused by switching cells between media and buffers), starved for 1 hour (as described previously), and induced by 1% (v/v) isoprene or 0.1% (w/v) epoxyisoprene (adapted from the protocol described in Section 2.10.1). It was previously shown that the *iso* metabolic gene cluster of *Rhodococcus* sp. AD45 responded to epoxyisoprene more rapidly than isoprene (Crombie *et al*. 2015), so the first sample from epoxyisoprene-induced cultures was harvested after only 20 minutes. An overlapping timepoint (2 hours) was selected in order to compare the level of induction by epoxyisoprene and isoprene. Epoxyisoprene degrades very quickly in water (Crombie, A., unpublished data), with less than half of the original concentration of epoxide present after only 1 hour. Therefore 4 hours was chosen as the final timepoint, as after 24 hours the epoxide would be likely to have broken down entirely. The decrease in the average expression of the *iso* genes after 4 hours in the presence of epoxyisoprene, compared to 2 hours, may be a result of the epoxide breaking down and resulting in less potent induction of the *iso* genes (Figure 7.13). Alternatively, the toxicity of the epoxide (as described in Chapter 3) may have caused *Variovorax* sp. WS11 to lose some viability during the extended incubation. A maximum level of expression of the *iso* metabolic genes was observed after 2 hours in the presence of

epoxyisoprene or after 6 hours in the presence of isoprene; approximately 3,600 for *isoG* (p≤0.01) and 2,200 for *isoA* (p≤0.01), relative to *rpoB* (Figure 7.13). The maximum expression of *isoG* was observed when *Variovorax* sp. WS11 was induced by epoxyisoprene (3,652.0 in epoxyisoprene-induced cells compared to 3,498.5 in isoprene-induced cells), while the maximum expression of *isoA* was observed when induced by isoprene (2,209.7 in isoprene-induced cells compared to 1,542.1 in epoxyisoprene-induced cells). The presence of epoxyisoprene alone would bypass the requirement for isoprene monooxygenase to be expressed, potentially accounting for the lower expression of *isoA* in epoxyisoprene-induced cells compared to isoprene-induced cells. The expression of *isoA* and *isoG* was statistically significant when compared to the succinate-grown baseline under all conditions (p≤0.05) except for the epoxyisoprene-induced condition after 4 hours, likely indicating degradation of the epoxide, and *isoG* expression induced by isoprene after 2 hours. The latter was likely due to the relatively large degree of error in the gene expression data, as *isoG* was expressed by 342.41±254.30 relative to *rpoB*.

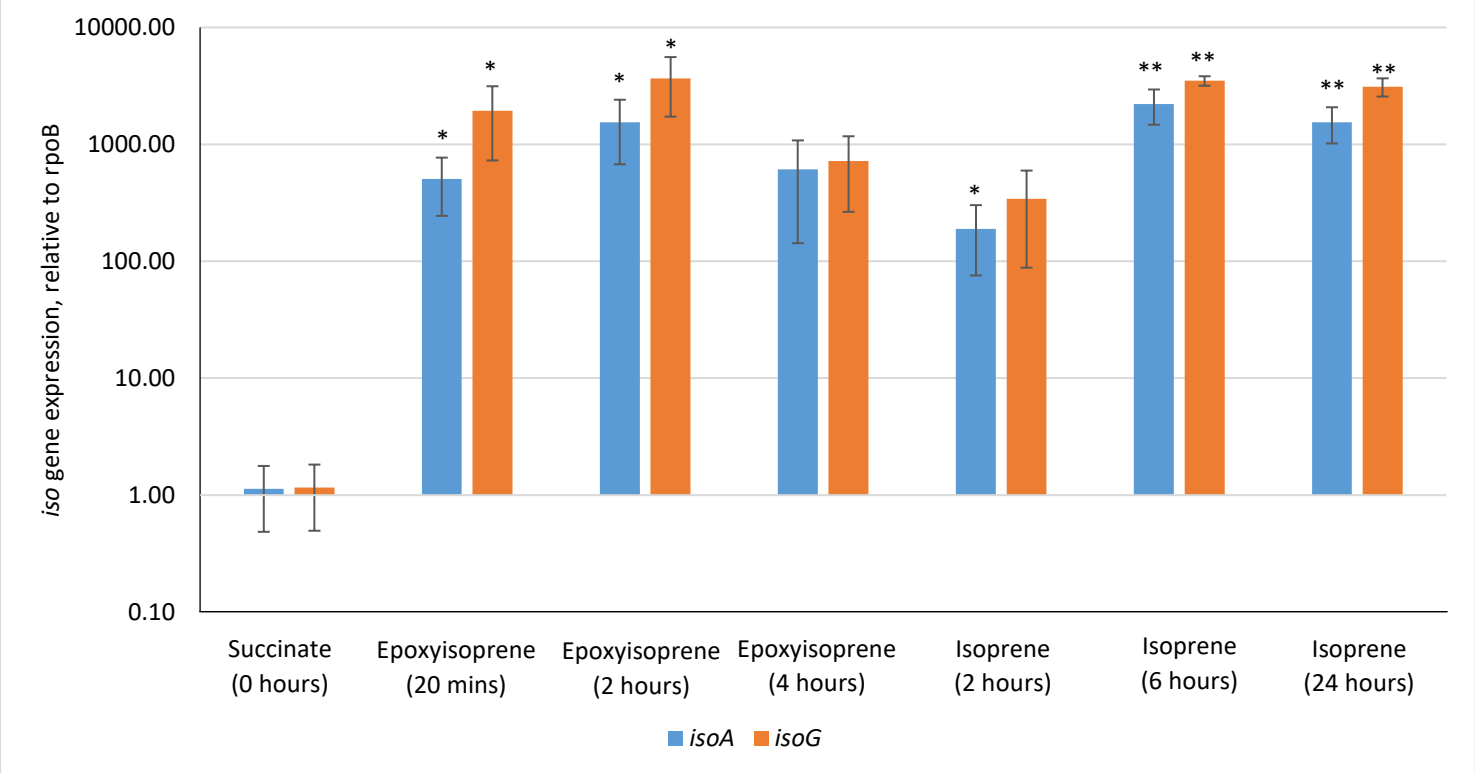

Figure 7.13. Induction of *iso* metabolic genes by isoprene and epoxyisoprene over time, relative to *rpoB*. Error bars represent the standard deviation about the mean of three biological replicates. An asterisk indicates statistically significant (* p≤0.05, ** p≤0.01) increases in gene expression with respect to succinate (0 hours).

The significant level of upregulation of *isoG* and *isoA* expression by epoxyisoprene after only 20 minutes (p≤0.05) indicated that an earlier timepoint may be more suitable for the analysis of *iso* gene expression over time. This was also true for the significant level of expression of *isoA* and *isoG* induced by isoprene after 2 hours. The final timepoints selected for the study of the transcriptome in *Variovorax* sp. WS11 are described in Section 2.10.1.

RNA extraction conditions were optimised sufficiently to allow the use of RNA sequencing (detailed in Section 7.5.4.1). Sequencing data were being prepared by Novogene (Cambridge, UK) at the time of writing this thesis, and therefore cannot be included in further discussions. However, a key difference between the transcriptomes of isoprene-grown *Variovorax* sp. WS11 and *Rhodococcus* sp. AD45 is already expected; enzymes which catalyse the methylcitrate pathway were significantly expressed in the proteome of isoprene-grown *Variovorax* sp. WS11 ($p \leq 0.01$), but the corresponding genes were not transcribed in isoprene-grown *Rhodococcus* sp. AD45. The level of transcription of the genes relating to the putative metabolic pathways identified in Section 3.5.7.4 will be very informative.

7.6. **Conclusions**

Prior to the start of this project, the regulation of isoprene metabolism had only been studied in *Rhodococcus* sp. AD45. Crombie *et al*. (2015) found that isoprene was not consumed by *Rhodococcus* sp. AD45 while succinate was present, while *Variovorax* sp. WS11 consumed isoprene at a reduced rate in the presence of a combination of succinate and isoprene when compared to isoprene-grown cells (Figure 7.8). Without further data available in *Rhodococcus* sp. AD45 and in other isoprene degrading bacteria, it is impossible to fully understand the effect of alternative growth substrates on isoprene metabolism. However, succinate may act as a repressor of isoprene metabolism, although the strength of this repression appears to vary between organisms. The repression of isoprene metabolism by sugars in *Variovorax* sp. WS11 was less simple than initially thought. Isoprene uptake assays in whole cells indicated that both fructose and glucose repressed isoprene metabolism (Figure 7.8), while only glucose repressed the expression of the *iso* metabolic genes at the transcriptional level (Figure 7.10), indicative of a role of CCR in the control of isoprene metabolism. Further work is required to fully understand the role of transcriptional regulation, post-transcriptional regulation, and post-translational regulation in the control of isoprene metabolism. Also requiring further study is the potential for some carboxylic acids to supplement the rate of isoprene metabolism in *Variovorax* sp. WS11. The rate of isoprene oxidation increased significantly when *Variovorax* sp. WS11 was grown on a combination of isoprene and pyruvate compared to isoprene alone (determined by *t* test, $p \leq 0.05$), indicating the role of pyruvate as a source of reducing power during isoprene oxidation.

Transcription of the metabolic gene cluster was influenced by the presence of isoprene-like compounds, with epoxyisoprene acting as a potent inducer of *iso* gene expression and 1,3-butadiene acting as a weak (but significant) inducer. The structure of the inducer was evidently important to the ability of the compound to influence *iso* gene expression, as 3-methyl-1,4-pentadiene and epoxyhexane were unable to induce transcription of the *iso* genes (Figure 7.12). Further experiments may focus on the affinity of inducing compounds for the specific transcriptional regulators of the *iso* metabolic gene cluster in *Variovorax* sp. WS11, DmlR_4 and DmlR_5.

A key aim of this project was to identify the metabolic reactions by which *Variovorax* sp. WS11 incorporated carbon derived from isoprene. These reactions were predicted due to the analysis of the proteome of isoprene-grown cells (described in Section 3.5.7.4), and it was hypothesised that the transcriptome of *Variovorax* sp. WS11 would give a

greater understanding of this metabolic pathway. The speed of transcription of *iso* metabolic genes in the presence of epoxyisoprene necessitated further study, as *isoG* was induced over 1000-fold (relative to *rpoB*) after only 20 minutes (Figure 7.13). Optimising the method of extraction of RNA for sequencing proved to be very challenging, as the RNA extracted from *Variovorax* sp. WS11 was partially degraded due to the length of time required at room temperature during preparation and purification. An optimised protocol was developed which used the TRIzol reagent (Thermo Fisher), allowing the extraction of high-quality RNA for sequencing. RNA sequence data will be analysed and prepared for publication at a later date.

In summary, the regulation of isoprene metabolism in *Variovorax* sp. WS11 varies according to the carbon sources present during growth. Non-growth-substrates can act as potent inducers of *iso* metabolic gene expression, with epoxyisoprene causing significant upregulation of these genes within minutes ($p \leq 0.05$). RNA-sequencing data will be used in combination with the data derived from the proteome of isoprene-grown *Variovorax* sp. WS11, providing a greater understanding of the mechanisms and regulation of the isoprene metabolic pathway.

8. Specific regulators of isoprene metabolism in *Variovorax* sp. WS11

8.1. Introduction

Transcriptional control of SDIMO-encoding genes is reported infrequently, with the transcription of the soluble methane monooxygenase representing one of the most well-characterised examples (as described in Section 7.1). The mechanism of regulation of isoprene metabolism is poorly understood. Epoxyisoprene, produced by the oxidation of isoprene by isoprene monooxygenase, is currently the most potent known inducer of isoprene metabolism (Crombie *et al*. 2015, Dawson *et al*. 2020), with isoprene and HGMB inducing the expression of the *iso* metabolic genes to a significantly smaller degree ($p \leq 0.05$) (Chapter 6, Figure 6.12, Figure 6.13). Different transcriptional regulators were located in the *iso* metabolic gene clusters of *Variovorax* sp. WS11 and *Rhodococcus* sp. AD45. Crombie *et al*. (2015) identified two *marR*-type transcriptional regulators in *Rhodococcus* sp. AD45, of which only *marR2* was upregulated in response to isoprene, and a single *gntR*-type transcriptional regulator which was only upregulated 4 hours after induction by isoprene or epoxyisoprene. The *iso* metabolic gene cluster of *Variovorax* sp. WS11 contains two LysR-type transcriptional regulators, initially identified by BLAST as *dmlR_4* and *dmlR_5* (Altschul *et al*. 1990), located 5' of *isoG* and 3' of *garB*, respectively (Chapter 1, Figure 1.8). The *iso* metabolic gene clusters of other Gram positive isoprene-degraders, *Nocardioides* sp. WS12 and *Gordonia* sp. i37, also contained *marR*-type transcriptional regulators (Gibson *et al*. 2020), indicating that Gram-positive isoprene-degraders probably use a conserved mechanism of regulation of isoprene metabolism. The use of LTTRs also appears to be conserved in Gram-negative isoprene-degraders. As in *Variovorax* sp. WS11, *Variovorax* sp. OPL2.2 contained two copies of *dmlR* in the same locations relative to the *iso* metabolic gene cluster (Carrión *et al*. 2020), while *Ramlibacter* sp. WS9 encoded a single copy of *dmlR* upstream of *isoG* (Chapter 1, Figure 1.8). *dmlR* was initially identified in *E. coli* for its essential role in regulating the metabolism of D-malate to tartarate (Reed *et al*. 2006, Lukas *et al*. 2010). Initially identified as YeaT, deletion of this gene prevented growth of *E. coli* on D-malate, and analysis by ChIP-seq confirmed that the regulator bound to the intergenic region upstream of the gene of interest, DmlA (YeaU), consistent with the typical model of transcriptional regulation by a LTTR (Figure 8.1).

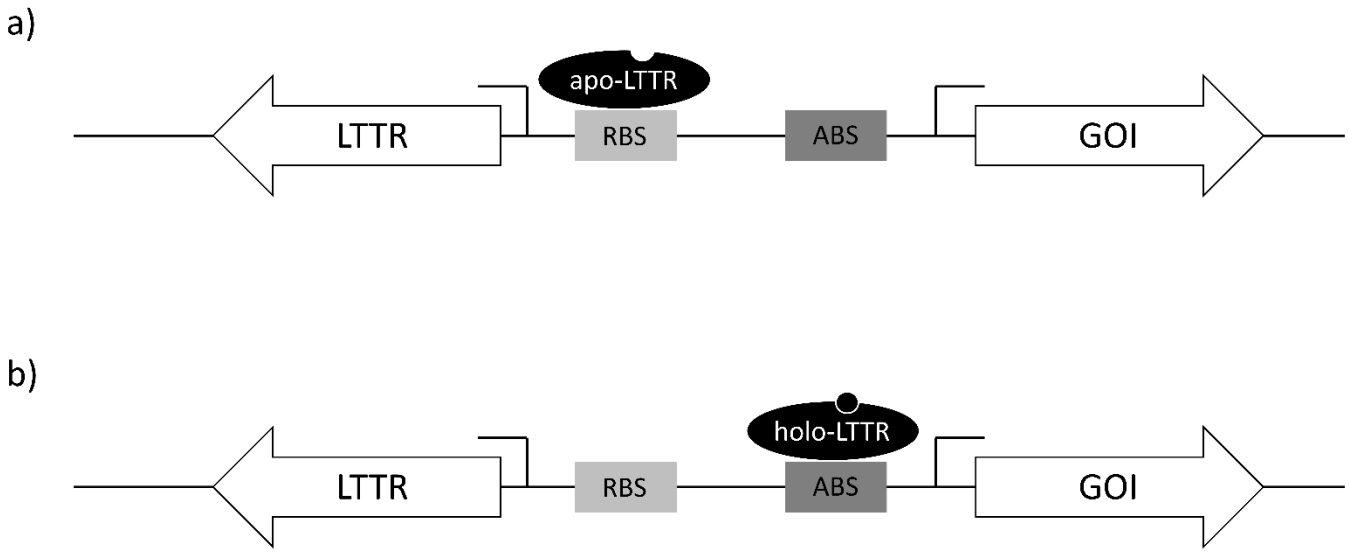

Figure 8.1. Schematic representation of transcriptional regulation by a LTTR, adapted from Maddocks & Oyston (2008). a) The apo-LTTR binds to the regulatory binding site (RBS) in the absence of a co-inducer or co-repressor, negatively autoregulating the expression of the LTTR. b) Binding of the co-inducer/co-repressor to the apo-LTTR forms the holo-LTTR which has an altered affinity for specific sequences of DNA, consequently binding to the activation binding site (ABS) and influencing the transcription of the gene of interest (GOI).

LTTRs are typically located directly upstream of, and divergently transcribed from, the target gene or gene cluster (Schell 1993). Contrary to this, *dmlR_5* was identified downstream of *garB* at the 3' end of the *iso* gene cluster of *Variovorax* sp. WS11, indicating that this putative transcriptional regulator may not influence the expression of the *iso* metabolic gene cluster. The work conducted in this chapter aimed to identify the functions of *dmlR_4* and *dmlR_5* in isoprene metabolism by *Variovorax* sp. WS11. A combination of *in silico* techniques and targeted mutagenesis were used to characterise the roles of these regulators, with planned chromatin immunoprecipitation with sequencing (ChIP-seq) potentially providing further insights into the mechanisms of these regulators.

8.2. **Specific chapter aims and objectives**

LTTRs were identified in the *iso* metabolic gene cluster of *Variovorax* sp. WS11 which were not present in the *iso* cluster of the model Gram positive isoprene degrader, *Rhodococcus* sp. AD45 (described in Chapter 4). Targeted mutagenesis was conducted with the aim of confirming the respective roles of each LTTR-encoding gene in isoprene metabolism. FLAG-tagged constructs of each LTTR were designed with the aim of conducting ChIP-seq, thereby leading to the identification the exact locations of DNA binding by each LTTR.

1. Determine the functions, if any, of *dmlR_4* and *dmlR_5* in the metabolism of isoprene by *Variovorax* sp. WS11.
2. Study the homology of *dmlR_4* and *dmlR_5* with transcriptional regulators from other isoprene degraders or, if not possible, with other well-characterised bacteria. Use this to infer the functions and origin of each LTTR.

3. Develop FLAG-tagged regulator constructs to facilitate a ChIP-seq experiment, thereby allowing the study of the locations of DNA binding of *dmlR_4* and *dmlR_5*.

8.3. **Hypothesis**

The location of *dmlR_4* and *dmlR_5* in close proximity to the core *iso* metabolic gene cluster in *Variovorax* sp. WS11 strongly indicated relevant transcriptional regulatory roles. However, close homologs of *dmlR_5* were located in the genomes of non-isoprene-degrading species of *Variovorax* (detailed in Section 8.5.1). Therefore, it was initially hypothesised that only *dmlR_4* played a role in transcriptional control of isoprene metabolism in *Variovorax* sp. WS11. Following the results of targeted mutagenesis experiments (detailed below), it was hypothesised that both *dmlR_4* and *dmlR_5* play roles in the transcription of the *iso* metabolic gene cluster, with *dmlR_5* superseding the role of *dmlR_4* when other carbon sources are present. This must be further studied by ChIP-seq or equivalent DNA-binding experiments to confirm the association of each transcriptional regulator with *iso*-specific promoters.

8.4. **Methods**

8.4.1. **Preparation of regulatory mutants by double-homologous recombination**

Inactivation of *dmlR_4* and *dmlR_5* by targeted mutagenesis was conducted as described in Section 6.4.2, with two primary exceptions. Firstly, DNA constructs were prepared with DNA inserts homologous to the 5' and 3' overlapping regions of either *dmlR_4* or *dmlR_5* (using the primers described in Table 8.1). These homologous regions were inserted into pK18mobsacB. Secondly, the gentamicin resistance gene inserted between the *dmlR* flanking regions was derived from pCM351 (Marx & Lidstrom 2002) rather than p34S-Gm (Dennis & Zylstra 1998). pCM351 was selected due to the presence of *loxP* sites upstream and downstream of *aacC1*, allowing excision of the gentamicin resistance gene after mutagenesis, generating marker-free mutants. Primers *aacC1*_fwd and *aacC1*_rev were designed to amplify *aacC1* and each *loxP* site, with *Xba*I sites included in the primer sequences to allow the ligation of the PCR-amplified gene into the suicide constructs in pK18mobsacB (Table 8.1). Recombination of each suicide construct into the genome of *Variovorax* sp. WS11 was confirmed using the primers described in Table 8.1. The second recombination event to remove the pK18mobsacB vector was confirmed by PCR using *dmlR_4*-up_fwd and *dmlR_4*-down_rev in *Variovorax* sp. WS11 Δ*dmlR_4*, and *dmlR_5*-up_fwd and *dmlR_5*-down_rev in *Variovorax* sp. WS11 Δ*dmlR_5*.

8.4.2. **Design of FLAG-tagged knock-ins of *dmlR_4* and *dmlR_5***

Initially, the wild-type copies of *dmlR_4* and *dmlR_5* had to be deleted from *Variovorax* sp. WS11 (as described in Section 8.4.2). Subsequently, FLAG-tagged copies of the respective regulatory proteins had to be re-introduced into the chromosome of *Variovorax* sp. WS11 under the control of the native promoters, complementing the regulatory mutants. DNA constructs which incorporated a *dmlR* gene, an N- or C-terminal 3X-FLAG tag, a $[Gly_4Ser]_3$ linker, and the native promoter of the *dmlR* gene (Figure 8.2) were directly synthesised (in collaboration with Dr Ben Miller, University of East Anglia, UK) with *Bam*HI and *Hind*III restriction sites for subsequent sub-cloning into pUC18miniTn7-Gm (Choi *et al*. 2005, Choi & Schweizer 2006). The multiple cloning site of pUC18miniTn7-Gm is located between two

Tn7 sequences, upstream of a gentamicin resistance gene. pUC18miniTn7-Gm facilitates the Tn7-based insertion of DNA into a broad range of bacterial chromosomes, with the insertion site located approximately 25 bp downstream of *glmS*, encoding a glutamine--fructose-6-phosphate aminotransferase (Choi & Schweizer 2006). This insertion site was previously confirmed in *Variovorax* sp. WS11 during an unrelated experiment (Carriòn-Fonseca, O., personal communication). pUC18miniTn7-Gm:*dmlR_4*-FLAG and pUC18miniTn7-Gm:*dmlR_5*-FLAG were used to transform *Variovorax* sp. WS11 by co-electroporation with pTNS2 (Choi *et al*. 2005, Choi & Schweizer 2006), which encoded the transposase necessary for Tn7-based insertion. Gentamicin was used as a selective agent. As the pUC18 backbone replicates using a ColE1-derived origin of replication (Choi & Schweizer 2006), *Variovorax* sp. WS11 Δ*dmlR_4*(-Gm) and Δ*dmlR_5*(-Gm) would only have gained resistance to gentamicin by receiving a DmlR-FLAG construct via knock-in. Primers were designed to amplify the region of DNA between *glmS* and *dmlR_4* or *dmlR_5* (Table 8.1), a product which would only exist if an insertion event had occurred. DNA bands were extracted from agarose gels and sequenced. *Variovorax* sp. WS11 Δ*dmlR_4* was confirmed to contain the *dmlR_4*-FLAG construct.

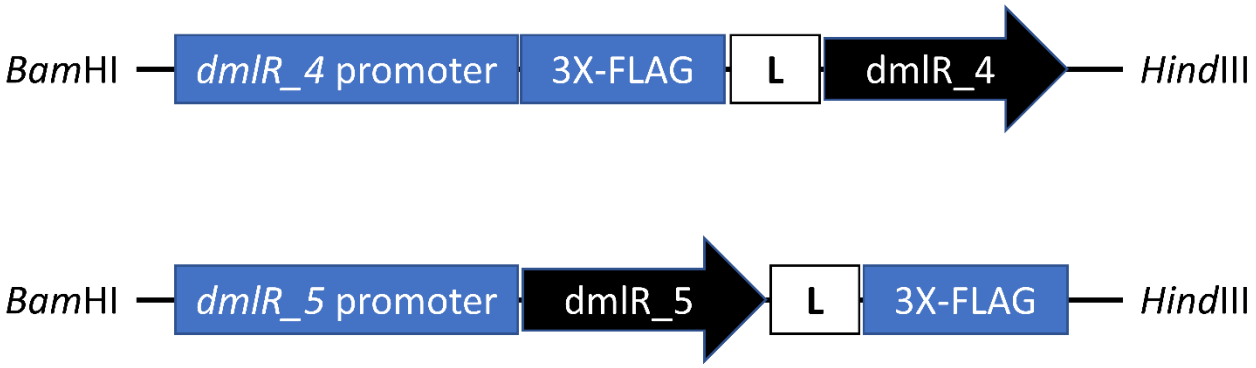

Figure 8.2. DNA-constructs designed to express N-terminal tagged DmlR_4-FLAG and C-terminal DmlR_5-FLAG in *Variovorax* sp. WS11. Fusion proteins were assembled using $(Gly_4Ser)_3$ linkers (L).

Table 8.1. Primers used in the experiments described in this chapter.

Primer	Sequence (5'--3')	Function
*dmlR_4-up*_fwd	TCTAGATAGAACGCGCTTCCTTCC	Synthesis of *dmlR_4* Flank A for the construction of a *dmlR_4* mutant of *Variovorax* sp. WS11.
*dmlR_4-up*_rev	AAGCTTCTTGTCTCCTGGTTGTCGCC	
*dmlR_4-down*_fwd	GGATCCGCGACCGACCGCATCACTAC	Synthesis of *dmlR_4* Flank B for the construction of a *dmlR_4* mutant of *Variovorax* sp. WS11.
*dmlR_4-down*_rev	TCTAGAATGGCGACCTCGTCCAACTG	
dmlR_4-A_fwd	TGACTGTGGAGGCAAGAAC	Identification of a single crossover at Flank A in the formation of a *dmlR_4* mutant of *Variovorax* sp. WS11.
GmR(4A)_rev	CTCAAACCTGGGCAGAACG	
dmlR_4-B_rev	AGTTCGCGACGCATACTTTC	Identification of a single crossover at Flank B in the formation of a *dmlR_4* mutant of *Variovorax* sp. WS11. Use in conjunction with *dmlR_4-down*_fwd.
*dmlR_5-up*_fwd	GGATCCTGTACTATGCCCTCACCGAACG	Synthesis of *dmlR_5* Flank A for the construction of a *dmlR_5* mutant of *Variovorax* sp. WS11.
*dmlR_5-up*_rev	TCTAGACGCGCATGGTGACGAATGG	
*dmlR_5-down*_fwd	TCTAGAGGCGCAACAGCGTGGTGTC	Synthesis of *dmlR_5* Flank B for the construction of a *dmlR_5* mutant of *Variovorax* sp. WS11.
*dmlR_5-down*_rev	AAGCTTGCGGTGAAGAGCGCCATGAGG	
*aacC1*_fwd	TCTAGAGTTCCGCGCACATTTCCC	Synthesis of GmR with flanking *loxP* sites, using pCM351 as a template.
*aacC1*_rev	TCTAGAAGCGCGTTTCCGAGAACC	
*garB*_fwd	TCAAGAGAACCGCTTTCGTCCC	Identification of a single crossover at Flank A in the formation of a *dmlR_5* mutant of *Variovorax* sp. WS11.
*aacC1*_rev	TGGTCGAAGGCAGCAAGCGC	
*garB*_fwd	As above	Identification of a single crossover at Flank B in the formation of a *dmlR_5* mutant of *Variovorax* sp. WS11.
KanR_rev	GTCTTGGAGTTCATTCAGGG	
*dmlR_4*_fwd	ACTAGTAGCGTGGTCGGGCGATATGG	Amplification of *dmlR_4* with a native flanking region, measuring 150 bp.
*dmlR_4*_rev	GAATTCGTTGTCGCCGCCGGTCTTTG	
*dmlR_5*_fwd	GGTACCGTCGCGCTGCTGCTGAATATC	Amplification of *dmlR_5* with varying lengths of native flanking region, measuring 200-1000 bp, to identify the native promoter.
*dmlR_5*_rev+200	AAGCTTAGCGCGTAGAGGCTGACC	
*dmlR_5*_rev+500	AAGCTTACCGTGAGGCCGGTAAAC	
*dmlR_5*_rev+1000	AAGCTTCCACGTAGACCTGCAGAC	
*dmlR_4*_fwd(PLMB)	GAATTCCCTCATGAAGGACCGTCTAC	Amplification of *dmlR_4* with 5' *Nde*I and 3' *Eco*RI restriction sites, allowing cloning in-frame into pLMB509 under the control of the *tauAp* promoter.
*dmlR_4*_rev(PLMB)	CATATGCGGCAGAATCGGACAATC	
*dmlR_5*_fwd(PLMB)	GAATTCGCGCTGCTGCTGAATATC	Amplification of *dmlR_5* with 5' *Nde*I and 3' *Eco*RI restriction sites, allowing cloning in-frame into pLMB509 under the control of the *tauAp* promoter.
*dmlR_5*_rev(PLMB)	CATATGTAGAAGCAGGCTCGAGTG	
*glmS*_fwd	GACGCGATCCCCGGGTTGAAC	Screening of insertions of *dmlR_4*-FLAG or *dmlR_5*-FLAG downstream of *glmS.*
dmlR_4(*glmS*)_rev	TCGCACAGTTGGCAGCATTCAGG	
dmlR_5(*glmS*)_rev	ACGAAGCACACGCTGCTGGG	

8.5. **Results and discussion**

8.5.1. ***in silico* analysis of the regulatory elements of the *iso* metabolic gene cluster**

BLASTp was used to predict the conserved domains in DmlR_4 and DmlR_5 (Altschul *et al*. 1990). Although these putative LTTRs share only 30.7% identity at the deduced amino acid level, each shared the conserved N-terminal helix-turn-helix (HTH) motif and C-terminal co-inducer binding pocket associated with this family of regulators (Maddocks & Oyston 2008). *dmlR_4* was likely to play a conserved role in isoprene metabolism due to its presence in the *iso* metabolic gene clusters of multiple Gram negative isoprene degrading bacteria. The translated DmlR_4 amino acid sequence shared 92.8% identity with DmlR from a metagenome-derived isoprene degrading *Variovorax* sp. (Crombie *et al*. 2018), 72.3% identity with the single copy of DmlR in the *iso* gene cluster from *Ramlibacter* sp. WS9 (Dawson *et al*. 2020), and 43.2% identity with the single copy of DmlR in the *iso* gene cluster from *Sphingopyxis* sp. OPL5 (Larke-Mejía *et al*. 2020). DmlR_5 shared surprisingly high homology with LTTRs in non-isoprene-degrading *Variovorax* spp., with the highest homology detected in *Variovorax* sp. RA8 (87.4%) (Altschul *et al*. 1990). The *dmlR_5* homolog in *Variovorax* sp. RA8 was detected immediately upstream of *dkgB* and *ydhP*, genes which were also detected in the genome of *Variovorax* sp. WS11 3' of the *iso* metabolic gene cluster. The identity of these peptides between *Variovorax* sp. WS11 and RA8 were very high (Figure 8.3), indicating that *dkgB*, *ydhP* and *dmlR_5* may commonly associate together in the genus *Variovorax*. The insertion of the *iso* metabolic gene cluster upstream of these genes may represent a rare genetic event. This brought the potential role of *dmlR_5* in the regulation of isoprene metabolism further into question, as this apparently *Variovorax*-specific cluster of genes (Figure 8.3) was not detected 3' of the *iso* gene clusters of other Gram negative isoprene degraders (Chapter 1, Figure 1.8). The high identity of DmlR_4 with the LTTRs in the *iso* gene clusters of other Gram negative bacteria indicated a specific role for this LTTR in the regulation of isoprene metabolism, while the identity of DmlR_5 with LTTRs in non-isoprene degrading bacteria indicated a non-specific regulatory role.

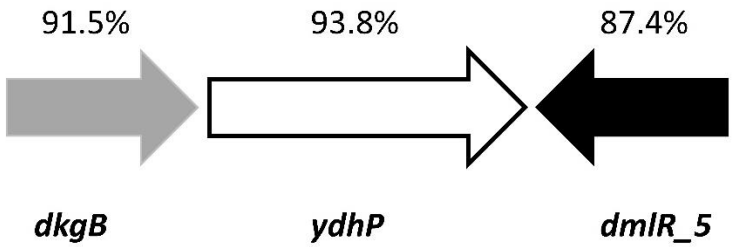

Figure 8.3. Arrangement of putative accessory genes from the *iso* metabolic gene cluster detected in *Variovorax* sp. RA8. The percentage identity of the translated amino acid sequences with the homologs from *Variovorax* sp. WS11 are shown above.

The conserved co-localisation of *dmlR_5*, *ydhP*, and *dkgB* in other species of *Variovorax* (Figure 8.3) indicated a role of this LTTR in the regulation of the activity of this putative inner membrane transporter (YdhP) and 2,5-diketo-D-gluconic acid reductase (DkgB). DkgB was expressed to a greater degree in isoprene-grown *Variovorax* sp. WS11

compared to succinate-grown cells (Chapter 3, Figure 3.20, Figure 3.21), indicating a role for this peptide in isoprene metabolism. In turn, the transcription of *dkgB* may be influenced by DmlR_5.

8.5.2. **Confirming the function of *dmlR_4* and *dmlR_5* in isoprene metabolism by targeted mutagenesis**

8.5.2.1. **Characterisation of *Variovorax* sp. WS11 with an inactive copy of *dmlR_4***

Variovorax sp. WS11 Δ*dmlR_4* was inoculated into Ewers medium with 10 mM pyruvate as the sole source of carbon and energy. Pyruvate was selected as this carbon source did not repress isoprene metabolism in wild-type *Variovorax* sp. WS11 (Chapter 7, Figure 7.8), making it a suitable substrate for generating initial biomass for subsequent subculturing into Ewers medium with isoprene. No growth of *Variovorax* sp. WS11 *ΔdmlR_4* was observed when isoprene was the only carbon source, indicating that DmlR_4 was essential for the growth of *Variovorax* sp. WS11 on isoprene (Figure 8.4). As *dmlR_4* was divergently transcribed from the *iso* metabolic gene cluster, and because the intergenic space containing the *isoG* promoter was intact (Chapter 6, Figure 6.15), it was highly unlikely that the cessation of isoprene metabolism was a result of a polar mutation causing inactivation of the transcription of the *iso* genes.

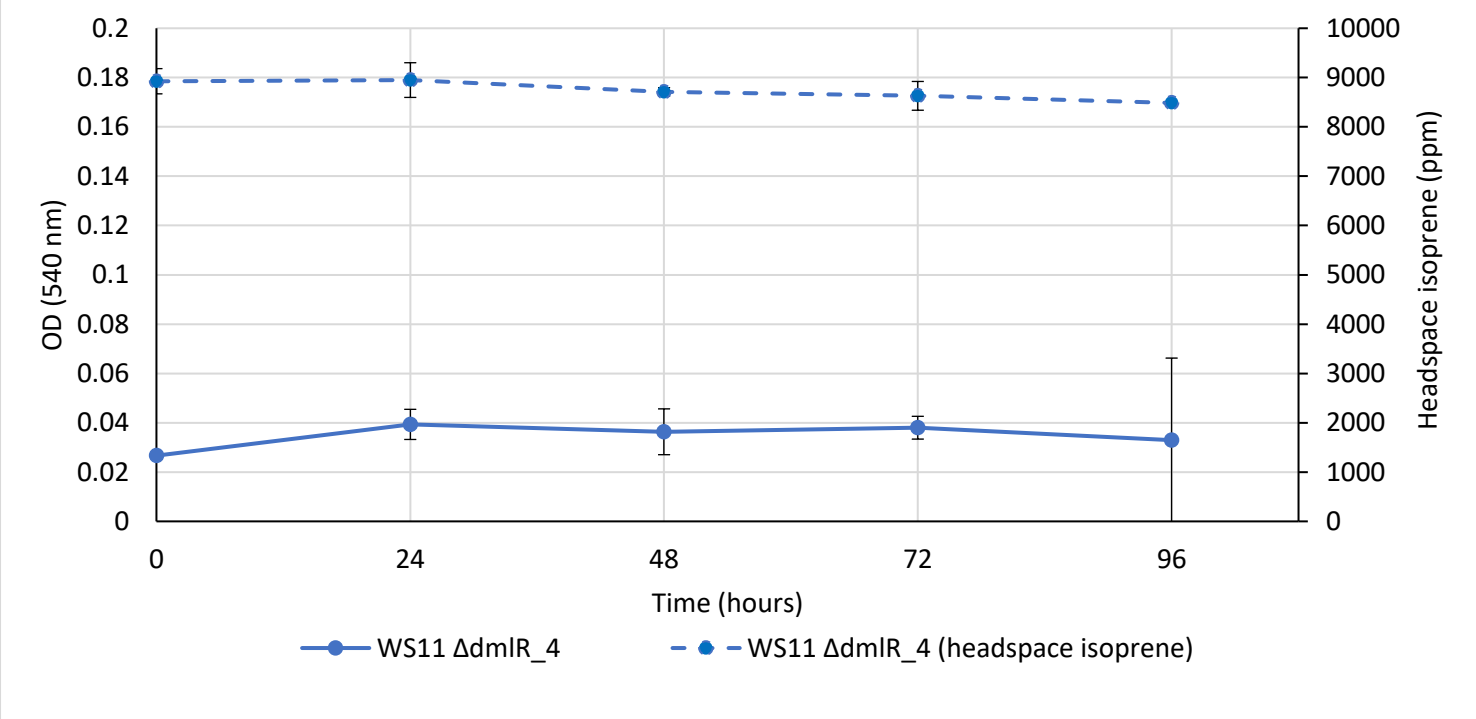

Figure 8.4. Deletion of *dmlR_4* prevented growth of *Variovorax* sp. WS11 Δ*dmlR_4* on isoprene, or the consumption of isoprene. Error bars represent the standard deviation about the mean of three biological replicates.

Previous studies of mutants of *dmlR* in *E. coli* indicated that this regulator acted as a transcriptional activator (Reed *et al*. 2006, Lukas *et al*. 2010), and the deletion of *dmlR_4* in *Variovorax* sp. WS11 appeared to confirm the same function. It was previously demonstrated that the *iso* metabolic gene cluster of *Variovorax* sp. WS11 contained two promoters (as described in Chapter 6). *dmlR_4* was located directly upstream of *isoG*, similar to the typical model of a LTTR (Figure 8.1). Depending on which promoter holo-DmlR_4 typically associates with, the lack of isoprene

metabolism by *Variovorax* sp. WS11 Δ*dmlR_4* may be explained in various ways. If DmlR_4 controls transcription from the *isoG1* promoter, the epoxide-detoxifying genes *isoI* and *isoH* may no longer be transcribed, leading to the accumulation of toxic epoxyisoprene. Alternatively, holo-DmlR_4 may control transcriptional activation from the *isoAp* promoter, preventing expression of IsoMO and therefore abolishing growth on isoprene, or may control transcriptional activation from both promoters, thereby preventing the expression of the whole *iso* metabolic gene cluster.

8.5.2.2. **Expression of *iso* metabolic genes in the absence of *dmlR_4***

The approximate mechanism of action of DmlR_4 was further investigated by RT-qPCR analysis. Succinate-grown *Variovorax* sp. WS11 Δ*dmlR_4* was incubated in the presence of 10 mM succinate, 1% (v/v) isoprene, or 0.1% (w/v) epoxyisoprene (as described in Section 2.10.2). Both *isoA* and *isoG* were significantly upregulated by isoprene and epoxyisoprene after 2 hours ($p \leq 0.05$, Figure 8.5), although the level of gene expression was smaller than in wild-type *Variovorax* sp. WS11. The level of expression induced by isoprene was similar to that of *Variovorax* sp. WS11 Δ*isoA* after induction by isoprene (Chapter 6, Figure 6.12). In the latter case, isoprene alone was sufficient to induce the expression of *isoG* by 6.6 (relative to *rpoB*, $p \leq 0.05$), while epoxyisoprene induced the expression of *isoG* by 151.8 (relative to *rpoB*, $p \leq 0.05$). By comparison, epoxyisoprene was only capable of inducing the expression of *isoA* and *isoG* by 12.8 ($p \leq 0.01$) and 11.2 ($p \leq 0.05$), respectively (relative to *rpoB*). There was no significant difference between the expression of *isoA* and *isoG* when induced by isoprene or epoxyisoprene ($p > 0.05$). The data presented in Figure 8.5 indicate that the previous observations in *Variovorax* sp. WS11 Δ*isoA*, in which epoxyisoprene retained its ability to induce *iso* gene expression despite the lack of active IsoMO, was in part due to the continued activity of DmlR_4. Therefore, DmlR_4 is likely to function as a transcriptional activator at the *isoG* promoter. A role of DmlR_4 in the activation of transcription at the *isoA* promoter is unclear, as *isoG* and was expressed to a similar degree in *Variovorax* sp. WS11 Δ*isoA* which lacked transcription of IsoMO.

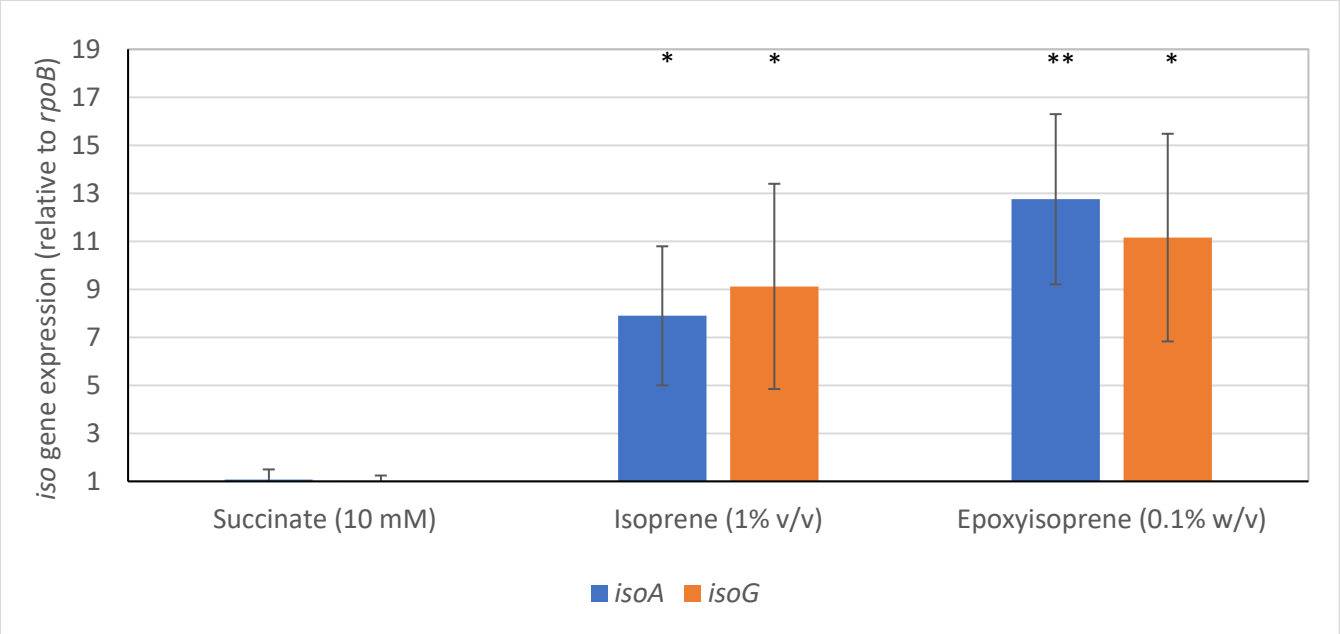

Figure 8.5. Expression of the *iso* metabolic genes by *Variovorax* sp. WS11 Δ*dmlR_4* (relative to *rpoB*) after 2 hours of incubation with 1% (v/v) isoprene or 0.1% (w/v) epoxyisoprene. Error bars represent the standard deviation about the mean of three biological replicates. Asterisks denote a statistically significant difference between the indicated condition and the succinate baseline (* p≤0.05, ** p≤0.01).

8.5.3. **Characterisation of *Variovorax* sp. WS11 with an inactive copy of *dmlR_5***

Variovorax sp. WS11 Δ*dmlR_5* was initially tested for its ability to grow using isoprene as the sole source of carbon and energy, as with *Variovorax* sp. WS11 Δ*dmlR_4*. However, the deletion of *dmlR_5* did not prevent the growth of *Variovorax* sp. WS11 on isoprene (Figure 8.6). In fact, this mutant strain consumed isoprene at a greater rate than the wild-type strain, with the mutant strain consistently growing to a higher OD_{540} from 0-54 hours (p≤0.05). It was hypothesised that the deletion of *dmlR_5* had de-repressed the expression of the *iso* metabolic gene cluster, allowing a more rapid response of this mutant strain to isoprene due to the greater initial abundance of the Iso peptides. If this was the case, then the uptake of isoprene by *Variovorax* sp. WS11 Δ*dmlR_5* under different growth conditions may differ from that of the wild-type strain. The wild-type and mutant strains were grown in Ewers medium using 10 mM glucose, 1% (v/v) isoprene, or a combination of 10 mM glucose and 1% (v/v) isoprene. The wild-type and mutant strains displayed stark differences in the relationship between growth substrate and the rate of isoprene uptake (Figure 8.7). Firstly, the growth of *Variovorax* sp. WS11 Δ*dmlR_5* using a combination of glucose and isoprene no longer repressed the oxidation of isoprene by IsoMO, indicating that DmlR_5 is required for the repression of the *iso* metabolic gene cluster in response to alternative growth substrates. There was no significant difference between the rate of isoprene uptake by *Variovorax* sp. WS11 Δ*dmlR_5* after growth on isoprene or a combination of glucose and isoprene (p>0.05), indicating that the IsoMO was expressed to approximately the same level under each condition. A small, statistically insignificant (p>0.05) decrease in the rate of isoprene uptake was observed when the mutant strain of *Variovorax* sp. WS11 was grown using a combination of 10 mM succinate and 1% (v/v) isoprene when compared to the wild-type strain, but the rate of isoprene uptake under the latter condition

was significantly lower than the isoprene-only condition ($p \leq 0.05$). A small rate of isoprene uptake was observed when the mutant strain was grown using glucose-only, while the wild-type strain demonstrated a negligible rate of uptake which was thought to be due to fluctuations in the baseline of the fast isoprene sensor (Figure 8.7). This may indicate that the baseline level of abundance of the Iso metabolic peptides was higher in *Variovorax* sp. WS11 Δ*dmlR_5* than in the wild-type during growth on glucose, as isoprene oxidation was apparently supported in the absence of isoprene.

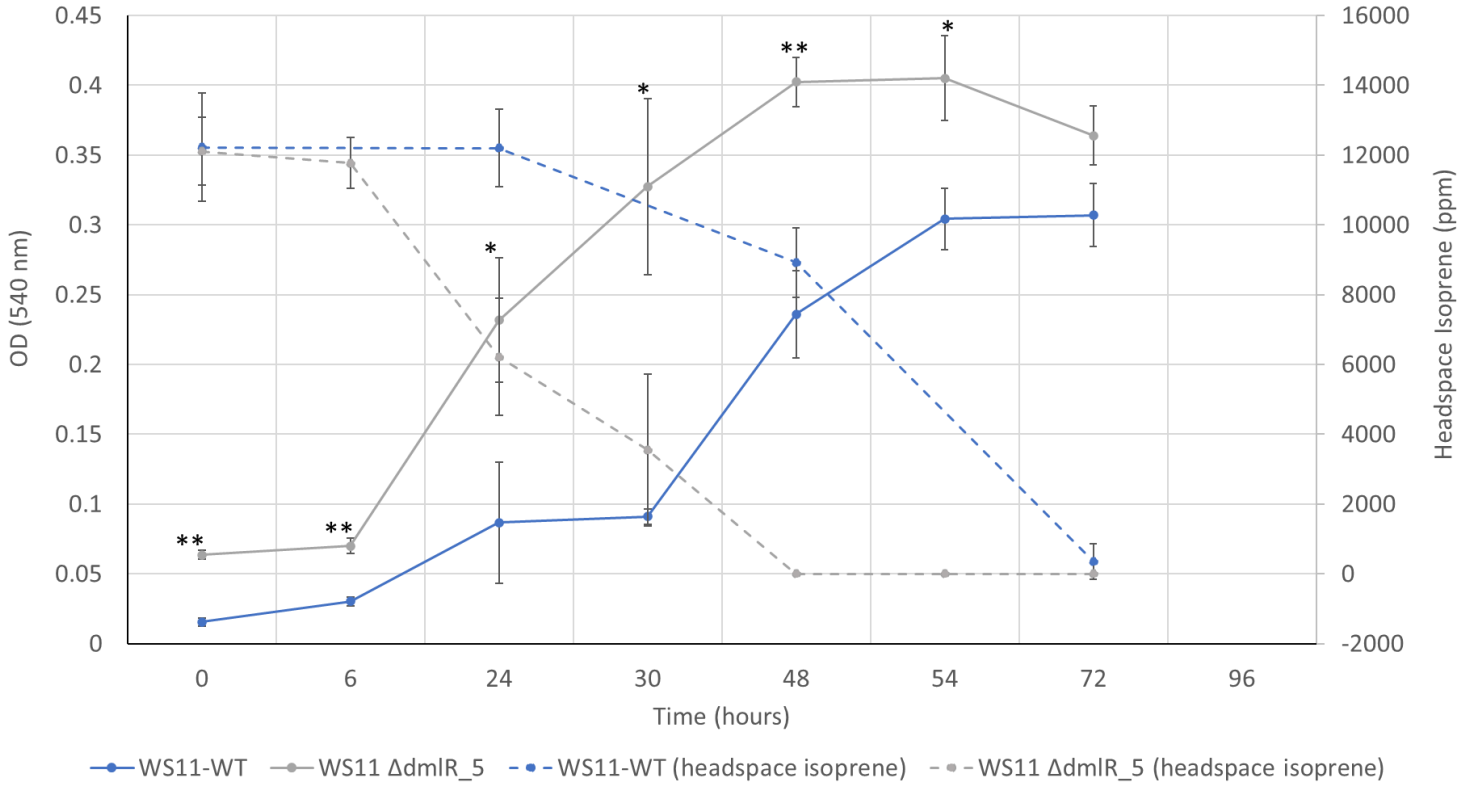

Figure 8.6. Growth of *Variovorax* sp. WS11 on 1% (v/v) isoprene, compared between wild-type or *dmlR_5* mutant strains. Error bars represent the standard deviation about the mean of three biological replicates. Asterisks denote statistically significant differences between growth conditions (* $p \leq 0.05$, ** $p \leq 0.01$).

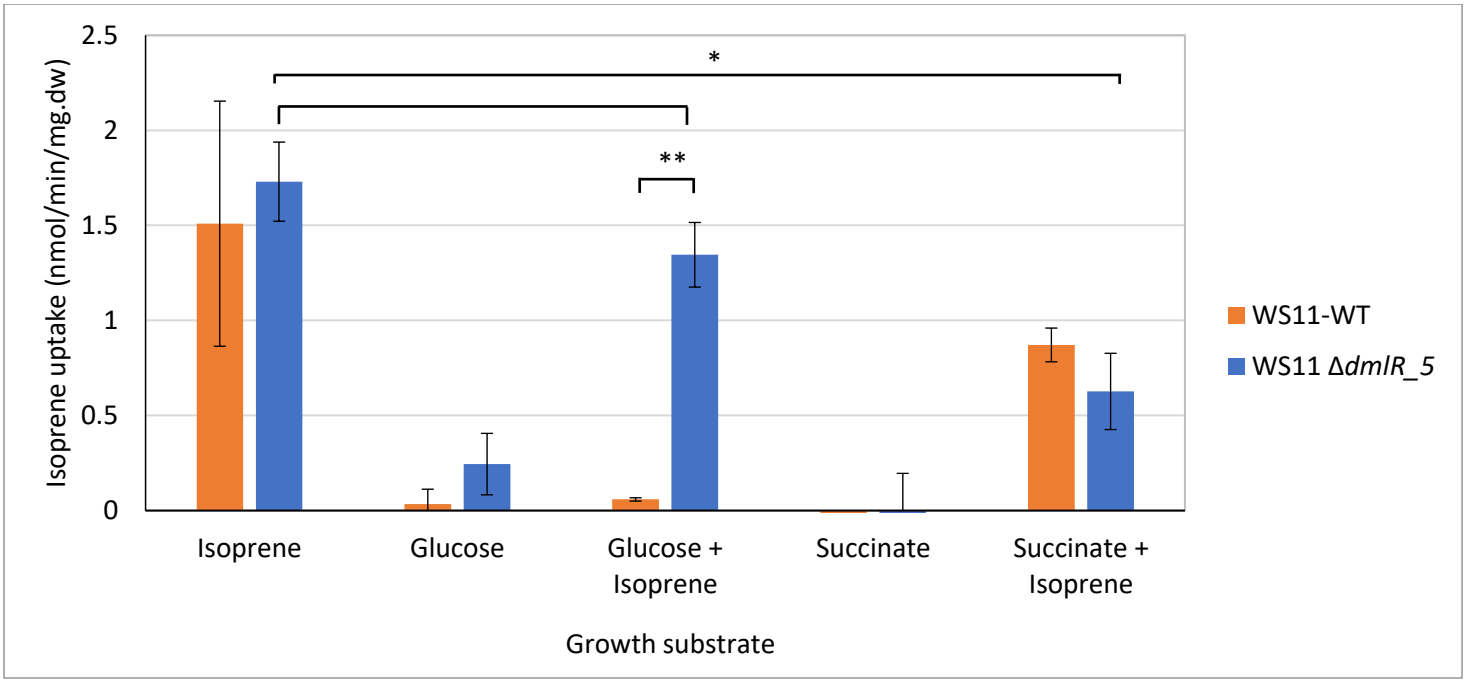

Figure 8.7. Consumption of isoprene by *Variovorax* sp. WS11 after growth on 1% (v/v) isoprene, 10 mM glucose, or a combination of 10 mM glucose and 1% (v/v) isoprene, compared between wild-type and *dmlR_5* mutant strains. Error bars represent the standard deviation about the mean of three biological replicates. Asterisks denote a statistically significant difference between the indicated conditions (* p≤0.05, ** p≤0.01).

8.5.4. Complementation of the function of *dmlR_4* and *dmlR_5* by expression *in trans* from the native promoters

In order to confirm that the altered phenotypes of *Variovorax* sp. WS11 Δ*dmlR_4* and Δ*dmlR_5* were specifically due to the deletion of these genes rather than due to non-specific effects caused by the mutagenesis process, each mutant phenotype was complemented by re-introduction of the deleted genes by expression *in-trans*. Each gene was amplified by PCR using a Q5 high-fidelity polymerase (NEB) with the native flanking region included upstream of the start codon (Table 8.1).

8.5.4.1. Complementation of *Variovorax* sp. WS11 Δ*dmlR_4*

dmlR_4 was amplified along with the native flanking region, measuring approximately 150 bp upstream of the start codon. The whole PCR product was ligated into pJET1.2 and subsequently was sub-cloned into pBBR1MCS-2. pBBR1:*dmlR_4* was used to transform *Variovorax* sp. WS11 Δ*dmlR_4*, and transformant colonies were grown in Ewers medium with 10 mM succinate, then sub-cultured into Ewers medium with 1% (v/v) isoprene. The complemented mutant regained the ability to grow using isoprene as the sole source of carbon and energy (Figure 8.8), confirming that *dmlR_4* is essential for growth on isoprene. This also confirmed that the promoter of *dmlR_4* was located in the intergenic space between *dmlR_4* and *isoG*, along with the *isoG1* promoter, consistent with the model of LysR-type transcriptional regulators (Figure 8.1).

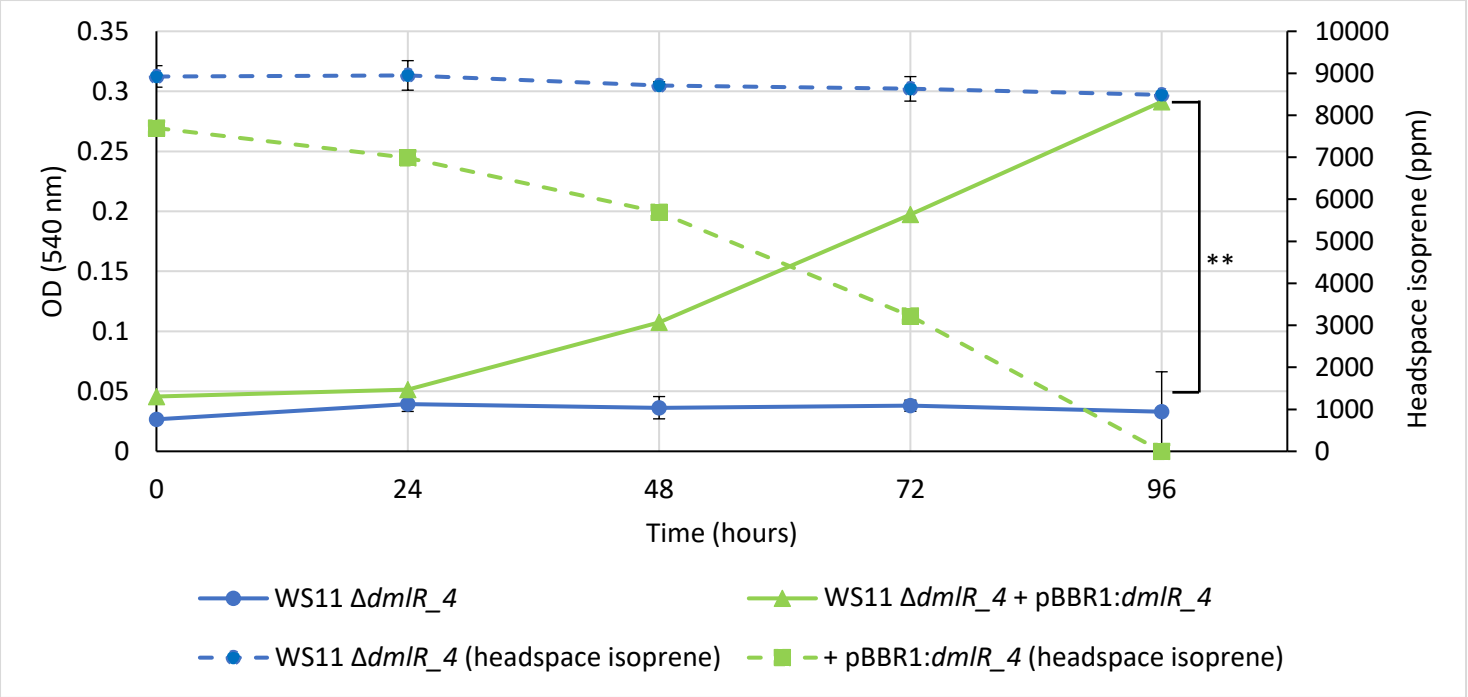

Figure 8.8. Growth of *Variovorax* sp. WS11 Δ*dmlR_4* on isoprene, with or without the re-introduction of *dmlR_4* by expression from pBBR1MCS_2 from the native *dmlR_4* promoter. Error bars represent the standard deviation about the mean of three biological replicates. Asterisks denote statistically significant differences between the indicated conditions (** p≤0.01).

8.5.4.2. **Complementation of *Variovorax* sp. WS11 Δ*dmlR_5***

dmlR_5 was initially amplified along with the native flanking region between *dmlR_5* and *garB*, measuring 106 bp upstream of the start codon (Table 8.1). This was cloned into pJET1.2 and subsequently was sub-cloned into pBBR1MCS-2. When this construct was used to transform *Variovorax* sp. WS11 Δ*dmlR_5*, the wild-type phenotype was not restored as the transformants continued to oxidise isoprene after growth using a combination of glucose and isoprene (data not shown). It was clear that the promoter of *dmlR_5* was not located within the intergenic space between *dmlR_5* and *garB*. New primers were designed to amplify incrementally larger flanking regions upstream of *dmlR_5,* extending past the stop codon of *garB*. These flanking regions were 200 bp, 500 bp, and 1000 bp long (Table 8.1). The native promoter of *dmlR_5* was not located within 200 bp of the start codon of *dmlR_5*, as evidenced by the continued oxidation of isoprene after *Variovorax* sp. WS11 Δ*dmlR_5* + pBBR1:*dmlR_5*(+200) was grown using a combination of glucose and isoprene (Figure 8.9). However, the rate of isoprene oxidation decreased significantly (p≤0.05) when *Variovorax* sp. WS11 Δ*dmlR_5* was transformed with pBBR1:*dmlR_5*(+500), indicating that the native promoter of *dmlR_5* was located between 200-500 bp upstream of the start codon of *dmlR_5*. The relative distance of the promoter from the start codon was larger than that of the *dmlR_4* promoter, indicating that additional regulatory elements may be located upstream of the *dmlR_5* promoter. Collectively, these data indicated that DmlR_5 acted as a transcriptional repressor of isoprene metabolism by *Variovorax* sp. WS11 in the presence of alternative carbon sources, but also that this transcriptional regulator was not essential to isoprene metabolism.

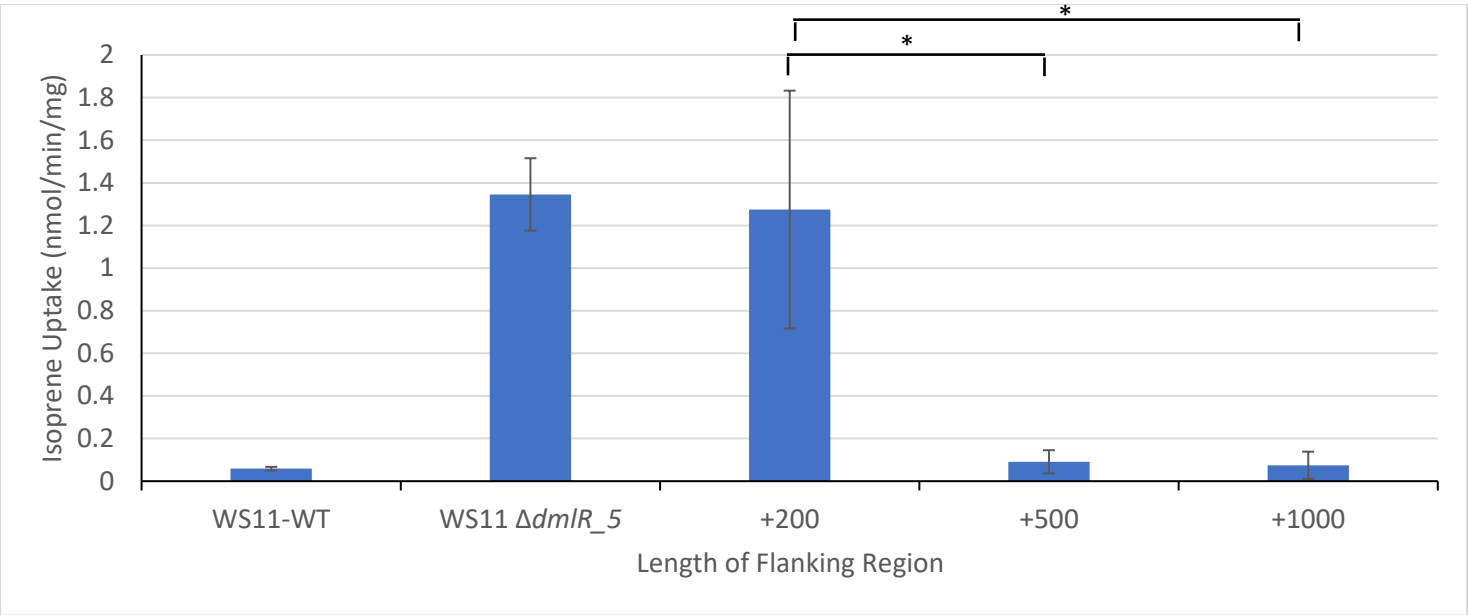

Figure 8.9. Isoprene uptake by wild-type *Variovorax* sp. WS11 or WS11 Δ*dmlR_5* after growth using a combination of glucose and isoprene. The native promoter of *dmlR_5* was located by the re-introduction of *dmlR_5* on pBBR1MCS-2 with varying lengths of native flanking region, extending 200, 500 or 1000 bp from the start codon of *dmlR_5*. Error bars represent the standard deviation about the mean of three biological replicates. Asterisks denote statistically significant differences between the indicated conditions (* p≤0.05).

The location of *dmlR_5* relative to the *iso* metabolic gene cluster is also a matter of interest; this gene is transcribed in the reverse orientation from the *iso* cluster but is not located upstream of the regulated genes (Chapter 1, Figure 1.8). Examples of LTTRs being located hundreds of bases from the regulated promoter are available. The NahR regulatory protein in *Pseudomonas putida* is located immediately upstream of the salicylate (*sal*) degradation gene cluster for which is controls transcription, but NahR also regulated expression of the naphthalene (*nah*) degradation gene cluster located 17 kbp upstream of the *nahR* gene (Schell 1993). Likewise, the LTTR protein GcvA from *E. coli* bound to regions up to 271 bp upstream of the transcription initiation site (Wilson *et al*. 1995).

8.5.4.3. **Expression of *dmlR_4* and *dmlR_5* from non-native promoters**

As both *dmlR_4* and *dmlR_5* were expressed from specific promoters, it was thought that these regulatory genes would be expressed under different conditions, and at different levels, during growth on isoprene. By expressing *dmlR_4* and *dmlR_5* from non-native promoters, the importance of the level of transcription of each gene to the specific regulatory function of the LTTR in question was tested. *dmlR_4* and *dmlR_5* were synthesised by PCR using a Q5 high-fidelity polymerase using primers which included *Nde*I and *Eco*R1 restriction sites at the 5' and 3' regions, respectively (Table 8.1). Each was ligated into pJET1.2 and sub-cloned into pLMB509 under the transcriptional control of the vector's taurine-inducible promoter, *tauAp* (Tett *et al*. 2012). Expression from *tauAp* is induced by taurine, typically supplied at a concentration of 10 mM (Tett *et al*. 2012). This was not suitable for testing the expression of *dmlR_4* or *dmlR_5* and the complementation of the respective mutants as taurine is a growth substrate for *Variovorax* sp. WS11 (Chapter 3, Table 3.2). However, leaky expression from this promoter was

previously identified (Pinchbeck 2016). It was hypothesised that *dmlR_4* or *dmlR_5* would be expressed from *tauAp* at a low constitutive level in the absence of taurine and may therefore restore the wild-type phenotype to *Variovorax* sp. WS11 Δ*dmlR_4* and Δ*dmlR_5*.

Variovorax sp. WS11 Δ*dmlR_4* and Δ*dmlR_5* both contained gentamicin resistance genes (*aacC1*) within the disrupted regulatory genes, preventing the use of pLMB509 (which confers resistance to gentamicin as a selectable trait) as a vector for intact copies of *dmlR_4* and *dmlR_5*. *aacC1* was derived from pCM351 along with *loxP* sites, allowing the removal of this gene from within *dmlR_4* and *dmlR_5* by expressing a Cre recombinase in each mutant strain (Marx & Lidstrom 2002). This was achieved by transformation of *Variovorax* sp. WS11 with pCM158, which contains a *cre* recombinase gene. Colonies were initially grown on Ewers agar with 10 mM succinate, with 50 µg/ml kanamycin included to select for the retention of pCM158. Expression of the *cre* recombinase was controlled by an *E. coli lac* promoter, thereby providing low-level constitutive *cre* expression and catalysing the loss of *aacC1* by recombination at the *loxp* sites (Marx & Lidstrom 2018). Colonies were picked and streaked onto Ewers agar with 10 mM succinate, supplemented with either kanamycin or gentamicin. Colonies which had retained resistance to kanamycin but which had lost resistance to gentamicin were grown in Ewers medium and prepared for electroporation as described in Section 2.4.3. Electrocompetent *Variovorax* sp. WS11 Δ*dmlR_4*(-Gm) and WS11 Δ*dmlR_5*(-Gm) were transformed by electroporation with pLMB509:*dmlR_4* and pLMB509:*dmlR_5*, respectively.

Variovorax sp. WS11 Δ*dmlR_4*(-Gm) regained the ability to grow using isoprene as the sole source of carbon and energy when *dmlR_4* was restored under the control of the *tauAp* promoter (Figure 8.10), reaching approximately the same final OD_{540} as wild-type *Variovorax* sp. WS11 when supplied with 1% (v/v) isoprene. This indicated that the level of expression of *dmlR_4* may not be essential to the activity of this putative transcriptional activator, or that DmlR_4 is only present at low abundance during growth on isoprene. Conversely, *Variovorax* sp. WS11 Δ*dmlR_5*(-Gm) was still able to oxidise isoprene after growth on a combination of glucose and isoprene, despite the presence of an intact copy of *dmlR_5* in pLMB509 (Figure 8.11). There were several possible explanations for the lack of activity. Firstly, the activity of DmlR_5 may depend more on the abundance of the regulatory peptide. LTTRs negatively autoregulate their own expression (Maddocks & Oyston 2008), and must be present in sufficient quantities to influence the expression of the regulated gene (in this case, the *iso* genes). The activity of *dmlR_5* is likely to depend on the presence of sugars such as glucose, although it is unknown whether glucose itself or a product of glucose catabolism may bind to *dmlR_5* to form a holo-LTTR repressor (Figure 8.1). This inhibition may occur through an allosteric mechanism. Secondly, the lack of activity may have been due to plasmid instability of pLMB509 in *Variovorax* sp. WS11. This is a less likely explanation due to the evident stability of pLMB509:*dmlR_4* in *Variovorax* sp. WS11 Δ*dmlR_4*(-Gm) over the course of at least 5 days (Figure 8.10). Likewise, the use of the same cloning strategy and restriction sites for the synthesis of pLMB509:*dmlR_4* and pLMB509:*dmlR_5* (*Eco*R1 and *Nde*I for expression in-frame) indicated an equal chance of success. Overall, these results indicate that abundance of DmlR_5 is more important than the abundance of DmlR_4 with respect to the transcriptional control exerted by these LTTRs.

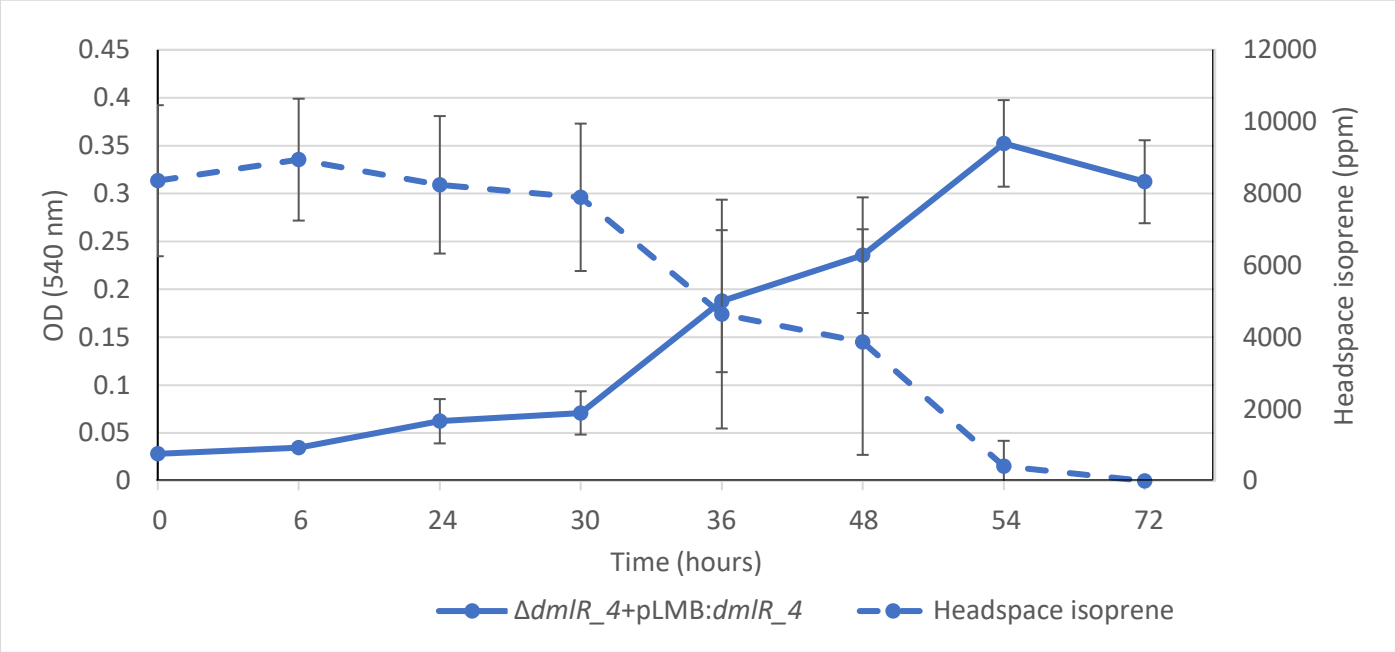

Figure 8.10. Growth of *Variovorax* sp. WS11 Δ*dmlR_4* on 1% (v/v) isoprene after the re-introduction of *dmlR_4* in pLMB509 under the control of a non-native (*tauAp*) promoter. Error bars represent the standard deviation about the mean of three biological replicates.

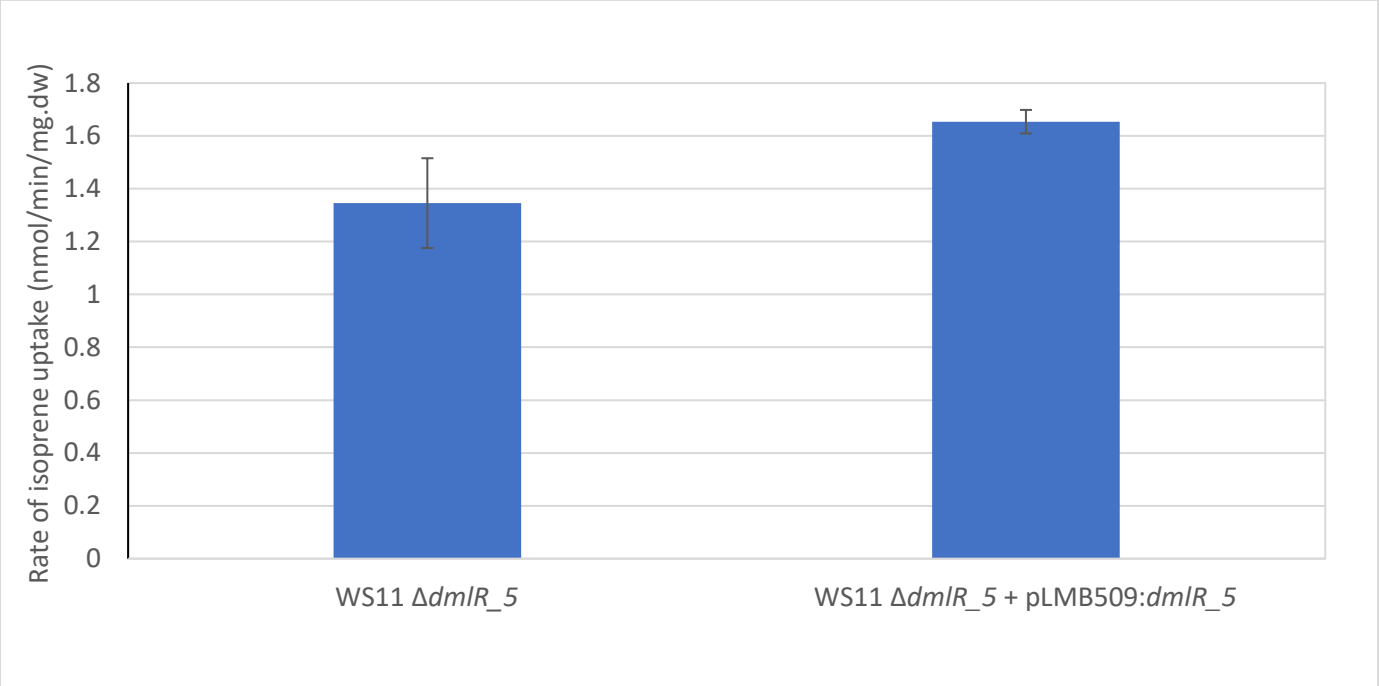

Figure 8.11. Uptake of isoprene by *Variovorax* sp. WS11 Δ*dmlR_5* after growth on a combination of 10 mM glucose and 1% (v/v) isoprene after the re-introduction of *dmlR_5* in pLMB509 under the control of a non-native promoter, compared to *Variovorax* sp. WS11 Δ*dmlR_5* in the absence of pLMB509. Error bars represent the standard deviation about the mean of three biological replicates.

8.5.5. **Identifying the regions of DNA binding by DmlR_4 and DmlR_5**

It was highly likely that DmlR_4 and DmlR_5 regulated the expression of the *iso* metabolic gene cluster by binding to either the *isoAp* or *isoG1* promoters. However, it was unknown which regulator would bind to which promoter, and under what conditions the regulation of gene expression would occur. Also, these putative LTTRs were likely to also bind to their own promoters, exerting negative autoregulation (Maddocks & Oyston 2008). Chromatin immunoprecipitation (ChIP) with sequencing (ChIP-seq) was selected as a method of identifying the regions of DNA binding by DmlR_4 and DmlR_5. Following the formation of DNA-protein interactions, sample DNA is fragmented and the protein-bound sections of DNA are selectively acquired by immunoprecipitation (Furey 2012). Immunoprecipitation of the DNA-binding proteins is made simpler by introducing selective tags, such as FLAG tags, to form fusion proteins. This allows the use of specific monoclonal anti-FLAG antibodies to purify the proteins and bound DNA.

DmlR_4-FLAG (described in Section 8.4.2) restored the wild-type phenotype as *Variovorax* sp. WS11 Δ*dmlR_4* was able to grow using isoprene as the sole source of carbon and energy (Figure 8.12), confirming that the chromosomal knock-in of *dmlR_4*-FLAG was active and capable of restoring the function of the transcriptional activator. No significant difference was observed between the growth of wild-type *Variovorax* sp. WS11 or WS11 Δ*dmlR_4* complemented by DmlR_4-FLAG (determined by *t* test, $p>0.05$).

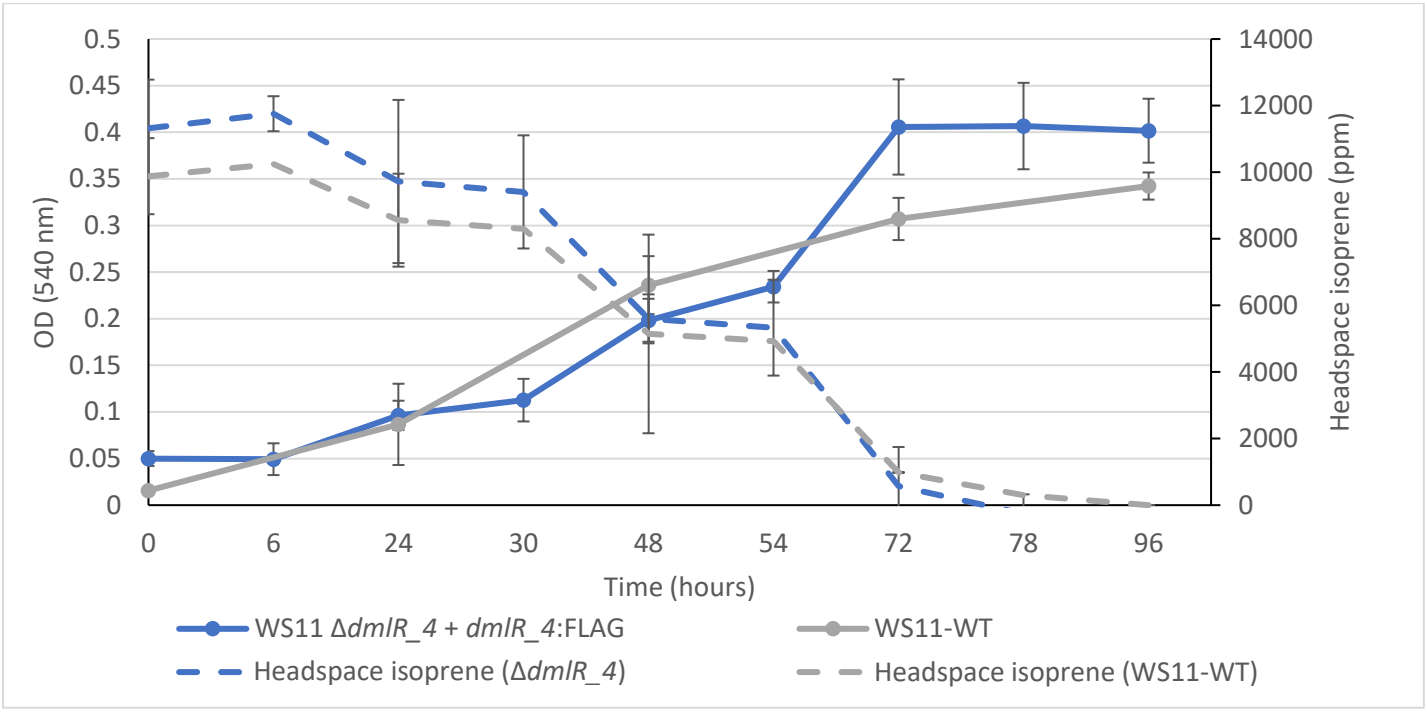

Figure 8.12. Growth of *Variovorax* sp. WS11 Δ*dmlR_4*:FLAG using isoprene as the sole source of carbon and energy. Error bars represent the standard deviation about the mean of three biological replicates.

DmlR_5-FLAG was initially prepared as an N-terminal tag, as with DmlR_4-FLAG (Figure 8.2), but insertions failed to complement the mutant phenotype. As such, the DNA construct was re-designed to include *dmlR_5* with a C-

terminal FLAG-tag (Figure 8.2). DmlR_5-FLAG(C-term) was inserted into *Variovorax* sp. WS11 Δ*dmlR_5* by co-electroporation with pUC18miniTn7-Gm:*dmlR_5*-FLAG(C-term) and pTNS2, as described above. Transformed cells were spread onto Ewers agar with 10 mM succinate and 10 µg/ml gentamicin, and colonies were used as the template in PCR reactions using primers *glmS_fwd* and *dmlR_5(glmS)_rev* (Table 8.1). Sequencing of the region of insertion indicated the receipt of a Tn7 sequence downstream of *glmS*, but the *dmlR_5*-FLAG was not detected in the sequencing results. Transformants retained the *dmlR_5* mutant phenotype, indicating that *dmlR_5*-FLAG was inactive or not received.

8.6. **Conclusions**

The roles of *dmlR_4* and *dmlR_5* in isoprene metabolism were confirmed by targeted mutagenesis. Distinct phenotypes were produced by the deletion of each LTTR-encoding gene, with *Variovorax* sp. WS11 Δ*dmlR_4* losing the ability to grow on (Figure 8.4) or respond to (Figure 8.5) isoprene, while isoprene oxidation by *Variovorax* sp. WS11 Δ*dmlR_5* was no longer repressed by glucose (Figure 8.7). These data indicated that DmlR_4 acted as a transcriptional activator which associated with the *isoG1* promoter, and possibly the *isoAp* promoter, while DmlR_5 acted as a transcriptional repressor.

The level of transcription of *dmlR_4* and *dmlR_5* differed, as only the deletion of *dmlR_4* could be complemented by the re-introduction of the native gene under the control of a non-native promoter (Figure 8.10, Figure 8.11). This indicated the importance of transcriptional control of *dmlR_5* expression in the activity of this regulator. Also, the locations of the promoters of *dmlR_4* and *dmlR_5* indicated differences in the transcription of each regulatory gene. The *dmlR_4* promoter was located in the intergenic space between *dmlR_4* and *isoG*, located in the opposite orientation compared to the *isoG1* promoter. This followed the same scheme as an archetypal LTTR (Figure 8.1). The *dmlR_5* promoter, however, was located between 200-500 bp upstream of the *dmlR_5* start codon (Figure 8.9). The homology of DmlR_5 with LTTRs from non-isoprene degrading bacteria indicated that this peptide, or homologs of this peptide, may act as regulators of more than one metabolic pathway (described in Section 8.5.1), particularly when considering the fact that this LTTR was absent from the *iso* metabolic gene clusters of the Gram negative isoprene degraders *Ramlibacter* sp. WS9 and *Sphingopyxis* sp. OPL5 (Dawson *et al*. 2020, Larke-Mejía *et al*. 2020).

DmlR_5 may act as a global regulator of various metabolic processes, indicated by the conserved co-localisation of the *dmlR_5* gene with *ydhP* and *dkgB*, combined with the role of *dmlR_5* as a transcriptional repressor of isoprene metabolism. This raises the question of how this LTTR became a repressor of the transcription of isoprene metabolism in *Variovorax* sp. WS11. ChIP-seq analysis of the DNA binding regions of DmlR_4 and DmlR_5 would provide greater insight into the scope of the roles of these LTTRs. However, the technical challenges associated with the preparation of FLAG-tagged LTTR constructs will currently only allow the study of DmlR_4 by ChIP-seq in this project.

9. Conclusions and Future Prospects

9.1. Development of *Variovorax* sp. WS11 as a model isoprene degrading bacterium

The work conducted in Chapter 3 initially detailed the development of *Variovorax* sp. WS11 as a model bacterium for the study of isoprene metabolism. The optimum conditions for the growth of *Variovorax* sp. WS11 were described and applied to large-scale cultures using an isoprene-fed fermentor, promoting the study of isoprene metabolism in whole-cell assays. The IsoMO of *Variovorax* sp. WS11 oxidised a wide range of substrates, consistent with previous observations in other SDIMO such as the sMMO (Green & Dalton 1989). The inclusion of alkyl side chains in aliphatic, aromatic or cyclic alkenes increased the rate of substrate oxidation by IsoMO when compared to alkenes without side chains. The influence of carbon chain length on IsoMO activity was demonstrated through both substrate oxidation assays and alkyne inhibition assays. Many SDIMO oxidised similar substrates when compared to IsoMO from *Variovorax* sp. WS11. For example, 1,3-butadiene was oxidised by the toluene 4-monooxygenase from *Pseudomonas mendocina* KR1, and also by the sMMO of *M. trichosporium* OB3b (Higgins et al. 1979, Green & Dalton 1989, Ono & Okura 1990, McClay et al. 2000). The inhibition of IsoMO by linear alkynes was compared with the inhibition of the sMMO from *M. capsulatus* (Bath) (Colby *et al*. 1977), demonstrating the capacity for alkynes to distinguish between functional populations of SDIMO-containing bacteria. Acetylene, known to be a potent inhibitor of substrate oxidation by sMMO (Prior & Dalton 1985), failed to significantly inhibit isoprene oxidation by IsoMO ($p>0.05$), but significantly inhibited the co-oxidation of isoprene by sMMO ($p=0.01$). Conversely, octyne was a potent inhibitor of isoprene oxidation by IsoMO from *Variovorax* sp. WS11 (Chapter 3, Figure 3.16) and *Rhodococcus* sp. AD45 (Sims 2020), but was a poor inhibitor of substrate oxidation by sMMO. Acetylene also failed to inhibit the IsoMO from *Rhodococcus* sp. AD45 or *Gordonia polyisoprenivorans* i37 (Johnston 2014, Sims 2020). This concept can be tested further in soils, as soils are the largest known sink for isoprene (Cleveland and Yavitt, 1997, 1998, Gray *et al*. 2015). The components of isoprene-oxidising communities could be estimated by using acetylene to selectively inhibit the co-oxidation of isoprene by methanotrophs, while octyne could be used to selectively inhibit true isoprene metabolism by inactivating the IsoMO. Further opportunities for the study of isoprene degradation have been provided due to the relative ease of maintaining large-scale cultures of *Variovorax* sp. WS11 in an isoprene-fed fermentor. Peptide components of isoprene metabolism could be purified from isoprene-grown cells according to the methods developed by van Hylckama Vlieg *et al*. (1998, 1999, 2000).

Study of the proteome of isoprene-grown *Variovorax* sp. WS11 provided valuable insights into the mechanism of isoprene metabolism by this bacterium, and also indicated considerable differences in the method of isoprene assimilation when compared to *Rhodococcus* sp. AD45 (Crombie *et al*. 2015). The transcriptome of isoprene-grown *Rhodococcus* sp. AD45 indicated that the methylmalonyl-CoA and methylcitrate pathways were not upregulated (Crombie *et al*. 2015). These pathways were highly expressed during the growth of *Variovorax* sp. WS11 on isoprene, indicating that different genera of isoprene degrading bacteria may have evolved disparate metabolic pathways for the incorporation of isoprene-derived carbon. Informed by the insights in Chapter 3, further work could focus on

confirming the roles of the methylcitrate and methylmalonyl-CoA pathways in isoprene metabolism, particularly in Gram negative bacteria. The metabolic intermediates generated during isoprene metabolism also require identification, and functional characterisations of *isoG*, *isoJ*, *aldH*, and *garB* are still required to improve our understanding of isoprene metabolism as a whole. To that end, mutants were being prepared with targeted deletions of the four genes described above at the time of writing this thesis, with purification and characterisation of each protein by Dr. L. Sims potentially aiding in the identification of unknown metabolic intermediates.

9.2. **Analysis of the genome of *Variovorax* sp. WS11**

The genome of *Variovorax* sp. WS11 was resolved to a sufficient degree to identify the presence of two megaplasmids, each greater than 1 Mbp. Diverse metabolic capabilities were indicated by genome annotation using RAST (Aziz *et al*. 2008, Overbeek *et al*. 2014, Brettin *et al*. 2015), although methanesulfonate metabolism and flagella-mediated motility indicated by observations in the genome were not observed in related experiments. The use of taurine as a source of carbon and energy indicated the expression of a taurine dioxygenase by *Variovorax* sp. WS11 (Eichhorn *et al*. 1997). The *iso* metabolic gene cluster of *Variovorax* sp. WS11 contained the core *iso* genes first identified in *Rhodococcus* sp. AD45 (van Hylckama Vlieg *et al*. 2000, Crombie *et al*. 2015), although the organisation of the genes and the selection of accessory and regulatory genes was distinct. The *iso* metabolic gene cluster from *Variovorax* sp. WS11 contained no duplicated copies of *isoGHIJ*, indicating different requirements for the metabolism of isoprene-derived intermediates after the production of epoxyisoprene by IsoMO. A lack of duplicated *isoGHIJ* was observed in the *iso* metabolic gene clusters of putative isoprene degraders identified in the metagenomes from isoprene-enriched samples (Carrión *et al*. 2020), indicating that the duplicated genes observed in *Rhodococcus* sp. AD45 and *Rhodococcus* sp. PD630 (Crombie *et al*. 2015) may be uncommon. Instead of *gshAB*, the *iso* metabolic gene cluster from *Variovorax* sp. WS11 contained *garB*, a putative glutathione disulfide reductase. The encoded enzyme was highly expressed during growth on isoprene (Chapter 3, Figure 3.20), leading to the prediction of a glutathione-recycling mechanism (as described in Section 3.5.7.2). A gene with a putative role in reductive synthesis of CoA-disulfide from CoA was identified in the *iso* metabolic gene cluster of *Rhodococcus* sp. AD45 (CoA-disulfide reductase). Functional characterisations of the mechanisms of glutathione synthesis and recycling of thiols by isoprene degrading bacteria would provide valuable insights into the requirement for anti-toxicity mechanisms in isoprene metabolism. Also identified was the difference in putative regulators of isoprene metabolism between *Variovorax* sp. WS11 and *Rhodococcus* sp. AD45, indicating that each bacterium had evolved different mechanisms of controlling the expression of the *iso* metabolic gene cluster. Analysis of these regulators by ChIP-seq (as described by Som *et al*. 2017) would provide valuable insights into the control of isoprene metabolism in different genera of isoprene degrading bacteria.

9.3. **Optimising genetics systems in *Variovorax* sp. WS11**

The work conducted in Chapter 5 aimed to develop *Variovorax* sp. WS11 as a model organism for molecular genetics studies. Electroporation-based and conjugation-based methods of DNA transfer were optimised, with electroporation selected as the primary method of transformation due to the relative ease and the lack of a counter-

selection step during growth to remove plasmid-donating bacteria (e.g. *E. coli*). Further work is required to expand the range of shuttle vectors suitable for use in both *E. coli* and in Gram negative isoprene degrading bacteria. *iso* metabolic genes were expressed from pBBR1MCS_2 (Kovach *et al*. 1995) in *Variovorax* sp. WS11, typically requiring the use of a native *iso* promoter. Further studies of the *iso* metabolic gene cluster in Gram negative bacteria would be aided by the development of broad host-range shuttle vectors which allow the expression of a gene, or genes, of interest under the control of an inducible promoter. An isoprene-inducible reporter strain of *Variovorax* sp. WS11 was prepared by transformation with pMHA200 (Ali & Murrell 2009) which carried a *gfp* gene under the control of the *isoG1* promoter (Carrión, O. unpublished). Further isoprene-inducible reporter strains could be prepared if additional *iso* promoters were identified in isoprene-degrading bacteria. These reporter strains could then be used to demonstrate the sensing of environmental concentrations of isoprene by bacteria according to detectable changes in *gfp* expression. To this end, transgenic isoprene-producing strains of tobacco have been prepared according to Vickers *et al*. (2009) (Carrión, O. unpublished).

9.4. **Molecular and biochemical analysis of isoprene metabolism by *Variovorax* sp. WS11**

Isoprene oxidation by *Variovorax* sp. WS11 occurred by the same mechanism first described in *Rhodococcus* sp. AD45 (van Hylckama Vlieg *et al*. 2000). The deletion of *isoA*, the active site-containing α-oxygenase component of IsoMO, prevented the growth of *Variovorax* sp. WS11 on isoprene. Unlike *Rhodococcus* sp. AD45 (Crombie *et al*. 2015), growth on isoprene by *Variovorax* sp. WS11 was restored by the expression of IsoMO from two *iso* promoters, *isoAp* and *isoG1*. Further work must focus on the regulation of isoprene metabolism from the two *iso* promoters in *Variovorax* sp. WS11, as it is unclear how transcriptional control from may differ between each promoter. However, the different levels of growth on isoprene by *isoAp*- and *isoG1*-complemented *Variovorax* sp. WS11 Δ*isoA* indicated differences in the level of transcription from each promoter (Chapter 6, Figure 6.15). These data proved that IsoMO from *Variovorax* sp. WS11 could be expressed in a homologous host, leading to further studies in the mutated isoprene degrader *Rhodococcus* sp. AD45-id and non-isoprene-degrading *E. coli* Rosetta 2. *E. coli* was consistently unable to express the full, functional IsoMO. This was unsurprising as van Hylckama Vlieg *et al*. (2000) previously attempted to express the whole *iso* metabolic gene cluster from *Rhodococcus* sp. AD45 in *E. coli* using a cosmid. At present, IsoD is the only IsoMO component from *Rhodococcus* sp. AD45 to be successfully expressed in, and purified from, *E. coli* (Sims 2020). Expression of *isoA-F* from *Variovorax* sp. WS11 (Chapter 6, Figure 6.16) and *Rhodococcus* sp. AD45 (Sims 2020) was successful in *Rhodococcus* sp. AD45-id, a derivative of *Rhodococcus* sp. AD45 which had lost the megaplasmid containing the *iso* metabolic gene cluster. The rate of isoprene oxidation by the heterologously expressed IsoMO was lower than in wild-type *Variovorax* sp. WS11, indicating that certain components of IsoMO may be less active in the heterologous system, or that the level of expression may be lower. This issue was also observed when homologously expressing IsoMO from *Rhodococcus* sp. AD45 in *Rhodococcus* sp. AD45-id (Sims 2020). Further studies of isoprene oxidation by IsoMO must focus on a shift from whole cell to cell free and pure protein assays. Kinetics experiments indicated that the IsoMO from *Variovorax* sp. WS11 had a K_m (apparent) of 10.5 μM for isoprene, considerably higher than the K_m calculated for other isoprene degrading bacteria (van Hylckama Vlieg *et al*. 1998, Larke-Mejía *et al*. 2020, Sims 2020). For example, IsoMO from *Rhodococcus* ps. AD45

had a K_m between 0.8-2.9 µM, while IsoMO from *Sphingopyxis* sp. OPL5 had a K_m of 2.53 µM. A greater number of isoprene degrading bacteria must be isolated with the aim of comparing the affinity of IsoMO for isoprene across terrestrial and aquatic environments. At present, only the IsoMO from *Rhodococcus* sp. AD45 has been characterised using the purified enzyme, with a rate of isoprene oxidation of 0.85 nmol min^{-1} mg $IsoABE^{-1}$ compared to 8.39 ± 1.26 nmol min^{-1} mg dry $weight^{-1}$ in whole cells (Sims 2020). The approximately 10-fold reduction in the rate of isoprene oxidation between whole cell and purified enzyme assays demonstrated the need for a greater understanding of the purification and reconstitution of this multi-component SDIMO.

9.5. **Regulation of isoprene metabolism by *Variovorax* sp. WS11**

Regulation of isoprene metabolism was only described by Crombie *et al*. (2015) prior to this work. Isoprene oxidation by *Rhodococcus* sp. AD45 was repressed by succinate, and the transcription of *marR* and *gntR*-type regulatory genes was upregulated at different stages during exposure to isoprene (Crombie *et al*. 2015). A combination of whole cell activity assays and gene expression studies by RT-qPCR identified differential expression of the components of isoprene metabolism in *Variovorax* sp. WS11 under different growth conditions. In an example of diauxic growth, glucose significantly repressed both the activity of IsoMO and the expression of *isoA* when isoprene was present ($p \leq 0.05$), confirming that isoprene metabolism was inducible in *Variovorax* sp. WS11. However, fructose repressed the activity of IsoMO but did not repress the transcription of *isoA*, indicating that unknown mechanisms of post-transcriptional regulation may inhibit isoprene metabolism under certain conditions. Further work is required to identify and characterise the different mechanisms of regulation of isoprene metabolism in *Variovorax* sp. WS11. Further to this, the regulatory mechanisms employed by different genera of isoprene degrading bacteria are yet to be studied. The presence of diverse regulatory genes in the *iso* metabolic gene clusters of different genera of isoprene degrading bacteria indicated alternative regulatory mechanisms. This was discussed further in Section 8.6. A greater understanding of the isoprene metabolic pathway will be achieved in further experiments by using a combination of 'omics approaches. Proteomic analysis has already led to the prediction of the metabolic reactions which may facilitate the incorporation of isoprene-derived carbon, particularly relating to the methylcitrate and methylmalonyl CoA-pathways. Analysis of the transcriptome of isoprene-grown and epoxyisoprene-induced *Variovorax* sp. WS11 will provide further insights into the mechanisms and control of isoprene metabolism, particularly when compared with the proteomic data, and these analyses are currently underway.

9.6. **Specific regulators of isoprene metabolism in *Variovorax* sp. WS11**

Two LysR-type transcriptional regulators were identified in the *iso* metabolic gene cluster of *Variovorax* sp. WS11. Comparisons with other Gram negative isoprene degrading bacteria indicated that *dmlR_4* was specific to isoprene degraders, while *dmlR_5* was not found in isoprene degrading bacteria from other genera. Instead, homologs of *dmlR_5* were detected in non-isoprene-degrading bacteria, with the same neighbouring genes (*dkgB* and *ydhP*) identified in *Variovorax* sp. RA8 (Öztürk *et al*. 2020). DmlR_4 and DmlR_5 both have functions in the control of the transcription of the *iso* metabolic gene cluster in *Variovorax* sp. WS11, as confirmed by targeted mutagenesis. *Variovorax* sp. WS11 Δ*dmlR_4* was unable to grow using isoprene as the sole source of carbon and energy, and the

transcription of *isoA* and *isoG* was greatly decreased in the presence of isoprene and epoxyisoprene when compared to the wild-type. This wild-type phenotype was restored by the expression of *dmlR_4* from the native promoter, which was located in the intergenic space between *dmlR_4* and *isoG*. Collectively, these data indicated that DmlR_4 functioned as a transcriptional activator, as the loss of this LysR-type transcriptional regulator prevented the transcription of the *iso* metabolic gene cluster. The deletion of *dmlR_5* alleviated the repression of isoprene metabolism normally observed in the presence of glucose. The wild-type phenotype was restored by the expression of *dmlR_5* from the native promoter, which was located between 200 and 500 bp from the start codon of *dmlR_5*. These data indicated that DmlR_5 functioned as a transcriptional repressor.

Further study of the mechanisms of action of DmlR_4 and DmlR_5 is warranted. Preliminary work was conducted with the aim of performing ChIP-seq analysis in order to identify the locations of binding of each LTTR to the genome of *Variovorax* sp. WS11. A FLAG-tagged DmlR_4 gene fusion was introduced into *Variovorax* sp. WS11 Δ*dmlR_4*. Future work will initially consist of confirmation of the activity of the FLAG-tag by Western blotting in order to demonstrate the specificity of anti-FLAG antibodies for the DmlR_4-FLAG fusion protein (Zhang *et al*. 2008). Once the mechanisms of the LTTRs specific to *Variovorax* sp. WS11 have been demonstrated, further work will be required to compare the roles of these regulators with the roles of the putative regulatory genes found in the *iso* metabolic gene clusters of other Gram negative and Gram positive bacteria. Putative *marR2* and *gntR* regulatory genes were upregulated in *Rhodococcus* sp. AD45 during growth on isoprene (Crombie *et al*. 2015), indicative of roles in isoprene metabolism. Analysis of these putative regulatory genes by targeted mutagenesis and ChIP-seq would provide valuable insights into the regulation of isoprene metabolism in different species of bacteria.

9.7. **Summary and future prospects**

This project led to the development of the first Gram negative model isoprene degrading bacterium, providing numerous comparative insights into the mechanism of isoprene metabolism at the genetic, molecular and biochemical levels. The relative ease of genetic manipulation of *Variovorax* sp. WS11, combined with the knowledge derived from the analysis of the proteome of this bacterium during growth on isoprene, will facilitate studies of the biochemical reactions which comprise the isoprene metabolic pathway. Further work must be conducted in order to identify the chemical intermediates of the isoprene metabolic pathway. To this end, purification of the Iso metabolic peptides and deletion of specific *iso* metabolic genes by targeted mutagenesis would greatly increase the ease of accumulating and identifying the currently uncharacterised intermediate compounds. The preparation of double-mutations may aid this process, as the expression of IsoMO was de-repressed in *Variovorax* sp. WS11 Δ*dmlR_5*, even in the presence of glucose. Targeted deletions of other *iso* genes in *Variovorax* sp. WS11 Δ*dmlR_5* may facilitate the accumulation of metabolic intermediates.

A greater understanding of isoprene metabolism would be achieved by purifying IsoMO, as current knowledge has been derived entirely from assays in whole cells. While the oxygenase (IsoABE), coupling (IsoD), and ferredoxin (IsoC) components of IsoMO were purified from *Rhodococcus* sp. AD45, the reductase component (IsoF) was not

successfully purified (Sims 2020), currently limiting the effectiveness of *in vitro* studies. The Iso metabolic peptides from *Variovorax* sp. WS11 may be simpler to express and purify, particularly in a Gram negative heterologous host such as *E. coli*. IsoGHIJ are also required as pure proteins to characterise the functions of these polypeptides and to isolate the metabolic products. Work is currently being conducted with the aim of purifying these accessory Iso peptides from *Variovorax* sp. WS11 (Sims, L. personal communication). Intermediate metabolites, predicted by the analysis of the proteome of *Variovorax* sp. WS11 (Chapter 3, Figure 3.24) may be accumulated by targeted mutagenesis of candidate genes. For example, the deletion of *isoJ* may cause the accumulation of the GMBA-CoA conjugate, while the deletion of *isoG* should result in the accumulation of GMBA (Chapter 3, Figure 3.24). At present, a role for AldH has not been adequately predicted for inclusion in Figure 3.24, but the preparation of a targeted mutant and subsequent analysis by LC-MS may lead to the identification of the product of this aldehyde dehydrogenase. Targeted deletions must be prepared in *isoG*, *isoJ*, *aldH*, and *garB* with the aim of fully characterising the *iso* metabolic gene cluster, identifying the functions of each Iso polypeptide, and accumulating and identifying the products of each metabolic reaction. Alterations to the supply of biotin and vitamin B12 to *Variovorax* sp. WS11 implied the roles of propionyl-CoA carboxylase, methylmalonyl-CoA mutase, and methylmalonyl-CoA carboxyltransferase in isoprene metabolism. The deletion of the corresponding genes may disrupt many metabolic pathways rather than simply the isoprene metabolic pathway, preventing the application of mutagenesis in the confirmation of these reactions in isoprene metabolism. However, the results of the proteome analysis will be considered in conjunction with the transcriptome of isoprene-grown *Variovorax* sp. WS11, potentially lending credence to the proposed metabolic pathway (Chapter 3, Figure 3.24).

Transcriptional regulation of the *iso* metabolic gene cluster was studied primarily by IsoMO activity assays and RT-qPCR. Expression of the *iso* metabolic gene cluster was significantly upregulated when *Variovorax* sp. WS11 was grown using a combination of fructose and isoprene ($p \leq 0.01$), but no isoprene uptake was detected under the same conditions. This disparity implied that a mechanism of post-transcriptional regulation was controlling the translation of IsoMO, or preventing the activity of the translated IsoMO, when fructose was present. Further experiments are required in order to determine why fructose should permit the transcription of the *iso* metabolic gene cluster while glucose, a structural isomer of fructose (Holesh *et al*. 2020), totally repressed *iso* gene expression. Initial experiments should examine differences in the soluble protein content of *Variovorax* sp. WS11 grown using isoprene, glucose, fructose, a combination of fructose and isoprene, and a combination of glucose and isoprene. This may indicate differences in the translation of the Iso polypeptides, and would further indicate the level (post-transcription or post--translation) at which the repression was occurring.

The transcriptome of *Variovorax* sp. WS11 was sequenced after induction by isoprene or epoxyisoprene, with succinate and no carbon source acting as uninduced controls. Further work must focus on the analysis of the transcriptome in conjunction with the proteome of isoprene-grown *Variovorax* sp. WS11, as this may indicate the levels of regulation of the *iso* metabolic gene cluster and of the whole isoprene metabolic pathway. Also required is the corroboration of the predicted isoprene metabolic pathway (Chapter 3, Figure 3.24), as evidence of the

transcription of the genes encoding the methylmalonyl-CoA and methylcitrate pathways in response to isoprene and epoxyisoprene would strongly indicate the involvement of these pathways in isoprene metabolism.

The specific transcriptional regulators of the *iso* metabolic gene cluster of *Variovorax* sp. WS11, *dmlR_4* and *dmlR_5*, require further characterisation. A FLAG-tagged copy of *dmlR_4* was synthesised with the aim of conducting ChIP-seq, but technical difficulties prevented the synthesis of an N-terminal or C-terminal FLAG-tagged copy of *dmlR_5*. Further work must initially focus on identifying the reason for this. An untagged copy of *dmlR_5*, including the 500 bp promoter region, will be introduced into pUC18miniTn7-Gm and used to complement the phenotype of *Variovorax* sp. WS11 Δ*dmlR_5* by re-introducing the intact *dmlR_5* gene via knock-in. Successful complementation would indicate that the previous issues stemmed from the incorrect assembly of the fusion protein, possibly due to steric hindrance of DmlR_5 activity caused by the FLAG-tag. This would be curious, as it is typically assumed that small tags such as FLAG-tags have little to no impact on the secondary and tertiary structures of the fusion protein (Bräuer *et al*. 2019). However, Bucher *et al*. (2002) reported the ability of these tags to influence the formation of protein crystals. Alternatively, the use of a different linker sequence, or the use of no linker at all due to the small size of the FLAG-tag, may improve the activity of tagged *dmlR_5*. With the use of ChIP-seq, the regions of DNA binding of DmlR_4 and DmlR_5 would be identified. This would provide a wealth of information regarding the functions of these LTTRs, particularly if multiple growth conditions were tested. For example, the binding of DmlR_4 to the *dmlR_4* promoter in the absence of isoprene would indicate negative autoregulation at this promoter (Maddocks & Oyston 2008). However, the proteome of isoprene-grown *Variovorax* sp. WS11 indicated that the abundance of DmlR_4 decreased when this bacterium was exposed to isoprene (Figure 3.20), indicating an alternative mechanism of regulation as it was expected that isoprene would act as a co-inducer by associating with DmlR_4, thereby causing the dissociation of DmlR_4 from its own promoter. ChIP-seq would greatly aid the characterisation of each transcriptional regulator, and would also aid in the identification of additional *iso* promoters.

Studies of the wider impact of the microbial degradation of isoprene must begin to take alternative isoprene metabolic pathways into account. Kronen *et al*. (2019) reported the first case of reductive isoprene metabolism in *Acetobacterium* spp., an anaerobe, in which isoprene was reduced to form a range of methyl butenes in a manner which was dependent on H_2 and HCO_3^-. It is unclear whether this process was a fortuitous mechanism derived from an otherwise established metabolic pathway or if it was a metabolic pathway specifically utilised for this purpose, particularly because none of the essential genes for this metabolic process have been identified. Rohwerder *et al*. (2020) suggested a lyase-dependent mechanism of isoprene oxidation via a 1,2-diol. It is unlikely that a functional redundancy exists between the *iso* metabolic gene cluster and the putative lyase gene cluster in *Rhodococcus* sp. AD45 due to the inability of *Rhodococcus* sp. AD45 Δ*isoA* to grow using isoprene (Crombie *et al*. 2015). Comparative genomics may identify the presence of lyase-dependent gene clusters in other isoprene degrading bacteria, and would indicate the need for molecular analysis of this putative isoprene metabolic pathway.

In summary, the work conducted in this project has provided a greater understanding of the metabolism of isoprene by bacteria. While many questions are yet to be answered, such as the roles of the currently uncharacterised *iso* metabolic genes (*isoG*, *isoJ*, *aldH*, *garB*), putative metabolic pathways for the incorporation of isoprene-derived carbon have now been identified. Molecular and biochemical analysis of these pathways, and the identification of metabolic intermediates, will aim to fully elucidate the isoprene metabolic pathway.

10. **References**

Acuña Alvarez L, Exton DA, Timmis KN, Suggett DJ, McGenity TJ (2009) Characterization of marine isoprene-degrading communities. Environ Microbiol 11:3280–3291.

Adegbola O (2008) High cell density methanol cultivation of *Methylosinus trichosporium* OB3b. Queen's University

Agnihotri G, Liu H (2003) Enoyl-CoA hydratase: Reaction, mechanism, and inhibition. Bioorg Med Chem 11:9–20.

Alanazi MQ, Alqahtani FY, Aleanizy FS (2018) An evaluation of E. coli in urinary tract infection in emergency department at KAMC in Riyadh, Saudi Arabia: retrospective study. Ann Clin Microbiol Antimicrob 17:doi: 10.1186/s12941-018-0255-z.

Albers P, Lood C, Özturk B, Horemans B, Lavigne R, van Noort V, De Mot R, Marchal K, Sanchez-Rodriguez A, Springael D (2018) Catabolic task division between two near-isogenic subpopulations co-existing in a herbicide-degrading bacterial consortium: consequences for the interspecies consortium metabolic model. Environ Microbiol 20:85–96.

Albertini RJ, Carson ML, Kirman CR, Gargas ML (2010) 1,3-Butadiene: II. Genotoxicity profile. Crit Rev Toxicol 40:12–73.

Alekshun MN, Levy SB (1999) The mar regulon: multiple resistance to antibiotics and other toxic chemicals. Trends Microbiol 7:410–413.

Ali H, Murrell JC (2009) Development and validation of promoter-probe vectors for the study of methane monooxygenase gene expression in *Methylococcus capsulatus* Bath. Microbiology 155:761–771.

Ali SL (1984) Tetracycline Hydrochloride. In: *Analytical Profiles of Drug Substrances*, 13th ed. Florey KBT-AP of DS (ed) Academic Press, New York, p 597–653

Allen JR, Ensign SA (1999) Two short-chain dehydrogenases confer stereoselectivity for enantiomers of epoxypropane in the multiprotein epoxide carboxylating systems of *Xanthobacter* strain Py2 and *Nocardia corallina* B276. Biochemistry 38:247–256.

Altschul SF, Gish W, Miller W, Myers EW, Lipman DJ (1990) Basic local alignment search tool. J Mol Biol 215:403–410.

Antoine R, Rivera-Millot A, Roy G, Jacob-Dubuisson F (2019) Relationships between copper-related proteomes and lifestyles in β proteobacteria. Front Microbiol 10:doi: 10.3389/fmicb.2019.02217.

Arenz S, Wilson DN (2016) Bacterial Protein Synthesis as a Target for Antibiotic Inhibition. Cold Spring Harb Perspect Med 6:a025361.

Arneth A, Monson RK, Schurgers G, Niinemets Ü, Palmer PI (2008) Why are estimates of global terrestrial isoprene emissions so similar (and why is this not so for monoterpenes)? Atmos Chem Phys 8:4605–4620.

Arneth A, Schurgers G, Lathiere J, Duhl T, Beerling DJ, Hewitt CN, Martin M, Guenther A (2011) Global terrestrial isoprene emission models: Sensitivity to variability in climate and vegetation. Atmos Chem Phys 11:8037–8052.

Arnold SR, Spracklen D V, Williams J, Yassaa N, Sciare J, Bonsang B, Gros V, Peeken I, Lewis AC, Alvain S, Alvain M (2009) Evaluation of the global oceanic isoprene source and its impacts on marine organic carbon aerosol. Atmos Chem Phys 9:1253–1262.

Asada K (1992) Ascorbate peroxidase – a hydrogen peroxide-scavenging enzyme in plants. Physiol Plant 85:235–241.

Ashizawa A, Roney N, Tucker PG, Harper C, Cronin D, Ingerman L, Klotzbach J, Diamond GL, Lumpkin M, Plewak DJ (2012) Toxicological profile for 1,3-butadiene. Agency for Toxic Substances and Disease Registry. Atlanta, Georgia.

Atkinson R, Arey J (2003) Atmospheric degradation of volatile organic compounds. Chem Rev 103:4605–4638.

Azam MS, Vanderpool CK (2018) Translational regulation by bacterial small RNAs via an unusual Hfq-dependent mechanism. Nucleic Acids Res 46:2585–2599.

Aziz FAA, Suzuki K, Moriuchi R, Dohra H, Tashiro Y, Futamata H (2020) Draft genome sequence of phenol-degrading *Variovorax boronicumulans* strain HAB-30. Microbiol Resour Announc 9:e01478-19.

Aziz RK, Bartels D, Best AA, Dejongh M, Disz T, Edwards RA, Formsma K, Gerdes S, Glass EM, Kubal M, Meyer F, Olsen GJ, Olson R, Osterman AL, Overbeek RA, Mcneil LK, Paarmann D, Paczian T, Parrello B, Pusch GD, Reich C, Stevens R, Vassieva O, Vonstein V, Wilke A, Zagnitko O (2008) The RAST Server: Rapid Annotations using Subsystems Technology. BMC Genomics 9:doi:10.1186/1471-2164-9-75.

Babitzke P, Baker CS, Romeo T (2009) Regulation of translation initiation by RNA binding proteins. Annu Rev Microbiol 63:27–44.

Bäck J, Aaltonen H, Hellén H, Kajos MK, Patokoski J, Taipale R, Pumpanen J, Heinonsalo J (2010) Variable emissions of microbial volatile organic compounds (MVOCs) from root-associated fungi isolated from Scots pine. Atmos Environ 44:3651–3659.

Bagley MC, Dale JW, Merritt EA, Xiong X (2005) Thiopeptide Antibiotics. Chem Rev 105:685–714.

Bai B, Ren J, Bai F, Hao L (2020) Selection and validation of reference genes for gene expression studies in *Pseudomonas brassicacearum* GS20 using real-time quantitative reverse transcription PCR. PLoS One 15:e0227927.

Baier M, Kandlbinder A, Golldack D, Dietz KJ (2005) Oxidative stress and ozone: Perception, signalling and response. Plant, Cell Environ 28:1012–1020.

Bailey LJ, Acheson JF, McCoy JG, Elsen NL, Phillips GN, Fox BG (2012) Crystallographic Analysis of Active Site Contributions to Regiospecificity in the Diiron Enzyme Toluene 4-Monooxygenase. Biochemistry 51:1101–1113.

Bailey LJ, Elsen NL, Pierce BS, Fox BG (2008a) Soluble expression and purification of the oxidoreductase component of toluene 4-monooxygenase. Protein Expr Purif 57:9–16.

Bailey LJ, McCoy JG, Phillips GN, Fox BG (2008b) Structural consequences of effector protein complex formation in a diiron hydroxylase. Proc Natl Acad Sci U S A 105:19194–19198.

Banerjee R, Jones JC, Lipscomb JD (2019) Soluble Methane Monooxygenase. Annu Rev Biochem 88:409–431.

Barket DJ, Grossenbacher JW, Hurst JM, Shepson PB, Olszyna K, Thornberry T, Carroll MA, Roberts J, Stroud C, Bottenheim J, Biesenthal T (2004) A study of the NOx dependence of isoprene oxidation. J Geophys Res D Atmos 109:doi.org/10.1029/2003JD003965.

Barletta B, Meinardi S, Simpson IJ, Khwaja HA, Blake DR, Rowland FS (2002) Mixing ratios of volatile organic compounds (VOCs) in the atmosphere of Karachi, Pakistan. Atmos Environ 36:3429–3443.

Barta C, Loreto F (2006) The relationship between the methyl-erythritol phosphate pathway leading to emission of volatile isoprenoids and abscisic acid content in leaves. Plant Physiol 141:1676–1683.

Behnke K, Ehlting B, Teuber M, Bauerfeind M, Louis S, Hänsch R, Polle A, Bohlmann J, Schnitzler JP (2007) Transgenic, non-isoprene emitting poplars don't like it hot. Plant J 51:485–499.

Behnke K, Kleist E, Uerlings R, Wildt J, Rennenberg H, Schnitzler JP (2009) RNAi-mediated suppression of isoprene biosynthesis in hybrid poplar impacts ozone tolerance. Tree Physiol 29:725–736.

Belimov AA, Dodd IC, Hontzeas N, Theobald JC, Safronova VI, Davies WJ (2009) Rhizosphere bacteria containing 1-

aminocyclopropane-1-carboxylate deaminase increase yield of plants grown in drying soil via both local and systemic hormone signalling. New Phytol 181:413–423.

Belimov AA, Safronova VI, Sergeyeva TA, Egorova TN, Matveyeva VA, Tsyganov VE, Borisov AY, Tikhonovich IA, Kluge C, Preisfeld A, Dietz K-J, Stepanok V V. (2001) Characterization of plant growth promoting rhizobacteria isolated from polluted soils and containing 1-aminocyclopropane-1-carboxylate deaminase. Can J Microbiol 47:642–652.

Bentlage B, Rogers TS, Bachvaroff TR, Delwiche CF (2016) Complex Ancestries of Isoprenoid Synthesis in Dinoflagellates Bastian. J Eukaryot Microbiol 63:123–137.

Berndt T, Hyttinen N, Herrmann H, Hansel A (2019) First oxidation products from the reaction of hydroxyl radicals with isoprene for pristine environmental conditions. Commun Chem 2:doi: 10.1038/s42004-019-0120-9.

Bers K, Leroy B, Breugelmans P, Albers P, Lavigne R, Sørensen SR, Aamand J, De Mot R, Wattiez R, Springael D (2011) A novel hydrolase identified by genomic-proteomic analysis of phenylurea herbicide mineralization by Variovorax sp. strain SRS16. Appl Environ Microbiol 77:8754–8764.

Bertoni G, Bolognese F, Galli E, Barbieri P (1996) Cloning of the genes for and characterization of the early stages of toluene and o-xylene catabolism in *Pseudomonas stutzeri* OX1. Appl Environ Microbiol 62:3704–3711.

Biesenthal TA, Wu Q, Shepson PB, Wiebe HA, Anlauf KG, Mackay GI (1997) A study of relationships between isoprene, its oxidation products, and ozone, in the Lower Fraser Valley, BC. Atmos Environ 31:2049–2058.

Biswas I (2015) Genetic tools for manipulating Acinetobacter baumannii genome: An overview. J Med Microbiol 64:657–669.

Blazyk JL, Gassner GT, Lippard SJ (2005) Intermolecular Electron-Transfer Reactions in Soluble Methane Monooxygenase: A Role for Hysteresis in Protein Function. J Am Chem Soc 127:17364–17376.

Bloemberg G V, Lugtenberg BJJ (2004) Bacterial Biofilms on Plants: Relevance and Phenotypic Aspects. In: *Microbial Biofilms*. O'Toole GA, Ghannoum MA (eds) American Society of Microbiology, Washington, DC, p 141–159

Blume AJ, Weber A, Balbinder E (1968) Analysis of polar and nonpolar tryptophan mutants by derepression kinetics. J Bacteriol 95:2230–2241.

Bolas CG, Ferracci V, Robinson AD, Mead MIMI, Nadzir MSM, Pyle JA, Jones RL, Harris NRP, Shahrul M, Nadzir MSM, Pyle A, Jones RL, Harris NRP, Pyle JA, Jones RL, Harris NRP (2020) IDirac: a field-portable instrument for long-term autonomous measurements of isoprene and selected VOCs. Atmos Meas Tech 13:821–838.

Bolger AM, Lohse M, Usadel B (2014) Trimmomatic: a flexible trimmer for Illumina sequence data. Bioinformatics 30:2114–2120.

Bolivar F, Rodriguez RL, Greene PJ, Betlach MC, Heyneker HL, Boyer HW, Crosa JH, Falkow S (1977) Construction and characterization of new cloning vehicles. II. A multipurpose cloning system. Gene 2:95–113.

Bondarczuk K, Piotrowska-Seget Z (2013) Molecular basis of active copper resistance mechanisms in Gram-negative bacteria. Cell Biol Toxicol 29:397–405.

Bonsang B, Polle C, Lambert G (1992) Evidence for marine production of isoprene. Geophys Res Lett 19:1129–1132.

Bragonzi A, Worlitzsch D, Pier GB, Timpert P, Ulrich M, Hentzer M, Andersen JB, Givskov M, Conese M, Doring G (2005) Nonmucoid *Pseudomonas aeruginosa* expresses alginate in the lungs of patients with cystic fibrosis and in a mouse model. J Infect Dis 192:410–419.

Brandt U, Deters A, Steinbüchel A (2015) A jack-of-all-trades: 2-mercaptosuccinic acid. Appl Microbiol Biotechnol 99:4545–4557.

Brandt U, Galant G, Meinert-Berning C, Steinbüchel A (2019) Functional analysis of active amino acid residues of the mercaptosuccinate dioxygenase of *Variovorax paradoxus* B4. Enzyme Microb Technol 120:61–68.

Brandt U, Hiessl S, Schuldes J, Thürmer A, Wübbeler JH, Daniel R, Steinbüchel A (2014a) Genome-guided insights into the versatile metabolic capabilities of the mercaptosuccinate-utilizing β-proteobacterium *Variovorax paradoxus*

strain B4. Environ Microbiol 16:3370–3386.

Brandt U, Schu M, Steinbüchel A (2014b) Mercaptosuccinate dioxygenase, a cysteine dioxygenase homologue, from *Variovorax paradoxus* strain B4 is the key enzyme of mercaptosuccinate degradation. J Biol Chem 289:30800–30809.

Bräuer M, Zich MT, Önder K, Müller N (2019) The influence of commonly used tags on structural propensities and internal dynamics of peptides. Monatshefte fur Chemie 150:913–925.

Brettin T, Davis JJ, Disz T, Edwards RA, Gerdes S, Olsen GJ, Olson R, Overbeek R, Parrello B, Pusch GD, Shukla M, Iii JAT, Stevens R, Vonstein V, Wattam AR, Xia F (2015) RASTtk : A modular and extensible implementation of the RAST algorithm for annotating batches of genomes. Sci Rep 5:doi: 10.1038/srep08365.

Breuer M, Ditrich K, Habicher T, Hauer B, Keßeler M, Stürmer R, Zelinski T (2004) Industrial methods for the production of optically active intermediates. Angew Chemie - Int Ed 43:788–824.

Browning DF, Busby SJW (2016) Local and global regulation of transcription initiation in bacteria. Nat Rev Microbiol 14:638–650.

Bru N, Zimmer I, Zhou G, Elobeid M, Janz D, Polle A, Behnke K, Grote R, Brüggemann N, Zimmer I, Zhou G, Elobeid M, Janz D, Polle A, Schnitzler JP (2012) Isoprene emission-free poplars - a chance to reduce the impact from poplar plantations on the atmosphere. New Phytol 194:70–82.

Brückner R, Titgemeyer F (2002) Carbon catabolite repression in bacteria: choice of the carbon source and autoregulatory limitation of sugar utilization. FEMS Microbiol Lett 209:141–148.

Brusseau GA, Tsien H, Hanson RS, Wackett LP (1990) Optimization of trichloroethylene oxidation by methanotrophs and the use of a colorimetric assay to detect soluble methane monooxygenase activity. Biodegradation 1:19–29.

Bucher MH, Evdokimov AG, Waugh DS (2002) Differential effects of short affinity tags on the crystallization of *Pyrococcus furiosus* maltodextrin-binding protein. Acta Crystallogr Sect D 58:392–397.

Byrne AM, Olsen RH (1996) Cascade regulation of the toluene-3-monooxygenase operon (*tbuA1UBVA2C*) of Burkholderia pickettii PKO1: role of the *tbuA1* promoter (PtbuA1) in the expression of its cognate activator, TbuT. J Bacteriol 178:6327–6337.

Cadoret F, Soscia C, Voulhoux R (2014) Gene Transfer: Transformation/Electroporation. In: *Methods in Molecular Biology*. Filoux A, Ramos J-L (eds) Springer Science, Clifton, N.J., p 11–15

Campbell EA, Korzheva N, Mustaev A, Murakami K, Nair S, Goldfarb A, Darst SA (2001) Structural Mechanism for Rifampicin Inhibition of Bacterial RNA Polymerase. Cell 104:901–912.

Canada KA, Iwashita S, Shim H, Wood TK (2002) Directed evolution of toluene ortho-monooxygenase for enhanced 1-naphthol synthesis and chlorinated ethene degradation. J Bacteriol 184:344–349.

Carbajal-rodríguez I, Sto N, Satola B, Wu JH, Steinbüchel A (2011) Aerobic Degradation of Mercaptosuccinate by the Gram-Negative Bacterium *Variovorax paradoxus* Strain B4. J Bacteriol 193:527–539.

Carey PR, Sönnichsen FD, Yee VC (2004) Transcarboxylase: one of nature's early nanomachines. IUBMB Life 56:575–583.

Carlton AGG, Wiedinmyer C, Kroll JH (2009) A review of secondary organic aerosol (SOA) formation from isoprene. Atmos Chem Phys 9:4987–5005.

Carrión O, Gibson L, Elias DMO, McNamara NP, Van Alen TA, Op Den Camp HJM, Supramaniam CV, McGenity TJ, Murrell JC (2020) Diversity of isoprene-degrading bacteria in phyllosphere and soil communities from a high isoprene-emitting environment: A Malaysian oil palm plantation. Microbiome 8:doi.org/10.1186/s40168-020-00860-7.

Carrión O, Larke-Mejía NL, Gibson L, Farhan Ul Haque M, Ramiro-garcía J, McGenity TJ, Murrell JC (2018) Gene probing reveals the widespread distribution, diversity and abundance of isoprene-degrading bacteria in the

environment. Microbiome 6:doi: 10.1186/s40168-018-0607-0.

Carver T, Harris SR, Berriman M, Parkhill J, Mcquillan JA (2012) Artemis: an integrated platform for visualization and analysis of high-throughput sequence-based experimental data. Bioinformatics 28:464–469.

Champreda V, Zhou N-Y, Leak DJ (2004) Heterologous expression of alkene monooxygenase components from *Xanthobacter autotrophicus* Py2 and reconstitution of the active complex. FEMS Microbiol Lett 239:309–318.

Chassy BM, Mercenier A, Flickinger J (1988) Transformation of bacteria by electroporation. Trends Biotechnol 6:303–309.

Chen I, Christie PJ, Dubnau D (2005) The ins and outs of DNA transfer in bacteria. Science (80-) 310:1456–1460.

Cheung S, McCarl V, Holmes AJ, Coleman N V., Rutledge PJ (2013) Substrate range and enantioselectivity of epoxidation reactions mediated by the ethene-oxidising *Mycobacterium* strain NBB4. Appl Microbiol Biotechnol 97:1131–1140.

Chiu ML, Viollier PH, Katoh T, Ramsden JJ, Thompson CJ (2001) Ligand-induced changes in the *Streptomyces lividans* TipAL protein imply an alternative mechanism of transcriptional activation for MerR-like proteins. Biochemistry 40:12950–12958.

Choi K, Gaynor JB, White KG, Lopez C, Bosio CM, Karkhoff-schweizer RR, Schweizer HP (2005) A Tn7-based broad-range bacterial cloning and expression system. Nat Methods 2:443–448.

Choi KH, Schweizer HP (2006) Mini-Tn7 insertion in bacteria with single attTn7 site: example Pseudomonas aeruginosa. Nat Protoc 1:153–161.

Chomczynski P, Sacchi N (1987) Single-step method of RNA isolation by acid guanidinium thiocyanate-phenol-chloroform extraction. Anal Biochem 162:156–159.

Choudhary A, Purohit H, Phale PS (2017) Benzoate transport in *Pseudomonas putida* CSV86. FEMS Microbiol Lett 364:doi: 10.1093/femsle/fnx118.

Chu KH, Alvarez-Cohen L (1999) Evaluation of toxic effects of aeration and trichloroethylene oxidation on methanotrophic bacteria grown with different nitrogen sources. Appl Environ Microbiol 65:766–772.

Ciok A, Dziewit L, Grzesiak J, Budzik K, Gorniak D, Zdanowski MK, Bartosik D (2016) Identification of miniature plasmids in psychrophilic Arctic bacteria of the genus *Variovorax*. FEMS Microbiol Ecol 92:doi.org/10.1093/femsec/fiw043.

Claeys M, Graham B, Vas G, Wang W, Vermeylen R, Pashynska V, Cafmeyer J, Guyon P, Andreae MO, Artaxo P, Maenhaut W (2004) Formation of Secondary Organic Aerosols Through Photooxidation of Isoprene. Science (80-) 303:1173–1176.

Clark DP, Pazdernik NJ, McGehee MR (2019) Protein Synthesis. In: *Molecular Biology*, Third Edit. Clark DP, Pazdernik NJ, McGehee MRBT-MB (Third E (eds) Academic Cell, p 397–444

Clark LC, Wolf R, Granger D, Taylor Z (1953) Continuous Recording of Blood Oxygen Tensions by Polarography. J Appl Physiol 6:189–193.

Cleveland C., Yavitt J. (1997) Consumption of atmospheric isoprene in soil. Geophys Res Lett 24:2379–2382.

Cleveland CC, Yavitt JB (1998) Microbial consumption of atmospheric isoprene in a temperate forest soil. Appl Environ Microbiol 64:172–177.

Colby J, Stirling DI, Dalton H (1977) The soluble methane mono-oxygenase of *Methylococcus capsulatus* (Bath). Biochem J 165:395–402.

Coleman N V., Bui NB, Holmes AJ (2006) Soluble di-iron monooxygenase gene diversity in soils, sediments and ethene enrichments. Environ Microbiol 8:1228–1239.

Conrad JC, Gibiansky ML, Jin F, Gordon VD, Motto DA, Mathewson MA, Stopka WG, Zelasko DC, Shrout JD, Wong GCL (2011) Flagella and pili-mediated near-surface single-cell motility mechanisms in *P. aeruginosa*. Biophys J

100:1608–1616.

Contzen M, Stolz A (2000) Characterization of the genes for two protocatechuate 3,4-dioxygenases from the 4-sulfocatechol-degrading bacterium *Agrobacterium radiobacter* strain S2. J Bacteriol 182:6123–6129.

Council NR (2010) Advancing the science of climate change. The National Academies Press, Washington, DC.

Criswell D, Tobiason VL, Lodmell JS, Samuels DS (2006) Mutations conferring aminoglycoside and spectinomycin resistance in *Borrelia burgdorferi*. Antimicrob Agents Chemother 50:445–452.

Crombie AT (2011) Metabolism of methane and propane and the role of the glyoxylate bypass enzymes in *Methylocella silvestris* BL2. University of Warwick

Crombie AT, Emery H, McGenity TJ, Colin J, Murrell JC (2017) Draft genome sequences of three terrestrial isoprene-degrading *Rhodococcus* strains. Genome Announc 5:4–5.

Crombie AT, Khawand M El, Rhodius VA, Fengler KA, Miller MC, Whited GM, McGenity TJ, Murrell JC (2015) Regulation of plasmid-encoded isoprene metabolism in *Rhodococcus*, a representative of an important link in the global isoprene cycle. Environ Microbiol 17:3314–3329.

Crombie AT, Larke-Mejia NL, Emery H, Dawson RA, Pratscher J, Murphy GP (2018) Poplar phyllosphere harbors disparate isoprene-degrading bacteria. Proc Natl Acad Sci 115:13081–13086.

Dani KGS, Silva Benavides AM, Michelozzi M, Peluso G, Torzillo G, Loreto F, Dani KGS, Silva AM, Michelozzi M, Peluso G, Torzillo G, Loreto F (2017) Relationship between isoprene emission and photosynthesis in diatoms, and its implications for global marine isoprene estimates. Mar Chem 189:17–24.

Dawson RA, Crombie AT, Pichon P, Mcgenity TJ, Murrell JC (2021) The microbiology of isoprene cycling in aquatic ecosystems. Aquat Microb Ecol 87:79–98.

Dawson RA, Larke-Mejía NL, Crombie AT, Farhan Ul Haque M, Murrell JC (2020) Isoprene oxidation by the Gram-negative model bacterium *Variovorax* sp. WS11. Microorganisms 8:doi: 10.3390/microorganisms8030349.

Dejonghe W, Berteloot E, Goris J, Boon N, Crul K, Maertens S, Höfte M, De Vos P, Verstraete W, Top EM (2003) Synergistic degradation of linuron by a bacterial consortium and isolation of a single linuron-degrading *Variovorax* strain. Appl Environ Microbiol 69:1532–1541.

delCardayre SB, Stock KP, Newton GL, Fahey RC, Davies JE (1998) Coenzyme A disulfide reductase, the primary low molecular weight disulfide reductase from *Staphylococcus aureus*. Purification and characterization of the native enzyme. J Biol Chem 273:5744–5751.

DeMaster EG, Nagasawa HT (1978) Isoprene, an endogenous constituent of human alveolar air with a diurnal pattern of excretion. Life Sci 22:91–97.

Deneris ES, Stein RA, Mead JF (1985) Acid-catalyzed formation of isoprene from a mevalonate-derived product using a rat liver cytosolic fraction. J Biol Chem 260:1382–1385.

Deng YW, Ro SY, Rosenzweig AC (2018) Structure and function of the lanthanide-dependent methanol dehydrogenase XoxF from the methanotroph *Methylomicrobium buryatense* 5GB1C. J Biol Inorg Chem 23:1037–1047.

Dennis JJ, Zylstra GJ (1998) Plasposons: Modular Self-Cloning Minitransposon Derivatives for Rapid Genetic Analysis of Gram-Negative Bacterial Genomes. Appl Environ Microbiol 64:2710–2715.

Deponte M (2013) Glutathione catalysis and the reaction mechanisms of glutathione-dependent enzymes. Biochim Biophys Acta - Gen Subj 1830:3217–3266.

Dolan SK, Wijaya A, Geddis SM, Spring DR, Silva-Rocha R, Welch M (2018) Loving the poison: The methylcitrate cycle and bacterial pathogenesis. Microbiol (United Kingdom) 164:251–259.

van Doorn MM, Merl-Pham J, Ghirardo A, Fink S, Polle A, Schnitzler J-P, Rosenkranz M (2020) Root isoprene formation alters lateral root development. Plant Cell Environ 43:2207–2223.

Dorn E, Hellwig I V, Reineke W, Knackmuss H-J (1974) Isolation and Characterization of a 3-chlorobenzoate Degrading Pseudomonad. Arch Microbiol 99:61–70.

Dumont MG, Murrell JC (2005) Stable isotope probing — linking microbial identity to function. Nat Rev Microbiol 3:499–504.

Durana N, Navazo M, Gómez MC, Alonso L, García JA, Ilardia JL, Gangoiti G, Iza J (2006) Long term hourly measurement of 62 non-methane hydrocarbons in an urban area: Main results and contribution of non-traffic sources. Atmos Environ 40:2860–2872.

Edney EO, Kleindienst TE, Jaoui M, Lewandowski M, Offenberg JH, Wang W, Claeys M (2005) Formation of 2-methyl tetrols and 2-methylglyceric acid in secondary organic aerosol from laboratory irradiated isoprene/NOX/SO 2/air mixtures and their detection in ambient PM2.5 samples collected in the eastern United States. Atmos Environ 39:5281–5289.

Egland KA, Greenberg EP (2001) Quorum sensing in Vibrio fischeri: Analysis of the LuxR DNA binding region by alanine-scanning mutagenesis. J Bacteriol 183:382–386.

Eichhorn E, Ploeg JR Van Der, Kertesz MA, Leisinger T (1997) Characterization of α-Ketoglutarate-dependent taurine dioxygenase from *Escherichia coli*. J Biol Chem 272:23031–23036.

Ellis EC, Klein Goldewijk K, Siebert S, Lightman D, Ramankutty N (2010) Anthropogenic transformation of the biomes, 1700 to 2000. Glob Ecol Biogeogr 19:589–606.

Ensign SA (2001) Microbial metabolism of aliphatic alkenes. Biochemistry 40:5845–5853.

Eoh H, Rhee KY (2014) Methylcitrate cycle defines the bactericidal essentiality of isocitrate lyase for survival of *Mycobacterium tuberculosis* on fatty acids. Proc Natl Acad Sci 111:4976–4981.

Ewers J, Freier-Schröder D, Knackmuss H (1990) Selection of trichloroethene (TCE) degrading bacteria that resist inactivation by TCE. Arch Microbiol 154:410–413.

Exton DA, Suggett DJ, McGenity TJ, Steinke M (2013) Chlorophyll-normalized isoprene production in laboratory cultures of marine microalgae and implications for global models. Limnol Oceanogr 58:1301–1311.

Fabre A-L, Colotte M, Luis A, Tuffet S, Bonnet J (2014) An efficient method for long-term room temperature storage of RNA. Eur J Hum Genet 22:379–385.

Faiz S, Zahoor AF (2016) Ring opening of epoxides with C-nucleophiles. Mol Divers 20:969–987.

Fall R, Copley SD (2000) Bacterial sources and sinks of isoprene, a reactive atmospheric hydrocarbon. Environ Microbiol 2:123–130.

Farhan Ul Haque M, Gu W, DiSpirito AA, Semrau JD (2016) Marker Exchange Mutagenesis of *mxaF*, Encoding the Large Subunit of the Mxa Methanol Dehydrogenase, in *Methylosinus trichosporium* OB3b. Appl Environ Microbiol 82:1549–1555.

Feng Z, Yuan X, Fares S, Loreto F, Li P, Hoshika Y, Paoletti E (2019) Isoprene is more affected by climate drivers than monoterpenes: A meta-analytic review on plant isoprenoid emissions. Plant Cell Environ 42:1939–1949.

Forouzanfar MH, Alexander L, Anderson HR, Bachman VF, Biryukov S (2015) Global, regional, and national comparative risk assessment of 79 behavioural, environmental and occupational, and metabolic risks or clusters of risks in 188 countries, 1990-2013: a systematic analysis for the Global Burden of Disease Study 2013. Lancet 386:2287–2323.

Fosdike WLJJ, Smith TJ, Dalton H (2005) Adventitious reactions of alkene monooxygenase reveal common reaction pathways and component interactions among bacterial hydrocarbon oxygenases. FEBS J 272:2661–2669.

Fox BG, Borneman JG, Wackett LP, Lipscomb J. (1990) Haloalkene oxidation by the soluble methane monooxygenase from *Methylosinus trichosporium* OB3b: mechanistic and environmental implications. Biochemistry 29:6419–6427.

Fox BG, Liu Y, Dege JE, Lipscomb JD (1991) Complex formation between the protein components of methane

monooxygenase from *Methylosinus trichosporium* OB3b. Identification of sites of component interaction. J Biol Chem 266:540–550.

Franje C, Chang S-K, Shyu C-L, Davis J, Lee Y-W, Lee R-J, Chang C-C, Chou C-C (2010) Differential heat stability of amphenicols characterized by structural degradation, mass spectrometry and antimicrobial activity. J Pharm Biomed Anal 53:869–877.

Fredendall RJ, Stone JL, Pehl MJ, Orwin PM (2020) Transcriptome profiling of *Variovorax paradoxus* EPS under different growth conditions reveals regulatory and structural novelty in biofilm formation. Access Microbiol 2:doi: 10.1099/acmi.0.000121.

Friedrich B, Hogrefe C, Schlegel HG (1981) Naturally occurring genetic transfer of hydrogen-oxidizing ability between strains of *Alcaligenes eutrophus*. J Bacteriol 147:198–205.

Froland WA, Andersson KK, Lee SK, Liu YY, Lipscomb JD (1992) Methane monooxygenase component B and reductase alter the regioselectivity of the hydroxylase component-catalyzed reactions. A novel role for protein-protein interactions in an oxygenase mechanism. J Biol Chem 267:17588–17597.

Fu D, Millet DB, Wells KC, Payne VH, Yu S, Guenther A, Eldering A (2019) Direct retrieval of isoprene from satellite-based infrared measurements. Nat Commun 10:doi: 10.1038/s41467-019-11835-0.

Furey TS (2012) ChIP-seq and beyond: New and improved methodologies to detect and characterize protein-DNA interactions. Nat Rev Genet 13:840–852.

Furuya T, Hayashi M, Kino K (2013) Reconstitution of active Mycobacterial binuclear iron nonooxygenase complex in *Escherichia coli*. Appl Environ Microbiol 79:6033–6039.

Furuya T, Hayashi M, Semba H, Kino K (2012) The mycobacterial binuclear iron monooxygenases require a specific chaperonin-like protein for functional expression in a heterologous host. FEBS J 280:817–826.

Futamata H, Nagano Y, Watanabe K, Hiraishi A (2005) Unique Kinetic Properties of Phenol-Degrading *Variovorax* Strains Responsible for Efficient Trichloroethylene Degradation in a Chemostat Enrichment Culture. Appl Environ Microbiol 71:904–911.

Gallagher SC, Cammack R, Dalton H (1997) Alkene monooxygenase from *Nocardia corallina* B-276 is a member of the class of dinuclear iron proteins capable of stereospecific epoxygenation reactions. Eur J Biochem 247:635–641.

Garcia S, Jardine K, de Souza VF, de Souza RAF, Junior SD, Gonçalves JF de C (2019) Reassimilation of leaf internal CO2 contributes to isoprene emission in the neotropical species *Inga edulis* Mart. Forests 10:doi.org/10.3390/f10060472.

Garcia Teijeiro R, Belimov AA, Dodd IC (2020) Microbial inoculum development for ameliorating crop drought stress: A case study of *Variovorax paradoxus* 5C-2. N Biotechnol 56:103–113.

Geissmann T, Marzi S, Romby P (2009) The role of mRNA structure in translational control in bacteria. RNA Biol 6:153–160.

George KW, Alonso-Gutierrez J, Keasling JD, Lee TS (2015) Isoprenoid Drugs, Biofuels, and Chemicals—Artemisinin, Farnesene, and Beyond BT - Biotechnology of Isoprenoids.Schrader J, Bohlmann J (eds) Springer International Publishing, Cham, p 355–389

Gibson DG, Glass JI, Lartigue C, Noskov VN, Chuang R-Y, Algire MA, Benders GA, Montague MG, Ma L, Moodie MM, Merryman C, Vashee S, Krishnakumar R, Assad-Garcia N, Andrews-Pfannkoch C, Denisova EA, Young L, Qi Z-Q, Segall-Shapiro TH, Calvey CH, Parmar PP, Hutchison CA, Smith HO, Venter JC (2010) Creation of a Bacterial Cell Controlled by a Chemically Synthesized Genome. Science (80-) 329:52–56.

Gibson DG, Young L, Chuang R-Y, Venter JC, Hutchison CA 3rd, Smith HO (2009) Enzymatic assembly of DNA molecules up to several hundred kilobases. Nat Methods 6:343–345.

Gibson L, Larke-Mejía NL, Murrell JC (2020) Complete genome of isoprene degrading Nocardioides sp. WS12. Microorganisms 8:doi.org/10.3390/microorganisms8060889.

Gilbert B, McDonald IR, Finch R, Stafford GP, Nielsen AK, Murrell JC (2000) Molecular analysis of the *pmo* (particulate methane monooxygenase) operons from two type II methanotrophs. Appl Environ Microbiol 66:966–975.

Van Ginkel CG, De Jong E, Tilanus JWRR, De Bont JAMM, Jong E De (1987) Microbial oxidation of isoprene, a biogenic foliage volatile and of 1,3-butadiene, an anthropogenic gas. FEMS Microbiol Lett 45:275–279.

Glick BR, Penrose DM, Li J (1998) A model for the lowering of plant ethylene concentrations by plant growth-promoting bacteria. J Theor Biol 190:63–68.

Goldstein AH, Goulden ML, Munger JW, Wofsy SC, Geron CD, Geron (1998) Seasonal course of isoprene emissions from a midlatitude deciduous forest. J Geophys Res 103:31045–31056.

Gómez MC, Durana N, García JA, de Blas M, Sáez de Cámara E, García-Ruiz E, Gangoiti G, Torre-Pascual E, Iza J, Blas M De, García-Ruiz E, Gangoiti G, Torre-Pascual E, Iza J (2020) Long-term measurement of biogenic volatile organic compounds in a rural background area: Contribution to ozone formation. Atmos Environ 224:doi: 10.1016/j.atmosenv.2020.117315.

Gray CM, Helmig D, Fierer N (2015) Bacteria and fungi associated with isoprene consumption in soil. Elementa 3:doi: 10.12952/journal.elementa.000053.

Green J, Dalton H (1989) Substrate specificity of soluble methane monooxygenase. Mechanistic implications. J Biol Chem 264:17698–17703.

Green MJ, Hill HAO (1984) Chemistry of dioxygen. Methods Enzymol 105:3–22.

Greve H-H (2000) Rubber, 2. Natural. In: *Ullmann's Encyclopedia of Industrial Chemistry*. Major Reference Works, Wiley, Weinheim, Germany

Guenther AB, Hewitt CN, Erickson D, Fall R, Geron C, Graedel T, Harley P, Klinger L, Lerdau M, McKay WA, Pierce T, Scholes B, Steinbrecher R, Tallamraju R, Taylor J, Zimmerman P (1995) A global model of natural volatile organic compound emissions. J Geophys Res 100:doi: 10.1029/94JD02950.

Guenther AB, Jiang X, Heald CL, Sakulyanontvittaya T, Duhl T, Emmons LK, Wang X (2012) The model of emissions of gases and aerosols from nature version 2.1 (MEGAN2.1): an extended and updated framework for modeling biogenic emissions. Geosci Model Dev 5:1471–1492.

Guenther AB, Karl T, Harley P, Wiedinmyer C, Palmer PI, Geron C (2006) Estimates of global terrestrial isoprene emissions using MEGAN (Model of Emissions of Gases and Aerosols from Nature). Atmos Chem Phys Discuss 6:107–173.

Gunarso P, Hartoyo ME, Agus F (2013) Oil Palm and Land Use Change in Indonesia , Malaysia and Papua New Guinea. In: *Reports from the Technical Panels of RSPOs 2nd Greenhouse Gas Working Group [Online]*. Killeen TJ, Goon J (eds) Kuala Lumpur, Malaysia, p 29–64

Haider S, Pal R (2013) Integrated analysis of transcriptomic and proteomic data. Curr Genomics 14:91–110.

Halarnkar PP, Blomquist GJ (1989) Comparative aspects of propionate metabolism. Comp Biochem Physiol Part B Comp Biochem 92:227–231.

Hamamura N, Yeager CM, Arp DJ (2001) Two distinct monooxygenases for alkane oxidation in *Nocardioides* sp. strain CF8. Appl Environ Microbiol 67:4992–4998.

Han J-I, Spain JC, Leadbetter JR, Ovchinnikova G, Goodwin LA, Han CS, Woyke T, Davenport KW, Orwin PM (2013) Genome of the Root-Associated Plant Growth-Promoting Bacterium *Variovorax paradoxus* Strain EPS. Genome Announc 1:doi: 10.1128/genomeA.00843-13.

Han J-II, Choi H-KK, Lee SYS-WW, Orwin PM, Kim J, LaRoe SL, Kim TG, O'Neil J, Leadbetter JR, Lee SYS-WW, Hur C-GG, Spain JC, Ovchinnikova G, Goodwin L, Han C (2011) Complete genome sequence of the metabolically versatile plant growth-promoting endophyte *Variovorax paradoxus* S110. J Bacteriol 193:1183–1190.

Hanson DT, Sharkey TD (2001a) Effect of growth conditions on isoprene emission and other thermotolerance-enhancing compounds. Plant, Cell Environ 24:929–936.

Hanson DT, Sharkey TD (2001b) Rate of acclimation of the capacity for isoprene emission in response to light and temperature. Plant, Cell Environ 24:937–946.

Hanson DT, Swanson S, Graham LE, Sharkey TD (1999) Evolutionary significance of isoprene emission from mosses. Am J Bot 86:634–639.

Hantson S, Knorr W, Schurgers G, Pugh TAM, Arneth A (2017) Global isoprene and monoterpene emissions under changing climate, vegetation, CO2 and land use. Atmos Environ 155:35–45.

Hardacre CJ, Palmer PI, Baumanns K, Rounsevell M, Murray-Rust D (2013) Probabilistic estimation of future emissions of isoprene and surface oxidant chemistry associated with land-use change in response to growing food needs. Atmos Chem Phys 13:5451–5472.

Harley P, Deem G, Flint S, Caldwell M (1996) Effects of growth under elevated UV-B on photosynthesis and isoprene emission in *Quercus gambelii* and *Mucuna pruriens*. Glob Chang Biol 2:149–154.

Harrison PW, Lower RPJ, Kim NKD, Young JPW (2010) Introducing the bacterial 'chromid': not a chromosome, not a plasmid. Trends Microbiol 18:141–148.

Harrison SP, Morfopoulos C, Dani KGS, Prentice IC, Arneth A, Atwell BJ, Barkley MP, Leishman MR, Loreto F, Medlyn BE, Niinemets Ü, Possell M, Peñuelas J, Wright IJ (2013) Volatile isoprenoid emissions from plastid to planet. New Phytol 197:49–57.

Harvey CM, Li Z, Tjellström H, Blanchard GJ, Sharkey TD (2015) Concentration of isoprene in artificial and thylakoid membranes. J Bioenerg Biomembr 47:419–429.

Harvey CM, Sharkey TD (2016) Exogenous isoprene modulates gene expression in unstressed *Arabidopsis thaliana* plants. Plant, Cell Environ 39:1251–1263.

He Y, Mathieu J, Yang Y, Yu P, da Silva MLB, Alvarez PJJ (2017) 1,4-Dioxane Biodegradation by *Mycobacterium dioxanotrophicus* PH-06 Is Associated with a Group-6 Soluble Di-Iron Monooxygenase. Environ Sci Technol Lett 4:494–499.

Heap JT, Ehsaan M, Cooksley CM, Ng Y-K, Cartman ST, Winzer K, Minton NP (2012) Integration of DNA into bacterial chromosomes from plasmids without a counter-selection marker. Nucleic Acids Res 40:e59.

Heine V, Meinert-Berning C, Lück J, Mikowsky N, Voigt B, Riedel K, Steinbüchel A (2019) The catabolism of 3,3'-thiodipropionic acid in *Variovorax paradoxus* strain TBEA6: A proteomic analysis. PLoS One 14:e0211876.

Hellén H, Tykkä T, Hakola H (2012) Importance of monoterpenes and isoprene in urban air in northern Europe. Atmos Environ 59:59–66.

Herrmann H, Janke D, Krejsa S, Kunze I (1987) Involvement of the plasmid pPGH1 in the phenol degradation of *Pseudomonas putida* strain H. FEMS Microbiol Lett 43:133–137.

Hewitt CN, MacKenzie AR, Di Carlo P, Di Marco CF, Dorsey JR, Evans M, Fowler D, Gallagher MW, Hopkins JR, Jones CE, Langford B, Lee JD, Lewis AC, Lim SF, McQuaid J, Misztal P, Moller SJ, Monks PS, Nemitz E, Oram DE, Owen SM, Phillips GJ, Pugh TAM, Pyle JA, Reeves CE, Ryder J, Siong J, Skiba U, Stewart DJ (2009) Nitrogen management is essential to prevent tropical oil palm plantations from causing ground-level ozone pollution. Proc Natl Acad Sci 106:18447–18451.

Hewitt CN, Street RA (1992) A qualitative assessment of the emission of non-methane hydrocarbon compounds from the biosphere to the atmosphere in the U.K.: Present knowledge and uncertainties. Atmos Environ Part A Gen Top 26:3069–3077.

Higgins IJ, Hammond RC, Sariaslani FS, Best D, Davies MM, Tryhorn SE, Taylor F (1979) Biotransformation of hydrocarbons and related compounds by whole organism suspensions of methane-grown *Methylosinus trichosporium* OB3b. Biochem Biophys Res Commun 89:671–677.

Holesh JE, Aslam S, Martin A (2020) Physiology, Carbohydrates. https://www.ncbi.nlm.nih.gov/books/NBK459280/ (accessed 9 June 2021)

Holmes DJ, Caso JL, Thompson CJ (1993) Autogenous transcriptional activation of a thiostrepton-induced gene in *Streptomyces lividans*. EMBO J 12:3183–3191.

Holo H, Nes IF (1989) High-Frequency Transformation, by Electroporation, of Lactococcus lactis subsp. cremoris Grown with Glycine in Osmotically Stabilized Media. Appl Environ Microbiol 55:3119–3123.

Hong CE, Jo SH, Jo IH, Jeong H, Park JM (2017) Draft genome sequence of the endophytic bacterium *Variovorax paradoxus* KB5, Which has antagonistic activity against a phytopathogen, *Pseudomonas syringae* pv. tomato DC3000. Genome Announc 5:doi: 10.1128/genomeA.00950-17.

Hou CT, Patel RN, Laskin N, Barnabe N, Barist I (1981) Epoxidation and hydroxylation of C4- and C5-branched-chain alkenes and alkanes by methanotrophs. Ind Microbiol 23:477–482.

Hu QH, Xie ZQ, Wang XM, Kang H, He QF, Zhang P (2013) Secondary organic aerosols over oceans via oxidation of isoprene and monoterpenes from Arctic to Antarctic. Sci Rep 3:doi: 10.1038/srep02280.

Huttner A, Verhaegh EM, Harbarth S, Muller AE, Theuretzbacher U, Mouton JW (2015) Nitrofurantoin revisited: a systematic review and meta-analysis of controlled trials. J Antimicrob Chemother 70:2456–2464.

van Hylckama Vlieg JET, Kingma J, Kruizinga W, Janssen DB (1999) Purification of a glutathione S-transferase and a glutathione conjugate-specific dehydrogenase involved in isoprene metabolism in *Rhodococcus* sp. strain AD45. J Bacteriol 181:2094–2101.

van Hylckama Vlieg JET, Kingma J, van den Wijngaard AJ, Janssen DBD. (1998) A glutathione S-transferase with activity towards cis-1,2-dichloroepoxyethane is involved in isoprene utilization by *Rhodococcus* sp. strain AD45. Appl Environ Microbiol 64:2800–2805.

van Hylckama Vlieg JET, De Koning W, Janssen DB (1997) Effect of chlorinated ethene conversion on viability and activity of *Methylosinus trichosporium* OB3b. Appl Environ Microbiol 63:4961–4964.

van Hylckama Vlieg JET, De Koning W, Janssen DB, Johan ET, Janssen DB (1996) Transformation kinetics of chlorinated ethenes by *Methylosinus trichosporium* OB3b and detection of unstable epoxides by on-line gas chromatography. Appl Environ Microbiol 62:3304–3312.

van Hylckama Vlieg JET, Leemhuis H, Jeffrey H, Spelberg L, Janssen DB (2000) Characterization of the gene cluster involved in isoprene metabolism in *Rhodococcus* sp. strain AD45. J Bacteriol 182:1956–1963.

Van Hylckama Vlieg JET, Poelarends GJ, Mars A, Janssen DB (2000) Detoxification of reactive intermediates during microbial metabolism of halogenated compounds. Curr Opin Microbiol 3:257–262.

Im WT, Liu QM, Lee KJ, Kim SY, Lee ST, Yi TH (2010) *Variovorax ginsengisoli* sp. nov., a denitrifying bacterium isolated from soil of a ginseng field. Int J Syst Evol Microbiol 60:1565–1569.

Ivashkiv E (1973) Ampicillin. In: *Analytical Profiles of Drug Substrances*, 2nd ed. Florey K (ed) Academic Press, New York, p 26

Jaishankar J, Srivastava P (2017) Molecular basis of stationary phase survival and applications. Front Microbiol 8:doi: 10.3389/fmicb.2017.02000.

Jamieson WD, Pehl MJ, Gregory GA, Orwin PM (2009) Coordinated surface activities in Variovorax paradoxus EPS. BMC Microbiol 9:doi: 10.1186/1471-2180-9-124.

Jamshad M, Marco P De, Pacheco CC, Hanczar T, Murrell JC (2006) Identification , Mutagenesis , and Transcriptional Analysis of the Methanesulfonate Transport Operon of *Methylosulfonomonas methylovora*. Appl Environ Microbiol 72:276–283.

Janes W, Schulz GE (1990) The binding of the retro-analogue of glutathione disulfide to glutathione reductase. J Biol Chem 265:10443–10445.

Jardine KJ, Zorzanelli RF, Gimenez BO, Oliveira Piva LR de, Teixeira A, Fontes CG, Robles E, Higuchi N, Chambers JQ, Martin ST (2020) Leaf isoprene and monoterpene emission distribution across hyperdominant tree genera in the Amazon basin. Phytochemistry 175:112366.

Jenkin ME, Hayman GD (1999) Photochemical ozone creation potentials for oxygenated volatile organic compounds: Sensitivity to variations in kinetic and mechanistic parameters. Atmos Environ 33:1275–1293.

Jenkin ME, Young JC, Rickard AR (2015) The MCM v3.3.1 degradation scheme for isoprene. Atmos Chem Phys 15:11433–11459.

Jimenez-Diaz L, Caballero A, Segura A (2017) Pathways for the Degradation of Fatty Acids in Bacteria. In: *Aerobic Utilization of Hydrocarbons, Oils and Lipids*. Rojo F (ed) Springer International Publishing, Cham, p 1–23

Jin L, Kim KK, Ahn CY, Oh HM (2012) *Variovorax defluvii* sp. nov., isolated from sewage. Int jounal Syst Evol Microbiol 62:1779–1783.

Johnson CM, Grossman AD (2016) The composition of the cell envelope affects conjugation in *Bacillus subtilis*. J Bacteriol 198:1241 LP – 1249.

Johnson T, Newton GL, Fahey RC, Rawat M (2009) Unusual production of glutathione in Actinobacteria. Arch Microbiol 191:89–93.

Johnston A (2014) Molecular ecology of marine isoprene degradation. University of Essex

Johnston A, Crombie AT, El Khawand M, Sims L, Whited GM, McGenity TJ, Murrell JC (2017) Identification and characterisation of isoprene-degrading bacteria in an estuarine environment. Environ Microbiol 19:3526–3537.

Kaiser J, Jacob DJ, Zhu L, Travis KR, Fisher JA, González Abad G, Zhang L, Zhang X, Fried A, Crounse JD, Clair JMS, Wisthaler A (2018) High-resolution inversion of OMI formaldehyde columns to quantify isoprene emission on ecosystem-relevant scales: Application to the southeast US. Atmos Chem Phys 18:5483–5497.

Kamala-Kannan S, Lee KJ, Park SM, Chae JC, Yun BS, Lee YH, Park YJ, Oh BT (2010) Characterization of ACC deaminase gene in *Pseudomonas entomophila* strain PS-PJH isolated from the rhizosphere soil. J Basic Microbiol 50:200–205.

Kanagawa T, Dazai M, Fukuoka S (1982) Degradation of O,O-Dimethyl Phosphorodithioate by *Thiobacillus thioparus* TK-1 and *Pseudomonas* AK-2. Agric Biol Chem 46:2571–2578.

Kane SR, Chakicherla AY, Chain PSG, Schmidt R, Shin MW, Legler TC, Scow KM, Larimer FW, Lucas SM, Richardson PM, Hristova KR (2007) Whole-genome analysis of the methyl tert-butyl ether-degrading beta-proteobacterium *Methylibium petroleiphilum* PM1. J Bacteriol 189:1931–1945.

Kaniga K, Delor I, Cornelis GR (1991) A wide-host-range suicide vector for improving reverse genetics in Gram-negative bacteria: inactivation of the *blaA* gene of *Yersinia enterocolitica*. Gene 109:137–141.

Keltjens JT, Pol A, Reimann J, Op den Camp HJM (2014) PQQ-dependent methanol dehydrogenases: rare-earth elements make a difference. Appl Microbiol Biotechnol 98:6163–6183.

Kennedy DO (2016) B Vitamins and the Brain: Mechanisms, Dose and Efficacy—A Review. Nutrients 8:doi.org/10.3390/nu8020068.

Kesselmeier J, Staudt M (1999) An Overview on Emission, Physiology and Ecology. J Atmos Chem 33:23–88.

El Khawand M, Crombie AT, Johnston A, Vavlline D V., McAuliffe JC, Latone JA, Primak YA, Lee SK, Whited GM, McGenity TJ, Murrell JC (2016) Isolation of isoprene degrading bacteria from soils, development of isoA gene probes and identification of the active isoprene-degrading soil community using DNA-stable isotope probing. Environ Microbiol 18:2743–2753.

Kim BY, Weon HY, Yoo SH, Lee SY, Kwon SW, Go SJ, Stackebrandt E (2006) *Variovorax* soli sp. nov., isolated from greenhouse soil. Int J Syst Evol Microbiol 56:2899–2901.

Kirschneck C, Batschkus S, Proff P, Köstler J, Spanier G, Schröder A (2017) Valid gene expression normalization by RT-qPCR in studies on hPDL fibroblasts with focus on orthodontic tooth movement and periodontitis. Sci Rep 7:doi: 10.1038/s41598-017-15281-0.

Kleindienst TE, Edney EO, Lewandowski M, Offenberg JH, Jaoui M (2006) Secondary Organic Carbon and Aerosol Yields from the Irradiations of Isoprene and α-Pinene in the Presence of NOx and SO2. Environ Sci Technol

40:3807–3812.

Kleindienst TE, Jaoui M, Lewandowski M, Offenberg JH, Lewis CW, Bhave P V., Edney EO (2007a) Estimates of the contributions of biogenic and anthropogenic hydrocarbons to secondary organic aerosol at a southeastern US location. Atmos Environ 41:8288–8300.

Kleindienst TE, Lewandowski M, Offenberg JH, Jaoui M, Edney EO (2007b) Ozone-isoprene reaction: Re-examination of the formation of secondary organic aerosol. Geophys Res Lett 34:doi:10.1029/2006GL027485.

Kotani T, Yamamoto T, Yurimoto H, Sakai Y, Kato N (2003) Propane monooxygenase and NAD+-dependent secondary alcohol dehydrogenase in propane metabolism by *Gordonia* sp. strain TY-5. J Bacteriol 185:7120–7128.

Kottegoda S, Waligora E, Hyman M (2015) Metabolism of 2-Methylpropene (Isobutylene) by the Aerobic Bacterium *Mycobacterium* sp. Strain ELW1. Appl Environ Microbiol 81:1966–1976.

Kovach ME, Elzer PH, Hill DS, Robertson GT, Farris MA, Roop RM, Peterson KM (1995) Four new derivatives of the broad-host-range cloning vector PBBR1MCS, carrying different antibiotic-resistance cassettes. Gene 166:175–176.

Krause SMB, Johnson T, Samadhi Karunaratne Y, Fu Y, Beck DAC, Chistoserdova L, Lidstrom ME (2017) Lanthanide-dependent cross-feeding of methane-derived carbon is linked by microbial community interactions. Proc Natl Acad Sci U S A 114:358–363.

Kroll JH, Ng NL, Murphy SM, Flagan RC, Seinfeld JH (2006) Secondary organic aerosol formation from isoprene photooxidation. Environ Sci Technol 40:1869–1877.

Kroll JH, Ng NL, Murphy SM, Flagan RC, Seinfeld JH (2005) Secondary organic aerosol formation from isoprene photooxidation under high-NOx conditions. Geophys Res Lett 32:1–4.

Kronen M, Lee M, Jones ZL, Manefield MJ (2019) Reductive metabolism of the important atmospheric gas isoprene by homoacetogens. ISME J 13:1168–1182.

Krum JG, Ensign SA (2001) Evidence that a linear megaplasmid encodes enzymes of aliphatic alkene and epoxide metabolism and coenzyme M (2-Mercaptoethanesulfonate) biosynthesis in *Xanthobacter* strain Py2. J Bacteriol 183:2172–2177.

Krum JG, Ensign SA (2000) Heterologous expression of bacterial epoxyalkane:coenzyme M transferase and inducible coenzyme M biosynthesis in *Xanthobacter* strain Py2 and *Rhodococcus rhodochrous* B276. J Bacteriol 182:2629–2634.

Kumar S, Stecher G, Tamura K (2016) MEGA7: molecular evolutionary genetics analysis version 7.0 for bigger datasets. Mol Biol Evoution 33:1870–1874.

Kuzma J, Nemecek-Marshall M, Pollock WH, Fall R (1995) Bacteria produce the volatile hydrocarbon isoprene. Curr Microbiol 30:97–103.

Kwan AJ, Chan AWH, Ng NL, Kjaergaard HG, Seinfeld JH, Wennberg PO (2012) Peroxy radical chemistry and OH radical production during the NO 3-initiated oxidation of isoprene. Atmos Chem Phys 12:7499–7515.

Lane D. (1991) 16S/23S rRNA sequencing. In: *Nucleic Acid Techniques in Bacterial Systematics*. Stackebrant E, Goodfellow M (eds) John Wiley & Sons, New York, p 115–175

Lantz AT, Allman J, Weraduwage S., Sharkey TD (2019a) Isoprene: new insights into the control of emission and mediation of stress tolerance by gene expression. Plant Cell Environ 42:2808–2826.

Lantz AT, Solomon C, Gog L, McClain AM, Weraduwage SM, Cruz JA, Sharkey TD (2019b) Isoprene Suppression by CO2 Is Not Due to Triose Phosphate Utilization (TPU) Limitation. Front For Glob Chang 2:1–13.

Laothawornkitkul J, Paul ND, Vickers CE, Possell M, Taylor JE, Mullineaux PM, Hewitt CN (2008) Isoprene emissions influence herbivore feeding decisions. Plant, Cell Environ 31:1410–1415.

Larke-Mejía NL, Carrión O, Crombie AT, McGenity TJ, Murrell JC (2020) *Sphingopyxis* sp. Strain OPL5, an isoprene-degrading bacterium from the sphingomonadaceae family isolated from oil palm leaves. Microorganisms 8:doi:

10.3390/microorganisms8101557.

Larke-Mejía NL, Crombie AT, Pratscher J, McGenity TJ, Murrell JC (2019) Novel isoprene-degrading proteobacteria from soil and leaves identified by cultivation and metagenomics analysis of stable isotope probing experiments. Front Microbiol 10:doi: 10.3389/fmicb.2019.02700.

Leadbetter JR, Greenberg EP (2000) Metabolism of acyl-homoserine lactone quorum-sensing signals by *Variovorax paradoxus*. J Bacteriol 182:6921–6926.

Leahy JG, Batchelor PJ, Morcomb SM (2003) Evolution of the soluble diiron monooxygenases. FEMS Microbiol Rev 27:449–479.

Leahy JG, Johnson GR, Olsen RH (1997) Cross-regulation of toluene monooxygenases by the transcriptional activators TbmR and TbuT. Appl Environ Microbiol 63:3736–3739.

Leak DJ, Aikens PJ, Seyed-Mahmoudian M (1992) The microbial production of epoxides. Trends Biotechnol 10:256–261.

Leak DJ, Dalton H (1987) Studies On The Regioselectivity And Stereoselectivity Of The Soluble Methane Monooxygenase From *Methylococcus capsulatus* (Bath). Biocatalysis 1:23–36.

Lee SJ, McCormick MS, Lippard SJ, Cho U-S (2013) Control of substrate access to the active site in methane monooxygenase. Nature 494:380–384.

Lehning A, Zimmer I, Steinbrecher R, Bruggemann N, Schnitzler J-P (1999) Isoprene synthase activity and its relation to isoprene emission in *Quercus robur* L. leaves. Plant Cell Environ 22:495–504.

Li J, Wang G, Wu C, Cao C, Ren Y, Wang J, Li J, Cao J, Zeng L, Zhu T (2018a) Characterization of isoprene-derived secondary organic aerosols at a rural site in North China Plain with implications for anthropogenic pollution effects. Sci Rep 8:doi: 10.1038/s41598-017-18983-7.

Li M, Nian R, Xian M, Zhang H (2018b) Metabolic engineering for the production of isoprene and isopentenol by *Escherichia coli*. Appl Microbiol Biotechnol 102:7725–7738.

Li Z, Sharkey TD (2013) Metabolic profiling of the methylerythritol phosphate pathway reveals the source of post-illumination isoprene burst from leaves. Plant, Cell Environ 36:429–437.

Liang AD, Lippard SJ (2014) Component interactions and electron transfer in toluene/o-xylene monooxygenase. Biochemistry 53:7368–7375.

Lienkamp AC, Heine T, Tischler D (2020) Glutathione: A powerful but rare cofactor among Actinobacteria. Adv Appl Microbiol 12.

Lipscomb JD (1994) Biochemistry of the soluble methane monooxygenase. Annu Rev Microbiol 48:371–399.

Liu C, Feng S, Van Heemst J, McAdam KG (2010) New insights into the formation of volatile compounds in mainstream cigarette smoke. Anal Bioanal Chem 396:1817–1830.

Liu KE, Valentine AM, Wang D, Huynh BH, Edmondson DE, Salifoglou A, Lippard SJ (1995a) Kinetic and spectroscopic characterization of intermediates and component interactions in reactions of methane monooxygenase from *Methylococcus capsulatus* (Bath). J Am Chem Soc 117:10174–10185.

Liu X, Mattes TE (2016) Epoxyalkane:coenzyme M transferase gene diversity and distribution in groundwater samples from chlorinated-ethenecontaminated sites. Appl Environ Microbiol 82:3269–3279.

Liu Y, Brito J, Dorris MR, Rivera-Rios JC, Seco R, Bates KH, Artaxo P, Duvoisin S, Keutsch FN, Kim S, Goldstein AH, Guenther AB, Manzi AO, Souza RAF, Springston SR, Watson TB, McKinney KA, Martin ST (2016) Isoprene photochemistry over the Amazon rainforest. Proc Natl Acad Sci 113:6125–6130.

Liu YY, Nesheim JC, Lee SK, Lipscomb JD (1995b) Gating effects of component B on oxygen activation by the methane monooxygenase hydroxylase component. J Biol Chem 270:24662–24665.

Liu Z-H, Cao Y-M, Zhou Q-W, Guo K, Ge F, Hou J-Y, Hu S-Y, Yuan S, Dai Y-J (2013) Acrylamide biodegradation ability

and plant growth-promoting properties of *Variovorax boronicumulans* CGMCC 4969. Biodegradation 24:855–864.

Lloyd JS, De Marco P, Dalton H, Murrell JC (1999) Heterologous expression of soluble methane monooxygenase genes in methanotrophs containing only particulate methane monooxygenase. Arch Microbiol 171:364–370.

Lock M, Nichol T, Murrell JC, Smith TJ (2017) Mutagenesis and expression of methane monooxygenase to alter regioselectivity with aromatic substrates. FEMS Microbiol Lett 364:doi.org/10.1093/femsle/fnx137.

Logan BA, Anchordoquy TJ, Monson RK, Pan RS (1999) The effect of isoprene on the properties of spinach thylakoids and phosphatidylcholine liposomes. Plant Biol 1:602–606.

Loreto F, Sharkey TD (1990) A gas-exchange study of photosynthesis and isoprene emission in *Quercus rubra* L. Planta 182:523–531.

Loreto F, Velikova V (2001) Isoprene Produced by Leaves Protects the Photosynthetic Apparatus against Ozone Damage, Quenches Ozone Products, and Reduces Lipid Peroxidation of Cellular Membranes. Plant Physiol 127:1781–1787.

Lukas H, Reimann J, Kim O Bin, Grimpo J, Unden G (2010) Regulation of aerobic and anaerobic D-malate metabolism of *Escherichia coli* by the LysR-type regulator DmlR (YeaT). J Bacteriol 192:2503–2511.

Lund J, Dalton H (1985) Further characterisation of the FAD and Fe2S2 redox centres of component C, the NADH: acceptor reductase of the soluble methane monooxygenase of *Methylococcus capsulatus* (Bath). Eur J Biochem 147:291–296.

Luo G, Yu F (2010) A numerical evaluation of global oceanic emissions of α-pinene and isoprene. Atmos Chem Phys 10:https://doi.org/10.5194/acp-10-2007-2010.

Lv H, Sahin N, Tani A (2020) *Methylotenera oryzisoli* sp. nov., a lanthanide-dependent methylotrophic bacteria isolated from rice field soil. Int J Syst Evol Microbiol:2713–2718.

Maceachran DP, Sinskey AJ (2013) The *Rhodococcus opacus* TadD protein mediates triacylglycerol metabolism by regulating intracellular NAD(P)H pools. Microb Cell Fact 12:doi: 10.1186/1475-2859-12-104.

Maddocks SE, Oyston PCF (2008) Structure and function of the LysR-type transcriptional regulator (LTTR) family proteins. Microbiology 154:3609–3623.

Madsen EL (2011) Stable Isotope Probing Techniques and Bioremediation. In: *Stable Isotope Probing and Related Technologies*. Murrell JC, Whiteley AS (eds) American Society for Microbiology Press, Washington, DC, p 186

Maness MJ, Foster GC, Sparling PF (1974) Ribosomal resistance to streptomycin and spectinomycin in *Neisseria gonorrhoeae*. J Bacteriol 120:1293–1299.

Marco PDE, Moradas-ferreira P, Higgins TP, Donald IANMC, Kenna EM, Murrell JC (1999) Molecular Analysis of a Novel Methanesulfonic Acid Monooxygenase from the Methylotroph *Methylosulfonomonas methylovora*. J Bacteriol 181:2244–2251.

Martirani-Von Abercron S-M, Marín P, Solsona-Ferraz M, Castañeda-Cataña M-A, Marqués S (2017) Naphthalene biodegradation under oxygen-limiting conditions: community dynamics and the relevance of biofilm-forming capacity. Microb Biotechnol 10:1781–1796.

Marx CJ, Lidstrom ME (2002) Broad-host-range cre-lox system for antibiotic marker recycling in Gram-negative bacteria. Biotechniques 33:1062–1067.

Marx CJ, Lidstrom ME (2018) Development of improved versatile broad-host-range vectors for use in methylotrophs and other Gram-negative bacteria. Microbiology 147:2065–2075.

Massey LK, Sokatch JR, Conrad RS (1976) Branched chain amino acid catabolism in bacteria. Bacteriol Rev 40:42–54.

Matthews KS, Nichols JC (1997) Lactose Repressor Protein: Functional Properties and Structure. In: *Progress in Nucleic Acid Research an Molecular Biology*. Moldave KBT-P in NAR and MB (ed) Academic Press, p 127–164

McCarl V, Somerville M V, Ly M, Henry R, Liew EF, Wilson NL, Holmes AJ, Coleman N V (2018) Heterologous expression of *Mycobacterium* alkene monooxygenases in Gram-positive and Gram-negative bacterial hosts. Appl Environ Microbiol 84:1–16.

McClain AM, Sharkey TD (2019) Triose phosphate utilization and beyond: From photosynthesis to end product synthesis. J Exp Bot 70:1755–1766.

McClay K, Fox BG, Steffan RJ (1996) Chloroform mineralization by toluene-oxidizing bacteria. Appl Environ Microbiol 62:2716–2722.

McClay K, Fox BG, Steffan RJ, McClay K, Fox BG, Steffan RJ, Clay KMC, Fox BG, Steffan RJ (2000) Toluene monooxygenase-catalyzed epoxidation of alkenes. Appl Environ Microbiol 66:1877–1882.

McCormick MS, Lippard SJ (2012) Analysis of Substrate Access to Active Sites in Bacterial Multicomponent Monooxygenase Hydroxylases: X-ray Crystal Structure of Xenon-Pressurized Phenol Hydroxylase from *Pseudomonas* sp. OX1. Biochemistry 51:573.

McGenity TJ, Crombie AT, Murrell JC (2018) Microbial cycling of isoprene, the most abundantly produced biological volatile organic compound on Earth. ISME J 12:931–941.

McLaggan D, Logan TM, Lynn DG, Epstein W (1990) Involvement of γ-glutamyl peptides in osmoadaptation of *Escherichia coli*. J Bacteriol 172:3631–3636.

McMillan M, Pereg L (2014) Evaluation of reference genes for gene expression analysis using quantitative RT-PCR in *Azospirillum brasilense*. PLoS One 9:e98162–e98162.

Meinert C, Schürmann M, Domeyer JE, Poehlein A, Daniel R, Steinbüchel A (2018) The unexpected function of a Flavin-dependent oxidoreductase from *Variovorax paradoxus* TBEA6. FEMS Microbiol Lett 365:doi: org/10.1093/femsle/fny011.

Men X, Wang F, Chen GQ, Zhang HB, Xian M (2019) Biosynthesis of natural rubber: Current state and perspectives. Int J Mol Sci 20:doi: org/10.3390/ijms20010050.

Michalska K, Chang C, Mack JC, Zerbs S, Joachimiak A, Collart FR (2012) Characterization of transport proteins for aromatic compounds derived from lignin: benzoate derivative binding proteins. J Mol Biol 423:555–575.

Misztal PK, Nemitz E, Langford B, Di Marco CF, Phillips GJ, Hewitt CN, MacKenzie AR, Owen SM, Fowler D, Heal MR, Cape JN (2011) Direct ecosystem fluxes of volatile organic compounds from oil palms in South-East Asia. Atmos Chem Phys 11:8995–9017.

Mitchell KH, Studts JM, Fox BG (2002) Combined Participation of Hydroxylase Active Site Residues and Effector Protein Binding in a Para to Ortho Modulation of Toluene 4-Monooxygenase Regiospecificity. Biochemistry 41:3176–3188.

Miura A, Dalton H (1995) Purification and characterization of the alkene monooxygenase from *Nocardia corallina* B-276. Biosci Biotechnol Biochem 59:853–859.

Molinier J, Ries G, Zipfel C, Hohn B (2006) Transgeneration memory of stress in plants. Nature 442:1046–1049.

Monks PS, Archibald AT, Colette A, Cooper O, Coyle M, Derwent R, Fowler D, Granier C, Law KS, Mills GE, Stevenson DS, Tarasova O, Thouret V, Von Schneidemesser E, Sommariva R, Wild O, Williams ML (2015) Tropospheric ozone and its precursors from the urban to the global scale from air quality to short-lived climate forcer. Atmos Chem Phys 15:8889–8973.

Monson RK, Fall R (1989) Isoprene emission from aspen leaves : influence of environment and relation to photosynthesis and photorespiration. Plant Physiol 90:267–74.

Monson RK, Neice AA, Trahan NA, Shiach I, McCorkel JT, Moore DJP (2016) Interactions between temperature and intercellular CO2 concentration in controlling leaf isoprene emission rates. Plant Cell Environ 39:2404–2413.

Moonen JH, Kamerbeek NM, Westphal AH, Boeren SA, Janssen DB, Fraaije MW, Berkel WJH Van (2008) Elucidation of the 4-Hydroxyacetophenone catabolic pathway in *Pseudomonas fluorescens* ACB. J Bacteriol 190:5190–5198.

Murrell JC, Gilbert B, McDonald IR (2000) Molecular biology and regulation of methane monooxygenase. Arch Microbiol 173:325–332.

Nakagawa T, Mitsui R, Tani A, Sasa K, Tashiro S, Iwama T, Hayakawa T, Kawai K (2012) A catalytic role of XoxF1 as La3+-dependent methanol dehydrogenase in *Methylobacterium extorquens* strain AM1. PLoS One 7:e50480.

Nakashima N, Tamura T (2004) Isolation and Characterization of a Rolling-Circle-Type Plasmid from *Rhodococcus erythropolis* and Application of the Plasmid to Multiple-Recombinant-Protein Expression. Appl Environ Microbiol 70:5557–5568.

Natsagdorj O, Sakamoto H, Santiago DMO, Santiago CD, Orikasa Y, Okazaki K, Ikeda S, Ohwada T (2019) *Variovorax* sp. has an optimum cell density to fully function as a plant growth promoter. Microorganisms 7:doi: 10.3390/microorganisms7030082.

Neretin LN, Schippers A, Pernthaler A, Hamann K, Amann R, Jørgensen BB (2003) Quantification of dissimilatory (bi)sulphite reductase gene expression in *Desulfobacterium autotrophicum* using real-time RT-PCR. Environ Microbiol 5:660–671.

Nestorowicz K, Jaoui M, Jan Rudzinski K, Lewandowski M, Kleindienst TE, Spólnik G, Danikiewicz W, Szmigielski R (2018) Chemical composition of isoprene SOA under acidic and non-acidic conditions: Effect of relative humidity. Atmos Chem Phys 18:18101–18121.

Newman LM, Wackett LP (1997) Trichloroethylene oxidation by purified toluene 2-monooxygenase: Products, kinetics, and turnover-dependent inactivation. J Bacteriol 179:90–96.

Nichol T, Murrell JC, Smith TJ (2015) Controlling the Activities of the Diiron Centre in Bacterial Monooxygenases: Lessons from Mutagenesis and Biodiversity. Eur J Inorg Chem 2015:3419–3431.

Nielsen AK, Gerdes K, Degn H, Murrell JC (1996) Regulation of bacterial methane oxidation: Transcription of the soluble methane mono-oxygenase operon of *Methylococcus capsulatus* (Bath) is repressed by copper ions. Microbiology 142:1289–1296.

Nieto PA, Covarrubias PC, Jedlicki E, Holmes DS, Quatrini R (2009) Selection and evaluation of reference genes for improved interrogation of microbial transcriptomes: case study with the extremophile *Acidithiobacillus ferrooxidans*. BMC Mol Biol 10:doi: 10.1186/1471-2199-10-63.

Nisbet EG, Dlugokencky EJ, Manning MR, Lowry D, Fisher RE, France JL, Michel SE, Miller JB, White JWC, Vaughn B, Bousquet P, Pyle JA, Warwick NJ, Cain M, Brownlow R, Zazzeri G, Lanoisellé M, Manning AC, Gloor E, Worthy DEJ, Brunke E-G, Labuschagne C, Wolff EW, Ganesan AL (2016) Rising atmospheric methane: 2007–2014 growth and isotopic shift. Global Biogeochem Cycles 30:1356–1370.

Nkongolo KK, Narendrula-Kotha R (2020) Advances in monitoring soil microbial community dynamic and function. J Appl Genet:249–263.

Nordlund I, Powlowski J, Shingler V (1990) Complete nucleotide sequence and polypeptide analysis of multicomponent phenol hydroxylase from *Pseudomonas* sp. strain CF600. J Bacteriol 172:6826–6833.

Nozire B, Gonzlez NJD, Borg-Karlson AK, Pei Y, Redeby JP, Krejci R, Dommen J, Prevot ASH, Anthonsen T (2011) Atmospheric chemistry in stereo: A new look at secondary organic aerosols from isoprene. Geophys Res Lett 38:doi: 10.1029/2011GL047323.

Oelschlägel M, Zimmerling J, Tischler D (2018) A Review: The Styrene Metabolizing Cascade of Side-Chain Oxygenation as Biotechnological Basis to Gain Various Valuable Compounds. Front Microbiol 9:doi: 10.3389/fmicb.2018.00490.

Oldenhuis R, Oedzes JY, Van Der Waarde JJ, Janssen DB (1991) Kinetics of chlorinated hydrocarbon degradation by *Methylosinus trichosporium* OB3b and toxicity of trichloroethylene. Appl Environ Microbiol 57:7–14.

Ono M, Okura I (1990) On the reaction mechanism of alkene epoxidation with *Methylosinus trichosporium* (OB3b). J Mol Catal 61:113–122.

Osterman IA, Dikhtyar YY, Bogdanov AA, Dontsova OA, Sergiev P V. (2015) Regulation of flagellar gene expression in

Bacteria. Biochem 80:1447–1456.

Otani H, Stogios PJ, Xu X, Nocek B, Li S-N, Savchenko A, Eltis LD (2016) The activity of CouR, a MarR family transcriptional regulator, is modulated through a novel molecular mechanism. Nucleic Acids Res 44:595–607.

Otu-Larbi F, Bolas CG, Ferracci V, Staniaszek Z, Jones RL, Malhi Y, Harris NRPP, Wild O, Ashworth K, Conor FO, Valerio GB, Zosia F, Jones RL, Malhi Y, Harris NRPP, Wild O, Ashworth K, Otu-Larbi F, Bolas CG, Ferracci V, Staniaszek Z, Jones RL, Malhi Y, Harris NRPP, Wild O, Ashworth K (2020) Modelling the effect of the 2018 summer heatwave and drought on isoprene emissions in a UK woodland. Glob Chang Biol 26:2320–2335.

Overbeek R, Olson R, Pusch GD, Olsen GJ, Davis JJ, Disz T, Edwards RA, Gerdes S, Parrello B, Shukla M, Vonstein V, Wattam AR, Xia F, Stevens R (2014) The SEED and the Rapid Annotation of microbial genomes using Subsystems Technology (RAST). Nucleic Acids Res 42:206–214.

Öztürk B, Werner J, Meier-Kolthoff JP, Bunk B, Spröer C, Springael D (2020) Comparative genomics suggests mechanisms of genetic adaptation towards the catabolism of the phenylurea herbicide linuron in *Variovorax*. Genome Biol Evol 12:827–841.

Palmer PI, Shaw SL (2005) Quantifying global marine isoprene fluxes using MODIS chlorophyll observations. Geophys Res Lett 32:doi: 10.1029/2005GL022592.

Park YR, Yoo HS, Song MY, Lee DH, Lee SJ (2018) Biocatalytic oxidations of substrates through soluble methane monooxygenase from *Methylosinus sporium*. Catalysts 8:doi: 10.3390/catal8120582.

Parke D (1996) Characterization of PcaQ, a LysR-type transcriptional activator required for catabolism of phenolic compounds, from *Agrobacterium tumefaciens*. J Bacteriol 178:266–272.

Parke D (1990) Construction of mobilizable vectors derived from plasmids RP4, pUC18 and pUC19. Gene 93:135–137.

Parke D (1995) Supraoperonic clustering of pca genes for catabolism of the phenolic compound protocatechuate in *Agrobacterium tumefaciens*. J Bacteriol 177:3808–3817.

Payankaulam S, Li LM, Arnosti DN (2010) Transcriptional repression: conserved and evolved features. Curr Biol 20:R764–R771.

Pehl M., Jamieson WD, Kong K, Forbester J., Fredendall R., Gregory G., Mcfarland J., Healy J., Orwin P. (2012) Genes That Influence Swarming Motility and Biofilm Formation in *Variovorax paradoxus* EPS. PLoS One 7:doi: 10.1371/journal.pone.0031832.

Pell EJ, Schlagnhaufer CD, Arteca RN (1997) Ozone-induced oxidative stress: Mechanisms of action and reaction. Physiol Plant 100:264–273.

Pelletier DA, Harwood CS (1998) 2-Ketocyclohexanecarboxyl coenzyme A hydrolase, the ring cleavage enzyme required for anaerobic benzoate degradation by *Rhodopseudomonas palustris*. J Bacteriol 180:2330–2336.

Perera IC, Grove A (2010) Molecular mechanisms of ligand-mediated attenuation of DNA binding by MarR family transcriptional regulators. J Mol Cell Biol 2:243–254.

Petkevičius V, Vaitekūnas J, Vaitkus D, Čėnas N, Meškys R (2019) Tailoring a soluble Diiron monooxygenase for synthesis of aromatic N-oxides. Catalysts 9:doi: 10.3390/catal9040356.

Pikus JD, Studts JM, Achim C, Kauffmann KE, Münck E, Steffan RJ, McClay K, Fox BG (1996) Recombinant toluene-4-monooxygenase: Catalytic and Mossbauer studies of the purified diiron and Rieske components of a four-protein complex. Biochemistry 35:9106–9119.

Pikus JD, Studts JM, McClay K, Steffan RJ, Fox BG (1997) Changes in the Regiospecificity of Aromatic Hydroxylation Produced by Active Site Engineering in the Diiron Enzyme Toluene 4-Monooxygenase. Biochemistry 36:9283–9289.

Pinchbeck BJ (2016) Regulation of Nitrate and Nitrite Assimilation in *Paracoccus denitrificans* at the Level of RNA. University of East Anglia

Plewka A, Gnauk T, Brüggemann E, Herrmann H (2006) Biogenic contributions to the chemical composition of

airborne particles in a coniferous forest in Germany. Atmos Environ 40:103–115.

Polikanov YS, Aleksashin NA, Beckert B, Wilson DN (2018) The Mechanisms of Action of Ribosome-Targeting Peptide Antibiotics. Front Mol Biosci 5:doi: 10.3389/fmolb.2018.00048.

Posman KM, DeRito CM, Madsen EL (2017) Benzene degradation by a *Variovorax* species within a coal tar-contaminated groundwater microbial community. Appl Environ Microbiol 83:doi: 10.1128/AEM.02658-16.

Poteete AR, Rosadini C, St. Pierre C (2006) Gentamicin and other cassettes for chromosomal gene replacement in *Escherichia coli*. Biotechniques 41:261–264.

Prasad B (2017) Biodegradation of ortho-dimethyl phthalate by a binary culture of *Variovorax* sp. BS1 and *Achromobacter denitrificans*. Int J Environ Sci Technol 14:2575–2582.

Prior SD, Dalton H (1985) Acetylene as a suicide substrate and active site probe for methane monooxygenase from *Methylococcus capsulatus* (Bath). FEMS Microbiol Lett 29:105–109.

Pyne ME, Moo-Young M, Chung DA, Chou CP (2013) Development of an electrotransformation protocol for genetic manipulation of *Clostridium pasteurianum*. Biotechnol Biofuels 6:50.

Quayle JR, Pfennig N (1975) Utilization of methanol by *Rhodospirillaceae*. Arch Microbiol 102:193–198.

Radajewski S, Ineson P, Parekh NR, Murrell JC (2000) Stable-isotope probing as a tool in microbial ecology. Nature 403:646–649.

Rasulov B, Copolovici L, Laisk A, Niinemets Ü (2009) Postillumination isoprene emission: in vivo measurements of dimethylallyldiphosphate pool size and isoprene synthase kinetics in aspen leaves. Plant Physiol 149:1609–1618.

Raux E, Lanois A, Levillayer F, Warren MJ, Brody E, Rambach A, Thermes C (1996) *Salmonella typhimurium* cobalamin (vitamin B12) biosynthetic genes: Functional studies in *S. typhimurium* and Esch*Escherichia coli*. J Bacteriol 178:753–767.

Reed JL, Patel TR, Chen KH, Joyce AR, Applebee MK, Herring CD, Bui OT, Knight EM, Fong SS, Palsson BO (2006) Systems approach to refining genome annotation. Proc Natl Acad Sci U S A 103:17480–17484.

Richards AO, Stanley SH, Suzuki M, Dalton H (1994) The Biotransformation of Propylene to Propylene Oxide by *Methylococcus capsulatus* (Bath): 3. Reactivation of Inactivated Whole Cells to Give a High Productivity System. Biocatalysis 8:253–267.

Rinaldo D, Philipp DM, Lippard SJ, Friesner RA (2007) Intermediates in dioxygen activation by methane monooxygenase: A QM/MM study. J Am Chem Soc 129:3135–3147.

Robinson AD, Millard GA, Danis F, Guirlet M, Harris NRP, Lee AM, McIntyre JD, Pyle JA, Arvelius J, Dagnesjo S, Kirkwood S, Nilsson H, Toohey DW, Deshler T, Goutail F, Pommereau J-P, Elkins JW, Moore F, Ray E, Schmidt U, Engel A, Müller M (2005) Ozone loss derived from balloon-borne tracer measurements in the 1999/2000 Arctic winter. Atmos Chem Phys 5:1423–1436.

Rohwerder T, Rohde M, Jehmlich N, Purswani J (2020) Actinobacterial Degradation of 2-Hydroxyisobutyric Acid Proceeds via Acetone and Formyl-CoA by Employing a Thiamine-Dependent Lyase Reaction. Front Microbiol 11:1–12.

Rojo F (1999) Repression of transcription initiation in bacteria. J Bacteriol 181:2987–2991.

Rosano GL, Ceccarelli EA (2014) Recombinant protein expression in *Escherichia coli*: advances and challenges. Front Microbiol 5:doi: 10.3389/fmicb.2014.00172.

Rosenkoetter KE, Kennedy CR, Chirik PJ, Harvey BG (2019) [4 + 4]-cycloaddition of isoprene for the production of high-performance bio-based jet fuel. Green Chem 21:5616–5623.

Rosenstiel TN, Ebbets AL, Khatri WC, Fall R, Monson RK (2004) Induction of poplar leaf nitrate reductase: a test of extrachloroplastic control of isoprene emission rate. Plant Biol (Stuttg) 6:12–21.

Rosenzweig AC, Brandstetter H, Whittington DA, Nordlund P, Lippard SJ, Frederick CA (1997) Crystal structures of the methane monooxygenase hydroxylase from *Methylococcus capsulatus* (Bath): Implications for substrate gating and component interactions. Proteins Struct Funct Genet 29:141–152.

Ross MOMO, Rosenzweig AC (2017) A tale of two methane monooxygenases. J Biol Inorg Chem 22:307–319.

Roth JR, Lawrence JG, Rubenfield M, Kieffer-Higgins S, Church GM (1993) Characterization of the cobalamin (vitamin B12) biosynthetic genes of *Salmonella typhimurium*. J Bacteriol 175:3303–3316.

Routledge SJ (2012) Beyond de-foaming: the effects of antifoams on bioprocess productivity. Comput Struct Biotechnol J 3:doi: 10.5936/csbj.201210014.

Rui L, Kwon YM, Fishman A, Reardon KF, Wood TK (2004) Saturation mutagenesis of toluene ortho-monooxygenase of *Burkholderia cepacia* G4 for enhanced 1-naphthol synthesis and chloroform degradation. Appl Environ Microbiol 70:3246–3252.

Ryan AC, Hewitt CN, Possell M, Vickers CE, Purnell A, Mullineaux PM, Davies WJ, Dodd IC (2014) Isoprene emission protects photosynthesis but reduces plant productivity during drought in transgenic tobacco (*Nicotiana tabacum*) plants. New Phytol 201:205–216.

Saeki H, Akira M, Furuhashi K, Averhoff B, Gottschalk G (1999) Degradation of trichloroethene by a linear-plasmid-encoded alkene monooxygenase in *Rhodococcus corallinus* (*Nocardia corallina*) B-276. Microbiology 145:1721–1730.

Sakuda A, Suzuki-Minakuchi C, Matsui K, Takahashi Y, Okada K, Yamane H, Shintani M, Nojiri H (2018) Divalent cations increase the conjugation efficiency of the incompatibility P-7 group plasmid pCAR1 among different *Pseudomonas* hosts. Microbiol (United Kingdom) 164:20–27.

Sanadze GA, Kalanadze AN (1966) Light and temperature curves of the evolution of C5H8. Fiziol Rastenii 13:458–461.

Sander R (2015) Compilation of Henry's law constants (version 4.0) for water as solvent. Atmos Chem Phys 15:4399–4981.

Sanderson MG, Jones CD, Collins WJ, Johnson CE, Derwent RG (2003) Effect of climate change on isoprene emissions and surface ozone levels. Geophys Res Lett 30:10–13.

Satola B, Wübbeler JH, Steinbüchel A (2013) Metabolic characteristics of the species *Variovorax paradoxus*. Appl Microbiol Biotechnol 97:541–560.

Satsuma K (2010) Mineralisation of the herbicide linuron by *Variovorax* sp. strain RA8 isolated from Japanese river sediment using an ecosystem model (microcosm). Pest Manag Sci 66:847–852.

Sazinsky MH, Bard J, Di Donato A, Lippard SJ (2004) Crystal structure of the toluene/o-xylene monooxygenase hydroxylase from *Pseudomonas stutzeri* OX1: Insight into the substrate specificity, substrate channeling, and active site tuning of multicomponent monooxygenases. J Biol Chem 279:30600–30610.

Schaefer JK, Goodwin KD, McDOnald IR, Murrell JC, Oremland RS (2002) *Leisingera methylohalidivorans* gen. nov., sp. nov., a marine methylotroph that grows on methyl bromide. Int jounal Syst Evol Microbiol 52:doi: 10.1099/00207713-52-3-851.

Schäfer A, Tauch A, Jsger W, Kalinowski JJ, Thierbachb G, Piihler A, Jager W, Kalinowski JJ, Thierbach G, Puler A (1994) Small mobilizable multi-purpose cloning vectors derived from the *Escherichia coli* plasmids pK18 and pK19: selection of defined deletions in the chromosome of *Corynebacterium glutamicum*. Gene 145:69–73.

Schell MA (1993) Molecular biology of the LysR family of transcriptional regulators. Annu Rev Microbiol 47:597–626.

Schmidt S, Christen P, Kiefer P, Vorholt JA (2010) Functional investigation of methanol dehydrogenase-like protein XoxF in *Methylobacterium extorquens* AM1. Microbiology 156:2575–2586.

Schmittgen TD, Livak KJ (2008) Analyzing real-time PCR data by the comparative CT method. Nat Protoc 3:1101–1108.

Schürmann M, Hirsch B, Wübbeler JH, Stöveken N, Steinbüchel A (2013) Succinyl-CoA:3-sulfinopropionate CoA-

transferase from *Variovorax paradoxus* strain TBEA6, a novel member of the class III coenzyme a (CoA)-transferase family. J Bacteriol 195:3761–3773.

Scott CE, Monks SA, Spracklen D V., Arnold SR, Forster PM, Rap A, Äijälä M, Artaxo P, Carslaw KS, Chipperfield MP, Ehn M, Gilardoni S, Heikkinen L, Kulmala M, Petäjä T, Reddington CLS, Rizzo L V., Swietlicki E, Vignati E, Wilson C (2018) Impact on short-lived climate forcers increases projected warming due to deforestation. Nat Commun 9:doi: 10.1038/s41467-017-02412-4.

Seinfeld JH, Pandis SN (2006) Atmospheric Chemistry and Physics. From air pollution to climate change, Second Edi. Seinfeld JH, Pandis SN (eds) John Wiley & Sons, Hoboken, NJ.

Sharkey TD, Chen X, Yeh S (2001) Isoprene increases thermotolerance of fosmidomycin-fed leaves. Plant Physiol 125:2001–2006.

Sharkey TD, Singsaas EL (1995) Why plants emit isoprene. Nature 374:doi: 10.1038/374769a0.

Sharkey TD, Singsaas EL, Vanderveer PJ, Geron C (1996) Field measurements of isoprene emission from trees in response to temperature and light. Tree Physiol 16:649–654.

Sharkey TD, Wiberley AE, Donohue AR (2008) Isoprene emission from plants: Why and how. Ann Bot 101:5–18.

Sharkey TD, Yeh S (2001) Isoprene emission from plants. Annu Rev Plant Physiol Plant Mol Biol 52:407–436.

Shaw SL, Gantt B, Meskhidze N (2010) Production and emissions of marine isoprene and monoterpenes: a review. Adv Meteorol 2010:doi: 10.1155/2010/408696.

Shehadul Islam M, Aryasomayajula A, Selvaganapathy PR (2017) A review on macroscale and microscale cell lysis methods. Micromachines 8:doi: 10.3390/mi8030083.

Shields MS, Montgomery SO, Chapman PJ, Cuskey SM, Pritchard PH (1989) Novel pathway of toluene catabolism in the trichloroethylene-degrading bacterium G4. Appl Environ Microbiol 55:1624–1629.

Shingler V, Franklin FC, Tsuda M, Holroyd D, Bagdasarian M (1989) Molecular analysis of a plasmid-encoded phenol hydroxylase from *Pseudomonas* CF600. J Gen Microbiol 135:1083–1092.

Shu K, Zhou W, Chen F, Luo X, Yang W (2018) Abscisic Acid and Gibberellins Antagonistically Mediate Plant Development and Abiotic Stress Responses. Front Plant Sci 9:doi: 10.3389/fpls.2018.00416.

Shu L, Nesheim JC, Kauffmann K, Münck E, Lipscomb JD, Que L (1997) An Fe2(IV)O2 Diamond Core Structure for the Key Intermediate Q of Methane Monooxygenase. Science (80-) 275:515–518.

Silva SJ, Heald CL, Geddes JA, Austin KG, Kasibhatla PS, Marlier ME (2016) Impacts of current and projected oil palm plantation expansion on air quality over Southeast Asia. Atmos Chem Phys 16:10621–10635.

Silver GM, Fall R (1995) Characterization of Aspen Isoprene Synthase, an Enzyme Responsible for Leaf Isoprene Emission to the Asmosphere. J Biol Chem 270:13010–13016.

Sims L (2020) Purification and characterisation of isoprene monooxygenase from *Rhodococcus* sp. AD45. University of East Anglia, Norwich, UK

Sindelarova K, Granier C, Bouarar I, Guenther A, Tilmes S, Stavrakou T, Müller JF, Kuhn U, Stefani P, Knorr W (2014) Global data set of biogenic VOC emissions calculated by the MEGAN model over the last 30 years. Atmos Chem Phys 14:9317–9341.

Singh A, Srivastava N, Dubey SK (2019) Molecular characterization and kinetics of isoprene degrading bacteria. Bioresour Technol 278:51–56.

Singsaas EL, Lerdau M, Winter K, Sharkey TD (1997) Isoprene increases thermotolerance of isoprene-emitting species. Plant Physiol 115:1413–1420.

Sirajuddin S, Rosenzweig AC (2015) Enzymatic oxidation of methane. Biochemistry 54:2283–2294.

Small FJ, Ensign SA (1997) Alkene monooxygenase from *Xanthobacter* strain Py2. J Biol Chem 272:24913–24920.

Smirnova A V, Dunfield PF (2018) Differential Transcriptional Activation of Genes Encoding Soluble Methane Monooxygenase in a Facultative Versus an Obligate Methanotroph. Microorganisms 6:doi: 10.3390/microorganisms6010020.

Smirnova G V., Oktyabrsky ON (2005) Glutathione in bacteria. Biokhimiya 70:1459–1473.

Smith AW, Iglewski BH (1989) Transformation of *Pseudomonas aeruginosa* by electroporation. Nucleic Acids Res 17:10509.

Smith TJ, Slade SE, Burton NP, Murrell JC, Dalton H (2002) Improved System for Protein Engineering of the Hydroxylase Component of Soluble Methane Monooxygenase. Appl Environ Microbiol 68:5265–5273.

Som NF, Heine D, Holmes NA, Munnoch JT, Chandra G, Seipke RF, Hoskisson PA, Wilkinson B, Hutchings MI (2017) The conserved actinobacterial two-component system MtrAB coordinates chloramphenicol production with sporulation in *Streptomyces venezuelae* NRRL B-65442. Front Microbiol 8:doi: 10.3389/fmicb.2017.01145.

Song WJ, Gucinski G, Sazinsky MH, Lippard SJ (2011) Tracking a defined route for O2 migration in a dioxygen-activating diiron enzyme. Proc Natl Acad Sci 108:14795–14800.

Squire OJ, Archibald AT, Griffiths PT, Jenkin ME, Smith D, Pyle JA (2015) Influence of isoprene chemical mechanism on modelled changes in tropospheric ozone due to climate and land use over the 21st century. Atmos Chem Phys 15:5123–5143.

Srivastva N, Shukla AK, Singh RS, Upadhyay SN, Dubey SK (2015) Characterization of bacterial isolates from rubber dump site and their use in biodegradation of isoprene in batch and continuous bioreactors. Bioresour Technol 188:84–91.

Srivastva N, Vishwakarma P, Bhardwaj Y, Singh A, Manjunath K, Dubey SK (2017) Kinetic and molecular analyses reveal isoprene degradation potential of *Methylobacterium* sp. Bioresour Technol 242:87–91.

Stabb E V., Ruby EG (2002) RP4-based plasmids for conjugation between *Escherichia coli* and members of the vibrionaceae. Methods Enzymol 358:413–426.

Stafford GP, Scanlan J, McDonald IR, Murell JC (2003) *RpoN*, *mmoR* and *mmoG*, genes involved in regulating the expression of soluble methane monooxygenase in *Methylosinus trichosporium* OB3b. Microbiology 149:1771–1784.

Steinbüchel A (2003) Production of rubber-like polymers by microorganisms. Curr Opin Microbiol 6:261–270.

Steinke M, Hodapp B, Subhan R, Bell TG, Martin-Creuzburg D (2018) Flux of the biogenic volatiles isoprene and dimethyl sulfide from an oligotrophic lake. Sci Rep 8:doi: 10.1038/s41598-017-18923-5.

Steinmetz M, Le Coq D, Aymerich S, Gonzy-Tréboul G, Gay P (1985) The DNA sequence of the gene for the secreted *Bacillus subtilis* enzyme levansucrase and its genetic control sites. Mol Gen Genet MGG 200:220–228.

Stephan L, Tilmes V, Hülskamp M (2019) Selection and validation of reference genes for quantitative Real-Time PCR in Arabis alpina. PLoS One 14:doi: 10.1371/journal.pone.0211172.

Stirling DI, Dalton H (1979) Properties of the methane mono-oxygenase from extracts of *Methylosinus trichosporium* OB3b and evidence for its similarity to the enzyme from *Methylococcus capsulatus* (Bath). Eur J Biochem 96:205–212.

Stone D, Evans MJ, Edwards PM, Commane R, Ingham T, Rickard AR, Brookes DM, Hopkins J, Leigh RJ, Lewis AC, Monks PS, Oram D, Reeves CE, Stewart D, Heard DE (2011) Isoprene oxidation mechanisms: Measurements and modelling of OH and HO2 over a South-East Asian tropical rainforest during the OP3 field campaign. Atmos Chem Phys 11:6749–6771.

Sun S, Yang W, Fang W, Zhao Y, Guo L, Dai Y (2018a) The Plant Growth-Promoting Rhizobacterium *Variovorax boronicumulans* CGMCC 4969 Regulates the Level of Indole-3-Acetic Acid Synthesized from Indole-3-Acetonitrile. Plant Microbiol 84:1–14.

Sun W, Alexander T, Man Z, Xiao F, Cui F, Qi X (2018b) Enhancing 2-Ketogluconate Production of *Pseudomonas*

plecoglossicida JUIM01 by Maintaining the Carbon Catabolite Repression of 2-Ketogluconate Metabolism. Molecules 23:2629.

Surette MA, Sturz A V., Lada RR, Nowak J (2003) Bacterial endophytes in processing carrots (*Daucus carota* L. var. *sativus*): Their localization, population density, biodiversity and their effects on plant growth. Plant Soil 253:381–390.

Sutcliffe JG (1979) Complete nucleotide sequence of the *Escherichia coli* plasmid pBR322. Cold Spring Harb Symp Quant Biol 43 Pt 1:77–90.

Takahashi-Iñiguez T, García-Hernandez E, Arreguín-Espinosa R, Flores ME (2012) Role of vitamin B12 on methylmalonyl-CoA mutase activity. J Zhejiang Univ Sci B 13:423–437.

Takaku H, Miyajima A, Kazama H, Sato R, Ara S, Matsuzawa T, Yaoi K, Araki H, Shida Y, Ogasawara W, Yamazaki H (2020) A novel electroporation procedure for highly efficient transformation of *Lipomyces starkeyi*. J Microbiol Methods 169:105816.

Tamura K, Nei M (1993) Estimation of the number of nucleotide substitutions in the control region of mitochondrial DNA in humans and chimpanzees. Mol Biol Evol 10:512–526.

Tao Y, Bentley WE, Wood TK (2005) Regiospecific oxidation of naphthalene and fluorene by toluene monooxygenases and engineered toluene 4-monooxygenases of *Pseudomonas mendocina* KR1. Biotechnol Bioeng 90:85–94.

Tao Y, Fishman A, Bentley WE, Wood TK (2004) Oxidation of benzene to phenol, catechol, and 1,2,3-trihydroxybenzene by toluene 4-monooxygenase of *Pseudomonas mendocina* KR1 and toluene 3-monooxygenase of *Ralstonia pickettii* PKO1. Appl Environ Microbiol 70:3814–3820.

Tavares L, Alves PM, Ferreira RB, Santos CN (2011) Comparison of different methods for DNA-free RNA isolation from SK-N-MC neuroblastoma. BMC Res Notes 4:3.

Taylor AE, Giguere AT, Zoebelein CM, Myrold DD, Bottomley PJ (2017) Modeling of soil nitrification responses to temperature reveals thermodynamic differences between ammonia-oxidizing activity of archaea and bacteria. ISME J 11:896–908.

Tett AJ, Rudder SJ, Bourdès A, Karunakaran R, Poole PS (2012) Regulatable vectors for environmental gene expression in Alphaproteobacteria. Appl Environ Microbiol 78:7137–7140.

ThermoFisher (2017) Proteome Discoverer User Guide. Software Version 2.2 (Revision A). https://assets.thermofisher.com/TFS-Assets/CMD/manuals/Man-XCALI-97808-Proteome-Discoverer-User-ManXCALI97808-EN.pdf

Thornton B, Basu C (2011) Real-time PCR (qPCR) primer design using free online software. Biochem Mol Biol Educ 39:145–154.

Tinberg CE, Lippard SJ (2011) Dioxygen activation in soluble methane monooxygenase. Acc Chem Res 44:280–288.

Tinberg CE, Lippard SJ (2010) Oxidation Reactions Performed by Soluble Methane Monooxygenase Hydroxylase Intermediates Hperoxo and Q Proceed by Distinct Mechanisms. Biochemistry 49:7902–7912.

Tinberg CE, Lippard SJ (2009) Revisiting the Mechanism of Dioxygen Activation in Soluble Methane Monooxygenase from *M. capsulatus* (Bath): Evidence for a Multi-Step, Proton-Dependent Reaction Pathway. Biochemistry 48:12145–12158.

Tingey DT, Evans RC, Bates EH, Gumpertz ML (1987) Isoprene emissions and photosynthesis in three ferns – The influence of light and temperature. Physiol Plant 69:609–616.

Tischler D, Schwabe R, Siegel L, Joffroy K, Kaschabek SRSR, Scholtissek A, Heine T (2018) VpStyA1/VpStyA2B of *Variovorax paradoxus* EPS: An Aryl Alkyl Sulfoxidase Rather than a Styrene Epoxidizing Monooxygenase. Molecules 23:doi: 10.3390/molecules23040809.

Trainer M, Williams E, Parrish D, Buhr M, Allwine E, Westberg H, Fehsenfeld F (1987) Models and observations of the

impact of natural hydrocarbons on rural ozone. Nature 329:705–707.

Tropel D, van der Meer JR (2004) Bacterial transcriptional regulators for degradation pathways of aromatic compounds. Microbiol Mol Biol Rev 68:474–500.

Tusher TR, Shimizu T, Inoue C, Chien MF (2020) Enrichment and analysis of stable 1,4-dioxane- degrading microbial consortia consisting of novel dioxane-degraders. Microorganisms 8:doi: 10.3390/microorganisms8010050.

Unger N (2014) Human land-use-driven reduction of forest volatiles cools global climate. Nat Clim Chang 4:907–910.

Vallenet D, Calteau A, Dubois M, Amours P, Bazin A, Burlot L, Bussell X, Gautreau G, Langlois J, Roche D, Rollin J, Rouy Z, Sabatet V, Médigue M (2019) MicroScope: an integrated platform for the annotation and exploration of microbial gene functions through genomic, pangenomic and metabolic comparative analysis. Nucleic Acids Res 48:D579–D589.

Vandecasteele SJ, Peetermans WE, Merckx R, Van Eldere J (2001) Quantification of expression of *Staphylococcus epidermidis* housekeeping genes with Taqman quantitative PCR during in vitro growth and under different conditions. J Bacteriol 183:7094–7101.

Velikova V, Loreto F, Tsonev T, Brilli F, Edreva A (2006) Isoprene prevents the negative consequences of high temperature stress in *Platanus orientalis* leaves. Funct Plant Biol 33:931–940.

Velikova V, Várkonyi Z, Szabó M, Maslenkova L, Nogues I, Kovács L, Peeva V, Busheva M, Garab G, Sharkey TD, Loreto F, Oa BTW, Sharkey TD, Loreto F, Peeva V, Busheva M (2011) Increased thermostability of thylakoid membranes in isoprene-emitting leaves probed with three biophysical techniques. Plant Physiol 157:905–916.

Velugula-Yellela SR, Williams A, Trunfio N, Hsu CJ, Chavez B, Yoon S, Agarabi C (2018) Impact of media and antifoam selection on monoclonal antibody production and quality using a high throughput micro-bioreactor system. Biotechnol Prog 34:262–270.

Větrovský T, Baldrian P (2013) The Variability of the 16S rRNA Gene in Bacterial Genomes and Its Consequences for Bacterial Community Analyses. PLoS One 8:doi: 10.1371/journal.pone.0057923.

Vickers CE, Possell M, Cojocariu CI, Velikova VB, Laothawornkitkul J, Ryan A, Mullineaux PM, Hewitt CN (2009) Isoprene synthesis protects transgenic tobacco plants from oxidative stress. Plant Cell Environ 32:520–531.

Wagner WP, Helmig D, Fall R (2000) Isoprene Biosynthesis in *Bacillus subtilis* via the Methylerythritol Phosphate Pathway. J Nat Prod 63:37–40.

Wallar BJ, Lipscomb JD (2001) Methane monooxygenase component B mutants alter the kinetics of steps throughout the catalytic cycle. Biochemistry 40:2220–2233.

Wang KY, Shallcross DE (2000) Modelling terrestrial biogenic isoprene fluxes and their potential impact on global chemical species using a coupled LSM-CTM model. Atmos Environ 34:2909–2925.

Wang S, Li R, Yi X, Fang T, Yang J, Bae H-J (2016) Isoprene Production on Enzymatic Hydrolysate of Peanut Hull Using Different Pretreatment Methods. Biomed Res Int 2016:4342892.

Wang VCC, Maji S, Chen PPY, Lee HK, Yu SSF, Chan SI (2017) Alkane Oxidation: Methane Monooxygenases, Related Enzymes, and Their Biomimetics. Chem Rev 117:8574–8621.

Wang W, Iacob RE, Luoh RP, Engen JR, Lippard SJ (2014) Electron transfer control in soluble methane monooxygenase. J Am Chem Soc 136:9754–9762.

Wang W, Lippard SJ (2014) Diiron oxidation state control of substrate access to the active site of soluble methane monooxygenase mediated by the regulatory component. J Am Chem Soc 136:2244–2247.

Weiland-Bräuer N, Kisch MJ, Pinnow N, Liese A, Schmitz RA (2016) Highly effective inhibition of biofilm formation by the first metagenome-derived AI-2 quenching enzyme. Front Microbiol 7:1–19.

Weise SE, Li Z, Sutter AE, Corrion A, Banerjee A, Sharkey TD (2013) Measuring dimethylallyl diphosphate available for isoprene synthesis. Anal Biochem 435:27–34.

Wen S, Chen X, Xu F, Sun H (2016) Validation of Reference Genes for Real-Time Quantitative PCR (qPCR) Analysis of *Avibacterium paragallinarum*. PLoS One 11:e0167736–e0167736.

Wennberg PO, Bates KH, Crounse JD, Dodson LG, McVay RC, Mertens LA, Nguyen TB, Praske E, Schwantes RH, Smarte MD, St Clair JM, Teng AP, Zhang X, Seinfeld JH (2018) Gas-phase reactions of isoprene and its major oxidation products. Chem Rev 118:3337–3390.

Werner J, Nour E, Bunk B, Spröer C, Smalla K, Springael D, Öztürk B (2020) PromA plasmids are instrumental in the dissemination of linuron catabolic genes between different genera. Front Microbiol 11:doi: 10.3389/fmicb.2020.00149.

West C. A, Salmond GP. PC, Dalton H, Murrell JCC (1992) Functional expression in Escherichia coli of proteins B and C from soluble methane monooxygenase of *Methylococcus capsulatus* (Bath). Microbiology 138:1301–1307.

Whited GM, Gibsont DT, Whited GM, Gibson DT (1991) Toluene-4-monooxygenase, a three-component enzyme system that catalyzes the oxidation of toluene to p-cresol in *Pseudomonas mendocina* KR1. J Bacteriol 173:3010–3016.

Whittenbury R (1981) The interrelationship of autotrophy and methylotrophy as seen in *Methylococcus capsulatus* (Bath). In: *Microbial growth on C1 compounds*. Dalton H (ed) Heyden, London, p 181–190

Whittenbury R, Phillips KC, Wilkinson JF (1970) Enrichment, isolation and some properties of methane-utilizing bacteria. J Gen Microbiol 61:205–218.

Wiberley AE, Donohue AR, Westphal MM, Sharkey TD (2009) Regulation of isoprene emission from poplar leaves throughout a day. Plant, Cell Environ 32:939–947.

Wick RR, Judd LM, Gorrie CL, Holt KE (2017) Unicycler: Resolving bacterial genome assemblies from short and long sequencing reads. PLOS Comput Biol 13:e1005595.

Wilkinson SP, Grove A (2006) Ligand-responsive transcriptional regulation by members of the MarR family of winged helix proteins. Curr Issues Mol Biol 8:51–62.

Willems A, De ley J, Gillis M, Kersters K (1991) Comamonadaceae, a new family encompassing the *Acidovorans* rRNA complex, including *Variovorax paradoxus* gen. nov., comb. Nov., for *Alcaligenes paradoxus* (Davis 1969). Int jounal Syst Bacteriol 41:445–450.

Wilson RL, Urbanowski ML, Stauffer G V (1995) DNA binding sites of the LysR-type regulator GcvA in the gcv and gcvA control regions of *Escherichia coli*. J Bacteriol 177:4940–4946.

Wohlleben W, Arnold W, Bissonnette L, Peiletier A, Tanguay A, Roy PH, Gamboa GC, Barry GF, Aubert E, Davies J, Kagan SA (1989) On the evolution of Tn21-1ike multiresistance transposons: Sequence analysis of the gene (*aacC1*) for gentamicin acetyltransferase-3-I(AAC(3)-I), another member of the Tn21-based expression cassette. Mol Genet Genomics 217:202–208.

Wolfe GM, Kaiser J, Hanisco TF, Keutsch FN, De Gouw JA, Gilman JB, Graus M, Hatch CD, Holloway J, Horowitz LW, Lee BH, Lerner BM, Lopez-Hilifiker F, Mao J, Marvin MR, Peischl J, Pollack IB, Roberts JM, Ryerson TB, Thornton JA, Veres PR, Warneke C (2016) Formaldehyde production from isoprene oxidation across NOx regimes. Atmos Chem Phys 16:2597–2610.

Wolfe MD, Altier DJ, Stubna A, Popescu C V, Münck E, Lipscomb JD (2002) Benzoate 1,2-Dioxygenase from Pseudomonas putida: Single Turnover Kinetics and Regulation of a Two-Component Rieske Dioxygenase. Biochemistry 41:9611–9626.

Wongkittichote P, Ah Mew N, Chapman KA (2017) Propionyl-CoA carboxylase - A review. Mol Genet Metab 122:145–152.

Wongsaroj L, Saninjuk K, Romsang A, Duang-nkern J, Trinachartvanit W, Vattanaviboon P, Mongkolsuk S (2018) *Pseudomonas aeruginosa* glutathione biosynthesis genes play multiple roles in stress protection, bacterial virulence and biofilm formation. PLoS One 13:1–18.

Wood WBWB, Woont WB, Wood WBWB (1966) Host Specificity of DNA produced by *Escherichia coli*: Bacterial

Mutations affecting the Restriction and Modification of DNA. J Mol Biol 16:118–133.

World Health Organization (2000) Air Quality Guidelines. Global update 2005, Second Edi. WHO Regional Publications.

Wu ML, Wessels HJCT, Pol A, Jetten MSM, Niftrik L Van, Keltjens JT (2015) XoxF-Type Methanol Dehydrogenase from the Anaerobic Methanotroph "*Candidatus Methylomirabilis oxyfera*". Appl Environ Microbiol 81:1442–1451.

Wübbeler JH, Hiessl S, Meinert C, Poehlein A, Schuldes J, Daniel R, Steinbüchel A (2015) The genome of *Variovorax paradoxus* strain TBEA6 provides new understandings for the catabolism of 3,3'-thiodipropionic acid and hence the production of polythioesters. J Biotechnol 209:85–95.

Xin X-F, He SY (2013) *Pseudomonas syringae* pv. tomato DC3000: A Model Pathogen for Probing Disease Susceptibility and Hormone Signaling in Plants. Annu Rev Phytopathol 51:473–498.

Xu J, Zhang W (2016) Strategies used for genetically modifying bacterial genome: site-directed mutagenesis, gene inactivation, and gene over-expression. J Zhejiang Univ Sci B 17:83–99.

Yang J, Zhao G, Sun Y, Zheng Y, Jiang X, Liu W, Xian M (2011) Bio-isoprene production using exogenous MVA pathway and isoprene synthase in *Escherichia coli*. Bioresour Technol 104:642–647.

Ye J, Coulouris G, Zaretskaya I, Cutcutache I, Rozen S, Madden TL (2012) Primer-BLAST: a tool to design target-specific primers for polymerase chain reaction. BMC Bioinformatics 13:134.

Yeager CM, Bottomley PJ, Arp DJ, Hyman MR (1999) Inactivation of Toluene 2-Monooxygenase in *Burkholderia cepacia* G4 by Alkynes. Appl Environ Microbiol 65:632–639.

Yen KM, Gunsalus IC (1985) Regulation of naphthalene catabolic genes of plasmid NAH7. J Bacteriol 162:1008–1013.

Yen KM, Karl MR, Blatt LM, Simon MJ, Winter RB, Fausset PR, Lu HS, Harcourt AA, Chen KK (1991) Cloning and characterization of a *Pseudomonas mendocina* KR1 gene cluster encoding toluene-4-monooxygenase. J Bacteriol 173:5315–5327.

Yoon JH, Kang SJ, Oh TK (2006) *Variovorax dokdonensis* sp. nov., isolated from soil. Int J Syst Evol Microbiol 56:811–814.

Zeaiter Z, Mapelli F, Crotti E, Borin S (2018) Methods for the genetic manipulation of marine bacteria. Electron J Biotechnol 33:17–28.

Zeidler J, Schwender J, Müller C, Wiesner J, Weidemeyer C, Beck E, Jomaa H, Lichtenthaler HK (1998) Inhibition of the Non-Mevalonate l-Deoxy-D-xylulose-5-phosphate Pathway of Plant Isoprenoid Biosynthesis by Fosmidomycin. A J Biosci Zeitschrift für Naturforsch C 53c:980–986.

Zhang X, Guo C, Chen Y, Shulha HP, Schnetz MP, LaFramboise T, Bartels CF, Markowitz S, Weng Z, Scacheri PC, Wang Z (2008) Epitope tagging of endogenous proteins for genome-wide ChIP-chip studies. Nat Methods 5:163–165.

Zhao L, Chang WW, Xiao Y, Liu HH, Liu P (2013) Methylerythritol phosphate pathway of isoprenoid biosynthesis. Annu Rev Biochem 82:497–530.

Zhao Y, Yang J, Qin B, Li Y, Sun Y, Su S, Xian M (2011) Biosynthesis of isoprene in *Escherichia coli* via methylerythritol phosphate (MEP) pathway. Appl Microbiol Biotechnol 90:1915–1922.

Zheng J, Feng JQ, Zhou L, Mbadinga SM, Gu JD, Mu BZ (2018) Characterization of bacterial composition and diversity in a long-term petroleum contaminated soil and isolation of high-efficiency alkane-degrading strains using an improved medium. World J Microbiol Biotechnol 34:doi: 10.1007/s11274-018-2417-8.

Zhou N, Fuenmayor SL, Williams PA (2001) *Nag* Genes of *Ralstonia* (Formerly *Pseudomonas*) sp. Strain U2 Encoding Enzymes for Gentisate Catabolism. J Bacteriol 183:700–708.

Zhou NY, Chan Kwo Chion CK, Leak DJ, Chan NZCK, Chion K (1996) Cloning and expression of the genes encoding the propene monooxygenase from *Xanthobacter*, Py2. Appl Microbiol Biotechnol 44:582–588.

Zhou NY, Jenkins A, Chan Kwo Chion CKN, Leak DJ (1999) The alkene monooxygenase from *Xanthobacter* strain Py2 is

closely related to aromatic monooxygenases and catalyzes aromatic monohydroxylation of benzene, toluene, and phenol. Appl Environ Microbiol 65:1589–1595.

Zhu L, Mickley LJ, Jacob DJ, Marais EA, Sheng J, Hu L, Abad GG, Chance K (2017) Long-term (2005-2014) trends in formaldehyde (HCHO) columns across North America as seen by the OMI satellite instrument: Evidence of changing emissions of volatile organic compounds. Geophys Res Lett 44:7079–7086.

Zuo ZZ-J, Weraduwage SM, Lantz AT, Sanchez LM, Weise SE, Wang J, Childs KL, Sharkey TD (2019) Isoprene acts as a signaling molecule in gene networks important for stress responses and plant growth. Plant Physiol 180:124–152.

11. Appendices

11.1. **Growth media and buffer preparation**

Growth media components were prepared using distilled water and sterilised by autoclaving for 15 minutes at 121 ^{o}C. Heat-sensitive solutions were sterilised by passage through a 0.2 µm syringe filter (Sartorius Ministart, Göttingen, Germany) before addition to the relevant growth medium. Rich solid media were prepared with 1.5% (w/v) agar granulated bacteriological grade (Formedium, Hunstanton, UK), while chemically defined solid media were prepared with 1.5% (w/v) bacto agar (Difco, Waltham, MA, USA). The minimal medium initially described by Dorn *et al*. (1974), herein Ewers medium, was prepared as follows.

(10x) mineral salts:

$(NH_4)_2SO_4$	10 g L^{-1}
$MgSO_4.7H_2O$	2 g L^{-1}
$Ca(NO_3)_2.4H_2O$	0.725 g L^{-1}

(100x) Fe Ammonium Citrate:

1 g L^{-1}

(1,000x) Trace Elements (SL-6 (Quayle & Pfennig 1975)**)**:

$ZnSO_4.7H_2O$	10 mg L^{-1}
$MnCl_2.4H_2O$	3 mg L^{-1}
H_3BO_3	30 mg L^{-1}
$CoCl_2.6H_2O$	20 mg L^{-1}
$CuCl_2.2H_2O$	1 mg L^{-1}
$NiCl_2.6H_2O$	2 mg L^{-1}
$Na_2MoO_4.2H_2O$	3 mg L^{-1}

1 M Phosphate Buffer (pH 6.0)

KH_2PO_4	0.5 M

Na_2HPO_4	0.5 M

(1,000x) MAMS (marine ammonium mineral salts) vitamins

(Kanagawa *et al*. 1982)

Thiamine hydrochloride	10 mg L^{-1}
Nicotinic acid	20 mg L^{-1}
Pyroxidine hydrochloride	20 mg L^{-1}
p-aminobenzoic acid	10 mg L^{-1}
Riboflavin	20 mg L^{-1}
Calcium pantothenate	20 mg L^{-1}
Biotin	1 mg L^{-1}
Cyanocobalamin B12	2 mg L^{-1}
Lipoic acid	5 mg L^{-1}
Folic acid	5 mg L^{-1}

Mineral salts, ferrous ammonium citrate, and trace elements were prepared to 1x concentration in distilled water and sterilised by autoclaving. Autoclaved phosphate buffer was added to 3% (v/v) and MAMS vitamins, sterilised by passage through a 0.2 µm syringe filter, was added to 1x.

Luria-Bertani (LB) medium was prepared in distilled water with the following components and sterilised by autoclaving.

Luria-Bertani (LB) medium

Tryptone	10 g L^{-1}
Yeast Extract	5 g^{-1}
NaCl	10 g L^{-1}

Chemical competence medium used in the preparation of chemically competent *Escherichia coli* was prepared as follows.

Chemical competence buffer (pH 6.4)

1M Potassium acetate	1% (v/v)
$MnCl_2.4H_2O$	4 g L^{-1}

$MgCl_2.6H_2O$	2 g L^{-1}
Glycerol	10% (v/v)

Super optimal broth (SOB) medium used in the preparation of chemically competent *E. coli* was prepared as follows.

Super optimal broth

Tryptone	20 g L^{-1}
Yeast Extract	4 g L^{-1}
NaCl	2 g L^{-1}
250 mM KCl	10% (v/v)
2M $MgCl_2$	0.5% (v/v)*
2M $MgSO_4$	0.5% (v/v)*

*Autoclaved separately and added to sterilised, cooled SOB medium.

Super optimal broth with catabolite repression (SOC) medium used in the recovery of chemically competent *E. coli* was prepared as follows.

SOC medium

Tryptone	20 g L^{-1}
Yeast Extract	5 g L^{-1}
NaCl	10 mM
KCl	2.5 mM
$MgCl_2$	10 mM
$MgSO_4$	10 mM
Glucose	20 mM